

✓ VOL. 102 DECEMBER 31, 1974

COMPLETE IN ONE ISSUE

**3rd Symposium on Ion Exchange,
Balatonfüred, May 28-31, 1974**

L. OF

CHROMATOGRAPHY

INTERNATIONAL JOURNAL ON CHROMATOGRAPHY, ELECTROPHORESIS AND RELATED METHODS

EDITOR, Michael Lederer (Rome)

ASSOCIATE EDITOR, K. Macek (Prague)

EDITORIAL BOARD

W. A. Aue (Halifax)
V. G. Berezkin (Moscow)
A. Bevenue (Honolulu, Hawaii)
P. Boulanger (Lille)
G. P. Cartoni (Rome)
K. V. Chmutov (Moscow)
G. Duyckaerts (Liège)
L. Fishbein (Jefferson, Ark.)
A. Frigerio (Milan)
C. W. Gehrke (Columbia, Mo.)
I. M. Hais (Hradec Králové)
N. G. L. Harding (Cambridge)
E. Heftmann (Berkeley, Calif.)
S. Hjertén (Uppsala)
E. C. Horning (Houston, Texas)
I. F. K. Huber (Vienna)
A. T. James (Sharnbrook, Beds)
J. Janák (Brno)
A. I. M. Keulemans (Eindhoven)
K. A. Kraus (Oak Ridge, Tenn.)
E. Lederer (Gif-sur-Yvette, S. et O.)
A. Liberti (Rome)
H. M. McNair (Neuchâtel)
Y. Marcus (Jerusalem)
G. B. Marini-Bettolo (Rome)
R. Neher (Basel)
G. Nickless (Bristol)
J. Novák (Brno)
O. Samuelson (Göteborg)
G.-M. Schwab (Munich)
G. Semenza (Zürich)
L. R. Snyder (Tarrytown, N.Y.)
H. Tuppy (Vienna)
A. Zlatkis (Houston, Texas)

EDITORS, BIBLIOGRAPHY SECTION

K. Macek (Prague), J. Janák (Brno), Z. Deyl (Prague)

EDITOR, BOOK REVIEW SECTION

R. Ar. os (Abingdon)

EDITOR, NEWS SECTION

J. F. K. Huber (Vienna)

COORD. EDITOR, DATA SECTION

J. Gasparič (Hradec Králové)

ELSEVIER SCIENTIFIC PUBLISHING COMPANY
AMSTERDAM

period.

CONTENTS

~~Third Symposium on Ion Exchange, Balatonfüred (Hungary), May 28-31, 1974~~

Contents	VII
Preface	1
<i>Plenary lectures</i>	
Recent progress in the field of synthetic inorganic exchangers having a layered or fibrous structure by G. Alberti and U. Costantino (Perugia, Italy)	5
The phenomenon of osmosis in permeable membranes by G. Dickel (Munich, G.F.R.)	31
Chemical equilibria in ion-exchange chromatography by J. Inczédy (Veszprém, Hungary)	41
Ion exchange, isotope exchange and isotope separation by H. Kakihana (Tokyo, Japan)	47
Liquid chromatography of organic compounds on ion-exchange resins by H. F. Walton (Boulder, Colo., U.S.A.)	57
The use of liquid ion exchangers in extraction chromatography by G. Werner (Leipzig, G.D.R.)	69
<i>Ion-exchange materials</i>	
Examination of ion-exchange resins by derivatography by O. Nagy, H. Gaál and J. Szabó (Budapest, Hungary)	77
Investigation of structure heterogeneity in ion-exchange membranes by M. S. Gorodnev, G. K. Saldadze, V. K. Varentsov and I. M. Abramova (Moscow, U.S.S.R.)	83
Selective properties and analytical use of an ion-exchange resin based on α -phenylvinylphosphonic acid by M. Marhol and J. Chmelíček (Prague, Czechoslovakia) and A. B. Alovitdinov and Ch. U. Kočkarova (Tashkent, U.S.S.R.)	89
The mobility of cerium ions in synthetic zeolites by A. Dyer and A. B. Ogden (Salford, Great Britain)	95
Zur Selektivität des Kationenaustauschs an kristallinen Ce(IV)-phosphat-sulfaten von K.-H. König (Frankfurt am Main, B.R.D.)	99
Preparation of some new inorganic ion exchangers by L. Szirtes and L. Zsinka (Budapest, Hungary)	105
Infrared and X-ray measurements on various inorganic ion exchangers by L. Zsinka, L. Szirtes, J. Mink and A. Kálmán (Budapest, Hungary)	109

© ELSEVIER SCIENTIFIC PUBLISHING COMPANY — 1974

All rights reserved. No part of this publication may be reproduced, stored in a retrieval system, or transmitted, in any form or by any means, electronic, mechanical, photocopying, recording, or otherwise, without permission in writing from the publisher.

Neue Ergebnisse über die Porosität von Styrol-Divinylbenzol-Copolymerisaten und Ionenaustauscherharzen von K. Häupke und V. Pienta (Bitterfeld, D.D.R.).	117
Untersuchung zur Herstellung stark saurer Kationenaustauscher auf der Basis von Styrol-Bis-(4-vinylphenyl)-methan-Copolymeren von G. Schwachula und D. Lukas (Bitterfeld, D.D.R.)	123
Synthesis and properties of some snake-cage ion-retardation resins by R. Bogoczek (Gliwice, Poland)	131
Beitrag zur Basizitätsprüfung von stark basischen Anionenaustauschern von H. Hecker (Bitterfeld, D.D.R.).	135
<i>Theory of ion exchange</i>	
A proposal for the nomenclature of exchangers by R. Hering (Güstrow, G.D.R.).	141
Comparison of experimental and theoretical rates of ion exchange by S. C. Duffy (Harrow, Great Britain) and L. V. C. Rees (London, Great Britain)	149
Chloride-sulphate exchange on anion-exchange resins. Kinetic investigations. I by L. Liberti and R. Passino (Rome, Italy)	155
Investigation of anion-exchange equilibria of maleic and fumaric acids by A. Marton and J. Inczédy (Veszprém, Hungary).	165
Kinetics of differential ion-exchange processes in a finite solution volume by K. Bunzl (Neuherberg, G.F.R.).	169
Transferts de masse d'échange d'ions minéraux perturbés par la fixation simultanée d'ions organiques volumineux par A. Abadie et H. Roques (Toulouse-Cédex, France)	181
Mechanism of cation exchange on silica gels by D. N. Strazhesko, V. B. Strelko, V. N. Belyakov and S. C. Rubanik (Kiev, U.S.S.R.)	191
Effect of cross-linking of a sulphonic cation-exchange resin and effect of temperature on the chromatographic separation of isomers of dinitrobenzene by J. Chmielowiec and W. Kemula (Warsaw, Poland)	197
Selective swelling of ion exchangers in mixed solvents and the effect of swelling on the sorption of ions by A. Lásztity and T. A. Belyavskaya (Budapest, Hungary)	203
Some aspects of ion-exchange in non-aqueous and mixed solvents by J. D. R. Thomas (Cardiff, Great Britain)	209
Anion exchange in ternary mixtures of aliphatic acids, mineral acids and water by S. K. Jha, F. de Corte and J. Hoste (Gent, Belgium).	217
The extraction of copper(II) ions with liquid anion exchangers using salicylate as complex-forming agent by E. Papp and J. Inczédy (Veszprém, Hungary)	225
Determination of the optimal conditions for ion-exchange processes by R. N. Rubinstein, M. M. Senyavin, E. V. Venitsianov, E. M. Makhalov, V. A. Alekseenko and V. A. Nikashina (Moscow, U.S.S.R.).	235
<i>Analytical applications</i>	
Chromatographic behaviour of amino acids on cation-exchange resin-coated chromatoshets in the H ⁺ form by I. Hazai, S. Zoltán, J. Salát, S. Ferenczi and T. Dévényi (Budapest, Hungary)	245
Chromatographic separation of dansyl amino acids and dansyl amines on Amberlite IRC-50 by T. Seki and H. Wada (Osaka, Japan)	251

(Continued overleaf)

Contents (continued)

Combined application of ion-exchange chromatographic methods for the study of "minor basic amino acids" by E. Tyihák (Budakalasz, Hungary) and S. Ferenczi, I. Hazai, S. Zoltán and A. Patthy (Budapest, Hungary)	257
The use of the amphoteric ion-exchange resin Retardion 11A8 for inorganic separations by R. Dybczyński and E. Sterlińska (Warsaw, Poland)	263
Separation of metal ions by mixed column ion-exchange chromatography by T. Yamabe and T. Hayashi (Tokyo, Japan)	273
Échange d'anions des éléments sur une résine échangeuse anionique de faible basicité en milieu de l'acide bromhydrique par L. Wódkiewicz et R. Dybczyński (Varsovie, Pologne)	277
Chelate sorbents for concentration and separation of noble metals by S. B. Savvin, I. I. Antokolskaja, G. V. Myasoedova, L. I. Bolshakova and O. P. Shvoeva (Moscow, U.S.S.R.)	287
Extraction chromatography with liquid ion exchangers as stationary phase by C. Testa and A. Delle Site (Rome, Italy)	293
Extraction chromatography with liquid ion exchangers by G. Ghersini (Milan, Italy)	299
The use of aqueous thiocyanate solutions in liquid-liquid extraction and reversed-phase extraction chromatography. I by U. A. Th. Brinkman, G. de Vries, R. Jochemsen and G. J. de Jong (Amsterdam, The Netherlands)	309
Separation of metals on ion-exchange resins by means of α -hydroxyisobutyronitrile as complexing agent by L. Légrádi (Füzfőgyártelep, Hungary)	319
Neuartige Kationenaustauscher auf Kieselgelbasis. I. Darstellung und Eigenschaften von N. Weigand, I. Sebastian and I. Halász (Saarbrücken, B.R.D.)	325
Separation of acidic compounds by high-pressure liquid-liquid chromatography involving ion-pair formation by J. C. Kraak and J. F. K. Huber (Amsterdam The Netherlands)	333
High-pressure liquid chromatography with ion-exchange celluloses and its application to the separation of estrogen glucuronides by Sj. van der Wal and J. F. K. Huber (Amsterdam, The Netherlands)	353
Separation of optical isomers by ion-exchange chromatography using copper(II) ions as complex-forming agents by J. Gaál and J. Inczédy (Veszprém, Hungary)	375
Separation of some chloramphenicol intermediates by high-pressure ion-exchange chromatography by Gy. Vigh and J. Inczédy (Veszprém, Hungary)	381
Application of ligands with sulphonic groups to the separation of metal ions on strongly basic anion exchangers by K. Brajter (Warsaw, Poland)	385

Ion-exchange technology

Prevention of calcium sulphate scale formation in evaporation plants by ion exchange by G. Boari, L. Liberti and R. Passino (Rome, Italy)	393
Some problems in the separation of copper and iron from mine waters by A. Sopková (Košice, Czechoslovakia), K. Vetejška (Prague, Czechoslovakia) and J. Bubanec (Košice, Czechoslovakia)	403

Puriwat® apparatus. A system of ion-exchange celluloses for the production of high-purity water by Zs. Horváth (Budapest, Hungary)	409
Échange d'ions en lit mobile à plusieurs constituants. Recherche d'une méthode de conception et de calcul pour des colonnes préparatives de petite dimension par M. Bailly et D. Tondeur (Villers-les-Nancy, France)	413
Fonctionnement cyclique d'un lit fixe d'échange d'ions avec trois constituants par G. Grevillot, D. Tondeur et J. A. Dodds (Villers-les-Nancy, France)	421
Elution of uranium from an anion-exchange resin by extraction with an organic extractant in the presence of an aqueous phase by M. Erdélyi and B. Czeglédi (Pécs, Hungary) and M. Vigvári (Budapest, Hungary) .	429
Countercurrent elution of uranium(VI) and iron(III) from an anion-exchange resin by M. Vigvári (Budapest, Hungary) and M. Erdélyi and B. Czeglédi (Pécs, Hungary) .	433
Ion exchange in agitated beds. Simulation of an ion-exchange column by model of agitated tanks in cascade by A. E. Rodrigues (Luanda, Angola)	437
The Akzo process for the removal of mercury from waste water by G. J. de Jong and C. J. N. Rekers (Hengelo, The Netherlands)	443
Einsatzmöglichkeiten von pulverförmigen Ionenaustauschern in der Kondensataufbereitung von R. Schaaf (Bitterfeld, D.D.R.)	451
The ion-exchange behaviour of arsenic(III) on VARION anion-exchange resins by I. Bálint-Ambró (Veszprém, Hungary)	457
Author Index	461
Subject Index	463

**Volume 2: Metals, Gaseous and
Industrial Pollutants**
of the 4 volume work

CHROMATOGRAPHY OF ENVIRONMENTAL HAZARDS

by **L. FISHBEIN**, Department of Health, Education and Welfare, Public Health Service, Food and Drug Administration, National Center for Toxicological Research, Jefferson, Ark., North Carolina State University, Raleigh, N.C., U.S.A.

1974. 650 pages. Dfl. 150.00 (about US\$54.60)
ISBN 0-444-41059-7

CONTENTS:

Introduction. Beryllium and chromium. Manganese, cobalt, nickel and cadmium. Tin and lead. Arsenic and phosphorus. Selenium and tellurium. Inorganic and organic mercury. Thallium and vanadium. Radionuclides: strontium-90, yttrium-91 and cesium-137. Radionuclides: actinides. Nitrogen gas (oxides of nitrogen, ammonia). Sulfur gases. Halogen gases. Carbon monoxide and carbon dioxide. Oxidants (ozone and peroxyacyl nitrates). Phosgene, cyanogen and hydrogen cyanide. Hydrocarbons (paraffinic and olefinic). Miscellaneous gaseous mixtures. Polycyclic aromatic hydrocarbons. Aromatic hydrocarbons. Chlorinated aliphatic hydrocarbons. Phenols. Aniline and derivatives. Polychlorinated biphenyls. Phthalate esters. Nitrilotriacetic acid. Miscellaneous industrial chemicals. Index.

Previously Published:

Volume 1: Carcinogens, Mutagens and Teratogens

1972. 508 pages. Dfl. 135.00 (about US\$49.10)
ISBN 0-444-40948-3

Elsevier

P.O. Box 211
Amsterdam, The Netherlands

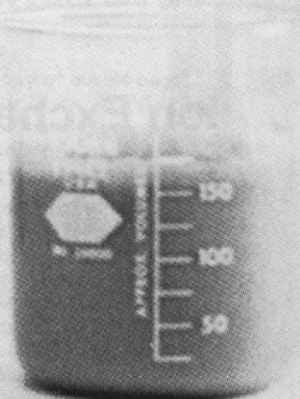
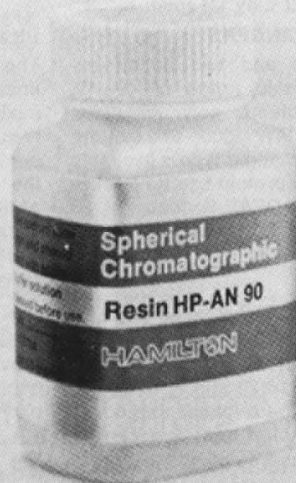
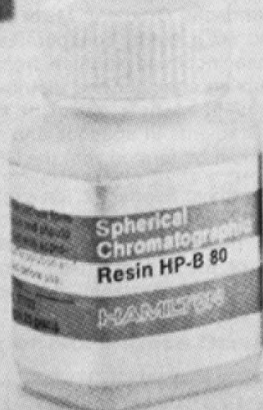


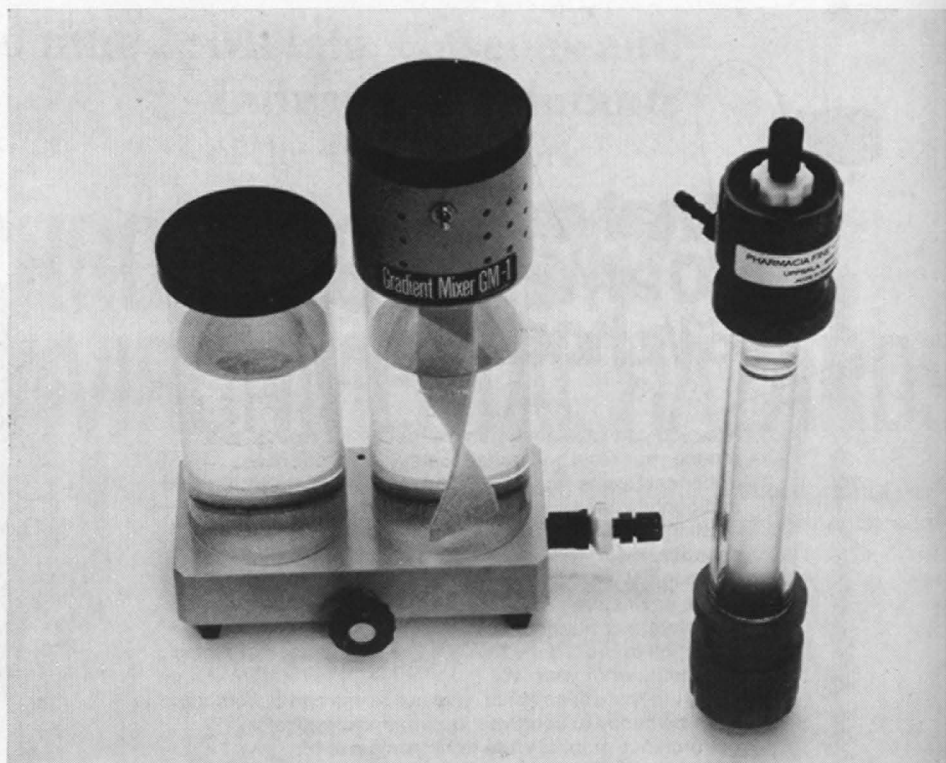
Analyze over 50 amino acids in 6 1/2 hours

Now you can save analysis time, get better results, and reduce your resin and buffer costs . . . with our new Spherical Resins for Column chromatography in amino acid and peptide analysis . . . and it's all compatible with your existing equipment. The key is our highly controlled spherical resin, with a reproducible, stable polymer bead. You can get three types of resins to handle the separation of acidic and neutral, and basic amino acids in either hydrolyzate or physiological procedures. With the reduction in procedure time, it's like having another amino acid analyzer in your lab.

If you analyze amino acids, give our resins and buffers a try. We'll be happy to send you literature and typical performance graphs. Write to Micromesure b.v., P.O. Box 205, The Hague 2076, Holland.

HAMILTON





Which?

Ion Exchanger • Column • Gradient Mixer

SEPHADEX® ION-EXCHANGERS

Two anion exchangers and two cation exchangers cover the whole range pH 2–12. High capacities for proteins, polynucleotides and other biopolymers MW 1000–200,000 are ensured as each ion-exchanger type is available in two porosities. 1 gram protein can be fractionated on a 30 ml bed of DEAE-Sephadex A-50 using only 10 % of its available capacity.

PHARMACIA COLUMNS

Fast separations using columns of the K15 and K16 series exploit to the full the high capacities and superior resolution of Sephadex ion-exchangers. Columns K 16/20 and K 15/30 are particularly suitable for bed volumes up to 40 or 50 ml. Thermostat jacket and flow control valve are standard on the K16 columns.

PHARMACIA GRADIENT MIXER GM-1

The prime requirement for the production of linear ionic strength gradients is efficient mixing of the components of the gradient. In the Pharmacia Gradient Mixer GM-1 this is achieved by a blade configuration which lifts the dense incoming solution from the bottom of the mixing chamber and distributes it evenly throughout the whole eluant at a low stirring speed. Gradients in aqueous and most organic solvents can be formed with the GM-1.

Used together, Sephadex ion-exchangers and apparatus from Pharmacia Fine Chemicals provide practical chromatographic systems capable of the highest resolution in the ion-exchange chromatography of biopolymers.

Pharmacia Fine Chemicals AB
Box 604
S-751 25 UPPSALA 1
Sweden



**Pharmacia
Fine Chemicals**

PIERCE



RAPID ONE-STEP PREPARATION OF TMS DERIVATIVES

TRI-SIL/BSA is a potent formulation for the rapid, one-step preparation of trimethylsilyl ("TMS") derivatives of polar organic compounds, such as alcohols, phenols, other hydroxy or polyhydroxy compounds, acids, amides and amines, for gas phase analysis and synthetic procedures. Prepared from the powerful silyl donor, BSA (N,O-bis-TMS-acetamide) and freshly distilled dry pyridine (Formula P) or dimethylformamide (Formula D). Packaged in convenient 25 ml Hypo-vials or 1 ml glass ampules.

- 49011 TRI-SIL/BSA, Formula P
25 ml Hypo-Vial™/\$18
10 x 1 ml Ampules/\$15 pkg
- 49010 TRI-SIL/BSA, Formula D
25 ml Hypo-Vial™/\$18
10 x 1 ml Ampules/\$15 pkg

Our silylation reagents are known the world over for their purity, efficiency and convenience. The ready for use TRI-SIL formulations rapidly produce volatile and thermally stable derivatives for gas phase analyses in simple one step procedures. Our free 48 page booklet *Handbook of Silylation* describes these and other reagents, solvents and standards, lists methods and references and provides numerous suggestions and practical ideas. If you don't have a copy we'll be glad to send you one.

We will also send you a copy of our 84 page *Pierce Unique Laboratory Aids and G.C. Accessories* that describes many clever and helpful items for your laboratory. Ask for a "G.C.Pack" and we'll send you both booklets.

SERVING YOU FROM 3 STRATEGIC LOCATIONS



PIERCE EUROCHEMIE B.V.

P.O. Box 1151,

Rotterdam, Holland



PIERCE & WARRINER (UK) LTD

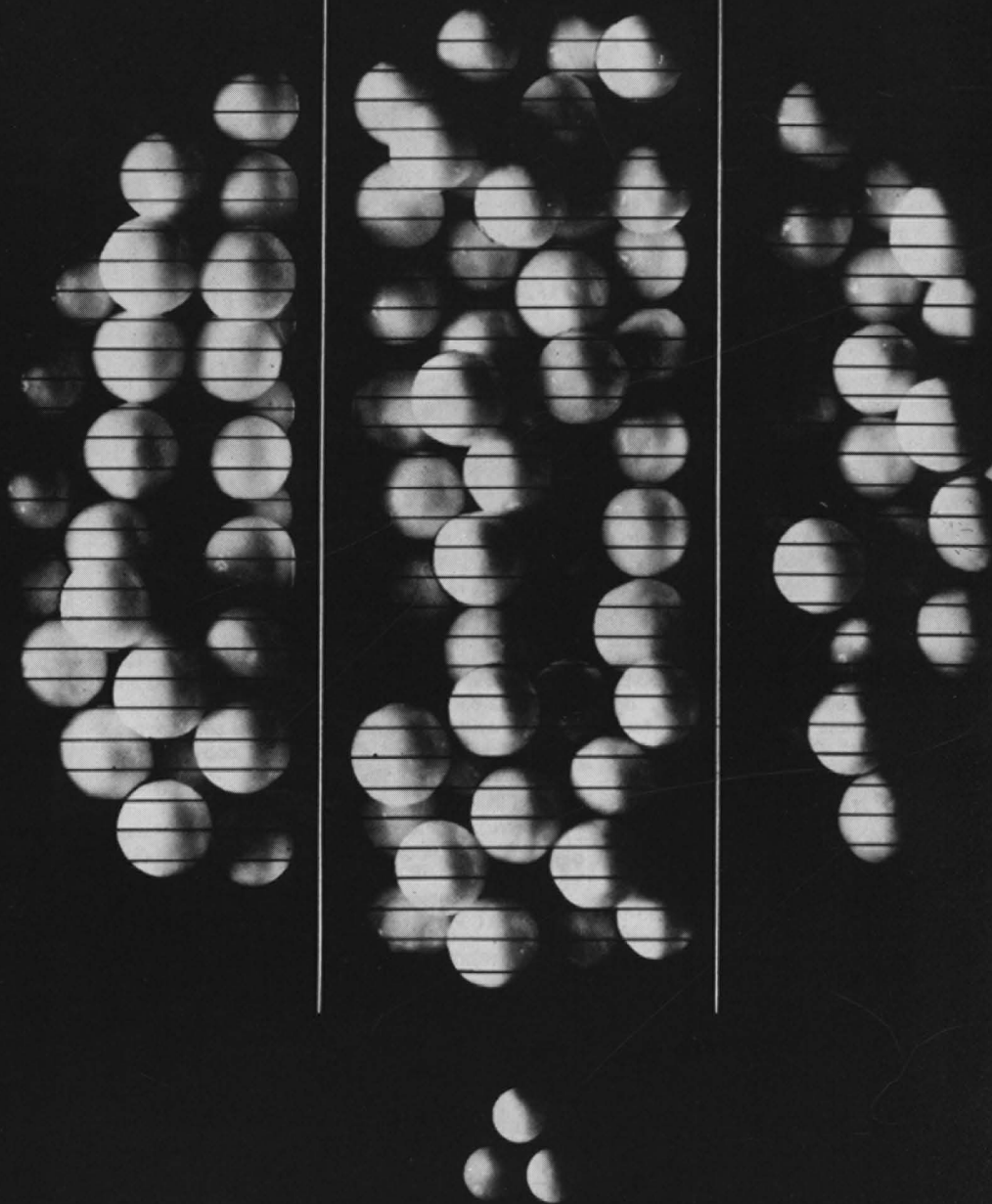
44 Upper Northgate Street, Chester, Cheshire CH1 4EF England



PIERCE

Box 117, Rockford, Illinois 61105, U.S.A.

 CHEMAPOL



MATERIALS FOR
GAS CHROMATOGRAPHY
THIN LAYER CHROMATOGRAPHY
PERMEATION GEL CHROMATOGRAPHY



GAS CHROMATOGRAPHY

CHROMATON N

White kieselguhr column support material of low density, small specific surface and relatively high porosity. The material is also available in acid-washed and silanized forms /DMCS, HMDS/, in seven different grain sizes from 0.10 to 0.63 mm. The support materials of this type exhibit very low adsorption and catalytic activity and are therefore suitable for the separation of strongly adsorbing polar substances.

CHROMATON N SUPER AND INERTON SUPER

Special silanized and deactivated column support materials showing a low catalytic and adsorption activity. They are suitable for difficult determinations and separation of trace amounts of substances decomposing readily at the analytical temperature /pesticides, steroids and substances of biological origin/. Chromaton N-Super and Inerton Super are available in two grain sizes, 125 - 0.15 mm and 0.16 - 0.20 mm, respectively.

CHEZASORB

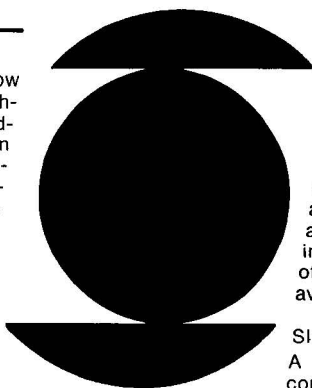
White kieselguhr column support materials of relatively higher apparent density, a larger specific surface area and relatively narrower pores. Chezasorb materials are likewise available in acid-washed and silanized forms /DMDS/ in four different grain sizes from 0.10 to 0.63 mm. The Chezasorb materials show high mechanical strength and a high efficiency in the separation of non-polar substances. The silanized form of Chezasorb is suitable for the separation of polar substances.

INERTON

White silicate column support materials of low apparent density, a very small specific surface and a narrow pore size distribution. Acid-washed and silanized forms /DMCS, HMDS/ in seven different grain sizes from 0.10 to 0.63 mm are also applied to order. The materials provide an advantageous combination of low adsorption and catalytic activity with high mechanical strength. They show high adsorption inertness towards polar compounds and a low catalytic activity towards readily decomposing substances.

READY-MADE COLUMN PACKINGS AND STATIONARY PHASES

All types of packing are supplied to special order with stationary phases in the form of ready-made column packings. A wide assortment of stationary phases is also supplied separately.



Make your choice from our wide range of materials and reagents for chromatography:

THIN-LAYER CHROMATOGRAPHY

SILICAGEL L 5/40

A high-purity adsorbent for thin-layer chromatography. In addition to the basic type, a type with added gypsum /LS 5/40/ and one with gypsum and an inorganic luminescent indicator for a wavelength of 254 nm /LSL 5/4/ are available.

SILUFOL

A reflexive silicagel sheet composed of aluminium foil and a coat of SILPEARL silicagel. The sheet material is supplied in sizes of 15x15 cm, 5x15 cm and 20x20 cm. Apart from the standard type we also supply SILUFOL with an inert inorganic luminescent indicator for the UV range of 254 nm or 366 nm or in mixture for both wavelengths, and SILUFOL 20 with a thicker silicagel coat /0.20mm/.

LUCEFOL

Reflecting sheets in which microcrystalline cellulose, free from any bonding agent, serves as adsorbent.

GEL PERMEATION CHROMATOGRAPHY

SPHERON P

A hydrophilic glycolmethacrylic gel of defined porosity for a wide range of separations. SPHERON has an outstanding mechanical strength and hydrolytic stability which makes it an ideal material for high-speed, high-resolution chromatography. Several types differentiated by elution limits and grain sizes are available.

SPHERON P is an universal gel suitable for separation of high-molecular substances in aqueous media as well as in polar organic solvents.



CHEMAPOL



All the above materials are manufactured by Lachema, National Corporation

Please mail me further technical information on your materials for



GAS CHROMATOGRAPHY



THIN-LAYER CHROMATOGRAPHY



GEL PERMEATION CHROMATOGRAPHY

Sole exporter
CHEMAPOL Co. Ltd.
Kodanská 46
Praha 10 /
Czechoslovakia
Telephone 715
Telex 122021

THE HPLC COLUMN -

Latest news on the Reeve Angel contribution to

High performance Liquid Chromatography

PRE-PACKED COLUMNS

Columns pre-packed with any of the stationary phases listed below are available from Reeve Angel. They are offered as original and replacement equipment for most leading commercial liquid chromatographs. Each column is carefully quality controlled for reproducible performance.

PARTISILS - SILICAS

Micro particulate silicas in three narrow size ranges: 5µm, 10µm, 20µm - developed specially for L.C. Plate heights less than 0.03mm are normal on 10µm Partisil.

PELLOSILS - SILICAS

Low band dispersion and rapid elution are important features of Pellosils. Each particle comprises a thin pellicle of silica bonded to a spherical vitreous core.

PELLUMINAS - ALUMINAS

Pellicular aluminas with applications in separating less polar substances, such as polycyclic hydrocarbons and fat soluble vitamins.

PELLIDON - POLYAMIDE

A porous polyamide pellicle which makes TLC separations normally done on polyamides now possible by HPLC. Very stable and non-compressible.

PELLIONEX - ION EXCHANGERS

Two pellicular cation exchangers and three anion, each having great stability and selectivity.

For further information send today to

REEVE ANGEL SCIENTIFIC LTD.,
SPRINGFIELD MILL, MAIDSTONE, KENT, ENGLAND
Telephone (0622) 61681, telex 96113

* Whatman S.a.r.l., Zone Industrielle, Ferrières en Gatinais 45, Loiret, France

Reeve Angel Scientific Ltd. is a member of the Whatman Reeve Angel Group
582vb

Books in Chromatography

Bibliography of Paper and Thin-Layer Chromatography 1961-1965

edited by K. MACEK, I. M. HAIS, J. KOPECKÝ and J. GASPARIČ

1968. 1040 pages. Out of print.

Only available on microfilm: Dfl. 150.00 (about US\$54)

Bibliography of Paper and Thin-Layer Chromatography 1966-1969

edited by K. MACEK, I. M. HAIS, J. KOPECKÝ, J. GASPARIČ, V. RÁBEK and J. CHURÁČEK

1972. 1008 pages. Dfl. 200.00 (about US\$72.70)

Bibliography of Column Chromatography 1967-1970

edited by Z. DEYL, J. ROSMUS, M. JUŘICOVÁ and J. KOPECKÝ

1973. 1088 pages. Dfl. 180.00 (about US\$65.50)

(Published as a supplement to the Journal of Chromatography)

Liquid Column Chromatography

edited by Z. DEYL, K. MACEK and J. JANÁK

1974. In preparation.

Practical Manual of Gas Chromatography

edited by J. TRANCHANT

1969. 407 pages. Dfl. 100.00 (about US\$36.40)

Chromatography of Environmental Hazards

by L. FISHBEIN

Vol. 1: Carcinogens, Mutagens and Teratogens

1972. 508 pages. Dfl. 135.00 (about US\$49.10)

Vol. 2: Metals, Gaseous and Industrial Pollutants

1973. 630 pages. Dfl. 150.00 (about US\$54.60)

Vol. 3: Pesticides

1974.

Vol. 4: Drugs

1975.

Chromatography of Antibiotics

by G. H. WAGMAN and M. J. WEINSTEIN

(Journal of Chromatography Library, Vol. 1)

1973. 248 pages. Dfl. 65.00 (about US\$23.60)

Elsevier

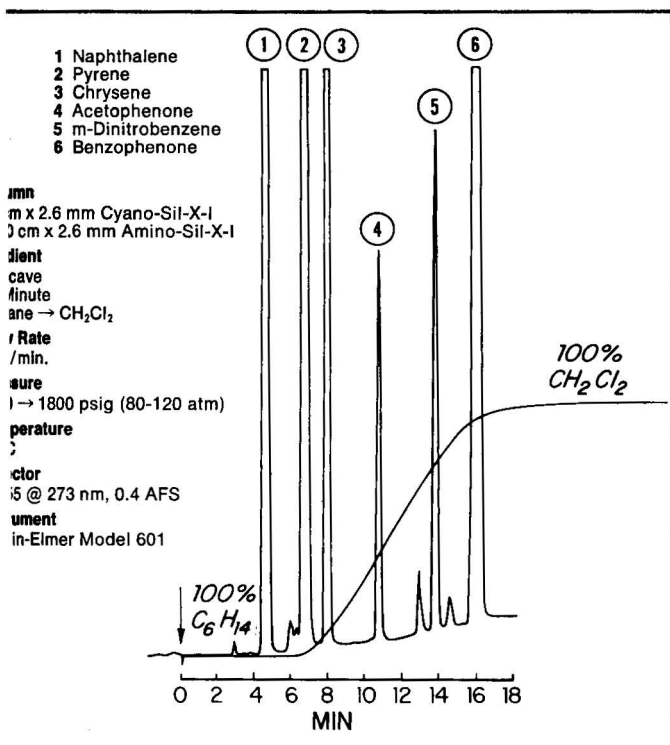
P.O. Box 211

Amsterdam, The Netherlands

1232 E



is chromatogram was run on the w Perkin-Elmer® Model 601 LC System. dy it. You'll be impressed.



n-Elmer's new Model 601 Chromatograph now joins 55 variable-wavelength UV and Perkin-Elmer's special packings, to produce the advanced liquid chromatography system available. Take a close look at the chromatogram of Figure 1, because the capabilities of the new are apparent from it. Close a necessity, because you must buy the Model 601 for its alone (Figure 2).

Wide gradient capability.

Mixture that was analyzed—aromatics, aromatic, and a nitro aromatic—separated by a wide-range gradient. We wanted to produce a chromatogram with evenly spaced peaks in less than 15 minutes.

How:

Perkin-Elmer's broad range of bonded-phase columns connected in series. One bonded Cyano-Sil-X™ packing, the other Amino-Sil-X.

2. A concave gradient was run, starting with 100% hexane. (In adsorption chromatography, a properly chosen concave gradient must be used to provide a linear change in solvent strength.) To achieve rapid results, the flow rate was set to 2 ml/minute. Note that, at this fast flow rate

and one meter of column, the back pressure was less than 1800 psi (120 atmospheres). This low pressure is a tribute to the proprietary method for packing efficiency of Perkin-Elmer's microparticulate columns.

- The LC-55 variable-wavelength detector was set to 273 nm, where neither solvent absorbs significantly, to yield a flat baseline. The chromatogram was then run.
- The LC-55 was then set to 239 nm, where methylene chloride absorbs much more than does hexane. The gradient was then rerun without a sample, yielding the true form of the gradient. Notice that this is quite different from the usual practice of indicating the gradient by recording the electrical impulses that drive the pumps, which may or may not have a real relationship to what actually happens. Here, you see the actual solvent composition at which each sample component elutes.

Syringe pumps without check valves are required.

Notice further that Peaks 1, 2, and 3 emerge during the first 10% of the gradient, while the pump delivering methylene chloride is accelerating smoothly from 0 to 0.2 ml/minute. For this, you need pulseless syringe pumps and a gradient system entirely free of check valves, because check valves would make it impossible to control very low rates accurately. Such performance represents an advance in the art of liquid chromatography.

Rapid refill, direct flow, and an oven.

One chromatogram can't show everything. This one doesn't show that you need the 601's air-bath oven to do first-rate reverse-phase and ion-exchange work; that you can record directly against solvent flow, rather than against time; and that the new rapid-refill feature can refill the 500-ml cylinders in less than 90 seconds.

Please send for literature and ask for a demonstration. Write to: Instrument Division, Perkin-Elmer Corporation, Main Avenue, Norwalk, Conn. 06856.

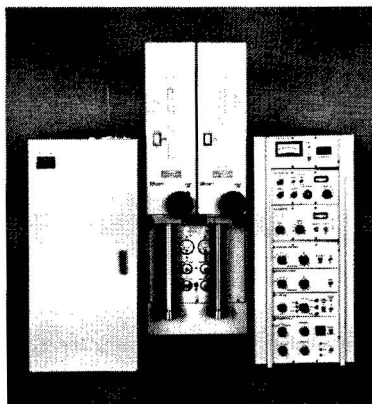


Figure 2

PERKIN-ELMER

Editor-in-Chief
U. CROATTO (Italy)

Associate Editors

A. W. Adamson (U.S.A.)
F. Basolo (U.S.A.)
F. A. Cotton (U.S.A.)
E. O. Fischer (Germany)
H. B. Gray (U.S.A.)
J. Halpern (U.S.A.)
J. A. Ibers (U.S.A.)
C. K. Jørgensen (Switzerland)
J. Lewis (U.K.)
L. Malatesta (Italy)
R. Mason (U.K.)
K. Nakamoto (U.S.A.)
G. Natta (Italy)
L. Sacconi (Italy)
F. G. A. Stone (U.K.)
L. Vaska (U.S.A.)
M. E. Vol'pin (U.S.S.R.)

MONTHLY frequency
provides rapid publication of
contributions

LETTERS SECTION offers
quick and concise
information on important
research developments in the
field of inorganic chemistry

Inorganica Chimica Acta

Incorporating Inorganica Chimica Acta Reviews

Scope of the Journal

Inorganica Chimica Acta, an international MONTHLY publication, provides a medium for original, high-level scientific contributions dealing with developments in inorganic chemistry from classic inorganic and coordination compounds to organometallic and bio-inorganic systems.

Subjects covered include

Synthesis, characterization and reactivity of coordination compounds

Synthesis and reactivity of organometallic compounds

Metals in biological systems

Metals in homogeneous catalysis

Metals in organic chemistry

Kinetics, reaction mechanisms, reaction intermediates and stereoselectivity

MO calculations — LCAO-CNDO — etc.

ESR, ESCA, NMR, PES and magnetic studies

Electron transfer, catalysis

Raman, IR, UV and CD spectra

X-ray and Neutron diffraction, Mössbauer spectra



Order form INORGANICA CHIMICA ACTA

Please enter my order for:

☐ 1974 SUBSCRIPTION, Vol. 8-11. Price SFr. 330.— (US\$112.— approx.)

☐ BACK VOLUMES 1-7. Price per volume SFr. 155.— (US\$52.50 approx.)

☐ check enclosed

☐ please bill me

Please send me:

☐ FREE SPECIMEN COPY



**Elsevier
Sequoia S.A.**

P.O. Box 851
CH-1001 Lausanne 1,
Switzerland

Name:

Address:

Country:

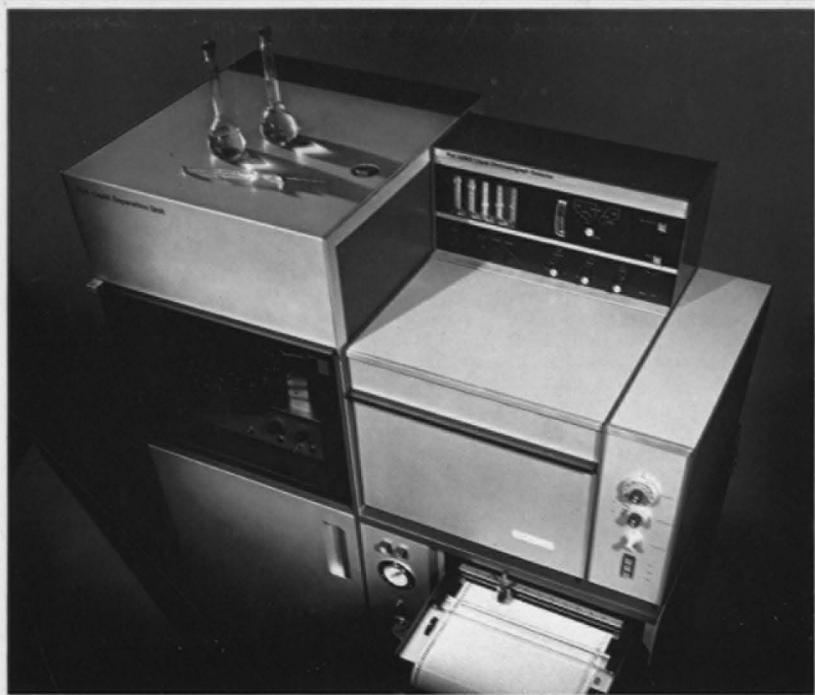
Date:

Signature:

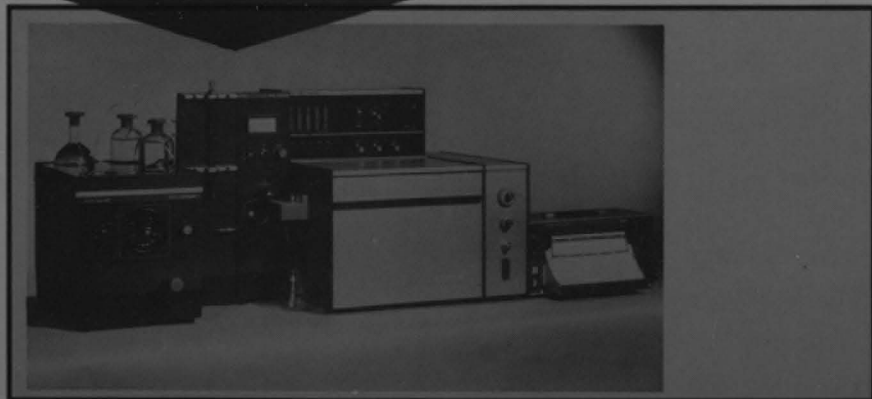
NEW

in Liquid Chromatography

Routine and research equality — that's what Pye Unicam has achieved with the new Model 20 Liquid Chromatograph. Modular design means systems can be built up to suit particular application requirements, whether they are for research or routine analysis. UV and phase transformation detectors are available and may be used separately or in combination. With comprehensive solvent and column systems and a minimum of controls, the Model 20UV is ideal for routine analyses of pharmaceuticals, food, oil and plastics additives. Model 20FD is particularly suited for carbohydrate and lipid analysis and, with the use of wide range gradient elution, the separation — characterisation of unknown mixtures can be achieved. Model 20UV/FD, with the simultaneous use of both detectors, provides for both selective high sensitivity and universal detection facilities.



LCM2 Detector



Model 20UV/FD Liquid Chromatograph

The phase transformation method of detection used both with the new Model 20FD and Model 20UV/FD was introduced originally with the Pye Unicam LCM2 Liquid Chromatograph, shown above. This well proven and highly successful detection method uses the unique Pye Unicam wire transport system — eminently suited for gradient elution work. For full information on all versions of the Model 20 Liquid Chromatograph please use the reader enquiry card or write or phone direct.

An Analysis of Liquid Chromatography from Pye Unicam

A Selection from the Pye Unicam range of . . .

Infrared spectrophotometers

SP1100 — An extremely versatile double-beam instrument with SPECTRASET, a control system providing repeatable and accurate spectra for any sampling technique in routine and research applications. Integral chart recorder, giving up to 10x%T expansion and 5x wavenumber expansion, extends flexibility even further. Spectral range is 400–4000 cm^{-1} .

Atomic absorption spectrophotometers

With low detection limits and high precision, the SP1900 incorporates double-beam optics, grating monochromator and digital display linear in absorbance and concentration. Auto-zero, integration, auto ignition and six-position lamp turret are standard features. A single lamp version, SP1950, is also available. Flameless sampling devices are included in a wide range of accessories.

UV spectrophotometers

SP1700 digital readout and SP1800 meter readout are double-beam, ratio

measurement spectrophotometers with presentation linear in absorbance and concentration. High resolution grating monochromator, and spectral range 190–850 nm, make both instruments ideal for every type of research and routine analytical application. A very wide range of accessories is available.

SP8000 — Precision, double-beam recording spectrophotometer, covering the spectral range 190–850 nm. Dual absorbance scales and a wider range zero back-off control, gives optimum

spectra presentation. Other standard facilities include constant wavelength operation, absorbance scale expansion and concentration readout.

Gas chromatographs

GCV, a modular gas chromatograph system, easily and quickly adapted to suit changing requirements. Exceptionally versatile with a range of detectors, columns, accessories and function modules, the GCV incorporates extremely stable column and detector ovens for high performance, precision, reliability and repeatability.



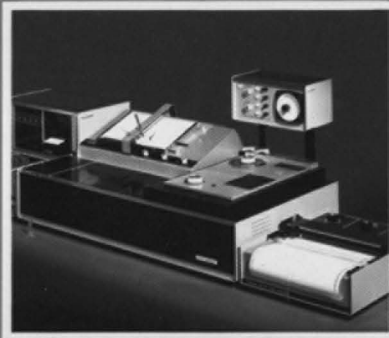
SP1700 and SP1800
SP8000



GCV
SP1900

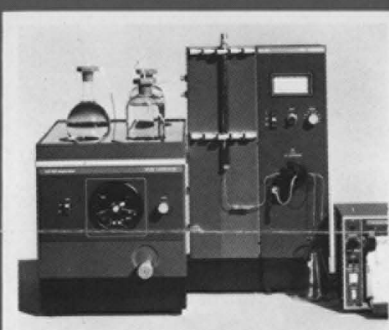


SP1100



The introduction of the Model 20 Liquid Chromatograph typifies the Pye Unicam philosophy of continuous development in the field of precision analytical instruments for research, general laboratory, industrial and educational applications.

Other recent introductions include the GCD Gas Chromatograph and S8 Autojector, AA Spectrophotometer SP190, UV/Visible Spectrophotometer SP30 and Infrared Spectrophotometer SP2000. For full information please use the reader reply service, write or telephone direct.



Model 20UV Liquid Chromatograph

Pye Unicam Ltd
York Street, Cambridge CB1 2PX
Tel (0223) 58866 Telex 817331



Pye Unicam Ltd

The Analytical World of Pye Unicam

Spectroscopy, chromatography, electrochemistry, electron microscopy, X-ray diffractometry and spectrometry, test and measuring equipment, cryogenics

JOURNAL OF CHROMATOGRAPHY

VOL. 102 (1974)

JOURNAL *of* CHROMATOGRAPHY

INTERNATIONAL JOURNAL ON CHROMATOGRAPHY,
ELECTROPHORESIS AND RELATED METHODS

EDITOR

MICHAEL LEDERER (Rome)

ASSOCIATE EDITOR

K. MACEK (Prague)

EDITORIAL BOARD

W. A. Aue (Halifax), V. G. Berezkin (Moscow), A. Bevenue (Honolulu, Hawaii),
P. Boulanger (Lille), C. P. Cartoni (Rome), K. V. Chmutov (Moscow), G.
Duyckaerts (Liège), L. Fishbein (Jefferson, Ark.), A. Frigerio (Milan), C. W.
Gehrke (Columbia, Mo.), I. M. Hais (Hradec Králové), N. G. L. Harding (Cam-
bridge), E. Heftmann (Berkeley, Calif.), S. Hjertén (Uppsala), E. C. Horning
(Houston, Texas), J. F. K. Huber (Vienna), A. T. James (Sharnbrook, Beds.),
J. Janák (Brno), A. I. M. Keulemans (Eindhoven), K. A. Kraus (Oak Ridge,
Tenn.), E. Lederer (Gif-sur-Yvette, S. et O.), A. Liberti (Rome), H. M. McNair
(Neuchâtel), Y. Marcus (Jerusalem), G. B. Marini-Bettolo (Rome), R. Neher
(Basel), G. Nickless (Bristol), J. Novák (Brno), O. Samuelson (Göteborg),
G.-M. Schwab (Munich), G. Semenza (Zürich), L. R. Snyder (Tarrytown, N.Y.),
H. Tuppy (Vienna), A. Zlatkis (Houston, Texas)

EDITORS, BIBLIOGRAPHY SECTION

K. Macek (Prague), J. Janák (Brno), Z. Deyl (Prague)

EDITOR, BOOK REVIEW SECTION

R. Amos (Abingdon)

EDITOR, NEWS SECTION

J. F. K. Huber (Vienna)

COORDINATING EDITOR, DATA SECTION

J. Gasparič (Hradec Králové)

VOL. 102

1974

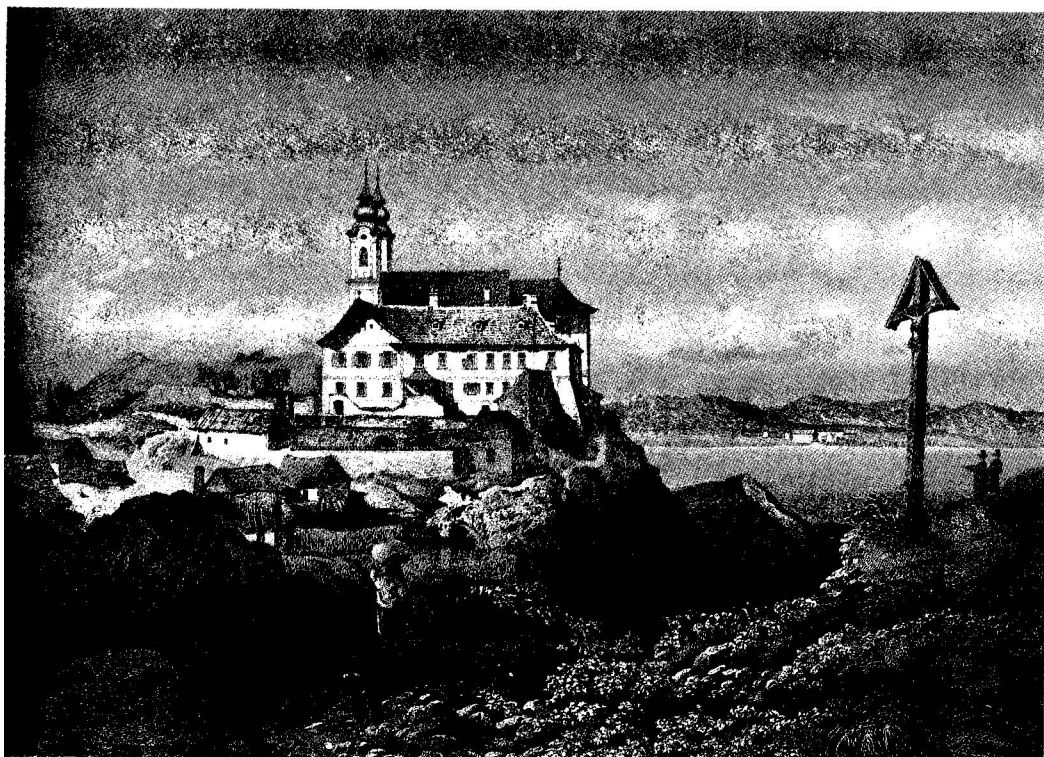


Handwritten text in Thai script, likely a library stamp or a note, located at the bottom of the page.

© ELSEVIER SCIENTIFIC PUBLISHING COMPANY — 1974

All rights reserved. No part of this publication may be reproduced, stored in a retrieval system, or transmitted, in any form or by any means, electronic, mechanical, photocopying, recording, or otherwise, without permission in writing from the publisher.

SPECIAL VOLUME



THIRD SYMPOSIUM ON ION EXCHANGE

Balatonfüred (Hungary), May 28-31, 1974

Edited by

J. INCZÉDY

(Budapest)

CONTENTS

THIRD SYMPOSIUM ON ION EXCHANGE, BALATONFÜRED (HUNGARY), MAY 28-31, 1974

J. Inczédy, Preface	1
-------------------------------	---

Plenary lectures

G. Alberti and U. Costantino, Recent progress in the field of synthetic inorganic exchangers having a layered or fibrous structure	5
G. Dickel, The phenomenon of osmosis in permeable membranes	31
J. Inczédy, Chemical equilibria in ion-exchange chromatography	41
H. Kakihana, Ion exchange, isotope exchange and isotope separation	47
H. F. Walton, Liquid chromatography of organic compounds on ion-exchange resins	57
G. Werner, The use of liquid ion exchangers in extraction chromatography	69

Ion-exchange materials

O. Nagy, H. Gaál and J. Szabó, Examination of ion-exchange resins by derivatography	77
M. S. Gorodnev, G. K. Saldadze, V. K. Varentsov and I. M. Abramova, Investigation of structure heterogeneity in ion-exchange membranes	83
M. Marhol, J. Chmelfíček, A. B. Alovitdinov and Ch. U. Kočkarova, Selective properties and analytical use of an ion-exchange resin based on α -phenylvinylphosphonic acid	89
A. Dyer and A. B. Ogden, The mobility of cerium ions in synthetic zeolites	95
K.-H. König, Zur Selektivität des Kationenaustauschs an kristallinen Ce(IV)-phosphat-sulfaten	99
L. Szirtes and L. Zsinka, Preparation of some new inorganic ion exchangers	105
L. Zsinka, L. Szirtes, J. Mink and A. Kálmán, Infrared and X-ray measurements on various inorganic ion exchangers	109
K. Häupke und V. Pientka, Neue Ergebnisse über die Porosität von Styrol-Divinylbenzol-Copolymerisaten und Ionenaustauscherharzen	117
G. Schwachula and D. Lukas, Untersuchung zur Herstellung stark saurer Kationenaustauscher auf der Basis von Styrol-Bis-(4-vinylphenyl)-methan-Copolymeren	123
R. Bogoczek, Synthesis and properties of some snake-cage ion-retardation resins	131
H. Hecker, Beitrag zur Basizitätsprüfung von stark basischen Anionenaustauschern	135

Theory of ion exchange

R. Hering, A proposal for the nomenclature of exchangers	141
S. C. Duffy and L. V. C. Rees, Comparison of experimental and theoretical rates of ion exchange	149
L. Liberti and R. Passino, Chloride-sulphate exchange on anion-exchange resins. Kinetic investigations. I	155
A. Marton and J. Inczédy, Investigation of anion-exchange equilibria of maleic and fumaric acids	165
K. Bunzl, Kinetics of differential ion-exchange processes in a finite solution volume	169
A. Abadie et H. Roques, Transferts de masse d'échange d'ions minéraux perturbés par la fixation simultanée d'ions organiques volumineux	181
D. N. Strazhesko, V. B. Strelko, V. N. Belyakov and S. C. Rubanik, Mechanism of cation exchange on silica gels	191
J. Chmielowiec and W. Kemula, Effect of cross-linking of a sulphonic cation-exchange resin and effect of temperature on the chromatographic separation of isomers of dinitrobenzene	197
A. Lásztity and T. A. Belyavskaya, Selective swelling of ion exchangers in mixed solvents and the effect of swelling on the sorption of ions	203

J. D. R. Thomas, Some aspects of ion-exchange in non-aqueous and mixed solvents	209
S. K. Jha, F. de Corte and J. Hoste, Anion exchange in ternary mixtures of aliphatic acids, mineral acids and water.	217
E. Papp and J. Inczédy, The extraction of copper(II) ions with liquid anion exchangers using salicylate as complex-forming agent	225
R. N. Rubinstein, M. M. Senyavin, E. V. Venitsianov, E. M. Makhalov, V. A. Alekseenko and V. A. Nikashina, Determination of the optimal conditions for ion-exchange processes	235

Analytical applications

I. Hazai, S. Zoltán, J. Salát, S. Ferenczi and T. Dévényi, Chromatographic behaviour of amino acids on cation-exchange resin-coated chromatoshets in the H ⁺ form	245
T. Seki and H. Wada, Chromatographic separation of dansyl amino acids and dansyl amines on Amberlite IRC-50	251
E. Tiyhák, S. Ferenczi, I. Hazai, S. Zoltán and A. Patthy, Combined application of ion-exchange chromatographic methods for the study of "minor basic amino acids"	257
R. Dybczyński and E. Sterlińska, The use of the amphoteric ion-exchange resin Retardion 11A8 for inorganic separations	263
T. Yamabe and T. Hayashi, Separation of metal ions by mixed column ion-exchange chromatography	273
L. Wódkiewicz et R. Dybczyński, Échange d'anions des éléments sur une résine échangeuse anionique de faible basicité en milieu de l'acide bromhydrique	277
S. B. Savvin, I. I. Antokolskaja, G. V. Myasoedova, L. I. Bolshakova and O. P. Shvoeva, Chelate sorbents for concentration and separation of noble metals	287
C. Testa and A. Delle Site, Extraction chromatography with liquid ion exchangers as stationary phase.	293
G. Ghersini, Extraction chromatography with liquid ion exchangers	299
U. A. Th. Brinkman, G. de Vries, R. Jochemsen and G. J. de Jong, The use of aqueous thiocyanate solutions in liquid-liquid extraction and reversed-phase extraction chromatography. I	309
L. Légrádi, Separation of metals on ion-exchange resins by means of α -hydroxyisobutyronitrile as complexing agent	319
N. Weigand, I. Sebastian und I. Halász, Neuartige Kationenaustauscher auf Kieselgelbasis. I. Darstellung und Eigenschaften	325
J. C. Kraak and J. F. K. Huber, Separation of acidic compounds by high-pressure liquid-liquid chromatography involving ion-pair formation	333
Sj. van der Wal and J. F. K. Huber, High-pressure liquid chromatography with ion-exchange celluloses and its application to the separation of estrogen glucuronides	353
J. Gaál and J. Inczédy, Separation of optical isomers by ion-exchange chromatography using copper(II) ions as complex-forming agents	375
Gy. Vigh and J. Inczédy, Separation of some chloramphenicol intermediates by high-pressure ion-exchange chromatography	381
K. Brajter, Application of ligands with sulphonic groups to the separation of metal ions on strongly basic anion exchangers	385

Ion-exchange technology

G. Boari, L. Liberti and R. Passino, Prevention of calcium sulphate scale formation in evaporation plants by ion exchange	393
A. Sopková, K. Vetejška and J. Bubanc, Some problems in the separation of copper and iron from mine waters	403
Zs. Horváth, PURIWAT® apparatus. A system of ion-exchange celluloses for the production of high-purity water	409
M. Bailly et D. Tondeur, Échange d'ions en lit mobile à plusieurs constituants. Recherche d'une méthode de conception et de calcul pour des colonnes préparatives de petite dimension	413
G. Grevillot, D. Tondeur et J. A. Dodds, Fonctionnement cyclique d'un lit fixe d'échange d'ions avec trois constituants	421

M. Erdélyi, B. Czeglédi and M. Vigvári, Elution of uranium from an anion-exchange resin by extraction with an organic extractant in the presence of an aqueous phase 429

M. Vigvári, M. Erdélyi and B. Czeglédi, Countercurrent elution of uranium(VI) and iron(III) from an anion-exchange resin 433

A. E. Rodrigues, Ion exchange in agitated beds. Simulation of an ion-exchange column by a model of agitated tanks in cascade 437

G. J. de Jong and C. J. N. Rekers, The Akzo process for the removal of mercury from waste water 443

R. Schaaf, Einsatzmöglichkeiten von pulverförmigen Ionenaustauschern in der Kondensat-aufbereitung. 451

I. Bálint-Ambró, The ion-exchange behaviour of arsenic(III) on VARION anion-exchange resins. 457

Author Index 461

Subject Index 463

CHROM. 7785

PREFACE

The Third Symposium on Ion Exchange was held on 28th-31st May, 1974, at Balatonfüred, Hungary. The first Symposium was held in 1963* and the second in 1969, both at Balatonszéplak. The Symposium was organized by the Hungarian Chemical Society with the co-operation of the Local Committee of Veszprém and the Local Committee of Pécs of the Hungarian Academy of Sciences, and supported by the Nitrochemical Works.

The aim of this Symposium, like that of the first and second, was to bring together experts from all over the world working on the development of ion-exchange materials, on the theory of ion exchange or on its applications. The lectures were delivered in the following four sections:

- (A) Ion-Exchange Materials;
- (B) Theory of Ion Exchange;
- (C) Analytical Applications;
- (D) Ion-Exchange Technology.

Corresponding to the above sections, the invited Plenary Lectures dealt with the main trends and developments in these fields. The Plenary Lectures were as follows:

G. Alberti (Perugia, Italy): Recent Progress in the Field of Synthetic Inorganic Exchangers Having a Layered or Fibrous Structure.

G. Dickel (Munich, G.F.R.): The Phenomenon of Osmosis.

J. F. K. Huber (Vienna, Austria): High-Efficiency Columns in Ion-Exchange Chromatography.

J. Inczédy (Veszprém, Hungary): Chemical Equilibria in Ion-Exchange Chromatography.

H. Kakihana (Tokyo, Japan): Ion Exchange, Isotope Exchange and Isotope Separations.

B. N. Laskorin (Moscow, U.S.S.R.): Ion-Exchange Processes in Hydrometallurgy.

G. V. Samsonov (Leningrad, U.S.S.R.): Equilibrium Kinetics and Dynamics of Organic Ions Interacting with Polyelectrolytes.

H. F. Walton (Boulder, Colo., U.S.A.): Liquid Chromatography of Organic Compounds on Ion-Exchange Resins.

G. Werner (Leipzig, G.D.R.): The Use of Liquid Ion Exchangers in Extraction Chromatography.

The Symposium was centred on the Hotel Marina, in the rooms of which the lectures were delivered and the discussions arranged.

Although lecturers and delegates from many countries (Austria, Belgium, Berlin, Czechoslovakia, Denmark, Finland, France, German Democratic Republic, German Federal Republic, Hungary, India, Iran, Italy, Japan, Poland, Portugal,

* *Ionenaustauscher und Anwendungen*, Symposium in Balatonszéplak (Hungary), 1963, Akadémiai Kiadó, Budapest.

Roumania, Switzerland, The Netherlands, United Kingdom, U.S.A., U.S.S.R. and Yugoslavia) took part in the Symposium, the recommended main language (English), the common interest in the problems of ion exchange and the pleasant surroundings kept all the guests and hosts together. Nevertheless, the lovely sunshine on Lake Balaton, as well as the taste of the Grey Monk from Badacsony, made significant contributions to the fruitful, multilateral discussions.

It can be concluded that the theory of ion exchange and the use of ion exchangers in laboratories and factories is still a flourishing discipline. The investigation of ion-exchange processes and the principles of the ion-exchange procedures established using inorganic and organic exchangers facilitate a deeper understanding of geological, geophysical and biophysical phenomena and the explanation of biological processes.

The application of ion exchangers in the laboratory has made possible the chromatographic separation of very complicated natural mixtures. By means of high-performance chromatographic techniques, not only most of the difficulties in separation procedures can be overcome, but the time required to obtain the desired information is also significantly reduced. The use of ion exchangers on a large scale may provide mankind with pure water and may be useful for the concentration and extraction of the most important metals and raw materials, the production of which is becoming more and more difficult.

Elsevier have undertaken to publish the papers from the Symposium in the *Journal of Chromatography*, so making accessible the whole proceedings to the participants and also to those who were not able to be present but are interested in new results on ion-exchange techniques.

We hope that by the publication of these papers, some contribution will be made to the scientific development of ion-exchange techniques and, by bringing together the results of workers from different countries, mutual co-operation and understanding can also be increased.

I would like to express my gratitude to Dr. Lederer and his co-workers for the tremendous amount of work which assured the publication of the full texts of the lectures in a reasonable time. Thanks are also due to the lecturers and contributors, whose valuable work, results and scientific enthusiasm led to the success of the Symposium.

J. INCZÉDY

PLENARY LECTURES

CHROM. 7714

RECENT PROGRESS IN THE FIELD OF SYNTHETIC INORGANIC EXCHANGERS HAVING A LAYERED OR FIBROUS STRUCTURE

GIULIO ALBERTI and UMBERTO COSTANTINO

Istituto di Chimica Inorganica, Università di Perugia, Via Elce di Sotto, Perugia (Italy)

SUMMARY

In the first part, recent results on crystalline insoluble acid salts of tetravalent metals having a layered structure are critically examined. The dependence of the inter-layer distance of crystalline zirconium phosphate on its water content and counter ions is discussed and an ion-exchange mechanism for monovalent and divalent ions, in both aqueous and molten salt media, is proposed. Furthermore, the effect of the degree of crystallinity of zirconium phosphate on its ion-exchange properties and electrical conductivity, the dependence of its selectivity for large cations on steric hindrance and the catalytic effect of small amounts of sodium ions on the exchange of large hydrated cations are also discussed. Other layered exchangers, such as zirconium arsenate and titanium phosphate, are also considered and some general points on their ion-exchange properties as a function of the tetravalent metal ion and polybasic acid groups involved are made.

The second part deals with the synthesis and ion-exchange properties of fibrous inorganic ion exchangers with special regard to fibrous cerium(IV) phosphate.

In the third part, some practical applications of the exchangers examined, in both ion-exchange and electrochemical processes, are reported.

INTRODUCTION

Ion exchange is now a well established technique in many industrial processes and is also widely employed in many chemical laboratories. However, the applications of ion exchange to some important processes that occur at high temperatures or in the presence of ionizing radiation or highly oxidizing media are severely limited at present, because commercially available ion-exchange resins undergo degradation under such drastic conditions.

The revived interest in inorganic ion exchangers is due primarily to their high resistance towards temperature and radiation, so that several new potential applications of ion-exchange technology can be expected.

A large number of new synthetic inorganic exchangers has been obtained and their ion-exchange properties investigated. Several of these exchangers were found to exhibit the expected chemical stability and sometimes they proved to be highly selective for certain ions.

These exchangers can conveniently be divided into the following principal groups:

- (1) Insoluble acid salts of polyvalent metals.
- (2) Hydrous oxides of polyvalent metals.
- (3) Salts of heteropolyacids.
- (4) Insoluble hexacyanoferrates(II).
- (5) Synthetic aluminosilicates.
- (6) Miscellaneous inorganic exchangers, *e.g.*, mercabide salts and potassium polyphosphate.

In the present paper, we are concerned exclusively with inorganic exchangers of the first group. Concerning the exchangers of the other groups, the interested reader is referred to recent reviews by Veselý and Pekárek^{1,2}.

Until recently, the insoluble acid salts of polyvalent metals have been obtained as gels with no definite composition and not very stable towards hydrolysis of their acid groups. Some of these compounds, particularly the amorphous zirconium phosphate, exhibit a high selectivity for some important cations such as Cs^+ and UO_2^{2+} and therefore extensive studies have been carried out on these exchangers. The ion-exchange properties of amorphous exchangers were reviewed in 1964 by Amphlett³. New developments in this field led to the synthesis of several exchangers having a fixed composition and a well defined crystalline structure⁴⁻²².

These crystalline exchangers can be divided into the following three sub-groups:

- (a) Exchangers having a layered structure.
- (b) Exchangers having a fibrous structure.
- (c) Exchangers having an as yet unknown structure.

We will consider here in detail only the insoluble acid salts of tetravalent metals having a layered or a fibrous structure, while some exchangers of sub-group (c) are briefly discussed only in connection with their practical applications. Additional information can be found in a recent review by Clearfield *et al.*²³.

EXCHANGERS HAVING A LAYERED STRUCTURE

Introduction

Some important exchangers of this sub-group are listed in Table I. Among these exchangers, crystalline zirconium phosphate is certainly the most widely investigated and therefore we shall consider in detail only this exchanger, while the remaining exchangers are briefly discussed with particular regard to their differences from crystalline zirconium phosphate.

TABLE I
INORGANIC ION EXCHANGERS HAVING A LAYERED STRUCTURE

Formula	Ion-exchange capacity (mequiv./g)	Interlayer distance d (Å)	References
$\text{Zr}(\text{HPO}_4)_2 \cdot \text{H}_2\text{O}$	6.64	7.56	24
$\text{Ti}(\text{HPO}_4)_2 \cdot \text{H}_2\text{O}$	7.76	7.56	5, 6
$\text{Zr}(\text{HAsO}_4)_2 \cdot \text{H}_2\text{O}$	5.14	7.82	8, 11, 25
$\text{Ti}(\text{HAsO}_4)_2 \cdot \text{H}_2\text{O}$	5.78	7.77	12

Synthesis of crystalline zirconium phosphate

The synthesis of crystalline zirconium phosphate is very important, as recent investigations have revealed that its ion-exchange properties depend on its degree of crystallinity, which, in turn, depends on the method of preparation used²⁶⁻²⁸. At present, there are two main methods of preparation. In the first method, crystalline zirconium phosphate is obtained by refluxing the amorphous product in concentrated phosphoric acid⁴. It was recently found by Alberti *et al.*²⁹ and Clearfield *et al.*³⁰ independently that the degree of crystallinity of the exchanger increases with the refluxing time and completely crystalline materials can be obtained only after about 20 days in 12-14 *M* orthophosphoric acid.

Until recently, most investigations on the ion exchange of crystalline zirconium phosphate have been carried out using materials prepared by refluxing for only 24-100 h in 10-12 *M* orthophosphoric acid, and which are therefore not completely crystalline; hence some of the results previously obtained must now be treated with caution. In some instances, there is a need to repeat some experiments using completely crystalline material, especially when the ion-exchange behaviour cannot be easily explained on the basis of a regular crystalline structure.

In the second method, first used by Alberti and Torracca⁹, zirconium is first complexed with hydrofluoric acid and then the fluoro-complex is slowly decomposed (*e.g.*, by decreasing the hydrofluoric acid concentration in solution) in the presence of orthophosphoric acid until crystalline zirconium phosphate starts to precipitate. By slowly evaporating the hydrofluoric acid at room temperature, large crystals, suitable for column applications, can be obtained, but the precipitation requires a long time. However, the decomposition rate of the zirconium fluoro-complex can be accelerated by warming the solution at *ca.* 80° and/or passing through it a stream of nitrogen; in order to avoid water evaporation, the nitrogen is pre-humidified by bubbling it through boiling water. Rapid precipitation is completed in about 4 days with a yield of *ca.* 80% and it still provides crystals larger than those obtained by the refluxing procedure^{29,31}. It was first found by Alberti *et al.*²⁹ and then confirmed by Horsley and Nowell³² that the direct precipitation method gives zirconium phosphate with high degree of crystallinity even when it is obtained by rapid precipitation. Thus, when crystalline zirconium phosphate with a high degree of crystallinity is required, precipitation in the presence of hydrofluoric acid is a more rapid method than the refluxing method (*ca.* 4 days compared with *ca.* 20 days); therefore, we are now almost exclusively using crystalline zirconium phosphate prepared according to the precipitation method in the presence of hydrofluoric acid.

Structural data for crystalline zirconium phosphate

The hydrogen form has been shown to be zirconium bis(monohydrogen orthophosphate), $\text{Zr}(\text{HPO}_4)_2 \cdot \text{H}_2\text{O}$, and its crystal structure has recently been established by Clearfield and Smith²⁴. This structure, shown schematically in Fig. 1, is a layered one and is similar in many respects to that of clay minerals. Each layer consists of zirconium atoms lying very nearly in a plane and bridged through phosphate groups located above and below this plane; each sandwich of this type can be considered as a giant molecule. The crystal structure of zirconium phosphate ($\text{Zr}_n(\text{HPO}_4)_{2n} \cdot n\text{H}_2\text{O}$) is built up by the bonding together of these sandwiches by long hydrogen bonds or Van der Waals forces. In this arrangement, each phosphorus atom in the lower sand-

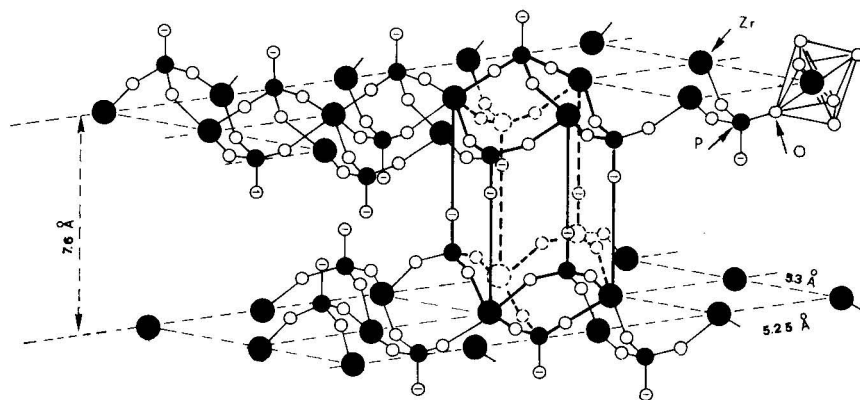


Fig. 1. Idealized crystal structure of zirconium phosphate. Solid lines show one of the zeolitic cavities created by the arrangement of the layers.

wich lies along a perpendicular line drawn from the zirconium atom of the upper sandwich. This arrangement creates zeolitic-type cavities that are interconnected by windows whose maximum diameter, for the hydrogen form, is 2.64 Å. Both hydrogen atoms can be exchanged with other cations so that the total ion-exchange capacity is 6.64 mequiv. of cation per gram of $\text{Zr}(\text{HPO}_4)_2 \cdot \text{H}_2\text{O}$.

In the following discussion, for the sake of brevity, the various ionic forms are simply indicated by their counter ions (under a bar) and water content, while their interlayer distances are reported in parentheses. Thus, for example, $\text{Zr}(\text{HPO}_4)_2 \cdot \text{H}_2\text{O}$ and $\text{ZrHNa}(\text{PO}_4)_2 \cdot 5\text{H}_2\text{O}$ will be written as $\overline{\text{HH}} \cdot \text{H}_2\text{O}$ (7.6 Å) and $\overline{\text{HNa}} \cdot 5\text{H}_2\text{O}$ (11.8 Å).

So far, the reticular position of the counter ions in the salt forms of crystalline zirconium phosphate has been determined only for the NH_4^+ form²⁵ owing to the difficulties involved in obtaining crystals of other ionic forms of a suitable size for structural determinations. Furthermore, the position of the water molecules in the hydrated salt forms of zirconium phosphate is as yet unknown.

On the other hand, the knowledge of the crystal structure of the various phases obtained in a given ion-exchange process is very important, as it provides the opportunity of relating the observed ion-exchange properties with the local structure. Therefore, research on the crystal structure of various salt forms is particularly necessary. At present, without the knowledge of the crystal structures of the salt forms, one can try to interpret the ion-exchange mechanism from other parameters such as the variation in the interlayer distance and water content in a given ion-exchange process.

Interlayer distance of crystalline zirconium phosphate in various ionic forms with different degrees of hydration

When the hydrogen ion in $\overline{\text{HH}} \cdot \text{H}_2\text{O}$ (7.6 Å) is exchanged with other counter ions, it is likely that the arrangement of zirconium atoms and phosphate groups, in each sandwich, remains about the same; consequently, the crystalline structure of the salt forms of zirconium phosphate will be essentially that of the dihydrogen form, with the layers at new distances in order to accommodate the exchanged counter

ions. Thus the first maximum of the X-ray powder pattern of a given ionic form of crystalline zirconium phosphate provides its interlayer distance. This view is now generally accepted and has recently been confirmed by working out the crystal structure of the $\text{NH}_4\text{NH}_4 \cdot \text{H}_2\text{O}$ (9.36 Å) phase²⁵.

The interlayer distances of several salt forms of crystalline zirconium phosphate containing two identical monovalent counter ions are given in Table II (column 3). A simple inspection of these values shows that the interlayer distance increases with the water content of the exchanger and that, for the same water content, it increases with increasing crystalline radius of the monovalent counter ion. Furthermore, it can easily be seen that the experimental difference between the interlayer distances of two monohydrated forms, $\overline{\text{MM}} \cdot \text{H}_2\text{O}$ and $\text{M}'\text{M}' \cdot \text{H}_2\text{O}$, is approximately equal to the dif-

TABLE II

EXPERIMENTAL AND CALCULATED INTERLAYER DISTANCES OF HYDRATED AND ANHYDROUS PHASES OF CRYSTALLINE ZIRCONIUM PHOSPHATE COMPLETELY EXCHANGED WITH THE SAME MONOVALENT ION

Phase composition	Drying conditions*	Interlayer distance, d (Å)	Interlayer distance (calculated value)**, d (Å)	References
$\overline{\text{HH}} \cdot 8\text{H}_2\text{O}$	r.t. ($P/P_0 = 1$)	10.4		21, 16, 20
$\overline{\text{HH}} \cdot \text{H}_2\text{O}$	r.t. over P_4O_{10}	7.56		4
$\overline{\text{HH}}$	110°	7.56		4
$\overline{\text{LiLi}} \cdot 4\text{H}_2\text{O}$	r.t. ($P/P_0 = 0.9$)	10.1; 9.98	10.0	33, 34, 35
$\overline{\text{LiLi}} \cdot 2\text{H}_2\text{O}$	r.t. over P_4O_{10}	8.84; 8.80; 8.87	8.8	35, 33, 36, 37
$\overline{\text{LiLi}} \cdot \text{H}_2\text{O}$	100–150°	8.87; 7.89; 7.91	7.9	37, 33, 34
$\overline{\text{LiLi}}$	300°	7.05; 7.0		33, 34, 38
$\overline{\text{LiLi}}$	400–800°	6.24		33
$\overline{\text{NaNa}} \cdot 3\text{H}_2\text{O}$	r.t. ($P/P_0 = 0.7$)	9.92; 9.83	9.9	34, 39
$\overline{\text{NaNa}} \cdot \text{H}_2\text{O}$	r.t. over P_4O_{10}	8.42	8.4	39, 37
$\overline{\text{NaNa}}$	165°	8.38		39
$\overline{\text{NaNa}}$	300–400°	7.63; 7.7		39, 38
$\overline{\text{KK}} \cdot 3\text{H}_2\text{O}$	r.t. ($P/P_0 = 0.7$)	10.74; 10.8	10.7	34, 35, 40
$\overline{\text{KK}} \cdot \text{H}_2\text{O}$	r.t. over P_4O_{10}	8.84; 8.90	8.9	40, 35, 36, 37
$\overline{\text{KK}}$	110–450°	8.93; 9.0; 9.02		34, 38, 40
$\overline{\text{RbRb}} \cdot \text{H}_2\text{O}$	r.t. ($P/P_0 = 0.9$)	9.20	9.1	31
$\overline{\text{RbRb}}$	150°	9.20		31
$\overline{\text{CsCs}} \cdot 6\text{H}_2\text{O}$	r.t. ($P/P_0 = 0.9$)	14.2	13.8	31
$\overline{\text{CsCs}} \cdot \text{H}_2\text{O}$	r.t. over P_4O_{10}	9.5	9.3	31
$\overline{\text{CsCs}}$	150°	9.20		31
$\overline{\text{NH}_4\text{NH}_4} \cdot 2\text{H}_2\text{O}$		9.02		36
$\overline{\text{NH}_4\text{NH}_4} \cdot \text{H}_2\text{O}$		9.36	9.0	25
$\overline{\text{AgAg}} \cdot \text{H}_2\text{O}$	r.t. ($P/P_0 = 0.7$)	8.41	8.8	41

* r.t. = room temperature.

** Calculated by eqn. 1 or 2 using the following values of crystalline ionic radius: Li^+ , 0.66 Å; Na^+ , 0.97 Å; K^+ , 1.33 Å; Rb^+ , 1.47 Å; Cs^+ , 1.67 Å; Ag^+ , 1.26 Å; NH_4^+ , 1.43 Å.

ference between the diameters of the two counter ions M and M' (a better agreement is obtained if the difference in diameters is multiplied by a factor of 1.1).

It can also be noted that the interlayer distances of $\overline{KK} \cdot H_2O$ (8.9 Å), $\overline{RbRb} \cdot H_2O$ (9.2 Å) and $\overline{CsCs} \cdot H_2O$ (9.5 Å) phases remain about the same when they lose their water molecule, while there is a slight decrease for $\overline{LiLi} \cdot H_2O$ (7.9 Å) and $\overline{NaNa} \cdot H_2O$ (8.4 Å) phases.

As the interlayer distances of several monohydrated forms do not decrease on dehydration, it can be assumed that the water molecule is situated near the centre of the cavity, where the available space is large enough to accommodate it without causing any change in the interlayer distance of the exchanger. This can easily be seen in Fig. 2, which shows the projection of oxygen atoms, carrying the fixed negative charges, in a plane perpendicular to the crystal axis c and passing in the middle point of the cavity.

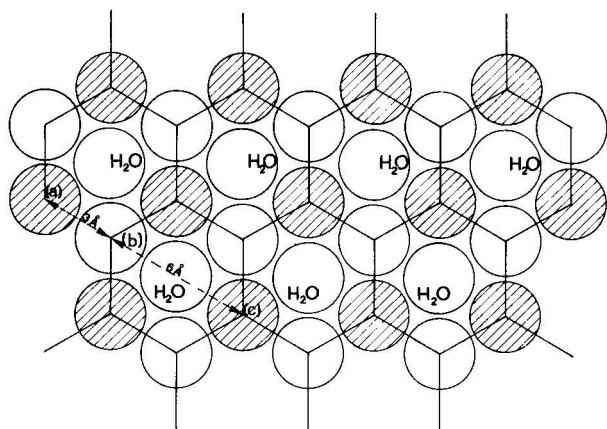


Fig. 2. Arrangement of oxygen atoms, carrying the fixed negative charges, and the water molecules inside the cavities of crystalline zirconium phosphate. The figure shows the projection of these oxygen atoms and water molecules in a plane perpendicular to the crystal axis c and crossing the cavities through their middle points. Hatched circles refer to oxygen atoms lying above the plane while open circles to those lying below the plane.

Thus the monovalent counter ions (two per cavity) should be placed around this water molecule and near two $P-O^-$ groups of the adjacent layers.

By assuming this reticular position for the counter ions and the water molecule, it was possible to show, from geometrical considerations, that the interlayer distance of the monohydrate salt forms of crystalline zirconium phosphate can be calculated as a function of the radius (r) of the counter ion according to the equation⁴¹

$$d = 2.8 + 3.4 \cos \alpha + (1.4 + r)^2 - 11.56 \sin^2 \alpha \quad (1)$$

where $\alpha = 46.9 - \arcsin(0.95 + 0.1r - 0.036r^2)$.

The calculated values of the interlayer distance are tabulated in column 4 of Table II. It can be seen that the agreement between the experimental and calculated

interlayer distances is very good, which supports our hypothesis about the reticular position of monovalent counter ions and water molecules.

A careful examination of Table II led to the observation that the interlayer distance of hydrated salt forms that have more than one water molecule is higher than that of the corresponding monohydrated phase by 1.8 Å for every two additional water molecules (one for each counter ion). Hence it is very likely that additional water molecules are situated between the counter ion and zirconium atom in order to reduce the electrostatic repulsions and accordingly the approximate interlayer distance, d , of a given salt form can simply be calculated by the relationship

$$d(\text{\AA}) = \text{interlayer distance of monohydrate form} + (0.9 \times \text{number of additional water molecules}) \quad (2)$$

where the interlayer distance of the monohydrated form can, in turn, be calculated by the eqn. 1.

In Table III are reported the interlayer distances of several phases of crystalline zirconium phosphate containing two monovalent counter ions of different sizes, at various degrees of hydration. It can be seen that the anhydrous mixed phases $\overline{MM'}$ (where M' is a larger counter ion than M) have an interlayer distance equal to or slightly higher than that of the pure \overline{MM} phase. This phenomenon could be explained assuming that, in the mixed salt forms, the larger counter ion is situated further inside the cavity and the smaller one is shifted further towards the sides of the cavity than in the pure salt forms $\overline{M'M'}$ and \overline{MM} , respectively, so as to allow only a minimum increase in the interlayer distance. If the two counter ions differ appreciably in their ionic radii, the larger one could even be accommodated near the centre of the cavity while the smaller one could approach a position very near to the side of the cavity. As an example, it can be seen from Table III that the interlayer distances of the anhydrous mixed forms \overline{HK} (7.5 Å), \overline{HRb} (7.6 Å) and \overline{HCs} (7.5 Å) are almost the same and very near to the value of the \overline{HH} (7.6 Å) form, in agreement with the above assumption. It was further supported from X-ray powder patterns, which show that mixed $\overline{M_1M'_1}$ or $\overline{M_{0.5}M'_{1.5}}$ phases have a more disordered structure than the pure phases. It can be pointed out that the interlayer distance of hydrated phases containing two different counter ions can also be calculated by eqn. 2 by using a factor of 1.0 instead of 0.9. The reason for this fact, which can be related to the relative positions of water molecules and counter ions, will be discussed elsewhere⁴¹.

Ion-exchange mechanism for zirconium phosphate for monovalent ions

The dependence of the interlayer distance of crystalline zirconium phosphate on water content, and the size of the counter ions involved as well as the shape of the titration curves (or ion-exchange isotherms) and the phase transitions in a given ion-exchange process, enable us to draw the following general conclusions on the ion-exchange mechanism of this exchanger.

Ion exchange in molten salts. Molten salts provide excellent media for investigating ion-exchange processes on zirconium phosphate, because in such media counter ions inside the exchanger are generally unsolvated⁴⁸; thus complications due to count-

TABLE III

INTERLAYER DISTANCES OF HYDRATED AND ANHYDROUS MIXED PHASES OF CRYSTALLINE ZIRCONIUM PHOSPHATE COMPLETELY EXCHANGED WITH TWO DIFFERENT MONOVALENT IONS

Phase composition	Drying conditions*	Interlayer distance, $d(\text{\AA})$	Ref.	Phase composition	Drying conditions*	Interlayer distance, $d(\text{\AA})$	Ref.
$\overline{\text{HLi}} \cdot 4\text{H}_2\text{O}$	r.t. ($P/P_0 = 0.9$)	10.1	29	$\text{H}_{1.5}\text{Cs}_{0.5} \cdot 0.5\text{H}_2\text{O}$	r.t. ($P/P_0 = 0.9$)	7.7	31
$\overline{\text{HLi}}$	300°	7.0	42	$\overline{\text{HCs}} \cdot 2\text{H}_2\text{O}$	r.t. ($P/P_0 = 0.9$)	11.3	31
$\overline{\text{H}_{0.67}\text{Li}_{1.33}} \cdot 4\text{H}_2\text{O}$	r.t. ($P/P_0 = 0.6$)	10.0	33	$\overline{\text{HCs}} \cdot 0.5\text{H}_2\text{O}$	r.t. over P_4O_{10}	8.03	31
$\overline{\text{H}_{0.67}\text{Li}_{1.33}} \cdot 3.3\text{H}_2\text{O}$	r.t. over P_4O_{10}	8.55	33	$\overline{\text{HCs}}$	150°	7.52	31
$\overline{\text{H}_{0.67}\text{Li}_{1.33}} \cdot 1.3\text{H}_2\text{O}$	80°	7.30	33	$\text{H}_{0.5}\text{Cs}_{1.5} \cdot 3\text{H}_2\text{O}$	r.t. ($P/P_0 = 0.9$)	11.7	31
$\overline{\text{H}_{0.67}\text{Li}_{1.33}} \cdot 0.7\text{H}_2\text{O}$	130°	7.84	33	$\overline{\text{H}}\text{NH}_4$		9.4	37
$\overline{\text{H}_{0.67}\text{Li}_{1.33}}$	400°	7.00	33	$\text{H}_{0.67}\text{NH}_{4\ 1.33}$		9.49	45
$\text{H}_{0.5}\text{Li}_{1.5} \cdot 4\text{H}_2\text{O}$	r.t. ($P/P_0 = 0.9$)	10.1	29	$\text{LiNa} \cdot 3.5\text{H}_2\text{O}$	r.t. ($P/P_0 = 0.9$)	10.0	46
$\overline{\text{HNa}} \cdot 5\text{H}_2\text{O}$	r.t. ($P/P_0 = 0.7$)	11.8	39, 43	LiNa	300°	7.5	38
$\overline{\text{HNa}} \cdot 4\text{H}_2\text{O}$	r.t. ($P/P_0 = 0.4$)	9.88	44	$\overline{\text{LiK}} \cdot 3\text{H}_2\text{O}$	r.t. ($P/P_0 = 0.9$)	10.0	35
$\overline{\text{HNa}} \cdot \text{H}_2\text{O}$	r.t. over P_4O_{10}	7.65	39	$\overline{\text{LiK}} \cdot 3\text{H}_2\text{O}$	r.t. ($P/P_0 = 0.9$)	9.3	35
$\overline{\text{HNa}}$	110°	7.33	39	$\overline{\text{LiK}} \cdot 2\text{H}_2\text{O}$	r.t. ($P/P_0 = 0.6$)	9.2	35
$\overline{\text{HK}} \cdot \text{H}_2\text{O}$	r.t. ($P/P_0 = 0.9$)	7.95	40, 43	$\overline{\text{LiK}} \cdot \text{H}_2\text{O}$	r.t. over P_4O_{10}	8.49	35
$\overline{\text{HK}}$	110°	7.50	40, 36	$\overline{\text{LiK}}$	300°	7.6	38
$\overline{\text{H}_{1.5}\text{Rb}_{0.5}} \cdot 0.5\text{H}_2\text{O}$	r.t. ($P/P_0 = 0.9$)	7.60	31	$\text{Li}_{0.3}\text{K}_{1.5} \cdot 3\text{H}_2\text{O}$	r.t. ($P/P_0 = 0.9$)	10.4	35
$\overline{\text{HRb}} \cdot \text{H}_2\text{O}$	r.t. ($P/P_0 = 0.9$)	8.20	31	$\overline{\text{NaK}} \cdot 3\text{H}_2\text{O}$	r.t. ($P/P_0 = 0.7$)	10.25	47
$\overline{\text{HRb}} \cdot 0.5\text{H}_2\text{O}$	r.t. over P_4O_{10}	8.20	31	$\overline{\text{NaK}}$	150°	8.04	47
$\overline{\text{HRb}}$	150°	7.60	31	$\overline{\text{NaK}}$	450°	7.9	49
$\overline{\text{H}_{0.5}\text{Rb}_{1.5}} \cdot 2\text{H}_2\text{O}$	r.t. ($P/P_0 = 0.9$)	10.6	31				
$\overline{\text{H}_{0.5}\text{Rb}_{1.5}} \cdot \text{H}_2\text{O}$	r.t. over P_4O_{10}	9.20	31				
$\overline{\text{H}_{0.5}\text{Rb}_{1.5}}$	150°	9.16	31				

* r.t. = room temperature.

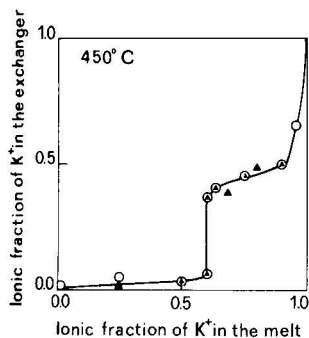
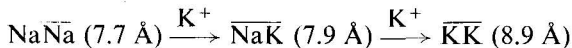


Fig. 3. Forward and reverse $\text{Na}^+ - \text{K}^+$ ion-exchange isotherms on crystalline zirconium phosphate in molten $\text{NaNO}_3 - \text{KNO}_3$ mixtures at 450° (From ref. 49). \circ , Na^+ displaces K^+ from $\overline{\text{KK}}$ (8.7 Å); \blacktriangle , K^+ displaces Na^+ from $\overline{\text{NaNa}}$ (7.7 Å).

er ion solvation are avoided and the interpretation of the ion-exchange mechanism is therefore usually simpler than in aqueous solution.

As an example, let us consider a two-step ion-exchange process, such as $\text{Na}^+ - \text{K}^+$ exchange⁴⁹, in which a smaller counter ion is replaced with a larger one. The relative ion-exchange isotherms are shown in Fig. 3 and the entire process can be summarized as follows:



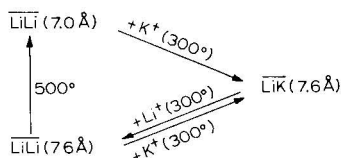
When the first Na^+ is replaced with K^+ , the interlayer distance increases, in agreement with the above considerations, and an immiscible $\overline{\text{NaK}}$ phase is formed. As two solid phases are present, the degree of freedom of the system (at constant temperature and pressure) becomes zero, and therefore the exchange must occur at a constant composition of the melt; a vertical portion of the isotherm is accordingly found (see Fig. 3). The replacement of the second Na^+ with K^+ must give a new immiscible phase having a larger interlayer distance and therefore a second vertical portion of the isotherm is obtained.

The $\text{Na}^+ - \text{K}^+$ ion exchange process at 450° seems to be reversible. However, in some ion-exchange processes, such as $\text{Li}^+ - \text{K}^+$ (ref. 38) or $\text{Li}^+ - \text{Na}^+$ (ref. 46) at 300° , very large hysteresis loops have been found. As already reported in a recent paper³⁸, the explanation could be as follows. When a larger counter ion is replacing a smaller one, the layers of the exchanger must be spread apart for space requirements. However, in the reverse process, where the smaller counter ion is replacing a larger one, the interlayer distance does not necessarily decrease again to the initial value, the formation of a metastable phase, with an interlayer distance larger than that in the original stable phase, being possible. In such a case, the exchange can occur without phase transition within a large range of the ionic composition of the solution.

A single solid phase being present, the system possesses one degree of freedom; the reverse isotherm is thus sloping and a large hysteresis loop is therefore found.

By heating the metastable solid solution at high temperature, the stable phase,

having a lower interlayer distance, is usually obtained. An example of the above considerations is the $\text{Li}^+ - \text{K}^+$ exchange process at 300° (ref. 38):



where the metastable $\overline{\text{LiLi}}$ (7.6 Å) phase is obtained.

As the phase transition $\overline{\text{LiK}}$ (7.6 Å)– $\overline{\text{LiLi}}$ (7.6 Å) is reversible, the knowledge of the enthalpies involved in the single steps of the cycle could give useful information on the energy difference of a given ion-exchange process, occurring with or without change in the interlayer distance of the exchanger⁵⁰.

Ion exchange in aqueous solutions. The ion-exchange behaviour of crystalline zirconium phosphate in aqueous solutions has been extensively investigated^{1,23}. Several considerations previously reported for ion-exchange processes in anhydrous media can be reconsidered here. However, in this case, one must take into account that in aqueous solution the counter ions are solvated, and consequently the interlayer distance also depends on the number of water molecules inside the exchanger. The number of the water molecules, in turn, depends on the hydration energy of the counter ion involved and on the lattice forces of the exchanger. Thus, some cases are also possible, e.g., $\overline{\text{LiLi}} \cdot 4\text{H}_2\text{O}$ (10.0 Å) $\xrightarrow{+\text{K}^+} \overline{\text{LiK}} \cdot 3\text{H}_2\text{O}$ (9.3 Å)³⁵, in which the interlayer distance decreases when a smaller counter ion is replaced with another ion having a larger radius but a lower hydration energy.

From a general point of view, when an ion-exchange process occurs with a phase transition, giving rise to an ionic form having a larger interlayer distance than the original one, the formation of a metastable supersaturated solid solution is possible in the reverse process and, as a consequence, a hysteresis loop can be obtained. Small hysteresis loops have been found for the $\text{Na}^+ - \text{K}^+$ exchange system^{34,47}, while very large hysteresis loops are found for systems such as $\text{Li}^+ - \text{K}^+$ (ref. 35), $\text{Rb}^+ - \text{H}^+$ and $\text{Cs}^+ - \text{H}^+$ (ref. 31). In the former case, the small hysteresis loop is explained by assuming, as in the case of zeolites⁵¹, that the phase rearrangement is delayed by a potential activation energy; therefore, phase transition takes place only when the original solid phase has been supersaturated by the incoming counter ion. Thus the forward and reverse isotherms do not coincide, as the phase rearrangement in the two opposite processes occurs at different ionic compositions of solution. In the latter cases, the large hysteresis loops were due to the formation of different phases in the two opposite processes, as already discussed for ion exchange in molten salts.

A comparison of titration curves of $\overline{\text{HH}} \cdot \text{H}_2\text{O}$ (7.6 Å) with alkali metal hydroxides is shown in Fig. 4. The X-ray analyses of samples at various stages of exchange have demonstrated that: (a) Na^+ and K^+ are exchanged in two steps in the approximate ranges 0–50% and 50–100% of conversion; (b) Li^+ is exchanged in three steps (0–50%, 50–75% and 75–100%); (c) Rb^+ is exchanged in three steps (0–25%, 25–75% and 75–100%); and (d) Cs^+ is exchanged in four steps (0–25%, 25–50%, 50–75% and 75–100%).

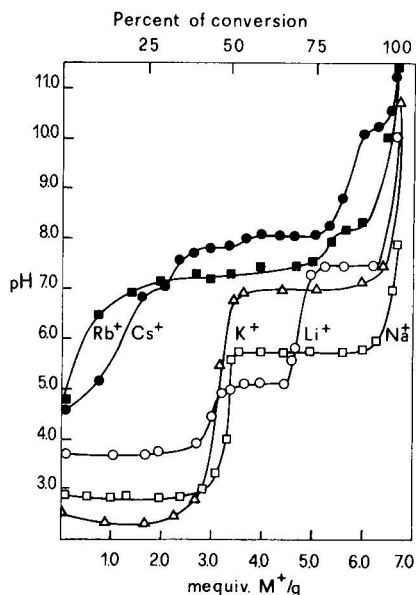
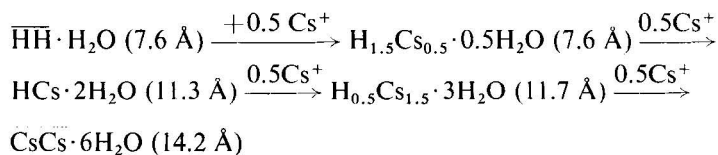


Fig. 4. Comparison of titration curves of crystalline zirconium phosphate with alkali metal ions. Conditions: 1 g of $\text{HH} \cdot \text{H}_2\text{O}$ (7.6 Å) in 200 ml of 0.1 N (MCl + MOH) solution at $25 \pm 1^\circ$.

The reasons for which crystalline zirconium phosphate exhibits different functionalities for the various alkali metal ions can most likely be ascribed to steric hindrance. As an example, we will try to explain the $\text{Cs}^+ - \text{H}^+$ exchange on the basis of the crystal structure of zirconium phosphate. As already reported in a previous paper³¹, this process can be summarized as:



It can be pointed out that in the first ion-exchange step, a solid solution is formed and the interlayer distance remains constant. By taking into account the spatial arrangement of the fixed O^- charges, it can easily be seen that this is possible only if a Cs ion enters inside the cavity where, for the interlayer distance of 7.6 Å, there is sufficient space to accommodate a Cs ion. Thus the water originally present near the centre of the cavity must be displaced, and therefore for each Cs^+ taken up by the exchanger, one molecule of water must be lost, as indeed is found³¹. Furthermore, owing to electrostatic repulsion, the unexchanged proton originally present in the cavity must be displaced away from the Cs ion, and it probably moves towards an adjacent cavity. At a degree of Cs^+ exchange of 25%, a situation similar to that shown schematically in Fig. 5 may be reached: 50% of the cavities are filled with a single Cs ion while the remaining cavities contain one water molecule and an average of three hydrogen ions.

In the second step, a degree of conversion of 50% is reached and each of the

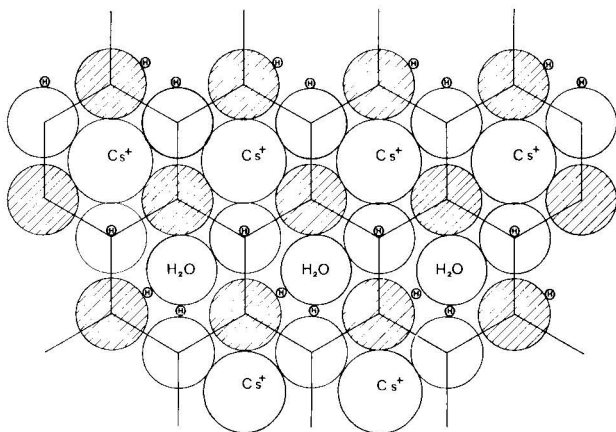


Fig. 5. Proposed arrangement of fixed charges, counter ions and water molecules in the phase $\overline{\text{H}}_{1.5}\text{Cs}_{0.5}\cdot 0.5\text{H}_2\text{O}$ (7.6 Å), viewed in a planar projection as described in Fig. 2.

cavities will therefore contain one Cs^+ placed near the centre, while the unexchanged protons, for electrostatic repulsion, are likely to be displayed towards the side of the cavities. The interlayer distance increases to 11.3 Å and water can enter inside the exchanger³¹.

As the pH is further increased other H^+ ions of the $\overline{\text{H}}\text{Cs}\cdot 2\text{H}_2\text{O}$ (11.3 Å) phase are exchanged and therefore more than one Cs^+ for each cavity has to be accommodated. In this case, Cs ions can no longer remain near the centre of the cavities and, for space requirements, the interlayer distance increases considerably. The presence of 25% of a small counter ion, such as H^+ , allows the Cs ions to remain further inside the cavities; consequently, the 75% loading Cs^+ phase can have an interlayer distance appreciably lower than that of the completely exchanged Cs^+ form in which, for space requirements, Cs ions are obliged to move towards the external part of the cavities⁴¹. The 75% Cs^+ -loaded phase must, however, be highly disordered, as confirmed by X-ray diffraction patterns³¹.

Finally, at very high pH values, the energy is sufficient to form the completely exchanged $\overline{\text{CsCs}}\cdot 6\text{H}_2\text{O}$ phase (fourth step). Using eqn. 2, it is possible to calculate that the interlayer distance of this phase must be 13.8 Å, which is in good agreement with the experimental value of 14.2 Å. This phase must again become ordered, as indeed is confirmed by its X-ray powder pattern.

Steric hindrance and ion selectivity for large cations on crystalline zirconium phosphate

As reported above, the maximum diameter of the windows interconnecting adjacent cavities of $\overline{\text{HH}}\cdot \text{H}_2\text{O}$ (7.6 Å) is 2.64 Å. Hence the ions that have a crystalline diameter greater than this value should not be exchanged for steric hindrance reasons. However, if sufficient energy is supplied, *e.g.*, by increasing the pH of the solution, the layers can spread apart and the large ions enter inside the exchanger. We have already seen that Rb^+ and Cs^+ can be taken up by $\overline{\text{HH}}\cdot \text{H}_2\text{O}$ (7.6 Å) until complete conversion occurs, although the exchange needs high pH values.

For this reason, crystalline zirconium phosphate has been regarded as a poor ion exchanger for large cations and, until recently, ion-exchange experiments have been

By employing $\text{HNa} \cdot 5\text{H}_2\text{O}$ (11.8 Å), it was not only observed that the Na^+ was easily replaced with Rb^+ , Cs^+ or Ba^{2+} (refs. 43 and 53), but also that large ions were strongly preferred by the exchanger. Taking into account that Na^+ is easily exchanged with $\text{HH} \cdot \text{H}_2\text{O}$, it can be concluded that the ion exchange of large cations by this exchanger requires a high activation energy due to steric hindrance. Once these steric hindrances are removed, the ion-exchange activation energy decreases and large cations can be exchanged. Now, it is well known that although the rate of a chemical reaction that needs a high activation energy is very low, its rate can be increased appreciably if a suitable catalyst is added. Therefore, it was worthwhile to investigate if an ion-exchange process that needs a high activation energy can be accelerated by adding a suitable ion-exchange catalyst.

We suggest the following mechanism, already reported⁵⁴ and confirmed by successive experiments⁵⁵, for the catalytic effect of Na^+ on the exchange of a large cation, M^+ .

$$\overline{\text{HH}} \cdot \text{H}_2\text{O} + \text{Na}^+ + 5 \text{H}_2\text{O} \rightarrow \overline{\text{HNa}} \cdot 5\text{H}_2\text{O} + \text{H}_3\text{O}^+ \quad (3)$$
$$\overline{\text{HNa} \cdot 5\text{H}_2\text{O}} + \text{H}_3\text{O}^+ + \text{Cs}^+ + \text{OH}^- \rightarrow \overline{\text{HCs}} + \text{Na}^+ + 7 \text{H}_2\text{O} \quad (4)$$

(11.8 Å) (8.0 Å)

Ion-exchange mechanism for crystalline zirconium phosphate for polyvalent ions

So far, very little experimental work on the ion exchange of polyvalent ions has been carried out^{36,56-58}. It was found that Mg^{2+} and Ba^{2+} are not appreciably exchanged by $\overline{\text{HH}}\cdot\text{H}_2\text{O}$ (7.6 Å) at room temperature⁵⁷; instead, Sr^{2+} and Ca^{2+} are

slowly exchanged at acidic pH values to form phases with the approximate composition $\text{H}_{0.9}\text{Sr}_{0.55} \cdot 3.5\text{H}_2\text{O}$ (10.2 Å) and $\text{H}_{0.74}\text{Ca}_{0.63} \cdot 3\text{H}_2\text{O}$ (10.0 Å), respectively. The complete conversion to Ca^{2+} or Sr^{2+} forms seems to require high pH values; however hydrolysis of the exchanger and precipitation of calcium or strontium phosphate occurs at pH values higher than about 5, so preventing the completely exchanged phases from being obtained.

Considerable progress in the ion exchange of divalent ions has recently been accomplished by using some zirconium phosphate phases having a large interlayer distance, such as the mixed salt form $\text{HNa} \cdot 5\text{H}_2\text{O}$ (11.8 Å)^{53,54}.

It has indeed been possible, using this exchanger, to obtain a completely converted $\text{Ba} \cdot 3.0\text{H}_2\text{O}$ (9.4 Å) phase⁵³ and some partially converted phases containing Mg^{2+} (ref. 54), UO_2^{2+} (ref. 52) and transition metal ions of the first series⁵⁹. Furthermore, these studies have shown that divalent ions are strongly preferred to Na^+ and therefore, as already discussed for large monovalent ions, the lack of exchange by $\text{HH} \cdot \text{H}_2\text{O}$ (7.6 Å) for Ba^{2+} , Mg^{2+} or transition metal ions should be essentially due to steric hindrance (*e.g.*, the large crystalline radius of Ba^{2+} or too large a hydrated ionic radius and high energy of hydration for other divalent ions).

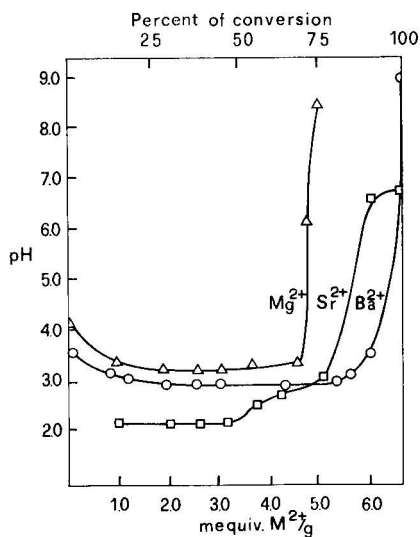


Fig. 6. Comparison of titration curves of crystalline zirconium phosphate with alkaline earth metal ions. Conditions: 1 g of $\text{HH} \cdot \text{H}_2\text{O}$ (7.6 Å) in 200 ml of 0.1 N ($\text{MCl}_2 + \text{M}(\text{OH})_2$) solution at $25 \pm 1^\circ$, in the presence of $5 \cdot 10^{-3}$ M NaCl as catalyst.

Hence the exchange of these ions by $\text{HH} \cdot \text{H}_2\text{O}$ could be made possible in the presence of small amounts of Na^+ , and this was indeed found true for Mg^{2+} and Ba^{2+} (refs. 53 and 54). It is interesting to compare the titration curves of alkaline earth metal ions on $\text{HH} \cdot \text{H}_2\text{O}$ (7.6 Å) in the presence of added Na^+ (see Fig. 6).

X-ray analyses showed that the following phase transitions take place at acidic pH values:

TABLE IV
INTERLAYER DISTANCES OF HYDRATED AND ANHYDROUS DIVALENT IONIC FORMS OF CRYSTALLINE ZIRCONIUM PHOSPHATE

Alkaline earth metal ions			Transition metal ions				
Phase composition	Drying conditions*	Interlayer distance, $d(\text{\AA})$	Ref.	Phase composition	Drying conditions	Interlayer distance, $d(\text{\AA})$	Ref.
$\overline{\text{Mg}}_{0.72}\text{H}_{0.56} \cdot 4\text{H}_2\text{O}$	r.t. ($P/P_0 = 0.9$)	9.85	54	$\overline{\text{Mn}}_{0.63}\text{H}_{0.74} \cdot n\text{H}_2\text{O}$	Wet sample	9.75	59
$\overline{\text{Mg}}_{0.72}\text{H}_{0.56}$	180°	7.69	53	$\overline{\text{Mn}}(\text{II})$	160°	7.41	60
$\overline{\text{Ca}}_{0.63}\text{H}_{0.74} \cdot 3\text{H}_2\text{O}$	r.t. ($P/P_0 = 0.7$)	9.98	57	$\overline{\text{Co}}_{0.57}\text{H}_{0.86} \cdot n\text{H}_2\text{O}$	Wet sample	10.30	59
$\overline{\text{Ca}}_{0.63}\text{H}_{0.74}$	200°	7.46	57	$\overline{\text{Co}}(\text{II})$	160°	9.93	60
$\overline{\text{Sr}}_{0.5}\text{H} \cdot 4\text{H}_2\text{O}$	r.t. ($P/P_0 = 0.9$)	10.2	53	$\overline{\text{Ni}}_{0.76}\text{H}_{0.48} \cdot n\text{H}_2\text{O}$	Wet sample	9.82	59
$\overline{\text{Sr}}_{0.5}\text{H}$	200°	7.46	53	$\overline{\text{Cu}}_{0.78}\text{H}_{0.44} \cdot n\text{H}_2\text{O}$	Wet sample	9.50	59
				$\overline{\text{Cu}}_{0.78}\text{H}_{0.44}$	320°	7.91	59
$\overline{\text{Ba}} \cdot 3.0\text{H}_2\text{O}$	r.t. ($P/P_0 = 0.9$)	9.4	53	$\overline{\text{Cu}}(\text{II})$	260°	7.87	60
$\overline{\text{Ba}}$	200°	7.55	53				
				$\overline{\text{Zn}}_{0.74}\text{H}_{0.52} \cdot n\text{H}_2\text{O}$	Wet sample	9.65	59
				$\overline{\text{Zn}}$	115°	7.41	60

* r.t. = room temperature.

ing the uptake of Cs^+ on $\text{HNa} \cdot 5\text{H}_2\text{O}$ (11.8 Å) phase or on $\overline{\text{HH}} \cdot \text{H}_2\text{O}$ (7.6 Å) in the presence of Na^+ as a catalyst.

In our laboratory, determinations of the electrical conductivity of zirconium phosphate of different degrees of crystallinity and in several ionic forms are also in progress. Preliminary results⁶² seem to indicate that the conductivity of $\overline{\text{HH}} \cdot \text{H}_2\text{O}$ (7.6 Å) increases with increasing degree of disorder in the crystal structure (see Table V).

TABLE V

SPECIFIC ELECTRICAL CONDUCTIVITY OF SOME IONIC FORMS OF ZIRCONIUM PHOSPHATE

<i>Exchanger</i>	<i>Preparation</i>	<i>Specific conductivity ($\text{ohm}^{-1} \text{cm}^{-1}$)</i>
$\text{Zr}(\text{HPO}_4)_2 \cdot n\text{H}_2\text{O}$	Amorphous	$8.4 \cdot 10^{-3}$
$\text{Zr}(\text{HPO}_4)_2 \cdot \text{H}_2\text{O}$	Refluxed for 100 h in 10 M H_3PO_4	$9.4 \cdot 10^{-5}$
$\text{Zr}(\text{HPO}_4)_2 \cdot \text{H}_2\text{O}$	HF method	$4.2 \cdot 10^{-5}$
$\text{Zr}(\text{NaPO}_4)_2 \cdot 3\text{H}_2\text{O}$	HF method	$2.2 \cdot 10^{-4}$
$\text{ZrMg}_{0.72}\text{H}_{0.56}(\text{PO}_4)_2 \cdot 4\text{H}_2\text{O}$	HF method	$1.3 \cdot 10^{-5}$

However, a comparison among the conductivity values is difficult because, owing to the low conductivity of truly crystalline materials, the surface conductivity becomes appreciable. On the other hand, the surface area also increases with decreasing crystallinity and this effect on the overall conductivity must be taken into account. Nevertheless, by determining the relative values of the surface areas of the various samples, it was possible to establish that the decrease in conductivity with increasing degree of crystallinity was greater than the decrease in surface area.

It can also be noted that the conductivity of the Ba^{2+} form of crystalline zirconium phosphate is very low. In agreement with this result, we have found that the rate of the ion-exchange processes



where $\text{M} = \text{Mg}, \text{Ca}$ or Sr is very low⁵³.

Other exchangers having a layered structure

In recent years, systematic investigations on the synthesis of insoluble crystalline acid salts of tetravalent metals led to the preparation of several new crystalline ion exchangers other than zirconium phosphate. The exchangers that have a layered structure are listed in Table I.

Their ion-exchange properties have been studied less frequently than those of zirconium phosphate; however, owing to the similarity between their crystalline structure and that of zirconium phosphate, we will try to discuss some expected ion-exchange behaviour.

In our opinion the ion exchange properties to be expected are:

(a) Dependence of the interlayer distances of exchanged ionic forms on the counter ion radius and water content.

(b) Occurrence of phase transitions and, consequently, ion exchange at fixed composition of the solution (plateau in the titration curves and vertical portions on the ion-exchange isotherms).

(c) Formation of metastable phases and, consequently, ion-exchange irreversibility and hysteresis loops between forward and reverse processes.

(d) High activation energy in the ion exchange of large cations and catalytic effect of small amounts of Na^+ or Li^+ .

Some properties already reported in previous papers⁸⁻¹² and some preliminary data on crystalline titanium phosphate⁶³ are in good agreement with the above expectations.

In our opinion, another interesting aspect of layered exchangers is the study of the relative variations in their ion-exchange behaviour as a function of the tetravalent metal and the polybasic acid involved.

Let us examine first the influence of the substitution of zirconium with other tetravalent metals. We have already seen that three oxygen atoms of each phosphate group are bonded to three tetravalent metal atoms lying in a plane. When zirconium is replaced with a smaller tetravalent metal such as titanium, smaller cavities (and consequently smaller windows connecting the cavities) have to be expected, as the Ti-O distance is shorter than the Zr-O distance and therefore the Ti-Ti distance in the plane of metal atoms should be shorter than Zr-Zr distance. It was recently reported by Clearfield *et al.*²³ that the Ti-Ti and Zr-Zr distances in the corresponding phosphates are 5.3 and 5.0 Å, respectively. Hence the ion exchange of large cations by crystalline titanium phosphate should require an even higher activation energy than in zirconium phosphate. As previously reported¹⁵, ion-sieve effects are higher in titanium than in zirconium phosphate.

The substitution of zirconium atoms with a larger tetravalent metal is expected to give an exchanger with slightly larger cavities. However, by substituting Zr with Ce(IV) or Th(IV), a fibrous structure has been obtained instead of the layered structure.

Let us now examine the effect of the substitution of the phosphate group with a larger polybasic acid group such as arsenate. We believe that the following changes in the ion-exchange properties could be expected:

(a) The Zr-Zr distance in zirconium arsenate should be longer than in zirconium phosphate; therefore, the cavities should also be larger, with a smaller steric hindrance than in zirconium phosphate. The Zr-Zr distances in zirconium arsenate and phosphate are 5.378 and 5.307 Å, respectively²³. The exchange of Ba^{2+} ion by zirconium arsenate⁸, but not by zirconium phosphate⁵⁷, could be related to the larger cavities in the former exchanger.

(b) The interlayer distance of M(IV) arsenates should be greater than in the corresponding M(IV) phosphates, as the As-O distance is greater than the P-O distance. As already shown in Table I, the interlayer distances of zirconium arsenate and phosphate are 7.82 and 7.56 Å, while those of titanium arsenate and phosphate are 7.77 and 7.56 Å, respectively.

(c) The hydrolysis should increase as the size of the polybasic acid group increases. In agreement with this view, it was found that crystalline titanium arsenate is a more hydrolyzable exchanger than crystalline titanium phosphate¹².

(d) Some differences in ion-exchange selectivity could also be expected be-

cause, according to the Eisenman theory⁶⁴, ion selectivity also depends on the field strength of the anions involved carrying the fixed charges.

Finally, the dimensions of the polybasic acid involved could play an important role in determining the crystalline structure of the exchanger. As an example, it can be pointed out that a phosphate group, with its small size, could be unable to bind three large tetravalent metals lying in a plane. Such a situation could instead be possible for other polybasic groups larger than phosphate, such as arsenate or antimonate. In this respect, it is interesting to note that cerium(IV) and thorium phosphates have a fibrous structure while the corresponding arsenates give microcrystals with as yet unknown structures (see Table VI). To understand the reasons for which a combination of a given tetravalent metal and a given polybasic acid gives a characteristic crystalline structure is of the utmost importance and studies in this field will also be very useful in the synthesis of new inorganic exchangers.

TABLE VI

ION EXCHANGERS HAVING AS YET UNKNOWN STRUCTURES

<i>Formula</i>	<i>Theoretical ion-exchange capacity (mequiv. H⁺/g)</i>	<i>First X-ray diffraction maxima, d (Å)</i>	<i>References</i>
Sn(HPO ₄) ₂ ·H ₂ O	6.08	7.76	17, 18
Sn(HAsO ₄) ₂ ·H ₂ O	4.80	7.77	17
Ce(HPO ₄) ₂ ·1.33H ₂ O	5.78	15.9	19
Ce(HAsO ₄) ₂ ·2H ₂ O	4.38	10.1	14
Th(HAsO ₄) ₂ ·H ₂ O	3.78	7.05	15

FIBROUS INORGANIC ION EXCHANGERS

Cerium(IV) phosphate¹⁰ and thorium phosphate⁶⁵ are the only two insoluble acid salts of tetravalent metals having a fibrous structure that have so far been synthesized. Fig. 7 shows an electron micrograph of a sample of cerium(IV) phosphate, showing its fibrous nature.

Fibrous inorganic ion exchangers are very interesting because they can be used to prepare inorganic ion-exchange papers or thin layers suitable for chromatographic separations as well as inorganic ion-exchange membranes without a binder. These applications will be discussed later, while below some properties of these exchangers, mainly referred to cerium(IV) phosphate, are reported.

Synthesis and composition of fibrous exchangers

These exchangers have been synthesized by adding slowly a solution of a Ce(IV) or Th(IV) salt to a hot solution (80–100°) of orthophosphoric acid with constant stirring. The effect of the temperature and digestion time, as well as of the molar ratio PO₄/Ce(IV) or PO₄/Th in solution, has already been reported in previous papers^{10,65}.

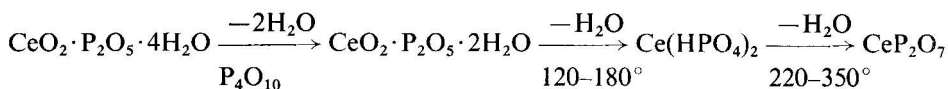
Unfortunately, so far it has not been possible to establish the structure of cerium(IV) or thorium phosphate because single fibres of suitable size for X-ray studies



Fig. 7. Electron micrograph of a sample of fibrous cerium(IV) phosphate (magnification 10,000 \times).

have not yet been obtained; even the chemical formula is not known for certain. However, some information has been derived from chemical and thermal analyses, ion-exchange properties, X-ray diffraction patterns and recently infrared spectroscopy^{66,67}.

The chemical composition of cerium(IV) phosphate is $\text{CeO}_2 \cdot \text{P}_2\text{O}_5 \cdot 4\text{H}_2\text{O}$ and its thermal behaviour can be summarized as:



The first step of the dehydration process does not cause significant changes in the X-ray powder pattern, but at 180° the material becomes almost amorphous and friable.

The molecule of water lost at about 180° is essential to the fibrous structure and, as infrared spectroscopy gives evidence for the formula $\text{Ce}(\text{HPO}_4)_2 \cdot 3\text{H}_2\text{O}$, this water molecule could join the fibres through hydrogen bonds.

Ion-exchange properties

Recently, extensive studies have been undertaken in this laboratory to determine the ion-exchange properties of fibrous cerium(IV) phosphate towards several monovalent, divalent and trivalent cations⁶⁷. In the preliminary results of these studies (Fig. 8), the ion uptake curves do not show any definite plateau, and the mechanism of exchange seems to occur without phase transitions and the exchangeable hydrogen ions display a large range of acidities like amorphous or semicrystalline exchangers. Fibrous cerium(IV) phosphate shows, at low loading, the sequence of the lyotropic series $\text{Cs}^+ > \text{K}^+ > \text{Na}^+ > \text{Li}^+$ or $\text{Ba}^{2+} > \text{Sr}^{2+} > \text{Ca}^{2+} > \text{Mg}^{2+}$, while, on increasing the loading of the exchanger, several reversals in selectivity occur until the sequence is almost completely reversed. It can be pointed out that with cations that

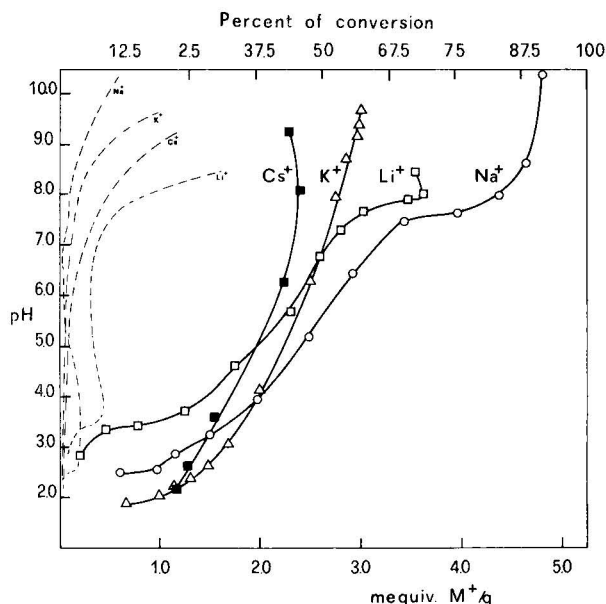


Fig. 8. Uptake and hydrolysis curves of fibrous cerium(IV) phosphate with alkali metal ions. Abscissae: uptake (solid lines), mequiv. M^+ per gram of exchanger; hydrolysis (dashed lines), mmoles of phosphate groups released by 1 g of exchanger to the solution. Conditions: 1 g of fibrous cerium(IV) phosphate in 200 ml of 0.1 N ($MCl + MOH$) solution at $25 \pm 1^\circ$.

have a large crystalline radius, such as K^+ and Cs^+ , conversions higher than 50% cannot be obtained in an acidic medium and, when the pH is increased to alkaline values, the exchanger hydrolyzes appreciably. As it is difficult to imagine that ion sieve exclusion would occur in a fibrous structure, this phenomenon could be ascribed, for example, to steric factors due to the closeness of adjacent fixed charges. It is notable that no sieving effect has been found for large divalent ions such as Ba^{2+} ; the X-ray powder pattern has only a few lines, of which the first is much more intense than the others. Its value ($d = 11.2 \text{ \AA}$) changes very little as the exchanging ion or the degree of exchange is changed, thus supporting the hypothesis that ion-exchange processes occur without phase transitions, as if a solid solution were formed.

Support-free fibrous cerium(IV) phosphate sheets have been used for the chromatographic separation of inorganic ions⁶⁸. In order to obtain more quantitative information on the selectivity of the fibrous cerium phosphate, K_d values of various inorganic ions at different concentrations have been determined⁶⁷. In Table VII, some of these results are reported. The marked selectivity towards ions such as Pb^{2+} , Ag^+ and Co^{2+} can be pointed out, so that this exchanger could be employed for several separations of analytical interest. Furthermore, as the increase in K_d values with decreasing concentration is different for the various ions, better separations could be obtained in diluted solution.

Owing to the presence of $Ce(IV)$ in the exchanger, redox reactions may take place with highly reducing ions. This behaviour, already found for Mn^{2+} in amorphous cerium phosphate⁶⁹, has also been confirmed for other ions such as Fe^{2+} and Cr^{3+} .

TABLE VII

DISTRIBUTION COEFFICIENT (mequiv. M^+ /g: mequiv. M^+ /ml) OF VARIOUS INORGANIC IONS ON FIBROUS CERIUM(IV) PHOSPHATE AT $25 \pm 1^\circ$ (g/ml = 25)

Ion	Concentration (N)		
	10^{-2}	$5 \cdot 10^{-3}$	10^{-3}
Na^+	32.2	50.3	122
Ag^+	215	325	550
Pb^{2+}	$7.8 \cdot 10^3$	10^6	10^6
Cu^{2+}	125	230	$1.3 \cdot 10^3$
Co^{2+}	33	43	100
Cr^{3+}	100	350	10^4

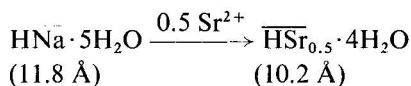
SOME PRACTICAL APPLICATIONS OF CRYSTALLINE INORGANIC ION EXCHANGERS OF THE CLASS OF INSOLUBLE ACID SALTS OF TETRAVALENT METALS

So far, very little experimental work on the practical applications of these crystalline exchangers has been carried out because, as already discussed, they have been considered to be, until recently, poor exchangers for large cations.

The discovery that these cations can be exchanged by enlarged phases of crystalline zirconium phosphate, indicates many new possibilities for the practical application of such exchangers.

Fig. 9 shows the Na^+ - Sr^{2+} isotherm obtained by using $ZrHNa(PO_4)_2 \cdot 5H_2O$ (11.8 Å).

The ion-exchange process takes place with the following single phase transition:



and the isotherm is therefore almost completely vertical. It can be seen that the phase transition occurs at a very low Sr^{2+} ionic fraction in solution and thus Sr^{2+} is strongly

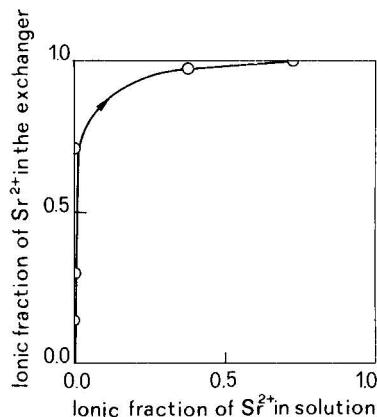


Fig. 9. Na^+ - Sr^{2+} forward ion-exchange isotherms on $\overline{HNa} \cdot 5H_2O$ (11.8 Å). Concentration: 0.01 N . Temperature: $25 \pm 1^\circ$.

preferred to Na^+ . Similar results have been obtained with Ca^{2+} , while the preference for Ba^{2+} is even greater⁵³. In our opinion, some practical applications of $\text{HNa} \cdot 5\text{H}_2\text{O}$ (11.8 Å) in water softening by alkaline earth metals or other divalent metal ions could be possible.

Further, we have seen above that $\text{HNa} \cdot 5\text{H}_2\text{O}$ can exchange several divalent transition metal ions; investigations on the catalytic activity of zirconium phosphate phases loaded with transition metal ions seem to be very promising⁷⁰. An interesting application of the layered exchangers could be to act as solid buffers. We have seen before that the conversion of $\text{HH} \cdot \text{H}_2\text{O}$ in a given salt form usually occurs with a phase transition and therefore the pH of the solution has to remain constant until all of the $\text{HH} \cdot \text{H}_2\text{O}$ phase is completely converted into the new ionic form. It can be pointed out that the conversion of a given salt form into another form occurs also with phase transition and, consequently, at constant composition of the solution. Hence the layered exchangers could also be employed in order to keep constant the ionic fraction of cations involved in the exchange.

The very high selectivity of fibrous exchangers towards Pb^{2+} and certain other divalent cations is also very promising for practical applications⁶⁷. At present, investigations are in progress in this laboratory in order to examine the practical application of fibrous cerium(IV) phosphate in the removal of some heavy metal ions from industrial waters. Inorganic ion-exchange papers are also suitable supports for carrying out good chromatographic or electrophoretic separations of inorganic ions.

Some exchangers that as yet have an unknown structure also possess interesting ion-sieve properties; *e.g.*, thorium arsenate behaves as a very narrow ion sieve: its protons being exchanged only by anhydrous Li^+ (ref. 15).

This interesting property has already been employed for carrying out good separations of Li^+ from other cations, even if present in high concentrations, and a practical application in the recovery of Li^+ from natural waters and dilute solutions can also be expected.

Finally, the insoluble acid salts of tetravalent metals have been employed for preparing inorganic ion-exchange membranes. These membranes are interesting from both a fundamental and a practical point of view. They represent a unique possibility for relating their electrochemical and osmotic properties to the known reticular arrangement of the fixed charges and counter ions or to steric factors. On the other hand, owing to the selectivity and stability of inorganic exchangers, these membranes could have applications as selective electrodes or in particular processes in which organic membranes cannot be employed because of their higher degradability. Particularly promising could be their employment in fuel cells at high temperatures or in the concentration of wastes containing fission products.

Extensive research on inorganic ion-exchange membranes is in progress in our laboratory under a C.N.R. contract, in order to investigate their electrochemical properties and particularly to examine their application in the desalting of brackish waters. Some of the membranes examined, in particular Ce(IV) phosphate membranes without a binder, seem to possess good electrochemical properties.

CONCLUSION

Recent advances with insoluble crystalline acid salts of tetravalent metals have

revealed several important fundamental aspects of these exchangers. However, further investigations, especially of a structural and thermodynamic nature, are still needed in order to understand in detail their ion-exchange mechanism and to make some predictions about their ion-exchange properties. Furthermore, as already discussed, the exchange of large cations by enlarged layered exchangers has opened new possibilities for the practical application of these exchangers and this will certainly be a stimulus for further investigations.

ACKNOWLEDGEMENTS

The authors thank Drs. M. G. Bernasconi, R. Bertrami, M. L. Luciani, and J. S. Gill for useful discussions and Mr. R. Giulietti for assistance in the experimental work.

This work was supported by Grant No. 72/00639 from the Istituto di Ricerca sulle Acque, C.N.R.

REFERENCES

- 1 V. Veselý and V. Pekárek, *Talanta*, 19 (1972) 219.
- 2 V. Veselý and V. Pekárek, *Talanta*, 19 (1972) 1245.
- 3 C. B. Amphlett, *Inorganic Ion Exchangers*, Elsevier, Amsterdam, 1964.
- 4 A. Clearfield and J. A. Stynes, *J. Inorg. Nucl. Chem.*, 26 (1964) 117.
- 5 A. Winkler and E. Thilo, *Z. Anorg. Allg. Chem.*, 346 (1966) 92.
- 6 G. Alberti, P. Cardini Galli, U. Costantino and E. Torracca, *J. Inorg. Nucl. Chem.*, 29 (1967) 571.
- 7 K. H. König and E. Meyn, *J. Inorg. Nucl. Chem.*, 29 (1967) 1153.
- 8 E. Torracca, U. Costantino and M. A. Massucci, *J. Chromatogr.*, 30 (1967) 584.
- 9 G. Alberti and E. Torracca, *J. Inorg. Nucl. Chem.*, 30 (1968) 317.
- 10 G. Alberti, U. Costantino, F. di Gregorio, P. Galli and E. Torracca, *J. Inorg. Nucl. Chem.*, 30 (1968) 295.
- 11 A. Clearfield, G. D. Smith and B. Hammond, *J. Inorg. Nucl. Chem.*, 30 (1968) 277.
- 12 G. Alberti and E. Torracca, *J. Inorg. Nucl. Chem.*, 30 (1968) 3073.
- 13 A. Clearfield, R. H. Blessing and J. A. Stynes, *J. Inorg. Nucl. Chem.*, 30 (1968) 2249.
- 14 G. Alberti, U. Costantino, F. di Gregorio and E. Torracca, *J. Inorg. Nucl. Chem.*, 31 (1969) 3195.
- 15 G. Alberti and M. A. Massucci, *J. Inorg. Nucl. Chem.*, 32 (1970) 1719.
- 16 E. Torracca, G. Alberti, R. Platania, P. Scala and P. Galli, in *Ion Exchange in the Process Industries*, Society of Chemical Industry, London, 1970, p. 315.
- 17 U. Costantino and A. Gasperoni, *J. Chromatogr.*, 51 (1970) 289.
- 18 M. J. Fuller, *J. Inorg. Nucl. Chem.*, 33 (1971) 559.
- 19 G. Alberti, U. Costantino and L. Zsinka, *J. Inorg. Nucl. Chem.*, 34 (1972) 3549.
- 20 A. Clearfield, A. M. Landis, A. S. Medina and J. M. Troup, *J. Inorg. Nucl. Chem.*, 35 (1973) 1099.
- 21 G. Alberti, S. Allulli, U. Costantino, P. Galli, M. A. Massucci and R. Platania, in J. A. Mikes (Editor), *IInd Symposium on Ion Exchange*, Vol. I, Magyar Kemikusok E., Budapest, 1969, p. 1.
- 22 G. Alberti, S. Allulli, U. Costantino, M. A. Massucci and E. Torracca, *Ion Exchange in the Process Industries*, Society of Chemical Industry, London, 1970, p. 318.
- 23 A. Clearfield, G. H. Nancollas and R. H. Blessing, in J. A. Marinsky and Y. Marcus (Editors), *Ion Exchange and Solvent Extraction*, Vol. 5, Marcel Dekker, New York, 1973, Ch. 1.
- 24 A. Clearfield and G. D. Smith, *Inorg. Chem.*, 8 (1969) 431.
- 25 A. Clearfield and W. L. Duax, *Acta Crystallogr.*, B25 (1969) 2658.
- 26 J. Albertsson, *Acta Chem. Scand.*, 20 (1966) 1689.
- 27 S. Ahrlund, J. Albertsson, A. Alnas, S. Hemmingsson and L. Kulberg, *Acta Chem. Scand.*, 21 (1967) 195.
- 28 A. Ruvarac and V. Veselý, *J. Inorg. Nucl. Chem.*, 32 (1970) 3939.
- 29 G. Alberti, S. Allulli, U. Costantino, M. A. Massucci and M. Pelliccioni, *J. Inorg. Nucl. Chem.*, 35 (1973) 1347.

- 30 A. Clearfield, A. Oskarsson and C. Oskarsson, *Ion Exchange and Membranes*, 1 (1972) 91.
- 31 G. Alberti, S. Allulli, U. Costantino and M. A. Massucci, *J. Inorg. Nucl. Chem.*, in press.
- 32 S. E. Horsley and D. V. Nowell, *J. Appl. Chem. Biotechnol.*, 23 (1973) 215.
- 33 A. Clearfield and J. Troup, *J. Phys. Chem.*, 74 (1970) 1314.
- 34 E. Torracca, *J. Inorg. Nucl. Chem.*, 31 (1969) 1189.
- 35 G. Alberti, S. Allulli, U. Costantino, M. A. Massucci and N. Tomassini, *J. Inorg. Nucl. Chem.*, 36 (1974) 653.
- 36 A. Dyer, D. Leigh and F. T. Ocon, *J. Inorg. Nucl. Chem.*, 33 (1971) 3141.
- 37 S. E. Horsley and D. V. Nowell, *Thermal Analysis, Proc. 3rd ICTA, Davos*, Vol. 2, 1971, p. 611.
- 38 G. Alberti, S. Allulli, U. Costantino, M. A. Massucci and N. Tomassini, *J. Inorg. Nucl. Chem.*, 36 (1974) 660.
- 39 A. Clearfield, D. L. Duax, A. S. Medina, G. D. Smith and J. R. Thomas, *J. Phys. Chem.*, 73 (1969) 3424.
- 40 A. Clearfield, W. L. Duax, J. M. Garces and A. S. Medina, *J. Inorg. Nucl. Chem.*, 34 (1972) 329.
- 41 G. Alberti and U. Costantino, in preparation.
- 42 G. Alberti, unpublished results.
- 43 G. Alberti, U. Costantino and J. P. Gupta, *J. Inorg. Nucl. Chem.*, 36 (1974) 2103.
- 44 A. Clearfield and A. S. Medina, *J. Inorg. Nucl. Chem.*, 32 (1970) 277.
- 45 Y. Hasegawa and H. Aoki, *Bull. Chem. Soc. Jap.*, 46 (1973) 836.
- 46 G. Alberti, S. Allulli, U. Costantino and M. A. Massucci, *Gazz. Chim. Ital.*, 103 (1973) 819.
- 47 G. Alberti, S. Allulli, U. Costantino and M. A. Massucci, *J. Inorg. Nucl. Chem.*, 35 (1973) 1339.
- 48 G. Alberti and S. Allulli, *J. Chromatogr.*, 32 (1968) 379.
- 49 G. Alberti, S. Allulli and G. Cardini, *J. Chromatogr.*, 45 (1969) 298.
- 50 S. Allulli, A. La Ginestra and N. Tomassini, *J. Inorg. Nucl. Chem.*, in press.
- 51 R. M. Barrer and L. Hinds, *J. Chem. Soc.*, (1953) 1879.
- 52 G. Alberti, U. Costantino and J. S. Gill, in preparation.
- 53 G. Alberti, R. Bertrami, U. Costantino and J. P. Gupta, in preparation.
- 54 G. Alberti, U. Costantino and J. P. Gupta, *J. Inorg. Nucl. Chem.*, 36 (1974) 2109.
- 55 G. Alberti, M. G. Bernasconi and U. Costantino, in preparation.
- 56 A. Clearfield and G. D. Smith, *J. Inorg. Nucl. Chem.*, 30 (1968) 327.
- 57 G. Alberti, U. Costantino and M. Pelliccioni, *J. Inorg. Nucl. Chem.*, 35 (1973) 1327.
- 58 S. J. Harvie and G. H. Nancollas, *J. Inorg. Nucl. Chem.*, 32 (1970) 3923.
- 59 S. Allulli, A. La Ginestra, M. A. Massucci, M. Pelliccioni and N. Tomassini, *Inorg. Nucl. Chem. Lett.*, 10 (1974) 337.
- 60 A. Clearfield and J. M. Troup, *J. Phys. Chem.*, 74 (1970) 2578.
- 61 A. Dyer and F. T. Ocon, *J. Inorg. Nucl. Chem.*, 73 (1971) 315.
- 62 G. Alberti, R. Bertrami and U. Costantino, in preparation.
- 63 G. Alberti, U. Costantino and M. L. Luciani, in preparation.
- 64 G. Eisenman, *Biophys. J.*, 2 (1962) 259.
- 65 G. Alberti and U. Costantino, *J. Chromatogr.*, 50 (1970) 482.
- 66 G. Alberti *et al.*, work in progress.
- 67 G. Alberti, U. Costantino, M. L. Luciani, in preparation.
- 68 G. Alberti, M. A. Massucci and E. Torracca, *J. Chromatogr.*, 30 (1967) 579.
- 69 W. A. Chylley, *Ph.D. Thesis*, University of Wisconsin, Madison, Wisc., 1963.
- 70 S. Allulli, A. La Ginestra and M. A. Massucci, personal communication.

CHROM. 7731

THE PHENOMENON OF OSMOSIS IN PERMEABLE MEMBRANES

GERHARD DICKEL

Physikalisch-Chemisches Institut, Universität München, Munich (G.F.R.)

SUMMARY

Two effects give rise to osmosis in a permeable membrane: the coupling effect between the ion streams and water, demonstrated by binary isotonic osmosis, and the osmotic difference between the outside solutions. But, in contrast to a semipermeable membrane, it is not the difference in the outside concentrations but the difference in the Donnan ions inside the membrane that produces the flux of water.

OSMOTIC PRESSURE

If a semipermeable membrane separates a solution from the pure solvent in an osmotic cell, a flux of water runs from the solvent into the solution. This flux is caused by the lower vapour pressure of the solution. On the other hand, the flux entering a closed osmotic cell gives rise to a hydrostatic pressure, which causes an increase in the vapour pressure of the solution and diminishes the decrease that arises from the solute. A state of equilibrium is reached if the vapour pressure has the same value on both sides of the membrane. This fact can be expressed by the equation

$$\mu_L^0 = \mu_L^{0'} + V_L P \quad (1)$$

which states that the chemical potential, μ_L^0 , of the pure solvent on one side of the membrane must be equal to the chemical potential, $\mu_L^{0'} + V_L P$, on the other side. Therefore, $\mu_L^{0'}$ represents the chemical potential of the water in a solution in the absence of a pressure (superscript zero) and $V_L P$ is an additional potential originating from the (hydrostatic) pressure P (V_L = molar volume).

Until equilibrium is reached, $\mu_L^0 > \mu_L^{0'} + V_L P$ and a flux of water from the higher to the lower potential is the result. Restricting the situation to a "strip dx ", i.e., a section of a membrane, Fick's first law can be written as

$$j_L/q = -D_H \text{grad} (\mu_L^0 + V_L P) \quad (2)$$

where D_H is the hydrodynamic permeability and q the cross-section of the membrane. Setting $j_L = 0$, we obtain

$$d\mu_L^0 = V_L dP \quad (3)$$

where

$$d\mu_L^0 = \mu_L^0 - \mu_L^{0'}$$

The hydrostatic difference dP (in the strip dx) which corresponds to the osmotic difference $d\mu_L^0$ between the pure solvent and the solution is called the osmotic pressure difference, dP_{os} .

OSMOSIS

In addition to semipermeable membranes, there are permeable membranes which are permeable for the solute also. In contrast to the semipermeable membranes, where the flux of solvent always runs in the direction of the osmotic gradient, we frequently observe in the case of permeable membranes a flux of water opposed to this gradient. Employing a pig's bladder to separate a concentrated solution of salicylic acid from pure water, both the salicylic acid and the water pass through the membrane in the same direction from the solution into the pure solvent. Surprisingly, the flux of water is 10,000 times greater than the flux of salicylic acid.

Effects in which water fluxes are opposed to the osmotic gradient are termed anomalous negative osmosis. In order to explain this behaviour, Graham¹ suggested that these effects originate from electric potentials.

ELIMINATION OF THE OSMOTIC PRESSURE: ISOTONIC OSMOSIS

In order to separate the flux of water originating in the osmotic difference from the flux, presumably caused by an electric potential, we used isotonic solutions, *i.e.*, solutions of different composition but equal activity of water. Our experiments were performed with membranes of condensed phenolsulphonic acid and binary isotonic mixtures of HCl with different alkalimetalchlorides². Although there was no osmotic difference, $d\mu_L$, between the solutions bordering the boundaries of the membrane, strong fluxes of water, j_L , were observed. Using small concentrations, the flux of water increases proportionally to the ion fluxes and the ratio j_L/j_i is given in Table I. However, on increasing the total concentration, c , the flux of water reaches a maximum and changes sign at $c > 4n$ (ref. 3) (see Fig. 1). In these experiments, pure solutions of HCl were used on one side of the membrane and mixtures of HCl and LiCl on the other side. By changing the $H^+ : Li^+$ ratio, a more or less steep gradient, $\Delta c_H/\Delta x$, which is the parameter of the family of curves in Fig. 1, was produced in the membrane. A surprising result was the independence of the inversion point on $\Delta c_H/\Delta x$ and on stirring of the solutions (plotted curve). This behaviour is explained in a further section on isotonic osmosis below.

APPLICABILITY OF THEORIES

While there is no lack of theories of osmosis, we have found no theory that is in accordance with our experiments. A large number of theories are based on an arrangement of the thermodynamics of irreversible processes (T.I.P.)⁴:

$$j_i = \sum_k L_{ik} X_k \quad (i = 1, 2, \dots, N) \quad (4)$$

where the unknown streams j_i are linear functions of arbitrary forces represented by X_k and L_{ik} are coefficients obeying the Onsager reciprocal relationship $L_{ik} = L_{ki}$.

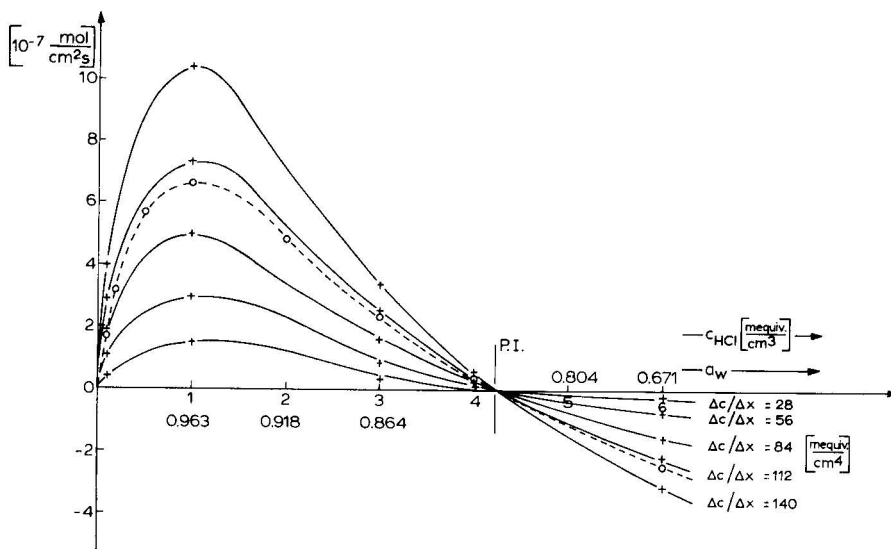


Fig. 1. Isotonic osmosis at higher concentrations. Water flux as a function of the concentration. System: LiCl + HCl-HCl. Parameter: concentration gradient.

Unrestricted confidence in the reciprocal relations can give rise to a failure of such theories. As stated by Gyarmati⁵, the Onsager relations do not need to be valid in the case of constraints. An example of a constraint is the condition

$$\sum z_i^{\pm} F j_i = I \quad (5)$$

which states that the electric current, I , is given by the number of elementary charges, $z_i^{\pm} F$ (F = Faraday constant), carried away with the ion fluxes. When $I = 0$, eqn. 5 is called the condition of electroneutrality, which gives rise to an electric field (Nernst's diffusion potential). As this field is not an independent and arbitrary force, it cannot be used on the right-hand side of eqn. 4.

The consequence of the above is that eqn. 4 and the Onsager equation can no longer be used and another principle must be sought. As all transport processes obey a variational principle (Fermat's principle of least time is the classical example) we have used this method to obtain correct equations of transport.

BRAUN-LE CHATELIER PRINCIPLE

The complete deduction of all transport equations requires an exhaustive knowledge of the calculus of variations. As such a procedure exceeds the scope of this paper, we give a short explanation of two equations which we have deduced elsewhere⁶.

If in a solution two fluxes j_1 and j_2 flow in opposite directions through a membrane, an interaction with the solvent (water) takes place. The water evades the constraint originating from the frictional interaction and moves so as to reduce the force

exerted on it to a minimum. In this case, the flux of water is given by the equation

$$j_L = \frac{c_L}{2} \frac{\sum R_i j_i}{\sum R_i c_i} \tag{6}$$

if R_i is the frictional coefficient of the ion i .

Imagining that the particles are electrically neutral and $R_1 > R_2$, the force K_1 necessary to transport particle 1 through the membrane must be greater than the force K_2 exerted on particle 2. In this case, a difference $dK = K_1 - K_2$ is the result. But in the case of ions, an electric field

$$c_F F \text{ grad } \varphi = - \frac{1}{2q} \sum R_i j_i \tag{7}$$

takes place and the result is that the difference dK disappears. This unexpected result is a consequence of the Braun–Le Chatelier principle of least constraint.

Comparing eqns. 6 and 7, the electric field as well as the flux of water can be expressed by the term $\sum R_i j_i$, which results in a formal connection between the osmosis and the electric field (eqn. 7). However, we cannot conclude from this fact that the osmosis arises from an electric field.

FURTHER CONSIDERATION OF ISOTONIC OSMOSIS

Eqn. 6 was used to evaluate the results of our experiments, presented in Table I. The frictional coefficients recorded in Table I were determined with the aid of reverse osmosis² by pressing the pure solvent through the membrane charged with ions 1 and 2. In addition to the ratio $(R_1 - R_2)/(R_1 + R_2)$, Table I gives the corresponding ratios of the ion mobilities, l_1 and l_2 , in solutions which do not differ essentially from the ratio found in the membrane. The last column gives the ratio f of the experimentally determined fluxes of water and the values calculated from eqn. 6. It is not clear whether there is a systematic error or an actual deviation from theory.

In order to understand the inversion of the water flux, it can be noted that eqns. 6 and 7 are valid for an arbitrary number of particles, N . In the case of the isotonic osmosis presented in Fig. 1, there are three particles, H^+ , Li^+ and Cl^- ,

TABLE I
ISOTONIC OSMOSIS AT LOW CONCENTRATIONS
Comparison of experimental and theoretical j_L/j_i values.

System	j_L/j_i (exptl.)	$\frac{R_1 - R_2}{R_1 + R_2}$	$\frac{l_2 - l_1}{l_2 + l_1}$	c_L/c_F	j_L/j_i (theor.)	f
Li-H	6.70	0.76	0.81	18.6	3.5	0.52
Na-H	4.80	0.57	0.76	16.3	2.3	0.48
K-H	3.60	0.47	0.67	16.0	1.9	0.52
Li-K	2.10	0.45	0.32	(13.0)	1.5	0.71
Na-K	1.40	0.14	0.19	(11.5)	0.4	0.20
NH ₄ -K	0.02	—	0.00	—	—	—

from which result the fluxes j_{H^+} and j_{Li^+} of the counter ions and j_{HCl} and j_{LiCl} of the Donnan ions. Eqn. 6 must be written in this case as

$$j_L \sum^N R_i c_i = \frac{c_L}{2} (R_H^+ j_H^+ + R_{HCl} j_{HCl} + R_{Li}^+ j_{Li}^+ + R_{LiCl} j_{LiCl}) \quad (8)$$

Using low outside concentrations, the Donnan fluxes can be ignored and osmosis flows in the direction of the Li^+ flux, as $R_{Li^+} > R_{H^+}$. Increasing the outside concentrations, a flux of Donnan ions takes place. As the experiments have shown³, a strong flux of HCl arises, whereas the flux of LiCl can be ignored. This behaviour results from the well known fact that the mobility of H^+ is more than ten times greater than the mobility of Li^+ . To this flux, the second term on the right-hand side of eqn. 8 is coordinated and as the flux j_{Cl^-} together with flux j_{H^+} is opposed to the flux j_{Li^+} , inversion of the osmosis takes place with an increasing concentration of Donnan ions. The independence of the inversion point on the parameter dc/dx follows from the fact that at this point the electric potential disappears and all fluxes j_i are dependent on dc/dx only. Having $j_L = 0$, we can divide both sides by dc/dx and obtain an equation that is independent of dc/dx at the inversion point. The osmotic inversion demonstrates that the electric field coordinated to the osmosis flux (see eqns. 6 and 7) is not Nernst's diffusion potential as assumed by Schlögl⁷. This is a consequence of the fact that $\text{grad } \varphi$ changes sign without the frictional coefficients or the gradients of chemical potentials changing sign, as would be necessary in the case of a diffusion potential.

ELECTROKINETIC RELATIONSHIPS

While on the one hand there is no agreement between our own results and those of prior concepts involving osmosis, on the other hand the investigations of Schmid⁸ on electrokinetic effects completely support our results.

Taking into consideration the definition

$$D_H = -c_L / \sum R_i c_i \quad (9)$$

and restricting eqns. 6 and 7 to a single ion $i = 1$, we obtain

$$\frac{j_L}{q} = -D_H c_F F \text{grad } \varphi \quad (10)$$

where D_H represents the hydrodynamic permeation, which is inversely proportional to the frictional coefficient. This equation, involving the correct coefficient $c_F F$, was first found by Schmid⁸.

A result of our theory is the following simple electrokinetic relationship. If any solution passes a sintered glass under the influence of a hydrostatic pressure, the velocities v_i and v_L of the solute i and solvent L fulfil the obvious relationship

$$v_L / v_i = 1 \quad (11)$$

If the sintered glass is replaced by a cation-exchange membrane and the pressure gradient by an electric field, it follows from the theory in the case of a single electrolyte^{2,6} that

$$v_L/v_i = 0.5 \quad (12)$$

The evaluation of earlier measurements⁹ yields a value of 0.54 (instead of 0.5), while more recent measurements¹⁰ give a value of 0.49.

PROBLEMS OF SUPERPOSITION OF FLUXES

Comparing eqns. 6 and 7, we can express the isotonic osmosis by an electric field. Proceeding to the non-isotonic osmosis, it seems obvious that the following equation results:

$$j_L/q = -D_H \text{ grad } (\mu_L^0 + V_L P) - \frac{c_L}{\sum R_i c_i} c_F F \text{ grad } \varphi \quad (13)$$

which gives a superposition of the water flux arising from the osmotic difference $d(\mu_L^0 + V_L P)$ (see eqn. 2) and the electric field (eqns. 6 and 7). This equation cannot be correct, however, as the first term on the right-hand side is related to a reversible process concerning a semipermeable membrane and the second term is related to an irreversible process concerning a permeable membrane. The correct equation results from the variational principles. In this paper, we will try to obtain the correct equation by means of phenomenological considerations.

CONSTRAINT RESULTING FROM THE MATRIX

It is the usual method in the theory of osmotic pressure to replace the osmotic difference, $d\mu_L^0$, by the concentration difference of the solute with the aid of the Gibbs-Duhem equation. Using this method for a permeable membrane, we obtain, in the case of a single counter ion 1, the equation

$$c_L \frac{d\bar{\mu}_L^0}{dc_L} \text{ grad } c_L = -c_{1F} \frac{d\mu_{1F}}{dc_{1F}} \text{ grad } c_{1F} - c_{1D} \frac{d\mu_{1D}}{dc_{1D}} \text{ grad } c_{1D} \quad (14)$$

In the following discussion, $\bar{\mu}_L^0$ represents the chemical potential of the solvent inside any membrane. The first term on the right-hand side includes the gradient of the counter ions, which must be zero in a membrane. In order to understand this very important fact, we must take into consideration that the concentration of the fixed ions in a membrane is constant, as is the concentration of the counter ions. Bearing in mind that the gradient implies differentiation and as the differentiation of a constant always results in zero, the term involving the fixed ions and the counter ions must also become zero in eqn. 14.

AN OSMOTIC PARADOX

At both boundaries of the membrane, the condition $\bar{\mu}_L^0 = \mu_L^0$ must be satisfied. From this it follows that $d\bar{\mu}_L^0 = d\mu_L^0$. But if the outside difference $d\mu_L^0$ is high and

as a result of a low concentration of the Donnan ions the difference $d\bar{\mu}_L^0$ is small, the latter condition cannot be satisfied and we have $d\bar{\mu}_L^0 < d\mu_L^0$. This paradox is an apparent one, as we have not paid attention to an essential condition which can be explained as follows. In contact with pure water, a membrane adsorbs water until the chemical potential of the water inside the membrane is equal to the chemical potential of the pure water. Taking the membrane for a simple polyelectrolyte, this state would first be attained at infinite dilution. Indeed, the non-cross-linked polystyrenesulphonic acid exhibits this behaviour. When divinylbenzene is added to the latter, a cross-linked gel is formed. The matrix of the membrane resulting from this reaction opposes a constraint P_c against the infiltrating water. The reaction against this stress is the swelling pressure P_s , which acts on the water according to the equation

$$P_s = -P_c \quad (15)$$

and increases the chemical potential of the latter according to eqn. 1. Hence the paradox mentioned above is resolved, as the phase equilibrium between both boundaries of the strip dx and the solutions must be written as

$$d\mu_L^0 = d(\bar{\mu}_L^0 + V_L P_s) \quad (16)$$

If there is an outside (hydrostatic) pressure gradient $\text{grad } P$, the expression $V_L dP$ must be added to both sides of eqn. 16. In contrast to an outside pressure gradient, a gradient of the swelling pressure does not perform any work, as P_c and P_s are constraining forces. It follows from these considerations that eqn. 13 is valid if we replace μ_L^0 by $\bar{\mu}_L^0$. The latter value results from the concentration gradient of the Donnan ions according to eqn. 14.

ILLUSTRATION OF A PERMEABLE MEMBRANE

In Fig. 2, curve A demonstrates the distribution of the concentration in an inactive membrane if the latter separates solutions of an electrolyte with different concentrations. This "normal" distribution breaks down if the membrane becomes "active" and adsorbs the bulk of ions (in exchange for other ions that diffuse away), as represented by curve C.

The remaining Donnan ions form a normal distribution (curve D). Curves B and E represent the osmotic gradients coordinated to curve A and D. The counter ions show a constant distribution of the concentration and do not give rise to any gradient.

OSMOTIC LAWS CONCERNING SEMIPERMEABLE AND PERMEABLE MEMBRANES

In order to emphasize the difference between a semipermeable and a permeable membrane, we can state that if a membrane separates two solutions showing an osmotic difference $d\mu_L^0$, the following effects take place in a closed osmotic cell:

(1) If the membrane is semipermeable, a hydrostatic pressure difference dP , given by eqn. 3 and called the osmotic pressure takes place in the equilibrium state.

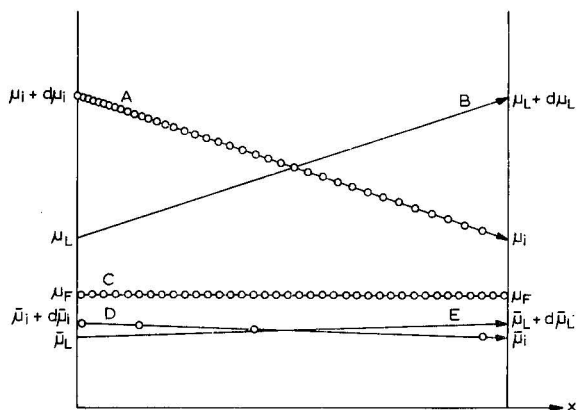


Fig. 2. Osmotic behaviour of semipermeable and permeable membranes. A, normal gradient $d\mu_i/dx$ of the ions; B, osmotic gradient $d\mu_L/dx$ in a semipermeable membrane; C, gradient of the fixed ions $d\mu_F/dx$ in a permeable membrane; D, gradient $d\bar{\mu}_i/dx$ of Donnan ions in a permeable membrane; E, intrinsic osmotic gradient $d\bar{\mu}_L/dx$ in a permeable membrane.

(2) Replacing the semipermeable membrane by a permeable membrane, a hydrostatic pressure difference dP is present in the stationary state. This pressure represents the apparent osmotic pressure and is given by the equation

$$\text{grad } P_a = -c_L \text{ grad } \bar{\mu}_L^0 - c_F F \text{ grad } \varphi \quad (17)$$

which follows from eqn. 13 if we write $\bar{\mu}_L^0$ instead of μ_L^0 , equate j_L to zero and take into consideration eqn. 9. The first term on the right-hand side of eqn. 17 represents the intrinsic osmotic difference which results from the gradient of the Donnan ions according to eqn. 14. From this arises the intrinsic osmotic pressure

$$\text{grad } P_i = -c_L \text{ grad } \bar{\mu}_L^0 = c_{iD} \text{ grad } \mu_{iD} \quad (18)$$

The second term in eqn. 17 represents the electroosmotic potential, which gives rise to the electroosmotic pressure difference

$$\text{grad } P_{el} = \frac{1}{2q} \sum R_i j_i \quad (19)$$

The right-hand side follows from eqns. 7.

(3) In all instances, the chemical potential of the water passes the boundaries of the membrane as stated by the condition

$$d(\mu_L^0 + V_L P) = d(\bar{\mu}_L^0 + V_L P_s + V_L P) \quad (20)$$

(4) In the case of a semipermeable membrane, dP_s vanishes and the intrinsic osmotic difference $d\bar{\mu}_L^0$ is equal to the outside osmotic difference.

(5) In the case of a permeable membrane, the outside osmotic difference performs a jump, which is given by the equation

$$d\mu_L^0 - d\bar{\mu}_L^0 = V_L dP_e \quad (21)$$

We call this effect the osmotic jump. It results from the fact that the constraining force dP_s represents a reaction against the outside osmotic difference $d\mu_L^0$, which reduces the latter to the inside osmotic difference, $d\bar{\mu}_L^0$.

CONCLUSION

In this paper we have considered a particular aspect in the field of osmosis, in as much as we have restricted ourselves to a "strip dx " of a membrane. The extension to a membrane of finite thickness is a further problem of the calculus of variations. The solution which we have found represents a function of the concentration on the boundaries of the membrane and not a function of the gradients, as is the case in the strip dx .

REFERENCES

- 1 T. H. Graham, *Phil. Trans. Roy. Soc. (London)*, 114 (1848) 178.
- 2 G. Dickel and F. Franke, *Z. Phys. Chem., (Frankfurt am Main)*, 80 (1972) 190.
- 3 G. Dickel and H. Hönig, *Z. Phys. Chem., (Frankfurt am Main)*, 90 (1974) 198.
- 4 S. R. Groot and P. Masur, *Non-Equilibrium Thermodynamics*, North-Holland, Amsterdam, 1962.
- 5 L. Gyarmati, *Non-Equilibrium Thermodynamics*, Springer Verlag, Berlin, 1970, p. 100.
- 6 G. Dickel, *Z. Phys. Chem., (Frankfurt am Main)*, 80 (1972) 173; 87 (1973) 260.
- 7 R. Schlögl, *Stofftransport durch Membranen*, Steinkopff Verlag, Darmstadt, 1952.
- 8 G. Schmid, *Z. Elektrochem. Ber. Bunsenges. Phys. Chem.*, 54 (1950) 424; 55 (1951) 229; 56 (1952) 181; 71 (1967) 778.
- 9 H. Krämer, *Diplomarbeit*, Göttingen, 1963.
- 10 H. Gohlke, *Z. Phys. Chem., (Frankfurt am Main)*, 87 (1973) 276.

CHROM. 7713

CHEMICAL EQUILIBRIA IN ION-EXCHANGE CHROMATOGRAPHY

JÁNOS INCZÉDY

Institute of Analytical Chemistry, University of Chemical Engineering, Veszprém (Hungary)

SUMMARY

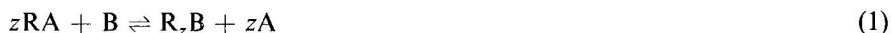
Equations for the calculation of distribution coefficients of cations, anions and basic molecules depending on the pH and composition of the eluent are given. Some general rules concerning anion-exchange equilibrium constants are also discussed.

INTRODUCTION

The rapid development and wide range of applications of ion-exchange chromatographic methods can be explained in terms of two main advantages. The first is the wide selectivity range. The distribution coefficient of the species to be separated can be influenced by chemical reactions, usually on a very large scale. The second advantage follows from the first, namely that the distribution coefficients and the related retention volumes can be calculated in most instances, and the optimum conditions of the separations can be predicted.

CALCULATION OF DISTRIBUTION COEFFICIENTS AND OPTIMUM CONDITIONS

The ion-exchange process taking place between an ion exchanger loaded with monovalent ions A and a solution containing B ions of valence z is described by the following equation (the charges being omitted for simplicity):



It was shown earlier¹ that the logarithm of the distribution coefficient of the B ions can be calculated to a good approximation using the following equation:

$$\log D_B = \log K^x + z \log Q - z \log [A] \quad (2)$$

where D_B is the distribution coefficient of the B ions, Q denotes the capacity of the resin and $[A]$ is the concentration of the monovalent eluent ions.

In the derivation of eqn. 2, it was considered that the concentration of the eluted B ions is much lower than that of the eluent ions, and the value of the mass action ratio of the ion-exchange reaction, K^x , can be assumed to be constant.

If there are side-reactions of the B ions, forming neutral or oppositely charged

species in the solution, eqn. 2 can be extended by using the side-reaction functions, introduced and widely used by Ringbom² in complex chemistry, to give

$$\log D_B = \log K^x - \log \alpha_{B(X)} + z \log Q - z \log [A] \quad (3)$$

where X denotes the species (ligands, protons, etc.) that reacts with the B ions to form complexes, protonated species, etc. If the concentration of the reacting species X and the equilibrium constants, β , of the side-reactions are known, the α values can easily be calculated:

$$\alpha_{B(X)} = 1 + [X] \beta_1 + [X]^2 \beta_2 + \dots \quad (4)$$

In those cases where the adsorption behaviour of the components to be separated is very similar, *i.e.*, the K^x values are very similar, in the presence of complex-forming ions (metal ions or ligands) the selectivity can be increased due to the side-reaction function.

The equations can be used for planning both cation-exchange and anion-exchange chromatography in general^{1,3,4}. In the case of organic bases, the ligand-exchange reactions, introduced by Helfferich⁵, can also be used successfully. As shown earlier⁶, the distribution coefficients and their dependence on the metal ion concentrations can also be in ligand exchange in the approximation

$$\log D_B \approx Q d_B \cdot \frac{\bar{\beta}_1}{\alpha_{B(M)}} \quad (5)$$

where d_B denotes the distribution constant of the ligand, $\bar{\beta}_1$ is the stability complex of the 1:1 complex and M is the complex-forming metal ion.

If the distribution coefficients of the species and their dependence on the pH or the concentration of the reagent X are known, the most suitable conditions for chromatographic separations, the elution volumes and the number of theoretical plates required for quantitative separations⁷ can be calculated.

ION-EXCHANGE EQUILIBRIUM CONSTANTS

If we wish to calculate the distribution coefficient of a substance using eqn. 2 or 3, one of the most important problems is to establish the proper value of the ion-exchange equilibrium constant, the logarithm of which is the first term on the right-hand side of eqns. 2 and 3.

Although several studies have been made in recent years on the elucidation of the general rules of the absorption behaviour of cations and anions, there has so far been a lack of data and rules that can be used in calculations. In the field of cation exchange on strongly acidic resins, the situation is better as extensive collections of distribution coefficients of metal ions in mineral acid solutions were given by Strelow and coworkers^{8,9} and also by other workers. In most instances, the selectivity order of the metal cations is in agreement with the classical theories of Gregor¹⁰ and Glueckauf¹¹. The field of anion exchange has been more neglected.

On account of these problems, and also on account of some separation prob-

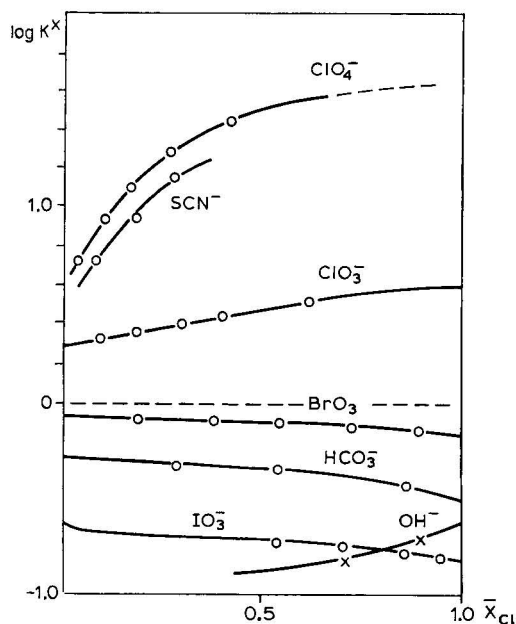


Fig. 1. Logarithm of K^x values of some monovalent ions relative to chloride as a function of the mole fraction of the chloride (\bar{X}_{Cl}) in the resin (Dowex 1-X8) at 28°.

lems, we carried out investigations on the ion-exchange equilibria of some anions¹². In Fig. 1, the logarithm of the K^x values of some monovalent ions referred to the chloride ion, found experimentally, are plotted against the mole fraction of the chloride ion inside the resin phase (\bar{X}_{Cl}). It can be seen that the selectivity of all ions that have a lower hydration tendency than that of the chloride ion increases with decreasing amount of the ion in question. The hydroxide ion shows the opposite behaviour, corresponding to the fact that its hydration tendency is greater than that of the reference ion.

For the calculation of chromatographic separations, $\log K^x$ values relating to high \bar{X}_{Cl} values are to be used.

The other important question in chromatographic separations is the order of adsorption strengths of the anionic species of the same polybasic acids and the dependence of the adsorption strength on valence. For metal cations, there is a general rule that on the sulphonic type of strongly acidic resins multivalent ions are bound more strongly than monovalent ions. According to our investigations, there is an opposite rule among anions, because on strongly basic anion-exchange resins the anion that has a lower valence has a greater K^x value if the counter ion is the same, e.g., chloride ion.

For example, the K^x value for the sulphate-chloride exchange is 0.1, while for the hydrosulphate-chloride exchange it is about 4 (ref. 13).

Nakamura *et al.*¹⁴ investigated the adsorption of different polyphosphate anions on anion-exchange resins at various pH values and at various chloride concentrations. Using their data, and eqns. 2 and 3, we calculated the $\log K^x$ values (Table I).

TABLE I

CALCULATED ION-EXCHANGE EQUILIBRIUM CONSTANTS OF POLYPHOSPHATE IONS OF VARIOUS VALENCES RELATIVE TO CHLORIDE ION

Resin: Dowex 1-X4.

Anion	Log K^x	Anion	Log K^x
$\text{H}_2\text{P}_3\text{O}_{10}^{3-}$	-1.1	$\text{HP}_4\text{O}_{13}^{5-}$	-2.7
$\text{HP}_3\text{O}_{10}^{4-}$	-1.7	$\text{P}_4\text{O}_{13}^{6-}$	-3.6
$\text{P}_3\text{O}_{10}^{5-}$	-2.25	$\text{HP}_5\text{O}_{16}^{6-}$	-3.1
		$\text{P}_5\text{O}_{16}^{7-}$	-5.0

It can be seen that the $\log K^x$ values decrease in the order of polymerization number, and for a given acid in the order of increasing valence.

This behaviour of the ions of polybasic acids is in agreement with the results obtained by thermoanalytical measurements. We found by thermal analysis that if we use slow heating, with increasing temperature the water content of the air-dried (conditioned) anion-exchange resin sample is removed in two distinct steps. The first step (rate maximum at 120°) corresponds to the removal of water of swelling, while the second step (rate maximum at 170°) corresponds to the water of hydration bound strongly to the ions. Thermal analysis curves are given in Fig. 2. By carrying out the measurements with resin samples loaded with different phosphate ions, the proportions of the two types of water were obtained from the *TG* curves.

From the data, the number of water molecules per equivalent of resin was calculated (Table II). It can be seen that the amount of the more strongly bound water molecules increases with valence (similar results were obtained with sulphate- and hydrosulphate-form resins). Hence the difference between the hydration ability of the

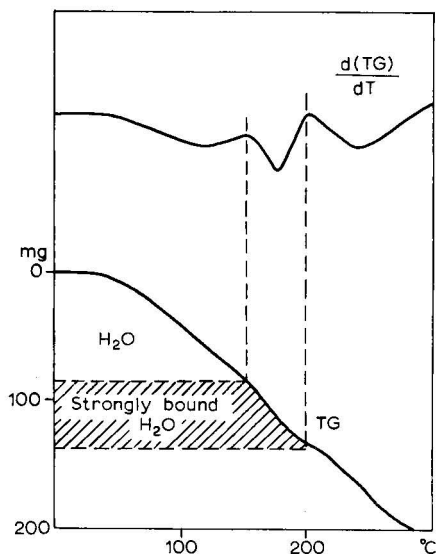


Fig. 2. Derivatogram of 500 mg of air-dried PO_4 -form Dowex 1-X8 resin sample. Heating rate: $3.0^\circ/\text{min}$.

TABLE II

STRONGLY AND LOOSELY BOUND WATER CONTENTS OF AIR-DRIED H_2PO_4^- , HPO_4^- AND PO_4^- FORM RESIN SAMPLES

Resin form	Strongly bound water (moles per equiv. resin)	Loosely bound water (moles per equiv. resin)
H_2PO_4^-	0.3	3.8
HPO_4^-	1.8	3.1
PO_4^-	2.1	3.0

ion in question and that of the chloride ion is an important factor in the selectivity. The volume of the hydrated ion is less important. Multivalent ions have a larger hydration tendency, and therefore their adsorption strength is lower.

EXPERIMENTAL

The determination of ion-exchange equilibrium constants of the monovalent and multivalent anions were determined by means of the dynamic method of Harvey *et al.*¹⁵. The description of the measurements and the results have been published elsewhere¹². The thermal analytical investigations were carried out with a derivatograph (Paulik–Paulik–Erdey system, MOM, Hungary).

REFERENCES

- 1 J. Inczédy, P. Klatsmányi-Gábor and L. Erdey, *Acta Chim. Hung.*, 61 (1969) 261.
- 2 A. Ringbom, *Complexation in Analytical Chemistry*, Interscience, New York, 1963.
- 3 J. Gaál and J. Inczédy, *Acta Chim. Hung.*, 76 (1973) 113.
- 4 J. Inczédy and L. Glósz, *Acta Chim. Hung.*, 62 (1969) 241.
- 5 F. Helfferich, *Nature (London)*, 189 (1961) 1001.
- 6 J. Inczédy, *Acta Chim. Hung.*, 69 (1971) 265.
- 7 J. Inczédy, *J. Chromatogr.*, 50 (1970) 112.
- 8 F. W. E. Strelow, *Anal. Chem.*, 32 (1960) 1185.
- 9 F. W. E. Strelow, R. Rethemeyer and C. J. C. Bothwa, *Anal. Chem.*, 37 (1965) 106.
- 10 H. P. Gregor, *J. Amer. Chem. Soc.*, 73 (1951) 642.
- 11 E. Glueckauf, *Proc. Roy. Soc. (London)*, A214 (1952) 207.
- 12 E. Fekete and J. Inczédy, *Acta Chim. Hung.*, in press.
- 13 B. J. Birch, J. Inczédy, R. J. Irwing and J. E. Salmon, *Trans. Faraday Soc.*, 65 (1969) 2886.
- 14 T. Nakamura, M. Kimura, H. Waki and S. Ohashi, *Bull. Chem. Soc. Jap.*, 44 (1971) 1302.
- 15 J. F. Harvey, J. P. Redfern and J. E. Salmon, *J. Chem. Soc. (London)*, (1963) 2861.

CHROM. 7892

ION EXCHANGE, ISOTOPE EXCHANGE AND ISOTOPE SEPARATION

HIDETAKE KAKIHANA

Tokyo Institute of Technology, O-okayama, Meguro-ku, Tokyo (Japan)

SUMMARY

Ion-exchange and isotope-exchange reactions are discussed mainly from the theoretical point of view in order to find a general expression for the isotope separation factor (eqn. 14). The theoretical expression for the separation factor of boron isotopes is derived from eqn. 14 for the system containing aqueous boric acid with an anion-exchange resin (eqn. 20). Some experimental results for boron isotopes are given and are discussed with the use of eqn. 20.

Results obtained from a small column are also presented in order to show a new, simple procedure for boron isotope separation, which needs only boric acid as raw material, a column of a weakly basic anion-exchange resin for chromatographic purposes and water as eluting agent.

INTRODUCTION

Since Taylor and Urey¹ proposed the possibility of ion-exchange separations of isotopes in 1937, many studies have been carried out, not only to acquire fundamental knowledge but also to find practical separation systems. Among these studies, the most important work might be the theoretical work of Glueckauf² and the successful separation of nitrogen isotopes by Powell *et al.*³.

In this paper, on the basis of fundamental facts of ion-exchange and isotope-exchange reactions, the further possibility of ion-exchange separation of isotopes is considered, using the case of boron isotopes as an example.

ION-EXCHANGE REACTION

The thermodynamics of pure ion-exchange reactions (with no complex formation in the system) have been intensively investigated by Gregor and Frederick⁴⁻⁶ and by Glueckauf⁷, who obtained different results. The reason for the difference has been discussed and the general expression for the equilibrium constant of pure ion-exchange reactions has been derived⁸.

The ion-exchange reaction is expressed in general as



where A and B are solvated cations having charges p and q , respectively, and R is the resinous anion.

The equilibrium constant of reaction 1, K , is given by

$$\ln K = \ln \frac{(\bar{a}_B)^p (a_A)^q}{(\bar{a}_A)^q (a_B)^p} = \frac{(\pi - P)}{RT} (q\bar{v}_{A'} - p\bar{v}_{B'}) - [q(\bar{h}_A - h_A) - p(\bar{h}_B - h_B)] \ln a_w \quad (2)$$

where a_A , a_B and a_w denote the activities of solvated cations A and B and free water W in the external solution, \bar{a}_A and \bar{a}_B are the activities of solvated cations A and B in the resin phase, π is a complicated function caused mainly by the structural strain of the resin and having the dimension of pressure, P is the external pressure, $\bar{v}_{A'}$ and $\bar{v}_{B'}$ are the partial molal volumes of the solvated cations A and B in the resin phase, and h and \bar{h} denote the solvation numbers of each cation in the external solution and the resin phases, respectively.

The definitions of the separation factor, S and the distribution coefficient, D are

$$S \equiv \frac{[\tilde{B}] \cdot [A]}{[\tilde{A}] \cdot [B]} \quad (3)$$

and

$$D \equiv \frac{[\tilde{B}]}{[B]} \quad (4)$$

where $[]$ and $[\tilde{ }]$ denote the concentrations of each species in the external solution and the resin phases, respectively.

Combining eqns. 2 and 3, we obtain

$$\ln S = \left(\frac{q}{p} - 1 \right) \ln \frac{[\tilde{A}]}{[A]} + \frac{1}{p} \ln \frac{(\bar{\gamma}_A)^q (\gamma_B)^p}{(\bar{\gamma}_B)^p (\gamma_A)^q} + \frac{1}{p} \cdot \frac{\pi - P}{RT} (q\bar{v}_{A'} - p\bar{v}_{B'}) - [q(\bar{h}_A - h_A) - p(\bar{h}_B - h_B)] \ln a_w \quad (5)$$

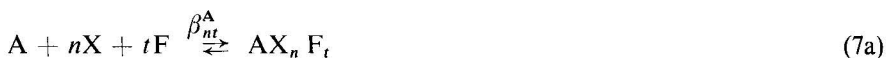
and combining eqns. 2 and 4, we obtain

$$\ln D = \frac{q}{p} \ln \frac{[\tilde{A}]}{[A]} + \frac{1}{p} \ln \frac{(\bar{\gamma}_A)^q (\gamma_B)^p}{(\bar{\gamma}_B)^p (\gamma_A)^q} + \frac{1}{p} \cdot \frac{\pi - P}{RT} (q\bar{v}_{A'} - p\bar{v}_{B'}) - [q(\bar{h}_A - h_A) - p(\bar{h}_B - h_B)] \ln a_w \quad (6)$$

where γ and $\bar{\gamma}$ denote the activity coefficients of each solvated ion in the external solution and the resin phases, respectively.

Eqns. 5 and 6 are the general expressions for the separation factor and the distribution coefficient of a pure ion-exchange reaction. The first term in each equation is the concentration term, which is very important when $p \neq q$, the second term is the activity coefficient term, the third is the pressure-volume term and the fourth is the solvation term.

If the system contains complex formation reactions such as



in the external solution and



in the resin phase, the general expression for the separation factor is⁹

$$\ln S_A^B = \ln S + \ln \frac{\sum_n \sum_t \beta_{nt}^A [X]^n [F]^t}{\sum_n \sum_t \beta_{nt}^B [X]^n [F]^t} - \ln \frac{\sum_n \sum_s \beta_{ns}^A [\bar{X}]^n [\bar{Y}]^s}{\sum_n \sum_s \beta_{ns}^B [\bar{X}]^n [\bar{Y}]^s} \quad (9)$$

where the β values are the stability constants of eqns. 7 and 8.

ISOTOPE-EXCHANGE REACTION

If A and B are the isotopes of a certain element M, the stability constants in reactions 7 and 8 can be expressed in terms of the isotopic reduced partition function ratio¹⁰:

$$\frac{f_{nt}}{f_{00}^0} = \frac{\beta_{nt}^A}{\beta_{nt}^B} \quad (10)$$

$$\frac{\bar{f}_{ns}}{\bar{f}_{00}^0} = \frac{\bar{\beta}_{ns}^A}{\bar{\beta}_{ns}^B} \quad (11)$$

where f_{nt} and \bar{f}_{ns} are the reduced partition function ratios of the chemical compounds $MX_n F_t$ and $MX_n Y_s$ and f_{00}^0 and \bar{f}_{00}^0 are the reduced partition function ratios of the atom (M) itself in the external solution and the resin phases, respectively.

The expression for the reduced partition function ratio was skillfully derived by Urey and Rittenberg¹¹ and Bigeleisen and Mayer^{12,13}:

$$\frac{s}{s'} f = \frac{s}{s'} f \left(\frac{m'}{m} \right)^{3n/2} = \prod_{i=1}^{3N-6} \left\{ \frac{u_i}{u'_i} \cdot \frac{e^{-u_i/2}}{1 - e^{-u_i}} \cdot \frac{1 - e^{-u'_i}}{e^{-u_i/2}} \right\} \quad (12)$$

or

$$\begin{aligned} \frac{s}{s'} f &= 1 + \sum_{i=1}^{3N-6} \left(\frac{1}{2} - \frac{1}{u_i} + \frac{1}{e^{u_{i-1}}} \right) \Delta u_i \\ &= 1 + \sum_{i=1}^{3N-6} G(u_i) \Delta u_i \end{aligned} \quad (13)$$

where $(s/s') f$ is the reduced partition function ratio, f is the partition function ratio, m and m' are the atomic weights for the heavy and light isotopes, n is the number of isotopic atoms exchanged, s and s' are the symmetry numbers, u_i and u'_i are equal to $h_c \nu_i / kT$ and $h_c \nu'_i / kT$ for the heavy and light isotopic compounds and Δu_i is equal to $u'_i - u_i$.

TABLE I

REDUCED PARTITION FUNCTION RATIOS OF BORON COMPOUNDS AND EQUILIBRIUM CONSTANTS FOR BORON ISOTOPE EXCHANGE REACTIONS AT 300°K

s_f/s'	$^{11}_0\text{B}^{19}\text{F}_3$	$^{11}_0\text{B}^{19}\text{F}$	$^{11}_0\text{B}(^{16}\text{O}^{17}\text{H})_3$	$^{11}_0\text{B}(^{16}\text{OH})_3$	$^{11}_0\text{B}(^{16}\text{OH})_4^-$	$^{11}_0\text{B}(^{12}\text{CH}_3)_3$	$^{11}_0\text{B}^{35}\text{Cl}_3$	$^{11}_0\text{B}^{35}\text{Cl}_3$	$^{11}_0\text{BH}_3\text{CO}$	$\text{HCN}^{11}_0\text{BCl}_3$	$^{11}_0\text{BH}_4^-$	$^{11}_0\text{B}^{79}\text{Br}_3$	$^{11}_0\text{B}^{35}\text{Cl}_4^-$	$^{11}_0\text{B}^{79}\text{Br}_4^-$	$^{11}_0\text{B}^{127}\text{I}_3$
	1.2387	1.2178	1.1979	1.1760	1.1693	1.1356	1.1319	1.1271	1.1190	1.1127	1.1072	1.0898	1.0893		
$^{11}_0\text{B}^{19}\text{F}_3$	1.0000	1.0172	1.0341	1.0533	1.0594	1.0908	1.0944	1.0990	1.1070	1.1132	1.1188	1.1366	1.1372		
$^{11}_0\text{B}^{19}\text{F}_4^-$	1.0000	1.0166	1.0355	1.0415	1.0724	1.0759	1.0805	1.0883	1.0945	1.0999	1.1175	1.1180			
$^{11}_0\text{B}(^{16}\text{OH})_3$		1.0000		1.0186	1.0245	1.0549	1.0583	1.0628	1.0705	1.0766	1.0819	1.0992	1.0997		
$^{11}_0\text{B}(^{16}\text{OH})_4^-$			1.0000		1.0057	1.0356	1.0390	1.0434	1.0509	1.0569	1.0621	1.0791	1.0796		
$^{11}_0\text{B}(^{12}\text{CH}_3)_3$				1.0000		1.0297	1.0330	1.0374	1.0450	1.0509	1.0561	1.0729	1.0734		
$^{11}_0\text{B}^{35}\text{Cl}_3$						1.0000	1.0033	1.0075	1.0148	1.0206	1.0257	1.0420	1.0425		
$^{11}_0\text{BH}_3\text{CO}$					-		1.0000	1.0043	1.0115	1.0173	1.0223	1.0386	1.0391		
$\text{HCN}^{11}_0\text{BCl}_3$								1.0000	1.0072	1.0129	1.0180	1.0342	1.0347		
$^{11}_0\text{BH}_4^-$									1.0000	1.0057	1.0107	1.0268	1.0273		
$^{11}_0\text{B}^{79}\text{Br}_3$										1.0000	1.0050	1.0210	1.0215		
$^{11}_0\text{B}^{35}\text{Cl}_4^-$											1.0000	1.0160	1.0164		
$^{11}_0\text{B}^{79}\text{Br}_4^-$												1.0000	1.0005		

Eqs. 12 and 13 make it possible to calculate the reduced partition function ratio, if the spectroscopic data are known for each isotopically different compound. Further, even if the spectroscopic data for the rarer isotopic compounds are not known, the approximate estimation of the reduced partition function is possible with use of the G and F matrix method¹⁴.

The reduced partition function ratios of boron compounds and the equilibrium constants of isotope exchange reactions between two boron compounds are calculated and shown in Table I.

ION-EXCHANGE SEPARATION OF ISOTOPES

Combining eqn. 9 with eqns. 10 and 11:

$$\ln S_A^B = \ln \sum_{n=0}^r \sum_{t=0}^T x_{nt} f_{nt} - \ln \sum_{n=0}^r \sum_{s=0}^S \bar{x}_{ns} \bar{f}_{ns} \quad (14)$$

where x_{nt} and \bar{x}_{ns} are the mole fractions of each chemical species in the external solution and the resin phases, respectively, and are expressed as

$$x_{nt} = \frac{\beta_{nt}^B [X]^n [F]^t}{\sum_{n=0}^r \sum_{t=0}^T \beta_{nt}^B [X]^n [F]^t} \quad (15)$$

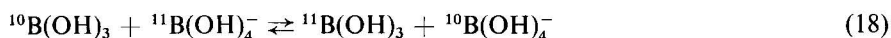
$$\bar{x}_{ns} = \frac{\bar{\beta}_{ns}^B [\bar{X}]^n [\bar{Y}]^s}{\sum_{n=0}^r \sum_{s=0}^S \bar{\beta}_{ns}^B [\bar{X}]^n [\bar{Y}]^s} \quad (16)$$

Eqn. 14 is the general expression for the isotope separation factor with complex formation reactions and describes the relationship among three different kinds of quantities, the separation factor, the reduced partition function ratio and the mole fraction, each of which can be measured experimentally by different methods.

In the case of boron isotopes, if boric acid is dissolved in water, the slight dissociation



will occur and the isotope exchange equilibrium



will be maintained.

The equilibrium constant of reaction 18 is simply the ratio of the reduced partition function ratio of B(OH)_3 to that of B(OH)_4^- and, as shown in Table I, the value is 1.0186 at 300°K.

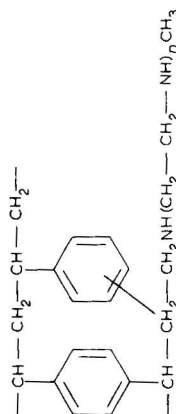
This means ^{11}B will prefer to move in the neutral species B(OH)_3 and ^{10}B in the anionic species B(OH)_4^- and the isotopic difference is 1.0186 which is very high as the isotopic standard. This high value, however, is not unexpected if it is remembered that the structural change between two species is very great, from a triangle in

TABLE II
VALUES FOR THE SEPARATION FACTOR OF BORON ISOTOPES OBTAINED BY EQUILIBRIUM AND BREAKTHROUGH EXPERI-
MENTS AT 25°C AND THE VALUES FOR THE MOLE FRACTION OF B(OH)_3 IN THE RESIN PHASE ESTIMATED BY EQN. 20

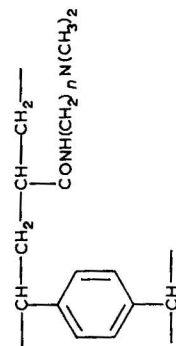
Parameter	Resin*			Diaion PA-312:		
	Diaion WA-21	Diaion WA-10:	Diaion PA-312:			
Boron concentration in the external solution (mole/l)	0.0107	0.102	0.518	0.0101	0.0991	0.501
Boron concentration in the resin phase (mole/l)	0.09	2.0	11	0.05	1.1	8.6
S^{10} ; equilibrium expt.	1.015	1.013	1.011	1.016	1.012	1.007
S^{10} ; breakthrough expt.	1.019	1.014	1.012	1.016	1.014	1.010
$\bar{x}_{\text{B(OH)}_3}$	0.10	0.31	0.42	0.16	0.31	0.52
pH in the resin phase	8	8	7	9	8	7
				10	8	7

* Structures:

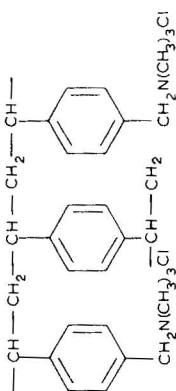
Diaion WA-21:



Diaion WA-10:



Diaion PA-312:



B(OH)_3 to a tetrahedron in B(OH)_4^- . This potentiality of isotopic difference in boric acid solution can be realized by the use of an anion-exchange resin, which prefers to pick up the anion B(OH)_4^- .

Involving only two chemical species, B(OH)_3 and B(OH)_4^- , a simple expression for the isotope separation factor can be derived from the general eqn. 14:

$$\ln S_{11}^{10} = \ln f_{\text{B(OH)}_3} - \ln [\bar{x}_{\text{B(OH)}_3} \bar{f}_{\text{B(OH)}_3} + (1 - \bar{x}_{\text{B(OH)}_3}) \bar{f}_{\text{B(OH)}_4}] \quad (19)$$

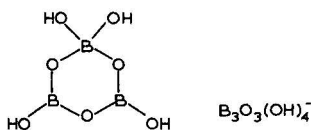
As the difference of the reduced partition function ratios of same chemical species between the external solution and the resin phases is very small, we can make the approximations $\bar{f}_{\text{B(OH)}_3} = f_{\text{B(OH)}_3}$ and $\bar{f}_{\text{B(OH)}_4} = f_{\text{B(OH)}_4}$ and, using the value 1.019 for $f_{\text{B(OH)}_3}/f_{\text{B(OH)}_4}$, eqn. 19 is reduced to

$$S_{11}^{10} = [\bar{x}_{\text{B(OH)}_3} + 1.019^{-1} (1 - \bar{x}_{\text{B(OH)}_3})]^{-1} \quad (20)$$

BORON ISOTOPE SEPARATION WITH USE OF ANION-EXCHANGE RESIN

The experimental results obtained by equilibrium and breakthrough experiments are summarized in Table II. The values for the mole fraction of B(OH)_3 in the resin phase, $\bar{x}_{\text{B(OH)}_3}$, are calculated by means of eqn. 20 and are shown in Table II. The separation factor of boron isotopes is not much influenced by the kind of anion-exchange resin used, but is very much influenced by the boric acid concentration in the external solution: the higher the concentration the lower is the separation factor or, in other words, the higher the value of $\bar{x}_{\text{B(OH)}_3}$ the lower is the separation factor.

The presence of the neutral species, B(OH)_3 , in the anion-exchange resin phase may be caused by the formation of polyborate anions such as



As observed in the above structure, the polyborate anions contain not only the B(OH)_4^- structure but also the B(OH)_3 structure and it is reported that the amount of polyborate is large at high concentrations of boric acid especially at pH 7–8 (ref. 15). In Table II, the high values for $\bar{x}_{\text{B(OH)}_3}$ can be seen in the resin phases of high boron concentrations and of pH 7–8.

As mentioned above, the separation factor is not much influenced by the kind of the anion-exchange resin, but if we use a weakly basic anion-exchange resin such as Diaion WA-21, the boric acid absorbed on the resin column can easily be eluted with water. This may be a very useful attribute in the practical separation of isotopes. If we used a strongly basic anion-exchange resin column, we must start by preparing the resin column in the free base form, then prepare a boric acid band, elute the band

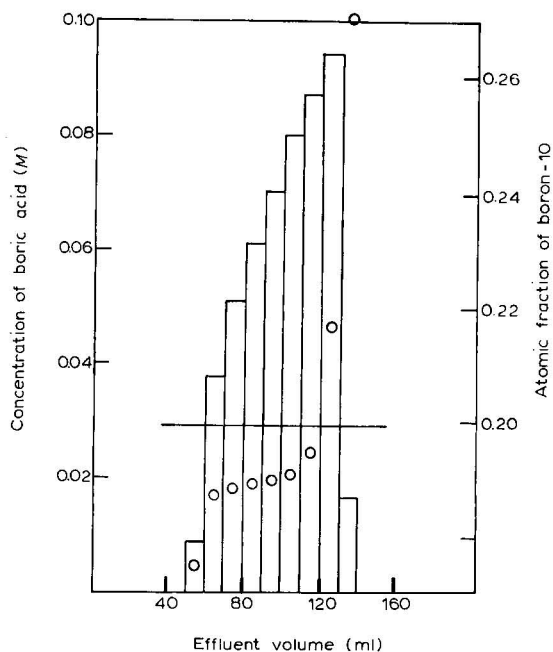


Fig. 1. Results obtained using a column of Diaion WA-21, 100–200 mesh, with a load of 10 ml of 0.501 *M* boric acid at a temperature of 40°C, flow-rate 10 ml/h·cm² and water as eluting agent. □, Concentration of boric acid; ○, atomic fraction of boron-10; —, atomic fraction of boron-10 in natural sample.

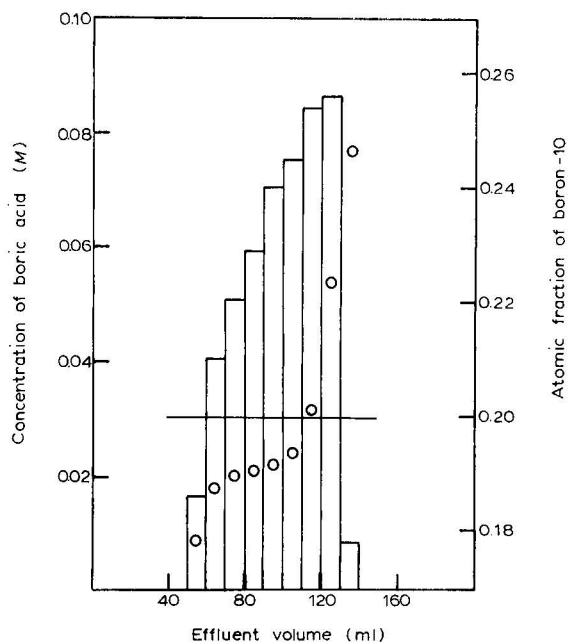


Fig. 2. Results obtained using a column of Diaion WA-21, 100–200 mesh, with a load of 10 ml of 0.497 *M* boric acid at a temperature of 40°C, flow-rate 19 ml/h·cm² and water as eluting agent. □, Concentration of boric acid; ○, atomic fraction of boron-10; —, atomic fraction of boron-10 in natural sample.

with a certain acid and regenerate it so as to prepare the column in the free base form. On the other hand, if we use a weakly basic anion-exchange resin column, the cycle is much simpler: We start from the free base form, prepare a boric acid band and elute the band with water, so that simultaneously the column is converted into the free base form.

Some results obtained on a small column of diameter 1 cm and about 50 cm long are shown in Figs. 1 and 2. The separation is so good and the procedure is so simple that it can be concluded that the system is particularly useful for the separation of boron isotopes.

REFERENCES

- 1 T. I. Taylor and H. C. Urey, *J. Chem. Phys.*, 5 (1937) 597.
- 2 E. Glueckauf, in H. London (Editor), *Separation of Isotopes*, Newnes, London, 1962, p. 209.
- 3 J. E. Powell, F. H. Spedding and H. J. Svec, *J. Amer. Chem. Soc.*, 77 (1955) 6125.
- 4 H. P. Gregor, *J. Amer. Chem. Soc.*, 70 (1948) 1293.
- 5 H. P. Gregor, *J. Amer. Chem. Soc.*, 73 (1951) 642.
- 6 H. P. Gregor and M. Frederick, *Ann. N.Y. Acad. Sci.*, 57 (1953) 87.
- 7 E. Glueckauf, *Proc. Roy. Soc., Ser., A* 214 (1952) 207.
- 8 H. Kakihana, *Bull. Tokyo Inst. Technol., Ser. B*, (1960) 1.
- 9 H. Kakihana and M. Hosoe, *Chemistry*, 28 (1973) 850, (in Japanese).
- 10 H. Kakihana and M. Aida, *Bull. Tokyo Inst. Technol.*, 116 (1973) 39.
- 11 H. C. Urey and D. Rittenberg, *J. Chem. Phys.*, 1 (1933) 137.
- 12 J. Bigeleisen and M. G. Mayer, *J. Chem. Phys.*, 15 (1947) 261.
- 13 J. Bigeleisen, *Proceedings of the International Symposium on Isotope Separation*, North-Holland, Amsterdam, 1958, p. 121.
- 14 H. Kakihana, Y. Yato and T. Amaya, *J. Nucl. Sci. Technol.*, 5 (1968) 36.
- 15 N. Ingri, *Sv. Kem. Tidskr.*, 75 (1963) 4.

CHROM. 7732

LIQUID CHROMATOGRAPHY OF ORGANIC COMPOUNDS ON ION-EXCHANGE RESINS

HAROLD F. WALTON

University of Colorado, Boulder, Colo. 80302 (U.S.A.)

SUMMARY

The use of ion-exchange resins for the chromatography of non-ionized organic compounds is reviewed, with special reference to work in the author's laboratory. Current work on ligand-exchange chromatography of drugs, alkaloids and amino sugars is reported, and an approach called "matrix-affinity chromatography" is described.

INTRODUCTION

In the early days of ion-exchange chromatography, around 1950, it occurred to Samuelson that organic compounds could be made to bind to ion-exchange resins through combination with inorganic ions. Thus, anion-exchange resins carrying bisulfite ions would bind aldehydes through the formation of aldehyde-bisulfite ions¹. Resins carrying borate ions would bind polyhydric alcohols and sugars as their cyclic, ionic borate complexes. Khym and Zill² separated sucrose, fructose and glucose by eluting them in this order from a short column of anion-exchange resin in the borate form, using potassium borate solution as the eluent.

Soon it was found that borate ions were not necessary; glucose would bind to a strong-base anion-exchange resin even in the absence of borate. In fact, it would bind to a cation-exchange resin too. The binding was greatly strengthened by adding alcohol. Rückert and Samuelson³ studied this effect and related it to the fact that, placed in water-alcohol mixtures, ion-exchange resins absorb water in preference to alcohol. The sugars are displaced out of the alcohol-rich liquid phase and into the water-rich resin phase. Elaborate, highly efficient techniques were developed for the chromatographic separation of mono-, di- and polysaccharides, the preferred stationary phase being an anion-exchange resin in the sulfate form⁴.

Simultaneously with the early researches of Samuelson and co-workers, Sargent and Rieman⁵ were developing "salting-out chromatography", in which salts like ammonium sulfate, added to water, pushed polar organic compounds out of the aqueous phase into the resin phase, which, again, was relatively water-rich owing to salt exclusion by the Donnan equilibrium. Then Sherma and Rieman⁶ pursued "solubilization chromatography", in which the ion-exchange resin, due to its own hydrocarbon-like character, absorbed and "dissolved" less polar organic compounds like

ethers, ketones and even aromatic hydrocarbons. These were eluted from the column by aqueous alcohol. The more alcohol was added to the solvent, the faster was the elution, for these solutes were more soluble in alcohol than in water.

Today, Rieman's principle of "solubilization chromatography" is widely used, and some current applications of this process will be described in this paper.

Another landmark in the application of ion-exchange resins to the separation of organic compounds was the discovery by Helfferich⁷ of "ligand-exchange chromatography". Helfferich used a column of cation-exchange resin loaded with ions of copper or nickel, ions that formed complexes with ammonia and amines. Such a column was used to absorb the compound 1,3-diamino-2-propanol from a dilute solution. It was stripped from the column in concentrated form by passing a concentrated ammonia solution. The ligand-exchange principle was applied to chemical analysis by Tsuji⁸, Shimomura *et al.*⁹ and others^{10,11}.

This paper will review recent progress in the author's laboratory, primarily in ligand-exchange chromatography, but also in the use of metal-free cation-exchange resin columns for the chromatography of non-ionic organic compounds.

LIGAND-EXCHANGE CHROMATOGRAPHY

In ligand-exchange chromatography a column of cation-exchange resin is used that carries ions of metals that form ammonia complexes, such as Cu(II), Ni(II), Zn(II), and Ag(I). Compounds that contain basic nitrogen atoms are absorbed on the column through coordination with the metal ions. They are displaced by passing solutions of ammonia, and the order of elution reflects their binding to the metal-loaded resin. Solutions of ammonia in alcohol-water mixtures may be used if the solutes are poorly soluble in water.

Ideally, the metal ions remain attached to the resin and do not move. In practice, aqueous ammonia solutions contain ammonium ions, and these ammonium ions displace the metal from the resin to some extent. As long as the metal-ion concentration in the effluent is small, say 10^{-4} M or less, this "bleeding" of metal ions can be tolerated, but if the concentration is higher, it is necessary to add metal salt to the influent. This introduces another variable; metal ions draw the complexing organic ligands out of the resin and into the solution, decreasing the retention volume.

If the resin is of the strong-acid polystyrene sulfonate type, only nickel ions are held sufficiently strongly to be useful in this type of chromatography. Resins with functional carboxyl groups hold metal ions much more strongly, and nickel, copper, zinc and cadmium ions can readily be used. The ligand-binding selectivity order varies with the metal ion, but in general, copper ions are the ions of choice because they form the most stable complexes (according to the Irving-Williams sequence).

Chelating resins hold metal ions very strongly, but they have the drawback that they use a large fraction of the ligand-binding capacity of the metals, so that the capacity available for chromatography is small. For most of the work described below we found carboxylic resins to be the most satisfactory, not only because they held the metal ions tightly, but also because commercial carboxylic resins are aliphatic-type, acrylate polymers, rather than styrene polymers, and do not absorb aromatic solutes so strongly that they cannot be eluted. Interactions between the solute molecules and the resin polymer backbone are very important, as will be seen.

Acrylate resins do have the disadvantage, however, that they are soft and cannot be used under high-pressure gradients.

Selectivity orders

Ligand-exchange selectivities of amines follow the rule that the binding is stronger, the less obstructed is the basic nitrogen atom. Primary amines are bound much more strongly than secondary, secondary amines are bound more strongly than tertiary. Substituents on nearby carbon atoms affect the binding, as is seen by comparing *n*-butylamine, isobutylamine, *sec*.-butylamine and *tert*.-butylamine¹⁰; distribution ratios between Dowex-50-Ni and 1.4 *M* ammonia are 21, 13, 11, and 9, respectively. Unsymmetrical dimethylhydrazine, monomethylhydrazine and hydrazine are eluted in that order, with hydrazine much more strongly bound than the others⁹. Similar sequences are found with aziridines and with ethanolamines, where the elution order is N-dimethylethanolamine, triethanolamine, diethanolamine, monoethanolamine¹², with monoethanolamine bound much more strongly than the others. These elution orders bear little relation to the base strengths of the amines.

The effects of various factors on elution orders are nicely seen with phenethylamine and its derivatives, which include the amphetamine drugs¹³. Some typical data are shown in Table I. Unsubstituted phenethylamine is held much more strongly than the other compounds. A methyl group on the carbon next to the amine nitrogen (in amphetamine) weakens the binding considerably, and a methyl group on the amine nitrogen itself (in metamphetamine) weakens it still more. The effect of the β -hydroxyl in ephedrine and norephedrine is to strengthen the binding, presumably through the formation of a chelate ring with $-\text{OH}$, $-\text{NH}-$ and the metal ion.

Table II shows more data. Tryptamine, with two basic nitrogens, is bound much more strongly than phenethylamine, while mescaline is bound much less strongly, probably because the three methoxy groups make the substance more soluble in the mobile phase.

TABLE I

ELUTION VOLUMES OF PHENETHYLAMINE DERIVATIVES

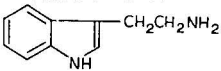
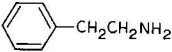
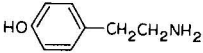
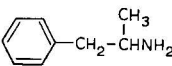
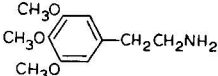
Bio-Rex 70 (methacrylate resin)-Cu, 0.10 *M* NH_3 , 33% ethanol.

Compound	Molecular formula	Relative elution volume
Phenethylamine	$\text{C}_6\text{H}_5\text{--CH}_2\text{--CH}_2\text{--NH}_2$	3.9
Norephedrine	$\begin{array}{c} \text{OH} \quad \text{CH}_3 \\ \quad \\ \text{C}_6\text{H}_5\text{--CH--CH--NH}_2 \\ \\ \text{CH}_3 \end{array}$	2.7
Amphetamine	$\begin{array}{c} \text{OH} \quad \text{CH}_3 \\ \quad \\ \text{C}_6\text{H}_5\text{--CH}_2\text{--CH--NH}_2 \end{array}$	2.15
Ephedrine	$\begin{array}{c} \text{CH}_3 \\ \\ \text{C}_6\text{H}_5\text{--CH--CH--NH--CH}_3 \\ \\ \text{CH}_3 \end{array}$	2.1
Metamphetamine	$\text{C}_6\text{H}_5\text{--CH}_2\text{--CH--NH--CH}_3$	1.75

TABLE II

ELUTION VOLUMES OF PHENETHYLAMINE DERIVATIVES

Bio-Rex 70-Ni (carboxylic), 33% ethanol, 0.1 M NH₃.

Compound	Structural formula	Relative elution volume
Tryptamine		5.2
Phenethylamine		2.8
Tyramine		2.75
Amphetamine		1.55
Mescaline		1.45

Alkaloids

It is logical to apply ligand-exchange chromatography to the alkaloids, but one difficulty is immediately evident. The alkaloids are all tertiary amines, which means they will be weakly bound. When we began work on alkaloids we used the commercial carboxylic resin, Bio-Rex 70 (Bio-Rad Labs., Richmond, Calif., U.S.A.), in its copper and nickel forms and found that the retention of alkaloids was slight, and separations were inefficient. Then we tested an experimental resin, Bio-Rex PC-20, in the copper form and found that it gave much better retention. We ordered more of this resin and the next batch we received was ineffective!

Seeking resins that would bind alkaloids, we took Poragel-PT, a highly polar resin made for liquid chromatography by Waters Ass. (Milford, Mass., U.S.A.), which carries ethylene glycol ester groups on a polystyrene base. We hydrolyzed this resin according to the suggestion of Freeman and Madamba¹⁴ and produced a resin with functional carboxyl groups. This was converted to its copper form, and was found to be effective in binding alkaloids.

We measured the ammonia uptake of the copper-loaded resins, and found that the bound ammonia to total copper ratio in the resin, for a given ammonia concentration in the solution, was about 50% higher in the resins that showed good alkaloid retention than it was in the resins that showed poor alkaloid retention. Evidently the environment of the metal ion in the carboxylic resins is very dependent on subtle details of the polymer structure.

Fig. 1 shows a chromatogram of a mixture of three alkaloids, morphine, codeine and strychnine, on hydrolyzed Poragel-PT-Cu. The alkaloids were introduced

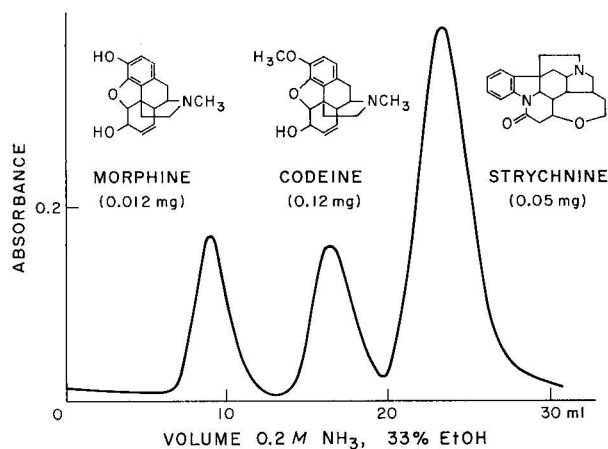


Fig. 1. Separation of alkaloids on Poragel-PT-Cu at 50°.

as their sulfate salts, and were converted to the free bases in the flowing stream of ammonia as soon as they entered the column; sulfate ions appeared in the effluent at one void volume. The solvent was 33 % ethanol, not water, because the alkaloid bases are almost insoluble in water.

The separation of these alkaloids is satisfactory, but the bands are undesirably broad, even though the column was run at 50° to raise diffusion rates. Table III lists elution volumes found with a number of alkaloids, and it is clear that, potentially, ligand-exchange chromatography could be an effective means of analysis of alkaloid mixtures if we could get narrower bands and better resolution. This work is still in progress, and details will be published later*. One difficulty must, however, be pointed

TABLE III

ELUTION SEQUENCE OF ALKALOIDS ON Cu- OR Ni-LOADED, HYDROLYZED PORAGEL-PT

Multiples of bulk column volume, 0.06 M NH₃, 33 % ethanol.

Compound	Relative elution volume
Morphine	1.0
Ethyl morphine	2.2
Codeine (methyl morphine)	2.3
Papaverine	3.8
Strychnine	4.0
Cocaine	4.5
Atropine	5.0
Narcotine	6.8
Nicotine	8.0
Methadone	8.0

* A preliminary report was presented at the American Chemical Society meeting in Chicago, August 1973.

out. Ligand-exchange chromatography is done in strongly alkaline solution. Some alkaloids hydrolyze rapidly under these conditions, while others are oxidized. Oxidation can be prevented, but hydrolysis cannot. Cocaine, for example, which has two ester groups in its molecule, hydrolyzes to a small but noticeable extent on the column, even when the solution is prepared just before injection. In 44 h, a solution of cocaine in 0.1 *M* ammonia hydrolyzes completely to ammonium benzoate. The same problem arises with heroin, which hydrolyzes to morphine.

Amino sugars

The aminohexoses, glucosamine, galactosamine and mannosamine, are strongly held on metal-loaded resins in spite of their "obstructed" amino groups. It is presumed that chelate rings are formed through the hydroxyl groups of the sugars. The sugars themselves—glucose, galactose and mannose—are not held at all, and elute at one void volume. Ligand exchange, therefore, separates amino sugars very effectively from other sugars.

We were surprised to find how great was the effect of the stereochemistry. Table IV shows data for a nickel-loaded resin. For copper-loaded resins the order of elution was the same, but there was more difference between mannosamine and galactosamine, less between galactosamine and glucosamine.

TABLE IV
ELUTION VOLUMES OF AMINO SUGARS

Bio-Rex 70-Ni (carboxylic), 0.68 *M* NH₃.

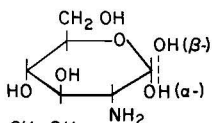
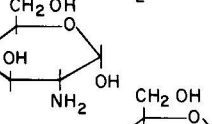
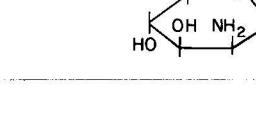
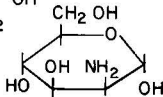
Compound	Structure	Relative elution volume
Glucose (at void volume)		1.00
Glucosamine		3.05
Galactosamine		4.30
Mannosamine		5.10

Fig. 2 shows a typical elution curve. The resin was of the acrylic type, copper-loaded Bio-Rex 70, size range 37–44 μ . The theoretical-plate height was about 0.25 mm, which is very good. Elution required 50 min, which is rather slow, but, as was noted above, resins of this type are soft and will not stand high-pressure gradients.

The ordinate in Fig. 2 is UV absorbance. Amino sugars do not absorb in the UV; however, they remove copper from the resin, and the copper complexes absorb at 254 nm. They absorb more strongly than the copper-ammonia ions themselves, and this method of detection is very sensitive. Moreover, it is free from the artifacts

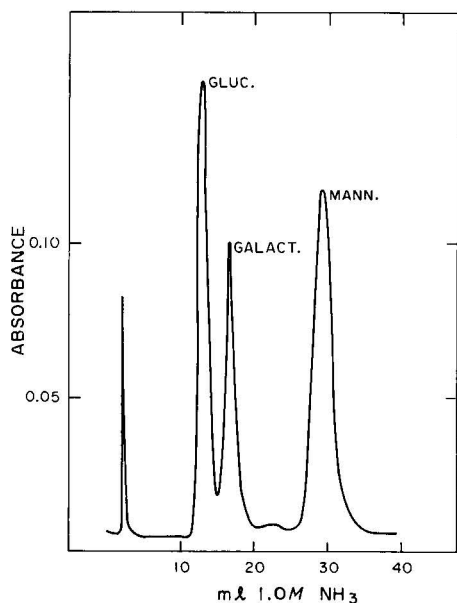


Fig. 2. Separation of amino sugars on Bio-Rex 70-Cu, 37–44 μ . Column, 6 mm \times 20 cm. Flow-rate, 0.7 ml/min; influent was 1×10^{-4} M in CuSO_4 ; absorbance at 254 nm. Weight of each sugar introduced was 50 μg as the hydrochloride.

that appear in refractive index curves. The sharp peak at one void volume is due to the conversion of the amino sugar chlorides to ammonium chloride, which displaces a little copper from the resin. To maintain the copper loading of the resin we added 10^{-4} M copper sulfate to the ammonia influent. Under these circumstances the peak area was proportional to the amount of amino sugar injected.

Amino sugars often occur together with amino acids, and we therefore studied the elution of several pure amino acids, as well as a standard mixture of twenty amino acids supplied by the Bio-Rad Labs. Most amino acids eluted between one and two void volumes, with 1 M ammonia as the eluent. Those that were more strongly retained were the basic amino acids lysine and histidine. In addition, tryptophan was retained strongly by hydrolyzed Poragel-PT-Cu, which has a polystyrene matrix, but not by Bio-Rex 70, which is an acrylic polymer. Fig. 3 shows an elution curve with Bio-Rex 70. With this resin lysine elutes just after glucosamine, but the two peaks can be distinguished, and moreover the intensity of the lysine peak is much less than the peak given by an equal weight of glucosamine. With hydrolyzed Poragel-PT at 60°, lysine elutes just after one void volume, while tryptophan elutes midway between galactosamine and mannosamine. It is thus possible, by careful work and using the appropriate resin, to distinguish amino sugars clearly from accompanying amino acids.

For a "real" analysis we took crab shells and hydrolyzed them with 6 M hydrochloric acid, and injected the hydrolyzate after evaporating most of the excess acid. We found a large peak at the void volume, two smaller peaks between one and two void volumes, then a well-isolated peak for glucosamine, followed by the histidine peak. The resin was Bio-Rex 70.

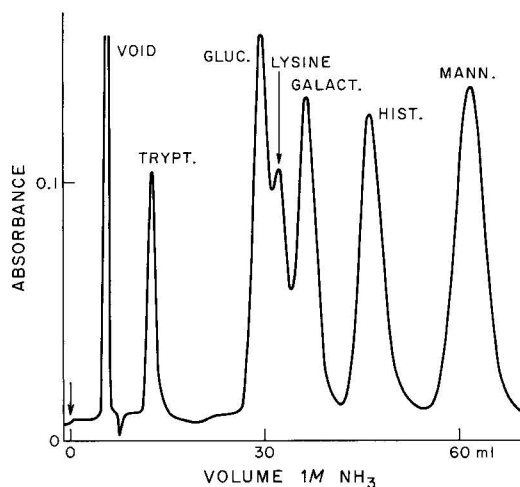


Fig. 3. Separation of amino sugars and amino acids on Bio-Rex 70-Cu, 37–44 μ . Column, same as in Fig. 2; flow-rate, 0.3 ml/min. Quantities introduced (μ g): tryptophan, 6; glucosamine \cdot HCl, 40; lysine \cdot HCl, 160; galactosamine \cdot HCl, 60; histidine, 80; mannosamine \cdot HCl, 50. Absorbance measured at 254 nm; influent 10^{-4} M in CuSO_4 .

This is a preliminary report. The work is in the process of development and will be the subject of a later publication.

MATRIX-AFFINITY CHROMATOGRAPHY: ANALGESIC DRUGS AND XANTHINES

Working with aromatic solutes in ion-exchange chromatography one is constantly aware that these solutes are strongly held by resins having a polystyrene matrix. This affinity is superimposed on other interactions, such as metal–ligand interactions. It is, for example, impossible to perform ligand-exchange chromatography of amphetamines on resins like Dowex-50. Broad bands result, with considerable tailing.

It was logical to exploit the matrix–solute affinity as a basis for chromatography in its own right. We therefore used cation-exchange resins in their ammonium and sodium forms, as well as anion-exchange resins, with water–alcohol mixtures, electrolyte-free, as eluents, and we obtained good chromatographic separations of non-ionized but polar aromatic compounds like ethyl benzoate and the drugs phenacetin (*p*-ethoxyacetanilide) and caffeine. The question then arises: Why use an ion-exchange resin at all? Why not use a styrene–divinylbenzene copolymer with no ionic groups? The answer is that the ions become solvated and make the resins permeable. One might achieve permeability by using a macroporous non-ionic resin, and such resins have, indeed, been used to absorb aromatic solutes¹⁵. For chromatography they have the drawback that the binding zones are not homogeneous. We have found that gel-type resins of small and uniform particle size, and particularly resins of low crosslinking, act as highly uniform, highly permeable stationary phases and can give theoretical-plate heights of 0.1 mm and less.

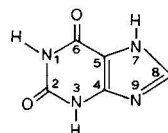
Our work in this area has been published^{16,17}, and what follows here is a summary and commentary.

Effects of counter-ions, crosslinking, solvent and pH

Working with phenacetin and caffeine as solutes and cation-exchange resins carrying as counter-ions Li, Na, K, and NH_4 , we found that the counter-ion had little effect on the elution volumes but a marked effect on the band width. Ammonium ions gave the sharpest bands, sodium ions the broadest. Later, however, when we learned how to get really narrow bands, we decided that the differences in band width were not significant. The difference between ammonium and sodium ions became important when the solute was a weak acid. The ionization of very weak acids within the resin, which is quite appreciable in a sodium-form resin, is suppressed in the more acidic ammonium-form resin, with a corresponding increase in the elution volumes: see Table V. This effect is related to the Donnan exclusion of co-ions, in this case the anions of the weak acids. It is important for acids having pK_a values around 7–8. Salicylamide, for instance, with $pK_a = 8.4$, had an elution volume (corrected) on an ammonium-form resin which was more than double that on the corresponding sodium-form resin. Acids that are much stronger, like acetylsalicylic acid, are excluded from the cation-exchange resin completely.

TABLE V

ACIDITY AND ELUTION VOLUMES OF XANTHINE DERIVATIVES:



4% crosslinking, 25% ethanol.

Compound	pK_a	k'		Ratio
		Na resin	NH_4 resin	
Uric acid (8-OH)	5.4	0	0.1	—
Xanthine	7.5	0.15	0.56	3.7
Theophylline (1,3- CH_3)	8.8	0.35	1.33	3.8
Hypoxanthine	8.9	0.75	2.25	3.0
Theobromine (3,7- CH_3)	10.0	1.42	1.60	1.13
Caffeine (1,3,7- CH_3)	14.0	1.9	1.8	0.95

Crosslinking affects the elution volumes of different solutes in different ways, and part of this effect may be due to Donnan equilibrium. Salicylamide is retained much more strongly by 8% than by 4% crosslinked resin (both in the ammonium form), and the reason may be that the higher ammonium ion concentration in the 8% resin represses the ionization more.

Singhal¹⁸ and Singhal and Cohn¹⁹, working with nucleic acid derivatives on ion-exchange columns, have found that very weak acids may be eluted from a cation-exchange resin at volumes greater than the void volume but smaller than the total volume of water in the column, as measured by injecting a trace of radioactive tritiated water. They call this effect "ion-exclusion chromatography". Elution volumes can, of course, be manipulated by changing the pH of the eluting buffer. We believe we have an example of ion-exclusion chromatography in our analysis of coffee, noted below.

It remains to mention the effect of solvent composition, that is, the ratio of alcohol to water. The more alcohol, the lower the elution volumes, and the effect is considerable. It would be easy to perform solvent-gradient elution if this were desired.

Applications

Refs. 16 and 17 describe applications of "matrix-affinity chromatography", as we may call it, to mixtures of analgesic drugs, xanthines, and coffee. Primarily we used electrolyte-free aqueous alcohol as the eluent, and we showed that we could change elution orders by changing from the ammonium form of the resin to the sodium form. For some applications the ammonium form was better, for others the sodium form. Best results were obtained with a sulfonated polystyrene resin of 4% crosslinking and a particle diameter of 20–30 μ , supplied by Bio-Rad Labs.

Electrolyte-free eluents have the advantage that it is easy to remove the solvent for preparative purposes or for mass spectrographic examination. One could, if one wished, use the resin bed as an internal buffer of any desired pH by equilibrating it beforehand with the proper solution. However, the resin would have to be regenerated, or reconditioned, at frequent intervals during use if one passed acid solutes that exchanged ions with the resin. A better practice, for most purposes, is to use a buffered eluent. We used a formic acid–ammonium formate buffer in 25% ethanol for the analysis of the UV-absorbing constituents of coffee, with excellent results. Adding electrolyte to the eluent causes the resin to shrink and become more rigid, an important advantage with resins of low crosslinking.

Using a glass column of 0.6×14 cm and a formate buffer of pH 3.65 at 60° we found six distinct peaks, three of which—caffeine, caffeic acid and trigonellin—were identified. With a longer column we could do better. We believe that this technique, which is really the same as Rieman's "solubilization chromatography" done with modern equipment, is a very powerful one for the examination of water-soluble and alcohol-soluble constituents of natural products.

ACKNOWLEDGEMENTS

This work was supported by the National Science Foundation, currently under Grant No. GP-37779X and a travel grant, GP-43414. I am very grateful to the Foundation for its support, and also to James Navratil, Eduardo Murgia and Jerry Harder, students at the University of Colorado, some of whose work is reported here.

REFERENCES

- 1 G. Gabrielson and O. Samuelson, *Sv. Kem. Tidskr.*, 62 (1950) 214; 64 (1952) 150.
- 2 J. X. Khym and L. P. Zill, *J. Amer. Chem. Soc.*, 73 (1951) 2399.
- 3 H. Rückert and O. Samuelson, *Acta Chem. Scand.*, 11 (1957) 303, 315.
- 4 L. I. Larsson and O. Samuelson, *Acta Chem. Scand.*, 19 (1965) 1357.
- 5 R. Sargent and W. Rieman, *J. Phys. Chem.*, 61 (1957) 354.
- 6 J. Sherma and W. Rieman, *Anal. Chim. Acta*, 20 (1959) 357.
- 7 F. Helfferich, *Nature (London)*, 189 (1961) 1001.
- 8 A. Tsuji, *Nippon Kagaku Zasshi (J. Chem. Soc. Jap., Pure Chem. Sect.)*, 81 (1960) 847, 1090.
- 9 K. Shimomura, L. Dickson and H. F. Walton, *Anal. Chim. Acta*, 37 (1967) 102.
- 10 H. F. Walton, in J. A. Marinsky and Y. Marcus (Editors), *Ion Exchange and Solvent Extraction*, Vol. 4, Marcel Dekker, New York, 1973, Ch. 4.

- 11 J. C. Welford, J. A. Dean and G. Goldstein, *J. Chromatogr.*, 62 (1971) 148.
- 12 K. Shimomura, Tong-Jung Hsu and H. F. Walton, *Anal. Chem.*, 45 (1973) 501.
- 13 C. M. de Hernandez and H. F. Walton, *Anal. Chem.*, 44 (1972) 890.
- 14 D. H. Freeman and A. Madamba, private communication.
- 15 A. K. Burnham, G. V. Calder, J. S. Fritz, G. A. Junk, H. J. Svec and R. Willis, *Anal. Chem.*, 44 (1972) 139.
- 16 P. Larson, E. Murgia, Tong-Jung Hsu and H. F. Walton, *Anal. Chem.*, 45 (1973) 2306.
- 17 E. Murgia, P. Richards and H. F. Walton, *J. Chromatogr.*, 87 (1973) 523.
- 18 R. P. Singhal, *Arch. Biochem. Biophys.*, 152 (1972) 800.
- 19 R. P. Singhal and W. E. Cohn, *Biochemistry*, 12 (1973) 1532.

CHROM. 7764

THE USE OF LIQUID ION EXCHANGERS IN EXTRACTION CHROMATOGRAPHY

GERHARD WERNER

Department of Chemistry, Karl-Marx-Universität, Leipzig (G.D.R.)

SUMMARY

A new development in separation science is the application of liquid ion exchangers. For the separation of metal ions, additional complexing in the aqueous phase can be favourable in some instances. The best method for increasing the efficiency of a separation is to impregnate an inert support with the exchanger.

A number of analytical problems can be solved, and reversed-phase chromatography is useful especially in the separation of rare earth elements. From the chromatographic data, conclusions on the behaviour of ion-exchange resins, extractants and reactions in the aqueous phase can be drawn.

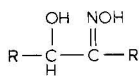
In the development of ion-exchange technology, new fields of application have been discovered that require ion-exchange materials which differ from conventional materials not only in their functional groups but also in physical form. The use of water-insoluble acidic and basic reagents as liquid ion exchangers was first proposed by Smith and Page¹ in a paper entitled "The acid-binding properties of long-chain aliphatic amines". Since then, increasing interest has been shown in the use of high-molecular-weight bases and acids as extractants.

The operation of liquid ion exchangers involves the selective transfer of electrolytes between two immiscible phases. In this process, the electrolytes undergo reactions that influence this distribution. In the aqueous phase, hydration (ion-dipole interaction), complex formation (covalent interaction) and ion association (electrovalent interaction) occur. In the organic phase, in addition to solvation, complex formation and ion association also occur. In general, ion associates are considered to be aggregates in which the different ions are separated by solvent molecules, while ion pairs, in which the ions are not separated by solvent molecules, are often referred to as complexes, even if the charges are still located on their original sites².

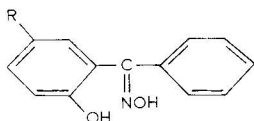
Of course, liquid cation exchangers effect extraction by exchanging protons for cations originally present in the aqueous phase and liquid anion exchangers effect extraction by exchanging their original anion with an anionic species in the aqueous phase. However, a number of additional effects must also be considered.

One of the most recent applications of liquid ion exchange is the recovery of

copper by the so called LIX reagents (LIX = liquid ion exchanger). These are hydroxyoximes:



LIX 63



LIX 64 N

which extract copper very selectively, and it is reported³ that the recovery of copper from low-grade ores is possible. This is not, of course, a pure ion-exchange reaction. The high selectivity is a consequence of complex formation.

As a first example of reversed-phase extraction chromatography, the application of LIX 64 will be mentioned. Cerrai and Ghersini⁴ treated paper or cellulose powder with LIX 64 and were able to separate copper from cobalt, nickel, manganese, chromium, molybdenum, tungsten, vanadium and iron (after aqueous phase complexing with fluoride).

In his Plenary Lecture, Prof. Laskorin⁵ pointed out the advantages and disadvantages of liquid ion exchangers. For analytical chemists, separation problems in which elements with very similar chemical properties are to be separated are mainly of interest. In some instances, the high selectivity of liquid ion exchangers is sufficient. Here the amine extraction of coloured anionic species (extraction photometry) can be mentioned. But in other instances, one requires better separation factors, and one possibility for obtaining them is by aqueous phase complexing. Here use is made from the different stabilities of coordination compounds in the aqueous phase. However, only in a few instances is a really good separation possible.

Another possibility for improving the separation is to combine liquid ion exchange with a chromatographic process, permitting an elementary separation step to be repeated many times. An inert support is treated with the liquid ion exchanger and a thin-layer or paper chromatographic or column operation is carried out. Because the organic phase is the stationary phase, the process is called reversed-phase extraction chromatography. An excellent review of the theory and applications of this technique was given by Cerrai and Ghersini⁶, and at this conference the most active workers in this field, Ghersini⁷, Testa and Delle Site⁸, and Brinkman *et al.*⁹, reported their latest results.

In liquid ion exchange, the ratio of the concentrations of a given element in the two phases at equilibrium is called the distribution coefficient. In the thin-layer or paper chromatographic application of reversed-phase chromatography, a relationship with the R_F value exists:

$$D = \frac{A_L}{A_S} \cdot \left(\frac{1}{R_F} - 1 \right)$$

$$R_M = \log \left(\frac{1}{R_F} - 1 \right)$$

where D is the distribution coefficient and A_L and A_S are the cross-sectional areas of the liquid (aqueous) and stationary (organic) phases, respectively.

In Table I, a list of liquid anion exchangers is given, based on primary, sec-

TABLE I
LIQUID ANION EXCHANGERS

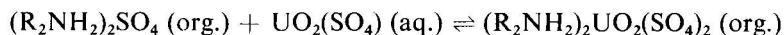
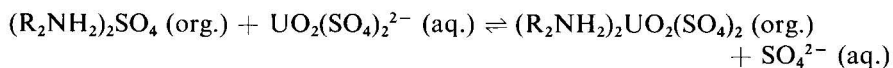
Type	Composition	Name/abbreviation
Primary amine	Trialkylmethylamine	Primene JM-T
Secondary amine	N-Dodecenytrialkylmethylamine	Amberlite LA-1
	N-Lauryltrialkylmethylamine	Amberlite LA-2
Tertiary amine	Tri- <i>n</i> -octylamine	TnOA
	Triisooctylamine	TiOA
	Tri- <i>n</i> -octylamine + tri- <i>n</i> -decylamine	Alamine 336
Quaternary ammonium salt	Methyltri- <i>n</i> -(octyl + decyl)ammonium chloride	Aliquat 336

ondary, tertiary and quaternary amines. In the following discussion, the different types of amines are not considered, but rather the different types of aqueous systems involved.

As an example of hydrochloric acid systems, the results of Neef and Grosse-Ruyken¹⁰ who separated trace concentrations of manganese, iron, cobalt, copper, nickel, zinc and cadmium, can be mentioned. Such a separation is possible only by use of a chromatographic procedure. Using TnOA on silica gel and by a gradient elution column technique, a complete separation of all these elements was possible, when the elution conditions were determined from liquid ion-exchange experiments.

The nitric acid system is often used in the separation of rare earths. In liquid ion exchange with TOA, the distribution coefficients of the rare earth elements decrease with atomic number¹¹. Hence it should be possible to increase the separation factors by aqueous phase complexing, because of the better extraction of the lanthanum which forms the less stable complexes with EDTA. However, little success was achieved¹¹. On the other hand, the R_F differences obtained in reversed-phase chromatography by Testa¹² using the same system are large enough for some separations to be obtained.

In liquid anion exchange, it is not clear whether real anion exchange or adduct formation occurs. In an investigation by Coleman and McDowell¹³, the amine extraction of uranium from acidic sulphate solutions was examined by interfacial tension measurements and by studying the transfer of ³⁵S-labelled sulphate between the two phases. In the system in question, in the aqueous phase the species UO_2SO_4 and $\text{UO}_2(\text{SO}_4)_2^{2-}$ exist and so two reactions are possible:

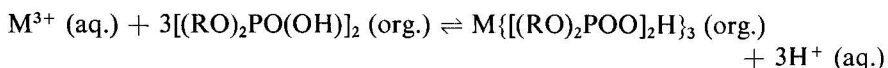


The difference is that if an anion is exchanged, a sulphate ion from the organic phase is transferred to the aqueous phase, which does not occur in neutral uranyl sulphate transfer. It was found that uranyl amine extraction from sulphate solutions proceeds by both anion exchange and neutral transfer, the proportion shifting according to the proportion of anionic uranium present, probably with some bias towards anion exchange.

TABLE II
LIQUID CATION EXCHANGERS

Composition	Abbreviation
Dinonylnaphthalenesulphonic acid	HDNS
Di-(2-ethylhexyl)orthophosphoric acid	HDEHP
Di- <i>n</i> -butylorthophosphoric acid	HDBP
2,6,8-Trimethylnonyl-4-phosphoric acid	H ₃ MiDP

In Table II, some liquid cation exchangers are listed. In addition to the compounds listed, carbonic acids must also be considered. Gindin *et al.*¹⁴ introduced liquid ion-exchange extraction, in which not only an exchange with hydrogen ions occurs but also an exchange between different metals. In the reversed-phase technique, phosphoric acids and dinonylnaphthalenesulphonic acid were mainly used as stationary phases. Extraction by dialkylphosphoric acids, for instance for a rare earth element, occurs according to the reaction



We obtained thin-layer chromatographic separations of the rare earth elements on silica gel impregnated with HDEHP^{15,16}, and it was shown that the anions in the aqueous phase have some influence on the exchange kinetics.

With organophosphorus liquid cation exchangers, in the rare earth series an increase in distribution coefficients usually occurs with increasing atomic number. In general, the separation of rare earths by liquid-liquid extraction is not very good, and we would therefore like to use the double effect of extraction and aqueous phase complexing. However, almost invariably the two effects tend to neutralize each other. The aqueous phase complexing favours the higher atomic numbers, and one will therefore have a partially nullifying effect rather than an enhancing effect. It is not very likely that there will be ligands in the aqueous phase that form less stable complexes with the heavier rare earth elements. Therefore, we looked for liquid cation exchangers that have the desired property. By analogy with sulphonic acid ion-exchange resins, dinonylnaphthalenesulphonic acid could be used¹⁷. According to Eisenman's theory, the reversal of selectivity between phosphoric or carbonic acid exchangers and sulphonic acid exchangers can be explained. In the first case, the gain in free energy

$$\Delta G_{1/2}^0 = \left(\frac{e^2}{r_A + r_2} - \frac{e^2}{r_A + r_1} \right) - (\Delta G_2 - \Delta G_1)$$

(where 1 and 2 are the exchanging ions, e is the charge, r_A and r_i are the radii of the fixed group and of the ions 1 and 2, and ΔG_1 and ΔG_2 are the standard free energies of hydration of the counter ions) is determined by the first terms in the equation because r_A is small. Hence the exchanger will prefer the ion with the smaller radius. In the case of sulphonic acids, where r_A is relatively large, the second terms are important. Because of the lanthanide contraction, the lighter elements are now pre-

ferred. Therefore, the addition of complex-forming agents to the aqueous phase is useful¹⁸. The effect is not very large but, in the separation of the alkaline earth elements, a separation factor for Sr/Ca of 120 was found¹⁹.

In the case of HDNS also, the reversed-phase technique in chromatography gives better results. With α -hydroxyisobutyric acid as eluent, a separation of the rare earth elements on paper impregnated with HDNS is possible²⁰. However, it must be mentioned that reproducible results can be achieved only if real elution chromatography is effected, *i.e.*, the paper strip must be in equilibrium with the eluent before the elements are spotted. The usual R_F and R_M values then cannot be obtained but, by introducing the velocity of the element and the velocity of the eluent, which can be determined, an analogous value is found. By this method, a complete separation of the rare earth ions was possible²¹. The chromatographic data can also be used to calculate the composition and stability of complexes between the metal ions and the eluent in the aqueous and stationary phases²². From the results, a very close analogy between reversed-phase liquid ion exchange and resinous ion exchange was obtained, and we obtained the same separation factors as on ion-exchange resins. Therefore, liquid ion exchangers fixed on an inert support can be used as models for ion-exchange resins and for solvent extraction, and are thus an invaluable analytical tool.

REFERENCES

- 1 E. L. Smith and J. E. Page, *Chem. Ind. (London)*, 61 (1948) 47.
- 2 H. M. Widmer in J. G. Gregory, B. Evans and P. C. Weston (Editors), *Proceedings of the International Solvent Extraction Conference, The Hague, 1971*, Vol. I, Society of Chemical Industry, London, 1971, p. 37.
- 3 K. L. Power in J. G. Gregory, B. Evans and P. C. Weston (Editors), *Proceedings of the International Solvent Extraction Conference, The Hague, 1971*, Vol. II, Society of Chemical Industry, London, 1971, p. 1409.
- 4 E. Cerrai and G. Ghersini, *Analyst (London)*, 94 (1969) 599.
- 5 B. N. Laskorin, *J. Chromatogr.*, in press.
- 6 E. Cerrai and G. Ghersini, *Advan. Chromatogr.*, 9 (1970) 3.
- 7 G. Ghersini, *J. Chromatogr.*, 102 (1974) 299.
- 8 C. Testa and A. Delle Site, *J. Chromatogr.*, 102 (1974) 293.
- 9 U. A. Th. Brinkman, G. de Vries, R. Jochemsen and G. J. de Jong, *J. Chromatogr.*, 102 (1974) 309.
- 10 B. Neef and H. Grosse-Ruyken, *J. Chromatogr.*, 79 (1973) 275.
- 11 G. Werner, R. Altendorf and H. Holzapfel, *J. Prakt. Chem.*, (4) 34 (1966) 201.
- 12 C. Testa, *Anal. Chem.*, 34 (1962) 1556.
- 13 C. F. Coleman and W. J. McDowell, in D. Dyrssen, J.-O. Liljenzin and J. Rydberg (Editors), *Solvent Extraction Chemistry*, North-Holland, Amsterdam, 1967, p. 540.
- 14 L. M. Gindin, P. I. Bobikov, G. M. Patjukov, A. M. Rosen, E. F. Kouba and A. W. Bugajewa, in A. P. Sefirov and M. M. Senjawin (Editors), *Ekstrakcija*, Vol. 2, Gosatomisdat, Moscow, 1962, p. 87.
- 15 H. Holzapfel, Le Viet Lan and G. Werner, *J. Chromatogr.*, 20 (1965) 580.
- 16 H. Holzapfel, Le Viet Lan and G. Werner, *J. Chromatogr.*, 24 (1966) 153.
- 17 G. Werner, *Z. Chem.*, 5 (1965) 147.
- 18 G. Werner, in D. Dyrssen, J.-O. Liljenzin and J. Rydberg (Editors), *Solvent Extraction Chemistry*, North-Holland, Amsterdam, 1967, p. 54.
- 19 G. Werner, R. Hannig, W. Dedek and H. Holzapfel, in J. Bűzas (Editor), *Proc. 3rd Anal. Chem. Conf. Budapest, 1970*, Vol. I, Akadémiai Kiadó, Budapest, 1970, p. 75.
- 20 G. Werner, *J. Chromatogr.*, 22 (1966) 400.
- 21 G. Werner, in preparation.
- 22 G. Werner, *Wiss. Z. Karl-Marx-Univ. Leipzig, Math.-Naturwiss. Reihe*, 21 (1972) 17.

ION-EXCHANGE MATERIALS

CHROM. 7733

EXAMINATION OF ION-EXCHANGE RESINS BY DERIVATOGRAPHY

O. NAGY, H. GAÁL and J. SZABÓ

Institute for Electrical Power Research (VEIKI), Zrinyi u. 1, Budapest, V. (Hungary)

SUMMARY

The possibility of observing the thermal behaviour of polymeric ion-exchange resins by means of a derivatographic method is considered. The thermal processes that take place during thermal decomposition are discussed and their nature is elucidated.

Information has been obtained on the process of thermal decomposition of the most frequently used Hungarian ion-exchange resins, and relationships are established between the thermal characteristics, the ionic form of the resin and its divinylbenzene content.

INTRODUCTION

In water treatment in thermal and nuclear power stations, the investigation of the thermal and radioactive stability of ion exchangers based on synthetic polymeric resins has great importance. We have obtained derivatographic results in order to be able to examine the correlation between the thermal characteristics of the resin samples by observation of the thermal behaviour of the ion-exchange resins submitted to radioactive irradiation at various dosages and, on this basis, to draw conclusions on the thermal and radioactive radiation stability of the resin structure¹.

In addition to the influence of the radioactive irradiation, we have also observed the influence of the ionic form and the divinylbenzene content of the resins and the influence of the quality of the gaseous medium applied when obtaining derivatographic results².

Mainly Hungarian ion-exchange resins were examined, but for comparison derivatographic results for some Lewatit products of the same type were also obtained. These results support the conclusions drawn in the course of testing the Hungarian resins^{3,4}.

EXPERIMENTAL

Anion exchangers of type Varion AT-400, AT-660, Varion AD, Varion ADM, Varion AD-P and cation exchangers of type Varion KS, Varion KSM and Varion KS-P were used. The resin samples were examined in various ionic forms (OH^- , Cl^- , BO_3^{3-} , Na^+ , K^+ , Fe^{3+} , H^+ and NH_4^+) and at different dosages of radioactive irradiation.

tion (0, 50, 100 and 150 Mrad). The derivatographic pictures of the samples were taken in air and nitrogen flows with a Paulik-Erdey derivatograph under identical experimental conditions in the temperature range 20–900° with the following parameters:

Calibration	from a 40-mg sample dried for 1 h at 40° and powdered.
Temperature curve (T)	instrument setting, 1000°.
Thermogravimetric curve (TG)	measuring range, 0–500 mg.
Differential thermogravimetric curve (DTG)	galvanometer sensitivity, 1/5.
Differential thermoanalytical curve (DTA)	galvanometer sensitivity, 1/15.
Heating velocity	10°/min.
Starting voltage	96 V.
Row of pins	3.
rpm of photographic drum	1/100 min.
220-V heating voltage	after 100 min.
Air or nitrogen flow-rate	30 l/h.

In addition to these pictures of the ion-exchange resins, samples of type Lewatit SP-120, MP-62, MP-500, MP-500-A and MP-600 and Varion ADA and ADAM were also examined. Of these samples, Lewatit SP-120 was a sulpho-acidic cation exchanger in the Na⁺ form and the others anion exchangers in the OH⁻ form.

Firstly, under our experimental conditions, on the basis of duplicate measurements, the limit of reproducibility of the individual pictures was determined and found to be 10°. This value of 10° can be considered as the threshold value for the identification of the DTG peaks obtained under the same conditions. That is, if the difference between the DTG peaks of two different samples examined under identical conditions does not exceed 10°, then the two peaks have occurred as a result of the same thermal process. If the difference between the two DTG peaks is greater than 10°, then different thermal processes have taken place or some effect of factors that cause dissimilarity in the samples has occurred.

RESULTS

The DTG peaks for the anion-exchange resins are distributed in four temperature ranges, as follows:

In temperature range I (68–157°):

- peak at 68°
- peak at 117°
- peak at 133°
- peak at 157°

In temperature range II (196–220°):

- peak at 196°
- peak at 220°

In temperature range III (260–277°):

- peak at 260°
- peak at 277°

In temperature range IV (396–430°):

peak at 396°

peak at 415°

peak at 430°

The individual temperature ranges are separated from one another by a minimum of 35°, in which region none of the samples examined gave a DTG peak. Thus the thermal process that takes place in the samples and results in variations of weight proceeds with maximum velocity in one of these four temperature ranges.

From a comparison of the pictures, it can be stated that the first temperature range is the band of water peaks. In this temperature range, the adsorbed moisture and the water of constitution are expelled from the samples. The temperature of the latter depends on the ionic form of the resin and the gas medium employed to a much greater extent than on the resin structure and on the intensity of the radioactive irradiation. The ionic OH^- form and nitrogen as the gas medium retard the expulsion of water.

In temperature ranges II and III, splitting off of the active groups takes place. This process involves the rupture of chemical bonds and the expulsion of low-molecular-weight gaseous products. Parallel with this endothermic process, exothermic recombination of the broken bonds of the resin structure also occurs.

It also can be seen in the pictures that the temperature of splitting off the active groups depends primarily on the ionic form of the ion-exchange resin. For example, the thermal stability resins in the Cl^- and BO_3^{3-} forms is greater by 40° than that of resins in the OH^- form.

Temperature range IV is the band of the decomposition of the skeletal structure. During this decomposition, some of the chemical bonds rupture in an endothermic process and gaseous products split off from the resin skeleton, and probably undergo combustion in the presence of air. Recombination of the broken bonds occurs which involves endothermic alteration of the structure corresponding to the stable form at higher temperatures. Thus the double peaks on the DTG curves resulted from endothermic bond rupture, exothermic recombination and endothermic alteration processes.

The interpretation of the DTG peaks of cation-exchange resins is not as unambiguous. The spectrum of the DTG peaks does not show a band arrangement (with the exception of the band of water peaks) similar to that for anion exchangers. This difference can be explained by the fact that with anion exchangers, after expulsion of the water of constitution in temperature ranges II and III, fission of the active groups occurs to give mainly gaseous products which leave the region under consideration, while with cation exchangers, after the departure of the water of constitution, mainly solid reaction products are formed, which do not leave the reaction area. Various compounds that contain sulphur, sodium, potassium, iron and oxygen suffer the greatest changes. The occurrence of DTG and DTA peaks showing these changes inhibits the band arrangement of the spectrum of DTG peaks.

EVALUATION OF THE RESULTS

On the basis of the derivatographic examinations, it can first be stated that the derivatographic methods can be used successfully for investigating the thermal

characteristics of ion-exchange resins and for performing comparative evaluations of the thermal stability of various products.

The results show that in the course of the thermal decomposition of the ion-exchange resins examined, first the adsorbed moisture and the water of constitution depart, then the active groups binding the ions split off from the skeletal structure of the resin and finally the skeletal structure decomposes. This three-stage decomposition process, especially in the case of anion exchangers, can be clearly followed on the DTG curves, where for each decomposition stage there is a corresponding DTG peak with a definite shape expressing the decrease in weight (Fig. 1). The DTG curves for cation exchangers show a more complicated picture (Fig. 2). Similarly, the enthalpy variations accompanying the thermal decomposition can also be followed on the DTG curves. These variations give information even about the modifications that often follow the individual decomposition cycles but are not accompanied by changes in weight.

Further, it has been shown that the positions of the DTG peak temperatures expressing the points of maximal velocities of the different decomposition processes in the temperature ranges are determined not by the radiation dosage, but by the ionic form of the resin sample, the divinylbenzene content of the resin structure and

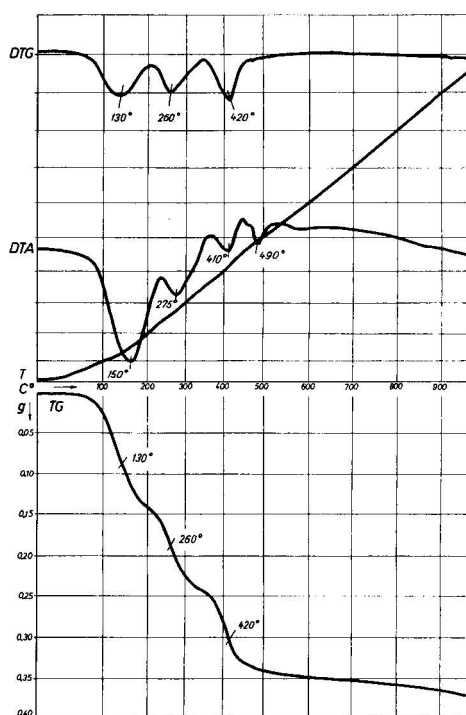


Fig. 1. Picture of a sample of Varion AT-660 (Cl^-) irradiated with 0 Mrad radiation dosage in a nitrogen flow.

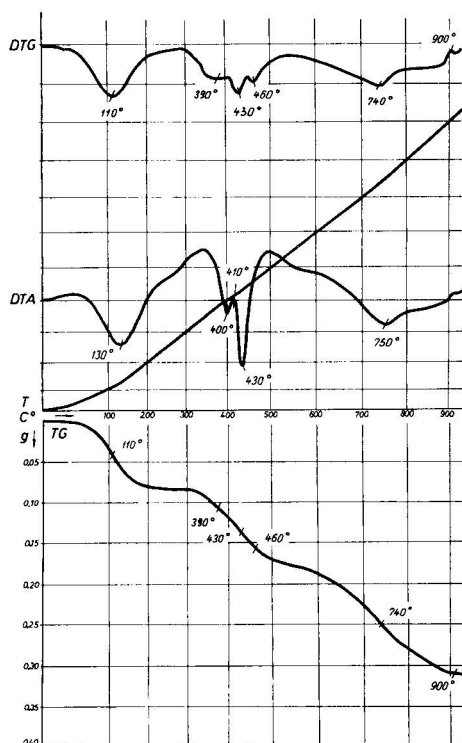


Fig. 2. Picture of a sample of Varion KS (K^+) irradiated with 50 Mrad radiation dosage in an air flow.

the gaseous medium employed when taking the pictures. Of these determining factors, the ionic form is of primary importance.

For example, in the first stage of the decomposition process, during the expulsion of water, the positions of the DTG peaks of the individual samples within the band of water peaks were determined by the ionic form of the resin and by the gaseous medium used. This can be illustrated by the following events connected with the band of water peaks (68–157°):

68°	Expulsion of adsorbed moisture from some badly prepared samples.
110°	Removal of the water of constitution of cation exchangers in the K^+ form in the case of air flow.
117°	Removal of the water of constitution of anion exchangers in the Cl^- and BO_3^{3-} forms in the case of air flow.
128°	Removal of the water of constitution of cation exchangers in the Na^+ , Fe^{3+} , NH_4^+ and H^+ forms in the case of air and nitrogen flows.
133° and 157°	Removal of the water of constitution of anion exchangers in the Cl^- form in the case of nitrogen flow and in the OH^- form in the case of air and nitrogen flows.

The role of the divinylbenzene content of the resin composition is shown by the results for cation exchangers. The cation-exchange resins examined contain more divinylbenzene (Varion KS, 8%; Varion KSM, 20%) than do the anion exchangers (Varion AT-400, 4%; Varion AT-660, 6.6%; Varion AD, 6.6%). The results showed that a larger divinylbenzene content results in fission of the active groups at lower temperatures, but the fission temperature is determined by the ionic form, as can be seen from the comparison in Table I.

In the fission of the active groups of anion exchangers, the decomposition temperature found in the case of ionic forms of the resin with lower molecular weight was lower by 40° than in the case of ionic forms with higher molecular weight. Thus the decomposition of resins in the OH^- form occurs at 196° and 220°, while that of resins in the Cl^- and BO_3^{3-} forms occurs at 280° and 277°.

TABLE I

FISSION TEMPERATURES OF CATION EXCHANGERS IN DIFFERENT IONIC FORMS

Ionic form	Fission temperature (°C)	
	Varion KSM (20% divinylbenzene)	Varion KS (8% divinylbenzene)
Na^+	350	430
K^+	320	390
Fe^{3+}	240	315
NH_4^+	355	395

CONCLUSION

From the results obtained, it can be stated that the thermal decomposition of ion exchangers based on styrene-divinylbenzene is influenced primarily by their

ionic form and secondly by their divinylbenzene content. The radioactive radiation used has no influence on the process.

As regards the practical application of the results obtained during this work, new possibilities have become apparent in the employment of derivatographic methods in the production and use of ion-exchange materials. Results and relationships can be obtained that may contribute to a great extent in solving the problems that arise in the application of ion-exchange materials in high-temperature condensate treatment (Powdex) and in other theoretical and practical aspects of ion exchangers.

REFERENCES

- 1 Zs. Ambrus and H. Gaál, *Examination of Ion-Exchange Resins by Derivatography*, VEIKI Report, Budapest, 1971.
- 2 H. Gaál, *Derivatographic Examination of the Most Frequently Used Hungarian Ion-Exchange Resins*, VEIKI Report, Budapest, 1971.
- 3 J. Szabó and H. Gaál, *Derivatographic Examinations for Determining the Thermal Stability of Varion Ion Exchangers*, VEIKI Report, Budapest, 1972.
- 4 Zs. Ambrus and H. Gaál, *Derivatographic Examinations of Macropore Ion-Exchangers*, VEIKI Report, Budapest, 1972.

CHROM. 7718

INVESTIGATION OF STRUCTURE HETEROGENEITY IN ION-EXCHANGE MEMBRANES

MIKHAIL S. GORODNEV, GRIGORI K. SALDADZE, VALERI K. VARENTSOV and IRINA M. ABRAMOVA

Scientific Research Institute for Plastics, 35 Perovsky Proyezd, Moscow E-112 (U.S.S.R.)

SUMMARY

Electron microscopy and local X-ray spectral analysis (utilizing an electron probe) have been used to evaluate structural heterogeneity in ion-exchange membranes. X-ray patterns, reflecting radiation intensity changes along the test sample proportional to the fixed charge density, can be obtained through X-ray microanalysis. Electron microscopic studies of ultra-thin sections of ion-exchange membranes indicated that the structural heterogeneity expressed by alternating zones with various electron densities associated with the presence of pores in the membranes is the basic feature of these membranes.

INTRODUCTION

Homogeneity of polymeric ion-exchange membranes is of prime importance for the interpretation of almost all of the physico-chemical properties of the membranes. This question is of particular importance in understanding the ion transfer mechanism and the electrochemistry of the membrane processes.

The existing division of the membranes into homogeneous and heterogeneous types is very arbitrary, and is not based on data reflecting the micro-structure of the membranes. The explanation of membrane properties is more often based on the assumption of their homogeneity. However, graft and block polymerization processes used for the manufacture of the membranes are mostly heterogeneous reactions proceeding with the formation of various supermolecular structures.

In previous work¹⁻³, the inevitability of the formation of a heterogeneous structure of ion-exchange materials at the expense of different concentrations of a cross-linking agent, the presence of micro-cavities, differences in the distribution of ionogenic groups, etc., was shown.

Morphological features of the structure of "homogeneous" membranes obtained by chemical grafting of 2,5-methylvinylpyridine-fluorlon copolymer in the shape of a film (membrane I) and in the shape of granules (membrane II) were studied in the present work by electron microscopy and local X-ray spectral analysis with an electron probe. The relationship between micro-structure of the membranes and certain properties was also studied.

EXPERIMENTAL

X-ray microanalysis utilizing an electron probe

The samples of anion-exchange membranes investigated by local X-ray spectral analysis were pre-saturated with PO_4^{3-} and thoroughly washed free from the non-exchange absorbed electrolyte; they were then dried and fixed in an air-dry state in a specially made mould with an epoxy resin. As the sample-making method affects the accuracy of the results, all of the membrane samples were fixed in one mould coated with a thin layer of graphite before making measurements. This mould was placed in the working chamber of an MS-46 microanalyzer (Cameca, Courbevoir, France), in which 10^{-5} -mmHg vacuum was maintained. The voltage on the probe was 20 kV and the current was $3 \cdot 10^{-8}$ A. X-ray patterns were taken from the sample areas free from mechanical defects observed with a $500\times$ power microscope.

Electron microscopy

An electron microscopic method utilizing ultra-thin sections prepared with ChMTP-2 ultramicrotome was used for the investigation of a thin structure of homogeneous ion-exchange membranes. The membrane samples, in the shape of a thin strip, were placed in a foil holder and filled with an epoxy resin. After polymerization, $0.2 \times 2 \times 0.2$ -mm samples were cut from the block obtained, and a section up to 1000 Å in thickness was made from the latter. Ethanol was used for making the above sections. The sections were observed with a $20,000\times$ magnification IEM-5V electron microscope with 10 Å resolution.

RESULTS AND DISCUSSION

Basic physico-chemical characteristics of the membranes under study are listed in Table I. Attention is drawn to the high resistivity of homogeneous membrane II. It is clear from Table I that the q for this membrane is considerably in excess of an electric resistivity value even for heterogeneous membrane III.

We decided to look for an explanation of this phenomenon by considering the distribution of active groups in a polymeric matrix. Information relating to the structure of the membranes obtained by using an X-ray microanalyzer with an electron probe is very convenient for this purpose. Fig. 1 shows the photographs obtained using characteristic PK_α radiation and shows the distribution of PO_4^{3-} ions in the membranes. These photographs make possible a qualitative estimation of the distribution

TABLE I
PHYSICO-CHEMICAL CHARACTERISTICS OF MEMBRANES

No.	Type of membrane	Static exchange capacity (mequiv./g dry membrane)	Degree of swelling, K (%)	Transfer number	Resistivity in 1 N HCl (ohm·cm)	$H_{m.sq}$ (%)
1	Homogeneous	2.0	109	0.95	17	36.7
2	Homogeneous	2.1	118	0.94	198	47.5
3	Heterogeneous	1.45	108	0.97	29.5	78.6

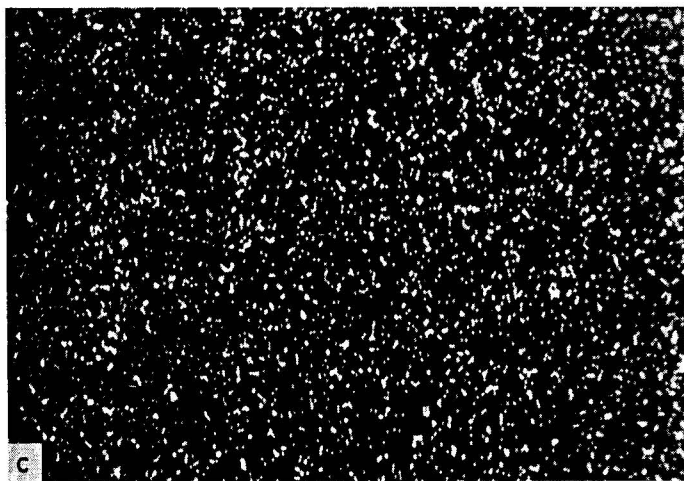
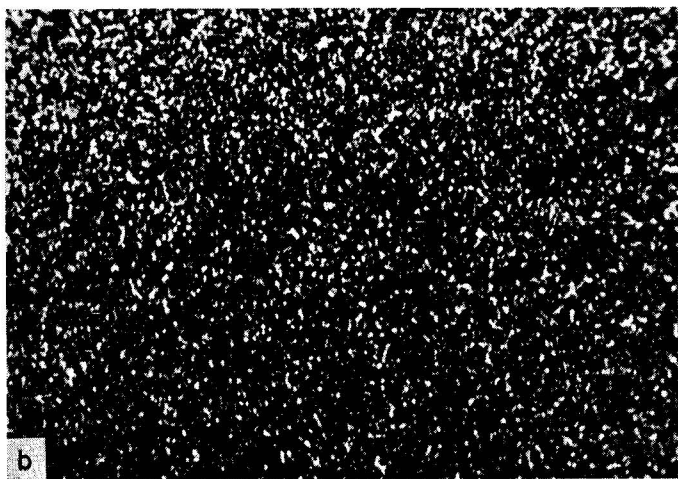
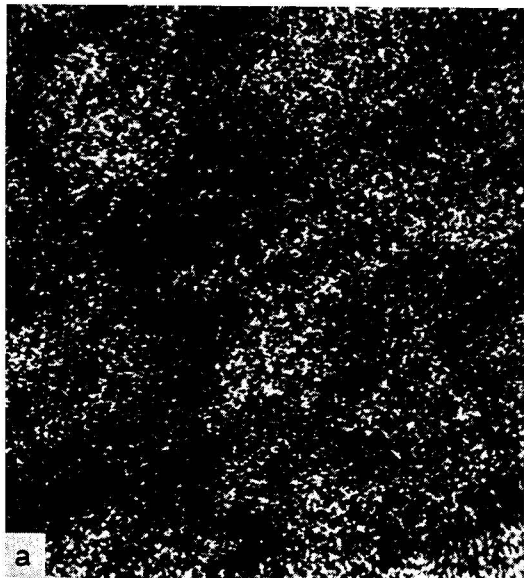


Fig. 1. Microphotographs obtained in characteristic PK_{α} radiation: (a) for heterogeneous membranes; (b) and (c) for homogeneous membranes.

of counter ions in homogeneous and heterogeneous membranes. Although the distribution of counter ions is of a discrete character in all instances, in homogeneous membranes, however, it is characterized by a sufficiently high degree of uniformity.

The quantitative estimation of the distribution of the ionogenic groups in the membrane was obtained through processing X-ray patterns (obtained with a microanalyzer) reflecting the changes in radiation intensity proportional to the fixed charge density.

When processing X-ray patterns by the method described earlier⁴, we calcul-

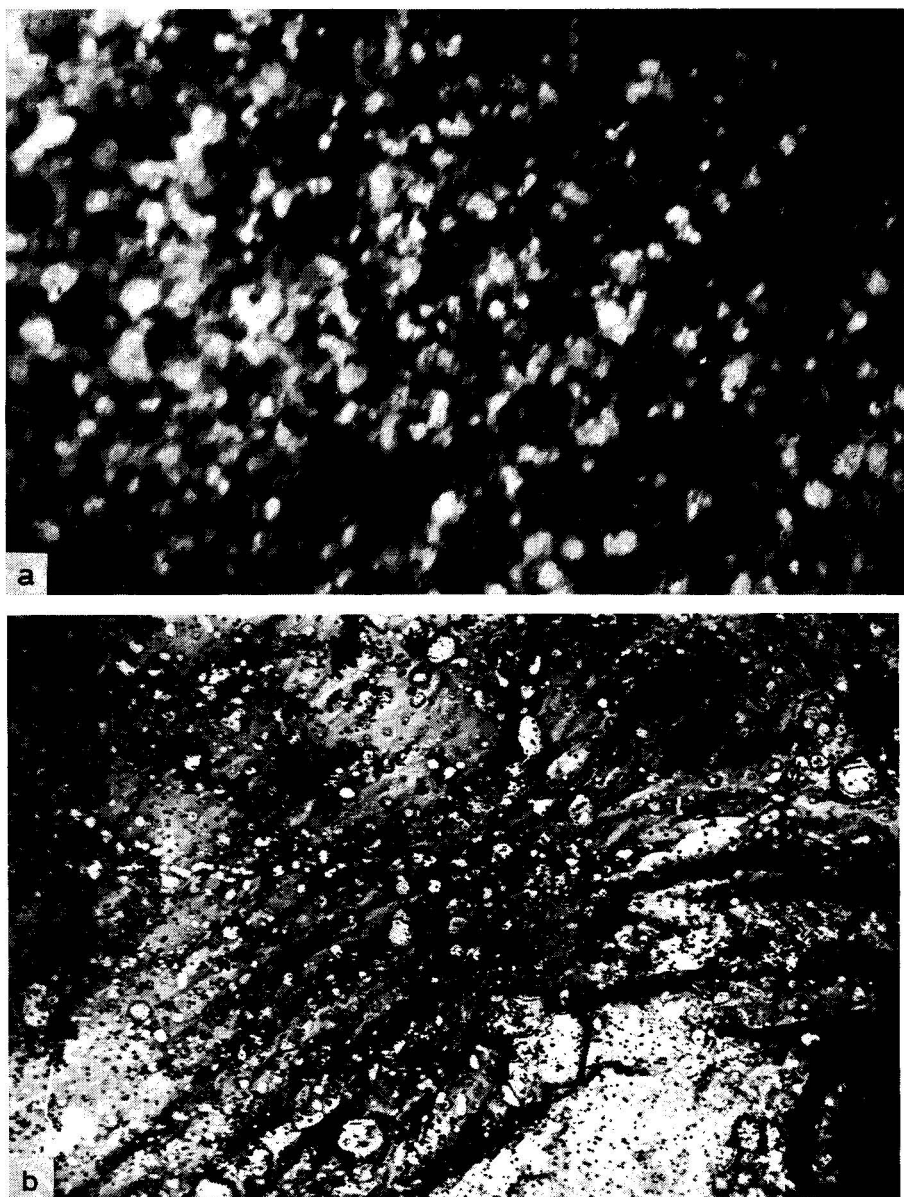


Fig. 2. Electron structure microphotograph of (a) membrane I and (b) membrane II.

ated the $H_{m.sq.}$ parameter, which shows the distribution non-uniformity of ionogenic groups in the membrane. The $H_{m.sq.}$ value for a heterogeneous membrane, given in Table I, substantially exceeds $H_{m.sq.}$ values for both homogeneous membranes. The $H_{m.sq.}$ value for membrane II is much higher than that for membrane I, which corresponds to a higher distribution non-uniformity of the active groups in membrane II, although the static exchange capacities are almost identical for both homogeneous membranes, thus indicating an equal amount of active groups in a macro-volume.

2,5-Methylvinylpyridine-*ftorlon* copolymerization processes differ depending upon the nature of the *ftorlon* (film or granules). It can be assumed that active groups are distributed in the surface layer of the granules when being chemically grafted on *ftorlon* granules. This is even more evident when taking into account the fact that the diffusion of 2,5-methylvinylpyridine molecules into *ftorlon* granules is difficult owing to steric effects.

A higher distribution non-uniformity of active groups in membrane II affects its electrochemical properties. Ion transfer in the ion-exchange membrane takes place, however, not only at the expense of available fixed active groups, but also at the expense of the electrolyte found in the membrane pores.

Using electron microscopy, we investigated the structural heterogeneity of homogeneous membranes represented by micro-cavities. Fig. 2 presents structural microphotographs of homogeneous membranes. It is clear from Table II that the structure of membrane I is more homogeneous at a supermolecular level compared with the structure of membrane II.

TABLE II

RESULTS FOR HOMOGENEOUS AND HETEROGENEOUS MEMBRANES

No.	Type of membrane	Size of micro-cavities (\AA)		Gas permeability ($\frac{\text{cm}^3 \cdot \text{cm}}{\text{cm}^2 \cdot \text{sec} \cdot \text{atm}}$)
		Electron microscopy	Low-angular X-ray scattering	
1	Homogeneous	150–250	230	$3.2 \cdot 10^{-8}$
2	Homogeneous	250–800 2000–4000	350	$4.5 \cdot 10^{-8}$
3	Heterogeneous	—	—	$9.6 \cdot 10^{-8}$

The presence of hydrophobic areas is possible in membrane II material owing to the non-uniform distribution of ionogenic groups. In this case, hydrophobic pores are not filled with the electrolyte, which leads to a disturbance of the ion contact between the active groups of the membrane and the electrolyte solution, and therefore to an abnormal decrease in electrical conductivity.

The combination of the two methods of investigation permits one to evaluate structural features of ion-exchange membranes; this structure makes a substantial contribution to the migration of ions in an electric field.

REFERENCES

- 1 F. Körösy and E. Zeigerson, *J. Appl. Polym. Sci.*, 11 (1967) 909.
- 2 J. Klinowski and M. Leszko, *Rocz. Chem.*, 42 (1968) 123.
- 3 V. K. Varentsov, K. H. Urusov, Yu. G. Lavrentiev and M. V. Pevnitskaya, *Dokl. Akad. Nauk SSSR*, 186, No. 2 (1969).
- 4 V. K. Varentsov and M. V. Pevnitskaya, *Izv. Sib. Akad. Nauk SSSR*, No. 2 (1972) 139.

CHROM. 7730

SELECTIVE PROPERTIES AND ANALYTICAL USE OF AN ION-EXCHANGE RESIN BASED ON α -PHENYLVINYLPHOSPHONIC ACID

M. MARHOL and J. CHMELÍČEK

Nuclear Research Institute, Řež near Prague (Czechoslovakia)

and

A. B. ALOVITDINOV and CH. U. KOČKAROVA

Polytechnic Institute of Tashkent, Tashkent (U.S.S.R.)

SUMMARY

The selective properties of a resin based on a copolymer of α -phenylvinylphosphonic acid with acrylic acid were investigated. The selectivity of the resin decreases in the order $\text{Th(IV)} > \text{Sc(III)} > \text{Fe(III)} > \text{U(VI)} > \text{divalent elements}$. Several interesting separations using the selectivity of this resin are discussed.

INTRODUCTION

Several papers have been published dealing with the synthesis and properties of various selective ion-exchange resins. For the synthesis of these resins, miscellaneous polymeric materials were used on which suitable ionogenic groups were fixed by additional reactions. Styrene–divinylbenzene copolymer has been the most commonly used carrier for these groups.

However, little interest has been shown in the preparation of resins obtained by polymerization or copolymerization of monomers containing suitable ionogenic groups, probably because of the difficulties involved in obtaining suitable monomers or the problems that occur during the polymerization of the monomers. Fortunately, these disadvantages are usually compensated by the fact that monofunctional resins with homogeneous structures are obtained.

For the preparation of selective ion-exchange resins containing phosphinic, phosphonic or phosphoric ionogenic groups by polymerization of suitable monomers, attention was focused particularly on various dichloroanhydrides of butadiene- or styrene-phosphonic acids^{1–3}, dialkyl esters of vinylphosphonic acids⁴, and diallylphosphates^{5,6}. Resins or membranes with good chemical and physical properties were obtained by copolymerization of α -phenylvinylphosphonic acid with divinylbenzene, acrylic acid or acrylonitrile^{7–9}. The radiation copolymerization of vinylphosphonic acid with different compounds has also been carried out¹⁰.

EXPERIMENTAL

The ion-exchange resin was prepared by the suspension copolymerization of α -phenylvinylphosphonic acid and acrylic acid^{7,8}. The molar ratio of phosphonic acid to acrylic acid was 0.40:0.60, which gave copolymers with good chemical and mechanical properties. The resin obtained was washed with water, a 5% solution of ammonium acetate and 5% hydrochloric acid. After washing with water, the resin was dried in air.

The titration curve of the exchanger was measured in a 2 *M* potassium chloride–0.10 *M* potassium hydroxide mixture at constant ionic strength (*I* = 2.0). The phosphorus content and swelling properties of the resin were determined by the method described earlier¹¹.

Distribution studies

A 0.120-g amount of air-dried resin in the H⁺ form was brought into equilibrium with 50.0 ml of a solution of nitric acid containing 0.50 mequiv. of the studied ion (as nitrate). This system was shaken mechanically for 180 h and then the concentration of the ion under investigation was determined in the aqueous phase.

The results are expressed as weight distribution coefficients, D_g , where

$$D_g = \frac{\text{mequiv. metal/g of dry resin}}{\text{mequiv. metal/ml of solution}}$$

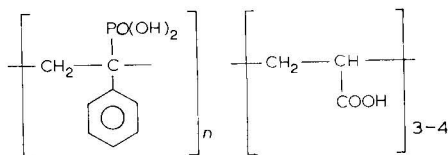
Breakthrough curves

A 1.780-g amount of air-dried exchanger in the H⁺ form (sieve fraction 0.10–0.20 mm) previously swollen in water was packed in a glass or plastic column (180 × 10 mm). After pre-treatment of the resin bed with 0.10 or 0.50 *M* nitric acid, 250 ml or more of a solution containing 20 mequiv./l of the element studied in 0.10 or 0.50 *M* nitric acid, respectively, was passed through the column at a flow-rate of 0.3 ml/min. The flow-rate was kept constant by using an Elutionspumpe H (Serva, Heidelberg, G.F.R.). Fractions of about 2.5 ml of the eluate were analysed. In some instances, ⁵⁹Fe or ⁶⁰Co were used as radioactive tracers.

Standard compleximetric or colorimetric procedures were employed for the determination of the elements. Radioactivity measurements were carried out with a Tesla NZQ 612 counter using an NaI(Tl) scintillator.

RESULTS AND DISCUSSION

From the IR spectra, phosphorus content and titration curve, the structure of the ion-exchange resin used could be written as^{7,8}



The phosphorus content in the resin was 8.88% (exchange capacity 5.7 mequiv./g,

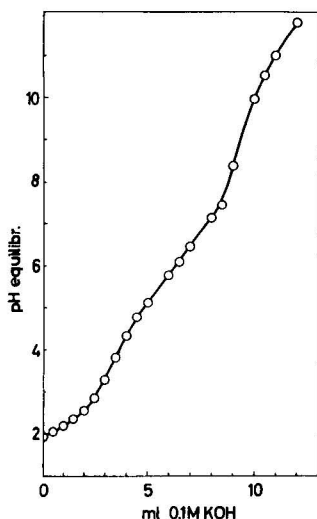


Fig. 1. Titration curve of the resin in 2.0 *M* KCl-0.10 *M* KOH.

based on phosphorus content). From the titration curve in Fig. 1, it can be seen that the resin has an overall potassium-hydrogen exchange capacity of 6.91 mequiv./g. The actual exchange capacities based on the phosphorus content are 2.54 mequiv./g and 4.73 mequiv./g, respectively. The remaining exchange is due to carboxylic groups.

The swelling properties of the exchanger in various media are summarized in Table I.

TABLE I

SWELLING PROPERTIES OF THE RESIN IN WATER AND NITRIC ACID

Ionic form	Swelling medium	Resin volume (ml/g)
NH_4^+	Water	2.24
H^+	Water	1.32
H^+	0.10 <i>M</i> HNO_3	0.93
H^+	0.50 <i>M</i> HNO_3	0.74
H^+	1.00 <i>M</i> HNO_3	0.67

Results showing the variation of distribution coefficients with the concentration of nitric acid are summarized in Fig. 2. The D_q values generally decrease with increasing nitric acid concentration. The selectivity of the exchanger decreases in the order $\text{Th(IV)} > \text{Sc(III)} > \text{Fe(III)} > \text{U(VI)} > \text{M(II)}$. A higher selectivity for Fe(III) than for U(VI) was observed compared with results on various exchangers containing the $-\text{PO}(\text{OH})_2$ group directly on the benzene ring, where the order of selectivity $\text{U(VI)} > \text{Fe(III)}$ was reported^{5,6}.

A strong dependence of the sorption of all the elements mentioned on the acidity of the solution was observed using 0.10–1.0 *M* nitric acid. With further increase in the acid concentration, the sorption of Th, Sc, Fe and U decreases only slowly.

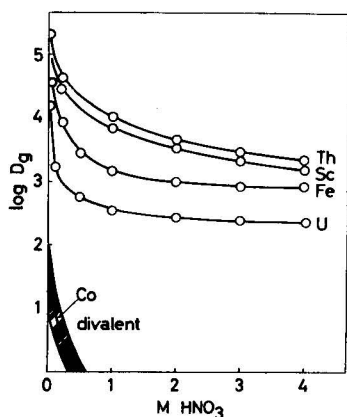


Fig. 2. D_g values of Th(IV), Sc(III), Fe(III), U(VI) and some divalent elements as a function of nitric acid concentration.

The adsorbability of the divalent elements (Ca, Mg, Sr, Co, Ni, Cd, Cu and Pb) is strongly affected by the concentration of the acid. It decreases to zero using nitric acid above 0.40 M for Pb and using nitric acid above 0.20–0.30 M for the other divalent elements.

The results of the column experiments, in the form of breakthrough curves in 0.10 and 0.50 M nitric acid, are given in Figs. 3 and 4. The results confirm the selectivity of the resin as derived from the batch experiments. All divalent elements

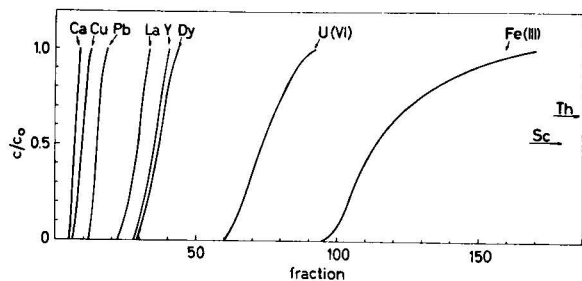


Fig. 3. Breakthrough curves of various elements in 0.10 M nitric acid. c = Actual concentration of the element; c_0 = initial concentration of the element.

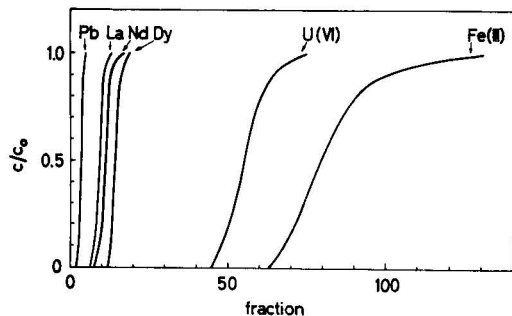


Fig. 4. Breakthrough curves of various elements in 0.50 M nitric acid.

penetrated through the resin bed in the first fractions when 0.50 *M* nitric acid was used. The selectivity of the resin for Y and lanthanides increases with increasing atomic number of the element sorbed. The sorbabilities of some lanthanides differ to such an extent that it could serve as a basis for separation without using complex-forming eluting agents.

The elution experiments show that the divalent elements are easily desorbed from the resin using nitric acid above 0.40 *M*; Y and lanthanides are quickly and quantitatively desorbed with nitric acid above 3.0 *M*. If Th, Sc, Fe or U was to be eluted, difficulties occurred because of high affinity of the resin for these elements. Fe(III) and U(VI) could be eluted effectively with the mixture 5.0 *M* nitric acid–1.0 *M* ammonium fluoride. No elution of Th and Sc was observed in 5.0 *M* nitric acid or 6–12 *M* hydrochloric acid and only a slow desorption was obtained by using 0.05 *M* EDTA solution at pH 2.5. After washing the resin with 0.5 *M* ammonium acetate solution, Th or U could be eluted with ammonium carbonate solution. Scandium was eluted very slowly with 1.0 *M* sulphuric acid.

From the D_g values and breakthrough curves, it is obvious that Th, Sc, Fe or U can be effectively separated from elements that have lower D_g values, *i.e.*, from Y, lanthanides and the divalent elements. Table II presents results showing the separation

TABLE II

SELECTIVE SEPARATIONS OF Fe, Sc, Th AND U FROM VARIOUS MIXTURES

<i>Metal</i>	<i>Taken (mg)</i>	<i>Found (mg)</i>	<i>Sorption or elution conditions</i>
Fe	1.860	1.866	Sorption from 0.3 <i>M</i> HNO ₃
Co	5 780.000	5 779.910	
Fe	34.646	34.708	Sorption from 0.3 <i>M</i> HNO ₃
Co	1.462	1.473	
Fe	9.300	9.260	Sorption from 0.3 <i>M</i> HNO ₃
Co	0.0070	0.0078	
Fe	20.000	20.000	Sorption from 0.3 <i>M</i> HNO ₃
Ni	0.0070	0.0075	
Zn, Cd, Cu	Σ100.000	Σ100.000	Sorption from 0.3 <i>M</i> HNO ₃
U	1.556	1.552	
Cu, Cd, Zn	Σ150.000	Σ150.000	Sorption from 0.15 <i>M</i> HNO ₃
La, Pr, Nd, Sm	Σ2.864	Σ2.860	
La, Pr, Nd	Σ4.600	Σ4.590	Sorption from 1.0 <i>M</i> HNO ₃
Sm, Gd, Eu			
Sc		—	
La, Pr, Nd, Sm, Gd, Eu	Σ15.900	Σ15.910	Sorption from 2.0 <i>M</i> HNO ₃
Th	2.867	—	
La, Pr, Nd, Sm, Gd, Eu	Σ2.864	Σ2.860	Rinsing with 2.0 <i>M</i> HNO ₃
Th, Sc in 1000 ml of 1.5 <i>M</i> HNO ₃	Σ125.000	—	

of grams down to a few micrograms of the elements mentioned, taken as representative of the use of the selectivity of the resin.

Analysis by means of this method offers the possibility of the rapid and easy determination of some impurities in thorium, scandium, iron or uranium nitrates. Rapid separation of the pairs Fe-Co and Fe-Ni suggest the possibility of using this resin in metallurgical laboratories also.

REFERENCES

- 1 U.S.S.R. Pat., No. 199 394 (1967).
- 2 U.S.S.R. Pat., No. 184 408 (1966).
- 3 Yu. A. Leikin, A. B. Davankov and V. V. Korshak, *Vysokomol. Soedin., Ser. A*, 9 (1967) 619.
- 4 V. A. Kargin, A. A. Efendiev, E. P. Cherneva and N. N. Tunickii, *Dokl. Akad. Nauk SSSR*, 144 (1962) 1307.
- 5 J. Kennedy, *Chem. Ind. (London)*, (1956) 378.
- 6 J. Kennedy, *Chem. Ind. (London)*, (1958) 950.
- 7 G. S. Kolesnikov, A. S. Tevlina and A. B. Alovitdinov, *Plast. Massy*, No. 2 (1966) 12.
- 8 A. B. Alovitdinov, A. S. Tevlina and G. S. Kolesnikov, *Plast. Massy*, No. 8 (1966) 21.
- 9 G. S. Kolesnikov, A. S. Tevlina, A. B. Alovitdinov and A. D. Korenov, in K. V. Chmutov (Editor), *Synthesis and Properties of Ion Exchange Materials*, Nauka, Moscow, 1968, p. 61.
- 10 J. Tsurugi, T. Fukumoto and M. Yamugami, *Annu. Rep. Radiat. Cent. Osaka Prefect.*, 13 (1972) 108; *C.A.*, 80 (1974) 83986B.
- 11 M. Marhol and K. L. Cheng, *Talanta*, 21 (1974) 751.

CHROM. 7729

THE MOBILITY OF CERIUM IONS IN SYNTHETIC ZEOLITES

A. DYER* and A. B. OGDEN**

Cockcroft Building, University of Salford, Salford M5 4WT, Lancs. (Great Britain)

SUMMARY

Radiochemical methods have been used to study the movement of cerium ions in three synthetic faujasites. Results are presented as self-diffusion parameters and conclusions are related to the possible ion migration pathways in the zeolite framework.

INTRODUCTION

The favourable catalytic properties¹ of rare earth forms of synthetic faujasites have prompted interest in their structure and ion-exchange reactions. Some single crystal work has been carried out by Olson *et al.*², and Hunter and Scherzer³, on cerium forms of X and similar materials; these give cation distributions in the unit cell at 25 °C.

Previous work from these laboratories^{4,5} has used radiochemical methods to study the behaviour over a range of temperatures of various ions (Sr, Ba, Zn) in synthetic faujasites having silicon/aluminium ratios of 1.26, 1.87, 2.62, respectively. Sherry comments from his ion-exchange experiments⁶ that only loosely bound sodium ions are exchanged by lanthanum in X (Si/Al \approx 1.2) at 25 °C because more thermal energy is required to remove waters of hydration from the lanthanum before it is able to pass through a six-membered oxygen ring to replace more tightly bound sodiums in the faujasite framework. Accordingly we have studied migrations of cerium in three faujasites in the temperature range 245 to 543 °K.

EXPERIMENTAL

Three sedimented samples of the faujasites were prepared in their ²²Na form. Portions (0.3 g) of these labelled zeolites were stirred for varying time intervals with 15 ml of 0.4 N cerium nitrate solution. This was carried out at 295 °K and 326 °K. These preliminary experiments showed that roughly one half of the sodium ions are easily exchanged, a further one fifth are more difficult and the remainder very difficult

* To whom correspondence should be directed.

** Present address: S. Martins College, Lancaster, Great Britain.

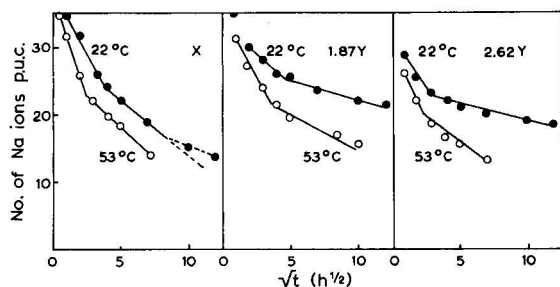


Fig. 1. Number of Na ions p.u.c. versus \sqrt{t} for X, 1.87Y, 2.62Y ($\text{Na}^+ \rightarrow \frac{1}{3}\text{Ce}^{3+}$).

TABLE I

ZEOLITE COMPOSITION

Zeolite	Si/Al ratio	Formula
CeX	1.26	$\text{Na}_{8.6} \text{Ce}_{25.5} (\text{AlO}_2)_{85} (\text{SiO}_2)_{107}$
Ce 1.87Y	1.87	$\text{Na}_{7.2} \text{Ce}_{18.9} (\text{AlO}_2)_{67} (\text{SiO}_2)_{125}$
Ce 2.62Y	2.62	$\text{Na}_{4.5} \text{Ce}_{16.0} (\text{AlO}_2)_{53} (\text{SiO}_2)_{137}$

to exchange (see Fig. 1). Cerium-exchanged samples were then prepared by successive heatings under vacuum as described elsewhere^{4,5}.

Finally these samples were heated at 85 °C with a 0.1 M ^{144}Ce nitrate solution, dried and heated under vacuum at 543 °K to homogeneously label the samples. Self-diffusion studies^{4,5} were then attempted in the the temperature ranges 244–268 °K and 359–412 °K.

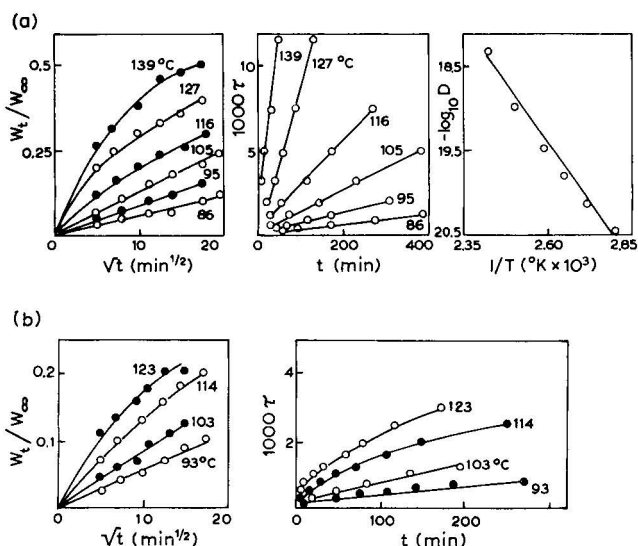


Fig. 2. (a) Percentage attainment of equilibrium (W_t/W_∞) versus \sqrt{t} , dimensionless time plot (τ versus t), and Arrhenius plot for Ce 2.62Y. (b) W_t/W_∞ versus \sqrt{t} and τ versus t plots for CeX.

TABLE II
MEASURED THERMODYNAMIC PARAMETERS

Zeolite	Temperature range ($^{\circ}\text{K}$)	E_a (kJ/mole)	ΔS^* (joule degree^{-1} mole^{-1})	ΔG^* (kJ/mole)
CeX	359–412	—	—	—
Ce 1.87Y		129 ± 7	+ 52	112
Ce 2.62Y		113 ± 6	+ 11	110
CeX	245–268	116 ± 6	+ 217	50
Ce 1.87Y		109 ± 5	+ 154	60
Ce 2.62Y		110 ± 6	+ 181	55

RESULTS

Analysis showed that the cerium zeolites were of the compositions shown in Table I.

Thermal analyses and scanning electron microscopy indicated some breakdown (roughly 30%) but X-ray powder patterns gave a clear indication of the faujasite framework and subsequent kinetic analysis showed that diffusion laws were obeyed (with one exception). Examples of the self-diffusion plots are shown in Fig. 2. From the plots estimates of E_a , ΔS^* , and ΔG^* for the migration of cerium in the zeolites could be made. Full description of the mathematical analysis used is recorded elsewhere⁷. Results are listed in Table II.

DISCUSSION

The sodium positions in hydrated NaX have been allocated⁸ as follows: Site I —9, Site I' —8, Site II' —0, Site II —24, with the remaining ions occupying less definite sitings in the large cavity. Fig. 3 is a sketch of the relevant element of the framework. Quick washing of our samples with inactive cerium nitrate solution, at room temperature, showed that the faujasites contain a proportion of loosely bound ions as expected^{2,3}. These were the ions which self-exchanged in the lower temperature range studied and the number of ions per unit cell exchanged corresponded to an original replacement of sodium in the large cavity (see Fig. 1). Comparison of the thermodynamic parameters observed in all three samples to those observed for zinc migrating in similar materials⁵ shows that they are almost identical. It is therefore suggested that the process observed at the low temperature is an analogous one to

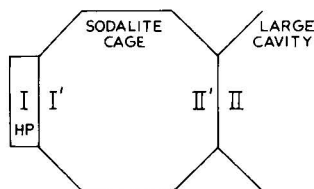


Fig. 3. Schematic representation of the hexagonal prism (HP), sodalite cage, and large cavity of the faujasite structure (with ion sites).

that for zinc —namely the migration of a hydrated ion. The high positive ΔS^* values observed are a consequence of this hydrated species disrupting ordered water molecules in the zeolite cavity as they move through the framework. The lack of correlation between E_a and the Si/Al ratio (*i.e.*, framework charge) tends to support this view.

The energy barrier to ion movement in the higher temperature range is presumed to be the cerium ion moving (in the absence of water) out of the sodalite cages (Site II' \rightarrow Site II) via a six-membered oxygen ring. The Ce 1.87Y and Ce 2.62Y results show a correlation between E_a and the Si/Al ratio in support of this thesis and the much lower positive ΔS^* values illustrate the absence of structured water and the ionic pathways available in 1.87Y relative to 2.62Y.

The fact that not all the activity is recovered from these zeolites indicates that ions in Site I' (or Site I) do not participate in these kinetics. This is not the case for CeX, where all the activity is recovered, but the diffusion kinetics indicate a complex process and no parameters were calculated for this case. It may be that ions from both Sites I' and I are migrating in CeX at this temperature range.

ACKNOWLEDGEMENT

One of us (A.B.O.) wishes to acknowledge the kind grant of a sabbatical leave during which this work was carried out.

REFERENCES

- 1 K. J. Veryard (Esso. Res. and Eng. Co), *Brit. Pat.*, 1090,563; appl., March 16, 1965.
- 2 D. H. Olson, G. T. Kokotailo and J. F. Charnell, *J. Colloid Interface Sci.*, 28 (1968) 305.
- 3 F. D. Hunter and J. Scherzer, *J. Catal.*, 20 (1971) 246.
- 4 A. Dyer, R. B. Gettins and J. G. Brown, *J. Inorg. Nucl. Chem.*, 32 (1970) 2389.
- 5 A. Dyer and R. P. Townsend, *J. Inorg. Nucl. Chem.*, 35 (1973) 2993.
- 6 H. S. Sherry, *J. Colloid Interface Sci.*, 28 (1968) 288.
- 7 A. Dyer, R. B. Gettins and R. P. Townsend, *J. Inorg. Nucl. Chem.*, 32 (1970) 2395.
- 8 D. H. Olson, *J. Phys. Chem.*, 74 (1970) 2798.

CHROM. 7972

ZUR SELEKTIVITÄT DES KATIONENAUSTAUSCHS AN KRISTALLINEN Ce(IV)-PHOSPHAT-SULFATEN

KARL-HEINZ KÖNIG

Institut für anorganische Chemie der Johann-Wolfgang-Goethe-Universität, Frankfurt am Main (B.R.D.)

SUMMARY

On the selectivity of the cation exchange on crystalline Ce(IV) phosphate-sulphates

The cation-exchange selectivity of crystalline cerium(IV) phosphate-sulphates is discussed. Examples of practical application in cation separations are given.

EINLEITUNG

Die Untersuchungen der Kationenaustauscheigenschaften kristalliner Ce(IV)-phosphat-sulfate sind mittlerweile in einem Stadium, in dem generelle Aussagen über die Selektivität möglich sind. Ihre Diskussion und Anwendung auf praktische Fragestellungen ist unter Berücksichtigung noch nicht publizierter Ergebnisse Gegenstand dieser Arbeit.

EXPERIMENTELLES

Darstellung kristalliner Ce(IV)-phosphat-sulfate

Kristalline Ce(IV)-phosphat-sulfate entstehen als säulenförmige Kristalle von 0.01 mm Dicke und 0.15 mm Länge bei Zusatz von *o*-Phosphorsäure zu heißen schwefelsauren Lösungen von Ce(IV)-sulfat^{1–3}. Eingehende Untersuchungen dieser Reaktion haben gezeigt, dass durch entsprechende Wahl der Schwefelsäurekonzentration das Verhältnis von Sulfat zu Phosphat in den Fällungen in relativ weiten Grenzen variiert werden kann.

Zusammensetzung und chemische Eigenschaften kristalliner Ce(IV)-phosphat-sulfate

Aus der Analyse lässt sich für die hier interessierenden Verbindungen die Formel $\text{Ce}_2(\text{HPO}_4)_{3-x}(\text{SO}_4)_x \cdot y\text{H}_2\text{O}$ angeben. Aus dieser Reihe wirken nur diejenigen als Kationenaustauscher, deren Sulfatgehalt $0 < x < 1$ ist. Innerhalb dieser Grenzen zeigen alle Verbindungen das gleiche Röntgenbeugungsdiagramm, das von dem reinen Ce(IV)-phosphate und von dem der höher substituierten Ce(IV)-phosphat-sulfate wesentlich verschieden ist¹.

Austauschverfahren

Der Kationenaustausch der Ce(IV)-phosphat-sulfate wurde im Säulenverfahren und im batch-Verfahren untersucht. Für die Säulenversuche wurden die feinkristallinen Syntheseprodukte in einer Tablettenpresse für die IR-Spektroskopie zu Ta-

bletten gepresst und diese anschliessend in einer Reibschale in säulengerechte Form zerkleinert. (Korndurchmesser 0.62 bis 0.41 mm, entsprechend DIN-Sieb Nr. 20/1171.) Die Packungen in den Austauschsäulen haben 5 mm Durchmesser und 70 mm Länge.

ERGEBNISSE UND DISKUSSION

Die stöchiometrische Kationenaustauschkapazität ist eine Funktion des Sulfatgehaltes der Verbindungen. In vielen Versuchen konnte sichergestellt werden, dass sie von einem Maximalwert bei kleinem Sulfatgehalt bis auf Null sinkt, wenn eine Phosphatgruppe des Austauschers durch Sulfat ersetzt wird². Zur Betonung dieser Eigenschaften liesse sich die oben angegebene Formel umschreiben in $\text{Ce}_2(\text{H}_2\text{O})(\text{PO}_4)_2 \cdot (\text{HPO}_4, \text{SO}_4) \cdot 3 \text{H}_2\text{O}$, wobei die Zahl der Wassermoleküle aus thermogravimetrischen Bestimmungen stammt. Eine endgültige Entscheidung über die Formulierung der Ce(IV)-phosphat-sulfate kann erst nach Abschluss der derzeit laufenden kristallographischen Strukturbestimmung gefällt werden. Für die weitere Diskussion wollen wir die Verbindungen dieses Typs mit "CePS I" bezeichnen.

Im Laufe der Untersuchungen wurde festgestellt, dass für die Kationenaustauscheigenschaften von CePS I Korrelationen zwischen Kristallstruktur des Austauschers und den Eigenschaften der hydratisierten Ionen bestehen³.

So wird zum Beispiel in 0.01 *N* Perchlorsäure die Sorption der Kationen durch einen Siebeffekt bestimmt, der in befriedigender Weise mit Hilfe der von Kielland⁴ für hydratisierte Ionen angegebenen Parameter a_i interpretiert werden kann. Das Experiment zeigt, dass unter den angegebenen Bedingungen Kationen mit $a_i \leq 6 \text{ \AA}$ vom Austauscher aufgenommen werden, während Kationen mit $a_i \geq 6 \text{ \AA}$ ausgeschlossen werden (Tabelle I).

TABELLE I

KATIONENAUSTAUSCHKAPAZITÄTEN VON CePS I ($\text{Ce}:\text{PO}_4:\text{SO}_4 = 2:2.64:0.36$) IN 0.01 *N* HClO_4

Berechnete Kapazität: 0.95 mequiv./g. a_i -Werte nach Kielland⁴ (K.-H. König und G. Eckstein³).

Kation	Austauschkapazität (mequiv./g)	a_i (Å)
Ag^+	0.90	2.5
Cs^+	0.51	2.5
Na^+	0.83	4
Sr^{2+}	0.41	5
Ba^{2+}	0.28	5
Ca^{2+}	0.43	6
Co^{2+}	0.04	6
Be^{2+}	0.00	8
Fe^{3+}	0.00	9
Sc^{3+}	0.00	>9
Y^{3+}	0.00	>9
Ce^{3+}	0.00	>9
Sm^{3+}	0.00	>9
Eu^{3+}	0.00	>9
Tb^{3+}	0.00	>9
Tm^{3+}	0.00	>9

TABELLE II

KATIONENAUSTAUSCHKAPAZITÄTEN VON CePS I ($\text{Ce:PO}_4\text{:SO}_4 = 2:2.64:0.36$) IN WÄSSRIGEN LÖSUNGENK.-H. König und G. Eckstein⁵.

Kation	Austausch- kapazität (mequiv./g)	% der maximalen Austausch- kapazität	Kation	Austausch- kapazität (mequiv./g)	% der maximalen Austausch- kapazität
Li ⁺	0.70	73.7	Mn ²⁺	0.65	68.4
Na ⁺	0.81	85.3	Pb ²⁺	0.86	90.6
K ⁺	0.78	82.2	Sc ³⁺	0.000	0.0
Rb ⁺	0.73	76.9	Y ³⁺	0.064	6.7
Cs ⁺	0.51	53.7	La ³⁺	0.18	18.9
NH ₄ ⁺	0.76	80.0	Ce ³⁺	0.22	23.2
Ag ⁺	0.85	89.6	Pr ³⁺	0.19	20.0
Tl ⁺	0.74	78.0	Nd ³⁺	0.18	18.9
Be ²⁺	0.004	0.4	Sm ³⁺	0.17	17.9
Mg ²⁺	0.10	10.5	Eu ³⁺	0.15	15.8
Ca ²⁺	0.75	79.0	Gd ³⁺	0.12	12.6
Sr ²⁺	0.72	75.8	Tb ³⁺	0.12	12.6
Ba ²⁺	0.14	14.7	Dy ³⁺	0.10	10.5
Zn ²⁺	0.65	68.4	Ho ³⁺	0.091	9.6
Cd ²⁺	0.53	55.8	Er ³⁺	0.084	8.8
Hg ²⁺	0.35	36.9	Tm ³⁺	0.078	8.2
Ni ²⁺	0.09	9.5	Yb ³⁺	0.078	8.2
Co ²⁺	0.53	55.8	Lu ³⁺	0.062	6.5

Dieser Siebeffekt verschwindet mit abnehmender Säurekonzentration der Salzlösungen, so dass aus normal wässrigen Lösungen auch Ionen mit $a_i > 6 \text{ \AA}$ absorbiert werden, wie dies in Tabelle II für eine grosse Zahl von Kationen gezeigt wird⁵. Unter diesen Bedingungen werden auch Seltenerd-kationen absorbiert. Nicht absorbiert wird das Sc³⁺, das starker Hydrolyse unterliegt, und Be²⁺, das stabile, grossvolumige Aquokomplexe bildet.

In den Reihen der Alkalimetalle und der Erdalkalien treten Austauschmaxima bei Natrium und Calcium auf. Dies wurde in Säulenexperimenten bestätigt, bei denen die Selektivitätsreihen $\text{Na} > \text{K} > \text{Li}$ und $\text{Sr}, \text{Ba} > \text{Ca} > \text{Mg}$ erhalten wurden⁶.

Besonders instruktiv ist der Gang des Austauschs der dreiwertigen Lanthanidionen, der in Fig. 1 gezeigt ist. Aus wässrigen Lösungen der Nitrate steigt die Aufnahme gegenläufig zur Lanthanidenkontraktion vom Lu³⁺ (0.062 mequiv./g) zum Ce³⁺ (0.22 mequiv./g) an⁵.

Für das Verständnis dieser stetigen Sequenz liefert schon die zur Lanthanidenkontraktion inverse Hydratation eine plausible Grundlage⁷. Es zeigte sich darüberhinaus, dass das Verhalten der vorher genannten Elemente mit Hilfe der Theorie von Eisenman⁸ zufriedenstellend diskutiert werden kann, wenn nicht wie beim Silber extrem feste Bindung zwischen Austauscher und gebundenem Kation vorliegt. In diesen Fällen muss beim CePS I genauso wie bei anderen Kationenaustauschern eine über rein elektrostatische Wechselwirkungen hinausgehende Bindung diskutiert werden.

In Säulenexperimenten haben die Austauschgeschwindigkeiten eine grosse

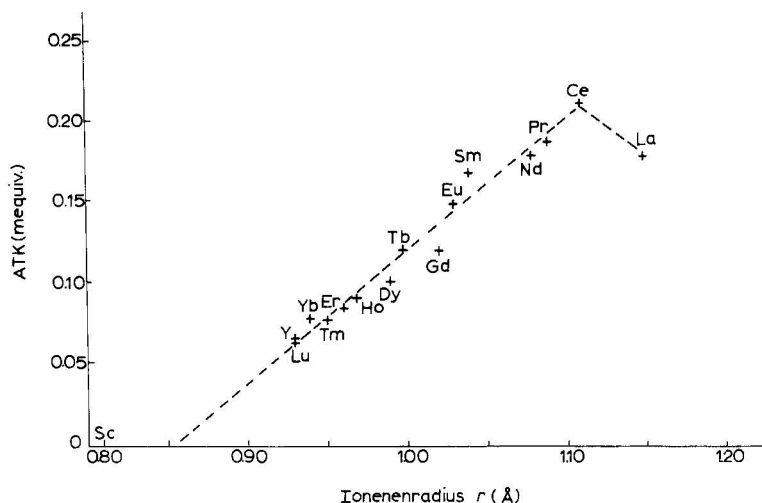


Fig. 1. Kationenaustauschkapazitäten der dreiwertigen Seltenerd-kationen an CePS I.

Bedeutung für eine gute Trennung. Für das CePS I konnte gezeigt werden⁹, dass in Salzlösungen mit Konzentrationen grösser 0.01 *N* die Diffusion im Austauscherkorn geschwindigkeitsbestimmend ist.

Kationentrennungen mit Ce(IV)-phosphat-sulfaten

Die grosse praktische Bedeutung der anorganischen Kationenaustauscher beruht in vielen Fällen auf der deutlichen Selektivität oder gar Spezifität für bestimmte Ionen. Allerdings ist es experimentell nicht immer leicht, die geeigneten Bedingungen zu finden. Wir benutzen hierzu eine Variante der Dünnschichtchromatographie, bei der das CePS I ohne Bindemittel auf aufgerauhte Glasplatten gestrichen wird und nach dem Trocknen auf diesen Platten aufsteigend chromatographiert wird¹⁰. Ein Beispiel gibt Tabelle III. Laufmittel war 0.2 *N* HCl bzw. 0.2 *N* HClO₄. Man sieht, dass in Übereinstimmung mit den Ergebnissen der Tabelle I Kationen mit $a_i < 6 \text{ \AA}$

TABELLE III

DÜNNSCHICHTCHROMATOGRAPHIE AN CePS I

Schichtdicke 0.2 mm; Laufmittel 0.2 *N* HCl oder 0.2 *N* HClO₄.

Kation	R_F -Wert
Ag ⁺	0.0
Na ⁺	0.0
Ca ²⁺	0.75
Hg ²⁺	0.9
Cd ²⁺	0.9
Co ²⁺	0.92
Ni ²⁺	0.91
Cr ³⁺	0.60
Fe ³⁺	0.35
Th ⁴⁺	0.0

den R_F -Wert Null haben. Kationen mit $a_i > 6 \text{ \AA}$ wandern in der Schicht und können voneinander getrennt werden. Die auf diese Weise erhaltenen Ergebnisse sind wesentliche Hilfen für die Planung von Experimenten in grösserem Masstab und wegen ihrer Übertragbarkeit wichtig für die Säulentechnik.

Eine instruktive Demonstration der Ionensiebeigenschaften von CePS I bietet die Trennung von ^{90}Sr und ^{90}Y im radioaktiven Gleichgewicht⁵. Nach Tabelle I wird aus mineral-sauren Lösungen Strontium vom Austauscher aufgenommen, nicht dagegen Yttrium. Wir erwarten also bei der Filtration der Gleichgewichtsmischung in 0.01 N HClO_4 über eine Austauschersäule aus CePS I im Eluat reines Yttrium. Tatsächlich ist das Verhältnis beider Elemente im Eluat $\text{Sr}:\text{Y} < 1:10^6$. Das ^{90}Sr wird vollständig im Austauscher festgehalten. Aus ihm bildet sich durch β -Zerfall das kürzerlebige ^{90}Y nach. In Anlehnung an das in der Radiochemie oft angewendete "Melken" von beladenen Ionenaustauschern zur Abtrennung der kurzlebigen Tochteraktivität aus einem stationären radioaktiven Gleichgewicht liegt es auch im vorliegenden Fall nahe, das gebildete ^{90}Y durch Elution der beladenen Säule mit Perchlorsäure von ^{90}Sr abzutrennen.

Dies ist aber selbst bei Verwendung von Perchlorsäure höherer Konzentration nicht möglich, weil das ^{90}Y nunmehr durch den Siebeffekt an einem Austritt vom Austauscherkorn in die umgebende Lösung gehindert wird.

Ein geläufiges Nuklidgemisch für radiochemische Trennoperationen ist das stationäre Gleichgewicht $^{137}\text{Cs}/^{137}\text{Ba}$, das sich wegen der kurzen Halbwertszeit des ^{137}Ba (2.55 min) sehr schnell einstellt und oft für die Beurteilung von Ionenaustausch-trennungen benutzt wird. In der überwiegenden Zahl der Fälle wird von diesem Gemisch das ^{137}Ba beim "Melken" aus dem Gleichgewicht eluiert. Im Fall des CePS I können wir, wiederum unter Benutzung von Tabelle I, vorhersagen, dass in mineral-sauren Lösungen keine Trennung der beiden Elemente möglich sein wird, da beide in grosser Menge vom Austauscher sorbiert werden. Das Experiment zeigt tatsächlich in 0.01 N HClO_4 vollständige Sorption beider Nuklide und selbst mit 0.1 N HClO_4 noch keine Elution.

Die beiden Beispiele demonstrieren nicht nur die Selektivität des CePS I, sondern auch die Gültigkeit der im Makrobereich gewonnenen Ergebnisse im Mikrobereich der Tracerchemie.

Bei Säulenexperimenten mit Makromengen gelangen Trennungen von Elementen der 1. Hauptgruppe des Periodensystems von denen der 2. Hauptgruppe⁶. Dabei wurde der Austauscher mit wässrigen Lösungen der Salzmischungen beladen und anschliessend mit 0.01 N oder 0.001 N HCl eluiert. Die besten Ergebnisse wurden bei der Abtrennung des Magnesiums erzielt, das schon bei der Elution mit der zweifachen Menge des Säulenvolumens quantitativ vom Natrium getrennt im Eluat erscheint.

Die schönsten Beispiele für die Selektivität eines Ionenaustauschers und für die Eleganz einer Trennmethode liefern Trennungen von Spuren eines Elements von grossem Überschuss eines anderen. In diesem Zusammenhang wurde die Trennung des Silbers von den Elementen der 1. und 2. Hauptgruppe des Periodensystems untersucht¹¹. Hier zeigte es sich, dass das Silber, wegen seiner bevorzugten Sorption am CePS I (vgl. die Tabellen I und II) selbst vom Natrium, das im Vergleich zu anderen Elementen ebenfalls fest gebunden wird, abgetrennt werden kann: Wässrige Lösungen von Silbersalzen, die etwa wie das Meerwasser einen rund 10^9 -fachen Überschuss an

Natriumsalzen enthielten ($2.3 \times 10^{-9} M$ AgNO_3 und $0.5 M$ NaClO_4 in der Mischung), wurden über Säulen von CePS I bis zu ca. 30% der totalen Austauschkapazität filtriert. Elution der beladenen Säulen mit $1 N$ HClO_4 führte zur Trennung der beiden Elemente, bei der das Natrium vom fest auf der Säule sorbierten Silber eluiert wurde.

DANK

Der Deutschen Forschungsgemeinschaft danke ich für die Förderung unserer Arbeiten durch die Gewährung von Sach- und Personalmitteln.

ZUSAMMENFASSUNG

Die Kationenselektivität von kristallinen Ce(IV)-phosphat-sulfaten wird diskutiert und an Beispielen von Kationentrennungen demonstriert.

LITERATUR

- 1 K.-H. König und E. Meyn, *J. Inorg. Nucl. Chem.*, 29 (1967) 1153.
- 2 K.-H. König und E. Meyn, *J. Inorg. Nucl. Chem.*, 29 (1967) 1519.
- 3 K.-H. König und G. Eckstein, *J. Inorg. Nucl. Chem.*, 31 (1969) 1179.
- 4 J. Kielland, *J. Amer. Chem. Soc.*, 95 (1937) 1675.
- 5 K.-H. König und G. Eckstein, *J. Inorg. Nucl. Chem.*, 34 (1972) 3771.
- 6 H. Schneider, *Statsexamensarbeit*, Frankfurt/M., 1973.
- 7 R. C. Vicery, *Chemistry of Yttrium and Scandium*, London, 1960.
- 8 G. Eisenman, *Biophys. J.*, 2 (1962) 259.
- 9 S. Schmidt, *Statsexamensarbeit*, Frankfurt/M., 1972.
- 10 K.-H. König und H. Graf, *J. Chromatogr.*, 67 (1972) 200.
- 11 R. Garten, *Diplomarbeit*, Johann-Wolfgang-Goethe-Universität, Frankfurt/M., 1974; *J. Chromatogr.*, im Druck.

CHROM. 7728

PREPARATION OF SOME NEW INORGANIC ION EXCHANGERS

L. SZIRTES and L. ZSINKA

Institute of Isotopes, Hungarian Academy of Sciences, Budapest (Hungary)

SUMMARY

The tellurates of titanium and chromium were investigated. The method of preparation of titanium tellurate is given. Chromium tellurate could not be obtained by the usual methods. Based on various experiments, the composition, solubility and ion-exchange data of amorphous titanium tellurate were obtained.

INTRODUCTION

Some years ago, experiments were carried out on the preparation of zirconium tellurate and during these investigations other ion exchangers based on tellurates were synthesized for comparison. The data concerning zirconium tellurate were reported earlier^{1,2}. This paper deals with the results obtained for titanium and chromium tellurates.

EXPERIMENTAL

Titanium tellurate was prepared as follows. Titanium tetrachloride in 15% hydrochloric acid and 2 *M* telluric acid were mixed with vigorous stirring. The mixture was evaporated on a water-bath with continuous stirring and the residue was cooled to room temperature, washed with re-distilled water to pH 4 and dried over phosphorus pentoxide.

Chromium tellurate was prepared in the same way as zirconium tellurate¹, except that hydrazine hydrate solution was used for the reduction of chromium and tellurium.

The titanium content was determined gravimetrically as titanium oxide, while chromium and tellurium were determined spectrophotometrically.

X-ray measurements were carried out using a Philips PW 1050 high-angle powder diffractometer with Cu K α (Ni filter) radiation ($\lambda = 1.5418 \text{ \AA}$).

The thermoanalytical investigations and the ion-exchange capacity measurements were carried out using methods described earlier^{3,4}. Solubility was controlled by a static method at room temperature.



Fig. 1. Microscope photograph of the titanium tellurate.

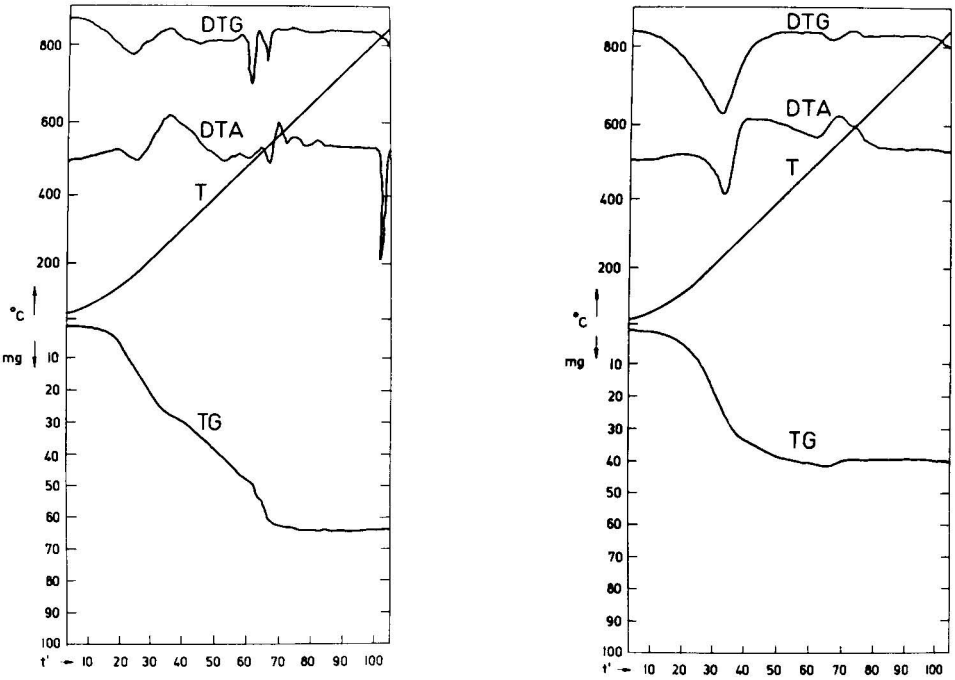


Fig. 2. Thermogram of titanium tellurate. T = Temperature (°C); TG = weight loss (mg) curve; DTG = differential thermogravimetric curve; DTA = differential thermoanalytical curve; t' = time (min).

Fig. 3. Thermogram of chromium tellurate.

RESULTS AND DISCUSSION

The preparation methods used earlier by us and other workers for the synthesis of other ion-exchange materials failed in the case of titanium tellurate. The X-ray diffractograms reveal no peaks for either material. The microscope photograph (Fig. 1) indicates that titanium tellurate is a transparent vitreous material (chromium is not), while both ion exchangers have a shell-like fracture. Based on these observations, we assume that amorphous materials were formed by the methods described.

Based on the analytical data, ratios of $\text{Te}:\text{Ti} = 2.06$ and $\text{Te}:\text{Cr} = 0.2$ were found.

It was found that chromium tellurate has a good solubility in all acids; titanium tellurate is virtually insoluble in alkalis and in various acids; thus it is insoluble in concentrated hydrofluoric and sulphuric acids and can be dissolved very slowly only in hot concentrated hydrochloric acid.

On the thermogram for titanium tellurate (Fig. 2), endothermic processes following weight loss were found with peaks at 170, 335, 500 and 560°. Exothermic peaks were found at 280, 370, 470, 525 and 545°. The first endothermic process is due to the loss of water of crystallisation. The weight losses up to 470° correspond to the release of structural water and the processes above this temperature are due to the reduction $\text{Te}^{6+} \rightarrow \text{Te}^{4+}$.

In Fig. 3 the thermogram for chromium tellurate is shown. Endothermic processes were found at 200 and 495°. The other processes found at 516, 547 and 832° are connected with reactions of tellurium. Comparing the curves found with those in the literature⁵, it can be postulated that we have chromium(III) oxide (Cr_2O_3) with some tellurium oxide adsorbed on the surface. This is supported by the rather weak processes above 500°.

In Fig. 4 the ion uptake data are shown. With titanium tellurate, the character of the curves and the approach of the capacity value to the maximum shows that this material is a real ion exchanger containing functional groups (HTeO_4^-) capable of exchanging H^+ .

With chromium tellurate, we obtained curves typical of oxyhydrates. Comparing these and the thermoanalytical data, it can be stated that the residue is a mixture of chromium and tellurium oxides.

From the above, it follows that the method described for the preparation of

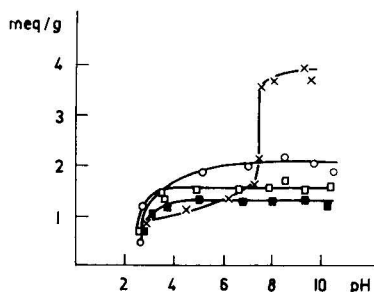


Fig. 4. Exchange capacity data of titanium tellurate: \times , Na^+ ; \circ , K^+ ; \blacksquare , Rb^+ ; \square , Cs^+ .

titanium tellurate is successful, but further investigations are necessary in order to clarify all details and to obtain crystalline titanium tellurate.

REFERENCES

- 1 L. Szirtes and L. Zsinka, *Proc. 2nd Symp. on Ion Exchange, Balatonszéplak, Hungary, 1969*, Vol. IIb, Magyar Kemikusok Egy., Budapest, 1969, p. 627.
- 2 L. Szirtes and L. Zsinka, *Radiochem. Radioanal. Lett.*, 7 (1971) 61.
- 3 L. Szirtes, L. Zsinka, K. B. Zaborenko and B. Z. Iofa, *Acta Chim. (Budapest)*, 54 (1967) 215.
- 4 L. Zsinka and L. Szirtes, *Acta Chim. (Budapest)*, 69 (1971) 249.
- 5 L. Erdey, *A Kémiai Analízis Szükszerinti Módszeret*, Akadémiai Kiadó, Budapest, 1960. p. 372.

CHROM. 7721

INFRARED AND X-RAY MEASUREMENTS ON VARIOUS INORGANIC ION EXCHANGERS

L. ZSINKA, L. SZIRTES and J. MINK

Institute of Isotopes, Hungarian Academy of Sciences, Budapest (Hungary)

and

A. KÁLMÁN

Central Research Institute for Chemistry, Hungarian Academy of Sciences, Budapest (Hungary)

SUMMARY

Investigations were carried out on crystalline cerium phosphate and arsenate in the lithium, sodium, potassium and caesium forms. The various salt forms were prepared according to the results obtained in ion uptake measurements. It was found that the water loss up to 150° is about one mole of water of crystallization. The bands belonging to structural water decrease with increase in the alkali metal content.

The stretching frequencies are characteristic of HAsO_4^{3-} and PO_4^{3-} groups, changing according to the ionic radii, *i.e.*, samples with different alkali metal contents have different structures.

INTRODUCTION

Investigations have been carried out on crystalline cerium arsenate and phosphate in the lithium, sodium, potassium, rubidium and caesium forms, and the results obtained with these samples are discussed in this paper. The samples were synthesized according to Alberti *et al.*¹. The X-ray and IR measurements were carried out as described elsewhere². The cerium content of the samples was determined by the method of Greenhous *et al.*³, the alkaline metal content with flame photometry.

RESULTS AND DISCUSSION

The ion uptake results for different forms of the ion exchangers are shown in Fig. 1. These results are in good agreement with those obtained analytically and calculated from the weight losses (Table I). According to these results, most of the samples were dried at 150° for the further investigations.

Based on the analytical measurements performed, the following compositions have been calculated:

CeAs-H	$\text{Ce}(\text{HAsO}_4)_2 \cdot 0.5\text{H}_2\text{O}$ main product
CeAs-Li/1	$\text{Ce}(\text{Li}_{0.37} \text{H}_{0.60} \text{AsO}_4)_2 \cdot 1.10\text{H}_2\text{O}$
CeAs-Li/2	$\text{Ce}(\text{Li}_{0.65} \text{H}_{0.39} \text{AsO}_4)_2 \cdot 0.67\text{H}_2\text{O}$
CeAs-Na/1	$\text{Ce}(\text{Na}_{0.40} \text{H}_{0.64} \text{AsO}_4)_2 \cdot 0.60\text{H}_2\text{O}$

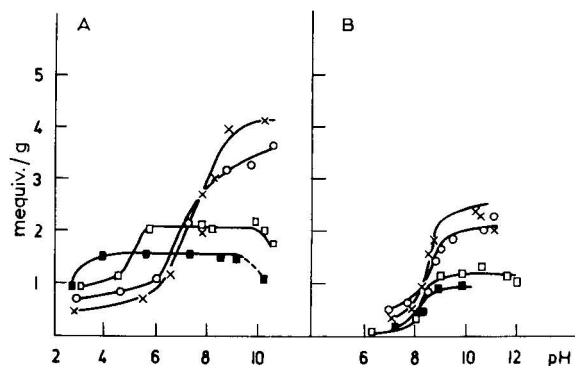


Fig. 1. Ion uptake curves: \times , Li^+ ; \circ , Na^+ ; \square , K^+ ; \blacksquare , Cs^+ . A, Cerium arsenate; B, cerium phosphate.

TABLE I
WEIGHT LOSSES AT VARIOUS TEMPERATURES

Sample	Weight losses (%)		
	150°	200°	400°
CeAs-H	0	2.10	4.20
CeAs-Li/1	2.20	4.59	6.53
CeAs-Li/2	—	2.82	4.53
CeAs-Na/1	1.08	2.57	5.41
CeAs-Na/2	0.31	0.43	0.51
CeAs-K/1	1.10	2.59	5.46
CeAs-Rb/1	1.16	2.60	5.90
CeAs-Cs/1	1.20	2.63	6.10
CeP-H	1.60	2.50	7.20
CeP-Li/1	1.40	2.63	4.30
CeP-Li/2	1.30	2.50	3.64
CeP-Na/1	1.80	3.60	4.95
CeP-K/1	1.61	3.08	6.10

TABLE II
FIRST INTERPLANAR DISTANCES

Sample	d (Å)	Sample	d (Å)	Sample	d (Å)
CeAs-H (25°)	9.25	CeAs-Li/2 (25°)	8.67	CeP-H (25°)	15.39
CeAs-Li/1 (25°)	8.92	CeAs-Li/2 (150°)	8.40	CeP-Li/1 (25°)	14.72
CeAs-Li/1 (150°)	7.97	CeAs-Na/2 (25°)	10.62	CeP-Li/1 (150°)	14.48
CeAs-Na/1 (25°)	8.33	CeAs-Na/2 (150°)	9.26	CeP-Na/1 (25°)	14.48
CeAs-Na/1 (150°)	9.02	CeAs-K/2 (25°)	—	CeP-Na/1 (150°)	14.06
CeAs-K/1 (25°)	8.76	CeAs-K/2 (150°)	—	CeP-K/1 (25°)	14.22
CeAs-K/1 (150°)	8.67	CeAs-Rb/1 (25°)	—	CeP-K/1 (150°)	13.80
CeAs-Rb/1 (25°)	8.96	CeAs-Cs/1 (25°)	—		
CeAs-Cs/1 (25°)	9.28				

CeAs-Na/2	$\text{Ce}(\text{Na}_{0.99} \text{H}_{0.01} \text{AsO}_4)_2 \cdot 0.10\text{H}_2\text{O}$
CeAs-K/1	$\text{Ce}(\text{K}_{0.43} \text{H}_{0.06} \text{AsO}_4)_2 \cdot 0.76\text{H}_2\text{O}$
CeAs-Rb/1	$\text{Ce}(\text{Rb}_{0.28} \text{H}_{0.70} \text{AsO}_4)_2 \cdot 0.87\text{H}_2\text{O}$
CeAs-Cs/1	$\text{Ce}(\text{Cs}_{0.23} \text{H}_{0.75} \text{AsO}_4)_2 \cdot 0.90\text{H}_2\text{O}$
CeP-H	$\text{Ce}(\text{HPO}_4)_2 \cdot 0.33\text{H}_2\text{O}$ main product
CeP-Li/1	$\text{Ce}(\text{Li}_{0.6} \text{H}_{0.4} \text{PO}_4)_2 \cdot 0.27\text{H}_2\text{O}$
CeP-Li/2	$\text{Ce}(\text{Li}_{0.75} \text{H}_{0.25} \text{PO}_4)_2 \cdot 0.25\text{H}_2\text{O}$
CeP-Na/1	$\text{Ce}(\text{Na}_{0.57} \text{H}_{0.43} \text{PO}_4)_2 \cdot 0.35\text{H}_2\text{O}$
CeP-K/1	$\text{Ce}(\text{K}_{0.22} \text{H}_{0.78} \text{PO}_4)_2 \cdot 0.31\text{H}_2\text{O}$

In Tables II–IV the X-ray data are collected. The data indicate that all the samples examined are crystalline. After heating to 150° , because of the loss of water, the lattices shrunk, which can be followed by comparing the first interplanar distances of the corresponding samples in Table II.

The results of the infrared (IR) investigations and conclusions that can be drawn concerning the structure are discussed below.

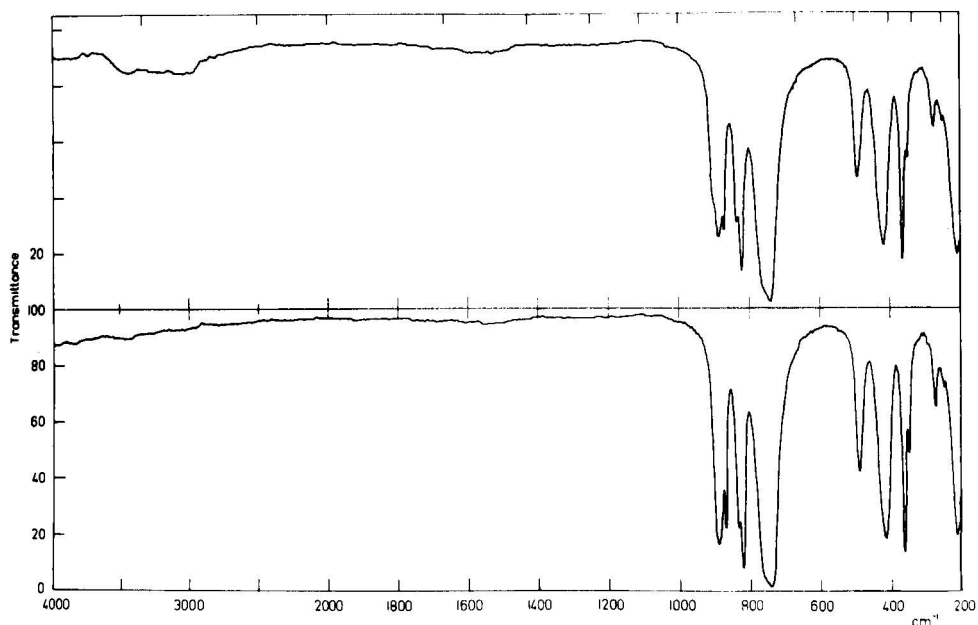


Fig. 2. IR spectra of cerium arsenate in the sodium form. 1, CeAs-Na/2 (25°); 2, CeAs-Na/2 (150°).

In Fig. 2 the IR spectra of arsenates in sodium form (normal and heated to 150°) are shown as an example. When the sample is heated, the band width decreases, giving a more definite band separation which, in accordance with X-ray data, indicates a higher degree of crystallinity. The above change in crystalline structure could be ascribed to the decrease in the water content of the sample, which is demonstrated by decreasing band intensities of molecular water at about 3600 and 1640 cm^{-1} .

The IR spectra of samples containing different amounts of alkali metals indicate that the relative band intensities (at about 2950 , 2340 and 1200 cm^{-1}) decrease

TABLE III

DATA FROM X-RAY MEASUREMENTS AT 25°

Abbreviations: vs = very strong; s = strong; m = medium; w = weak; vw = very weak.

<i>CeAs-H</i>	<i>CeAs-Li 1</i>	<i>CeAs-Li 2</i>	<i>CeAs-Na 1</i>	<i>CeAs-Na 2</i>	<i>CeAs-K 1</i>	<i>CeAs-Rb 1</i>	<i>CeAs-Cs 1</i>
—	—	—	9.18 vw	—	11.18 vw	—	—
—	—	—	—	—	9.61 vw	—	—
9.25 vs	8.92 vs	8.67 vs	8.33 vs	10.62 vs	8.76 vs	8.96 vs	9.28 vs
—	8.19 w	—	—	9.24 w	—	—	—
3.80 w	—	—	—	3.95 v w	—	—	—
3.75 vw	—	—	—	—	—	—	—
—	—	3.60 vw	3.66 w	—	—	—	—
—	—	—	—	—	—	—	—
—	—	—	—	—	—	—	—
—	—	3.33 vw	—	—	—	—	3.33 w
—	3.29 w	—	—	—	—	3.28 w	—
—	—	—	—	3.24 w	3.23 w	—	—
—	—	—	—	3.18 w	—	—	—
—	—	—	—	—	3.10 w	3.10 w	3.12 m
3.09 m	3.09 w	3.06 w	3.08 w	3.06 w	—	3.06 w	3.07 w
—	—	—	—	—	3.02 vw	—	—
2.94 w	—	—	—	—	2.94 w	—	—
—	—	—	2.90 w	2.91 vw	2.92 vw	—	—
—	—	—	2.72 vw	—	—	—	—
—	—	—	—	2.68 m	—	—	—
—	—	—	—	2.57 w	—	—	—
2.46 w	—	—	—	—	2.49 vw	—	—
2.43 vw	—	—	—	2.45 vw	—	2.41 vw	2.59 vw
—	—	—	—	—	—	—	—
2.31 w	—	—	—	—	—	—	—
—	—	—	2.28 vw	2.23 vw	2.18 vw	—	—
2.05 vw	2.04 vw	—	2.04 vw	—	2.05 vw	2.05 vw	2.05 vw
<i>CeP-H</i>	<i>CeP-Li 1</i>	<i>CeP-Li 2</i>	<i>CeP-Na 1</i>	<i>CeP-Na 2</i>	<i>CeP-K 1</i>	<i>CeP-Rb 1</i>	<i>CeP-Cs 1</i>
—	—	—	—	—	14.67 m	—	—
15.39 vs	14.72 vs	—	14.48 vs	—	14.22 vs	—	—
7.86 m	—	—	—	—	—	—	—
—	7.34 w	—	7.30 w	—	7.31 m	—	—
—	—	—	—	—	—	—	—
—	6.41 vw	—	—	—	—	—	—
—	—	—	—	—	5.95 vw	—	—
5.54 w	5.54 vw	—	—	—	—	—	—
5.26 m, s	—	—	—	—	—	—	—
—	4.88 m	—	4.87 m	—	—	—	—
—	—	—	4.69 vw	—	—	—	—
4.43 m	—	—	—	—	4.59 m	—	—
—	—	—	—	—	—	—	—
3.95 s	—	—	—	—	3.99 vw	—	—
3.66 w	3.65 m	—	3.66 m, s	—	3.66 m, s	—	—
—	—	—	3.51 vw	—	—	—	—
3.41 m	3.41 vw	—	3.40 vw	—	3.42 vw	—	—
—	—	—	—	—	—	—	—
—	3.29 vw	—	—	—	—	—	—
3.16 m	—	—	—	—	—	—	—
3.10 vw	—	—	—	—	—	—	—
2.94 m	2.95 vw	—	2.92 vw	—	2.94 vw	—	—
—	—	—	—	—	2.87 vw	—	—
2.71 vw	—	—	—	—	—	—	—
2.64 vw	—	—	—	—	—	—	—
—	2.43 w	—	—	—	2.44 w	—	—

TABLE IV

DATA FROM X-RAY MEASUREMENTS AT 150°

<i>CeAs-H</i>	<i>CeAs-Li/1</i>	<i>CeAs-Li/2</i>	<i>CeAs-Na/1</i>	<i>CeAs-Na/2</i>	<i>CeAs-K/1</i>	<i>CeAs-Rb/1</i>	<i>CeAs-Cs/1</i>
—	—	—	9.02 vw	—	—	—	—
—	—	—	—	—	—	—	—
—	7.97 vs	8.40 vs	9.02 vs	9.26 vs	8.67 vs	—	—
—	—	4.18 w	—	4.60 vw	—	—	—
—	3.97 vw	—	—	3.74 vw	—	—	—
—	—	—	—	—	—	—	—
—	3.55 w	3.60 w	3.63 w	—	—	—	—
—	—	—	—	3.39 w	—	—	—
—	3.36 vw	—	—	3.34 w	—	—	—
—	—	—	—	—	—	—	—
—	—	3.29 vw	—	—	—	—	—
—	—	3.24 vw	—	—	3.21 w	—	—
—	—	3.18 vw	—	—	—	—	—
—	3.13 w	—	—	—	3.10 w	—	—
—	3.08 w	3.04 w	3.08 w	3.06 m	—	—	—
—	—	—	—	—	—	—	—
—	—	—	—	—	2.94 w	—	—
—	—	—	2.89 w	2.90 s	2.90 vw	—	—
—	—	2.72 w	2.71 vw	2.74 m	—	—	—
—	2.64 w	—	—	2.69 m	—	—	—
—	—	—	—	—	—	—	—
—	—	—	—	—	2.47 vw	—	—
—	2.41 vw	—	—	—	—	—	—
—	—	—	2.34 vw	2.37 vw	2.36 vw	—	—
—	—	—	—	2.30 w	—	—	—
—	—	—	—	—	2.16 vw	—	—
—	2.04 vw	2.05 vw	2.04 vw	—	2.05 vw	—	—
<hr/>							
<i>CeP-H</i>	<i>CeP-Li/1</i>	<i>CeP-Li/2</i>	<i>CeP-Na/1</i>	<i>CeP-Na/2</i>	<i>CeP-K/1</i>	<i>CeP-Rb/1</i>	<i>CeP-Cs/1</i>
—	—	—	—	—	14.25 m	—	—
—	14.48 vs	—	14.06 vs	—	13.80 vs	—	—
—	—	—	—	—	—	—	—
—	7.26 w	—	7.02 w	—	7.14 vw	—	—
—	—	—	—	—	6.83 w	—	—
—	6.38 vw	—	—	—	—	—	—
—	—	—	5.92 vw	—	5.94 vw	—	—
—	5.45 vw	—	5.42 vw	—	—	—	—
—	—	—	—	—	—	—	—
—	4.84 m	—	—	—	4.77 w	—	—
—	—	—	4.69 m	—	—	—	—
—	—	—	—	—	4.52 w	—	—
—	—	—	4.03 vw	—	—	—	—
—	—	—	—	—	—	—	—
—	3.64 m	—	—	—	—	—	—
—	3.54 w	—	3.52 m	—	3.57 vw	—	—
—	—	—	3.41 vw	—	3.42 w	—	—
—	—	—	—	—	3.38 w	—	—
—	3.28 vw	—	—	—	—	—	—
—	—	—	—	—	—	—	—
—	—	—	3.10 vw	—	—	—	—
—	2.91 vw	—	2.90 vw	—	2.94 vw	—	—
—	—	—	—	—	2.86 vw	—	—
—	—	—	—	—	—	—	—
—	—	—	—	—	—	—	—
—	2.45 vw	—	—	—	2.43 vw	—	—

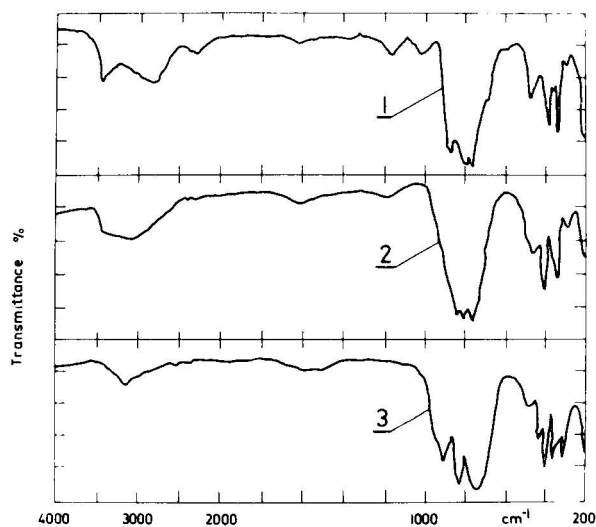


Fig. 3. IR spectra of cerium arsenate in the hydrogen and lithium forms. 1, CeAs-H; 2, CeAs-Li/1; 3, CeAs-Li/2.

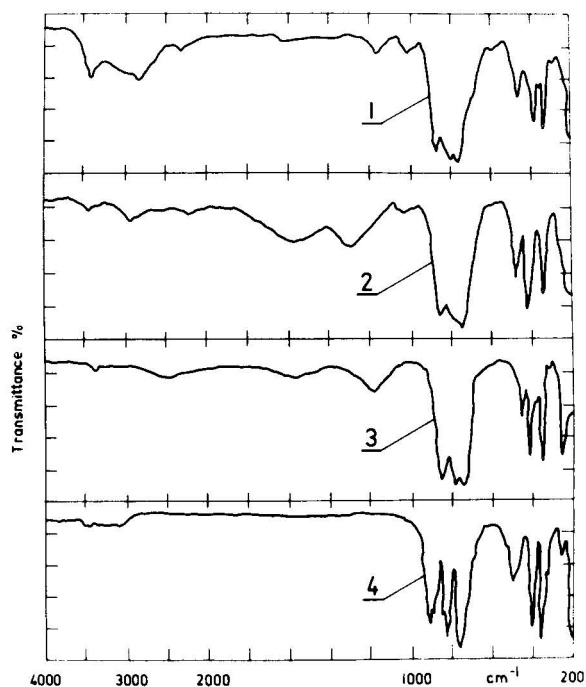


Fig. 4. IR spectra of cerium arsenate in the hydrogen, potassium and sodium forms. 1, CeAs-H; 2, CeAs-K/1; 3, CeAs-Na/1; 4, CeAs-Na/2.

proportionally with increasing alkali metal content of the sample, as is shown for the Li^+ form of cerium arsenate in Fig. 3. The relative intensity of the bands assigned to AsO_4^{3-} groups becomes more characteristic with increasing Li^+ content. This IR pattern unambiguously verified the H^+ exchange of the acidic HAsO_4^{2-} groups.

Comparison of the spectra of samples assigned under $\text{Me}^+/1$ (Fig. 4) indicates that these materials have a similar type of lattice. In the spectra of all samples, bands relating to acidic HAsO_4^{2-} groups (3000 , 2320 , 1300 – 1200 and 1050 cm^{-1}) can be found. If the alkali metal content approaches the total capacity value, these frequencies virtually disappear and only the bands relating to water of crystallization evaporating at 150° (3150 and *ca.* 1600 cm^{-1}) are visible.

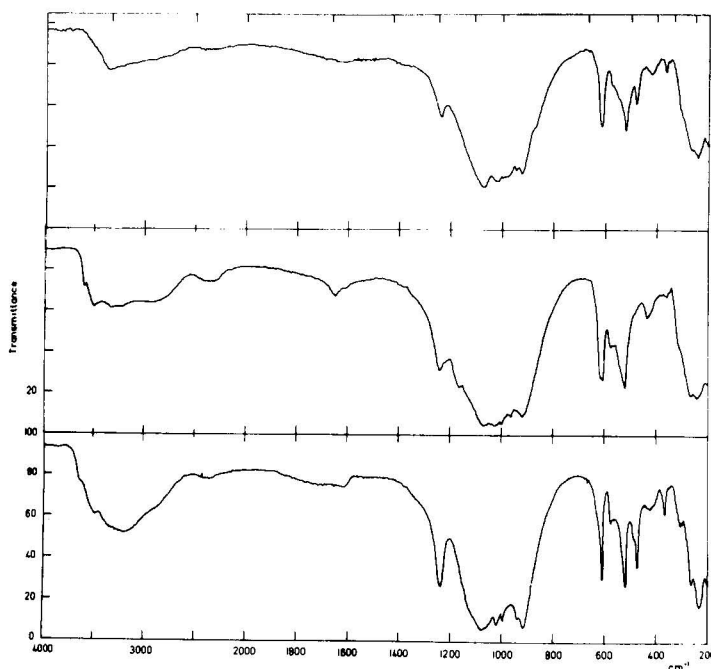


Fig. 5. IR spectra of cerium phosphate in the hydrogen and sodium forms. 1, CeP-H; 2, CeP-Na/1 (25°); 3, CeP-Na/1 (150°).

The IR spectra of cerium phosphates are shown in Fig. 5. The bands assigned to acidic HPO_4^{2-} groups (2350 and 1230 cm^{-1}) were established. Comparing the IR spectroscopic behaviour of cerium arsenates and phosphates, similar conclusions can be drawn. The decreasing intensities of HPO_4^{2-} bands according to the alkali metal content and the considerable water loss at 150° in the Na^+ form cerium phosphate can be seen in Fig. 5 (see the bands at 3500 and 1650 cm^{-1}). It may be noticed that sodium–hydrogen exchange is less stoichiometric than those with cerium arsenate (see the band at 1240 cm^{-1}). The influence of the alkali metal cation content on the IR spectra of arsenates and phosphates has been investigated and the characteristic bands are given in Table V.

It can be seen from Table V that the stretching frequencies of As–O at about

TABLE V
FREQUENCY DATA

Species	Frequency					
CeAs-Me ⁺ /1	<i>Li</i>	<i>Na</i>	<i>K</i>	<i>Rb</i>	<i>Cs</i>	
	850 w	840 w	845 w	848 w	848 w	} As-O stretching
	760 vs	790 vs	765 vs	785 vs	784 vs	
		750 vs				
	470 w	482 w	478 w	481 w	476 w	} O-As-O deformation
	408 w	416 w	416 w	418 w	413 w	
	354 w, m	347 w, m	350 w, m	350 w, m	344 w, m	
	260 m	220 m	~200 m	~200 m	~200 m	Lattice vibration
CeAs-Me ⁺ /2	<i>Li</i>	<i>Na</i>				
	921 m	892 m				
	896 w	870 w				
	825 m	822 m	} As-O stretching			
	740 vs	752 vs				
	420 m	418 m				
	370 w	364 w				
	326 m	275 m	Lattice vibration			
CeP-Me ⁺ /1	<i>Li</i>	<i>Na</i>	<i>K</i>			
	1035 vs	1065 vs	1070 vs			
		1025 m	1020 m			
	915 vs	915 vs	915 vs			
	600 m	610 m	610 m			
	520 m, w	518 m	518 m			
	455 vw	480 w	472 m			
	421 vw	430 w	418 w			
	370 vw	365 w	364 w			
	250 m	240 m	232 m			

760 cm⁻¹ and P-O at about 1060 cm⁻¹, characteristic of AsO₄³⁻ and PO₄³⁻ groups, respectively, changed as the ionic radii varied; at the same time, the lattice vibrations (200–260 cm⁻¹) decrease, probably because of the increase in the distance between the anions. The other frequencies can probably be assigned to such types of AsO₄³⁻ and PO₄³⁻ vibrational forms that have no influence on the cation-anion interaction. The crystal lattice interaction should decrease, *i.e.*, we approach nearer to the fundamental frequencies of “free” anionic groups (having no perturbation). The above consideration seems to be true for the samples marked Me⁺/2 (arsenates), and it is evident from the character of the spectra that the completely saturated samples should have a different crystalline structure.

REFERENCES

- 1 G. Alberti, U. Costantino, F. di Georgio and E. Torracca, *J. Inorg. Nucl. Chem.*, 31 (1969) 3195.
- 2 L. Zsinka, L. Szirtes, J. Mink and A. Kálmán, *J. Inorg. Nucl. Chem.*, 36 (1974) 1147.
- 3 H. C. Greenhous, E. M. Feibush and L. Gordon, *Anal. Chem.*, 29 (1957) 1531.

CHROM. 7727

NEUE ERGEBNISSE ÜBER DIE POROSITÄT VON STYROL-DIVINYLBENZOL-COPOLYMERISATEN UND IONENAUSTAUSCHERHARZEN

KLAUS HÄUPKE und VOLKER PIENTKA

VEB Chemiekombinat Bitterfeld, Forschungsbereich Ionenaustauscher, Bitterfeld (D.D.R.)

SUMMARY

New results on the porosity of styrene-divinylbenzene copolymers and ion-exchange resins

The porous structure of styrene-divinylbenzene copolymers formed in the presence of an aliphatic hydrocarbon consists of a permanent and an instable part. Together these two parts constitute maximum porosity, which is found to be in a better relationship to the properties of ion exchangers made from the polymers than the stable part alone.

EINLEITUNG

Makroporöse Polymerisate auf Styrolbasis finden heute eine breite Anwendung, z.B. zur Herstellung von Ionenaustauscherharzen. Zu ihrer Herstellung werden meist Styrol und Divinylbenzol in Gegenwart einer inerten Flüssigkeit, die sich mit den Monomeren mischt, das Polymere aber nicht quillt, copolymerisiert. Bei bestimmten Verhältnissen zwischen Styrol, Divinylbenzol und der inerten Flüssigkeit resultieren dabei Polymere mit messbarer Porosität und innerer Oberfläche. Aus ihnen können dann Austauscherharze mit ähnlicher Porenstruktur hergestellt werden.

Ebenso wie andere Autoren (z.B. Lit. 1-5) haben auch wir solche Polymerisate hergestellt und ihre Porositäten gemessen. Dabei hatten wir aber immer die inerte Flüssigkeit mit einem quellenden Lösungsmittel extrahiert oder unter Anwendung hoher Temperaturen entfernt^{6,7}.

Wenn wir nun versuchen, die inerte Flüssigkeit, in unserem Falle ein Gemisch aliphatischer Kohlenwasserstoffe, mit einem nichtquellenden Lösungsmittel (z.B. Methanol) zu extrahieren und das Polymerisat anschliessend bei Raumtemperatur zu trocknen, finden wir bei gegebenen Verhältnissen zwischen Styrol, Divinylbenzol und der inerten Flüssigkeit vielfach höhere Porositäten (und auch höhere spezifische Oberflächen), als bei unseren früheren Messungen. Dieser Porositätsanstieg ist jedoch nicht stabil. Durch Erwärmen der Polymerisate über 80° oder durch Quellen in einem guten Quellmittel und anschliessendes Trocknen verschwindet er und es verbleiben nur die bekannten Werte.

Wir müssen also eine nur durch spezielle Behandlung realisierbare Maximal-

porosität und deren stabilen Anteil, der aus älteren Untersuchungen bekannt ist, unterscheiden.

EXPERIMENTELLE ERGEBNISSE

Zuerst arbeiteten wir einen besseren Weg, als den oben angedeuteten, aus, um die Maximalporosität zu realisieren: In üblicher Weise hergestellte poröse Polymerisate, die also nur den stabilen Anteil der Porosität aufwiesen, wurden in Toluol gequollen und das Toluol mit Methanol ausgewaschen. Die Polymerisate wurden dann bei Raumtemperatur in strömender Luft getrocknet. Diese Behandlung wollen wir im Folgenden kurz "Porenöffnen" und die so behandelten Polymerisate "maximal porös" nennen. Wir behandelten eine Anzahl von Styrol-Divinylbenzol-Copolymerisaten (vernetzt mit 5–50 Gew. % Divinylbenzol, bezogen auf das Monomergewicht), die durch Suspensionspolymerisation in Gegenwart von unterschiedlichen Mengen (10–60 Gew. %, bezogen auf die Gesamtmasse der organischen Phase) eines Gemisches aliphatischer Kohlenwasserstoffe hergestellt worden waren, in dieser Weise. Tabelle I zeigt die Porositäten (ml Porenvolumen/g Polymerisat) der Polymerisate vor und nach

TABELLE I

POROSITÄTEN (ml/g) VON POLYMERISATEN IM ZUSTAND DER STABILEN (OBERE WERTE) UND DER MAXIMALEN (UNTERE WERTE) POROSITÄT

% DVB = Vernetzungsgrad in Gew. % Divinylbenzol der Monomerenmasse; % I.L. = Gehalt an inerter Flüssigkeit in Gew. %, bezogen auf die Gesamtmasse Monomere + inerte Flüssigkeit.

% I.L.	% DVB							
	5	10	15	20	25	35	42.5	50
60		4.00*		2.66*		3.25*		2.48
		2.38		2.94		3.33		2.48
55			2.74*		2.32		2.28	
			2.61		2.38		2.38	
50	0.19	1.79		1.75		1.72		1.62
	1.63	1.86		1.80		1.83		1.70
45					1.34			
					1.35			
40	0.03	0.53						
	0.54	1.00						
35	0	0.04	0.83	0.67	0.88	0.46	0.79	0.73
	0	0.80	0.88	0.72	0.93	0.85	0.93	0.85
30	0	0						
	0	0.33						
25		0	0.12	0.31	0.45			
		0.06	0.30	0.36	0.58			
20	0	0	0			0		0.27
	0	0	0.07			0.25		0.34
15					0	0	0.08	
					0.09	0.13	0.10	0.25
10			0			0		0.04
			0			0		0.07

* Polymerisate mangelhafter Stabilität (vgl. Fig. 2, Bereich V).

der Behandlung, d.h.,¹ der maximal porösen und der stabil porösen Polymerisate.

In allen Fällen, in denen für die Ionenaustauschersynthese brauchbare Zwischenprodukte erhalten worden waren, zeigt das Polymerisat mit geöffneten Poren zumindest die gleiche, meist aber eine höhere Porosität, als das normale Polymerisat.

Wir beobachteten also eine Erweiterung des Feldes der "echten Makroporosität" (vgl. Lit. 6 und 7) und eine Porositätserrhöhung bei vielen nach älterer Auffassung "echt makroporösen" Polymerisaten durch das Porenöffnen. In Fig. 1 sind die Bereiche der "stabilen" und der "maximalen" Porosität in Abhängigkeit vom Vernetzungsgrad und vom Gehalt an inerte Flüssigkeit dargestellt.

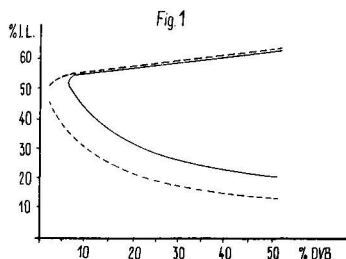


Fig. 1. Bereiche der stabilen (—) und der maximalen (---) Porosität in Abhängigkeit vom Vernetzungsgrad und vom Gehalt an inerte Flüssigkeit (angegeben wie bei Tabelle I).

Hieraus ergibt sich auch die Möglichkeit einer korrekteren Definition der "Halbporosität"^{6,7} als des Bereiches, in dem keine stabile Porosität vorliegt, durch das Porenöffnen aber messbare Porosität erzeugt werden kann.

Mit steigendem Vernetzungsgrad sinkt der Effekt des Porenöffnens. Die hochvernetzten Polymerisate sind in ihrer Porosität also stabiler.

Für die Diskussion dieser Ergebnisse ist es notwendig, noch eine andere Beobachtung darzulegen: Wir fanden, dass solche "nichtquellenden" Lösungsmittel wie unser Kohlenwasserstoffgemisch bei Temperaturen über 80° durchaus Quellmittel für poröse Polymerisate sind. Das Ergebnis dieser Quellung bei hoher Temperatur ist ein Zustand, der dem des noch heißen Polymerisates bei beendeter Polymerisation entspricht. 80° muss eine kritische Temperatur für das Styrol-Divinylbenzol-Copolymerisat sein, bei der eine Strukturveränderung, die das Eindringen von "Nichtquellmitteln" erlaubt, vor sich geht. Es ist sicher kein Zufall, dass die niedrigsten Werte für den Schmelzpunkt von linearem Polystyrol, die in der Literatur angegeben werden⁸, bei der gleichen Temperatur liegen.

Wenn also z.B. Toluol schon bei Raumtemperatur die intermicellaren Räume in unseren Polymerisaten füllen und ausserdem intramicellar die Polystyrolketten solvatisieren kann, so können aliphatische Kohlenwasserstoffe oberhalb 80° die Intermicellarräume füllen und das Polymerisat auf diese Weise quellen lassen.

DISKUSSION

Wir erklären die beobachteten Erscheinungen durch das Zusammenwirken verschiedener Mechanismen der Entmischung während der Polymerisation:

Die hohe Temperatur bei der Polymerisation bewirkt eine gewisse Quellung des

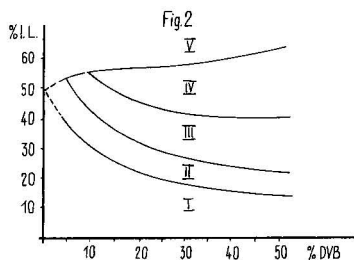


Fig. 2. Bereiche der verschiedenen Entmischungsmechanismen, dargestellt analog Fig. 1.

Polymeren durch den inerten Hilfsstoff, deren maximaler Grad von der Vernetzung abhängt und der Grenze zwischen den Gebieten I und II in Fig. 2 entspricht.

Im Gebiet I entsteht also keine Porosität. Die inerte Flüssigkeit diffundiert spätestens bei ihrer Entfernung aus dem Polymerisat heraus und hinterlässt es in einem "modifiziert gelartigen" Zustand. Die Toluolquellung ist erhöht, oberhalb 80° ist eine Quellung in Aliphaten möglich.

Im Gebiet II wird bei einem gewissen Grad des Monomerenverbrauchs, und zwar nach dem Gelpunkt, die Gleichgewichtsquellung des Polymerisates in der inerten Flüssigkeit überschritten und es scheiden sich Mikrotropfen derselben aus. Bei der Entfernung dieses Hilfsstoffes diffundieren sie aus der kohärenten Matrix heraus, die dabei (wenn Quellmittel zugegen sind oder hohe Temperaturen angewendet werden) völlig kollabiert, so dass die Poren nur potentiell vorhanden bleiben, aber z.B. durch das Porenöffnen jederzeit wieder erzeugt werden können. Hier liegt also "Halbporosität" vor.

Im Gebiet IV erfolgt die Entmischung dagegen nach einem anderen Mechanismus: Noch vor dem Gelpunkt scheiden sich Polymerteilchen mit einem sehr geringen Gehalt an inerten Flüssigkeit ab, die dann später zu einer kohärenten Phase verwachsen. Diese ist von dem ebenfalls kohärenten Porensystem durchzogen, dessen Volumen dem Volumenbruch des inerten Hilfsstoffes nahezu entspricht. Es entsteht eine weitgehend stabile Struktur, die durch das Porenöffnen nicht mehr wesentlich verändert werden kann.

Im Gebiet III laufen die für II und IV beschriebenen Mechanismen nebeneinander ab, so dass ein stabiler (analog Gebiet IV) und ein instabiler (analog Gebiet II) Anteil der Porosität resultiert.

Bei sehr hohen Mengen an inerten Flüssigkeit (Gebiet V) ist schliesslich deren Anteil zu hoch, um ein ausreichend festes poröses Polymerisat entstehen zu lassen. Das Porenöffnen hat hier inverse Effekte, diese Zusammensetzungen sind aber uninteressant, weil die Polymerisate für die Ionenaustauschersynthese zu instabil sind.

AUSBLICK

Abschliessend sollen einige Fakten angedeutet werden, die zeigen, dass die Kenntnis der Maximalporosität einen praktischen Nutzen haben kann:

Es ist bekannt, dass Anionenaustauscher, die aus "nicht porösen" Polymerisaten (d.h., solchen ohne stabile Porosität) hergestellt werden, echt makroporös sein können. Wir fanden, dass alle Anionenaustauscher, die wir hergestellt haben, eine

der Maximalporosität der Polymerisates qualitativ analoge Porosität hatten. Andererseits fanden wir bei stark sauren Kationenaustauschern eine Porosität, die recht genau 50% der Maximalporosität des entsprechenden Polymerisates betrug. Zwischen der stabilen Porosität des Polymerisates und der des Endproduktes hatten sich solche Zusammenhänge nicht ergeben⁷.

Wir können also aus der Kenntnis der Maximalporosität eines Polymerisates mehr Eigenschaften eines daraus hergestellten Austauscherharzes vorhersagen, als aus dem stabilen Porositätsanteil.

ZUSAMMENFASSUNG

Die Porosität von Styrol-Divinylbenzol-Copolymerisaten, die in Gegenwart eines aliphatischen Kohlenwasserstoffes hergestellt wurden, setzt sich aus einem permanenten und einem instabilen Anteil zusammen. Beide zusammen bilden die Maximalporosität, von der gefunden wurde, dass sie in einem besseren Zusammenhang zu den Eigenschaften der aus den Polymerisaten hergestellten Ionenaustauscher steht, als der permanente Anteil allein.

LITERATUR

- 1 G. O. Roberts und J. R. Millar, *Ion Exchange in the Process Industry, Conf., London, 1969*, Society of Chemical Industry, London, 1970, S. 42–46.
- 2 R. Kunin, *Ion Exchange in the Process Industry, Conf., London, 1969*, Society of Chemical Industry, London, 1970, S. 10–15.
- 3 J. A. Mikes, *Ion Exchange in the Process Industry, Conf., London, 1969*, Society of Chemical Industry, London, 1970, S. 16–23.
- 4 J. Seidl, J. Malinský, K. Dušek und W. Heitz, *Advan. Polym. Sci.*, 5 (1967) 113.
- 5 F. Krska, *Dissertation*, Pardubice, 1970.
- 6 K. Häupke und H. Hoffmann, in H. Reuter (Herausgeber), *Ionenaustauscher in Einzeldarstellungen*, Bd. 8, *Symposiumsbericht, Leipzig, 1968*, Akademie-Verlag, Berlin, 1970, S. 158–165.
- 7 K. Häupke und H. Hoffman, in J. A. Mikes (Herausgeber), *Symp. Ion Exchange*, 2, Budapest, 1969, Vol. I, S. 155–162.
- 8 A. J. Staverman und F. Schwarzl, in H. A. Stuart (Herausgeber), *Die Physik der Hochpolymeren*, Bd. IV, *Theorie und molekulare Deutung technologischer Eigenschaften von hochpolymeren Werkstoffen*, Springer, Berlin, Göttingen, Heidelberg, 1956, S. 18.

CHROM. 7712

UNTERSUCHUNG ZUR HERSTELLUNG STARK SAURER KATIONEN-AUSTAUSCHER AUF DER BASIS VON STYROL-BIS-(4-VINYLPHENYL)-METHAN-COPOLYMEREN

G. SCHWACHULA und D. LUKAS

VEB Chemiekombinat Bitterfeld, 44-Bitterfeld (D.D.R.)

SUMMARY

Study on the preparation of strongly acidic cation exchangers based on copolymers of styrene and bis-(4-vinylphenyl)-methane

Strongly acidic cation-exchange resins based on copolymers of styrene and bis-(4-vinylphenyl)-methane were synthesized and their characteristics were compared with strongly acidic cation-exchange resins based on styrene and technically obtained divinylbenzene. The comparison was made with a particular view to the mechanical stabilities. The higher mechanical stability of resins formed with bis-(4-vinylphenyl)-methane is ascribed to the more uniform structure of the cross-linked copolymer matrix, as appears from the more favourable r values of styrene and bis-(4-vinylphenyl)-methane.

EINFÜHRUNG

Eigene Untersuchungen haben uns gezeigt, dass Copolymere aus Styrol und Divinylbenzol grosse Inhomogenitäten hinsichtlich der Vernetzungsstellen in Styrol-Divinylbenzol-Copolymeren besitzen¹. Dies hat, wie wir zeigen konnten², seine Ursache in den ungünstigen Reaktivitätsverhältnissen des Styrols mit p - und m -Divinylbenzol (DVB), denn die von Wiley und Mitarbeitern gemessenen Reaktivitätsverhältnisse (r -Werte) lauten für die Copolymerisation von Styrol (M_1) und m -DVB³ (M_2): $r_1 = 0.65$ und $r_2 = 0.60$ und für die Copolymerisation von Styrol (M_1) mit p -DVB⁴ (M_2): $r_1 = 0.14$ und $r_2 = 0.50$.

Entsprechend diesen r -Werten kommt es zu Beginn der Copolymerisation zum Einbau von weit mehr Divinylbenzol in das Copolymere, als es der anfänglichen Zusammensetzung der Monomerenmischung entspricht. Dadurch bewirken die anfangs dichter eingebauten Divinylbenzolbausteine die Bildung von Bereichen engmaschiger, stark verknäulter Netzwerke, zwischen denen langkettige, weniger dicht vernetzte Glieder eingelagert sind, die sich im späteren Stadium der Copolymerisation bilden, wenn der grösste Teil der Divinylbenzolmonomeren bereits verbraucht ist.

Diese bei der Copolymerisation sich bildende Inhomogenität der Verteilung der Vernetzungsstellen zum Beispiel in Styrol- p -DVB-Copolymeren bewirkt eine

schlechte mechanische Beständigkeit der auf Basis Styrol-*p*-DVB-Copolymeren hergestellten stark sauren Kationenaustauscher. So nimmt mit steigendem Divinylbenzolgehalt die mechanische Beständigkeit der stark sauren Kationenaustauscher ab², weil im Copolymerendiagramm von Styrol mit *p*-DVB die Polymerisationskurve bis etwa 16 Mol-% *p*-DVB immer weiter von der idealen Geraden abweicht. Damit lässt sich aber auch postulieren, dass bei Verwendung eines Vernetzers zur Copolymerisation mit Styrol, der dem Styrol nahekommende Reaktivitätsverhältnisse besitzt, die Inhomogenitäten in den Copolymerisaten geringer werden, sowie die daraus hergestellten Kationenaustauscher eine höhere mechanische Festigkeit gegenüber solchen auf Basis Styrol-techn. DVB aufweisen müssten. Als solcher Modellvernetzer kann das Bis-(4-vinylphenyl)-methan für Untersuchungen herangezogen werden, dessen *r*-Werte im System mit Styrol (M_1) von Wiley und Mayberry⁵ bestimmt wurden: $r_1 = 1.0$ und $r_2 = 0.91$.

Sie lassen eine wesentlich bessere Homogenität der Copolymerisate mit Styrol gegenüber solchen aus Styrol mit *p*- oder *m*-DVB erwarten, wie auch aus Fig. 1, in der die Abweichungen von der idealen Geraden im Copolymerendiagramm dieser drei binären Systeme in Abhängigkeit von der Monomerenzusammensetzung im Bereich 0 bis 20 Mol-% Vernetzer dargestellt sind, gut ersichtlich ist. Vor allem im Bereich niedriger Vernetzung, der für die Synthese von Ionenaustauschern besonders wichtig ist, sind die Abweichungen im System Styrol-Bis-(4-vinylphenyl)-methan wesentlich geringer als die von Styrol-*p*-DVB oder Styrol-*m*-DVB.

Ziel unserer Untersuchungen war es, festzustellen, ob auf der Basis eines Copolymerisates von Styrol mit Bis-(4-vinylphenyl)-methan ein stark saurer Kationen-

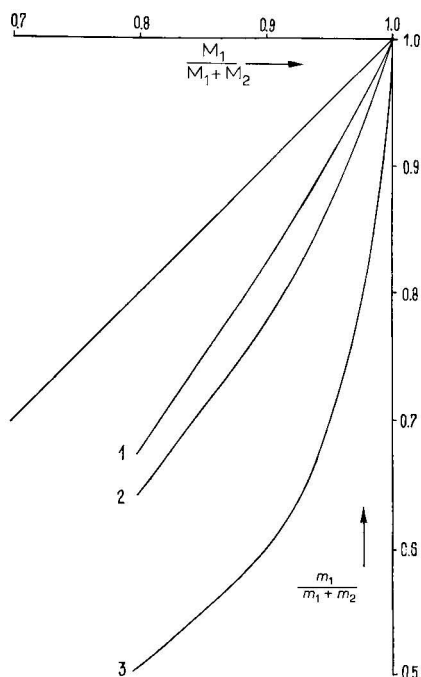


Fig. 1. Ausschnitt aus dem Copolymerendiagramm der drei binären Systeme. 1 = Styrol (M_1)-Bis-(4-vinylphenyl)-methan (M_2); 2 = Styrol (M_1)-*m*-DVB (M_2); 3 = Styrol (M_1)-*p*-DVB (M_2). $M_1/(M_1+M_2)$ = Molenbruch des Monomeren 1; $m_1/(m_1+m_2)$ = Molenbruch des Polymeren 1.

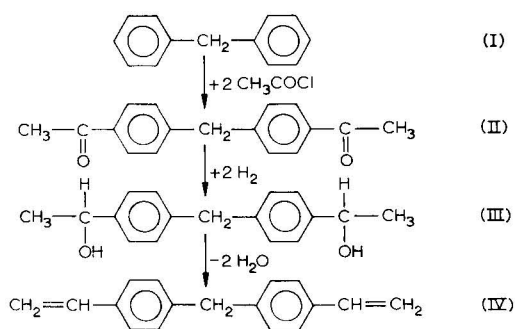
austauscher herstellbar ist, der eine bessere mechanische Festigkeit besitzt als Produkte auf Basis eines Copolymerisates von Styrol mit Divinylbenzol.

EXPERIMENTELLER TEIL

Synthese des Bis-(4-vinylphenyl)-methan

Die Darstellung des Bis-(4-vinylphenyl)-methan als Vernetzer für die Copolymerisation mit Styrol basiert im wesentlichen auf der Vorschrift, die bei Wiley und Mayberry⁵ angegeben wird:

Ausgegangen wird vom Diphenylmethan (I), das nach Friedel und Crafts zur Bisacetylverbindung (II) acetyliert wird. Die Bisacetylverbindung (II) wird nach Meerwein-Ponndorf-Verley mit Aluminiumisopropylat zum entsprechenden Dicarbinol (III) reduziert und dieses durch Dehydratisierung in die Bisvinylverbindung (IV) überführt. Diese Reaktion wurde von uns nicht, wie in Lit. 5, katalytisch bei erhöhter Temperatur durchgeführt, sondern erfolgte nach Traynelis *et al.*⁶ mit wenig konz. Schwefelsäure in Dimethylsulfoxid bei 180° in Anwesenheit von etwas Hydrochinon.



Das erhaltene Produkt wurde mit Isooktan extrahiert und nach Abdampfen des Extraktionsmittels der kristalline Rückstand aus Methanol und Äthanol umkristallisiert.

Herstellung von Massecopolymerisaten

Die Herstellung der Copolymeren aus Styrol und Bis-(4-vinylphenyl)-methan erfolgte mit 0.15 Mol-% Azoisobuttersäuredinitril als Initiator nach der in Lit. 1 angegebenen Methode b in Reagenzgläsern.

Quellungsmessungen

Die Copolymeren aus Styrol und Bis-(4-vinylphenyl)-methan wurden nach der Zerlegung in einzelne Scheiben nach der in Lit. 1 bereits erläuterten Methode zur Messung der maximalen Aufnahme an Dichloräthan und der Ermittlung der Abweichung der Gleichgewichtsquellung Q innerhalb eines Stabes herangezogen.

Es wurden Stäbe aus Styrol und 3 Mol-% Bis-(4-vinylphenyl)-methan, sowie 6 Mol-% Bis-(4-vinylphenyl)-methan hergestellt, in Scheiben zerlegt und von den einzelnen Scheiben die Gleichgewichtsquellung in Dichloräthan bestimmt. Tabelle I

TABELLE I

GLEICHGEWICHTSQUELLUNG Q VON POLYMERISATSTÄBEN AUS 3 BZW. 6 MOL-% BVPM MIT STYROL UND 0.15 MOL-% AZOISOBUTTERSÄUREDINITRIL NACH ZERLEGUNG IN EINZELNE SCHEIBEN

Nr. der Scheibe	Q (mg/g)	
	3 Mol-% BVPM	6 Mol-% BVPM
1	1690.5	1068
2	1706.5	1092
3	1704.5	1089
4	1691.0	1079
5	1708.5	1073
6	1700.0	1076
7	1705.5	1067
8	1703.0	1073
9	1705.0	—
Mittl. Quellung	1701.6	1077
ΔQ	18	25

zeigt die gemessenen Werte für die mit 3 und 6 Mol-% Bis-(4-vinylphenyl)-methan (BVPM) vernetzten Copolymerisate.

Die maximale Quellungsdifferenz ΔQ zwischen zwei Scheiben innerhalb eines Stabes wurde von uns als ein Mass für die Inhomogenität herangezogen.

Herstellung von stark sauren Kationenaustauschern

Die Herstellung von stark sauren Kationenaustauschern auf Basis Styrol und Bis-(4-vinylphenyl)-methan, sowie mit techn. DVB, erfolgte entsprechend den Vorschriften: Die Suspensions-Copolymerisationen wurden in einem Volumenverhältnis von wässriger zu ölgiger Phase wie 5:1 durchgeführt. In einem 1 l-Planschliffbecher mit Rührer, Kontaktthermometer, Rückflusskühler und Tropftrichter wurden 1.5 g $\text{MgSO}_4 \cdot 7 \text{H}_2\text{O}$ in 225 ml dest. Wasser gelöst, die wässrige Phase wurde unter Rühren auf 60° erwärmt. Dann wurde mit einer Lösung aus 0.525 g NaOH in 25 ml dest. Wasser, die langsam zugestropft wurde, Magnesiumhydroxid gefällt. Anschliessend wurde die ölige Phase, die aus den berechneten Mengen Styrol, Vernetzer und jeweils 0.125 Mol-% Initiator N bestand, zugegeben und mittels des Rührers eine Monomerenröpfchengrösse zwischen 0.3 und 0.8 mm eingestellt. Danach wurde das System mit einer Geschwindigkeit von 2.5° pro 15 min auf 95° hochgeheizt und weitere 4 h bei dieser Temperatur gehalten.

Das Copolymerisat wurde anschliessend von der wässrigen Phase getrennt, durch Waschen mit 5%iger Salzsäure von Magnesiumhydroxid befreit und im Trockenschrank 10 h bei 85° nachgehärtet. Das bei der Copolymerisation verwendete technische Divinylbenzol hatte die in Tabelle II angegebene Zusammensetzung.

Danach wurden die Copolymerisate wie folgt in stark saure Ionenaustauscher überführt: 25 g der Copolymerisate (Siebfraktion zwischen 0.3 bis 0.8 mm) wurden mit 20 g 1,2-Dichloräthan 2 h lang in einer Schliffflasche auf einer Rollbank vorgequollen und anschliessend mit 100 ml reiner 96%iger Schwefelsäure unter Rühren innerhalb 1 h auf 100° erhitzt. Nach einer Reaktionszeit von 6 h wurde die Schwefel-

TABELLE II

ZUSAMMENSETZUNG DES ZUR COPOLYMERISATION VERWENDETEN TECHNISCHEN DIVINYLBENZOL NACH GASCHROMATOGRAPHISCHER ANALYSE⁷

Substanz	Anteil (Gewicht-%)
<i>p</i> -Methylstyrol	4.0
<i>m</i> -Diäthylbenzol	9.1
<i>p</i> -Diäthylbenzol	2.9
Inden	0.6
<i>m</i> -Äthylstyrol	30.3
<i>p</i> -Äthylstyrol	5.9
<i>m</i> -Divinylbenzol	37.9
<i>p</i> -Divinylbenzol	9.3

säure über einer G-1-Glasfritte innerhalb von 1.5 h vom sulfierten Produkt abgesaugt, bevor das erkaltete Produkt mit einer kaltgesättigten Kochsalzlösung restlos hydratisiert wurde. Danach wurde der Austauscher mit dest. Wasser sulfat- und chlo-
ridfrei gewaschen und an der Luft getrocknet.

Zur Prüfung der mechanischen Beständigkeit der gefertigten Kationenaustauscher wurde folgende Methode der Abriebsbestimmung angewendet: 50 ml Ionenaustauscherharz der Fraktion 0.3–1.0 mm Durchmesser (Dmr) wurden zusammen mit 100 ml dest. Wasser 30 min in einer Kugelmühle (0.63 l Inhalt) mit 40 Kugeln (Dmr = 16 mm) und 40 Kugeln (Dmr = 11 mm) bei 150 rpm gerollt. Anschließend wurde der Anteil unter 0.3 mm Dmr ermittelt, der als Abrieb angegeben wird:

$$\text{Abrieb (\%)} = \frac{\text{ml Harz unter 0.3 mm}}{\text{ml eingesetztes Ionenaustauscherharz}} \cdot 100$$

Die Bestimmung der Gesamtgewichtskapazität (GGK) der stark sauren Ionenaustauscher und die Bestimmung des Wassergehaltes erfolgte nach den bei Helferich⁸ beschriebenen Methoden. Tabelle III zeigt die Eigenschaftskennwerte der Kationenaustauscher aus Bis-(4-vinylphenyl)-methan und Styrol, während Tabelle IV die Eigenschaftskennwerte der vergleichbar aufgearbeiteten Kationenaustauscher auf Basis Styrol-techn. DVB enthält.

TABELLE III

EIGENSCHAFTSKENNWERTE DER KATIONENAUSTAUSCHER AUF BASIS STYROL-BIS-(4-VINYLPHENYL)-METHAN

Vernetzergehalt (Mol-%)	GGK (mequiv./g)	Wassergehalt (%)	Abrieb (%)
2	5.4	76.8	7.0
3	5.3	70.6	12.0
6	5.2	56.2	38.0
10	5.0	43.8	56.0

TABELLE IV

EIGENSCHAFTSKENNWERTE DER KATIONENAUSTAUSCHER AUF BASIS STYROL-TECHN. DIVINYLBENZOL

Vernetzergehalt (Mol-%)	GGK (mequiv./g)	Wassergehalt (%)	Abrieb (%)
2	5.3	77.0	12.0
3	5.3	68.6	40.0
6	5.0	53.1	76.0
10	5.0	43.0	98.0

DISKUSSION

Ein Vergleich der Quellwerte der mit Bis-(4-vinylphenyl)-methan hergestellten Copolymerisate mit den Quellwerten von Copolymerisaten aus Styrol mit *m*- oder *p*-DVB oder techn. DVB⁹ zeigt, dass die Heterogenität innerhalb der Polymerisatstäbe ΔQ in folgender Reihenfolge abnimmt:

$$p\text{-DVB} > m\text{-DVB} > \text{techn. DVB} > \text{BVPM}$$

wie auch aus der Fig. 2 zu ersehen ist. Die Heterogenität ΔQ ist sowohl bei 3 als auch bei 6 Mol-% BVPM am geringsten und entspricht damit den aus den Copolymerendiagramm (Fig. 1) ersichtlichen geringen Abweichungen, die eine hohe Homogenität der Vernetzungsstellen erwarten lässt.

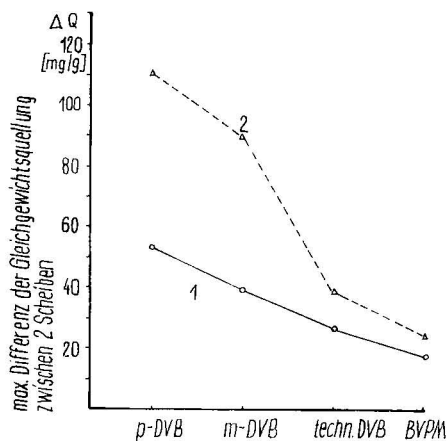


Fig. 2. Abhängigkeit der Inhomogenität innerhalb eines Copolymerenstabes von der Art der vernetzenden Komponente. Initiatorgehalt: 0.15 Mol-% Azoisobuttersäuredinitril. 1 = 3 Mol-% vernetzt; 2 = 6 Mol-% vernetzt. ΔQ = maximale Differenz der Gleichgewichtsquellung zwischen zwei Scheiben.

Dies wird noch durch die Bestimmung der mechanischen Festigkeit von stark sauren Kationenaustauschern auf Basis Styrol-Bis-(4-vinylphenyl)-methan im Vergleich mit solchen auf Basis Styrol-techn. DVB bestätigt. Aus Fig. 3 ist zu entnehmen, dass die mechanische Festigkeit der Austauscher auf Basis Styrol-BVPM wesentlich höher ist gegenüber solchen auf Basis Styrol-techn. DVB, während sie

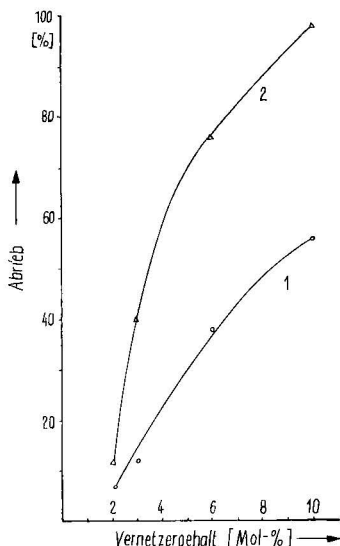


Fig. 3. Abhängigkeit der mechanischen Festigkeit von stark sauren Kationenaustauschern von der Art und Menge des Vernetzers. 1 = Styrol-Bis-(4-vinylphenyl)-methan; 2 = Styrol-techn. Divinylbenzol.

sich hinsichtlich Gesamtgewichtskapazität und Wassergehalt weitgehend gleichen (siehe Tabelle III und IV).

Stark saure Kationenaustauscherharze auf Basis Styrol-*p*-Divinylbenzol-Copolymeren bzw. auf Basis Styrol-*m*-Divinylbenzol-Copolymeren besitzen, wie wir in einer späteren Veröffentlichung zeigen werden⁹, noch geringere mechanische Festigkeiten als Produkte auf Basis von Styrol-techn. Divinylbenzol-Copolymeren.

Damit haben diese Versuche die These erhärtet, dass die wesentliche Ursache der Festigkeitsbeeinflussung von Polymerisationsionenaustauscherharzen schon in dem Reaktionsverhalten der Monomeren zueinander begründet ist, da Austauscher, die auf einem Copolymeren basieren, das eine weitgehend homogene Verteilung der Vernetzungsstellen aufweist, bessere mechanische Beständigkeiten besitzen.

ZUSAMMENFASSUNG

Es wurden stark saure Kationenaustauscherharze auf Basis von Copolymeren des Styrols mit Bis-(4-vinylphenyl)-methan hergestellt und ihre Eigenschaften, vor allem hinsichtlich der mechanischen Festigkeit, mit stark sauren Kationenaustauschern auf Styrol-techn. Divinylbenzol-Basis verglichen. Als Ursache für die bessere mechanische Festigkeit der mit Bis-(4-vinylphenyl)-methan hergestellten Austauscher wird der gleichmässiger Aufbau der vernetzten Copolymerenmatrix angesehen, der sich durch die günstigen *r*-Werte von Styrol und Bis-(4-vinylphenyl)-methan ergibt.

LITERATUR

- 1 G. Schwachula, *Symp. 30 Jahre Kunstharz-Ionenaustauscher, Leipzig, 4-7 Juni, 1968*, Akademie-Verlag, Berlin, 1970, S. 73-93.

- 2 G. Schwachula, F. Wolf und H. Gatzmanga, *Plaste Kaut.*, 17 (1970) 255.
- 3 R. H. Wiley und E. E. Sale, *J. Polym. Sci.*, 42 (1960) 491.
- 4 R. H. Wiley und B. Davis, *Polym. Lett.*, 1 (1963) 463.
- 5 R. H. Wiley und G. L. Mayberry, *J. Polym. Sci., Part A*, 1 (1963) 217.
- 6 V. J. Traynelis, W. L. Hergenrother, J. R. Livingstone und J. A. Valincenti, *J. Org. Chem.*, 27 (1962) 2377.
- 7 G. Schwachula, M. Henke und H. Seidenschnur, *Chem. Tech. (Leipzig)*, 22 (1970) 485.
- 8 F. Helfferich, *Ionenaustauscher*, Bd. 1, Verlag-Chemie, Weinheim, 1959, S. 81, 220.
- 9 G. Schwachula, zur Veröffentlichung vorgelegt.

CHROM. 7741

SYNTHESIS AND PROPERTIES OF SOME SNAKE-CAGE ION-RETARDATION RESINS

R. BOGOCZEK

Institute for Organic Chemistry and Technology, Silesian Polytechnic University, Gliwice (Poland)

SUMMARY

In certain separation processes, snake-cage amphoteric retardation resins undergo a decrease in chemical stability followed by loss of their separation ability.

A means has been found of preventing this decay by cross-linking the "snake" polymer within the matrix. New ion-exchange resins have been synthesized on this basis and are termed "net-cage" resins. Their most important properties are tabulated.

INTRODUCTION

Snake-cage ion-retardation resins have found industrial applications in many separation processes involving highly concentrated solutions, such as the separation of ionizable, slightly ionizable and non-ionizable organic and inorganic compounds, splitting of complexes and in processing waste water in the Sirotherm Project^{1–3}. The absorbed solutes are displaced from the resin and the resin is regenerated merely by rinsing it with water. A snake-cage resin is a cross-linked polymer system containing a physically constrained mixture of linear polymers^{4,5}. The main separation properties of an amphoteric snake-cage resin depend, above all, on the correct proportion of anionic to cationic sites. Amphoteric snake-cage resins can also act as true ion-exchange resins, but only at certain pH ranges.

Investigations have been performed in order to explain the origin of the deterioration of these resins, which occurs during their working life.

EXPERIMENTAL AND RESULTS

A glass column of 9 cm I.D. and 105 cm height was surrounded with a jacket of warm water and filled with an amphoteric ion-retardation resin based on Wofatit SBW and polyacrylic acid. This arrangement was used in the following separations.

(1) Sodium thiocyanate was separated from sodium thiosulphate in a solution with a total starting concentration of 400–900 g/l. After 40–50 separation cycles, the ion-retardation resin had completely lost its separation abilities.

(2) Calcium maltobionate–calcium bromide, a complex compound, was split in order to obtain a very pure concentrated solution of calcium maltobionate for use

TABLE I

PROPERTIES OF NET-CAGE RESINS BASED ON WOFATIT SBW-X4 AND POLY-(ACRYLIC + α % SORBIC) ACID

Test solution: cane sugar + NaCl.

No.	Sorbic acid content, α (%)	Separation ability, $100 \cdot \frac{\Delta V_{max}}{V_T}$	Capacity max., $V_{soln.}$ V_T	Regeneration ability by water, V_{water} V_T	Water content of resin (%)	Swelling volume in saturated NaCl _{aq.} (%)	Comparative swelling half-time in water*
1	0.0	57	136	30.0	41.0	+35	100
2	2.0	62	143	25.0	42.5	+30	110
3	5.0	53	103	16.0	50.5	+30	105
4	10.0	39	88	13.5	58.5	+15	90
5	15.0	31	90	10.5	58.0	+6	88
6	25.0	24	92	9.0	55.6	-4	95
7	50.0	20	97	12.0	52.5	-10	97
8	100.0	16	101	16.5	45.0	-10	100

* 100 represents 28 sec.

in pharmaceutical preparations. Before each following separation cycle, the resin bed was thoroughly rinsed with boiling water so as to effect complete regeneration and to remove any bromide ions present inside the resin. Leakage appeared within 6-8 cycles and increased rapidly, rendering impossible any further cleavage of the complex compound.

(3) The used ion-retardation resins from the above columns were subjected to batchwise saturation with acrylic acid and, by using peroxy polymerization initiators, were polymerized to give amphoteric snake-cage resins. The reconstructed resin beds were used repeatedly in the above separation processes with good results.

TABLE II

PROPERTIES OF NET-CAGE RESINS BASED ON WOFATIT SBW-X4 AND POLY-(ACRYLIC ACID + α % DIVINYLBENZENE)

Test solution: cane sugar + NaCl.

No.	Divinylbenzene content in relation to acrylic acid (mole:mole)	Separation ability, $100 \cdot \frac{\Delta V_{max}}{V_T}$	Capacity max., $V_{soln.}$ V_T	Regeneration ability by water, V_{water} V_T	Water content of resin (%)	Swelling volume in saturated NaCl _{aq.} (%)	Comparative swelling half-time in water*
1	0% DVB	57	136	30	41.0	+35	100
2	1:40	59	142	20	38.0	+30	91
3	1:30	53	118	15	36.5	+28	97
4	1:20	47	101	15	37.0	+25	100
5	1:15	44	95	22	37.5	+22	105
6	1:10	41	92	33	37.2	+20	118
7	1:7	38	86	40	36.0	+15	116
8	1:4	25	76	45	33.5	+10	104
9	1:2	16	72	42	32.0	+6	103

* 100 represents 28 sec.

Nevertheless, after the same number of cycles, the resin beds again lost their separation abilities.

New ion-retardation resins have been synthesized in the following way. Basic resins such as Wofatit SBW, Wofatit SBK and Wofatit SBU in the hydroxide form were subjected to successive batchwise neutralization and polymerization using mixtures of acrylic acid and a cross-linking agent (2–33% divinylbenzene, 2–100% sorbic acid and 2–100% muconic acid. In a further series of experiments, acidic resins such as Wofatit KPS and Wofatit CP in the hydrogen form were neutralized using mixtures of monovinylpyridines and 2–100% divinylpyridine or 2–33% divinylbenzene as cross-linking agent. After polymerization and subsequent de-solvation of unpolymerized raw materials, the resins obtained were subjected to detailed investigation, and the results are given in Tables I and II.

The best resins were used in the separation processes described above. After 50 separation cycles, no significant deterioration occurred and no leakage appeared.

DISCUSSION

In certain separation processes, known snake-cage resins undergo a decrease in durability owing to de-solvation of "snake" molecules out of the matrix "cage". The resulting unfavourable relation between cationic and anionic sites can be restored to a satisfactory extent by soaking the used retardation resins with the "snake" monomer and by subsequent polymerization, but the stability of the reconstructed resin is still not adequate. It has been shown that one can obtain stable retardation resins by cross-linking the "snake" polymer. The "snakes" thus form "nets" and so cannot leave the resin "cage".

It was possible to increase the stability of retardation resins by modifying their synthesis route to give a composition with a cross-linked "snake" structure within a cross-linked matrix cage. These new ion-retardation resins do not exhibit the tendency to lose their "snakes" as do the previous products. They show also different selectivities towards many solutes, which can be regulated by changing the degree of "snake" cross-linking. There is a distinct sieve effect in their behaviour.

As the "snakes" are now cross-linked, it is more appropriate to name these products "net-cage" resins. Net-cage resins are produced in Poland under the name "Saturion", and a patent application has been filed describing a method of producing them.

REFERENCES

- 1 A. Kopecký, *Collect. Czech. Chem. Commun.*, 26 (1961) 3160.
- 2 R. Bogoczek, Z. Wałaszek, W. Szeja, J. Krawczyk, J. Słaboń, J. Próżdzsk and W. Ziobro, *Polish Patent Application*, July 3rd, 1969, Nos. P 135137, P 135138, P 135139; 1971, No. P 146634.
- 3 B. A. Bolto, A. S. Macpherson, R. Siudak, R. E. Warner, D. E. Weiss and D. Willis, in *Ion Exchange in the Process Industries*, Society of Chemical Industry, London, 1969, p. 270.
- 4 M. J. Hatch, J. A. Dillon and H. B. Smith, *Ind. Eng. Chem.*, 49 (1957) 1813.
- 5 F. Wolf and H. Mlytz, *J. Chromatogr.*, 34 (1968) 59.

CHROM. 7706

BEITRAG ZUR BASIZITÄTSPRÜFUNG VON STARK BASISCHEN ANIONENAUSTAUSCHERN

HANS HECKER

VEB Chemiekombinat Bitterfeld, 44 Bitterfeld (D.D.R.)

SUMMARY

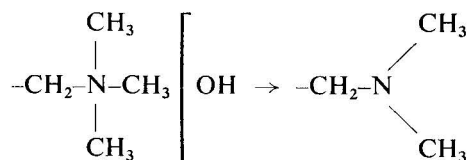
Contribution to basicity testing of strongly basic anion exchangers

A new method is developed for determination of the amounts of different strongly basic groups present in currently used strongly basic anion exchangers. The method involves conversion into the base form of the weakly basic groups present in the exchange resin, which is in the chloride form. This is done by reaction with an ammonia solution containing sodium chloride under stirring. Because of the chloride added, the strongly basic groups are practically not affected by the ammonia. The results are therefore more illustrative of the basicity ratios present in ion-exchange resins than with older methods of determination.

EINLEITUNG

Auf Grund von Wechselwirkungen mit den im Rohwasser enthaltenen Huminsäuren können stark basische Anionenaustauscher, die zur Entkieselung eingesetzt sind, in ihrer Funktion bekanntlich mehr oder weniger stark beeinträchtigt werden. Hierüber finden sich in der Fachliteratur der letzten 15 Jahre zahlreiche Veröffentlichungen. Bei näherer Untersuchung erkannte man, dass diesen Erscheinungen, abgesehen von weiteren gleichfalls massgebenden elementaren Veränderungen, folgende Vorgänge am Austauschergerüst zugrunde liegen:

(1) Ein Teil der quaternären Trialkylammoniumgruppen wird zu wesentlich schwächer basischen Aminogruppen von niedrigerem Substitutionsgrad abgebaut, z.B.:



(2) Der Austauscher hält adsorbierte Huminsäuren unter den normalen Regenerierungsbedingungen irreversibel fest, so dass ein Teil der aktiven Gruppen nicht mehr in Funktion treten kann. Stattdessen wirken nun die schwächer basischen Amino-

gruppen der fixierten Huminsäuren gegenüber der flüssigen Phase ionenaustauschend.

Den beiden hier genannten Vorgängen ist somit gemeinsam, dass sie dem Austauschermaterial einen schwächer basischen Charakter verleihen im Vergleich zum ursprünglichen Zustand. Dieses Phänomen gestattet es, an Hand einer entsprechenden Laboruntersuchung den Nachweis über eine Schädigung von Austauschern durch Huminsäuren zu führen. Der Nutzen einer solchen Basizitätsprüfung geht allerdings darüber noch hinaus. Um während der Benutzung geschädigte Anionenaustauscher von sehr fest adsorbierter Huminsäure zu befreien, bedient man sich Spezialregenerierungen mit Natriumchloridlösung. Die Wirksamkeit einer derartigen Behandlung lässt sich im Labor dadurch überprüfen, dass man den Anstieg an Basizität ermittelt, der auf die Freilegung von bisher durch Huminsäuren blockierten aktiven Gruppen zurückzuführen ist.

Mehrere Autoren haben sich in methodischer Hinsicht mit der Basizitätsprüfung beschäftigt (siehe z.B. Lit. 1–5). Da in mancher Beziehung die vorgeschlagenen Verfahren nicht voll befriedigen, erschien es lohnend, das Problem noch einmal aufzugreifen. Die Zielstellung bestand dabei, abgesehen von anderen Gesichtspunkten, im wesentlichen in der Forderung, dass die Methode bei Anwendung auf ungebrauchte stark basische Austauscher nicht zu Ergebnissen führen darf, die im Widerspruch zu allgemeinchemischen Tatsachen stehen. In diesen Fällen müssen nämlich angesichts der hohen Basizität der quaternären Ammoniumgruppen Zahlenwerte in der Nähe von 100% resultieren, was den Anteil an stark basischen Gruppen anbelangt. Es sei darauf hingewiesen, dass demgegenüber nach der Methode von Fisher und Kunin¹ in der durch Wilson² abgewandelten Form erhebliche Anteile an schwach basischen Gruppen vorgetäuscht werden. Diese Tatsache gab bereits Štamberg und Juračka³ Anlass, die Methode dieser Autoren zu überarbeiten.

GRUNDLAGEN DER NEUEN METHODE

Wie es von Fisher und Kunin¹ einleuchtend begründet wird, ist die Chloridform als Bezugszustand für die Bestimmung der Gesamtkapazität von Anionenaustauschern besonders gut geeignet. Damit erscheint es sinnvoll, zur Reaktion an den schwach basischen Gruppen entsprechend dem Vorschlag der beiden Autoren die Einwirkung von Ammoniaklösung vorzusehen. Hierbei wird jedoch auch ein gewisser Teil der quaternären Ammoniumgruppen in die Basenform übergeführt, was die eben erwähnte Vortäuschung entsprechender Mengen an schwach basischen Gruppen nach sich zieht. Dies gilt es durch eine geeignete Massnahme von vornherein zu verhindern. Angesichts des ausserordentlich starken Unterschiedes in der Chlorid/Hydroxid-Selektivität von stark und schwach basischen Gruppen sollte dieser Effekt durch einen Zusatz an Chloridionen zur Ammoniaklösung erzielbar sein, während eine solche Massnahme bei ausreichend hoch gewähltem pH-Wert auf die schwach basischen Gruppen ohne Einfluss bleiben müsste. Als Mass für den Anteil schwach basischer Gruppen würde dann die infolge des Kontaktes mit dem Austauscher eingetretene Erhöhung der Chloridkonzentration in der Lösung dienen.

In orientierenden Versuchen an definierten ungebrauchten Austauschermaterialien stark und schwach basischen Charakters wurden die erforderlichen Arbeitsbedingungen ermittelt. Auf der Grundlage der Ergebnisse kam die nachstehend beschriebene Arbeitsvorschrift zustande.

BESTIMMUNG DES ANTEILS AN STARK BASISCHEN GRUPPEN (KURZBESCHREIBUNG)

20 ml des stark basischen Anionenaustauschers werden durch Dekantieren mit Wasser von Trübstoffen befreit. In einer Austauschersäule wird die Probe durch Behandeln mit verdünnter Natronlauge von Kieselsäure befreit. Nach Zwischenwaschen mit Wasser werden mittels verdünnter Salzsäure säurelösliche Verunreinigungen beseitigt und der Austauscher in die Chloridform übergeführt. Es folgt ein kurzes Auswaschen mit Wasser.

5 ml des so behandelten Austauschers werden abgemessen und in einer Säule mit wenig verdünnter Salzsäure nachregeneriert, mit Methanol bis zur Säurefreiheit ausgewaschen und mit Natriumsulfatlösung behandelt. Die hierbei eluierten Chloridionen werden bestimmt. Das Ergebnis dient zur Berechnung der Gesamtvolumenkapazität (GVK).

Eine zweite Probe des behandelten Austauschers von 5 ml wird auf einer Glasfritte mit wenig verdünnter Salzsäure behandelt und mit Methanol ausgewaschen. Die Probe wird trocken gesaugt und 1 Std. in 100 ml 1%iger Ammoniaklösung, die genau 0.1 N an Natriumchlorid ist, gerührt. Anschliessend ist die Chloridkonzentration der überstehenden Lösung zu bestimmen. Aus ihrem Anstieg wird die Menge an schwach basischen Gruppen berechnet. Durch Einbeziehung der GVK lässt sich der prozentuale Anteil an stark basischen Gruppen ermitteln.

DISKUSSION DER ERGEBNISSE

Bei Anwendung der Methode auf ungebrauchten Wofatit SBW*, einen Austauscher mit quaternären Trimethylammoniumgruppen (Typ I), findet man Werte zwischen 96 und 99 %. Im Falle des Wofatit SBK* mit quaternären Dimethylhydroxyäthylammoniumgruppen (Typ II) liegen die Werte zwischen 94 und 97 %. Hierbei handelt es sich um Zahlenbereiche, die für stark basische Anionenaustauscher industrieller Herstellung durchaus plausibel erscheinen. Die engen, nahe bei 100 % liegenden Wertespanssen bringen noch den Vorteil mit sich, dass es bei der Untersuchung geschädigter Austauscher in der Regel nicht erforderlich ist, das chargengleiche ungebrauchte Material zum Vergleich ebenfalls der Basizitätsprüfung zu unterziehen. Demgegenüber erscheint dies aber bei Anwendung der Methode von Wilson sehr ratsam.

Nach der beschriebenen Methode wurden in Gebrauch befindliche Reaktorfüllungen von Wofatit SBW und SBK untersucht, die durch eine Funktionsminderung auffielen. Neben der Frage nach deren Ursache stand dabei im Vordergrund, die Wirksamkeit einer aufbessernden Behandlung mit Natriumchloridlösung festzustellen.

In Tabelle I sind für vier Austauschermaterialien die Prüfergebnisse aufgeführt und zwar vor und nach einer labormässigen Natriumchloridbehandlung. Zusätzlich wird jeweils die Differenz der erhaltenen Werte angegeben als eines der Masse —unter anderen— für die Wirksamkeit dieser Behandlung. Zum Vergleich erscheint noch die entsprechende Differenz, die bei Anwendung der Methode von Wilson resultiert.

* Hersteller: VEB Chemiekombinat Bitterfeld, D.D.R.

TABELLE I

ERGEBNISSE VON BASIZITÄTSUNTERSUCHUNGEN AN GEBRAUCHTEN STARK BASISCHEN ANIONENAUSTAUSCHERN VOR UND NACH EINER BEHANDLUNG MIT NaCl-LÖSUNG

Wofatit	Stark basischer Anteil (%)		Differenz (%)	Differenz nach Wilson (%)
	Unbehandelt	Behandelt		
SBW (Typ I)	67	83	16	11
SBW (Typ I)	60	75	15	10
SBW (Typ I)	68	72	4	7
SBK (Typ II)	29	39	10	9

Aus den erhaltenen Ergebnissen lassen sich für die Betriebspraxis wertvolle Schlüsse ziehen. So sollte sich im Falle der ersten beiden Materialien eine betriebliche Behandlung mit Natriumchloridlösung lohnen, da ein merklicher Reinigungseffekt zu verzeichnen ist. Letzterer fehlt dagegen bei dem dritten Material. Bei der Probe des Wofatit SBK beobachtet man zwar einen relativ starken Anstieg der Basizität, doch dürfte auch nach der Natriumchloridbehandlung der Entkieselungseffekt noch zu wünschen übrig lassen.

Die nach der Methode von Wilson erhaltenen Differenzen liegen vergleichsweise im allgemeinen etwas niedriger, sind jedoch von gleicher Größenordnung.

Die hier beschriebene, wenig aufwendige und verhältnismässig schnelle Untersuchungsmethode dürfte gut geeignet sein für eine bei ungünstigen Rohwasserbedingungen erforderliche turnusmässige Kontrolle des Gebrauchswertes stark basischer Anionenaustauscher im Kraftwerkslabor.

ZUSAMMENFASSUNG

Zur Bestimmung der Anteile an verschiedenen stark basischen Gruppen in gebrauchten stark basischen Anionenaustauschern wurde eine neue Methode entwickelt. Nach dieser werden die schwach basischen Gruppen des in der Chloridform vorliegenden Austauschers im Rührverfahren durch Einwirkung einer natriumchloridhaltigen Ammoniaklösung in die Basenform übergeführt. Infolge des Chloridzusatzes bleiben hierbei die stark basischen Gruppen vom Ammoniak praktisch unbeeinflusst. Die Ergebnisse spiegeln daher die Basizitätsverhältnisse im Austauscher besser wider als es nach älteren Bestimmungsmethoden der Fall ist.

DANK

Herrn E. Hintsche und Frau C. Stark sei für die sorgfältige Durchführung der Versuche bestens gedankt.

LITERATUR

- 1 S. Fisher und R. Kunin, *Anal. Chem.*, 27 (1955) 1191.
- 2 A. L. Wilson, *J. Appl. Chem.*, 9 (1959) 466.
- 3 J. Štamberg und F. Juračka, *Zh. Prikl. Khim.*, 35 (1962) 2295.
- 4 F. Martinola, in *Speisewassertagung, 1965*, Vereinigung der Grosskesselbetreiber, Essen, 1965, S. 17.
- 5 H. Berg, *Mitt. Ver. Grosskesselbetr.*, 48 (1968) 458.

THEORY OF ION EXCHANGE

CHROM. 7723

A PROPOSAL FOR THE NOMENCLATURE OF EXCHANGERS

RUDOLF HERING

Pädagogische Hochschule, Güstrow (G.D.R.)

SUMMARY

The proposed nomenclature for exchangers is able to reflect up to six aspects of any exchange material. The central part of the nomenclature characterizes that it is an exchanger with a typical exchanging function. Two main parts reflect the anchor group and the adsorbate by means of the directives of the IUPAC. Two further parts indicate the chemical nature of the matrix and any secondary exchanging function of the adsorbate. Further, there is a complete system for chemical formulae.

INTRODUCTION

With ion exchangers and other sorbents there are increasing problems with terminology. The main cause is that the large number of commercial names for new chemical products is continuously increasing, and producers are often not willing to specify the exact chemical composition of their products.

This paper represents an attempt to formulate a uniform nomenclature for exchanging sorbents. This nomenclature includes suitable parts of traditional terminology and is in accordance with the principles of nomenclature laid down by IUPAC that any chemical nomenclature has to be concise, should be easily pronounced, should be written without additional symbols or the need for special type and should be equally applicable to Germanic, Roman and Slavonic languages.

The central part of the nomenclature (I) is given by the *Type* of exchanger. It may be expressed in more detail by two additional main parts (II), the *Anchor group* and the *Adsorbate*, as well as by two further parts (III), the *Matrix* and the *Modification* of the function of the anchor group by special adsorbates:

(Matrix)–(Anchor group)–(Type)–(Adsorbate)–(Modification)
(III) (II) (I) (II) (III)

Furthermore there is a complete system for chemical formulae.

SYMBOLIC CHARACTERIZATION OF THE MATRIX

A common factor in all exchangers is the matrix. Therefore, the matrix must be given a general symbol for chemical formulae so as to be certain that no confusion will occur. It is proposed that the symbol § should be used for this purpose,

because it cannot be confused with the usual chemical symbols and it can also be written, typed and printed without difficulty.

CHARACTERIZATION OF THE FUNCTION OF EXCHANGERS

The function of exchangers is principally based on steric as well as chemical interactions with all species of the medium; both always act together.

The chemical interaction may be effected by reactive matrix atoms, or by attaching reactive groups to the matrix, the so-called *Anchor groups (A)*. This type of exchanger should be characterized as *Exchange reagents* and their symbolic sign should be §A and §-A.

Steric interactions decide the permeability. Exchangers with a decisive permeation function should generally be designated as *Permeation exchangers*, and their general chemical formula could also be given by the symbol §.

CHARACTERIZATION OF THE TYPE OF EXCHANGE REAGENT

In recent years exchange reagents have been developed for all types of reactions, whereas the anchor groups and the reactive matrix atoms characterize the type of exchange reagent. The following types of reactions are mainly connected with particular anchor groups:

acid, base and salt-reactions, *e.g.*, $-\text{SO}_3^-$, $-\text{COO}^-$, $-\text{PO}_3^{2-}$, $-\text{NR}_3^+$;

complex-forming and amphoteric reactions, *e.g.*, $-\text{N}(\text{CH}_2\text{COOH})_2$,

$-\text{NR}(\text{CH}_2)_n\text{COOH}$, $-\text{S}(\text{CH}_2)_n\text{COOH}$;

electron-transfer reactions, *e.g.*, -quinone, -ferrocene;

ligand-exchange reactions, *e.g.*, $-\text{Hg}-\text{OOC}-\text{CH}_3$.

These typical functions constitute the central part of the nomenclature, although the many exchange reagents are able to react in other types of reactions also.

A terminology that includes the final syllable *it*, which is sometimes used nowadays, is efficient, concise and unambiguous.

The conventional designations *ion exchanger*, *cation exchanger*, *anion exchanger*, *electron exchanger* and *ligand exchanger* may also be used besides the nomenclature names, provided that they are used without any further attributes.

Chemical formulae

In accordance with the chemistry of solutions, the type of exchange reagent should be characterized by adequate chemical symbols in addition to the symbol § (see Table I).

CHARACTERIZATION OF THE ANCHOR GROUP

Nomenclature

The general or the special name of the anchor group should be placed in front of the name of the type. The anchor group and the name of the type should be connected with a hyphen.

If possible, only covalent attached anchor groups should be specified, but never in connection with any adsorbate (*e.g.*, exactly: *sulphonate*-cationit; not exactly: *sulphonic-acid*-cationit). This principle will not be practicable in all cases (*e.g.*, *amino-acid*-ampholit), but it should be used if possible.

TABLE I

NAMING OF THE TYPE OF EXCHANGE REAGENT

<i>Typical functions</i>	<i>Conventional names</i>	<i>Nomenclature</i>	<i>General formulae</i>
Ion exchange	Ion exchanger	<i>Ionit</i>	
Cation exchange	Cation exchanger	<i>Cationit</i>	
by matrix atoms			$\$^{-}$
by anchor groups			$\$A^{-}$
Anion exchange	Anion exchanger	<i>Anionit</i>	
by matrix atoms			$\$^{+}$
by anchor groups			$\$A^{+}$
Chelating reactions	Chelating exchanger	<i>Chelit</i>	$\$Y$
Amphoteric properties	Amphoteric exchanger	<i>Ampholit</i>	$\$X$
Electron exchange	Electron exchanger	<i>Redoxit</i>	$\$redox, \$red, \$ox$
Ligand exchange	Ligand exchanger	<i>Ligandit</i>	$\$M, \ML_n
Permeation	Special names	<i>Permit</i>	$\$$
Synthetic intermediate	Special names	<i>Synthit</i>	<i>e.g.</i> , $\$-Cl, \$-NH_2$
Inclusion by crown structures	—	<i>Crownit</i>	

Since anchor groups are substituents of the matrix, they may be marked by a final *o* (*e.g.*, *amino-anionit*; *sulphonato-cationit*).

Chemical formulae

The formula of the anchor group follows the symbol of the matrix ($\$$) directly (in general: $\$A$) or after a hyphen (in general: $\$-A$). (Table II).

CHARACTERIZATION OF THE ADSORBATE IN CONNECTION WITH THE EXCHANGE REAGENT

As a rule, exchange reagents are not applied without an adsorbate, but as a suitable state of adsorption (in general: $\$AB, \$AC, \$AD$, etc.).

TABLE II

NOMENCLATURE OF ANCHOR GROUPS IN CONNECTION WITH THE TYPE

<i>Nomenclature</i>	<i>Formulae</i>
<i>Sulphonate-cationit</i>	$\$SO_3^{-}$
<i>Carboxylate-cationit</i>	$\$COO^{-}$
<i>Quaternary ammonium anionit</i>	$\$NR_3^{+}$
<i>e.g.</i> , trimethylammonium anionit	$\$N(CH_3)_3^{+}$
<i>Amine-anionit</i> (in general)	$\$NR_2$
<i>Primary-amine anionit</i>	$\$NH_2$
<i>Secondary-amine-anionit</i>	$\$NRH$
<i>Tertiary-amine-anionit</i>	$\$NR_2$
<i>e.g.</i> , dimethylamine-anionit	$\$N(CH_3)_2$
<i>Iminodiacetate-chelit</i> (<i>IDA-chelit</i>)	$\$N(CH_2COO^{-})_2$ ($\$IDA$; $\$Y$)
<i>Mercaptoacetate-chelit</i>	$\$SCH_2COO^{-}$
<i>Amino-acid-ampholit</i>	$\$NR(CH_2)_nCOOH$ ($\$X$)
<i>e.g.</i> , methylaminopropionate-ampholit	$\$N(CH_3)CH_2CH_2COOH$ ($\$MAP$)
<i>Quinone-redoxit</i>	$\$C_6H_4O_2, \$C_6H_4(OH)_2, \$-quinone$
<i>Mercury(II)-acetate-ligandit</i>	$\$HgOOCCH_3, \$Hg-ac$
<i>Chlormethyl-synthit</i>	$\$-Cl$
<i>(Dibenzo-18-crown-6)-crownit</i>	$\$-DB18C6$

Nomenclature

The state of adsorption is designated by the chemical name of the adsorbate which is placed after the name of the type. The most concise and unambiguous form is attachment by a hyphen (see Table III) instead of the usual term *...in form of...*

States of incomplete (partial) adsorption can be designated by the term *-part.-*, which is placed between the name of the type and the name of the adsorbate (see Table III: 22–24).

Oxidation states of redoxits should be characterized as modified exchange reagents by means of the abbreviations *-red* and *-ox* (see Table III: 31 and 32).

TABLE III

NOMENCLATURE OF ADSORBATES IN CONNECTION WITH THE TYPE AND THE ANCHOR GROUP

No.	Nomenclature	Formulae
1	Sulphonate-cationit-acid	$\text{\$SO}_3^- \text{H}_3\text{O}^+$
2	Sulphonate-cationit-potassium	$\text{\$SO}_3^- \text{K}^+$
3	Sulphonate-cationit-calcium	$(\text{\$SO}_3^-)_2 \text{Ca}^{2+}$
4	Carboxylate-cationit-acid	$\text{\$COOH}$
5	Carboxylate-cationit-sodium	$\text{\$COO}^- \text{Na}^+$
6	Carboxylate-cationit-magnesium	$(\text{\$COO}^-)_2 \text{Mg}^{2+}$
7	Carboxylate-cationit-iron(III)	$(\text{\$COO})_3 \text{Fe}$ or $[(\text{\$COO})_3 \text{Fe}]$
8	Quaternary-ammonium-anionit-hydroxide	$\text{\$NR}_3^+ \text{OH}^-$
9	Quaternary-ammonium-anionit-chloride	$\text{\$NR}_3^+ \text{Cl}^-$
10	Quaternary-ammonium-anionit-sulphate	$(\text{\$NR}_3^+)_2 \text{SO}_4^{2-}$
11	Amine-anionit-base	$\text{\$NR}_2, \text{H}_2\text{O}$ or $\text{\$NR}_2$
12	Amine-anionit-hydrochloride	$\text{\$NR}_2, \text{HCl}$ or $\text{\$NR}_2 \text{H}^+ \text{Cl}^-$
13	Amine-anionit-hydrosulphate	$(\text{\$NR}_2)_2, \text{H}_2\text{SO}_4$ or $(\text{\$NR}_2 \text{H}^+)_2 \text{SO}_4^{2-}$
14	IDA-chelit-acid (acid form)	$\text{\$N}(\text{CH}_2\text{COOH})_2 \text{\$YH}_2$
15	IDA-chelit-sodium (neutral form)	$\text{\$NH}(\text{CH}_2\text{COO}^-)_2 \text{Na}^+; \text{\$YH}^- \text{Na}^+$
16	IDA-chelit-disodium (alkaline form)	$\text{\$N}(\text{CH}_2\text{COO}^- \text{Na}^+)_2; \text{\$Y}^{2-}, 2\text{Na}^+$
17	IDA-chelit-hydrochloride (strong acid)	$\text{\$N}(\text{CH}_2\text{COOH})_2, \text{HCl}; \text{\$YH}_2, \text{HCl}$
18	IDA-chelit-copper(II) (chelate form)	$\text{\$N}(\text{CH}_2\text{COO})_2 \text{Cu}; \text{\$YCu}$
19	Amino-acid-ampholit-acid (neutral form)	$\text{\$NR}(\text{CH}_2)_n \text{COOH}; \text{\$XH}$
20	Amino-acid-ampholit-sodium (alkaline form)	$\text{\$NR}(\text{CH}_2)_n \text{COO}^- \text{Na}^+; \text{\$X}^- \text{Na}^+$
21	Amino-acid-ampholit-hydrochloride	$\text{\$NR}(\text{CH}_2)_n \text{COOH}, \text{HCl}; \text{\$XH}, \text{HCl}$
22	MAP-ampholit-part.-hydroiodide	$\text{\$NRCH}_2\text{CH}_2\text{COOH}(\text{HI}); \text{\$XH}(\text{HI})$
23	Amine-anionit-part.-copper(II)	$\text{\$NR}_2(\text{Cu}^{II})$
24	Amine-anionit-part.-hydrochloride	$\text{\$NR}_2(\text{HCl}, \text{pH } 9)$ (buffer form)
25	Amine-anionit-hydrochloride sulphate	$\text{\$NR}_2 \text{H}^+(\text{Cl}^-, \text{SO}_4^{2-})$ (mixed adsorbate)
26	Sulphonate-cationit-acid, copper(II), (1:2 moles)	$\text{\$SO}_3^-(\text{H}_3\text{O}, \text{Cu}^{2+} = 1:2)$ (mixed adsorbate)
27	Carboxylate-cationit-acid sodium (pH 4)	$\text{\$COO}^-(\text{H}^+, \text{Na}^+, \text{pH } 4)$ (buffer form)
28	Mixture of 1 vol. of sulphonate-cationit-acid and 2 vol.s of quaternaryammonium-anionit-hydroxide	$(\text{\$SO}_3^- \text{H}_3\text{O}^+, \text{\$NR}_3^+ \text{OH}^-, 1:2 \text{ vol.})$
29	Mixture of 1 mole of carboxylate-cationit-acid and 2 moles of carboxylate-cationit-potassium	$(\text{\$COOH}, \text{\$COO}^- \text{K}^+, 1:2 \text{ moles})$
30	Stratified beds of carboxylate-cationit-acid, sulphonate-cationit-acid, amine-anionit-base, and quaternary-ammonium-anionit-hydroxide (1:1:1:1 vol.)	$(\text{\$COOH}/\text{\$SO}_3^- \text{H}_3\text{O}^+/\text{\$NR}_2/\text{\$NR}_3^+ \text{OH}^- 1:1:1:1 \text{ vol.})$
31	Quinone-redoxit-red	$\text{\$Quinone-red}; \text{\$C}_6\text{H}_4(\text{OH})_2$
32	Quinone-redoxit-ox	$\text{\$Quinone-ox}; \text{\$C}_6\text{H}_4\text{O}_2$
33	DB18C6-crownit-potassium thiocyanate	$\text{\$DB18C6}, \text{K}^+ \text{SCN}^-$

Chemical formulae (for examples, see Table III)

In any example, the formula of the adsorbate must be placed after the anchor group, mainly to make sure that there can be no errors regarding the anchor group and adsorbate. However, when hydrogen is the adsorbate, this principle must often be broken.

Predominantly electrovalently bound adsorbates should be characterized by indicating the charge if possible. Predominantly covalent and coordination bonds can usually be indicated without any special marking.

The formulation of acidic and basic forms should in principle designate the type of chemical bonding also (e.g., $\text{\$SO}_3^-\text{H}_3\text{O}^+$ and $\text{\$NR}_3^+\text{OH}^-$, but $\text{\$COOH}$ and $\text{\$NR}_2\text{H}_2\text{O}$ and $\text{\$NR}_2$).

Polyvalent adsorbates are formulated so that the anchor group together with the symbol $\text{\$}$ are given in parentheses, i.e., (...). As usual, coordination states can be indicated by brackets, i.e., [...]. As brackets do not characterize the stoichiometric value, a symbol $\text{\$}$ can be placed outside or inside the brackets, e.g., $\text{\$}_3[(-\text{COO})_3\text{Fe}]$ or $[(\text{\$COO})_3\text{Fe}]$; however, it seems more advantageous to place the symbol $\text{\$}$ inside the bracket.

States of incomplete or partial adsorption can be designated such that the formula of the adsorbate is placed in parentheses. In these cases, there are no stoichiometric formulae (see Table III; 22–24).

Mixtures of different adsorbates should also be included in parentheses (see Table III: 25–27).

The stoichiometric ratio of a mixture of different adsorbates as well as the pH of the adsorption, as they are needed in order to define buffer forms exactly, can also be placed within parentheses (see Table III: 24, 26 and 27).

Mixed exchange reagents should be included in parentheses, separated by a comma (see Table III: 28). In addition, any ratio of moles or volumes can also be indicated within parentheses (see Table III: 28 and 29).

Mixtures of different adsorbate forms of the same exchange reagent should be treated as mixed exchange reagents.

Stratified-beds and multi-column systems can be characterized by naming the layers and columns in the sequence of the direction of flow separated by oblique strokes. Further, it is possible to place any ratio of moles or volumes within parentheses also.

CHARACTERIZATION OF MODIFIED EXCHANGE REAGENTS

The term modified exchange reagent indicates that the exchange reaction is caused not by the anchor group but by the adsorbate. In this way, it is possible to use ionits for the purpose of electron exchange, to use chelits for ligand exchange, etc. Therefore, the nomenclature must be able to indicate any modification of the anchor group. The modified function of the anchor group can be characterized by means of suitable abbreviations. In the case of full nomenclature, the abbreviation should be placed after the adsorbate, following a hyphen. In the case of the fundamental characterization of any modified type, the abbreviation can be placed in front of the type, followed by a hyphen, or the full modified function can be named without a hyphen (see Tables IV–VI).

TABLE IV
ABBREVIATION SYMBOLS FOR MODIFIED EXCHANGE REAGENTS

<i>Function of the adsorbate</i>	<i>Modification symbol</i>
Reversible electron exchange	-Redox
Irreversible reducing agent	-Red
Irreversible oxidizing agent	-Ox
Ligand exchange	-Ligex
Chelating agent	-Chel
Precipitation	-Prec
Anion exchange	-Anex
Cation exchange	-Catex
Intermediate of synthesis	-Syn
Permeation	-Perm

TABLE V
NAMING THE MODIFICATION IN CONNECTION WITH THE TYPE (EXAMPLES)

<i>Modified type</i>	<i>Nomenclature</i>
Redox-reversible cationit	Redox-cationit
Reducing anionit	Red-anionit
Oxidizing chelit	Ox-chelit
Chelation anionit	Chel-anionit
Ligand-exchanging chelit	Ligex-chelit
Precipitating anionit	Prec-anionit
Anion-exchanging chelit	Anex-chelit
Intermediate anionit	Syn-anionit
Cationit for permeation	Perm-cationit

TABLE VI
FULL NOMENCLATURE OF MODIFIED EXCHANGE REAGENTS

<i>Nomenclature</i>	<i>Formula</i>
Trialkylammonium-anionit-indigodisulphonate-redox	$\$NR_3^+(Ind^{2-})-redox$
Trimethylammonium-anionit-dithionite-red	$(\$N(CH_3)_3^+)_2S_2O_4^{2-}-red$
Sulphonate-cationit-thallium(III)-ox	$(\$SO_3^-)_3Tl^{3+}-ox$
IDA-chelit-copper(II)-ligex	$[\$YCu(H_2O)]-ligex$
Quaternary-ammonium-anionit-EDTA-chel	$\$NR_3^+(EDTA)-chel$
IDA-chelit-lanthan(III)-anex	$[\$YLa]^+Cl^- -anex$
IDA-chelit-lanthan(III)-catex	$[(\$Y)_2La]^-K^+-catex$
Primary-amine-anionit-base-syn	$\$NH_2-syn$
Sulphonate-cationit-barium-prec	$(\$SO_3^-)_2Ba^{2+}-prec$
Polystyrene-sulphonate-cationit-potassium-perm	$Pst\$SO_3^-K^+-perm$

CHARACTERIZATION OF THE CHEMICAL NATURE OF THE MATRIX

The chemical nature of the matrix should be characterized only by chemical names and not by trivial or commercial names.

Nomenclature

The chemical name of the matrix should be placed in front of the anchor group (e.g., *dextran-amine-anionit*).

Combined chemical names of the matrix are included in parentheses [e.g., (*phenol-formaldehyde*)-sulphonate-cationit].

Exchange reagents containing reactive matrix atoms as well as exchange reagents, which have been synthesized from monomers containing complete anchor groups, must be characterized by naming the matrix, in same instances connected with its type [e.g., (*zirconylphosphate*)-cationit; (*m-phenylene-resorcinol-formaldehyde*)-anionit]. In other instances, the well known designation of an exchange reagent reflects the chemical nature of the matrix (e.g., *zeolite*; *cross-linked polymethacrylate*, etc.)

Anchor groups that are kept at a distance by means of a spacer-chain can be indicated by the term *-spacer-* between the name of the matrix and the name of the anchor group (e.g., *dextran-spacer-carboxylate-synthit*). The length of the spacer-chain can be indicated by means of the number of carbon atoms it contains (e.g., *dextran-C₆-spacer-amine-anionit*).

Chemical formulae

Exchange reagents containing ionic matrix atoms should generally be designated without an anchor group, but together with an indication of the charge (e.g., §⁺; §⁻).

The chemical nature of the matrix can be indicated by special abbreviation symbols, which are placed in front of the symbol § without a hyphen.

Spacer-groups can be indicated by the abbreviation *-sp-*, which is placed between the symbol § and the anchor group (see Table VII).

Examples of exchange reagents with anchor groups: *PV*§COOH; *Pst*§NR₂; *Cel*§COOH; *Cond*§SO₃⁻K⁺; *Dex*§OPO₃²⁻.

Examples of exchange reagents with reactive matrix atoms: *Zeo*§⁻K⁺; *AMP*§⁻Rb⁺; *ZrO*§⁺Cl⁻; *ZrP*§⁻(Ca²⁺).

Examples of exchange reagents with spacer-groups: *Dex*§-*sp*-COOH; *Dex*§-*sp*-NH₂; *Dex*§-*sp*-Prot (protein).

TABLE VII

ABBREVIATIONS OF THE CHEMICAL NATURE OF MATRICES

<i>Chemical nature of the matrix</i>	<i>Abbreviation</i>
Cross-linked polystyrene	<i>PSt</i>
Cross-linked polyvinyl-	<i>PV</i>
Cellulose	<i>Cel</i>
Cross-linked polysaccharide	<i>PSac</i>
Cross-linked dextran	<i>Dex</i>
Cross-linked agarose	<i>Agar</i>
Synthetic zeolites	<i>Zeo</i>
Hydrated zirconium oxide	<i>ZrO</i>
Condensation resin	<i>Cond</i>
Ammoniummolybdate phosphate	<i>AMP</i>
Zirconyl phosphate	<i>ZrP</i>
Spacer-groups	§- <i>sp</i> -

CHARACTERIZATION OF PERMEATION FUNCTIONS

Most kinds of gel-like exchange reagents not only can act as exchange reagents, but can also be used as permeation exchangers. For some of them, their main function occurs by permeation.

A gel matrix without anchor groups and without reactive matrix atoms can be designated as *gel* or *permit* (e.g., dextran-*gel* or dextran-*permit*; polystyrene-*gel* or polystyrene-*permit*; polyacrylamide-*gel* or polyacrylamide-*permit*).

A gel matrix with anchor groups is characterized in accordance with its usual function or with the function for which it is used. (e.g., polystyrene-*gel*-sulphonate-cationit or polystyrene-sulphonate-*permit*).

A matrix with reactive matrix atoms can be characterized in the same way, but as a rule this kind of exchanger is well known by trivial names which also characterize their permeation function (e.g., zeolites, molecular sieves, silica gel).

COMPLETE CHARACTERIZATION OF EXCHANGE REAGENTS

Contrary to the nomenclature of monomeric substances, the nomenclature of exchange reagents cannot indicate all chemical and structural details of commercial products, which are often unknown to the producers themselves. In order to complete the information given by the nomenclature, further details in parentheses should be placed after the nomenclature.

The most exact method is to use the commercial name together with the data of production or a batch number [e.g., sulphonate-cationit (*Wofatit KPS 200, 1958*)]. One should avoid giving a commercial name in direct combination with the nomenclature.

Further, the characterization of exchange reagents can be completed by mentioning physical, chemical, structural, technical and functional properties connected with the use of the exchange reagent. (e.g., exchange capacity; degree of swelling in different solutions; macroreticular or gel-like state of the matrix; porosity; degree of cross-linking, mesh size; beads or granulate or powder; thermal resistance; oxidation resistance).

In order to specify the chemical nature of exchange reagents exactly, the unit of the polymer connected with the cross-linking reagent should be given by means of structural formulae or by naming the polymer unit by means of the IUPAC nomenclature.

CHROM. 7720

COMPARISON OF EXPERIMENTAL AND THEORETICAL RATES OF ION EXCHANGE

STEPHEN C. DUFFY

Kodak Ltd., Harrow, Middlesex (Great Britain)

and

LOVAT V. C. REES

Physical Chemistry Laboratories, Imperial College of Science and Technology, London, SW7 2AY (Great Britain)

SUMMARY

The theoretical rates of the forward and backward ion-exchange reactions



have been calculated. In these calculations the concentration dependencies of D_{Na}^* and D_{K}^* , the respective self-diffusion coefficients of sodium and potassium in (Na,K)-chabazites, have been taken into account. When these theoretical rates are compared with rates determined experimentally for these two reactions, the introduction of concentration-dependent self-diffusion coefficients has been shown to be of prime importance.

INTRODUCTION

For spherical symmetry the diffusion equation can be written as:

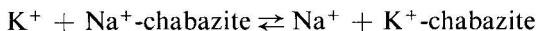
$$\frac{\partial C_A}{\partial t} = \frac{1}{r^2} \cdot \frac{\partial}{\partial r} \left(r^2 D_{AB} \frac{\partial C_A}{\partial r} \right) \quad (1)$$

where t is time, r is the distance from the centre of the sphere, and C_A is the concentration in mole fractions of the ion A in the sphere. This diffusion equation has been solved for a binary ion-exchange system using a finite difference method^{1,2}. The inter-diffusion coefficient, D_{AB} , used includes activity gradient terms and is given by

$$D_{AB} = \frac{D_A^* D_B^* \left(C_A Z_A^2 \frac{\partial \ln a_B}{\partial \ln C_B} + C_B Z_B^2 \frac{\partial \ln a_A}{\partial \ln C_A} \right)}{D_A^* C_A Z_A^2 + D_B^* C_B Z_B^2} \quad (2)$$

D_A^* , D_B^* are the self-diffusion coefficients of the ions A and B in the exchanger phase whose valencies and activities are Z_A , Z_B and a_A , a_B , respectively.

In this paper the theoretical rates of the forward and backward ion-exchange reactions



have been calculated and are compared with the corresponding experimental rates. Chabazite is a zeolite whose composition in the Na^+ form was



and in the K^+ form was



RESULTS AND DISCUSSION

To calculate theoretical rates it is necessary to determine the concentration dependencies of D_{Na}^* and D_{K}^* in the chabazite exchanger. The coefficients were determined using radiochemical techniques with ^{24}Na and ^{42}K as tracers³. The results obtained are shown in Fig. 1. This figure shows that there is a smooth decrease in both D_{Na} and D_{K}^* as the K^+ content of the exchanger decreases.

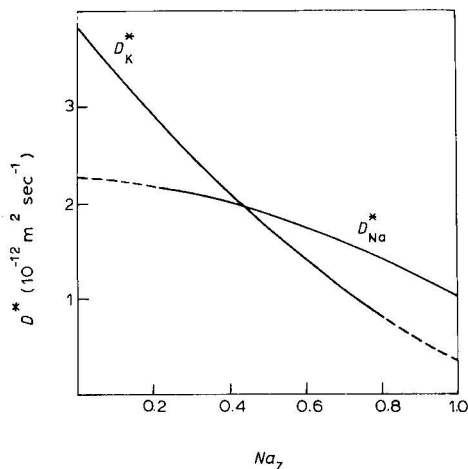


Fig. 1. Concentration dependence of self-diffusion coefficients.

The $(\partial \ln a)/(\partial \ln C)$ terms were obtained from a thermodynamic analysis⁴ of the equilibrium isotherm shown in Fig. 2a. This isotherm shows that K^+ is the preferred ion in the chabazite lattice. In Fig. 2b the plot of $\log_{10} K_C$ against K_Z is shown, where

$$K_C = \frac{K_Z \cdot m_{\text{NaCl}} \cdot \gamma_{\text{NaCl}}^2}{Na_Z \cdot m_{\text{KCl}} \cdot \gamma_{\text{KCl}}^2} \quad (3)$$

Na_Z and K_Z are the mole fractions of Na^+ and K^+ ions in the chabazite phase, respectively; m and γ represent the molality and mean molal activity coefficient of the subscripted electrolyte in the mixed solution phase.

In previous theoretical studies D_A and D_B have always been assumed constant equal to their values in the respective pure A and B forms of the exchanger. In one of these studies¹ it was found that the introduction of the $(\partial \ln a)/(\partial \ln C)$ terms reversed the predicted rates of exchange and produced kinetics which were in qualitative agreement with experiment.

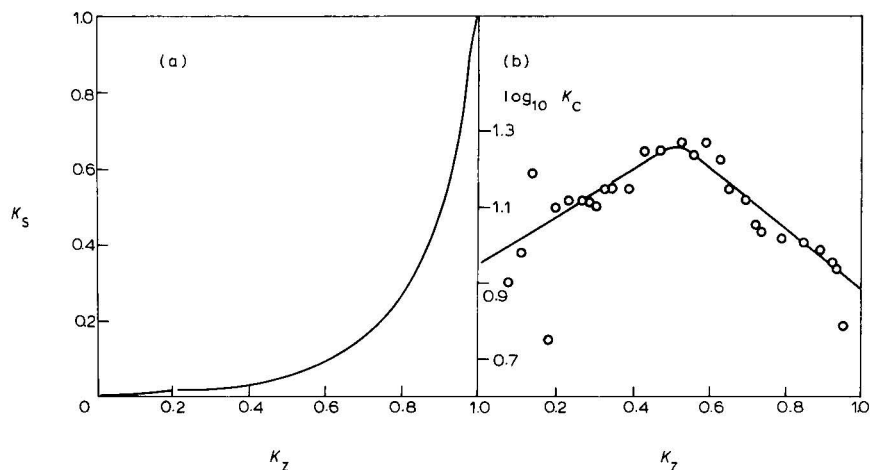


Fig. 2. (a) Na/K equilibrium exchange isotherm in chabazite (K_S and K_Z represent the mole fraction of K^+ in the solution and zeolite phase, respectively). (b) Plot of $\log_{10} K_C$ against K_Z (i.e. Kielland plot).

In the present study, however, Fig. 3 shows that if the self-diffusion coefficients are held constant and only activity corrections applied, the theoretical rates are the reverse of the experimental rates.

When, however, allowance is made for the concentration dependence of the self-diffusion coefficients as well as the non-ideality of the exchanger, the theoretical rates are reversed and these rates now agree qualitatively with the experimental rates. The introduction of concentration-dependent self-diffusion coefficients into the theoretical equations is obviously of prime importance.

In Fig. 4, D_{AB} as a function of Na_Z is shown for the case (a) where the self-diffusion coefficients are constant but the zeolite is thermodynamically non-ideal and (b) where these coefficients are concentration dependent in the non-ideal zeolite.

The exchange in the peripheral layers contributes principally to the overall exchange rate because, for spherical particles, the spherical shell of thickness dr and volume $4\pi r^2 \cdot dr$ is greatest at the periphery and contains, therefore, the largest fraction of the exchangeable cations. Secondly, in the exchange $A^+ \rightarrow B^+$ the outward passage of A^+ ions through the B^+ -rich outer layers is rate controlling.

When the exchange Na-chabazite \rightarrow K-chabazite is considered, the D_{AB} values in the rate-controlling peripheral layers are the high values shown in Fig. 4 around the 100% K^+ region. The rate-controlling D_{AB} values for the reverse exchange are the low values of the 100% Na^+ region. Thus, when concentration-dependent self-diffusion coefficients are used, the above argument indicates that the exchange

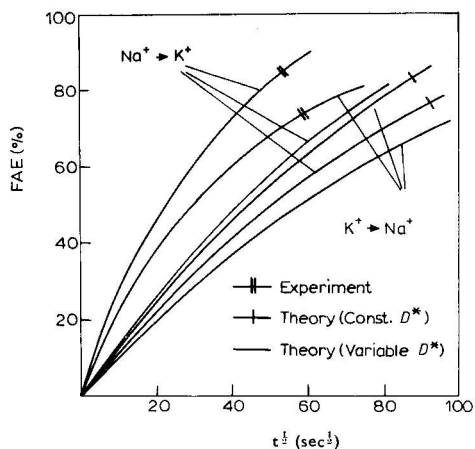


Fig. 3. Comparison of theoretical and experimental rates of forward and backward exchange. (Fractional attainment of equilibrium vs. $t^{1/2}$).

Na-chabazite \rightarrow K-chabazite should be the faster of the two. Similar analysis of the D_{AB} values for the situation where the self-diffusion coefficients are assumed constant indicates that the reverse exchange should now be the faster. This is also the situation for a thermodynamically ideal exchanger phase and constant self-diffusion coefficients, *i.e.* the conditions of the simple theory of Helfferich and Plesset⁵.

The smooth decrease in both D_{Na}^* and D_K^* as the K^+ content of the exchanger decreases as shown in Fig. 1 can be explained as follows. As Na^+ ions replace K^+ ions in the K-chabazite these Na^+ ions are forced to occupy sites least favourable to K^+ ions since the isotherm shows that K^+ is the preferred cation of the two in the chabazite lattice. Thus D_K^* decreases as this replacement proceeds since the K^+ ions remaining and participating in the diffusion process are occupying the most favourable

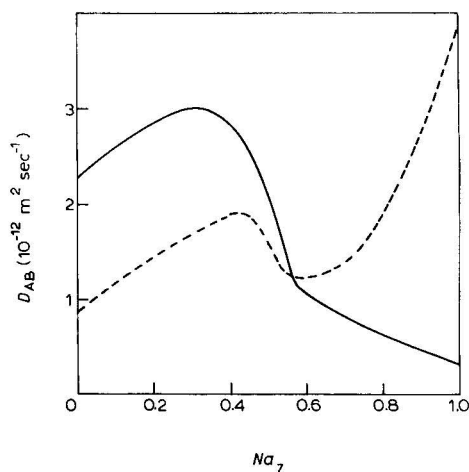


Fig. 4. D_{AB} as a function of concentration for constant (---) and concentration-dependent D_{Na} and D_K^* (—).

sites and require a larger and larger activation energy for their movement. The converse situation explains the increase in D_{Na}^* as Na^+ ions are replaced by K^+ ions.

It is interesting to note that similar behaviour to that found for Na^+/K^+ exchange in chabazite has been observed in all ion-exchange reactions in zeolites so far studied. In all cases the faster rate of exchange has always been obtained when the cation with the higher affinity for the lattice is diffusing into the exchanger from the solution phase. The rates are not dependent on whether $D_{\text{A}}^* > D_{\text{B}}^*$ or not (where D^* here refers to the homoionic form of the exchanger). The elementary theory of Helfferich and Plesset always predicts that the exchange $\text{A} \rightarrow \text{B}$ should be the faster if $D_{\text{A}}^* > D_{\text{B}}^*$. It would be interesting, therefore, to measure the concentration dependence of the self-diffusion coefficients of many more binary exchange systems to see if they behave similar to the Na/K-chabazite system.

REFERENCES

- 1 N. M. Brooke and L. V. C. Rees, *Trans. Faraday Soc.*, 64 (1968) 3383.
- 2 N. M. Brooke and L. V. C. Rees, *Trans. Faraday Soc.*, 65 (1969) 2728.
- 3 S. C. Duffy and L. V. C. Rees, *J. Chem. Soc. Faraday I*, 70 (1974) 777.
- 4 R. M. Barrer and L. V. C. Rees, *J. Phys. Chem. Solids*, 25 (1964) 1035.
- 5 F. Helfferich and M. S. Plesset, *J. Chem. Phys.*, 28 (1958) 418.

CHROM. 7722

CHLORIDE-SULPHATE EXCHANGE ON ANION-EXCHANGE RESINS KINETIC INVESTIGATIONS. I

LORENZO LIBERTI* and ROBERTO PASSINO**

Istituto di Ricerca Sulle Acque, Rome (Italy)

SUMMARY

The exchange rates for the complete conversion of many anion-exchange resins from the chloride to the sulphate form when particle diffusion is the controlling mechanism have been measured. Infinite solution volume conditions were adopted, using the centrifugal stirrer-reactor technique. The exchange rates were found to be greatly dependent on the basicity of the functional groups of the resins, according to the “kinetic sequence” quaternary > tertiary > secondary > primary amino-type resins, which is the reverse of the “selectivity sequence” previously found for the same resins under equilibrium conditions. On this basis, it was found to be advantageous to use a weak anion-exchange resin of intermediate selectivity in the process for the desulphation of sea-water feed to evaporation plants.

INTRODUCTION

The formation of calcium sulphate scales on heat-transfer surfaces greatly reduces the performance of evaporation plants. Studies conducted at IRSA since 1969 to prevent this problem led to the development of a process for sea-water desulphation using anion-exchange resins regenerated by the brine discharged from such plants¹. Investigations on the chloride-sulphate equilibrium on anion-exchange resins indicated that the selectivity of the resin toward sulphates is strongly dependent on the basicities of the amino-type fixed charges of the resins, according to the “selectivity sequence”²

quaternary < tertiary < secondary < primary amino-type resins (1)

Investigations have also been conducted on the kinetics of the system using both commercial and experimental resins, all with amino-type functional groups. Experimental conditions (solution concentration, temperature, liquid-solid contact time, etc.) were widely varied throughout the study.

* Present address: IRSA-CNR, Via De Blasio, 70122 Bari, Italy.

** Present address: IRSA-CNR, Via Reno I, 00198 Rome, Italy.

This paper describes an investigation of kinetics at high solution concentration (1.8 *N*), where the experimental conditions allow ion interdiffusion within the particles to be assumed as the rate-controlling mechanism. As the regeneration step (in which 1.2–2.0 *N* brine is used) is the least efficient part of the desulphation process, a knowledge of resin performance under such conditions is of extreme importance in the evaluation of the process.

EXPERIMENTAL

The infinite batch technique was adopted, using a modified version of the Kressman–Kitchener stirrer–reactor³, as shown in Fig. 1, which allows the beads to be uniformly flushed by the solution aspirated by centrifugal action. The stirring rate was 2000 rpm. The rotating reactor, filled with about 0.01 g of resin in the chloride form, was rapidly immersed in a jacketed vessel, pre-agitated by a supplementary stirrer, containing 800 ml of sodium sulphate–sulphuric acid solution with a total sulphate concentration of 1.8 *N* and a pH of 3.0, at $25 \pm 0.1^\circ$.

The resin exchange capacities ranged from 2 to 7 mequiv./g, so that an

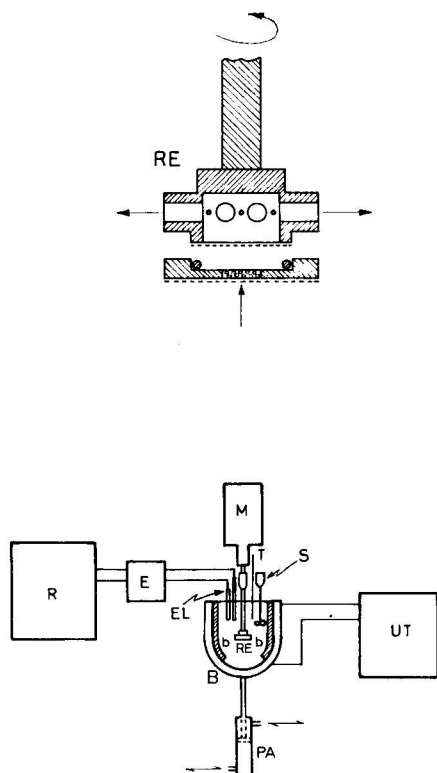


Fig. 1. Schematic diagram of the apparatus for kinetic measurements. R = potentiometric recorder; E = potentiometer; M = stirrer; T = thermometer; EL = electrodes; RE = centrifugal stirrer reactor; PA = pneumatic piston; UT = ultrathermostat; B = jacketed vessel; bb = baffles; S = supplementary stirrer.

"equivalent ratio" less than 10⁻⁷ equiv. of resin per equiv. of solution was used consistently. The infinite solution volume condition was assumed under these conditions. The chloride release was followed potentiometrically by means of ion-selective electrodes, the potential variations recorded and, by suitable reference curves, the Cl⁻ concentration *versus* time curves obtained. In order to account for electrode response delays, the reference curves were determined "dynamically" before each set of experiments, adding to the vessel an appropriate amount of standard sodium chloride solution with an automatic constant-speed burette.

After preliminary acid-base cycles, the resins were converted into the chloride form with sodium chloride-hydrochloric acid solution having the same pH and ionic strength as the reacting sodium sulphate-sulphuric acid solution, in order to prevent hydrolysis during the exchange. Fractions of 16-18, 20-30, 30-35 and 60-70 (U.S.) mesh were collected for each resin, using the same sodium chloride-hydrochloric acid solution as screening carrier, the mesh size being assumed to be the average radius of each fraction of the wet resin, r_0 .

The resins were then washed with methanol and heated to constant weight in a vacuum oven at 60°. The broken beads were removed by rolling on an inclined plane, and the imperfect particles were discarded after final microscopic observation. Before each kinetic experiment, a weighed amount of dry resin was allowed to re-swell completely for 12 h in a saturated humidity box. For each mesh fraction, about 1 g of dry resin was thoroughly regenerated with an excess of warm 2 *N* sodium hydroxide solution, in order to obtain its chloride exchange capacity. This was used to calculate [Cl⁻]_∞, the chloride solution concentration after an infinite time, assuming complete conversion from the chloride to the sulphate form of the resin. The variation of Cl⁻ concentration with time was expressed as the fractional attainment of equilibrium: $U = [\text{Cl}^-]_t / [\text{Cl}^-]_\infty$.

Interruption tests performed on each resin confirmed that particle diffusion was the rate-controlling mechanism in all experiments.

RESULTS

As an illustration of the reproducibility of the system, Fig. 2 shows the kinetics obtained with one resin, under the same experimental conditions, over a period of several months. Fig. 2 also shows the kinetics obtained with the resin previously immersed for 4 h in distilled water (as it is a strong resin, hydrolysis was virtually undetectable). In Table I are reported the main physico-chemical characteristics of the resins investigated, and Table II gives the half-exchange times and the corresponding values of the interdiffusion coefficients, $\bar{D}_{0.5}$. The latter were calculated according to the well known solution to Fick's diffusional model for spherical particles, with a constant boundary condition (infinite solution volume), and a constant interdiffusion coefficient, as given by Barrer and Cranck (see ref. 4):

$$U = 1 - (6/\pi^2) \sum_{n=1}^{\infty} (1/n^2) \exp(-\bar{D}t \pi^2 n^2 / r_0^2) \quad (2)$$

which, for $U = 0.5$, gives

$$\bar{D}_{0.5} = 0.03 r_0^2 / t_{0.5} \quad (3)$$

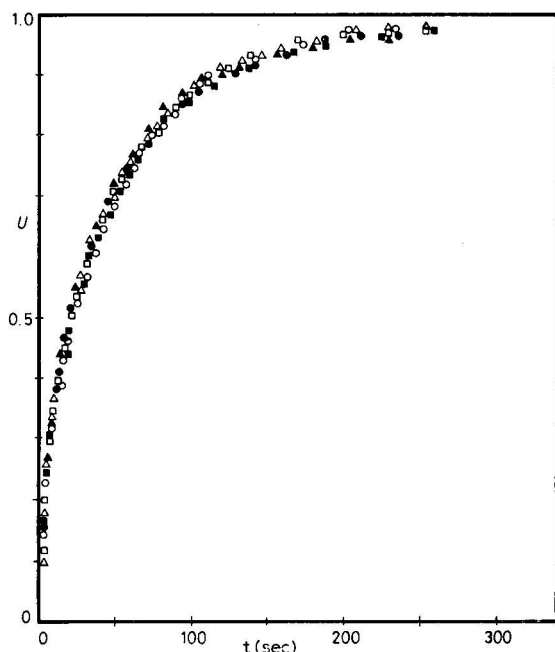


Fig. 2. Typical high-salinity kinetics. Resin: Kastel A-500, 30-35 mesh. Temperature, 25°; stirring speed 2000 rpm; concentration, 1.8 *N*. ●, Test 160; ○, 161; ■, 289; □, 290; △, 313; ▲, 314. Tests 160 and 161 dated November, 1973; tests 289, 290, 313 and 314, January, 1974. Tests 313 and 314: resin previously immersed in distilled water for 4 h.

TABLE I

MAIN PHYSICO-CHEMICAL PROPERTIES OF THE RESINS INVESTIGATED

Concentration = 1.8 *N*; temperature = 25°.

Resin	Predominant functional group	Matrix	Porosity	Exchange capacity (equiv./kg)		
				16-18 mesh	20-30 mesh	30-35 mesh
Kastel A-500	Quaternary (type I)	Styrenic	Gel	3.05	3.22	3.48
Lewatit M-500	Quaternary (type I)	Styrenic	Gel		4.05	
Amberlite IRA-400	Quaternary (type I)	Styrenic	Gel	3.94	3.89	3.72
Relite 3A	Quaternary (type I)	Styrenic	Gel		3.75	
Kastel A-300	Quaternary (type II)	Styrenic	Gel		3.28	
Lewatit M-600	Quaternary (type II)	Styrenic	Gel		3.35	
Relite 2A	Quaternary (type II)	Styrenic	Gel		3.63	
Kastel A-101	Tertiary	Styrenic	Gel		3.90	
Amberlite IRA-93	Tertiary	Styrenic	Macroreticular	3.97	3.88	3.81
Relite 4-MS	Tertiary	Styrenic	Gel		3.89	
Lewatit MP-60	Tertiary	Styrenic	Macroporous		4.23	
Relite MS-170	Tertiary	Styrenic	Gel		4.65	
Amberlite IRA-68	Tertiary	Acrylic	Gel		4.70	
Kastel A-105	Tertiary	Acrylic	Gel	5.28	5.80	5.32
Lewatit Ca-9222	Tertiary	Acrylic	Gel		4.70	
Wofatit AK-40	Secondary	Styrenic	Porous	5.38	5.35	5.33
Kastel A-102	Secondary	Acrylic	Gel	6.20	6.20	6.20
Relite MG-1	Secondary	Acrylic	Gel		6.49	
Duolite A-366	Secondary	Acrylic	Gel		6.75	
Kastel A-103/1	Primary	Styrenic	Gel	3.13	2.88	2.33
Duolite S-2002	Primary	Styrenic	Porous		3.45	

TABLE II

KINETIC DATA FOR THE Cl⁻-SO₄²⁻ EXCHANGE IN THE PARTICLE DIFFUSION REGION

Concentration = 1.8 N; temperature = 25°; stirring rate 2000 rpm.

Resin	16-18 mesh		20-30 mesh		30-35 mesh		$\bar{D}_{0.5,av.} \cdot 10^7$ (cm ² /sec)
	$t_{0.5}$ (sec)	$\bar{D}_{0.5} \cdot 10^7$ (cm ² /sec)	$t_{0.5}$ (sec)	$\bar{D}_{0.5} \cdot 10^7$ (cm ² /sec)	$t_{0.5}$ (sec)	$\bar{D}_{0.5} \cdot 10^7$ (cm ² /sec)	
Kastel A-500	45	20	28	13.7	23	10	15.7
Lewatit M-500			55	7.1			
Amberlite IRA-400			34	11.3			
Relite 3A			35	11			
Kastel A-300			55	7.0			
Lewatit M-600			94	4.1			
Relite 2A			45	8.5			
Kastel A-101			51	7.5			
Amberlite IRA-93	107	8.4	39	9.8	24	9.3	8.8
Relite 4-MS			50	7.7			
Lewatit MP-60			73	5.3			
Relite MS-170			42	9.1			
Amberlite IRA-68			41	9.4			
Kastel A-105	114	7.9	58	6.6	29	7.4	7.5
Lewatit Ca-9222			40	9.6			
Wofatit AK-40	105	8.6	38.5	10.1	25	8.9	8.9
Kastel A-102	124	7.2	59	6.5	38	6.0	6.8
Relite MG-1			38	10.1			
Duolite A-366			62	6.2			
Kastel A-103/1	174	5.2	118	3.2	75	3.0	4.5
Duolite S-2002			108	3.6			

The third condition for the application of eqn. 2 (*i.e.*, constancy of \bar{D}), in fact, did not prove to be valid in this experiment. Further examination of the experimental results, based on the application of the Nernst-Planck model, is currently being carried out⁵. $\bar{D}_{0.5}$ is therefore merely one value of \bar{D} during that experiment, and not even the most representative value for the resin under the conditions used. Fig. 3 shows the general dependence of the exchange rates on the predominant fixed charge of the resins (closed circles indicate the potential resins for use in the sea-water desulphation process).

The same dependence in Fig. 4 is restricted to strong anion-exchange resins with a type I or type II quaternary ammonium group. In Fig. 5 the exchange rates of resins of intermediate basicity with tertiary amino groups are compared, according to the nature of the matrix. Fig. 6 shows the half-exchange times of different mesh fractions of some resins.

DISCUSSION

The difficulty of making valid comparisons among different resins must be recognized. When comparing, for instance, resins with the same kind of matrix, porosity, degree of cross-linking, charge density, etc., which differ only in the predominant functional groups, in principle it cannot be excluded that other, less appar-

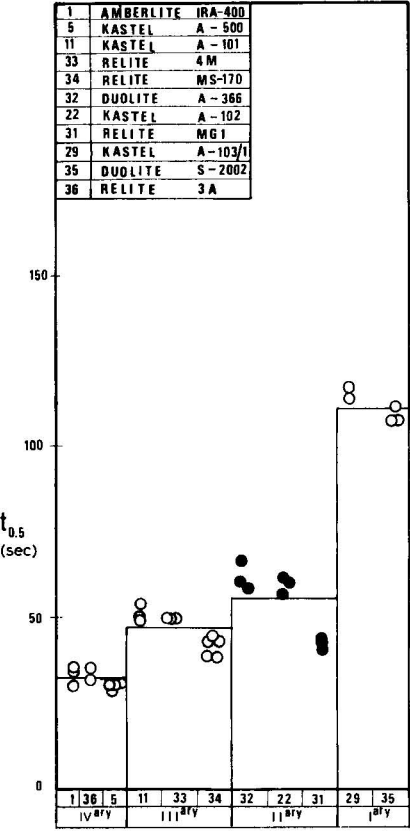


Fig. 3. Half-exchange times of polystyrenic gel resins with different amino-type functional groups (20-30 mesh).

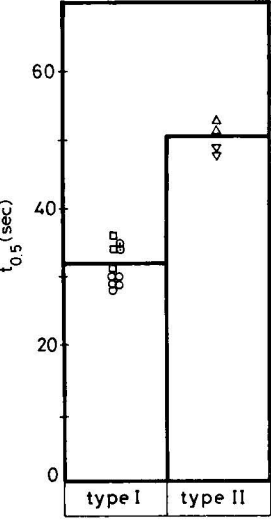


Fig. 4. Half-exchange times of polystyrenic gel strong anion-exchange resins with type I or type II ammonium groups (20-30 mesh). \circ , Kastel A-500, type I; \square , Amberlite IRA-400, type I; \odot , Relite 3A, type I; \triangle , Kastel A-300, type II; ∇ , Relite 2A, type II.

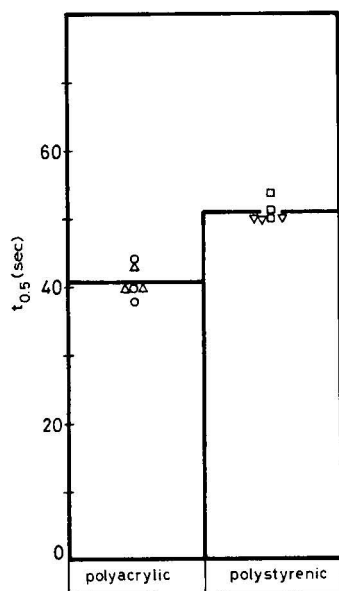


Fig. 5. Half-exchange times of tertiary gel resins with different matrices (20-30 mesh). ○, Lewait Ca-9222; △, Amberlite IRA-68; □, Kastel A-101; ▽, Relite 4-MS.

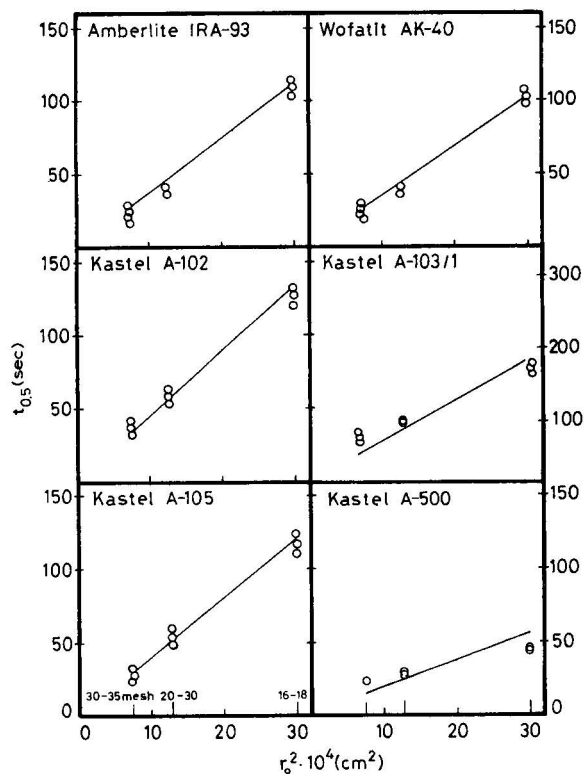
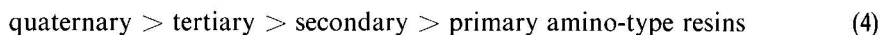


Fig. 6. Half-exchange times of different mesh fractions as a function of the average particle radius of the resins.

ent, physical differences in the resin morphology may have been introduced by the type of fixed charge itself. However, the hypothesis of physical homogeneity in groups of resins seems to be valid if one observes the reproducibility obtained over each group of similar resins.

The main result of this study was the finding of a close dependence of the Cl^- - SO_4^{2-} exchange rate on the nature of the amino-type functional group in the anion-exchange resins. According to the results in Fig. 3, the following "kinetic sequence" occurs:



which is the reverse of the selectivity sequence in eqn. 1.

It must be noted that strongly basic anion-exchange resins, (*i.e.*, with quaternary ammonium groups) have often been reported to show higher exchange rates than weakly basic ones in deionization and similar processes. In such cases, however, the parallel neutralization reaction of OH^- ions influences the overall exchange rate of the weaker resins. This is not the case in this work, where strict pH control prevents exchange reactions other than Cl^- - SO_4^{2-} from occurring.

The co-existence of the selectivity and kinetic sequences 1 and 4 may be considered to be reasonable if one simply examines the particular pattern of ion transfer inside the resin. In order to allow for further sulphate ions to be adsorbed by the particle, the exchanged sulphate ions migrate towards the inner parts of the bead, jumping from one fixed charge to another, with an iterative attach-detach mechanism. As the exchange process proceeds, each fixed charge repeatedly exchanges its sulphate ion with new sulphate ions. According to the established collision theory, this can be described by the following reaction:



where $\text{X}^- = \frac{1}{2} \text{SO}_4^{2-}$, $\text{Y}^- = \frac{1}{2} \text{SO}_4^{2-}$ (except in the first exchange, where $\text{Y}^- = \text{Cl}^-$) and R = amino-type fixed charge. Assuming that approximately the same energy content applies to the activated complex, irrespective of the type of amino group, the activation energy required for such a reaction to proceed is inversely proportional to the energy content of the sulphate form of the amino groups themselves.

It follows that the reaction rate is lower with the more selective resins, characterized by lower values of the energy content of the sulphate form and, therefore, by higher values of the activation energy involved in reaction 5. This helps to explain the large rate differences found between type I and type II quaternary ammonium resins. Type II strong anion-exchange resins (with a dimethylethanolammonium group) are often preferred to the stronger type I resins (with a trimethylammonium group) in industrial applications, because of their hydrophilic nature, which would enable faster rates to be obtained. Our findings, which contrast with this general statement, may be explained on the basis of a selectivity-kinetic correlation, the selectivity towards sulphate ions of the type II ammonium resins (like their basicity) lying between the first and second positions in sequence 1.

Our results agree with the data of Eliasek and Talasek⁶, who studied several

anion-exchange kinetics in the particle diffusion region and found a strong superiority of type I over type II anion-exchange resins in exchange reactions such as OH⁻-Cl⁻ and OH⁻-SO₄²⁻.

In full agreement with the expectations are the higher kinetics showed by polyacrylic over polystyrenic matrix resins, according to the hydrophobic nature of the latter. This result, among other considerations, confirms the possibility of using a polyacrylic product for the desulphation process.

Finally, as shown in Fig. 6 for some of the resins investigated, the half-exchange times lie on a straight line when plotted against the square of the particle radius. While definitely confirming the particle diffusion control, this allowed for the $\bar{D}_{0.5,av}$ values in Table II to be calculated for these resins by the least-squares method applied to eqn. 3. As confirmed by further investigations, however, although useful for comparison purposes, $\bar{D}_{0.5,av}$ is not yet suitable for quantitative measurements of the Cl⁻ and SO₄²⁻ diffusivities within the resins.

CONCLUSIONS

The basicity of functional groups has been seen to influence greatly both the equilibrium and the kinetic features of the Cl⁻-SO₄²⁻ exchange on anion-exchange resins. For the sea-water desulphation process, thermodynamic considerations and laboratory runs⁷ suggested the selection of intermediate weak anion-exchange resins, with predominantly secondary amino functional groups and a polyacrylic matrix, for substantially removing sulphates from sea-water, being capable of regeneration by the limited amount of brine available in the evaporation plants. This choice is now supported by kinetic considerations, which indicate that weaker resins (such as primary amino-type anionic resins), being extremely selective towards sulphates, would exhibit too low exchange rates. Due also to the hydrophilic nature of the polyacrylic matrix, with the selected resins half-exchange times less than 1 min can be expected, while 90% exchange can be reached in less than 5 min. These figures ensure high over-all kinetics coupled with high selectivity in the desulphation process.

In general, according to the diffusive nature of the ion-exchange mechanism, it can be concluded that selectivity may adversely influence the over-all kinetics of ion-exchange processes. This must be accounted for each time one is dealing with selective applications of ion exchange.

ACKNOWLEDGEMENT

The experimental part of the study was conducted by Mr. Antonio Pinto.

REFERENCES

- 1 G. Boari, *Ital. Pat. No. 39657-A/69*.
- 2 G. Boari, L. Liberti, C. Merli and R. Passino, *Desalination*, 15, No. 2 (1974).

- 3 T. R. E. Kressman and J. A. Kitchener, *Discuss. Faraday Soc.*, 7 (1949) 90.
- 4 F. Helfferich, *Ion Exchange*, McGraw-Hill, New York, 1962, p. 260.
- 5 L. Liberti and R. Passino, *J. Chromatogr.*, submitted for publication.
- 6 J. Eliasek and V. Talasek, *Collect. Czech. Chem. Commun.*, 33 (1968) 3866.
- 7 A. Aveni, G. Boari, L. Liberti, B. Monopoli and M. Santori, *Proc. 4th Int. Symp. Fresh Water from the Sea*, Vol. 2, Heidelberg, 1973, pp. 13-31.

CHROM. 7711

INVESTIGATION OF ANION-EXCHANGE EQUILIBRIA OF MALEIC AND FUMARIC ACIDS

A. MARTON and J. INCZÉDY

Department of Analytical Chemistry, University of Chemical Engineering, Veszprém (Hungary)

SUMMARY

The effect of pH on the distribution coefficients of maleic and fumaric acids on Dowex 1-X8 (Cl^-) anion-exchange resin has been investigated. From the dependence of the overall distribution coefficient on the pH of the solution, the ion-exchange selectivity coefficients for the monovalent and bivalent anions of maleic and fumaric acids have been calculated. The selectivity series observed follows the decreasing order of protonation constants. The nuclear magnetic resonance spectra of the resin in various ionic forms have also been investigated qualitatively.

INTRODUCTION

Chromatography on anion-exchange resins in the hydroxide, chloride, nitrate, acetate, borate, sulphate and carbonate forms has been widely used for the separation of organic acids. The various methods have been reviewed recently by Jandera and Churáček¹. Relatively few data are available, however, for the selectivity coefficients of *cis-trans* isomeric dicarboxylic acids. A study of the anion-exchange behaviour of maleic and fumaric acids was therefore undertaken in an attempt to obtain more information about the factors underlying the selective sorption of these acids on an ion-exchange resin in the chloride form.

EXPERIMENTAL

Dowex 1-X8 (Cl^-), 100-200 mesh, ion-exchange resin was obtained from Serva (Heidelberg, G.F.R.). The weight capacity of the resin was determined by the standard column technique².

A 10^{-1} M stock solution of maleic acid and a $2 \cdot 10^{-2}$ M stock solution of fumaric acid were prepared from reagent-grade chemicals. The pH values of these solutions were adjusted by the following method. A 20-ml volume of 0.5 M hydrochloric acid was pipetted into a 100-ml calibrated flask. For the investigation of the equilibrium of maleic acid 10 ml, and for fumaric acid 50 ml, of the above stock solution were added to the calibrated flask. Before filling the flask to the mark with distilled water, the required volume of saturated sodium hydroxide solution was added to it.

The overall distribution coefficients were measured by a batch method. A 50-ml volume of the above mixture was added to 0.5 g of the resin in a 100-ml glass-stoppered flask and allowed to stand with intermittent shaking for 24 h at room temperature. After the attainment of equilibrium, the final pH of the solution was determined by using a glass electrode.

After the liquid phase had been filtered free from the resin, an aliquot of the liquid was analyzed for the organic acid present. The distribution coefficient was calculated from the difference in concentration of organic acid before and after attainment of equilibrium. The concentration of the organic acid was determined by the polarographic method described by Elving and Rosenthal⁸.

Nuclear magnetic resonance (NMR) spectra were obtained with a Varian A-60 spectrometer. The chloride form of the resin was converted into the desired ionic form by a standard column procedure. For the conversion, the pH of a $10^{-1} M$ solution of maleic acid was adjusted to 3.9 or 10.0 and that of $2 \cdot 10^{-2} M$ fumaric acid to 3.8 or 7.65. After conversion, the resin was carefully air-dried and the dry resin was transferred into an NMR tube filled with a solution of appropriate concentration. The weight ratio of the resin and solution was approximately 1:1.

RESULTS AND DISCUSSION

The overall distribution coefficients were calculated using the following equation:

$$D = \frac{\text{amount of acid on resin}}{\text{amount of acid in solution}} \cdot \frac{\text{ml of solution}}{\text{g of dry resin in chloride form}}$$

The calculated distribution coefficients for maleic and fumaric acids are plotted against the pH in Fig. 1.

For the calculation of the ion-exchange selectivity coefficients, the following equation was derived earlier⁴:

$$D = \frac{K_{BH}^x K_1 Q [H^+] [Cl^-]^{-1} + K_B^x Q^2 [Cl^-]^{-2}}{1 + K_1 [H^+] + K_1 K_2 [H^+]^2}$$

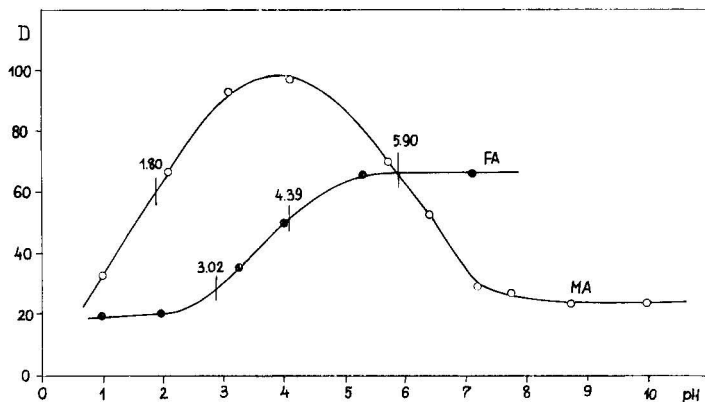


Fig. 1. Change of the distribution coefficients of maleic and fumaric acids as a function of pH. Resin: Dowex 1-X8. $c_{MA} = c_{FA} = 10^{-2} M$; $[Cl^-] = 10^{-1} M$.

where: D = overall distribution coefficient;
 K_{BH}^x, K_B^x = ion-exchange selectivity coefficients for the monovalent and bivalent anions, respectively;
 K_1, K_2 = protonation constant of the anions;
 $[H^+]$ = hydrogen ion concentration (mequiv./ml);
 $[Cl^-]$ = chloride ion concentration (mequiv./ml);
 Q = resin capacity (mequiv./g).

The values of the ion-exchange selectivity coefficients were calculated using the above equation by an Algol computer program based on the principles of least squares. Details of the computation and the program have been described elsewhere⁵.

The calculated ion-exchange selectivity coefficients for the monovalent and bivalent anions of maleic and fumaric acids are given in Table I.

TABLE I

ION-EXCHANGE SELECTIVITY COEFFICIENTS FOR THE MONOVALENT AND BIVALENT ANIONS OF MALEIC AND FUMARIC ACIDS AND THE LOGARITHM OF THE PROTONATION CONSTANTS⁶ OF THE ANIONS AT ROOM TEMPERATURE

Compound	K_{BH}^x	K_B^x	Log K_1	Log K_2
Maleic acid	2.96	0.022	5.90	1.80
Fumaric acid	1.70	0.063	4.39	3.02

From a comparison of the selectivity coefficients, it can be seen that the selectivity increases in the following order: $M^{2-} < F^{2-} < FH^- < MH^-$. This selectivity series follows the decreasing order of the protonation constants of the anions. This observation can be explained by the specific ion hydration effect, discussed by Chu *et al.*⁷. The value of the protonation constant is a measure of the base strength of the anion. A strong base has a strong interaction with water and is strongly hydrated, while a weak base has a weak interaction with water and is less hydrated. Hence it would be expected that the strong base would prefer the aqueous phase rather than the exchanger phase, while the weak base is preferentially adsorbed by the resin.

In the resin phase, the degree of hydration of the monovalent and bivalent anions was studied by NMR spectrometry and typical NMR spectra are shown in Fig. 2.

An aqueous suspension of the resin gives a well defined NMR spectrum exhibiting two peaks corresponding to the protons of water inside and outside the resin particles. The ion shift, relative to the peak of the outside water, can be explained in terms of structure-breaking and structure-making effects of the ions on the bulk solvent. Breaking of the hydrogen bonds by ions results in an upfield shift of the peak, while polarization of the water molecules by ions results in a downfield shift of the peak. The value of the shift, as pointed out by Reichenberg and Lawrenson⁸, is determined by the swelling of the resin. The shift is largest when the swelling is low.

The spectra in Fig. 2 indicate that the shift is negative (downfield shift) and is large when the resin is in the monovalent ionic form. These ions are less well hydrated and are preferentially adsorbed. The two peaks appear, however, when the resin is converted into the bivalent ionic form, such ions being more hydrated and less preferentially adsorbed by the resin.

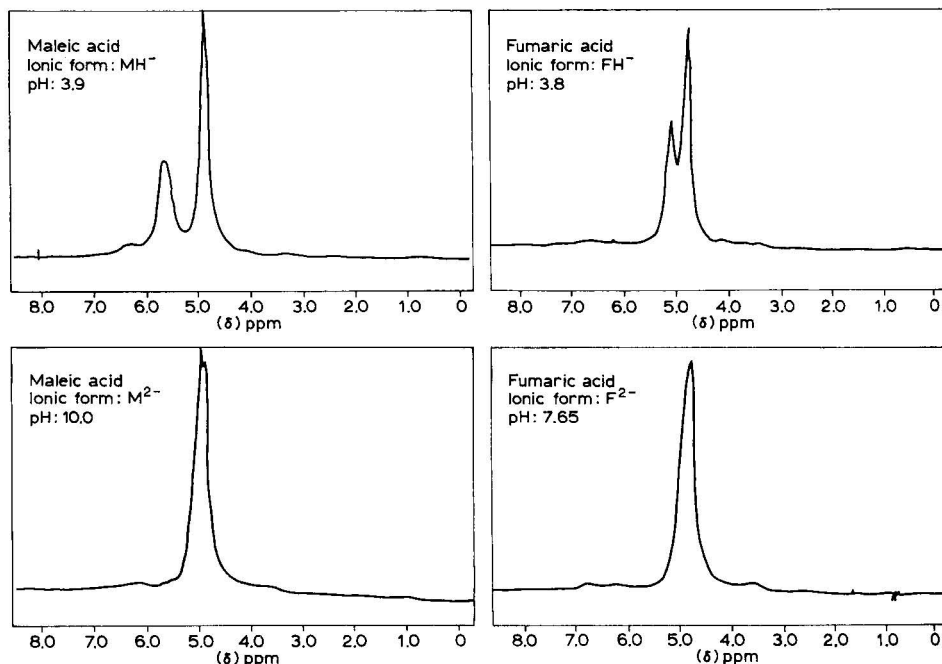


Fig. 2. NMR spectra of the aqueous resin suspension. Resin: Dowex I-X8 (100–200 mesh). Resin: water ratio = 1:1.

ACKNOWLEDGEMENT

The authors thank Serva (Heidelberg, G.F.R.) for supplying the ion-exchange resin. Thanks are also due to Dr. Ervin Kerényi, Leader of the Analytical Department of the Hungarian Oil and Gas Research Institute, and to Dr. Zoltan Décsy for making available the Varian A-60 NMR spectrometer.

REFERENCES

- 1 P. Jandera and J. Churáček, *J. Chromatogr.*, 86 (1973) 351.
- 2 J. Inczédy, *Analytical Applications of Ion Exchangers*, Pergamon Press, Oxford, 1964.
- 3 P. J. Elving and J. Rosenthal, *Anal. Chem.*, 26 (1954) 1454.
- 4 J. Inczédy and L. Glósz, *Acta Chim. Acad. Sci. Hung.*, 62 (1969) 241.
- 5 A. Marton and J. Inczédy, *Magy. Kém. Foly.*, 80 (1974) 145.
- 6 J. Inczédy, *Komplex egyensúlyok analitikai alkalmazása*, Műszaki Könyvkiadó, Budapest, 1970.
- 7 B. Chu, D. C. Whitney and R. M. Diamond, *J. Inorg. Nucl. Chem.*, 24 (1962) 1405.
- 8 D. Reichenberg and I. J. Lawrenson, *Trans. Faraday Soc.*, 59 (1963) 141.

CHROM. 7770

KINETICS OF DIFFERENTIAL ION-EXCHANGE PROCESSES IN A FINITE SOLUTION VOLUME

K. BUNZL

Gesellschaft für Strahlen- und Umweltforschung mbH München, Institut für Strahlenschutz, Gruppe Radiochemie und Analytik, 8042 Neuherberg (G.F.R.)

SUMMARY

Rate equations are given for film diffusion-controlled, differentially small ion-exchange processes in a finite solution volume. Two possibilities of performing differential ion-exchange reactions were considered: (1) reactions in which, independent of the initial ionic composition of the sample, the same small amount of counter ions is added, and (2) reactions in which, depending on the initial ionic composition of the sample, the amount of counter ions added is adjusted so as always to yield the same differential conversion of the sample. The theory shows in which way the rate of a differential ion-exchange process, which may involve ions of arbitrary valency, depends on the diffusion coefficients of the ions in the film, on the selectivity of the ion exchanger, on the initial ionic composition of the sample and on the extent of each differential reaction. It is shown that at any given initial ionic composition of the sample, the ratio of the initial rate of the forward to that of the corresponding reverse differential ion-exchange process is independent of the diffusion coefficients of the ions.

INTRODUCTION

Investigations on the kinetics of ion-exchange processes are important not only for the economic employment of synthetic ion exchangers in industry, but also to give a better understanding of many of the ion-exchange processes that occur in nature, e.g., in the soil or in biological membranes. Contrary to investigations on the rates of complete conversions of ion exchangers, which have been carried out over many years, determinations of the rates of differentially small ion-exchange reactions have been studied only recently. These studies, in which the ion exchanger is, independent of its initial ionic composition, converted only to a very small extent, offer several advantages: (1) information is obtained on the dependence of the rate of ion exchange as a function of the initial ionic composition of the ion exchanger; (2) quantities such as the separation factor, the diffusion coefficients or the water content of the sample, which, in general, depend on the ionic composition of the ion exchanger, can be considered to be constant within the small range of a differential ion-exchange process; and (3) a better understanding of many of the ion-exchange processes that

occur in nature, during which, in many instances, only very small amounts of ions are exchanged at a time, can be expected.

The kinetics of differential ion-exchange processes under infinite solution conditions were investigated first by Dickel and Körner¹ for particle diffusion-controlled and by Bunzl and Dickel²⁻⁴ for film diffusion-controlled ion-exchange processes. For many substances with ion-exchange properties, e.g., soil constituents, however, the experimental procedures of simulating an infinite solution by a streaming solution are not applicable, as their particle size is too small to enclose them in a wire screen cage.

For this reason, it seemed appropriate to us to investigate differential ion-exchange reactions under the finite solution conditions of a batch procedure. For this purpose, ion exchanger particles of a given initial ionic composition are first suspended in well-stirred pure water in a thermostated reaction vessel. The differential ion-exchange process, the rate of which one wants to determine, is then started by adding only a very small amount of counter ions, B, to this mixture. When investigating the rates of differential ion-exchange processes according to this method as a function of the initial ionic composition of the ion exchanger, the following two possibilities controlling the extent of each reaction are conceivable. (1) The amount of ions B added in each experiment to the ion exchanger, which contains initially ions B and D, is always the same. In this case, the total concentration, c , of all counter ions B and D in the solution will be constant throughout every differential ion-exchange process, but the extent of each differential ion-exchange reaction decreases as the initial equivalent fraction of B in the sample increases. (2) The counter ions B are always added to the ion exchanger in such an amount that the extent of each differential ion-exchange reaction is constant, regardless of the initial ionic composition of the sample. In this case, increasing amounts of counter ions B have to be added to each experiment as the initial equivalent fraction of B in the sample increases.

In this paper, the theory describing the rates of differential ion-exchange processes under finite solution volume conditions is considered. As the concentration of the solution must always be very dilute in order to yield only differential ion-exchange processes, film diffusion was considered as the rate-determining step. Both possibilities for performing differential reactions as mentioned above are considered. In addition to calculating the rates of such reactions as a function of the initial ionic composition of the sample, of the selectivity coefficient and of the diffusion coefficients, the ratios of the rates for forward and reverse differential ion-exchange processes at a given initial composition were also investigated.

THEORY

Differential batch ion-exchange processes, initiated by adding small, but always constant, amounts of counter ions ($\Delta c = \text{constant}$)

Equilibria. The experimental procedure is as follows. The ion exchanger particles are loaded with counter ions B (subscript 1) and D (subscript 2) and suspended in well-stirred pure water in a thermostated reaction vessel. A small amount of B ions (dissolved in water) is added to this suspension at time $t = 0$. If this amount of B ions added is small compared to the total ion-exchange capacity of the sample, the ion-exchange reaction thus initiated will convert the sample towards the B form

only by a small differential amount (*e.g.*, a few percent). The rate of this differential reaction is measured by conventional procedures. In order to obtain the desired information on the rate of ion exchange as a function of the ionic composition, the above experiments are carried out with different initial equivalent fractions of B in the ion exchanger. This set of differential measurements can be carried out most conveniently if one starts with the pure D form of the resin and uses (after washing with water) the equilibrium ionic composition of the sample attained in the first experiment as the initial ionic composition of the next experiment, and so on. As the same amount of ions is added every time in this type of measurement, regardless of the initial ionic composition of the sample, the extent of each differential reaction will become smaller the higher is the initial equivalent fraction of B in the resin. The equilibrium values and hence the extent of each differential ion-exchange reaction as a function of the initial equivalent fraction and of the equivalent separation factor, α_2^1 , can be derived for arbitrary valent ions from the equation

$$\alpha_2^1 = \frac{C_{1,\infty} \cdot c_{2,\infty} \cdot r_{2c}}{C_{2,\infty} \cdot c_{1,\infty} \cdot r_{1c}} = \frac{\bar{\gamma}_{1,\infty} \cdot \gamma_{2,\infty}}{\bar{\gamma}_{2,\infty} \cdot \gamma_{1,\infty}} \quad (1)$$

where $C_{1,\infty}$ and $C_{2,\infty}$, and $c_{1,\infty}$ and $c_{2,\infty}$, are the concentrations of the counter ions B and D (in moles of ion per litre) in the ion exchanger phase after attainment of equilibrium (*i.e.*, $t = \infty$) and the concentrations of these ions (in moles of electrolyte per litre) in the solution at $t = \infty$, respectively; r_{1c} and r_{2c} are the stoichiometric coefficients for ionization of the two electrolytes $B_{r_{1c}}A_{r_{1a}}$ and $D_{r_{2c}}A_{r_{2a}}$ present in solution (A is the common co-ion); and $\bar{\gamma}_{1,\infty}$ and $\gamma_{1,\infty}$ are the equilibrium equivalent fractions of the counter ions in the ion exchanger and in the solution, respectively.

The initial equivalent fractions of the counter ions in the resin at $t = 0$ are given by

$$\bar{\gamma}_{i,0} = z_i C_{i,0}/C \quad (2)$$

($i = 1$ or 2), where z_i are the valencies of the counter ions and $C_{i,0}$ denotes C_i at $t = 0$. Eqn. 2 holds, of course, also at the equilibrium if one replaces the subscript 0 by ∞ . C (mequiv./ml) is the total volume ion-exchange capacity of the water-swollen sample, given by

$$C = z_1 C_{1,t} + z_2 C_{2,t} \quad (0 \leq t \leq \infty) \quad (3)$$

As to V_0 ml of water, in which the ion exchanger particles are suspended by stirring, a small amount of B ions is added, the total equivalent concentration of counter ions in solution (in mequiv./ml) will increase from zero at $t = 0$ by a small amount Δc to an equivalent concentration, which is constant throughout the entire experiment and given by

$$\Delta c = z_1 r_{1c} c_{1,t} + z_2 r_{2c} c_{2,t} \quad (0 \leq t \leq \infty) \quad (4)$$

where $c_{i,t}$ are the concentrations (in moles of electrolyte per litre) of the ions B and D in solution at time t . According to the above experimental conditions, we have $c_{2,0} = 0$ and thus $\Delta c = r_{1c} z_1 c_{1,0}$. Note that for consistency with the diffusion coeffi-

cients introduced later according to the theory of irreversible thermodynamics⁵, $c_i(t)$ has the unit moles of electrolyte per litre and c has the unit milliequivalents per litre. After addition of the small amount of the electrolyte solution containing B ions, the final solution volume is now given by V (ml). The boundary condition of the batch system under consideration is then given by

$$r_{2c} z_2 c_2(t) = w z_1 [C_1(t) - C_{1,0}] = w C [\bar{\gamma}_1(t) - \gamma_{1,0}] \quad (5)$$

where $w = \bar{V}/V$ (\bar{V} ml = volume of the ion exchanger suspended in the reaction vessel in V ml of solution). Inserting eqns. 4 and 5, which also hold, of course, at $t = \infty$, into eqn. 1, we obtain for the equilibrium equivalent fraction, $\bar{\gamma}_{1,\infty}$, of a differential ion-exchange reaction, which started at $\bar{\gamma}_{1,0}$, the equation

$$\bar{\gamma}_{1,\infty} = [\sqrt{(b^2 + 4aH)} - b]/2a \quad (6)$$

where

$$a = w(1 - \alpha_2^1);$$

$$H = \alpha_2^1(w\bar{\gamma}_{1,0} + \Delta c/C);$$

and

$$b = w[\alpha_2^1 - \bar{\gamma}_{1,0}(1 - \alpha_2^1)] + \alpha_2^1 \Delta c/C$$

The extent of a differential ion-exchange reaction is then given by $\Delta\bar{\gamma}_1 = \bar{\gamma}_{1,\infty} - \bar{\gamma}_{1,0}$. The dependence of $\Delta\bar{\gamma}_1$ on the initial ionic composition and on the equivalent separation factor α_2^1 , as calculated according to eqn. 6, is shown in Fig. 1. The constants

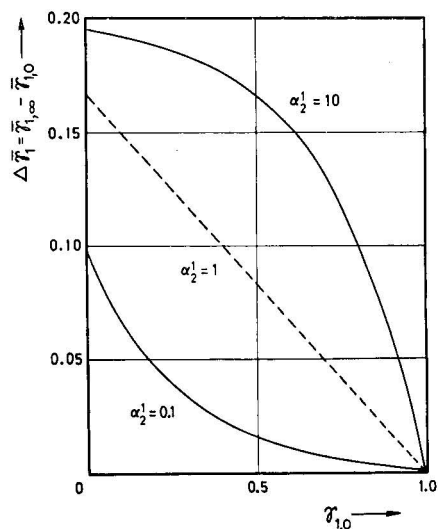


Fig. 1. Extent $\Delta\bar{\gamma}_1$ of differential ion-exchange processes as a function of the initial equivalent fraction $\bar{\gamma}_{1,0}$ of the ion exchanger, calculated according to eqn. 6. The values of the constants in this equation were taken as $w = 0.0001$, $V = 200$ ml, $c = 0.0001$ mequiv./ml and $C = 5$ mequiv./ml.

used for the system were: $w = \bar{V}/V = 0.0001$; $V = 200$ ml; $\Delta c = 0.0001$ mequiv./ml; and $C = 5$ mequiv./ml, which corresponds always to adding (independent of the initial ionic composition of the resin) 1 ml of a 0.02 N solution of B ions to 0.1 mequiv. of ion exchanger suspended in 199 ml of water. Fig. 1 shows how the extent of a differential ion-exchange reaction decreases the more the sample contains initially the ion to be taken up.

Rate equations. In order to obtain only differentially small ion-exchange reactions, the amount of counter ions added must be small (Δc will be about 0.0001 N , see above). For ordinary ion-exchange resins, the rate-determining step will thus be diffusion of the ions through the Nernst film surrounding the ion exchanger particles (film diffusion)⁶.

The differential equation of a film diffusion-controlled ion-exchange process is given⁷ for ions of arbitrary valency by

$$\frac{d\bar{\gamma}_1}{dt} = R' \cdot \frac{\alpha_2^1 r_{1c} c_1 z_1 (1 - \bar{\gamma}_1) - z_2 c_2 r_{2c} \bar{\gamma}_1}{\alpha_2^1 D_2 (1 - \bar{\gamma}_1) + D_1 \bar{\gamma}_1} \quad (7)$$

where

$$\begin{aligned} \gamma_1 &= z_1 C_1 / C; \\ R' &= \bar{F} D_1 D_2 / \bar{V} \delta C; \\ \bar{F} / \bar{V} &= \text{surface to volume ratio of the ion exchanger, which for spherical particles} = 3/r \text{ (} r = \text{particle radius)}; \\ D_1, D_2 &= \text{diffusion coefficients, which are functions of the four diffusion coefficients, } D_{ij}, \text{ describing isothermal diffusion in the corresponding ternary electrolyte solution involving the counter ions 1 and 2 and the common co-ion 3. They can be determined by independent measurements, but as yet very few data are available;} \\ \delta &= \text{film thickness.} \end{aligned}$$

Inserting the boundary and initial conditions (eqns. 4 and 5) of differential batch ion-exchange processes, we obtain

$$\frac{z_1 dC_1}{C dt} = R' \cdot \frac{\alpha_2^1 [\Delta c - w (z_1 C_1 - z_1 C_{1,0})] (C - z_1 C_1) - w z_1 (C_1 - C_{1,0}) z_1 C_1}{\alpha_2^1 D_2 (C - z_1 C_1) + D_1 z_1 C_1} \quad (8)$$

Eqn. 8 is the differential equation for the rate of uptake of B ions by the ion exchanger. It can be solved analytically, but as the solution is rather complicated for practical applications, it will not be reproduced here. As a more convenient characterization of the time dependence of the ion-exchange reaction we will use the initial rate, $(z_1 dC_1/dt)_{t=0}$, with which each differential ion-exchange process starts at a given $\gamma_{1,0}$. This quantity is obtained from eqn. 8 as

$$\left(\frac{z_1 dC_1}{C dt} \right)_{t=0} = R' \cdot \frac{\alpha_2^1 \Delta c (C - z_1 C_{1,0})}{\alpha_2^1 D_2 (C - z_1 C_{1,0}) + D_1 z_1 C_{1,0}} \quad (9)$$

or, in terms of the equivalent fraction of the ions in the ion exchanger, as

$$\begin{aligned} \left(\frac{d\bar{y}_1}{dt} \right)_{t=0} \cdot \frac{D_1}{R' \Delta c} &= \left(\frac{dQ_1}{dt} \right)_{t=0} \cdot \frac{D_1}{Q_{\text{tot}} R' \Delta c} = \\ &= \frac{\alpha_2^1 (1 - \bar{y}_{1,0})}{\bar{y}_{1,0} (1 - \alpha_2^1 D_2/D_1) + \alpha_2^1 D_2/D_1} \quad (10) \end{aligned}$$

where $Q_1 = z_1 C_1 \bar{V}$ = the total amount of ions, in milliequivalents, exchanged at time t by the sample and $Q_{\text{tot}} = C \bar{V}$ is the total amount of exchangeable ions in the sample. The value of $(dQ_1/dt)_{t=0}$ can be determined experimentally from the initial slope of a graph of Q_1 versus t .

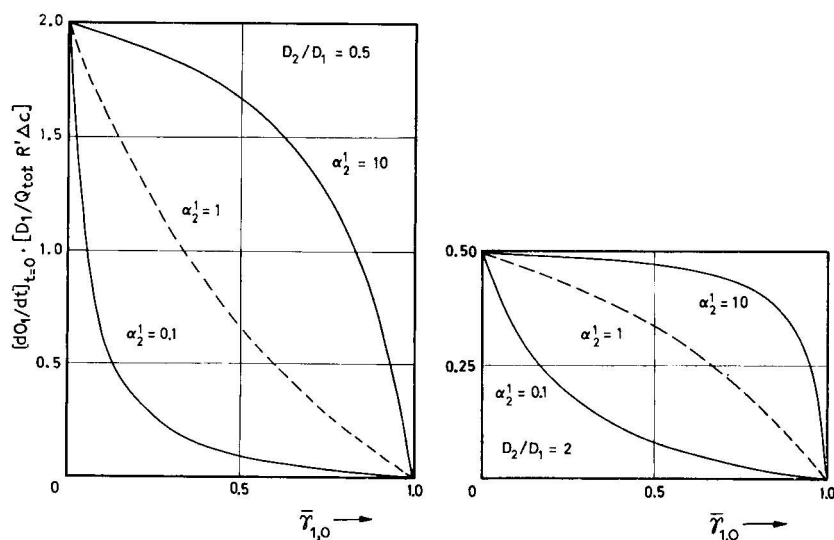


Fig. 2. Initial rates of differential ion-exchange processes plotted as the dimensionless quantity $(dQ_1/dt)_{t=0} \cdot (D_1/Q_{\text{tot}} R' \Delta c)$, according to eqn. 10, as a function of the initial equivalent fraction $\bar{y}_{1,0}$ of the ions in the sample. Parameters are the separation factor α_2^1 and the diffusion coefficients D_2/D_1 . $\Delta c = \text{constant}$.

Several important characteristics of the initial rate of differential ion-exchange processes can be seen from eqn. 10 and from Fig. 2, where the dependence of the initial rate (plotted as the dimensionless quantity on the left-hand side of eqn. 10) on the initial composition $\bar{y}_{1,0}$ of the ion exchanger is plotted as calculated according to eqn. 10; parameters in these plots are D_2/D_1 and α_2^1 :

(1) The initial rate of each differential ion-exchange process is directly proportional to Δc (*i.e.*, to the amount of B ions added) and to R' (*i.e.*, to the surface to volume ratio of the ion exchanger). It is inversely proportional to the film thickness, δ , which is determined mainly by the rate of agitation in the reaction vessel.

(2) The initial rate of each differential ion-exchange reaction decreases if the ion exchanger contains initially more of the B ions to be taken up.

(3) At a given initial composition of the ion exchanger and for given ions B and D (which determine the value of D_1/D_2), the initial rate of a differential ion-

exchange process is faster if α_2^1 is high, i.e., if the B ions are taken up preferentially compared with the D ions.

(4) Eqn. 10 and a comparison of the graphs in Fig. 2 show that the initial rate of each differential ion-exchange process increases as D_2/D_1 decreases.

Besides calculating, as above, the time dependence of the equivalent fraction of the ions in the ion exchanger during a differential reaction, it is even more revealing to calculate the time dependence of the fractional attainment, U , of the equilibrium of each process. U is defined as

$$U = \frac{C_1 - C_{1,0}}{C_{1,\infty} - C_{1,0}} = \frac{\bar{\gamma}_1 - \bar{\gamma}_{1,0}}{\bar{\gamma}_{1,\infty} - \bar{\gamma}_{1,0}} \quad (11)$$

Differentiation of eqn. 11 with respect to t yields

$$\frac{dU}{dt} = \frac{1}{\bar{\gamma}_{1,\infty} - \bar{\gamma}_{1,0}} \cdot \frac{d\bar{\gamma}_1}{dt} = \frac{1}{Q_{1,\infty} - Q_{1,0}} \cdot \frac{dQ_1}{dt} \quad (12)$$

which also holds, of course, for the initial rates. As the initial rates $(d\bar{\gamma}_1/dt)_{t=0}$ are given by eqn. 10 and the extent $\Delta\bar{\gamma}_1$ as a function of $\bar{\gamma}_{1,0}$ by eqn. 6, the initial rate of U , i.e., $(dU/dt)_{t=0}$, can be calculated for each differential ion-exchange process. According to eqn. 12, dU/dt is given by $(d\bar{\gamma}_1/dt)_{t=0}$ divided by the extent $\Delta\bar{\gamma}_1$ of each differential reaction. As both quantities decrease with increasing values of $\bar{\gamma}_{1,0}$ (see Figs. 1 and 2), one can expect $(dU/dt)_{t=0}$ to depend less on the initial composition of the ion exchanger than $(dQ_1/dt)_{t=0}$. That this is indeed the case can be seen from Fig. 3, in which $(dU/dt)_{t=0} \cdot D_1/R'\Delta c$ is plotted as a function of the initial composition of differential ion-exchange processes. The parameters are D_2/D_1 and α_2^1 . The values of the constants are the same as used in Fig. 1. Again, the rates for the attainment of the fractional equilibrium U are higher if D_2/D_1 is small.

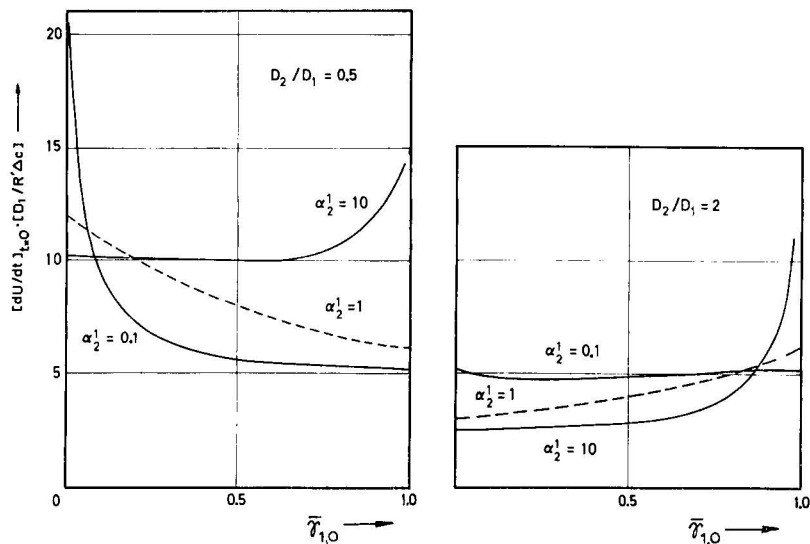


Fig. 3. Initial rates of the fractional attainment of equilibrium of differential ion-exchange processes plotted as the dimensionless quantity $(dU/dt)_{t=0} D_1/R'\Delta c$ according to eqn. 12 as a function of the initial equivalent fraction $\bar{\gamma}_{1,0}$ of the ions in the sample. Parameters are the separation factor α_2^1 and the diffusion coefficients D_2/D_1 . $\Delta c = \text{constant}$.

Forward and reverse ion-exchange reactions. As yet we have only considered differential ion-exchange processes, in which counter ions B were added to the ion exchanger of a given initial ionic composition $\bar{\gamma}_{1,0}$. The sample thus absorbed B ions and released D ions. In order to obtain the rate for the reverse ion-exchange reaction, in which D ions are added and B ions released by the resin, we must calculate $(\overrightarrow{dQ_1/dt})_{t=0}$ at the same initial ionic composition $\bar{\gamma}_{1,0}$ as for the forward reaction. $(\overrightarrow{dQ_1/dt})_{t=0}$ is given by eqn. 10. $(\overleftarrow{dQ_1/dt})_{t=0}$ at $\bar{\gamma}_{1,0}$ is obtained by exchanging in eqn. 10 D_2 and D_1 and substituting $\alpha_2^1 = 1/\alpha_2^2$ for α_2^1 , and $1 - \bar{\gamma}_{1,0}$ for $\bar{\gamma}_{1,0}$. We then obtain

$$\left| \left(\overleftarrow{dQ_1/dt} \right)_{t=0} \right| = \frac{Q_{\text{tot}} R' \Delta c}{D_2} \cdot \frac{\bar{\gamma}_{1,0}}{(1 - \bar{\gamma}_{1,0})(\alpha_2^1 - D_1/D_2) + D_1/D_2} \quad (13)$$

The ratio of the initial rate of a differential forward reaction to that of the corresponding reverse reaction at the same initial ionic composition $\bar{\gamma}_{1,0}$ is obtained from eqns. 10 and 13 as

$$\frac{\overrightarrow{dQ_1/dt}}{\overleftarrow{dQ_1/dt}}_{t=0} = \frac{\alpha_2^1 (1 - \bar{\gamma}_{1,0})}{\bar{\gamma}_{1,0}} \quad (14)$$

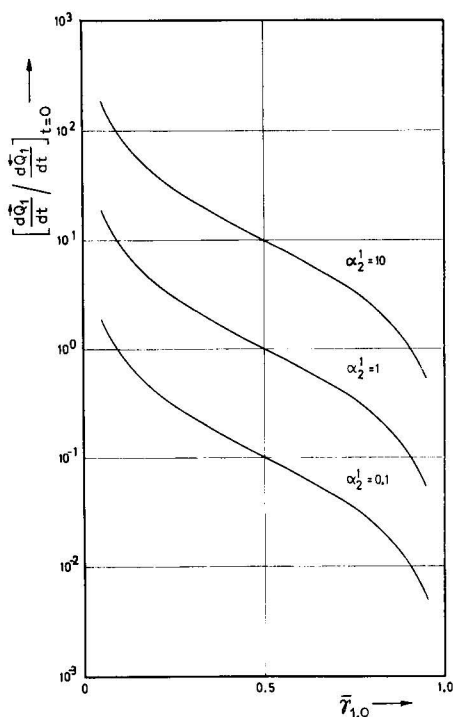


Fig. 4. Ratio of the initial rates of forward and reverse ion-exchange reactions as a function of the initial ionic composition $\bar{\gamma}_{1,0}$ of the sample according to eqn. 14. Parameter is the separation factor α_2^1 . $\Delta c = \text{constant}$.

As an illustration, this quantity is plotted in Fig. 4 for different values of α_2^1 as a function of $\bar{\gamma}_{1,0}$.

It can be seen that if the ion exchanger shows no preference for either B or D ions ($\alpha_2^1 = 1$), the forward reaction is faster than the reverse reaction provided that the initial value of $\bar{\gamma}_{1,0}$ is less than 0.5; if $\bar{\gamma}_{1,0}$ is greater than 0.5, the opposite is true. If the ion exchanger prefers the counter ion B compared with the counter ion D ($\alpha_2^1 > 1$), the forward reaction, in which B ions are taken up by the resin, will be faster (except at high values of $\bar{\gamma}_{1,0}$) than the reverse reaction. If the ion exchanger shows a selectivity for the counter ion D compared with the counter ion B ($\alpha_2^1 < 1$), the forward reaction, in which B ions are taken up, will be slower (except at low values of $\bar{\gamma}_{1,0}$) than the reverse reaction. Note that the ratio of the initial rate of the forward reaction to that of the reverse reaction, as given by eqn. 14, does not depend on either the diffusion coefficients or the concentration Δc . As we kept the latter quantity constant for the forward and the reverse reactions, the extent of the forward reaction, $\Delta \bar{\gamma}_1$, will be different from that of the corresponding reverse reaction, $\Delta \bar{\gamma}_1$, starting at the same initial ionic composition $\bar{\gamma}_{1,0}$. This can be taken into account by calculating the ratio of the initial rates for attainment of the fractional equilibrium U for the forward and the reverse reaction, which are given at $\bar{\gamma}_{1,0}$ by

$$\left| \frac{d\bar{U}}{dt} \right|_{t=0} / \left| \frac{d\bar{U}}{dt} \right|_{t=0} = \left| \frac{dQ_1}{dt} \right|_{t=0} / \left| \frac{dQ_1}{dt} \right|_{t=0} \cdot \frac{|\Delta \bar{\gamma}_1|}{|\Delta \bar{\gamma}_1|} \quad (15)$$

As the values of $(dQ_1/dt)/(dQ_1/dt)_{t=0}$ are given by eqn. 14 and $\Delta \bar{\gamma}_1$ by eqn. 6, $(d\bar{U}/dt)/(d\bar{U}/dt)_{t=0}$ was calculated for different values of α_2^1 using the values of $\Delta \bar{\gamma}_1$ shown in

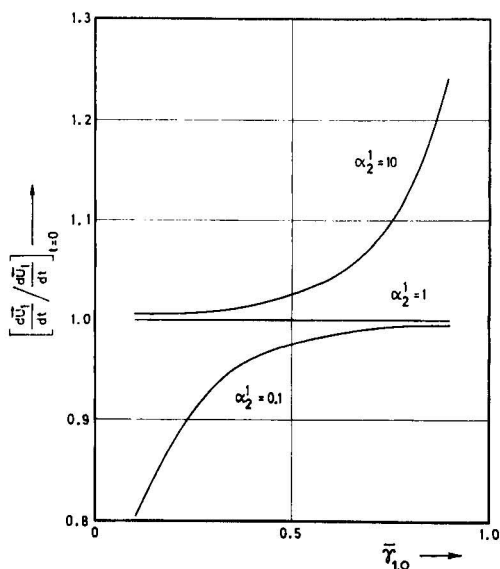


Fig. 5. Ratio of the initial rates for the fractional attainment of equilibrium of forward and reverse ion-exchange processes as a function of the initial ionic composition $\bar{\gamma}_{1,0}$ of the sample according to eqn. 15. Parameter is the separation factor α_2^1 . $\Delta c = \text{constant}$.

Fig. 1. Note that if $\overrightarrow{\Delta\bar{\gamma}_1}$ for the forward reaction is taken at $\bar{\gamma}_{1,0}$ from the curve of a given value of α_2^1 , the value of $\overleftarrow{\Delta\bar{\gamma}_1}$ of the reverse reaction has to be taken from the curve of $1/\alpha_2^1$ at $1 - \bar{\gamma}_{1,0}$. The ratio of the rates of the forward and reverse reactions for the attainment of the fractional attainment U are shown in Fig. 5. It can be seen that if the ion exchanger shows no selectivity for the two counter ions ($\alpha_2^1 = 1$), the forward and reverse rates for the attainment of fractional equilibrium U are identical. If the resin prefers the counter ions B compared with the counter ions D ($\alpha_2^1 > 1$), the rate of the forward reaction will always be higher than that of the corresponding reverse reaction. If the ion exchanger prefers the counter ions D compared with the counter ions B ($\alpha_2^1 < 1$), the opposite will be true.

Differential batch ion-exchange reactions, initiated by adding counter ions always in such amounts that the extent of each ion-exchange process remains constant ($\Delta\bar{\gamma}_1 = \text{constant}$)

Equilibria. The ion exchanger particles of a given initial ionic composition $\bar{\gamma}_{1,0}$ are again stirred in pure water in a reaction vessel at time $t = 0$ as in the first section *Equilibria*. The amount of counter ions B added to this mixture however, is now, depending on the initial ionic composition of the resin, selected in such a way that the extent $\Delta\bar{\gamma}_1$ of each differential ion-exchange reaction is always the same. This means, in general, addition of increasing amounts of counter ions B as long as $\bar{\gamma}_{1,0}$ increases. The exact amount of B ions to be added, i.e., the value of Δc as a function of the initial ionic composition $\bar{\gamma}_{1,0}$ in order to achieve a given $\Delta\bar{\gamma}_1$, can be calculated from eqn. 6.

Rate equations. If we again use the initial and boundary conditions used in the first section *Equilibria* but now express the rate as a function of $\Delta\bar{\gamma}_1$, we obtain for the initial rate of the uptake of B ions the equation

$$\begin{aligned} \left(\frac{dU}{dt}\right)_{t=0} \cdot \frac{D_1}{R'wC} &= \left(\frac{dQ_1}{dt}\right)_{t=0} \cdot \frac{D_1}{Q_{\text{tot}} \Delta\bar{\gamma}_1 R'wC} = \\ &= \frac{[\alpha_2^1 - (\alpha_2^1 - 1)(\Delta\bar{\gamma}_1 + \bar{\gamma}_{1,0})] \cdot (1 - \bar{\gamma}_{1,0})}{(1 - \bar{\gamma}_{1,0} - \Delta\bar{\gamma}_1) [\alpha_2^1 (D_2/D_1) (1 - \bar{\gamma}_{1,0}) + \bar{\gamma}_{1,0}]} \quad (16) \end{aligned}$$

As dU/dt and dQ/dt differ in this case only by a constant factor, it is sufficient to show in Fig. 6 only the dependence of dU/dt as a function of $\bar{\gamma}_{1,0}$ for different values of α_2^1 and D_2/D_1 , as calculated according to eqn. 16. As one can see from these figures (calculated for differential ion-exchange reactions of $\Delta\bar{\gamma}_1 = 0.05$), the rates at low values of $\bar{\gamma}_{1,0}$ can, depending on the values of α_2^1 and D_2/D_1 , either increase or decrease with increasing values of $\bar{\gamma}_{1,0}$. All curves converge, however, asymptotically to infinitely high rates at $\bar{\gamma}_{1,0} = 0.95$, because at this point the addition of an infinite amount of counter ions B to the solution would be required in order to convert the sample by a further step of $\Delta\bar{\gamma}_1 = 0.05$ completely into the B form ($\bar{\gamma}_{1,\infty} = 1$). This is, however, an unrealistic case, because at such high concentrations, film diffusion would no longer be the rate-determining step.

Forward and reverse ion-exchange reactions. The ratio of the rates of the forward and reverse reactions at the initial ionic composition $\bar{\gamma}_{1,0}$ is obtained in the same way as in the first section *Forward and reverse ion-exchange reactions*, and one obtains

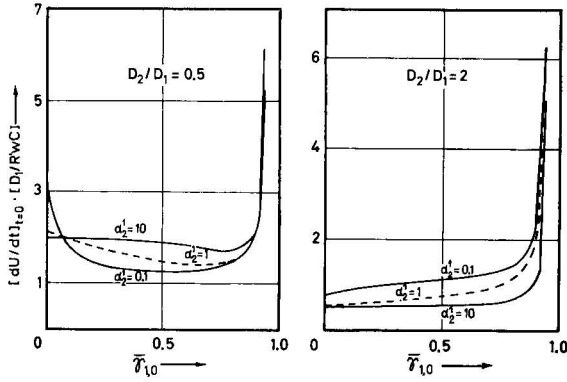


Fig. 6. Initial rates for the fractional attainment of equilibrium of differential ion-exchange processes plotted as the dimensionless quantity $(dU/dt)_{t=0} \cdot D_1/RwC$ as a function of the initial equivalent fraction $\bar{r}_{1,0}$ of the ions in the sample (eqn. 16). Parameters are the separation factor α_2^1 and the diffusion coefficients D_1/D_2 . $\Delta\bar{r}_1 = 0.05$.

$$\left| \frac{d\vec{U}}{dt} \right| / \left| \frac{dU}{dt} \right|_{t=0} = \frac{(1 - \bar{r}_{1,0})(\bar{r}_{1,0} - \Delta\bar{r}_1)}{\bar{r}_{1,0}(1 - \bar{r}_{1,0} - \Delta\bar{r}_1)} \times \frac{\Delta\bar{r}_1(1 - \alpha_2^1) + \alpha_2^1(1 - \bar{r}_{1,0}) + \bar{r}_{1,0}}{\Delta\bar{r}_1(\alpha_2^1 - 1) + \alpha_2^1(1 - \bar{r}_{1,0}) + \bar{r}_{1,0}} \quad (17)$$

i.e., a quantity that again is independent of the diffusion coefficients.

The ratio of the rates of the forward and reverse reactions, as calculated ac-

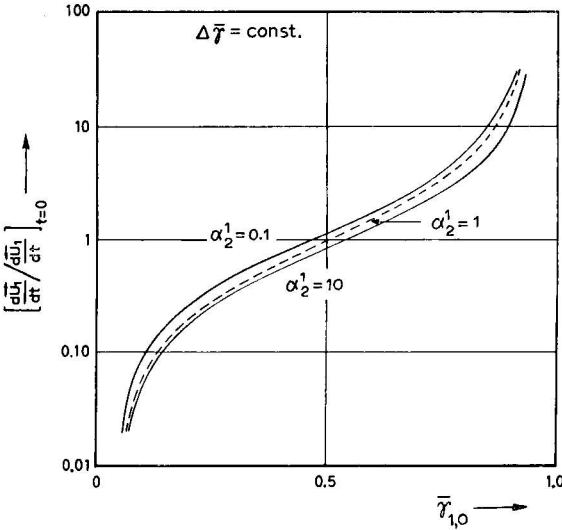


Fig. 7. Ratio of the initial rates for the fractional attainment of equilibrium of forward and reverse ion-exchange reactions as a function of the initial equivalent fraction $\bar{r}_{1,0}$ of the ions in the sample (eqn. 17). Parameter is the separation factor α_2^1 . $\Delta\bar{r}_1 = \text{constant} = 0.05$.

according to eqn. 17 for a value of $\Delta\bar{\gamma}_1 = 0.05$, is shown in Fig. 7 as a function of $\gamma_{1,0}$ for different values of α_2^1 .

As expected, the rate of the forward reaction is higher than that of the reverse reaction if $\bar{\gamma}_{1,0}$ is larger than about 0.5, because in order to convert the ion exchanger further towards the B form, a higher concentration of these ions in solution is necessary compared with the ion-exchange reaction in which the resin is converted by the same amount towards the D form. If $\bar{\gamma}_{1,0}$ is less than about 0.5, the opposite behaviour is found. The selectivity of the ion exchanger, *i.e.*, the value of α_2^1 , in this case has a comparatively small influence on the shape of the curves. At $\bar{\gamma}_{1,0} = 0.95$ and 0.05, the rate of the forward reaction compared with that of the reverse reaction becomes infinite and zero, respectively, for reasons which were explained in the previous section. If $\Delta\gamma_1$ approaches zero, $|(dU/dt)/(dU/dt)|_{t=0}$ approaches unity.

DISCUSSION

In all of the above figures, in which the dependence of the rates of differential ion-exchange processes on the initial ionic composition $\bar{\gamma}_{1,0}$ of the sample is shown, the equivalent separation factor α_2^1 was, for simplicity, always assumed to be independent of $\bar{\gamma}_{1,0}$. In many experiments, more complicated behaviour will be observed, however. In this case one can, nevertheless, apply all of the above rate equations because, and this is the advantage of considering only differential ion-exchange processes, within the small range $\Delta\bar{\gamma}$ of each reaction, α_2^1 can still be considered to be constant, although different for different values of $\bar{\gamma}_{1,0}$.

A similar situation arises for the diffusion coefficients D_1 and D_2 . As the four diffusion coefficients D_{ij} in the ternary solution of the film, which determine the values of D_1 and D_2 (eqn. 18 in ref. 7), depend to some extent on the equivalent fraction⁵, D_1 and D_2 are not strictly constant. This effect, however, probably need be considered only if the counter ions involve H^+ ions.

Finally, if one compares experimental results for forward and reverse reactions with the above theoretical predictions, one should first check if both reactions are actually film diffusion-controlled. As pointed out by Helfferich⁸, the rate-determining step of forward and reverse reactions need not necessarily always be the same.

Preliminary experimental results obtained in our laboratory are in satisfactory accordance with the above theory.

REFERENCES

- 1 G. Dickel and D. Körner, *Z. Phys. Chem. (Frankfurt am Main)*, **58** (1964) 64.
- 2 K. Bunzl and G. Dickel, *Z. Phys. Chem. (Frankfurt am Main)*, **61** (1968) 109.
- 3 K. Bunzl and G. Dickel, *Z. Naturforsch. A*, **24** (1969) 109.
- 4 K. Bunzl, *Z. Naturforsch. A*, **24** (1969) 900.
- 5 D. G. Miller, *J. Phys. Chem.*, **71** (1967) 616.
- 6 G. E. Boyd, *J. Amer. Chem. Soc.*, **69** (1947) 2836.
- 7 K. Bunzl, *Z. Phys. Chem. (Frankfurt am Main)*, **75** (1971) 118.
- 8 F. Helfferich, in J. A. Marinsky (Editor), *Ion Exchange*, Vol. 1, Marcel Dekker, New York, 1966, Ch. 2, p. 65.

CHROM. 7724

TRANSFERTS DE MASSE D'ÉCHANGE D'IONS MINÉRAUX PERTURBÉS PAR LA FIXATION SIMULTANÉE D'IONS ORGANIQUES VOLUMINEUX

A. ABADIE et H. ROQUES

Institut National des Sciences Appliquées de Toulouse, Département de Chimie, Avenue de Rangueil, 31077 Toulouse-Cédex (France)

SUMMARY

Mass transfers in ion-exchange systems perturbed by simultaneous fixation of an organic pollutant

Pollution of ion exchangers by organic matter takes place in two steps: dynamic fixation and accumulation of the organic matter in the network of the resin. We studied the first step in the light of mass transfer. For the determination of the two elementary mass transfer coefficients ak_L and ak_R (without and with organic pollutant in the solution) we built a laboratory unit by which a semicontinuous counter-current between a solution and an ion exchanger could be effected. The system studied was cationic, $RSO_3^- - NH_4^+ - K^+$, and the organic pollutant chosen was the cetyl pyridinium ion. We found that the *HUT* (height of the transfer unit) and the overall resistance were increased by a factor of 2.3. The two elementary mass transfer coefficients were perturbed.

INTRODUCTION

L'empoisonnement des résines échangeuses d'ions par des matières organiques est un phénomène qualitativement très bien connu¹⁻⁶ qui se manifeste généralement sur les anioniques fortes par une augmentation du temps de régénération, une consommation accrue d'eau de rinçage, une perte de capacité, une fuite en silice plus forte et une faible fixation des matières organiques.

Cet empoisonnement est dû à l'accumulation dans le temps de grosses molécules organiques dans les pores de la résine. Ces molécules généralement ioniques ou ionisables au contact de la résine peuvent être des acides humiques ou (et) fulviques, des polluants industriels divers (colorants, tensioactifs).

Les effets mentionnés ci-dessus, provoqués par l'état encrassé des résines par effet d'accumulation sont à distinguer du phénomène de perturbation instantané qui intervient par exemple sur une résine neuve traitant une solution minérale contenant une certaine concentration d'un polluant organique ionique. La distinction entre les deux phénomènes que l'on peut appeler respectivement perturbation statique et dynamique, tient compte de ce que: (i) La perturbation dynamique cesse dès que l'on sup-

prime la présence du polluant organique dans la solution. (ii) La perturbation statique est indépendante de la concentration instantanée en polluant organique dans la solution seule compte la quantité accumulée dans le temps par la résine. (iii) Les deux perturbations ne sont décelables qu'à partir d'une certaine concentration dans l'influent (dynamique) ou quantité accumulée (statique). (iv) Si la concentration en polluant est suffisante, on constate que la résine étant neuve, c'est la perturbation dynamique qui apparaît seule la première, dans le temps la perturbation statique vient s'y rajouter.

Cette perturbation dynamique récemment signalée et étudiée qualitativement⁷⁻¹⁰ nous semble mériter une étude plus fondamentale du type de celles menées pour l'étude d'autres phénomènes de transferts solide-liquide (électrodialyse), gaz-liquide, liquide-liquide modifiés par la présence de tensio-actifs aux interfaces ou (et) dans la masse.

De ces travaux antérieurs on peut retenir que l'empoisonnement dynamique des résines est lié à la présence d'un ion organique polluant dans la solution, est d'autant plus marqué que cette pollution est grande, se manifeste lorsque l'ion organique est susceptible de se fixer sur la résine et peut atteindre aussi bien les anioniques que les cationiques.

Ces expériences qualitatives tendraient à montrer aussi que les perturbations se situent à la fois à la périphérie et dans les grains de résine, mais cette conclusion demande confirmation.

Ces récents résultats laissant donc encore un doute sur la localisation de la perturbation et n'apportant aucune information quantitative sur les variations subies par les coefficients de transfert locaux et sur les *HUT* (hauteurs d'unités de transfert) il nous a paru utile d'engager une recherche pour aborder ces deux points.

Après un bref rappel théorique des phénomènes de transfert en échange d'ions et de la méthode choisie pour déterminer séparément les deux coefficients de transfert de masse locaux nous présenterons le dispositif expérimental à contre courant séquentiel construit pour cette étude. Ce dispositif sera testé avant d'aborder les résultats expérimentaux et leur discussion.

RAPPELS THÉORIQUES

Sur le modèle classique du transfert de masse au travers d'un double film appliqué à l'échange d'ions, on peut écrire que le nombre de milliéquivalents transférés par unité de temps et de surface est donné par

$$n = k_L Co (x - x_i) = k_R Q (y_i - y) \quad (1)$$

Dans le cas d'une courbe d'équilibre linéaire du type

$$y = ex^* + b \quad (2)$$

et en admettant l'équilibre à l'interface $y_i = ex_i + b$, l'équation 1 devient

$$n = K_{oL} Co (x - x^*) \quad (3)$$

avec

$$\frac{1}{K_{oL}} = \frac{1}{k_L} + \frac{Co}{k_R Q e}$$

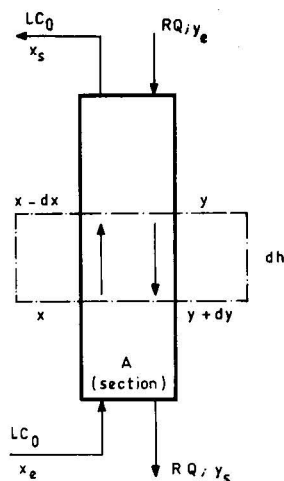


Fig. 1. Schéma des bilans de masse.

En régime permanent dans un dispositif à contre-courant, solution-résine, le bilan ionique sur une tranche de colonne s'écrit (Fig. 1)

$$A dh a Co K_{oL} (x - x^*) = L Co dx$$

qui conduit à la relation de dimensionnement classique

$$h = HUT \cdot NUT = \frac{L}{Aa K_{oL}} \int_{x_1}^{x_2} \frac{dx}{x - x^*} \quad (4)$$

Le fait de travailler avec un système qui possède une courbe d'équilibre linéaire dans l'intervalle $x_1 \rightarrow x_2$ permet une utilisation plus rigoureuse de l'équation 4 ainsi qu'une intégration mathématique car la courbe de travail est une droite, $y = tx + b'$, et dans ces conditions, la NUT est donnée par

$$NUT = \frac{e}{e - t} 2.3 \left[\log_{10} \left(\frac{tb - b'e}{e} \right) + \left(\frac{e - t}{e} \right) y \right]_{y_1}^{y_2}$$

L'observation de l'équation de la HUT suggère¹¹ une méthode simple pour la détermination séparée de ak_L et ak_R ; en effet, l'expression :

$$HUT = \frac{u}{ak_L} + \frac{uCo}{ak_R Qe}$$

reportée dans le plan $[HUT, (Co)]$ doit conduire à une droite dont l'ordonnée à l'origine et la pente contiennent les coefficients recherchés indissociables de a . En pratique il suffira de déterminer la HUT sur un dispositif à contre-courant pour quatre ou cinq valeurs de Co en présence, puis en l'absence d'ion organique perturbateur.

APPAREILLAGE ET EXPERIMENTATION

Le dispositif réalisé est à classer dans la catégorie des colonnes forcées, l'avancement de la résine et la circulation de la solution étant alternatifs.

et 3b qui schématisent les deux périodes d'un cycle complet, 3 min 30 sec, en position de travail et 30 sec en séquence d'avancement de la résine. La partie supérieure de la zone h de travail est délimitée par un contre-courant d'eau déminéralisée L' , la séparation des deux flux L et L' étant linéaire, et dans l'axe de la crépine de sortie.

Pour les essais avec perturbation dynamique, il était nécessaire que la résine entre dans la zone de travail déjà perturbée par l'ion organique, par souci d'homogénéité le long de la colonne. C'est la raison pour laquelle un volume de résine égal à celui évacué par cycle est sollicité par trois injections ($\lambda/3$) de solution d'ion organique polluant dans la zone d'attente A à la concentration égale à la pollution choisie pour la solution à traiter (compte tenu de la dilution L'). De même, lors de la séquence d'avancement de la résine le débit d'eau de poussée I sera dopé par l'ion organique [$3(\lambda/3)$ et I'] toujours à la concentration choisie et compte-tenu de la dilution par I , de manière à ne pas "déperturber" la résine. Pour les essais sans perturbation les injections λ et I' n'existent pas.

Toute l'installation a été automatisée. Le temps de mise en régime n'a jamais excédé 60 min.

Le développement théorique nous ayant montré la nécessité d'avoir une courbe d'équilibre linéaire ou assimilable à une droite dans l'intervalle d'intégration (équation 4) nous avons choisi le système RSO_3^- [cationique forte standard (Duolite C-20), 0.63–0.80 mm]– NH_4^+ – K^+ , qui admet l'équation $y \approx I x^*_{\text{K}^+} + 0.035$ comme droite d'équilibre dans l'intervalle $y = 0.25$ à 1 (Fig. 4) ($C_0 = 0.1 N$). La résine d'entrée était donc toujours conditionnée à $y_e \approx 0.25$.

Les dosages ont été effectués sur l'ion ammonium par le réactif de Nessler. Le débit ionique de résine RQ était mesuré par pHmétrie (capacité d'échange de R , débité par cycle).

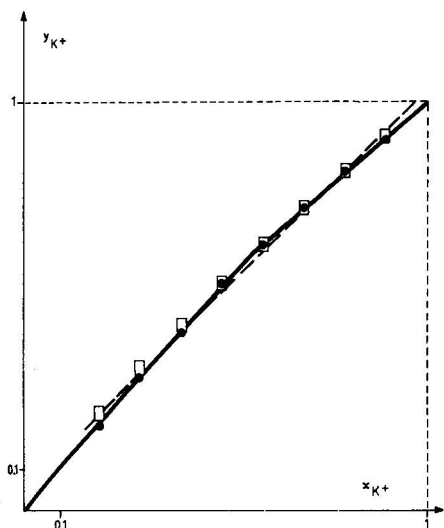
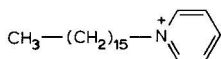


Fig. 4. Courbe d'équilibre $y = f(x)$ pour le système résine cationique forte (Duolite C-20)– KCl – NH_4Cl (24°; $C_0 = 0.1 N$).

L'espèce organique perturbatrice choisie a été le cation cétyl pyridinium (CP^+)



que l'on peut doser par absorption UV.

RÉSULTATS ET DISCUSSION

Fiabilité de l'installation

Après les mises au point mécaniques et hydrauliques de notre appareillage nous avons testé les résultats qu'il était susceptible de nous donner en déterminant l'exposant b de l'équation

$$HUT = M u^b$$

où u représente la vitesse spécifique ($cm \cdot sec^{-1}$) de la solution. Ce terme b a été utilisé et mesuré par plusieurs auteurs, qui ont proposé: $b = 0.50$ (Michaels¹⁵); 0.44 (Bieber *et al.*¹⁶); 0.44 (Moison et O'Hern¹¹); 0.54 (Shiryaev *et al.*¹⁷; valeur déterminée à partir d'un graphe figurant dans la publication); 0.36 (Gondo¹⁸); 0.54 (Nikashina et Rubinshtein¹⁹).

Entre les valeurs 0.708 et 2.472 cm/sec de u nous trouvons

$$HUT = 2.84 u^{0.46}$$

La valeur $b = 0.46$ s'incère donc parfaitement dans l'ensemble de valeurs précédemment citées. Les essais ont été faits à Co constant: $0.021 N$.

Détermination des coefficients de transfert de masse

Nous avons choisi un débit spécifique liquide voisin de 2 cm/sec (1.98 exactement) essentiellement pour que la pente de la droite $HUT = f(Co)$ soit mesurable avec une précision convenable¹¹. Il y avait à priori deux possibilités de travail permises en ce qui concerne le débit ionique de résine (RQ):

$$\text{soit avoir } t = \frac{LCo}{RQ} = cte, \text{ avec } RQ \text{ variable}$$

$$\text{soit avoir } t \text{ variable avec } Co, \text{ avec } RQ = cte$$

Pour les tests normaux, sans perturbation, les deux techniques de travail conduisent normalement à des résultats très voisins (Fig. 5, courbe I) par contre, pour les essais perturbés par CP^+ avec la possibilité $t = cte$ (soit RQ variable) nous avons obtenu des résultats inexploitable pour la détermination des deux coefficients de transfert locaux ceci étant dû principalement au fait que l'état perturbé de la résine n'est pas identique d'un essai à l'autre (RQ à $R'Q$) car la quantité de CP^+ injectée, elle, reste constante (L , λ et l'). En travaillant donc à RQ constant ($\approx 11,934$ méquiv./cycle) nous obtenons la courbe II (Fig. 5) qui montre très nettement que ce sont les deux coefficients élémentaires de transfert qui sont modifiés, le taux de pollution choisi en CP^+ étant 100 mg/l , $M = 358$ g (chlorure à 1 H_2O): soit 0.279 méquiv./l, soit 1.3% de la concentration en ions minéraux à $Co = 0.021 N$.

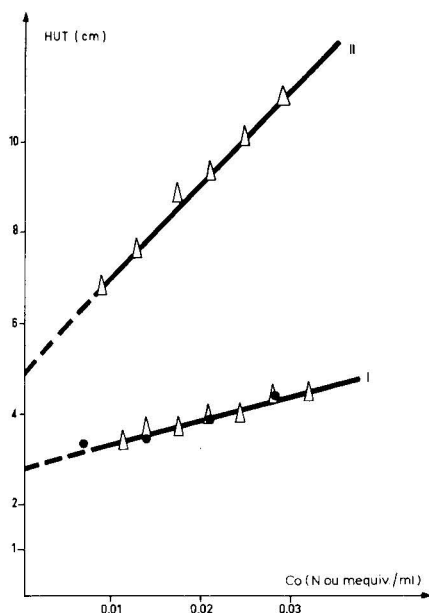


Fig. 5. Évolution linéaire de la HUT en fonction de Co . ●, Essais à $(LCo)/(RQ)$ constant, soit RQ variable; △, essais à $(LCo)/(RQ)$ variable, avec RQ constant. Courbe I, sans perturbation; courbe II, avec perturbation: 100 mg/l CP^+ .

L'expression de la HUT passe de $HUT = 52.4 Co + 2.82$ sans perturbation à $HUT = 208 Co + 4.90$ avec perturbation ce qui donne les deux séries de valeurs résumées dans le Tableau I.

TABLEAU I

	Perturbation		Rapport	Validité
	Sans	Avec		
HUT , cm	3.90	9.22	2.35	$Co = 0.021 N$
$\frac{1}{aK_{oL}}$, sec	1.98	4.66	2.35	$Co = 0.021 N$
ak_L , sec^{-1}	0.70	0.40	0.57	Indépendant de Co
ak_R , sec^{-1}	0.018 ₇	0.004 ₇	0.25	Indépendant de Co

Les conditions expérimentales et les résultats obtenus amènent un certain nombre de remarques pour situer cette étude tant sur le plan fondamental que pratique.

Nous dirons tout d'abord que dans nos essais, en présence de CP^+ la résine n'est pas dans un état identiquement perturbé entre l'entrée et la sortie de la zone de travail malgré le fait que nous ayons prévu une préperturbation en A (Fig. 3a).

En effet, on a pu mesurer que la concentration en ion cétyl pyridinium sur la résine, y_{CP^+} , passe de 0.0035 à l'entrée de la zone de travail à 0.0134 en sortie de colonne ($Co = 0.021 N$, $[CP^+]_{\text{entrée}} = 100 \text{ mg/l}$) ceci pour des temps de séjour respec-

tivement de 3 min 30 sec (A) et de 14 min environ ($A + h$). Mais ce qui est important, c'est que d'un essai à l'autre, cet état de perturbation dynamique incomplet et évolutif dans la colonne se conserve à peu de choses près. Il existe d'ailleurs également un gradient sur $[CP^+]_{\text{solution}}$ de 100 à 40 mg/l environ. Il faut donc considérer les valeurs des coefficients de transfert locaux comme des valeurs moyennes.

D'autre part, sur un plan pratique, il est évident que la concentration polluante appliquée, 100 mg/l, ne représente pas un cas réel possible. Nous avons donc étudié l'effet global de cette perturbation dynamique en fonction de $[CP^+]_{\text{solution influente}}$. La Fig. 6 indique qu'à partir d'une résine neuve, sur le plan empoisonnement organique, on note encore une exaltation d'environ 10% de la HUT pour 25 mg/l de CP^+ . Il est très probable que sur une résine ayant déjà accumulé une pollution organique, l'effet de la perturbation dynamique soit plus net, notamment vers les basses teneurs en polluant organique dans la solution influente.

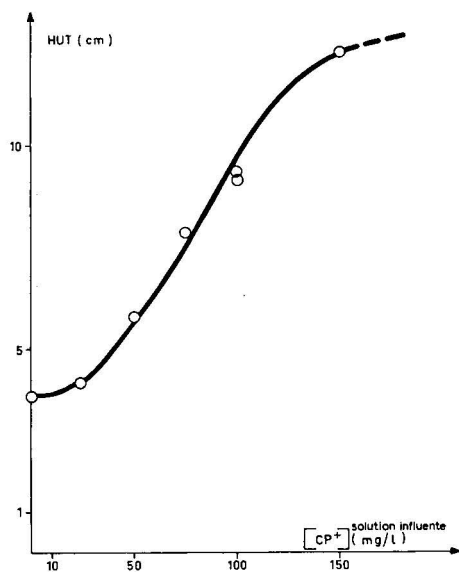


Fig. 6. Influence de la concentration en ion CP^+ dans la solution influente sur la HUT ($Co = 0.021$ N; $RQ \neq 12$ méquiv./cycle).

Des essais effectués avec un tensio-actif non ionique (Simulsol 9300 P, 50 mg/l) n'ont montré aucune perturbation, ceci rejoint un résultat de Small⁸, qui constate un résultat semblable en empêchant la fixation du polluant organique ionique.

CONCLUSIONS

L'empoisonnement des échangeurs d'ions par des polluants organiques peut se manifester de deux manières différentes: par effet dynamique et par effet statique. Si la résine est suffisamment agée, les deux effets peuvent se cumuler.

Par analogie avec d'autres phénomènes de transfert de masse perturbés par

des tensio-actifs, nous avons engagé une étude sur la perturbation dynamique d'une réaction d'échange d'ions minéraux par un polluant organique ionique susceptible de se fixer sur la résine en visant essentiellement deux objectifs: la localisation des perturbations et la mesure de leur amplitude. Le développement théorique permet d'établir une technique simple de séparation des deux coefficients de transfert de masse mais avec nécessité d'utiliser un dispositif d'échange d'ions à contre-courant ainsi que de travailler sur un couple qui admette pour courbe d'équilibre une droite dans l'intervalle de travail.

Nous avons conçu, réalisé et mis au point ce dispositif expérimental avec lequel on obtient la relation de forme classique $HUT = 2.84 u^{0.46}$. Le système $RSO_3^- - NH_4^+ - K^+$ peut admettre la droite

$$y_{K^+} = I x_{K^+} + 0.035$$

comme courbe d'équilibre dans l'intervalle $y \approx 0.25$ à 1.

En utilisant l'ion cétyl pyridinium comme agent perturbateur, nous avons montré que les deux étapes du transfert étaient perturbées, le coefficient ak_R était plus fortement diminué que ak_L et la résistance globale de transfert était multipliée par 2.3.

Nos résultats associés à ceux de Small⁸ montrent la nécessité d'avoir fixation de l'espèce polluante pour observer le phénomène.

NOMENCLATURE

- A = section de la colonne, cm^2 ;
 a = surface spécifique des grains de résine par ml de lit, on suppose $a_{liq.} = a_{résine}$, cm^2/ml ;
 Co = concentration ionique minérale totale de la solution, méquiv./ml;
 e = pente de la courbe d'équilibre assimilée à une droite;
 HUT = hauteur de l'unité de transfert, cm;
 h = hauteur du lit de résine, cm;
 k_L, k_R = coefficients de transferts de masse résine et liquide, cm/sec;
 K_{oL} = coefficient global de transfert de masse, cm/sec;
 L = débit volumique de la solution influente, ml/sec;
 NUT = nombre d'unités de transfert;
 Q = capacité d'échange de la résine, méquiv./ml de lit de résine (résine immergée, 50% K^+ , 50% NH_4^+);
 R = débit volumique de résine, ml/sec ou ml/cycle;
 u = vitesse spécifique du liquide, cm/sec;
 x et y = fractions ioniques équivalentes dans la solution et la résine (K^+);
 t = pente de la droite de travail $= \frac{LCo}{RQ} = \frac{y_{sortie} - y_{entrée}}{x_{sortie} - x_{entrée}}$.

RÉSUMÉ

Nous distinguons deux états dans l'empoisonnement des échangeurs d'ions par les matières organiques: un état dynamique et un état statique (résultant d'une

accumulation). Nous abordons l'étude fondamentale du premier effet en termes de transfert de masse. Nous avons conçu, construit et mis au point un dispositif d'échange d'ions à contre-courant séquentiel. Cet appareil nous a permis de déterminer les deux coefficients de transfert élémentaires ak_L et ak_R sans et avec perturbation par l'espèce organique additionnée dans la solution. On étudie le système $\text{RSO}_3^- - \text{NH}_4^+ - \text{K}^+$ perturbé par le cation cétyl pyridinium. La *HUT* (hauteur d'une unité de transfert) et la résistance globale de transfert sont multipliées par 2.3. Les deux transferts élémentaires sont perturbés.

BIBLIOGRAPHIE

- 1 F. X. McGarvey et J. W. Moffett, *Power Eng.*, 60 (1956) 97.
- 2 N. W. Frisch et R. Kunin, *J. Amer. Water Works Ass.*, 52 (1960) 875.
- 3 J. Ungar, *Effluent Water Treat.*, 6 (1962) 331.
- 4 J. J. Wolff et I. M. Abrams, *Ind. Water Eng.*, 12 (1969) 40.
- 5 I. M. Abrams, *Ann. Liberty Bell Corrosion Course*, 8th, Drexel University, Philadelphia, Pa., septembre 1970.
- 6 R. Kunin, *Amber-hi-lites*, (1973) 134.
- 7 A. G. Baranova et P. R. Taube, *Sb. Nauch. Rab. Penz. Inzh.-Stroit. Inst.*, 4 (1970) 117; *C.A.*, 69 (1968) 90057a.
- 8 H. Small, *J. Amer. Chem. Soc.*, 90 (1968) 2217.
- 9 A. Abadie et H. Roques, *Rapport D.G.R.S.T.*, Contrat No. 69.01.676 (1969).
- 10 A. Abadie et H. Roques, *Bull. Soc. Chim. Fr.*, 5 (1972) 1932.
- 11 R. L. Moison et H. A. O'Hern, Jr., *Chem. Eng. Prog., Symp. Ser.*, 55 (1959) 71.
- 12 L. S. Stanton, *M.S. Thesis*, Université de Washington, 1950.
- 13 N. K. Hiester, E. F. Fields, R. C. Phillips et S. B. Radding, *Chem. Eng. Prog.*, 50 (1954) 139.
- 14 L. Pawlowski, *Ion Exch. Membrane Technol.*, 1 (1972) 113.
- 15 A. S. Michaels, *Ind. Eng. Chem.*, 44 (1952) 1922.
- 16 H. Bieber, F. E. Steidler et W. A. Selke, *Ion Exch. Chem. Eng. Prog., Symp. Ser.*, 50 (1954) 17.
- 17 V. K. Shiryayev, M. S. Safonov, V. I. Gorshkov et V. A. Lipasova, *Russ. J. Phys. Chem.*, 45 (1971) 1294.
- 18 S. I. Gondo, *Mem. Fac. Eng. Kyushu Univ.*, 26 (1967) 123.
- 19 V. A. Nikashina et R. N. Rubinshtein, *Zh. Fiz. Khim.*, 45 (1971) 2842.

CHROM. 7726

MECHANISM OF CATION EXCHANGE ON SILICA GELS

DEMETRIUS N. STRAZHESKO, VLADIMIR B. STRELKO, VLADIMIR N. BELYAKOV
and SVETLANA C. RUBANIK

*L. V. Pisarzhevsky Institute of Physical Chemistry, Ukrainian SSR Academy of Sciences, Kiev
(U.S.S.R.)*

SUMMARY

The results of potentiometric studies of the polymerization of silicic acid and the mechanism of cation exchange on different ionic forms of silica gel are considered in terms of modern concepts of the properties of siloxane bonds.

INTRODUCTION

It is well known^{1,2} that orthosilicic acid is an extremely weak acid ($pK_1 \approx 9.8$). On the other hand, silica gel (polysilicic acid) and other highly dispersed silicas can exchange cations not only in neutral solutions, but even in acidic solutions (at pH 3–4 and higher)^{3–6}. This fact, as well as the location of the isoelectric point of sols and gels of silicic acid near pH 2 (refs. 6 and 7), shows that these more complex forms of silica contain strongly acidic centres or groups.

In order to ascertain the reason for this discrepancy and to study in more detail the mechanism of cation exchange on dispersed silicas, the changes in pK values of silicic acids in the initial stages of the polymerization of $\text{Si}(\text{OH})_4$ were followed potentiometrically; the same method was used to determine the pK of silica gel. The results obtained were then compared with our values and literature values for the adsorbabilities of various cations, ions of the elements of sub-groups I–IIIA of the periodic system, d - and f -cations, on different cation-substituted forms of silica gel. All the results thus obtained are considered in this paper in terms of modern concepts of the properties of Si–O bonds^{8,9}.

EXPERIMENTAL

A coarse porous silica gel with a specific surface area (B.E.T.) of *ca.* $600 \text{ m}^2 \cdot \text{g}^{-1}$ was prepared, as described earlier³. By means of ion exchange, we obtained from this sample a completely substituted calcium form and a mixed aluminium–hydrogen form of silica. Separate weighed portions of the hydrogen form of silica gel were titrated potentiometrically with solutions of LiOH, NaOH, KOH, $\text{Ca}(\text{OH})_2$ and $\text{Ba}(\text{OH})_2$ in 0.1 *N* solutions of the corresponding perchlorates.

In the sorption experiments, we traced the cations of salt solutions by means of the corresponding radioisotopes and measured their adsorption radiometrically.

RESULTS AND DISCUSSION

In our previous work¹⁰⁻¹², the high protogeneity of the surface silanol groups of silicas, which enables cation exchange to occur on them in acidic media, was attributed to the well known^{8,9,13} effect of $(p \rightarrow d)_\pi$ conjugation in the chain of siloxane bonds. In particular, it was shown¹² that the influence of this factor becomes apparent in the first stages of polymerization, *i.e.*, in the formation of oligomers of silicic acids; on going from the dimer to the tetramer, the ionization constant increased, in our tests, by an order of magnitude. This may be explained by the relatively greater contribution of $(p \rightarrow d)_\pi$ conjugation to the decrease in the negative charge on the oxygen atoms of terminal Si-OH groups with lengthening of the chain of Si-O bonds¹³.

A further development of the polymerization process must obviously lead to an even greater strengthening of the silicic acids formed. In fact, although when titrating with various bases we obtained different pK values for silica gel (NaOH, 7.7; KOH, 7.3; $\text{Ca}(\text{OH})_2$, see Fig. 1; $\text{Ba}(\text{OH})_2$, 6.5), they all showed that hydrogen in the silanol groups of polysilicic acid is much more mobile than in monomeric orthosilicic acid. It should also be noted that our results agree satisfactorily with the pK value of 7.1 ± 0.5 obtained recently by an independent IR spectral method¹⁴.

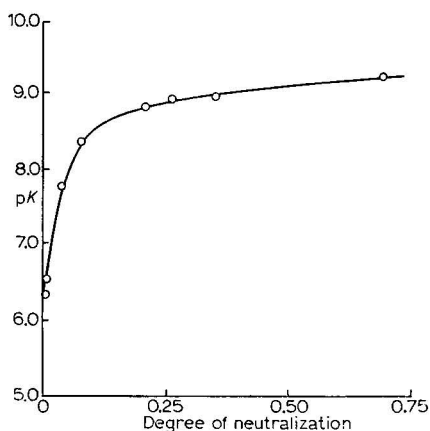


Fig. 1. Dependence of pK values of the silanol groups of silica gel on the degree of their neutralization (α) when titrating the gel with a solution of $\text{Ca}(\text{OH})_2$ in 0.1 N $\text{Ca}(\text{ClO}_4)_2$.

The results of the potentiometric measurements, which revealed a considerable mobility and hence the ability of the protons of the silanol groups of silica gel to undergo cation exchange, as well as their interpretation as cited above, are strongly supported by our sorption data. In accordance with other work³⁻⁶, these experiments showed that on both the hydrogen and the aluminium forms of silica gel (Fig. 2), which have compensating ions that are similar by nature (see below), the adsorbability of highly basic alkali metal and alkaline earth metal cations at $\text{pH} \leq 7$ increases regularly* with increase in their crystallographic radii, *i.e.*, from Li^+ to Rb^+ and from Ca^{2+} to Ba^{2+} .

* As on strongly acidic cation-exchange resins¹⁵.

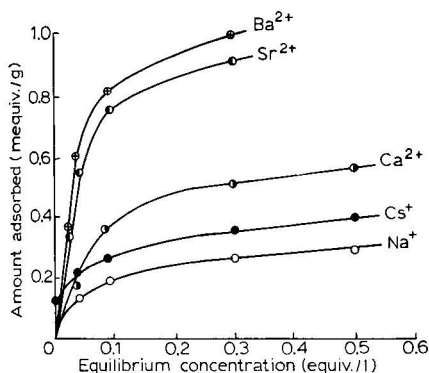


Fig. 2. Sorption isotherms of Na^+ , Cs^+ , Ca^{2+} , Sr^{2+} and Ba^{2+} cations on silica gel in the aluminium form; aqueous nitrate solutions at pH 4.5.

On the contrary, on the calcium^{16,17} and sodium forms of silica gel¹⁸, the order of sorption of these ions is reversed: $\text{Li}^+ > \text{Na}^+ > \text{K}^+ > \text{Rb}^+$ and $\text{Be}^{2+} > \text{Mg}^{2+} > \text{Sr}^{2+} \approx \text{Ba}^{2+}$. A similar reversal of the usual sequence of adsorbabilities of these metal cations was also observed in potentiometric titrations of silica gel in the hydrogen form with various alkalis at pH > 10 (Fig. 3).

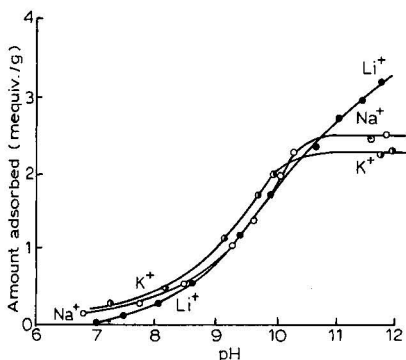


Fig. 3. Reversal of the adsorbability order of alkali metal cations in the high pH range when titrating silica gel with LiOH, NaOH and KOH solutions.

This reversal of the sorption series of cations of alkali metals and alkaline earth metals, *i.e.*, elements that have the lowest electronegativities⁸, X , with a change in the type of exchangeable cation (H^+ , $\text{Al}^{3+} \rightarrow \text{Na}^+$, Ca^{2+}) can, in our opinion, be given a convincing explanation in terms of the effects of $(p \rightarrow d)\pi$ conjugation on the properties of surface Si-O bonds.

It is known¹ that the surface of the common hydrogen form of silica gel can be represented schematically as shown in Fig. 4a. An exchange of the protons of a small (in acidic media) proportion of the surface Si-OH groups on strongly basic alkali metal or alkaline earth metal cations, Me_1^+ (Fig. 4b), leads to the appearance, on the oxygen atoms of the Si-O⁻Me₁⁺ groups, of a negative charge which increases with the basicity of the sorbed ion, Me_1^+ . This is due to the presence of OH groups

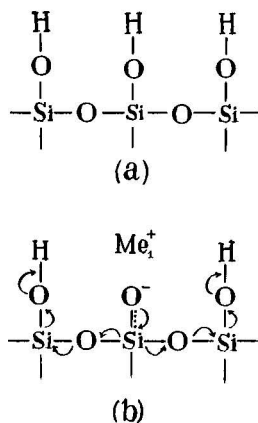


Fig. 4. Schematic representation of the surface of silica gel in acidic solutions (a) before and (b) after sorption of basic cations, Me_1^+ , on it. Me_1 : Li, Na, K, Rb, Cs, Ca, Sr, Ba with $X \leq 1$.

with a high electronegativity⁸ near every exchange centre, and the possibility of the electronic influence being transferred through the chain of Si–O bonds. Therefore, even from energy considerations*, on a silica surface with acceptor compensating ions (H^+ , Al^{3+} , etc.) from a group of alkali metal or alkaline earth metal cations, the ions with the lowest ionization potential must be sorbed preferably; this is, in fact, observed experimentally.

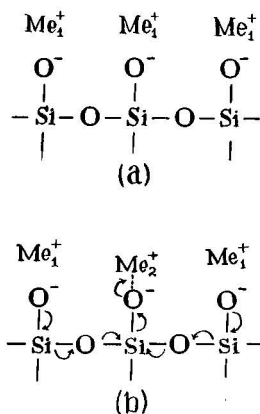


Fig. 5. Schematic representation of the surface of a silica gel salt form with basic counter ions, Me_1^+ , (a) before and (b) after the sorption of acceptor ions, Me_2^+ , on it. Me_1 : see Fig. 4; Me_2 : Be, Mg, Al, elements of *d*- and *f*-series with $X > 1$.

A different case occurs when cations are sorbed on the salt forms of silica gel with basic counter ions, Me_1^+ (e.g., Na^+ or Ca^{2+}), which are bound mainly electrostatically to the anionic oxygen in $\text{Si}-\text{O}^-\text{Me}_1^+$ groups (Fig. 5a). On such forms of silica, the ions sorbed most effectively will be those Me_2^+ ions which can compete

* Because of the increased ($p \rightarrow d$) _{π} interaction in $\text{Si}-\text{O}^-$ bonds^{8,9}.

most successfully with the silicon atom for the electronic density on the oxygen, thus providing a maximum degree of π interaction in the whole system of surface siloxane bonds near the exchange centre (Fig. 5b). These are, in fact, the most acceptor (least basic) ions, which explains, in particular, the reversal of the sorption series of alkali metal and alkaline earth metal cations on some silica gel salt forms¹⁶⁻¹⁸.

It is of interest to note that, unlike the cations of alkali metals and alkaline earth metals, the multivalent acceptor ions, e.g., of the rare-earth metals, gave the same sorption series on all investigated ionic forms of silica gel: $\text{La}^{3+} < \text{Ce}^{3+} < \text{Nd}^{3+} < \text{Gd}^{3+} < \text{Tb}^{3+} \approx \text{Y}^{3+} < \text{Er}^{3+} < \text{Tm}^{3+} < \text{Yb}^{3+} < \text{Lu}^{3+} < \text{Sc}^{3+}$.

In the light of above considerations, the independence of the affinity order of trivalent acceptor cations (and of similar, in this sense, d -element ions¹⁷) of the nature of the silica surface, acceptor (Fig. 4) or anionic (Fig. 5), could be explained only by the fact that the π interaction in the $\text{O}^- - \text{Me}_2^+$ bonds of these ions far exceeds the energy changes in the surface siloxane bonds. Therefore, the sorbed acceptor ion is unable to "feel" the nature of the exchanged counter ion separated from it by a chain of Si-O bonds.

The results of our potentiometric and ion-exchange studies are also in good agreement with IR spectral data for cation-substituted silica gels¹⁶ and results for the adsorption of different substances (acetic acid, dioxan, pyridine) on them¹¹.

REFERENCES

- 1 R. K. Iler, *The Colloid Chemistry of Silica and Silicates*, Cornell, New York, 1955, Ch. 3, p. 56.
- 2 A. G. Volosov, I. L. Khodakovskii and B. Ryzhenko, *Geokhimiya*, No. 5 (1972) 575.
- 3 D. N. Strazhesko and G. Ph. Jankowskaya, *Ukr. Khim. Zh.*, 25 (1959) 471.
- 4 S. Ahrland, I. Grenthe and B. Noren, *Acta Chem. Scand.*, 14 (1960) 1059 and 1077.
- 5 D. L. Dugger, J. H. Stanton, B. N. Irby, B. L. McConnell, W. W. Cummings and R. W. Maatman, *J. Phys. Chem.*, 68 (1964) 757.
- 6 Z. Z. Vysotsky and D. N. Strazhesko, in D. N. Strazhesko (Editor), *Adsorbtsiya i Adsorbenty*, Vol. 1, Naukova Dumka, Kiev, 1972, p. 36.
- 7 G. A. Parks, *Chem. Rev.*, 65 (1965) 177.
- 8 W. Noll, *Angew. Chem.*, 75 (1963) 123.
- 9 A. N. Lazarev, in N. A. Toropov and A. E. Porai-Koshits (Editors), *Structural Transformations in Glasses at Elevated Temperatures*, Nauka, Moscow, Leningrad, 1965, p. 233.
- 10 D. N. Strazhesko, Z. D. Skripnik and V. B. Strelko, *Trudy III Vsesojuznogo Sovestchaniya po Adsorbentam*, Nauka, Leningrad, 1971, p. 105.
- 11 V. B. Strelko and S. C. Rubanik, in D. N. Strazhesko (Editor), *Adsorbtsiya i Adsorbenty*, Vol. 2, Naukova Dumka, Kiev, 1974, p. 82.
- 12 V. N. Belyakov, N. M. Soltivsky, D. N. Strazhesko and V. B. Strelko, *Ukr. Khim. Zh.*, 40 (1974) 236.
- 13 C. T. Mortimer, *Reaction Heats and Bond Strengths*, Pergamon Press, Elmsford, N.Y., Oxford, Paris, 1962, Ch. 10.
- 14 M. L. Hair and W. Hertl, *J. Phys. Chem.*, 74 (1970) 91.
- 15 R. Kunin, *Ion Exchange Resins*, Wiley, New York, 2nd ed., 1958, Ch. 2, p. 30.
- 16 S. C. Rubanik, A. A. Baran, D. N. Strazhesko and V. B. Strelko, *Teor. Eksp. Khim.*, 5 (1969) 361.
- 17 V. B. Strelko, D. N. Strazhesko, N. I. Soloshenko, S. C. Rubanik and A. A. Baran, *Dokl. Akad. Nauk SSSR*, 186 (1969) 1362.
- 18 M. Milone and G. Cetini, *Atti Accad. Sci. Torino*, 90 (1956) 3.

CHROM. 7958

EFFECT OF CROSS-LINKING OF A SULPHONIC CATION-EXCHANGE RESIN AND EFFECT OF TEMPERATURE ON THE CHROMATOGRAPHIC SEPARATION OF ISOMERS OF DINITROBENZENE

JAN CHMIELOWIEC and WIKTOR KEMULA

Institute of Physical Chemistry, Polish Academy of Sciences, 01-224 Warsaw (Poland)

SUMMARY

The effect of resin cross-linking and temperature on the elution of the *o*-, *m*- and *p*-isomers of dinitrobenzene from a chromatographic column was investigated. It was found that longitudinal diffusion in the resin phase affects the total plate height.

An example of the separation of isomers of dinitrobenzene is described.

INTRODUCTION

Aromatic compounds are strongly sorbed on ion-exchange resins. The sorption of uncharged molecules by ion-exchange resins that differ in their degree of cross-linking¹ and the effect of resin cross-linking on ion-exchange separations²⁻⁴ have been investigated previously. Various nitro-compounds, including isomers, have been separated by elution development on a sulphonic cation exchanger⁵.

It seemed interesting, therefore, to study the effect of resin cross-linking on the chromatographic separation of organic compounds. This paper describes part of studies on the effect of resin cross-linking and temperature on the distribution and chromatographic separation of *o*-, *m*- and *p*-dinitrobenzene (DNB).

EXPERIMENTAL

Ion-exchange resins

Wofatit KPS (H⁺) of 4, 6, 8, 10 and 16% divinylbenzene (DVB) nominal cross-linking, containing sulphonic acid functional groups was used.

The air-dried resins were ground in a mortar and sieved, and the gradual sedimentation method from a suspension in water⁶ was employed to separate particles of 200-400 mesh for column experiments.

The resins were treated in a column successively with 1 *N* hydrochloric acid and 1 *N* sodium chloride solution. After several such cycles, the cation exchanger was washed with ethanol and then with water. The resins were then air-dried and stored in the H⁺ form. Their water contents were determined by drying them in an oven at 105° to constant weight. The exchange capacity was determined⁷ by adding exactly 200 ml of standard 0.1 *N* sodium hydroxide solution in 5% (w/w) sodium

TABLE I
PROPERTIES OF THE RESINS USED

% DVB	Exchange capacity (mequiv./g dry resin, H^+)	Maximum water content (g water/g dry resin, H^+)	Density of H^+ form
4	4.15	2.48	0.328
6	4.00	1.80	0.388
8	5.45	1.32	0.516
10	5.10	1.08	0.630
16	6.65	1.02	0.713

chloride solution to *ca.* 1 g of resin, weighed into a dry 250-ml erlenmeyer flask. After standing overnight in the stoppered flask, 50-ml aliquots of the supernatant solution were back-titrated with standard 0.1 *N* hydrochloric acid with phenolphthalein as indicator. The bed density, d_z (grams of the dry resin per millilitre of the bed), was determined by introducing a known amount of the resin in deionized water into a graduated cylinder and measuring the volume occupied by the resin bed after settling. The properties of the resins used are summarized in Table I.

Apparatus and procedure

The technique of chromato-polarography^{8,9} was chosen to monitor the effluent from the thermostatted 7×65 mm glass column filled with ion exchanger. The flow-rate used in all instances was 0.4 ml/min. A de-aerated aqueous solution (10% acetone + 0.05 *M* sulphuric acid) was used as eluent⁵. Methanolic solutions of isomers of DNB ($1 \cdot 10^{-2}$ *M*) were prepared, injected separately into the column and eluted at 15, 25, 35 and 50°. The amount of the isomers of DNB injected was $1.7 \cdot 10^{-6}$ g in a volume of 5 μ l.

TABLE II
WEIGHT-DISTRIBUTION COEFFICIENTS (λ) FOR ISOMERS OF DINITROBENZENE

% DVB	DNB isomer	λ			
		15°	25°	35°	50°
4	<i>p</i> -	14.5	11.7	11.2	7.5
	<i>m</i> -	17.8	15.5	13.0	10.3
	<i>o</i> -	22.6	20.1	16.2	11.9
6	<i>p</i> -	12.8	10.9	7.7	6.8
	<i>m</i> -	15.2	12.6	9.5	8.1
	<i>o</i> -	18.0	16.2	12.3	9.1
8	<i>p</i> -	9.8	7.7	6.5	5.9
	<i>m</i> -	12.9	9.8	8.6	6.9
	<i>o</i> -	18.1	14.3	10.7	8.3
10	<i>p</i> -	7.1	5.8	5.3	6.0
	<i>m</i> -	8.9	7.4	6.4	7.0
	<i>o</i> -	11.7	9.1	7.9	8.3
16	<i>p</i> -	6.0	5.3	4.6	3.3
	<i>m</i> -	7.4	6.0	5.3	3.7
	<i>o</i> -	10.6	8.0	6.3	3.8

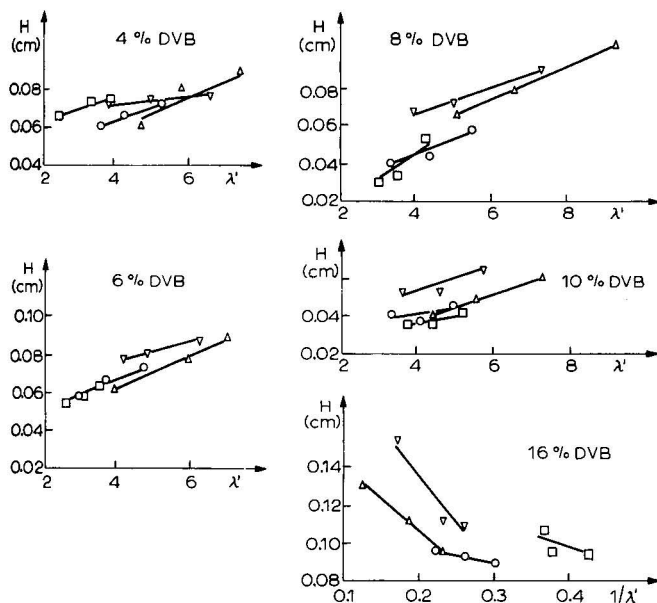


Fig. 1. Plate height (H) as a function of the bed distribution coefficient (λ'), and as a function of $1/\lambda'$ for resin of 16% DVB cross-linking. \triangle , 15° ; ∇ , 25° ; \circ , 35° ; \square , 50° .

RESULTS

The weight distribution coefficients, λ (summarized in Table II), and experimental plate heights were calculated¹⁰ from the elution curves.

Plate heights, H , are plotted as a function of the bed distribution coefficient, λ' , where, $\lambda' = \lambda \cdot d_z$, in Fig. 1. It can be seen that there is almost strictly linear de-

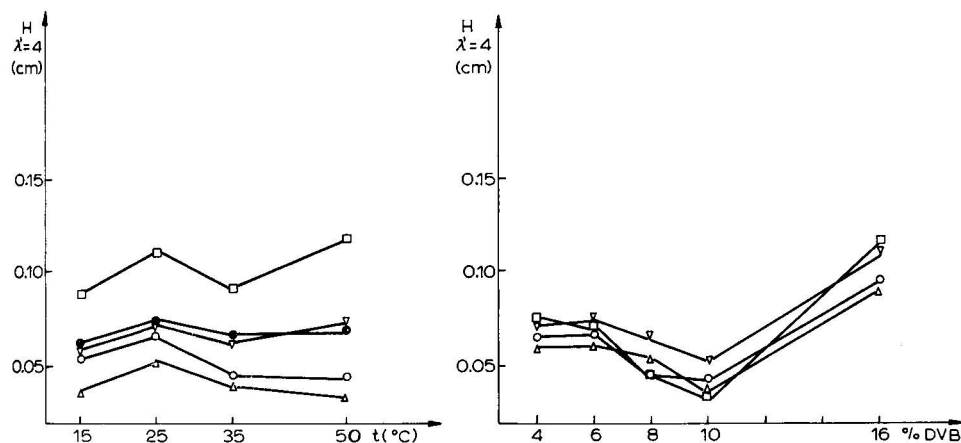


Fig. 2. Plate height ($H_{\lambda'=4}$), normalized for a bed distribution coefficient of 4, as a function of temperature. ∇ , 4% DVB; \bullet , 6% DVB; \circ , 8% DVB; \triangle , 10% DVB; \square , 16% DVB.

Fig. 3. Plate height ($H_{\lambda'=4}$), normalized for a bed distribution coefficient of 4, as a function of the degree of cross-linking. \triangle , 15° ; ∇ , 25° ; \circ , 35° ; \square , 50° .

pendence between H and λ' for resins of 4, 6, 8 and 10% DVB cross-linking, and also between H and $1/\lambda'$ for the resin of 16% DVB cross-linking. Plate heights, normalized for a bed distribution coefficient of 4 by extrapolating the linear dependences, are plotted as a function of temperature in Fig. 2 and as a function of the degree of cross-linking in Fig. 3.

DISCUSSION

It has been found, that the sorption of dinitrobenzenes is less at higher temperatures for all the degrees of cross-linking examined. The weight-distribution coefficients tend to decrease with increasing degree of cross-linking at all temperatures.

The plate height, H , changes slightly with increase in temperature for three isomers, independent of the resin cross-linking. In most instances, H tends to decrease. For all elution temperatures, H decreases with a decrease in the bed distribution coefficient (*cf.*, Fig. 1), which may be a reason for the tendency of the plate height to decrease with increasing temperature.

The plate height, normalized for a bed distribution coefficient of 4, depends less on the increase in temperature in comparison with the effect of cross-linking (*cf.*, Figs. 2 and 3). The changes in the normalized plate height with temperature can be neglected. For all elution temperatures, H decreases with the increase in the degree of cross-linking up to 10% DVB, where a minimum was observed, and H subsequently increases with further increase in the degree of cross-linking up to 16% DVB.

The origin of the changes in plate height with resin cross-linking in the system examined is of interest. The shape of the $H_{\lambda'=4}$ versus % DVB plot can be explained by the theoretical equation for the plate height in ion-exchange chromatography^{3,4}:

$$H = A + \frac{B}{\bar{D}} + C + E + F \cdot \bar{D} \quad (1)$$

where A , B , C , E and F are constants under particular experimental conditions and \bar{D} is the diffusion coefficient. Diffusion coefficients of isomers of DNB in the resin phase are not available, but usually diffusion coefficients decrease with an increase in the degree of cross-linking¹¹. Assuming that the diffusion coefficients decrease approximately linearly with an increase in the degree of cross-linking and the diffusional mass transfer in the resin phase (the second and fifth terms on the right-hand side of eqn. 1) is the main factor determining the plate height, it is easy to conclude that when \bar{D} decreases with an increase in the degree of cross-linking from 4% to 10% DVB, the significant contribution of longitudinal diffusion in the stationary phase for the less cross-linked resins is the reason why the plate height decreases. For Wofatit KPS of 10% DVB, a minimum occurs and $\bar{D} = \sqrt{B/F}$. A further decrease in \bar{D} with increase in the degree of cross-linking up to 16% DVB indicates that the second term must be operative and must be a reason for the increase in the plate height.

Such an explanation of the H versus % DVB dependence seems to be reasonable, although it is possible that the effect of differences in particle size distribution in the broad range of mesh size used (200–400 mesh) may interfere. After consider-

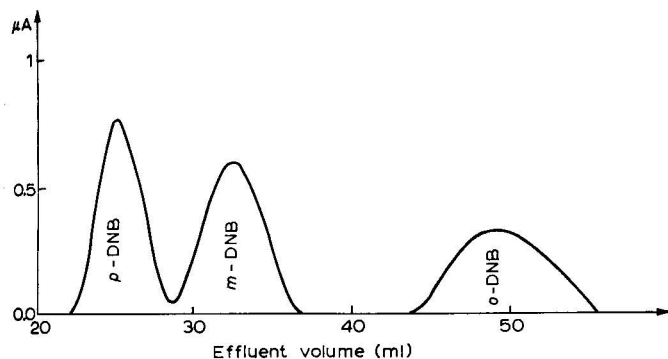


Fig. 4. Separation of the isomers of dinitrobenzene. Wofatit KPS of 8% DVB (7×300 mm) column. Eluent, 10% acetone + 0.05 M H_2SO_4 . Flow-rate, 0.4 ml/min. Temperature, 30° . Ordinate, intensity of the reduction current.

ation of the dependence of the calculated resolution¹⁰ on the degree of cross-linking and on temperature, the resin of 8% DVB nominal cross-linking and a temperature of 30° were chosen for the separation, and the isomers of DNB were separated (Fig. 4).

REFERENCES

- 1 D. Reichenberg and W. F. Wall, *J. Chem. Soc.*, (1956) 3364.
- 2 R. Dybczyński, Institute of Nuclear Research, Report No. 1115 (VIII) C, 1969.
- 3 R. Dybczyński, *J. Chromatogr.*, 50 (1970) 487.
- 4 R. Dybczyński, *J. Chromatogr.*, 71 (1972) 507.
- 5 W. Kemula and S. Brzozowski, *Rocz. Chem.*, 35 (1961) 711.
- 6 J. Minczewski and R. Dybczyński, *J. Chromatogr.*, 7 (1962) 98.
- 7 P. Helfferich, *Ion Exchange*, McGraw-Hill, New York, 1962, p. 91.
- 8 W. Kemula, *Rocz. Chem.*, 26 (1952) 281.
- 9 W. Kemula, in *Progress in Polarography*, Vol. 2, Wiley-Interscience, New York, 1962, p. 397.
- 10 R. Dybczyński, *J. Chromatogr.*, 31 (1967) 155.
- 11 G. E. Boyd, B. A. Soldano, *J. Amer. Chem. Soc.*, 75 (1953) 6091.

CHROM. 7855

SELECTIVE SWELLING OF ION EXCHANGERS IN MIXED SOLVENTS AND THE EFFECT OF SWELLING ON THE SORPTION OF IONS

A LÁSZTITY and T. A. BELYAVSKAYA*

Institute of Inorganic and Analytical Chemistry, L. Eötvös University, H 1443 Budapest, P.O. Box 123 (Hungary)

SUMMARY

The swelling of KU-2 cation exchanger and AV-17 anion exchanger in the hydrogen, chloride, nitrate, sulphate and perchlorate forms were measured in mixed solvents. In mixed aqueous–organic solvents, preferential swelling by water was found. For the perchlorate form of the resin, the selective uptake of organic solvent was observed at $N_{\text{MeOH}} < 0.2$ and at $N_{\text{Me}_2\text{O}} < 0.5$. The addition of mineral acids decreased the selective uptake of water by resins, especially in the case of resins in the sulphate form. This can be explained by the capability of the anion exchanger to take up mineral acids. The preferential sorption of water strongly influences the sorption of Ni(II), Co(II) and Cu(II) ions.

INTRODUCTION

The swelling behaviour of ion exchangers has been measured by numerous workers^{1–8} using mixed solvents. Most of them found that up to fairly high mole fractions of solvent in the solvent–water mixture there is a strong preference for water in the resin phase. The selective uptake of water by the exchanger is lower for anion exchangers than for cation exchangers² and depends on the ionic form of the exchanger^{1,2} and the degree of cross-linking of the resin³. Rückert and Samuelson⁴ determined the swelling of the Li^+ , Na^+ and K^+ forms of Dowex 50 resin and the Cl^- , SO_4^{2-} and ClO_4^- forms of Dowex 2 resin in ethanol–water mixtures. The order of swelling found for Dowex 50 was $\text{Li}^+ > \text{Na}^+ > \text{K}^+$ and for Dowex 2 $\text{SO}_4^{2-} > \text{Cl}^- > \text{ClO}_4^-$. However, with decreasing water content, the order of swelling for the SO_4^{2-} and Cl^- forms was reversed, which was explained by the different degrees of hydration of counter ions and their different salting-out effects with ethanol. An empirical equation valid in the mole fraction of organic solvent range 0.2–0.8, in the intermediate region of solvent mixtures, was found to describe the swelling of ion exchangers. This equation was used to describe swelling in other solvent mixtures also^{5,7}. Marcus and Naveh⁷ determined the swelling of the Cl^- and ClO_4^- forms of Dowex 1 resin of various degrees of cross-linking in several solvents and their mixtures in water. In mixed aqueous–organic solvents, alcohols are sorbed preferentially at low mole fractions (up to about 0.2). The same behaviour was ob-

* Present address: Department of Analytical Chemistry, Moscow State Lomonosov University, U.S.S.R.

served for an isopropanol–water mixture⁸. At higher mole fractions, water was sorbed to a greater extent. The results were explained in terms of the effect of the organic solvent on the structure of water and the selective ion solvation effects. The selective sorption of acetone was observed on the strongly basic anion exchanger AV-17 (CdI_4^{2-}) up to 0.5 mole fraction of acetone, whereas in the Cl^- form water was preferentially sorbed⁶.

Although many investigations have been carried out on the sorption and separation of ions in water–organic solvent–mineral acid mixtures, there have been no investigations on the effect of mineral acids on the distribution of organic solvents and water between the resin and the liquid phase. We therefore determined the swelling of ion exchangers in the presence of mineral acids in mixtures which we have investigated previously⁹. Because of the lack of swelling data in the literature for all the systems investigated, for comparison we studied binary mixtures also.

EXPERIMENTAL

The swelling of KU-2-X8 cation exchanger and AV-17-X8 anion exchanger in the hydrogen, chloride, nitrate, sulphate and perchlorate forms was measured in water and in methanol–water and acetone–water mixtures and in solutions of different mineral acids (perchloric, sulphuric, nitric and hydrochloric) in methanol–water and acetone–water mixtures.

We also studied systematically the sorption of Cu(II), Co(II) and Ni(II) ions from organic solvent–mineral acid–water mixtures by the cation exchanger KU-2-X8 and the anion exchanger AV-17-X8.

The weight swelling of exchangers was determined by the standard centrifugation method (1500 g for 45 min). After centrifugation, the components were measured in the swollen resin phase. The acetone and methanol were determined by the iodine¹⁰ and potassium dichromate¹¹ methods, respectively. The sorbed acid was titrated with alkali. In some instances, the Karl Fischer method was adopted for determining the water bound by the ion exchanger. Equilibrium ion-exchange measurements were performed under static conditions.

RESULTS AND DISCUSSION

The selective swelling of KU-2 cation exchanger is shown in Fig. 1. The curves are asymmetrical to the diagonal drawn in the \bar{N}_0/N_0 diagram. This effect is greater for an acetone–water mixture, and the positive deviation from ideal behaviour is higher in the case of this mixture. In the presence of perchloric acid, the preferential sorption of water decreases, especially at higher N_0 values and at higher acid concentrations. The uptake of perchloric acid is small ($2.7 \cdot 10^{-2}$ – $8.3 \cdot 10^{-1}$ mole per kilogram of resin). The same result was observed in nitric acid solution.

Fig. 2 demonstrates the sorption of Ni(II) ions on KU-2 cation exchanger from organic solvent–water–nitric acid mixtures as a function of organic solvent content. The distribution coefficients, D , increase in the order methanol < ethanol < propanol < acetone, and so does the selective uptake of water by the resin.

Selective swelling of an anion exchanger depends on the nature of the solvent mixture, the structure of the solution, the ionic form of the ion exchanger and the type

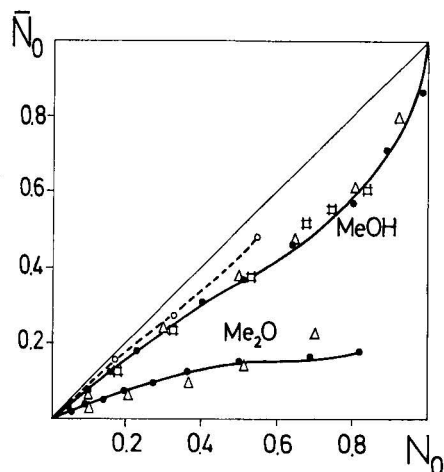


Fig. 1. Solvent selectivity, \bar{N}_0 , as a function of N_0 for KU-2-X8 (H^+) resin in water-organic solvent-perchloric acid mixtures, with methanol and acetone as the organic solvents. \bar{N}_0 and N_0 = mole fraction of organic solvent in the resin and in solution, respectively. Concentration of perchloric acid in both solvents: \bullet , 0; \triangle , 0.5 N; \square , 1.0 N; \circ , 2.0 N.

of hydration of the counter ion. The uptake of water by anion exchangers depends on the counter ion: it increases in the order $ClO_4^- < NO_3^- < Cl^- < SO_4^{2-}$ form of the resin and is greater from acetone-water mixtures than from methanol-water mixtures, especially for higher N_0 values. The sorption of methanol in different forms of anion exchangers exhibits the same order as that of water, *i.e.*, $ClO_4^- < NO_3^- < Cl^- \approx SO_4^{2-}$, whereas the uptake of acetone by the anion exchanger is very low and

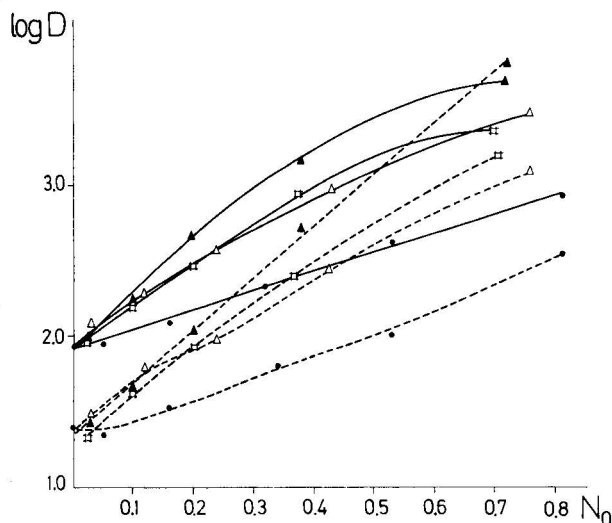


Fig. 2. Sorption of Ni(II) ions on KU-2-X8 cation exchanger from organic solvent-water-nitric acid mixtures. Solvent: \bullet , methanol; \triangle , ethanol; \square , propanol; \blacktriangle , acetone. Solid lines, 0.5 N nitric acid; broken lines, 1.0 N nitric acid. $D = (\mu g \text{ ion/g resin}) / (\mu g \text{ ion/ml solution})$.

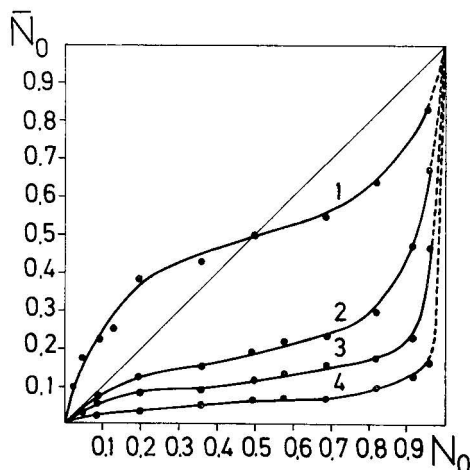


Fig. 3. Solvent selectivity, \bar{N}_0 , as a function of N_0 for different forms of AV-17-X8 resin in water-acetone mixtures. Form of resin: 1, ClO_4^- ; 2, NO_3^- ; 3, Cl^- ; 4, SO_4^{2-} .

varies only slightly with the mole fraction of solvent in the solution, and the order is opposite to that with water and methanol. This phenomenon is related to the different solvating ability of the two solvents¹². Fig. 3 shows the $\bar{N}_0 - N_0$ curves obtained with different forms of the anion exchanger in an acetone-water mixture. The greater the hydration energy and the stronger the positive hydration of the counter ion, the higher is the selective water sorption coefficient, K_0^w , of the resin:

$$K_0^w = \frac{\bar{N}_w \cdot N_0}{\bar{N}_0 \cdot N_w}$$

where \bar{N}_w and N_w are the mole fraction of water in the resin and in solution, respectively. For N_0 values lower than 0.5 on the perchlorate form of the resin, selective adsorption of acetone can be observed. The component present in a smaller amount is better sorbed. Perchlorate ion does not show a salting-out effect with acetone because, as its hydration is negative, it shows a water structure breaking effect. Similarly, in a methanol-water mixture, for $N_0 < 0.2$, selective sorption of methanol was observed. The same result was obtained by Marcus and Naveh⁷ on Dowex 1 resin, and they attributed this result to the effect of the low methanol concentration on the structure of water.

The presence of mineral acid affects the selective uptake of water by anion exchangers to a greater extent than that by cation exchangers. This difference is related to the higher acid uptake by anion exchangers. Figs. 4 and 5 show the water uptake by different forms of the anion exchanger from methanol-water and acetone-water mixtures, respectively, and from 1 *N* solutions of mineral acids in the same solvent mixtures. The water uptake by the SO_4^{2-} form of the resin decreased to a great extent in the presence of sulphuric acid. There is virtually no difference between the two curves for the perchlorate form of the resin. Sulphuric acid is bound to a greater extent with formation of HSO_4^- ions in the resin phase: 0.8–1.0 equiv. acid/equiv. resin. Negative hydration is characteristic of the HSO_4^- ion in contrast to the SO_4^{2-}

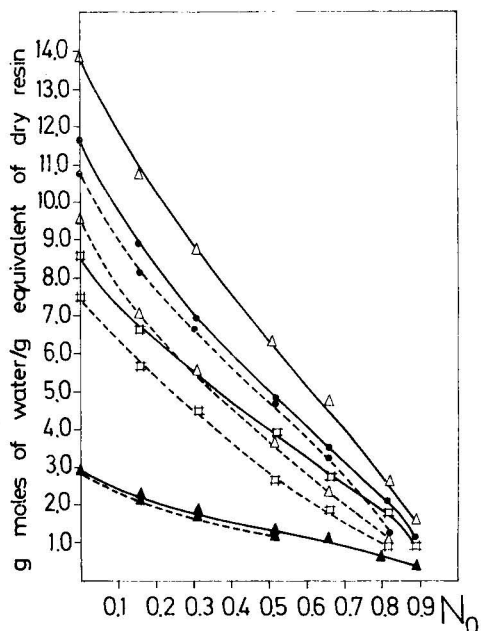


Fig. 4. Water uptake (moles of water per equivalent of dry resin) by different forms of the resin: \blacktriangle , ClO_4^- ; \square , NO_3^- ; \bullet , Cl^- ; \triangle , SO_4^{2-} . Solid lines, water-methanol; broken lines, water-methanol-1 N acid (HClO_4 , HNO_3 , HCl or H_2SO_4 , corresponding to the salt form of the anion exchanger).

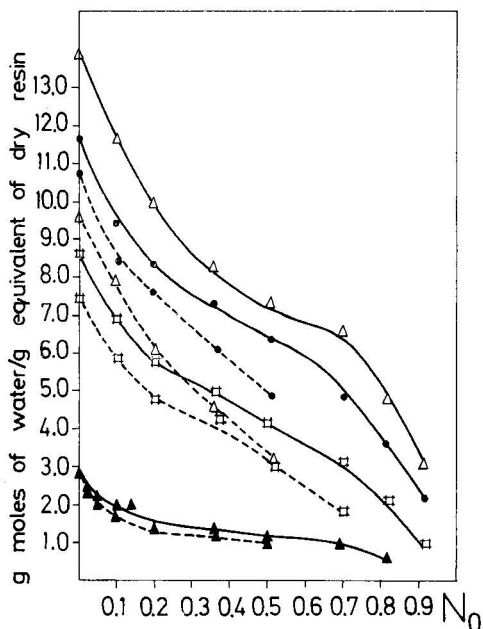


Fig. 5. Water uptake (moles of water per equivalent of dry resin) in different salt forms of the resin. Symbols for salt forms as in Fig. 4. Solid lines, water-acetone; broken lines, water-acetone-1 N acid (HClO_4 , HNO_3 , HCl or H_2SO_4 , corresponding to the salt form of the anion exchanger).

ion, and therefore the water uptake by the former is even less than that of the Cl^- form of the resin (Figs. 4 and 5).

The sorption of hydrochloric and nitric acid can be explained by the formation of HCl_2^- and $\text{H}(\text{NO}_3)_2^-$ ions, respectively, particularly at higher acid concentrations, in a similar manner to the result with liquid anion exchangers^{13,14}. The uptake of perchloric acid is very low (ca. 0.07 mole per equivalent of resin). Increasing the solvent concentration may enhance both the association and the acid sorption. The methanol uptake decreases in mixtures containing sulphuric acid compared with the binary mixtures, but it remains virtually unchanged in the Cl^- , ClO_4^- and NO_3^- forms of the resin. By addition of acid, the acetone uptake increases in the case of the SO_4^{2-} form of the resin, the salting-out effect of the HSO_4^- ion being weaker than that of the SO_4^{2-} ion.

The sorption of ions in the anion exchanger depends considerably on the selective swelling of the resin. Without the addition of acid, metal nitrates are sorbed only from acetone at very high concentrations, as the addition of water does not allow the formation of $\text{CoX}_3(\text{NO}_3)_3^-$ ions (X = acetone) in the resin phase because of selective adsorption of water by the resin. From sulphuric acid solutions, the elements are sorbed only at low acid concentrations ($<0.1 N$) and at high organic solvent concentrations ($N_0 > 0.5$). Under such conditions, the difference in solvent mixture composition is greatest between the resin and solution phase. Metal sulphates prefer the water-rich ion exchanger phase. The solubility of metal sulphates is much greater in water than in organic solvents. The distribution coefficients in acetone–water–hydrochloric acid mixtures are lower for Co(II) and Cu(II) than in mixtures containing alcohol, as the sorption of ions is hindered by the lower organic solvent content of the resin phase, which in turn is lower in acetone–water mixtures because of the enhanced water adsorption. Ions are not sorbed on the perchlorate form of the resin because neither complex formation nor a distribution mechanism is possible. The presence of metal ions (maximum 500 μg per 0.200 g of ion exchanger) has virtually no effect on the selective swelling of the ion exchangers.

REFERENCES

- 1 O. D. Bonner and J. C. Moorefield, *J. Phys. Chem.*, **58** (1954) 555.
- 2 H. P. Gregor, D. Noble and M. H. Gottlieb, *J. Phys. Chem.*, **59** (1955) 10.
- 3 C. W. Davies and B. D. R. Owen, *J. Chem. Soc.*, (1956) 1676.
- 4 H. Rückert and O. Samuelson, *Acta Chem. Scand.*, **11** (1957) 703.
- 5 V. A. Akulich and G. L. Starobinets, *Vestsi Akad. Navuk Belarus. SSR, Ser. Khim. Navuk*, (1968) 35.
- 6 O. R. Skorohod and T. N. Kuzhelevich, *Zh. Fiz. Khim.*, **43** (1969) 2899.
- 7 Y. Marcus and I. Naveh, *J. Phys. Chem.*, **73** (1969) 591.
- 8 C. H. Jensen, A. Partridge, T. Kenjo, J. Bucher and R. M. Diamond, *J. Phys. Chem.*, **76** (1972) 1040.
- 9 A. Lásztity and T. A. Belyavskaya, *Proceedings of the IIIrd Conference on Analytical Chemistry, Budapest*, Publishing House of the Hungarian Academy of Sciences, Budapest, 1970, p. 59.
- 10 D. K. Bauer, *Die organische Analyse*, Akademische Verlagsgesellschaft, Leipzig, 1950, p. 245.
- 11 E. Schulek and E. Szeghő, *Z. Anal. Chem.*, **117** (1939) 400.
- 12 A. I. Parker, *Quart. Rev. Chem. Soc.*, **16** (1962) 163.
- 13 A. S. Kertes and I. T. Platzner, *J. Inorg. Nucl. Chem.*, **24** (1962) 1417.
- 14 D. H. McDaniel and R. E. Vallée, *Inorg. Chem.*, **2** (1963) 996.

CHROM. 7852

SOME ASPECTS OF ION-EXCHANGE IN NON-AQUEOUS AND MIXED SOLVENTS

J. D. R. THOMAS

Chemistry Department, University of Wales Institute of Science and Technology, Cardiff CF1 3NU (Great Britain)

SUMMARY

The author's published work has been used to illustrate certain aspects of ion-exchange resin stability and sorption behaviour in non-aqueous and mixed solvent media. Solvent and thermal stability studies have confirmed that even strong-base ion-exchange resins are sufficiently stable in methanol and heptane media at ambient temperature to permit their use in analytical separations. The enhanced selectivity differences of ion-exchange resins for inorganic ions in mixed media is illustrated by the sorption of alkali metal ions on Zeo-Karb 225 (hydrogen form) from aqueous methanol, aqueous ethanol, and aqueous acetone. Finally, on the organic side, the discussion of work on the separation principles of phenols from methanolic media with De-Acidite FF (acetate form) is extended to the wider context of ion-exchange fractionation of peat and petroleum constituents.

INTRODUCTION

It has long been known that water is by no means the only solvent from which sorption by ion-exchange resins can take place; over a quarter of a century ago some of the general principles of ion exchange in mixed solvents had been established¹. For example, Na^+ , K^+ , Ba^{2+} , and Ca^{2+} ions were claimed to show greater affinity for a cation exchanger in aqueous solutions of increasing ethanol or acetone content¹. Enhanced sorption and selectivity trends have since been confirmed and recent reviews²⁻⁴ summarise the several systematic investigations demonstrating the versatility of non-aqueous solvents and aqueous-organic solvent mixtures for metal separations.

Rather more striking is the fact that many organic compounds can ionize sufficiently or are sufficiently polar to permit sorption by ion exchangers. This phenomenon even extends to the sorption by orthodox ion-exchange resins of naphthenic acids, alkylphenols and certain non-basic and basic nitrogen compounds present in non-ionising petroleum fractions⁵.

The use of non-aqueous and mixed solvent media therefore offer a greatly extended scope for ion-exchange resins and illustrations of the sorption principles of inorganic and organic materials and of ion-exchange resin stability are centred on the author's published work.

STABILITY AND SWELLING CONSTRAINTS

Stabilities of ion-exchange resins have recently been reviewed from the mechanical⁶, chemical⁶, radiation⁷, solvent⁸, and thermal⁸ standpoints. Solvent and thermal stabilities are of special interest in the present context and observations in aqueous systems that salt forms of the resins are more able to withstand high temperatures than are free-base and free-acid forms^{8,9} also apply to basic resins in non-aqueous media like methanol and heptane⁸. This pattern presumably extends to acidic resins in non-aqueous media as might also be the trend for free-base resins less resistant to capacity loss than the free-acid types. Weak-base and weak-acid resins are generally more stable thermally than their strong-base and strong-acid counterparts⁹.

Just as in water, ion-exchange resins are degraded in non-aqueous solvents by normal erosive forces, but in organic solvent media the hydrocarbon resin matrix might be expected to be especially sensitive to erosion. This could account for the tendency to particle attrition and emulsification at higher temperature ($>50^{\circ}$) in methanol and heptane¹⁰. The greater incidence of this feature in macroreticular resins lends support to this susceptibility of the hydrocarbon matrix¹⁰. Nevertheless, stability studies at ambient temperature indicate that resins have adequate stability in non-aqueous media¹⁰ for a wide range of studies and applications.

Provided the desired separation objective is achieved, the relatively slow exchange rate imposed by low swelling characteristics in non-aqueous media can be tolerated and in this respect it is now appreciated that considerable ion-exchange capacity is possible without resin swelling¹¹. Thus, even the microporous or gel-type resins are sufficiently porous to permit ready access of solvents and polar species. Here, the studies of Inczédy and Pásztlér¹² with strongly acidic and strongly basic resins in seven water-miscible solvents are interesting. They confirm earlier reports that swelling is at a maximum with water, with alcohols and glycols also producing significant swelling. However, there is a surprising difference between solvent sorption by the hydrogen and sodium forms of cation exchangers in ethanol with a lesser difference in methanol¹². This is significant, and in the low swelling of the sodium form in ethanol (0.3 for Dowex 50-X8 in sodium form compared with 2.5 for the hydrogen form) there may well be a clue to pronounced selectivity patterns in non-aqueous over aqueous media. Similar swelling patterns were observed for macroporous or macroreticular resins¹³.

SELECTIVE SORPTION OF INORGANIC MATERIALS

Much of the work on ion exchange from non-aqueous and mixed solvent media has been aimed at developing new and improved methods for separating and purifying lanthanides and actinides, mostly by anion exchange in mixed solvents containing water^{14,15}. Experimental studies undertaken to learn more of the ion-exchange process have been mainly based on straightforward cation exchange, especially of univalent cations, and useful data on ion selectivities for cation exchangers have been accumulated. Recent studies¹⁶ demonstrate that while selectivity differences of Zeo-Karb 225 (8% divinylbenzene) in the hydrogen form were not very marked for alkali metal ions in water, there were strikingly different extents of increase in resin affinity

TABLE I

SELECTIVITY COEFFICIENTS, K_H^M , FOR HYDROGEN FORM OF ZEO-KARB 225 (8% DVB) IN WATER AND ORGANIC SOLVENT-WATER AT 30°¹⁶

Volume fraction water	Organic solvent	K_H^M					
		Li-H	Na-H	K-H	Rb-H	Cs-H	NH ₄ -H
1.0*	Methanol	0.92	1.61	2.34	2.12	2.29	1.86
	Ethanol	0.83	1.62	2.29	1.64	1.71	1.13
	Acetone	1.03	1.50	1.89	1.89	2.06	1.89
0.1	Methanol	2.08	33.5	978	147	79	15.6
	Ethanol	7.5	83	183	99	67	8.5
	Acetone	15.2	53	15.2**	173	21.4**	16.3**

* Three sets of figures arise for water because the preliminary resin treatment involves washing with organic solvent.

** These figures may be low because of poor solubility.

for the alkali metal ions with increasing organic solvent (Table I). This leads to increasing and very substantial selectivity differences between one ion and another, as is illustrated by the data of Table I, in passing from purely aqueous media to 90% by volume of methanol, ethanol or acetone in water.

Although polarity of the medium as expressed by the dielectric constant is an important factor, the breakdown of the linear relation between $\log K_H^M$ and $1/D$ through the tendency of selectivities to maximise suggests that several factors may be responsible for selectivities. These include solvation, hydrogen bonding, ion-pair formation, and the coordinating abilities of the solvent. Also meriting consideration are the standard molar free energies of transfer for single cations between various media¹⁷. As seen from the data of Table II, such free energies of transfer between water and water-methanol media become increasingly lower with increasing methanol content of the medium. This pattern is relevant in the light of the observation¹⁸ that the medium associated with the resin phase is predominantly aqueous. Thus, the fact that the alkali metal ions, Li⁺, Na⁺, and K⁺, are sequentially in a higher (more positive) free energy state than hydrogen (Table II) has been used¹⁶ to suggest that hydrogen ions prefer the more organic liquid medium. This leads to an increase in K_H^M with increasing organic solvent content of the medium and to increasingly higher K_H^M in the series Li⁺, Na⁺, K⁺ as the free energy of the ion relative to hydrogen becomes more positive.

TABLE II

STANDARD FREE ENERGY OF TRANSFER (J/mole) AT 25° OF SINGLE CATIONS FROM WATER TO WATER-METHANOL MEDIA¹⁷

Ion	Water-10% (w/v) methanol	Water-43.12% (w/v) methanol
H ⁺	-2060	-11 760
Li ⁺	-1390	-8 400
Na ⁺	-920	-5 900
K ⁺	-800	-5 000
	(±250 J/mole)	(±2 500 J/mole)

No amount of theoretical explanation will disguise the feature of potential analytical interest, namely, that mixed organic solvent–water media are capable of creating large differences in selectivity coefficients with the effect of also bringing about changes in the order of selectivities with consequent interesting separation possibilities (Table III).

TABLE III

AFFINITY ORDER OF HYDROGEN FORM OF ZEO-KARB 225 (8% DVB) FOR ALKALI METAL/AMMONIUM IONS IN VARIOUS ORGANIC SOLVENT–WATER MEDIA AT 30° (REF. 16)

<i>Solvent composition</i> (% organic solvent)	<i>Affinity (decreasing) →</i>					
Methanol						
0	K	Cs	Rb	NH ₄	Na	Li
10	K	Cs =	NH ₄	Rb	Na	Li
30	K	Rb	Cs =	NH ₄	Na	Li
50	K	Rb	Na	Cs	NH ₄	Li
70	K =	Rb	Cs	Na	NH ₄	Li
90	K	Rb	Cs	Na	NH ₄	Li
Ethanol						
0	K	Cs	Rb	Na	NH ₄	Li
10	K	Cs	Rb	Na	NH ₄	Li
30	K	Na	Rb	Cs	NH ₄	Li
50	K	Na	Rb	Cs	NH ₄	Li
70	K	Na	Rb	Cs	NH ₄	Li
90	K	Rb	Na	Cs	NH ₄	Li
Acetone						
0	Cs	Rb =	K =	NH ₄	Na	Li
10	Cs =	Rb =	K	Na	NH ₄	Li
30	Rb	K	Cs	Na	NH ₄	Li
50	Rb	K =	Na	Cs	NH ₄	Li
70	Rb	K	Na	Cs	NH ₄	Li
90	Rb	Na	Cs	NH ₄	K =	Li

SEPARATION OF ORGANIC MATERIALS

An important area of application of ion-exchange resins in non-aqueous solvent media is in the separation of organic acids and bases¹⁹. One reason for this is the facility in overcoming the insolubility problems frequently characteristic of aqueous systems as exemplified by precipitation trapping free phenols on columns of free-base resins during an attempted desorption stage with aqueous hydrochloric acid²⁰.

The principles of separations using ion-exchange resins in non-aqueous media may be illustrated with reference to phenols, where elution of a mixture of phenols from an anion-exchange resin column with amine–acetic acid buffer solutions leads to a separation pattern parallel to the aqueous pK_a values of the weakly acidic phenols. Thus, according to the pattern shown in Table IV, Logie²⁰ isolated the constituents of crude 2,4-dichlorophenol with a column of De-Acidite FF (acetate form) from a solution of 0.2% by volume of triethylamine in methanol (pH 9.2). By sequential elution with various methanol–triethylamine–acetic acid systems of decreasing pH (arbitrary only for these non-aqueous systems) *p*-chlorophenol (pK_a 9.38), 2,4-di-

TABLE IV

SEPARATION OF CONSTITUENTS OF CRUDE 2,4-DICHLOROPHENOL ON DE-ACIDITE FF (ACETATE FORM)²⁰

Sorption medium: 0.2% triethylamine in methanol (pH 9.2).

Elution order and phenol eluted	Eluent
1. <i>p</i> -Chloro- ($pK_a = 9.38$)	200 ml of 0.2% triethylamine acetate in methanol per litre of 0.2% triethylamine in methanol (pH 8.6)
2. 2,4-Dichloro- ($pK_a = 7.51$)	0.2% triethylamine acetate in methanol (pH 8.0)
3. 2,6-Dichloro- ($pK_a = 6.79$)	0.2% acetic acid in methanol (pH 3.5)
4. 2,4,6-Trichloro- ($pK_a = 6.41$)	5% acetic acid in methanol

chlorophenol (pK_a 7.51), 2,6-dichlorophenol (pK_a 6.79) and 2,4,6-trichlorophenol (pK_a 6.41) were eluted²⁰ in the order of decreasing pK_a (Table IV).

The separation illustrated by Table IV may also be effected with a longer ion-exchange resin column using gradient elution²¹. The gradient is effected by replenishing an eluent reservoir initially of pure methanol, with 0.2% acetic acid in methanol. This releases *p*-chlorophenol, 2,4-dichlorophenol and 2,6-dichlorophenol according to the order of their pK_a values, while 2,4,6-trichlorophenol may be released with a final elution with 5% acetic acid in methanol²¹.

When the pK_a values of the phenols are close, fixed concentration elution is ruled out because of the amount of experimentation required. A more effective solution is a rigorous combination of the use of amine-acetic acid buffer solutions in methanol combined with gradient elution²². Thus, *m*, *o* and *p*-nitrophenols of pK_a 8.39, 7.22 and 7.15, respectively, may be loaded on to a column of De-Acidite FF (acetate form) in 4% triethylamine in methanol and sequentially eluted during gradient elution involving replenishment of a reservoir of 4% triethylamine in methanol with 4% of 1 *M* triethylamine acetate in methanol together with 80 ml 1 *M* triethylamine in methanol plus 10 ml acetic acid per litre.

The same principles of ion-exchange separation by gradient elution combined with judicious use of amine-acetic acid buffer systems can be extended²² to the very weakly acidic cresols (pK_a 10.1 to 10.33) and xylenols (pK_a 10.20 to 10.62). The buffer systems must now include the more basic diethylamine instead of triethylamine. The xylenols must represent the limit to which the method can extend, that is, to a phenol pK_a of about 10.5, for 2,3-xylene (pK_a 10.54), 2,4-xylene (pK_a 10.60) and 2,6-xylene (pK_a 10.62) defy sorption on the acetate form of De-Acidite FF—even from 25% of diethylamine in methanol²².

Application of the above principles to technological situations is interesting. For example, IR analysis suggests that a methanolic extract of peat bitumen fractionated on the acetate form of De-Acidite FF gives ethers, aliphatic esters, and other weakly ionised substances on elution with methanol; aromatic esters on elution with methanol-acetic acid (3:1); and evidence of phenolic type materials in the fraction eluted with glacial acetic acid^{23,24}.

A fractionation scheme (Table V) of petroleum constituents using macro-

TABLE V

FRACTIONATION OF PETROLEUM CONSTITUENTS USING MACRO-RETICULAR ANION-EXCHANGE RESINS²⁵

Stage	Resin form	Step	Directions	Fraction eluted
A.	CO_3^{2-}	1	Add mixture of naphthenic acids, alkylphenols, pyrrolic compounds and nitrogen bases dissolved in toluene to column.	Nitrogen bases (not adsorbed)
		2	Elute with methanol.	Alkylphenols Pyrrolic compounds
		3	Elute with methanol- CO_2 .	Naphthenic acids
B.	OH^-	1	Add fraction A.2 to column and elute with methanol.	Pyrrolic compounds (not adsorbed)
		2	Elute with methanol- CO_2 .	Alkylphenols

reticular anion-exchange resin²⁵ can have an important role in the petroleum field and it is pertinent to mention here that, apart from the strict ion-exchange mechanism which is probably characteristic of the phenol separations described above, sorption can also be effected by a more physical mechanism through the polar site facilities on the resin phase. The separation shown in Table V is potentially capable of refinement¹⁹ and an elution immediately following stage A.1 with methanol-ammonia could well provide a sub-fraction of the alkylphenols/pyrrolic compounds fraction of A.2. Also, a gradient elution with methanol-carbon dioxide immediately after stage B.1 might sub-fractionate the alkylphenols.

CONCLUSION

The possibilities of enhancing and reversing selectivities of ion-exchange resins by the addition or exclusive use of organic solvents can clearly extend the application of ion-exchange resins as a separation tool. In this a quantitative knowledge of the forces of solvation and sorption, the polar effects of substituent atoms and groups in organic molecules, and other physical phenomena can be of considerable value in establishing practical principles.

REFERENCES

- 1 E. I. Akeroyd, T. R. E. Kressman and A. T. Cooper, *Manuf. Chem.*, 19 (1948) 394.
- 2 G. J. Moody and J. D. R. Thomas, *Analyst (London)*, 93 (1968) 557.
- 3 G. J. Moody and J. D. R. Thomas, *Lab. Pract.*, 19 (1970) 378.
- 4 W. R. Heumann, *CRC Crit. Rev. Anal. Chem.*, (1971) 425.
- 5 W. A. Munday and A. Eaves, *World Petrol. Congr., Proc.*, 5th, New York, 1959, 1960, Sect. V, Paper 9.
- 6 G. J. Moody and J. D. R. Thomas, *Lab. Pract.*, 21 (1972) 632.
- 7 G. J. Moody and J. D. R. Thomas, *Lab. Pract.*, 21 (1972) 717.
- 8 M. A. Minto, G. J. Moody and J. D. R. Thomas, *Lab. Pract.*, 21 (1972) 797.
- 9 G. R. Hall, J. T. Klaschka, A. Nellestyn and M. Streat, in *Ion Exchange in the Process Industries*, Soc. Chem. Ind., London, 1970, p. 62.

- 10 M. A. Minto, *M.Sc. Thesis*, University of Wales, Uwist, Cardiff, 1971.
- 11 R. Kunin, *Ion Exchange Resins*, Wiley, London, 2nd ed., 1963.
- 12 J. Inczédy and E. Pásztler, *Acta Chim. (Budapest)*, 56 (1968) 9.
- 13 J. Inczédy and I. Högye, *Acta Chim. (Budapest)*, 56 (1968) 109.
- 14 J. Korkisch, *Modern Methods for the Separation of Rarer Metal Ions*, Pergamon Press, Oxford, 1969.
- 15 Y. Marcus and A. S. Kertes, *Ion Exchange and Solvent Extraction of Metal Complexes*, Interscience, New York, 1969.
- 16 J. G. Jones and J. D. R. Thomas, *Talanta*, 19 (1972) 961.
- 17 D. Feakins and P. Watson, *Chem. Ind. (London)*, (1962) 2008.
- 18 C. W. Davies and J. J. Thomas, *J. Chem. Soc.*, (1952) 1607.
- 19 G. J. Moody and J. D. R. Thomas, *Lab. Pract.*, 19 (1970) 487.
- 20 D. Logie, *Analyst (London)*, 82 (1957) 563.
- 21 N. E. Skelly, *Anal. Chem.*, 33 (1961) 271.
- 22 D. E. Thomas and J. D. R. Thomas, *Analyst (London)*, 94 (1969) 1099.
- 23 J. D. R. Thomas, *Nature (London)*, 193 (1962) 975.
- 24 J. D. R. Thomas, *J. Appl. Chem.*, 12 (1962) 289.
- 25 P. V. Webster, J. N. Wilson and M. C. Franks, *Anal. Chim. Acta*, 38 (1967) 193.

CHROM. 7725

ANION EXCHANGE IN TERNARY MIXTURES OF ALIPHATIC ACIDS, MINERAL ACIDS AND WATER

S. K. JHA*, F. DE CORTE** and J. HOSTE

Institute for Nuclear Sciences, Rijksuniversiteit Gent, Proeftuinstraat, 9000 Gent (Belgium)

SUMMARY

The anion-exchange behaviour of bivalent cobalt, copper, zinc and cadmium towards the strong base anion exchanger Dowex 1-X8 is studied as a function of the composition of ternary mixtures of aliphatic acids (acetic acid, propionic acid and butyric acid), mineral acids (hydrochloric and nitric) and water. The experimental data could be interpreted on a qualitative physico-chemical basis in terms of the gradual building-up of metal-ligand complexes (including those with a ligand number less than 2) and of the dielectric constant of the solvent.

INTRODUCTION

Aliphatic organic acids with low dielectric constants (ϵ) and a wide range of miscibility with water are interesting media, as they favour metal-complex formation and can thus enhance adsorbabilities in ion-exchange systems; this has been shown for both anion and cation exchangers in previous studies from this laboratory¹⁻⁵. The present work was aimed at comparing the effects of acetic acid, propionic acid and butyric acid (HAc, HPr and HBu, respectively) on the distribution coefficients of some metals in ternary mixtures of these organic acids with mineral acids (hydrochloric and nitric acids) and water. The adsorption isotherms at 25° have been examined as a function of the aliphatic and mineral acid concentration for the bivalent transition metals copper, cobalt, zinc and cadmium, and an attempt has been made to interpret the experimental results on a physico-chemical basis, taking into account additional information from the results of a spectrophotometric investigation of the metal complexes involved.

EXPERIMENTAL

Resin

Dowex 1-X8 (Cl^- or NO_3^- ; 100-200 mesh) was conditioned before use⁶ and dried *in vacuo* over phosphorus pentoxide; after conversion into nitrate form, the

* Present address: Department of Chemistry, Agra College, Agra, India.

** Research Associate of the Nationaal Fonds voor Wetenschappelijk Onderzoek.

residual chloride content was determined by activation analysis⁷; it was found to be 0.5% of the original capacity.

Solvents

The solvents were prepared by mixing appropriate amounts of the aliphatic acids (purity 99%), mineral acids (analytical grade) and water. The metal under investigation was introduced into the system as a solution of its acetate, propionate or butyrate in a mineral or aliphatic acid. The composition of the solvent is expressed in terms of mole fractions for the organic acids (compared with the sum of organic acid and water) and of molarities for the mineral acids.

Radioactive tracers

Tracers of copper-64, cobalt-60, zinc-69m and cadmium-115 were obtained by neutron irradiation in the Thetis reactor (Gent, Belgium).

Radiometric analysis

The activity in the solvent phase was counted by means of a NaI(Tl) well-type detector coupled to a single-channel analyser. Purity checks were made with the use of a lithium-drifted germanium detector coupled to a 4000-channel analyser. For cadmium-115–indium-115m, an appropriate decay period was allowed to ensure transient mother–daughter equilibrium.

Determination of K_d values

The adsorbabilities were expressed as weight-distribution coefficients (K_d = amount of metal per g of dry resin/amount of metal per ml of solution). They were determined by the batch-equilibration technique, with use of 100 mg of resin and 21 ml of solvent. Agitation times of 15 h and metal loadings below 1% of the total exchange capacity were used.

Spectrophotometry

Absorption spectra of the solvent phase for Cu(II) were obtained by using 1.00-cm silica cells and the visible source and detection mode of a Beckman DK-1A recording spectrophotometer. The blank solutions were solvents treated identically but not containing the metal.

RESULTS AND DISCUSSION

The K_d values at constant chloride or nitrate molarity were plotted as a function of the aliphatic acid mole fraction. From these curves it was possible to plot K_d versus chloride or nitrate molarity; the results are shown in Figs. 1–3.

An attempt was made to give a qualitative physico-chemical interpretation of the phenomena observed, based on the theories of Marcus and Coryell⁸ for media with high ϵ values (dissociated species) and of Penciner *et al.*⁹ for media with low ϵ values (ion-paired species).

It follows from the former theory that, at high values of ϵ , *e.g.*, in aqueous media, the distribution curves can be described in terms of the gradual building-up of cationic, neutral and anionic metal–ligand complexes with increasing ligand con-

tent, respectively corresponding to positive, zero and negative slopes of the adsorption isotherms [\log (distribution coefficient) *versus* \log (ligand content)]. The highest value of the distribution coefficient (corrected for ligand invasion⁸), and thus zero slope, occurs at a ligand content such that the neutral metal–ligand complex predominates in the solution.

At low ϵ values⁹, *e.g.*, in acetone or ethanol medium, the metal is introduced into the system as, for instance, its chloride (if chloride is the ligand); thus, the adsorption isotherm begins horizontally with zero slope. When the ligand content is increased, formation of higher metal–ligand complexes commences, resulting in a negative slope.

In the present work, however, the metal is introduced into the system as its acetate, propionate or butyrate; this means that:

(1) The existence of lower metal–ligand complexes (with a ligand number less than 2) becomes possible, so that the adsorption isotherm will show a positive slope at low ligand concentration.

(2) The metal acetates, propionates or butyrates are gradually transformed into higher metal–ligand complexes with increasing ligand content. This means that an increase in the aliphatic acid mole fraction (lower value of ϵ) will influence the distribution not only because of the transition from dissociated to ion-paired species, but also because the aliphatic acids contribute to the equilibria.

(3) The maximum of the adsorption isotherms will no longer exactly correspond to the predominance of neutral metal–ligand complexes in the solvent phase, unless the distribution coefficient is corrected for ligand invasion as well as for solvent invasion.

If these considerations are taken into account together with the fact that the presence of an organic solvent with a low ϵ value favours the formation of metal complexes, the distribution curves can be interpreted as follows. Fig. 1 shows a typical example of dependence of K_d for Cu(II) on the aliphatic acid mole fraction for six discrete values of hydrochloric acid molarity. The plots for the other metals investigated showed the same qualitative picture. At low mole fractions of the organic acids, where the ϵ values of the mixed solvents are still relatively high ($\epsilon_{\text{H}_2\text{O}} = 78.5$, $\epsilon_{\text{HAc}} = 6.2$, $\epsilon_{\text{HPr}} = 3.4$ and $\epsilon_{\text{HBu}} = 3.0$ at 25°), and at low ligand concentration, the fraction of the neutral metal complex does not attain a maximum. This fraction increases, and thus the K_d values become higher with increasing hydrochloric acid molarity at a constant mole fraction, and with increasing mole fraction at a constant hydrochloric acid molarity. At very high mole fractions (low ϵ values), the neutral complex predominates in the solution even at low hydrochloric acid concentration. Addition of hydrochloric acid leads to the formation of higher complexes and thus results in a decrease in K_d values. Even so, the increase in the organic solvent mole fraction at constant (preferably high) chloride molarity should eventually result in decreasing K_d values. Although this effect was not observed for Cu(II) and Zn(II) up to the mole fractions investigated, it did occur with Cd(II). Obviously, the region of the above-mentioned sequence inversion should be positioned at a higher mole fraction when the ϵ value of the aliphatic acid is higher, *i.e.*, $\text{HBu} < \text{HPr} < \text{HAc}$.

Graphs of K_d *versus* chloride molarity for Cu(II) at aliphatic acid mole fractions of 0.55 and 0.80 are shown in Fig. 2. At the lower mole fraction (highest ϵ values) and low chloride concentrations, formation of the neutral complex is still incomplete and is further enhanced by increasing chloride concentration, thus giving higher K_d

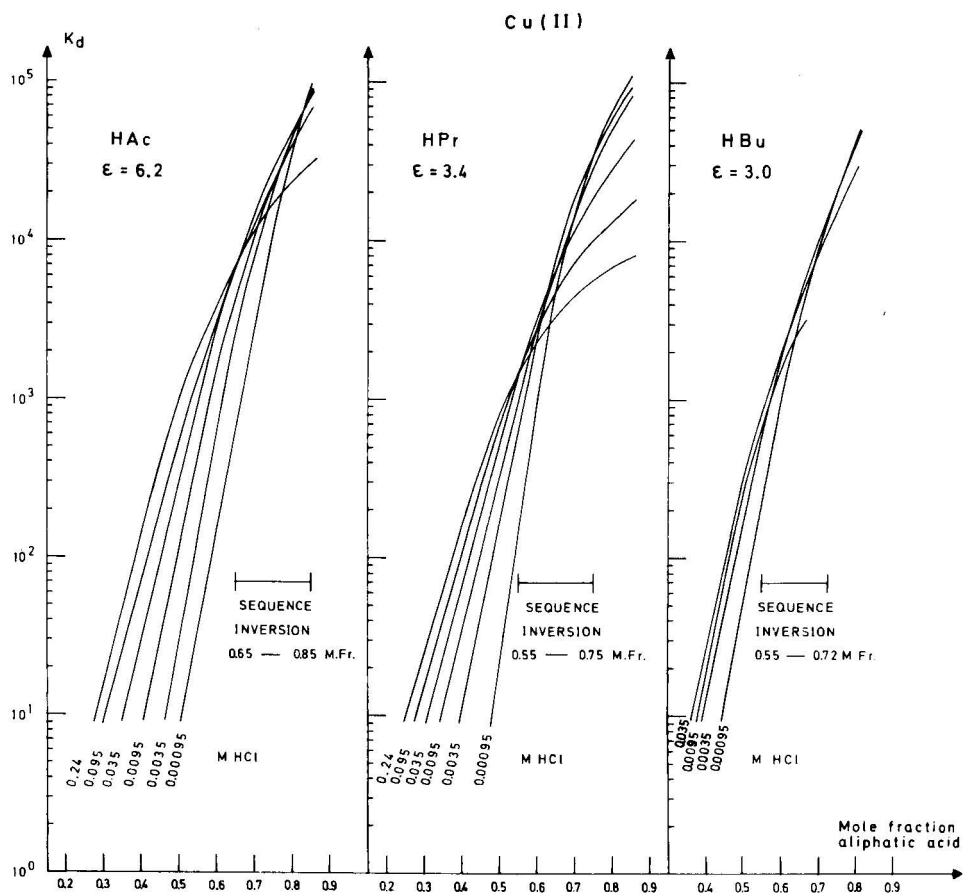


Fig. 1. K_d for Cu(II) versus aliphatic acid mole fraction at different hydrochloric acid molarities.

values. Moreover, the fraction of the neutral complex (and thus the value of K_d) is lower at higher ϵ values, so that in this region the K_d values follow the sequence $\text{HAc} < \text{HPr} < \text{HBu}$. An analogous reasoning leads to the K_d sequence $\text{HBu} < \text{HPr} < \text{HAc}$ at lower mole fractions and at very high chloride concentrations; this explains the observed inversion at intermediate chloride concentrations. On the hydrochloric acid molarity scale, the transition from increasing to max. and then decreasing K_d values will therefore follow the sequence $\text{HBu} < \text{HPr} < \text{HAc}$. At the higher mole fraction (lowest ϵ value), the adsorption is very high even in the absence of chloride ligand in the solvent. This is due to another adsorption mechanism, not involving metal-complex formation in the solution, but based on solvent extraction into the resin phase, followed by complex formation with the chloride counter-groups of the resin¹⁰. Because of this complication, the K_d sequence order at zero or extremely low ligand concentration can no longer be described in the same terms as mentioned above. However, with increasing hydrochloric acid content, the K_d sequence is again $\text{HAc} < \text{HPr} < \text{HBu}$ at low (and $\text{HBu} < \text{HPr} < \text{HAc}$ at high) ligand concentrations. As the ϵ values are low, the inversion occurs at a ligand concentration lower than a mole fraction of 0.55, thereby following the same sequence as on the hydrochloric acid molarity scale, viz., $\text{HBu} < \text{HPr} < \text{HAc}$.

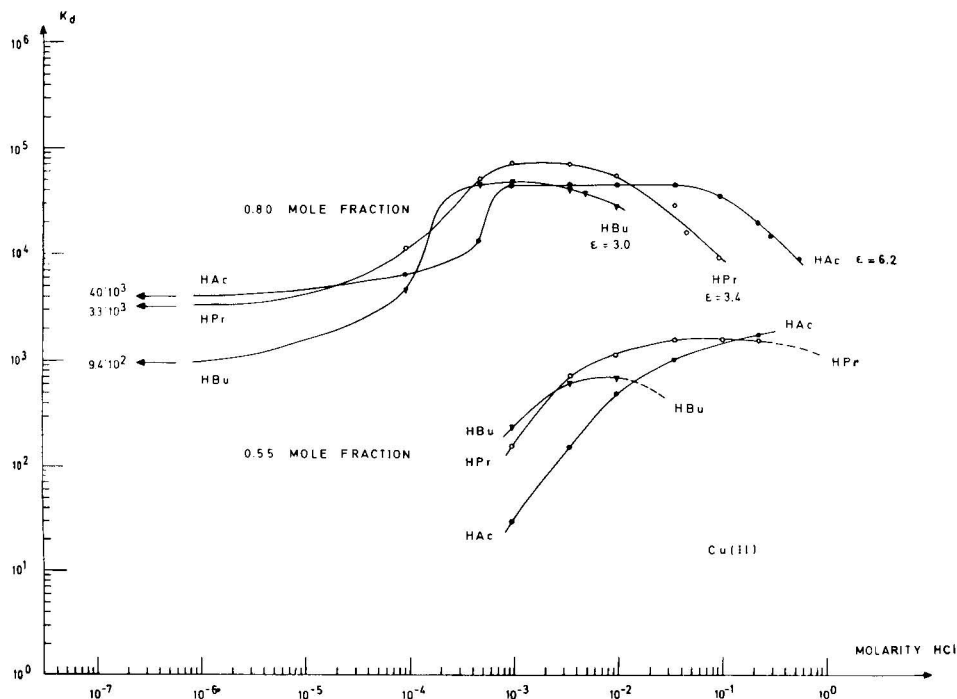


Fig. 2. K_d for Cu(II) versus chloride molarity at low and high aliphatic acid mole fraction.

Fig. 3 represents the dependence of K_d for Cu(II) on the nitrate molarity. As may be expected from the anion-exchange distribution behaviour of the elements in aqueous nitric acid¹¹, metal-complex formation with nitrate will occur with more difficulty, and thus only at a higher ligand concentration or at a higher aliphatic acid mole fraction (lower ϵ value) than with hydrochloric acid. At low mole fractions, no complexes are formed even at high nitrate concentrations; thus, no adsorption occurs. Even at high mole fractions (Fig. 3) and low nitrate concentrations, only the lower species are present, so that K_d first increases to a max. and then decreases with increasing nitrate molarity. This represents the gradual building-up of lower, neutral and higher metal nitrate complexes. As with low chloride concentration at low mole fraction of aliphatic acid, formation of the neutral complex is enhanced by lowering the ϵ value, thus resulting in the same K_d sequence, viz., HAc < HPr < HBu. It should be noted that sequence inversion should occur at high nitrate molarity; this tendency is indeed observed in Fig. 3, but it was more marked in the case of Zn(II). Logically, as the nitrate concentration increases, predominance of the neutral metal species is reached earlier in a low- ϵ medium, so that the sequence of the max. is HBu < HPr < HAc.

Evidence of the above-outlined interpretation is obtained from spectrophotometric determination of the complex species in the solvent phase. Fig. 4 shows that, for Cu(II) in HAc-hydrochloric acid-water, the height of the absorption band at 383 nm, which can be ascribed to $[\text{CuCl}_4]$ (ref. 12), increases with increasing chloride concentration; this corresponds to a decreasing K_d value (see Fig. 2).

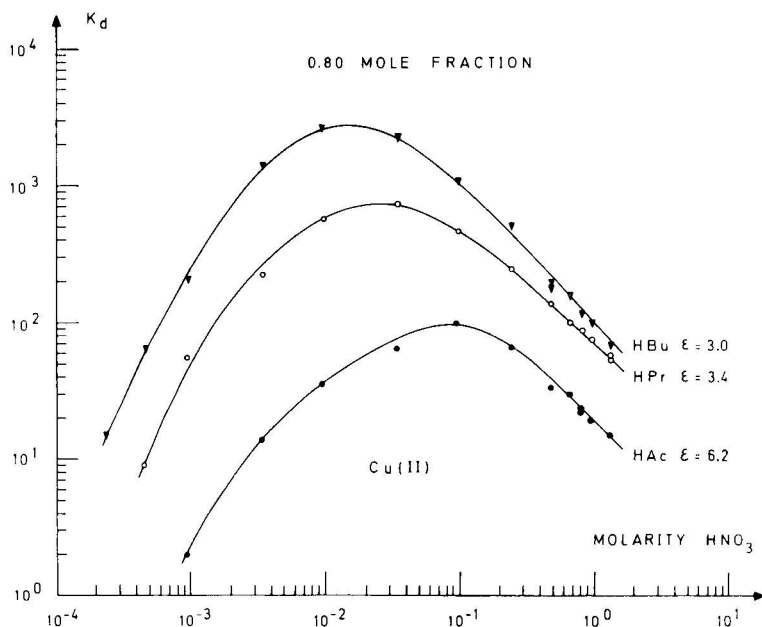


Fig. 3. K_d for Cu(II) versus nitrate molarity at high aliphatic acid mole fraction.

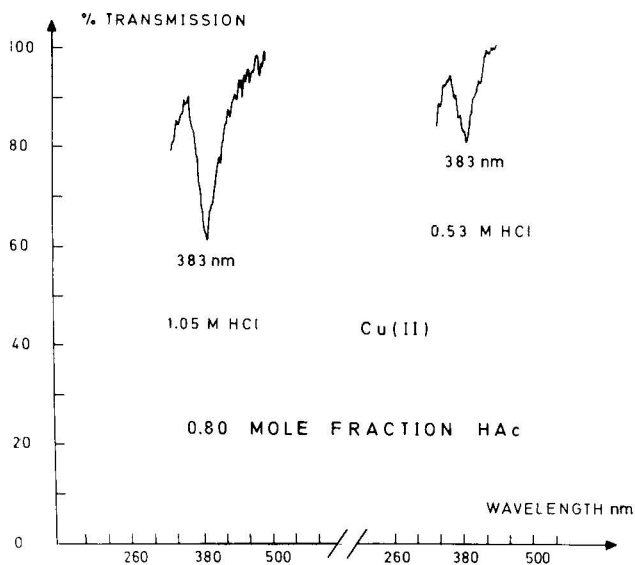


Fig. 4. Spectrophotometric absorption bands for Cu(II) in acetic acid (0.80 mole fraction) as a function of hydrochloric acid molarity.

CONCLUSION

It has been shown that anion exchange in ternary mixtures of aliphatic acids, mineral acids and water can be interpreted (at least qualitatively) in terms of the

gradual building-up of metal complexes and of the dielectric constant of the solvent. However, to obtain a quantitative treatment, it will be necessary to perform more refined experimental work, such as determination of solvent uptake, electrolyte invasion and spectrophotometric investigation of the metal complexes adsorbed on the resin. This work is in progress and will be reported in due course.

ACKNOWLEDGEMENTS

We are grateful to the Ministerie van Nationale Opvoeding en Nederlandse Cultuur and the Nationaal Fonds voor Wetenschappelijk Onderzoek for financial assistance. We are also indebted to Mrs. S. Jha for technical assistance.

REFERENCES

- 1 P. van den Winkel, F. de Corte, A. Speecke and J. Hoste, *Anal. Chim. Acta*, 42 (1968) 340.
- 2 P. van den Winkel, F. de Corte and J. Hoste, *Anal. Chim. Acta*, 56 (1971) 241.
- 3 P. van den Winkel, F. de Corte and J. Hoste, *J. Radioanal. Chem.*, 10 (1972) 139.
- 4 S. K. Jha, F. de Corte and J. Hoste, *Anal. Chim. Acta*, 62 (1972) 163.
- 5 P. van Acker, F. de Corte and J. Hoste, *Anal. Chim. Acta*, 64 (1973) 177.
- 6 W. Rieman, III and H. F. Walton, *Ion Exchange in Analytical Chemistry*, Pergamon Press, Oxford, 1970, p. 64.
- 7 F. de Corte and J. Hoste, *J. Inorg. Nucl. Chem.*, 35 (1973) 2049.
- 8 Y. Marcus and C. D. Coryell, *Bull. Res. Council. Isr., Sect. A*, 8 (1959) 1.
- 9 J. Penciner, I. Eliezer and Y. Marcus, *J. Phys. Chem.*, 69 (1965) 2955.
- 10 P. van Acker, F. de Corte and J. Hoste, *J. Inorg. Nucl. Chem.*, in press.
- 11 J. P. Faris and R. F. I. Buchanan, *Anal. Chem.*, 36 (1964) 1158.
- 12 L. I. Katzin, *J. Chem. Phys.*, 36 (1962) 3034.

CHROM. 7763

THE EXTRACTION OF COPPER(II) IONS WITH LIQUID ANION EXCHANGERS USING SALICYLATE AS COMPLEX-FORMING AGENT

E. PAPP and J. INCZÉDY

Institute of Analytical Chemistry, University of Chemical Engineering, Veszprém (Hungary)

SUMMARY

The extraction of copper(II) ions in the presence of salicylate ions, using a solution of the salicylate form of Aliquat 336 in chloroform, involves two simultaneous processes depending on the pH and on the salicylate concentration of the aqueous phase. The composition of the species formed in the chloroform phase can be described as follows: $\text{Cu}(\text{HL})_3\text{R}_4\text{N}$ and $\text{Cu}(\text{HL})\text{LR}_4\text{N}$, where HL is the monovalent salicylate anion. The corresponding extraction constants are: $\log K_1^e = 6.47 \pm 0.03$; $\log K_2^e = 1.80 \pm 0.01$. In solutions of $\text{pH} > 9$, if the chloride form of Aliquat 336 is used, a compound of composition $\text{CuL}_2(\text{R}_4\text{N})_2$ is also formed; the extraction constant found for this species is $\log K_3^e = 3.85 \pm 0.05$.

INTRODUCTION

It was shown earlier¹ that the separation of several metal ions in the presence of the chelate-forming compound tiron could be achieved by using a liquid anion exchanger. In the present work, the liquid-liquid distribution of copper(II) ions in the presence of salicylate ions was investigated, with use of a quaternary-ammonium-group-containing liquid anion exchanger (Aliquat 336) in chloroform solution.

EXPERIMENTAL

Reagents

In all experiments reagent-grade chemicals were used; aqueous solutions were prepared with deionised water.

Chloroform solution of Aliquat 336 (chloride), about 0.1 M. Fifty grams of Aliquat 336 (methyltriocetylammmonium chloride; Serva Entwicklungslabor, Heidelberg, G.F.R.) were dissolved in 680 ml of chloroform. To determine the concentration of the quaternary ammonium chloride 10 ml of the solution were shaken several times with excess of a solution of sodium salicylate, and the concentration of chloride ions in the aqueous solution after separation was determined by potentiometric titration with silver nitrate solution.

Chloroform solution of Aliquat 336 (salicylate). Fifty millilitres of the chloroform solution of Aliquat 336 (chloride) and 50 ml of 0.5 M sodium salicylate (in

aqueous solution) were shaken together. After equilibration, the phases were separated, a fresh solution of salicylate was added to the chloroform solution, and the mixture was shaken again. This procedure was repeated until chloride in the aqueous phase was not detectable by means of silver nitrate. The aqueous layer was discarded.

Sodium salicylate, 0.1 M. A 16.0120-g portion of sodium salicylate was dissolved in water, and the solution was diluted to 1 litre.

Copper(II) sulphate, 0.01 M. A 2.4968-g portion of copper sulphate pentahydrate was dissolved in water, and the solution was diluted to 1 litre.

Sodium chloride, 0.5 M. A 29.224-g portion of sodium chloride was dissolved in water, and the solution was diluted to 1 litre.

Polarographic base solution for determination of copper(II) ions. A 26.2-g portion of ammonium chloride was dissolved in water, 38 ml of concentrated aqueous ammonia were added, and the solution was diluted with water to 500 ml.

Instruments

An OH-104 square-wave polarograph (Radelkis).

An SP-700 spectrophotometer (Unicam).

A pH meter, model 25 (Radiometer, Copenhagen, Denmark).

Distribution experiments

In these experiments, 10 ml of aqueous and 10 ml of chloroform solutions were pipetted into a shaking bottle. The time of shaking was 3 min. After settling and separation of the phases, the aqueous phase was centrifuged. The equilibrium pH of the solution was determined by using glass and calomel electrodes, and the concentrations of the ions being investigated were determined in the aqueous phase, copper ions by square-wave polarography and salicylate by spectrophotometry.

Investigation of the distribution of salicylate and some other anions between water and the chloroform solution of Aliquat 336 (chloride)

To determine the ion-exchange equilibrium constant of the salicylate referred to the chloride ions ($K_{\text{Cl,HL}}^x$), the stoichiometry of the exchange, *i.e.*, the form in which the salicylate was bound to the quaternary amine in the pH range of 4–11, had to be established. The ratio of salicylate and Aliquat 336 was determined by distribution measurements. In a series of experiments, the concentration of salicylate in the aqueous solution was varied from 0.02 to 0.25 *M* while the concentration of Aliquat 336 was kept constant at 0.072 *M* (pH \approx 6). After equilibration, the concentration of salicylate (after acidification of the solution with hydrochloric acid) was determined spectrophotometrically at 300 or 237 nm. The concentration of salicylate in the organic phase was calculated from the original and equilibrium concentrations of salicylate in the aqueous phase. The calculated ratio of the salicylate concentration and Aliquat 336 concentration in the organic phase was plotted against the original concentration of salicylate in the aqueous phase (C_{sal}^0). The graph is shown in Fig. 1, from which it can be seen that, above a certain concentration of salicylate, the molar ratio of salicylate to the amine is 1:1. Thus, the composition of the compound formed can be written R_4NHL , where HL denotes the once-protonated, monovalent, salicylate ion.

The distribution of salicylate was also investigated at various pH values

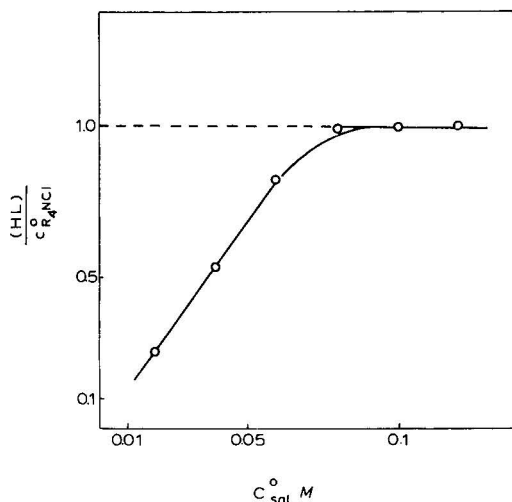


Fig. 1. Ratio of salicylate and amine concentrations in the organic phase plotted against the initial salicylate concentration in the aqueous phase: $C_{R_4NCl}^0 = 0.072 M$; $pH \approx 6$.

of the solution. The distribution coefficient was practically independent of pH in the pH range 4–10. The distribution coefficient was also determined at various initial concentrations of salicylate, but at constant concentration of chloride. The results were used to calculate the values of $K_{Cl,HL}^x$.

In order to compare the ion-exchange constants of some other anions referred to chloride, experiments were also carried out with these other anions. Aqueous solutions of these anions were shaken with a chloroform solution of Aliquat 336 (chloride). After equilibration, the pH of the aqueous phase and the concentration of chloride ion in the aqueous phase were determined. The concentration of the anion in question in the organic phase, and its distribution coefficient, were also calculated. For sulphosalicylate ions, a portion of the aqueous phase was diluted to a known volume with hydrochloric acid, the optical density of the acid solution was measured spectrophotometrically at 237 nm, and the concentration was determined by reference to a calibration graph.

Investigation of the distribution of copper(II) ions in the presence of salicylate

During the investigation of the extraction of copper ions, the concentration of metal ions was kept low (1 to 5 mg-ions per litre) compared with that of the salicylate ions ($>0.01 M$) and with that of the quaternary amine ($>0.05 M$). After equilibration and separation of the phases, the concentration of Cu(II) ions in the aqueous phase was determined by square-wave polarography using calibration graphs, and the distribution coefficient of copper (D_{Cu}) was calculated.

Investigation of the distribution of copper(II) ions using Aliquat 336 (salicylate) in chloroform solution

The values of D_{Cu} were investigated at different pH values of the solution, the concentrations of salicylate and Aliquat 336 (salicylate) being kept constant. The

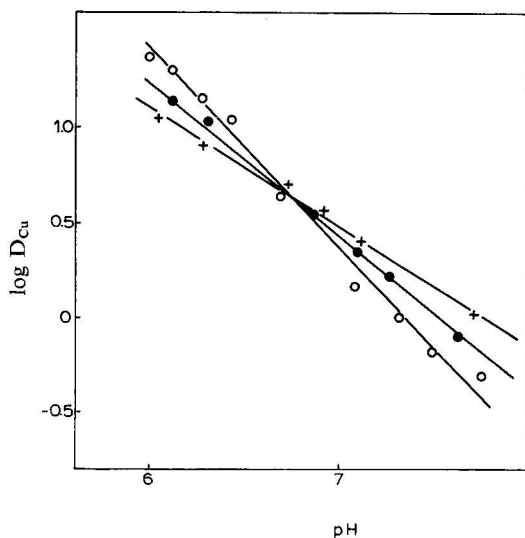


Fig. 2. Logarithmic diagram of the dependence of D_{Cu} on pH at different concentrations of salicylate: $C_{\text{Cu}}^0 = 1 \text{ mM}$; $C_{\text{R}_4\text{NHL}}^0 = 0.071 \text{ M}$; $C_{\text{sal}}^0 = 0.1 \text{ M}$ ($\circ-\circ$); 0.06 M ($\bullet-\bullet$); 0.04 M ($+--+$).

values obtained for $\log D_{\text{Cu}}$ were plotted against pH for different initial concentrations of sodium salicylate; the results are shown in Fig. 2, from which it can be seen that $\log D_{\text{Cu}}$ decreases with increasing pH. However, the slope of the curve depends on the concentration of salicylate in the aqueous phase. The colour of the chloroform phase gradually changes from bluish-green to green with increasing pH; this can be explained by the fact that different extraction processes take place simultaneously, depending on the pH and on the salicylate concentration.

The change in $\log D_{\text{Cu}}$ plotted against the log of the concentration of Aliquat 336 (salicylate) gave a linear graph with a slope of 1.28. This showed that the concentration of copper ions in the organic phase increased almost in proportion with the increasing concentration of the quaternary ammonium salicylate.

Investigation of the distribution of copper(II) ions using Aliquat 336 (chloride) in chloroform solution

It was found by the distribution measurements using Aliquat 336 (chloride) that the extent of extraction of copper ions increased with increasing pH; the colour of the chloroform phase was yellowish-green. The values of $\log D_{\text{Cu}}$ plotted against pH at different initial concentrations of salicylate are shown in Fig. 3. The concentration of chloride (0.5 M) in the original solution was relatively high. From the results obtained, it can be seen that $\log D_{\text{Cu}}$ is nearly constant above pH 9, and that, at lower concentrations of salicylate, higher values of $\log D_{\text{Cu}}$ can be obtained. The change in D_{Cu} as a function of the concentration of the quaternary ammonium salt at $\text{pH} > 9$ was also investigated. Using the determined ion-exchange constant value for the salicylate-chloride exchange reaction, the fraction of Aliquat 336 was calculated for any given condition. Thus, using the values for D_{Cu} and the concentration

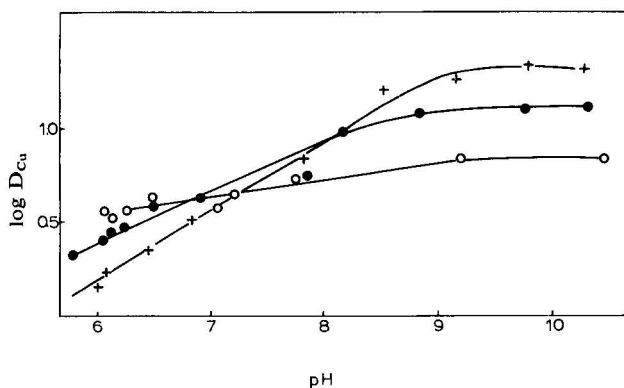
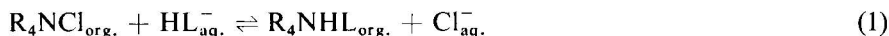


Fig. 3. Logarithmic diagram of the dependence of D_{Cu} on pH at different concentrations of salicylate: $C_{\text{Cu}}^0 = 1 \text{ mM}$; $C_{\text{R}_4\text{NCl}}^0 = 0.072 \text{ M}$; $C_{\text{Cl}^-}^0 = 0.5 \text{ M}$; $C_{\text{sal}^-}^0 = 0.06 \text{ M}$ (\circ — \circ); 0.05 M (\bullet — \bullet); 0.04 M ($+$ — $+$).

of the chloride form of Aliquat 336 in the organic phase, a logarithmic diagram was constructed; this was a straight line with a slope of *ca.* 2. It was also found that $\log D_{\text{Cu}}$ decreased with increasing concentration of chloride in the aqueous phase.

RESULTS AND DISCUSSION

The ion-exchange process between the chloride and monovalent salicylate anions can be described by the equation



The equilibrium constant is given by

$$K_{\text{Cl,HL}}^x = \frac{(\text{R}_4\text{NHL}) [\text{Cl}^-]}{(\text{R}_4\text{NCl}) [\text{HL}^-]} = \frac{D_{\text{HL}} [\text{Cl}^-]}{C_{\text{R}_4\text{NCl}}^0 - (\text{R}_4\text{NHL})} \quad (2)$$

in which the concentrations shown in square brackets refer to the aqueous phase and those shown in parentheses refer to the organic phase, D_{HL} is the distribution coefficient of salicylate, and $C_{\text{R}_4\text{NCl}}^0$ denotes the initial concentration of quaternary ammonium chloride in the organic phase.

The ion-exchange equilibrium constant was calculated from eqn. 2 using the experimentally found value of D_{HL} , the concentration of salicylate anion in the organic phase (R_4NHL), the concentration of chloride in the equilibrated aqueous phase and the initial concentration of Aliquat 336 in the chloroform phase. The ion-exchange equilibrium constants of the other anions were calculated in a similar way. The results are presented in Table I.

The Cu(II) ions in the presence of salicylate may form complexes having the compositions CuL and CuL_2^{2-} , depending on the pH and the concentration of salicylate. We calculated the mole fractions of the various species in the aqueous

TABLE I

ION-EXCHANGE EQUILIBRIUM CONSTANTS OF DIFFERENT ANIONS REFERRED TO CHLORIDE

Anions (A^{n-})	Equilibrium constant ($\log K^x$)
Salicylate (HL^-)	2.43 ± 0.02
Sulphosalicylate (HA^{2-})	2.24 ± 0.05
Bromide (A^-)	1.34 ± 0.04
Nitrate (A^-)	1.33 ± 0.06
Oxalate (A^{2-})	-1.28 ± 0.07
Acetate (A^-)	-1.74 ± 0.05
Sulphate (A^{2-})	-3.6 ± 0.2

phase in the pH range investigated (pH 4–8), using the “ α ” functions introduced by Ringbom². Thus,

$$\alpha_{Cu} = \frac{C_{Cu}}{[Cu^{2+}]} = 1 + [L] \beta_1 + [L]^2 \beta_2 = 1 + \frac{C_{sal.}^0}{\alpha_{L(H)}} \beta_1 + \left(\frac{C_{sal.}^0}{\alpha_{L(H)}} \right)^2 \beta_2 \quad (3)$$

where C_{Cu} is the concentration of Cu(II) ions in the aqueous phase, $C_{sal.}^0$ is the initial concentration of sodium salicylate in the aqueous phase, β_1 and β_2 are the overall stability constants of the copper-salicylate complexes ($\log \beta_1 = 10.6$ and $\log \beta_2 = 18.45$; see ref. 3), and $\alpha_{L(H)}$ is the side-reaction function of protonation of the salicylate ligand. The value of $\alpha_{L(H)}$ can be calculated using the following equation

$$\alpha_{L(H)} = 1 + [H^+] K_1 + [H^+]^2 K_1 K_2 \quad (4)$$

in which K_1 and K_2 are protonation constants of the divalent salicylate ion. The value of $\log K_1$ is 13.6, whereas $\log K_2 = 3$ (see ref. 3). Thus,

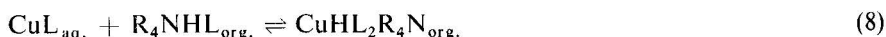
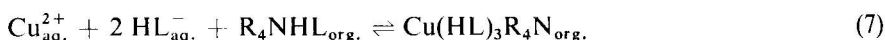
$$\alpha_{CuL} = \frac{C_{Cu}}{[CuL]} = 1 + \frac{\alpha_{L(H)}}{C_{sal.}^0 K_{CuL}} + \frac{C_{sal.}^0 K_{CuL}}{\alpha_{L(H)}} \quad (5)$$

and

$$\alpha_{CuL_2} = \frac{C_{Cu}}{[CuL_2^{2-}]} = 1 + \left(\frac{\alpha_{L(H)}}{C_{sal.}^0} \right)^2 \frac{1}{\beta_2} + \frac{\alpha_{L(H)}}{C_{sal.}^0 K_{CuL_2}} \quad (6)$$

where K_{CuL} and K_{CuL_2} are the stability constants of the copper-salicylate complexes.

The values of α_{Cu} , α_{CuL} and α_{CuL_2} were calculated at various pH and at various concentrations of salicylate (0.1, 0.06 and 0.04 M); their reciprocal values are the mole fractions of the species. The calculations showed that in the pH range 4–6, mainly Cu^{2+} and complex of composition CuL are present in the aqueous phase. At the extraction, using a chloroform solution of Aliquat 336 (salicylate) therefore, the following reactions were assumed



The corresponding extraction equilibrium constants are

$$K_1^e = \frac{\text{Cu}(\text{HL})_3 \text{R}_4\text{N}}{[\text{Cu}^{2+}] [\text{HL}^-]^2 (\text{R}_4\text{NHL})} = \frac{D_{1\text{Cu}} \alpha_{\text{Cu}}}{C_{\text{sal}}^0{}^2 (\text{R}_4\text{NHL})} \quad (9)$$

$$K_2^e = \frac{(\text{Cu HL}_2\text{R}_4\text{N})}{[\text{CuL}] (\text{R}_4\text{NHL})} = \frac{D_{2\text{Cu}} \alpha_{\text{CuL}}}{(\text{R}_4\text{NHL})} \quad (10)$$

where

$$D_{1\text{Cu}} = \frac{(\text{Cu}(\text{HL})_3\text{R}_4\text{N})}{C_{\text{Cu}}} = \frac{(\text{Cu}(\text{HL})_3\text{R}_4\text{N})}{[\text{Cu}^{2+}] \alpha_{\text{Cu}}} \quad (11)$$

and

$$D_{2\text{Cu}} = \frac{(\text{Cu HL}_2\text{R}_4\text{N})}{C_{\text{Cu}}} = \frac{(\text{CuHL}_2\text{R}_4\text{N})}{[\text{CuL}] \alpha_{\text{CuL}}} \quad (12)$$

By combining eqns. 9 and 10, the equation for the overall distribution coefficient of the copper can be obtained

$$D_{\text{Cu}} = (\text{R}_4\text{NHL}) \left[\frac{K_1^e (C_{\text{sal}}^0)^2}{\alpha_{\text{Cu}}} + \frac{K_2^e}{\alpha_{\text{CuL}}} \right] \quad (13)$$

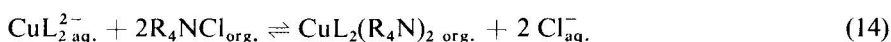
The D_{Cu} values were determined by experiment and the values of α , the side-reaction functions, were calculated by using the known pH value and the concentration of salicylate. By substituting these values at various experimental conditions in eqn. 11, an equation system with two unknown quantities was obtained; by solving this system, the values of the K_1 and K_2 extraction constants were calculated. These were

$$\log K_1^e = 6.47 \pm 0.03$$

$$\log K_2^e = 1.80 \pm 0.01$$

To verify the assumptions and calculations, we compared the calculated and experimentally found values of $\log D_{\text{Cu}}$ at various pH values; these are shown in Fig. 4, from which it can be seen that the calculated and experimental values are in close agreement. Thus the assumption was correct.

In the distribution experiments carried out at $\text{pH} > 9$ we found that the D_{Cu} values increased with the concentration of the quaternary ammonium chloride in the organic phase. It was found also, by calculation, that in the pH range mentioned and under the given concentration conditions, the CuL_2^{2-} complex was predominant in the aqueous phase. Therefore the following extraction reaction was assumed



The extraction equilibrium constant is given by

$$K_3^e = \frac{(\text{CuL}_2(\text{R}_4\text{N})_2)}{[\text{CuL}_2^{2-}] (\text{R}_4\text{NCl})^2} = \frac{D_{3\text{Cu}} \alpha_{\text{CuL}} [\text{Cl}^-]^2}{(\text{R}_4\text{NCl})^2} \quad (15)$$

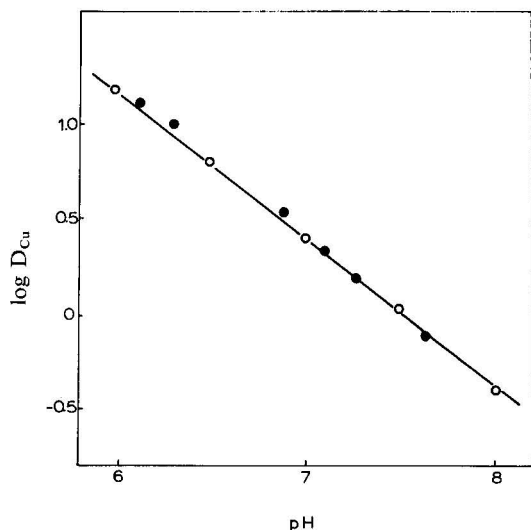


Fig. 4. Calculated and experimentally found values of $\log D_{\text{Cu}}$ at various pH values: $C_{\text{Cu}}^0 = 1 \text{ mM}$; $C_{\text{sal}}^0 = 0.06 \text{ M}$; $C_{\text{R}_4\text{NHL}}^0 = 0.071 \text{ M}$; calculated (\circ — \circ), measured (\bullet — \bullet).

where

$$D_{3\text{Cu}} = \frac{(\text{CuL}_2(\text{R}_4\text{N})_2)}{C_{\text{Cu}}} = \frac{(\text{CuL}_2(\text{R}_4\text{N})_2)}{[\text{CuL}_2^{2-}] \alpha_{\text{CuL}_2}} \quad (16)$$

By using eqn. 15, we calculated, from known quantities, the value of the third extraction constant; this was

$$\log K_3^e = 3.85 \pm 0.05$$

So, if we want to calculate the distribution coefficient of the copper in the pH range 6–10, the process described by eqn. 8 must be taken into consideration. Thus, the

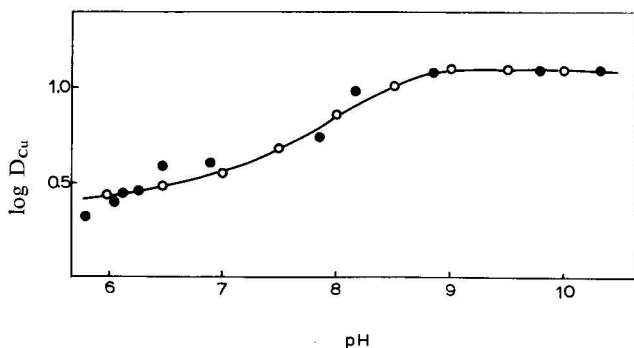


Fig. 5. Calculated and experimentally found values of D_{Cu} at various pH values: $C_{\text{Cu}}^0 = 1 \text{ mM}$; $C_{\text{sal}}^0 = 0.05 \text{ M}$; $C_{\text{Cl}}^0 = 0.5 \text{ M}$; $C_{\text{R}_4\text{NCl}}^0 = 0.02 \text{ M}$; calculated (\circ — \circ), measured (\bullet — \bullet).

overall distribution coefficient, D_{Cu} is the sum of $D_{2\text{Cu}}$ and $D_{3\text{Cu}}$. The calculated and experimentally found values for D_{Cu} are shown in a logarithmic diagram in Fig. 5; it can be seen that agreement between them was reasonably good.

REFERENCES

- 1 J. Inczédy and E. Zimonyi, *Acta Chim. Acad. Sci. Hung.*, 67 (1971) 391.
- 2 A. Ringbom, *Complexation in Analytical Chemistry*, Wiley, New York, 1963.
- 3 D. D. Perrin, *Nature (London)*, 182 (1958) 741.

CHROM. 7915

DETERMINATION OF THE OPTIMAL CONDITIONS FOR ION-EXCHANGE PROCESSES

R. N. RUBINSTEIN, M. M. SENYAVIN, E. V. VENITSIANOV, E. M. MAKHALOV, V. A. ALEKSEENKO and V. A. NIKASHINA

V.I. Vernadsky Institute of Geochemistry and Analytical Chemistry, U.S.S.R. Academy of Sciences, Moscow (U.S.S.R.)

SUMMARY

The theory of the use of the basic parameters of mathematical process models is discussed. In the calculations, it is assumed that the equilibrium is described by the law of mass action and the kinetics have a diffusional nature. Solutions of ion-exchange dynamics for film, particle and mixed diffusion in the case of linear and non-linear isotherms are given. As examples, theoretical curves and experimental results are compared graphically.

INTRODUCTION

Up to the present, an empirical approach has been mainly used to study the problem of the optimal conditions for ion-exchange processes. However, this approach does not enable the true optimal conditions for ion-exchange processes to be found, as a consequence of the many independent parameters that define real systems. In the calculations, it is assumed that the equilibrium is described sufficiently accurately by the law of mass action and the kinetics have a diffusional nature, so that in the description of any ion-exchange system it is possible to use as initial data the ion-exchange capacity, selectivity coefficients, film diffusion and particle diffusion coefficients. In this paper are discussed the principles and results of the creation of such models for single-component systems suitable for optimization purposes. It should be noted that the calculation of the sorption stage for some multicomponent systems may be reduced to the single-component dynamic problem (deionization until the break-through point of a component with the lowest selectivity coefficient, dynamics of ion-exchange of a micro-component with a macro-component¹).

THEORETICAL

Ion-exchange dynamics are described by a system of three equations for each component in a mixture: balance, kinetics and isotherm. For the purpose of solving

these equations simply, they are written in dimensionless variables below:
balance equation:

$$\frac{\partial U}{\partial X} + \frac{\partial V}{\partial T} = A \cdot \frac{\partial^2 U}{\partial X^2} \quad (1)$$

kinetic equation:

$$\frac{\partial V}{\partial T} = F(U, V, V^{(s)}, U_{\text{eq}}) \quad (2)$$

isotherm equation:

$$V_{\text{surface}}^{(s)} = f(U_{\text{eq}}) \quad (3)$$

where

- $U \equiv c/c_0$ = non-dimensional concentration of the exchanged ion in the liquid;
- $V \equiv a/a_0$ = non-dimensional concentration of the exchanged ion in the resin, mean amount within the volume of the resin particle;
- $V^{(s)} \equiv a^{(s)}/a_0$ = non-dimensional local concentration of the ion in the resin;
- $U_{\text{eq}} \equiv c_{\text{eq}}/c_0$ = non-dimensional concentration of the ion in the liquid, being in equilibrium with $V^{(s)}$ on the particle surface of the resin;
- c_0, a_0 = characteristic concentrations of the exchanged ion in the liquid and in the resin, respectively;
- $X \equiv l/l_0$ = non-dimensional size;
- $T \equiv t/t_0$ = non-dimensional time;
- l_0, t_0 = characteristic values of size and time, connected with the peculiarities of each concrete problem;
- D_l = longitudinal diffusion coefficient;
- w = flow-rate, calculated for the pure section of the column;
- $A \equiv D_l/wl_0$ = non-dimensional longitudinal diffusion coefficient.

In the calculations, it is assumed that the equilibrium is described accurately by the law of mass action, which has the following form under the conditions of an absence of any additional chemical interaction:

$$\frac{V}{(1-V)^\mu} = \bar{K} \cdot \frac{U}{(1-U)^\mu} \quad (4)$$

where

- $\mu \equiv Z/Z_0$ = ratio of ionic charges;
- \bar{K} = non-dimensional selectivity coefficient.

The ion-exchange kinetics are determined by the mass transport in the liquid and in the resin. The film diffusion equation has the form

$$\frac{\partial V}{\partial T} = U - U_{\text{eq}} \quad (5)$$

and the scale factors are

$$l_0 = \frac{w}{\beta}; t_0 = \frac{a_0}{c_0 \cdot \beta} \quad (5a)$$

The kinetic coefficient, β , for aqueous solutions and resins with spherical particles at 20° can be calculated according to the equation (ref. 2, p. 68)

$$\beta = 7.5 \cdot 10^{-4} \left(\frac{z}{\lambda} + \frac{z_0}{\lambda_0} \right)^{-2/3} w^{0.47} (2R)^{1.53} \quad (6)$$

where

R = radius of the resin particles;

λ, λ_0 = equivalent conductivities of ions.

It was shown (ref. 2, p. 84) that relative contributions of longitudinal diffusion and film diffusion to erosion of the front was determined by the factor Δ :

$$\Delta = \frac{D_i}{\beta R^2}$$

When $\Delta \gg 1$, the contribution of longitudinal diffusion is the most important, but when $\Delta \ll 1$, film diffusion predominates. It is further assumed that $\Delta \ll 1$ for the most commonly used conditions in practical ion-exchange and $D_i = 0$ in eqn. 1.

Diffusion in particles is determined by Fick's laws, which have the following form for spherical particles:

$$\frac{\partial}{\partial T} (\varrho V^{(s)}) = \frac{\partial^2}{\partial \varrho^2} (\varrho V^{(s)}) \quad (7)$$

where

$\varrho = r/R$ = non-dimensional variable radius in particle. In this case, characteristic scales of size and time are:

$$l_0 = \frac{w c_0}{a_0 D_i}; t_0 = \frac{R^2}{D_i} \quad (7a)$$

where

D_i = particle diffusion coefficient.

The particle diffusion is described by an equation similar to eqn. 5 for the final stages of sorption at the time when the greatest volume of the particle is removed:

$$\frac{\partial V}{\partial T} = V^{(s)} - V \quad (8)$$

The characteristic scales of size and time are:

$$l_0 = \frac{c_0 w}{a_0 \beta_i}; t_0 = \frac{1}{\beta_i} \quad (8a)$$

where

$$\beta_i = \frac{\gamma D_i}{R^2}$$

$\gamma = \text{constant}$.

The true kinetic process is the mixed diffusion process, and correlation of the contributions of film and particle diffusion is determined by the factor H :

$$H = \frac{\beta R^2 c_0}{a_0 D_i} \quad (9)$$

When $H \ll 1$, the kinetics are defined by film diffusion and it is possible to assume that redistribution of the concentration occurs instantly in the particle, *i.e.*, $V^{(s)} = V$.

The solutions stated below were obtained within the limitations indicated.

Linear isotherm

$$V^{(s)} = U \quad (3')$$

(1) In the case of film diffusion ($H = 0$), tables of certain solutions³ were obtained for a wide range of values of X and T by means of a computer and the solutions of sorption and desorption problems for chromatographic variants were also found⁴.

(2) In the case of particle diffusion ($H = \infty$) (eqns. 1, 3' and 7), the particular solution⁵ was supplemented with an asymptotic equation (ref. 2, p. 38). For comparison of the theory with experimental results, we investigated the sorption of copper(II) ions by oxidized coal⁶. The theoretical curve and experimental points are plotted logarithmically in Fig. 1.

The superposition of the non-dimensional theoretical curve on the experi-

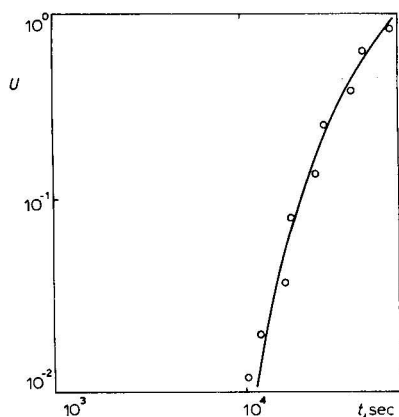


Fig. 1. Comparison of the theoretical curve and experimental results for the sorption of copper ions from a solution containing $5 \cdot 10^{-4}$ mg-equiv./ml of Cu^{2+} and 1.25 mg-equiv./ml of $\text{Na}^+(\text{NaNO}_3)$ by oxidized coal ($w = 0.08$ cm/sec; $R = 0.02$ cm; $l = 11$ cm; $D_i = 9.6 \cdot 10^{-9}$ cm²/sec; $a_0/c_0 = 300$; $X = 0.99$).

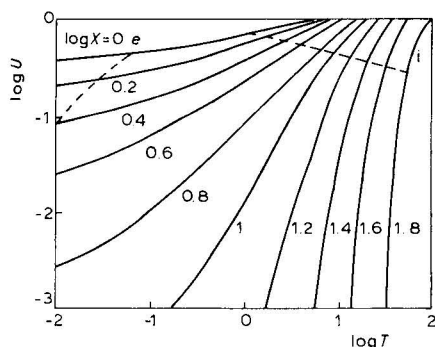


Fig. 2. Theoretical curves in the range of mixed diffusion and linear isotherm; $H = 10$.

mental results on a graph of $\log c/c_0$ versus $\log t$ gives the possibility of finding the characteristic scales of size and time by the intercept on the abscissa equal to $\log t/T$. It is then possible to calculate the parameters a_0/c_0 , D_i or β , knowing the conditions of the experiment (w , R).

(3) In the case of mixed diffusion (eqns. 1, 3', 5 and 7), the exact solution for the dynamic sorption problem was found by means of a computer⁷. As it was found that the influence of film diffusion prevails in the initial stages of sorption, whereas particle diffusion prevails in the final stages, there must exist a stage of the process at which the rates of these two processes are equal and the duration of this stage depends on H and X . Graphs of $U(X, T)$ for $H = 10$ are given in non-dimensional logarithmic co-ordinates in Fig. 2. The ranges described by film or particle diffusion to within 10% are shown by dotted lines. Fig. 3 gives a comparison of the theoretical curve and experimental results⁸.

Non-linear isotherms

(1) *Film diffusion.* By means of a computer, the solution of the system of eqns. 1, 4, 5 and 5a for $U(X, T)$ was found⁹ for selectivity constants, \bar{K} , changing over a wide

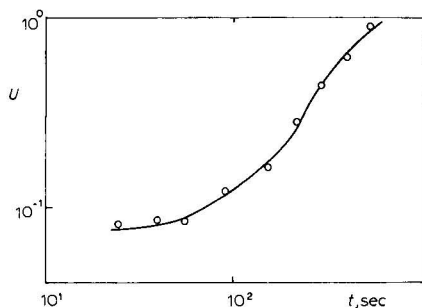
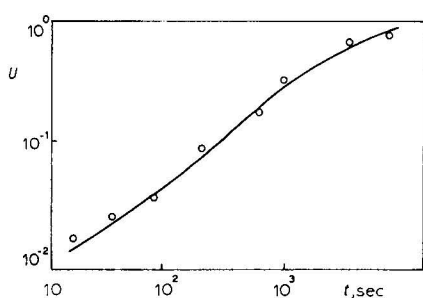


Fig. 3. Comparison of the theoretical curve and experimental results for the sorption of yttrium from a solution containing 0.1 mg-equiv./ml of Ca^{2+} and 10^{-5} mg-equiv./ml of Y^{3+} by oxidized coal in the Ca^{2+} form (pH = 3; $w = 0.35$ cm/sec; $R = 0.01$ cm; $l = 2.8$ cm; $D_i = 2.1 \cdot 10^{-9}$ cm²/sec; $H = 68.5$; $a_0/c_0 = 500$; $X_e = 5.76$).

Fig. 4. Comparison of the theoretical curve and experimental results for the sorption of calcium by cationite KU-2 (H^+) ($\bar{K} = 2$; $w = 5.3$ cm/sec; $R = 0.024$ cm; $l = 8$ cm; $\beta = 2.3$ sec⁻¹; $X = 3.5$).

range (from 0.1 to ∞). As an example, the theoretical curve and the experimental results are given in Fig. 4.

(2) *Particle diffusion, described by eqns. 1, 4, 8 and 8a.* In this case, the solution can be expressed by the solution of the film diffusion problem by means of the following calculations. Let us designate the solution of the film diffusion problem (see section (1), above) with a selectivity coefficient \bar{K}_e and a ratio of charges μ_e by $U(X, T, \bar{K}_e, \mu_e)$ and $V(X, T, \bar{K}_e, \mu_e)$. Then, the solution for the sorption problem in the case of particle diffusion $U^{(i)}$ and $V^{(i)}$ with a selectivity coefficient \bar{K}_i and a ratio of charges μ_i is expressed by the equations

$$\begin{aligned} U^{(i)}(X_i, T_i, \bar{K}_i, \mu_i) &= 1 - V\left(T_i, X_i, \bar{K}_i^{\mu_i}, \frac{1}{\mu_i}\right) \\ V^{(i)}(X_i, T_i, \bar{K}_i, \mu_i) &= 1 - U\left(T_i, X_i, \bar{K}_i^{\mu_i}, \frac{1}{\mu_i}\right) \end{aligned} \quad (10)$$

By means of eqn. 10, it is possible to plot easily the solutions of the problems in section (1) in the case of particle diffusion. Fig. 5 shows a comparison of the theoretical curve and experimental results.

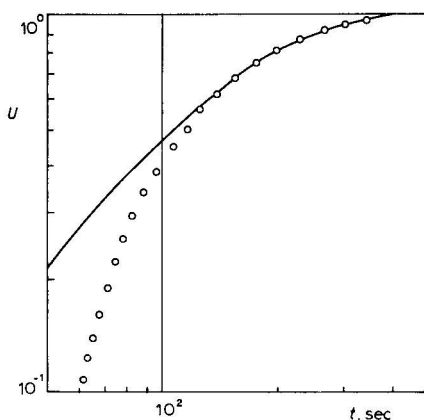


Fig. 5. Comparison of the theoretical curve and experimental results for hydrogen in the regeneration of KU-2 (Na^+) by 1 *N* acid ($w = 0.25$ cm/sec. $R = 0.03$ cm; $l = 15.8$ – 17.5 cm (H^+ form); $\bar{R} = 0.8$; $a_0 = 1.5$ mg-equiv./ml; $X = 5$).

(3) We found the approximate solution¹⁰ for the case of S-shaped isotherms, to which the ion-exchange dynamics may be reduced, for example, when complex formation occurs or in the case of resin mixtures. The isotherm is divided into two parts by drawing a tangent at the point (c_0, a_0) (Fig. 6). The initial part is approximated by the isotherm in eqn. 4 with $\mu = 1$ and the selectivity coefficient

$$\bar{K}_1 = \frac{c_1}{a_1} \left(\frac{da}{dc} \right)_{c=0} < 1$$

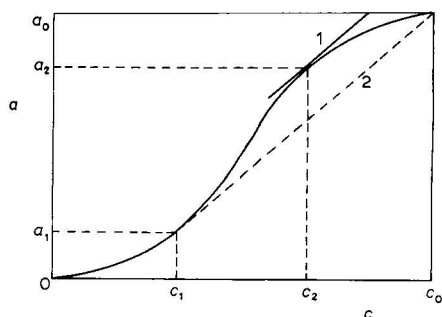


Fig. 6. Method of division of S-shaped isotherm into two parts (straight line 2 is parallel to tangent 1).

The second convex part of the isotherm is also approximated by the isotherm in eqn. 4 with $\mu = 1$ and the selectivity coefficient

$$\bar{K}_2 = \left(\frac{a_2 - a_1}{a_0 - a_2} \right)^2$$

The method of finding a_2 is shown in Fig. 6.

For the first part, the solution could be found from the equation

$$\frac{c}{c_1} = U(X, T, \bar{K}_1, 1)$$

and for the second part, it could be found from the equation

$$\frac{c - c_2}{c_0 - c_2} = U(X, T, \bar{K}_2, 1) \quad (11)$$

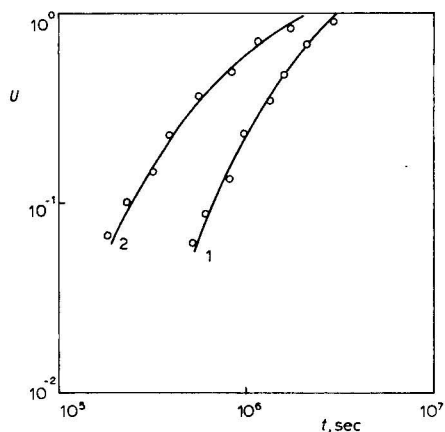


Fig. 7. Comparison of the theoretical curves and experimental results for the sorption of calcium from natural carbonated water by cationite Kb-4p-2 (1: $w = 0.03$ cm/sec; $l = 14.6$ cm; $\bar{K}_2 = 2$; $X = 0.07$. 2: $w = 0.04$ cm/sec; $l = 29.2$ cm; $\bar{K}_2 = 2$; $X = 0.1$).

where $U(X, T, \bar{K}, 1)$ is the solution for the cases in section (1) or (2) depending on the kind of kinetics. Fig. 7 shows a comparison of the data obtained by eqn. 11 and the theoretical curves corresponding to them.

The solutions given above are used for the calculation of the sorption dynamics and the regeneration dynamics of different true single-component and multicomponent systems. These models are also the basis for the calculation of the optimal conditions for ion-exchange processes. It is appropriate to mention here that information on the systems studied (selectivity coefficients; coefficients of film diffusion and particle diffusion) could be obtained for use in calculations in ion-exchange processes by superimposing the theoretical curves and experimental results.

REFERENCES

- 1 N. K. Galkina and M. M. Senyavin, *Zh. Fiz. Khim.*, 43 (1969) 1783.
- 2 M. M. Senyavin, R. N. Rubinstein, E. V. Venitsianov, N. K. Galkina, I. V. Komarova and V. A. Nikashina, *Essentials of Calculation and Optimization of Ionexchange Processes*, Nauka, Moscow, 1972.
- 3 A. A. Zhukhovitsky, I. L. Zabezhinsky, and A. N. Tikhonov, *Zh. Fiz. Khim.*, 19 (1945) 253.
- 4 E. V. Venitsianov, B. A. Volkov, V. P. Ioffe, G. M. Kolosova and R. N. Rubinstein, *Zavod. Lab.*, 37 (1971) 513.
- 5 I. A. Myasnikov and K. A. Golbert, *Zh. Fiz. Khim.*, 26 (1953) 1311.
- 6 V. A. Alekseenko, V. A. Nikashina, M. M. Senyavin, I. A. Tarkovskaya, L. N. Grashchenkova and V. E. Goba, *Adsorption and Adsorbents*, Vol. 2, Naukova Dumka, Kiev, 1974.
- 7 E. V. Venitsianov, E. M. Makhalov and R. N. Rubinstein, *Zh. Fiz., Khim.*, 47 (1973) 665.
- 8 V. A. Alekseenko, V. A. Nikashina and E. V. Venitsianov, *Zh. Fiz. Khim.*, 47 (1973) 1033.
- 9 V. A. Nikashina, B. A. Volkov, R. N. Rubinstein and M. M. Senyavin, *Zh. Fiz. Khim.*, 46 (1972) 686.
- 10 R. N. Rubinstein, A. M. Sorochan, V. A. Alekseenko and A. K. Kunbazarov, *Izv. Akad. Nauk SSSR, Ser. Khim.*, No. 7 (1973) 1461.

ANALYTICAL APPLICATIONS

CHROM. 7832

CHROMATOGRAPHIC BEHAVIOUR OF AMINO ACIDS ON CATION-EXCHANGE RESIN-COATED CHROMATOSHEETS IN THE H^+ FORM

I. HAZAI, S. ZOLTÁN, J. SALÁT, S. FERENCZI

Chinoin Pharmaceuticals Ltd., Budapest (Hungary)

and

T. DÉVÉNYI

Enzymology Department, Institute of Biochemistry, Hungarian Academy of Sciences, Budapest (Hungary)

INTRODUCTION

Modern analysis of amino acids is based on ion-exchange chromatography, which has become a common method after the work of Moore and Stein¹. Several efforts have been made to combine the excellent separation capacity of ion-exchange chromatography with the simplicity of paper and thin-layer chromatography. Using resin-impregnated filter-papers², tailing caused by diffusion has to be considered. Thin layers prepared from a mixture of ion-exchange resin and cellulose powder^{3–8} have not been applied to the separation of amino acids. The manufacture of Dowex 50-X8 resin-coated chromatoplates and chromatoshets (in the Na^+ form) made it possible to study the possibilities of using ion-exchange chromatography in the separation of amino acids by applying the thin-layer technique^{9–11}. When the circumstances are similar to those which apply in column chromatographic procedures, thin-layer chromatoshets coated with ion-exchange resin of the same type yield analogous separations. Tomasz¹² applied the ion-exchange thin-layer chromatographic technique to the separation of nucleic acid components using sheets of cation exchanger in the H^+ form. We were interested in investigating the adaptability of this method to the separation of amino acids.

In this paper, we describe studies on the behaviour of amino acids on chromatoshets in the H^+ form.

EXPERIMENTAL

The chromatoshets used were produced by Chinoin (Budapest, Hungary) under the tradename Fixion 50-X8 in the sodium form*. The sheets were converted into the H^+ form by two methods. The first method was continous chromatography⁹, while the following second, more efficient, procedure gave the same results. Some 20 × 50-cm strips were cut from filter-paper and placed on horizontally positioned chromatoshets with 15 cm hanging down each side. In this way, about 15–20 chromatoshets could be superposed with the filter-paper strips between them. One

end of the filter-paper was placed in 1 *N* hydrochloric acid and the other in an empty vessel, as shown in Fig. 1. The procedure was carried out for 24 h, after which the wet chromatoshets were dried and the filter-paper strips were replaced with new ones. The chromatoshets were washed until the filter-paper strips became neutral in the second vessel.

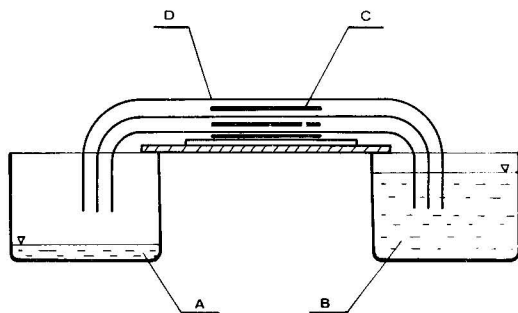


Fig. 1. Method of converting chromatoshets into the H^+ form. A, Empty vessel; B, vessel containing 1 *N* HCl; C, chromatoshet; D, filter-paper.

Detection on the chromatograms was carried out by the ninhydrin reaction. A stock solution was prepared by dissolving 5 g of ninhydrin and 1 g of cadmium acetate in a mixture of 95 ml of 96% ethanol and 5 ml of glacial acetic acid. The spray reagent was prepared by adding four volumes of carbon tetrachloride to the alcoholic stock solution together with 10% collidine. In each case, development was carried out at 45°. The migration distance was 18 cm.

RESULTS AND DISCUSSION

When using weak acids such as formic or acetic acid at concentrations of 0.1–2.0 *N*, the amino acids hardly moved from the origin. As strong acids, sulphuric and hydrochloric acids were used. Sulphuric acid was found to be unsatisfactory as even at low concentrations the layers were badly damaged.

The relationship between the hydrochloric acid concentration and the hR_F value was investigated in detail, and the results are shown in Table I. It can be seen that the best separation is obtained at concentrations between 0.8 and 1.0 *N*. Basic amino acids showed a tailing effect in 1.2 *N* hydrochloric acid. At higher concentrations, basic amino acids preceded aromatic amino acids.

If the development is repeated in the same direction with the same eluting solution, better separations can be achieved. This type of separation is shown in Fig. 2.

It was found that the presence of organic solvents does not improve the effectiveness of the separation of components with high R_F values (see Table I).

* Ionex 25 SA-Na, produced by Macherey, Nagel & Co. (Düren, G.F.R.) is identical with Fixion 50-X8.

TABLE I

hR_F VALUES OF AMINO ACIDS ON A CATION-EXCHANGE RESIN-COATED CHROMATOSHEET IN THE H^+ FORM

The hR_F of Asp was assigned the value 100 and the values for other amino acids are given relative to this value. Eluting solutions: 1 = 0.5 *N* HCl; 2 = 0.8 *N* HCl; 3 = 1.0 *N* HCl; 4 = 1.2 *N* HCl; 5 = 1.4 *N* HCl; 6 = 1.6 *N* HCl; 7 = 1.8 *N* HCl; 8 = 2.0 *N* HCl; 9 = 2.2 *N* HCl; 10 = 3.0 *N* HCl; 11 = 4.0 *N* HCl; 12 = 0.8 *N* HCl, 1 development; 13 = 0.8 *N* HCl, 2 developments; 14 = 0.8 *N* HCl, 3 developments; 15 = 1.0 *N* HCl containing 10% methanol; 16 = 1.0 *N* HCl containing 10% ethanol; 17 = 1.0 *N* HCl containing 10% ethylene glycol; 18 = 1.0 *N* HCl containing 10% glycerine.

Amino acid	Eluting solution																	
	1	2	3	4	5	6	7	8	9	10	11	12	13	14	15	16	17	18
Asp	100	100	100	100	100	100	100	100	100	100	100	100	100	100	100	100	100	100
Ser	97	98	100	100	100	101	101	100	101	104	103	100	100	99	99	100	100	100
Thr	96	92	93	96	96	99	97	96	99	97	97	94	94	96	97	95	96	92
Glu	86	89	89	95	95	99	96	96	96	95	97	85	91	95	90	93	93	92
Gly	69	80	86	91	91	94	95	93	93	95	94	74	82	90	77	75	79	81
Ala	61	72	77	83	82	87	87	88	88	87	87	67	74	81	73	70	71	69
Val	40	50	54	60	61	66	66	70	76	67	67	46	55	60	59	52	53	50
Met	26	37	38	44	45	50	51	58	63	51	57	32	40	45	41	36	34	33
Ile	26	34	34	41	41	45	46	51	57	45	48	29	36	41	40	36	34	33
Leu	23	30	31	38	37	41	42	47	53	42	45	27	34	38	36	35	30	31
Tyr	14	25	25	30	29	33	35	41	45	34	39	19	24	31	30	28	25	25
Phe	10	15	15	18	19	21	23	27	31	23	28	12	16	20	20	18	14	16
Lys	1	8	11	27	25	27	33	43	62	60	75	6	10	12	11	10	14	11
His	1	8	10	26	22	23	30	38	55	55	70	5	7	10	10	7	7	8
Arg	1	4	6	14	12	13	18	25	36	39	55	2	4	6	6	3	2	4

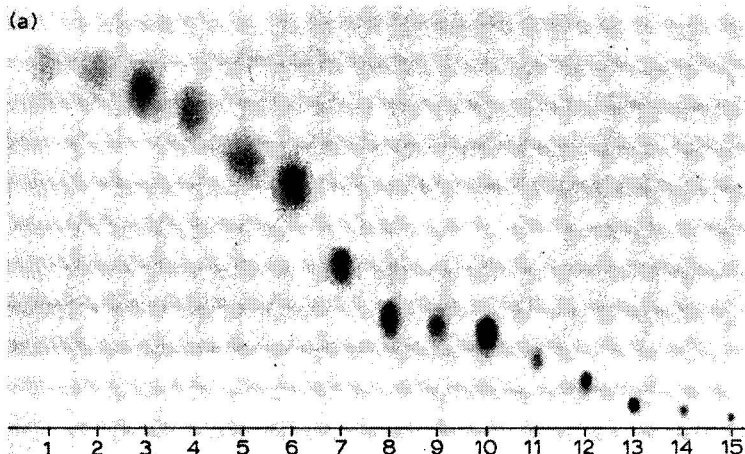


Fig. 2.

(Continued on p. 248)

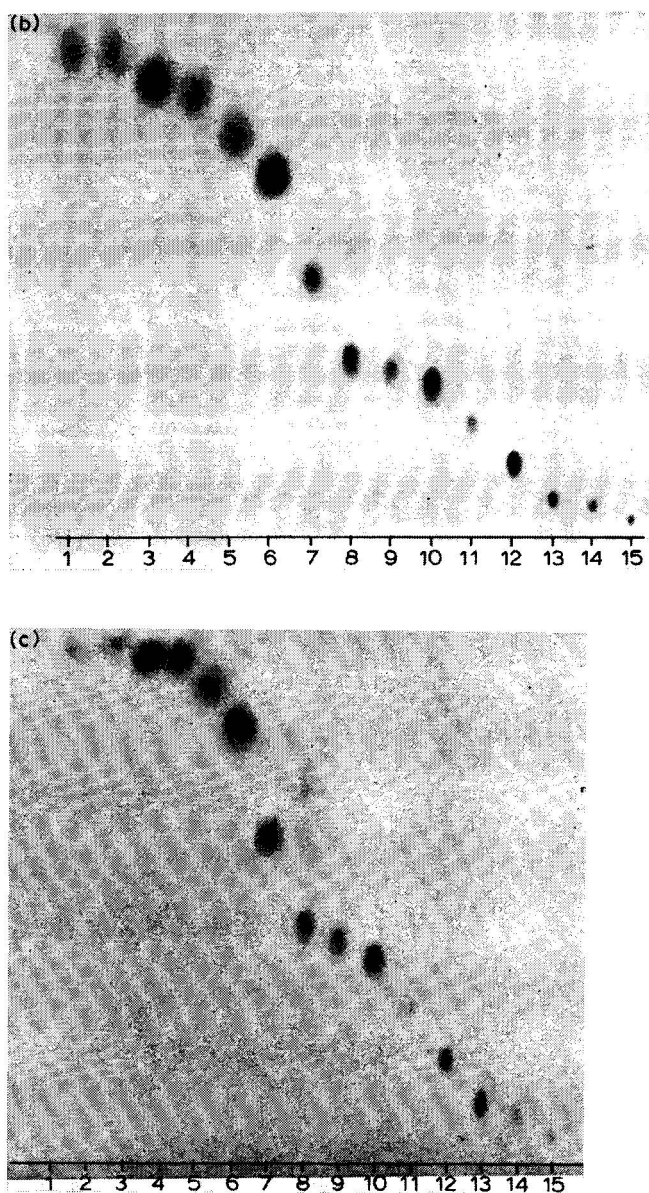


Fig. 2. Development with repeated running: (a) 1 development with 1.0 *N* HCl; (b) 2 developments with 1.0 *N* HCl; (c) 3 developments with 1.0 *N* HCl. Amino acids, from left to right: 1, Asp; 2, Ser; 3, Thr; 4, Glu; 5, Gly; 6, Ala; 7, Val; 8, Met; 9, Ile; 10, Leu; 11, Tyr; 12, Phe; 13, Cys; 14, His; 15, Arg.

Ion-exchange thin-layer chromatography using cation-exchange resins in the H^+ form might be a useful method for the separation of amino acid derivatives, oligopeptides, etc., with one- or two-dimensional development.

REFERENCES

- 1 S. Moore and W. H. Stein, *Anal. Biochem.*, 30 (1958) 1190.
- 2 C. S. Knight, *Chromatogr. Rev.*, 4 (1962) 69.
- 3 J. A. Berger and P. Blanquet, *Bull. Soc. Chim. Biol.*, (1963) 2662.
- 4 J. A. Berger and P. Blanquet, *Bull. Soc. Chim. Biol.*, (1964) 3179.
- 5 J. A. Berger, *C.R. Acad. Sci., Paris*, 259 (1964) 2231.
- 6 L. Lepri, P. G. Desideri and V. Coas, *J. Chromatogr.*, 52 (1970) 421.
- 7 L. Lepri, P. G. Desideri and V. Coas, *J. Chromatogr.*, 64 (1972) 271.
- 8 L. Lepri, P. G. Desideri and R. Mascherini, *J. Chromatogr.*, 70 (1972) 212.
- 9 T. Dévényi, *Acta Biochim. Biophys. Acad. Sci. Hung.*, 5 (1970) 435.
- 10 T. Dévényi, I. Hazai, S. Ferenczi and J. Bati, *Acta Biochim. Biophys. Acad. Sci. Hung.*, 6 (1971) 385.
- 11 T. Dévényi, J. Bati and F. Fábián, *Acta Biochim. Biophys. Acad. Sci. Hung.*, 6 (1971) 133.
- 12 J. Tomasz, *J. Chromatogr.*, 84 (1973) 208.

CHROM. 7709

CHROMATOGRAPHIC SEPARATION OF DANSYL AMINO ACIDS AND DANSYL AMINES ON AMBERLITE IRC-50

TOKUICHIRO SEKI and HIROSHI WADA

*Department of Genetics and Department of Pharmacology II, Osaka University School of Medicine,
Osaka 530 (Japan)*

SUMMARY

A column chromatographic method for the separation of dansyl amino acids and dansyl amines is described in which Amberlite IRC-50 equilibrated with the eluent is used as the stationary phase and six solvent mixtures, which are composed of a buffer or 2% acetic acid and tetrahydrofuran, methyl ethyl ketone and acetone, are used as eluents. Neutral and acidic dansyl derivatives were separated at low pH, and those having a positive charge or present as the dipolar ion at pH 5.60 were separated at high pH. Quantitative determination of histamine as its monodansyl derivative was successful, and an analysis for histamine in a rat liver extract is described.

INTRODUCTION

1-Dimethylaminonaphthalene-5-sulphonyl(dansyl) derivatives of amino acids and amines are highly fluorescent compounds and nanogram amounts of amino compounds can be determined by converting them into their dansyl derivatives¹⁻³.

We have tried to use ion-exchange resins as the column material for the chromatographic separation of dansyl derivatives and a carboxylic acid type resin, Amberlite IRC-50, was found to be useful for this purpose.

EXPERIMENTAL

Reagents

The dansyl amino acids were purchased from Seikagaku Kogyo Co. (Tokyo, Japan), and dansyl chloride from Tokyo Kasei Kogyo Co. (Tokyo, Japan). Biogenic amines were obtained from commercial sources. Dipeptides of the branched chain amino acids, Val-Val, Ile-Val, Val-Ile and Ile-Ile, were supplied by Dr. T. Inui. Citric acid monohydrate, formic acid (99% and 85%), acetone, methyl ethyl ketone, tetrahydrofuran and acetic acid were of special grade and thiodiglycol was of reagent grade for amino acid analyzer.

Dansylation of the dipeptides

The above dipeptides were dansylated according to the procedure recommended by Gray⁴, and purified on a 0.6×10 – 15 -cm column of Amberlite IRC-50 (H^+), using a mixture of 2% acetic acid and acetone (3:2, v/v) as the eluent.

Dansylation of amines

Serotonin and catecholamines. Ten nanomoles of each amine in $10 \mu\text{l}$ of 0.2% acetic acid were mixed with $30 \mu\text{l}$ of dansyl chloride solution in acetone (10 mg/ml) and $10 \mu\text{l}$ of carbonate buffer (pH 10, 0.4 *N*). Then 10 – $20 \mu\text{l}$ of acetone were added in order to clarify the reaction mixture. After incubation at 25° for 5 h, the mixture was neutralized with $60 \mu\text{l}$ of 0.1 *N* formic acid, diluted with $200 \mu\text{l}$ of eluent E (Table I) and added to the column.

Histamine. One to five nanomoles of histamine dihydrochloride in $10 \mu\text{l}$ of 0.2% acetic acid were mixed with $20 \mu\text{l}$ of dansyl chloride solution (2.5 mg/ml) and $10 \mu\text{l}$ of sodium hydrogen carbonate solution (0.4 *N*), and $10 \mu\text{l}$ of dansyl chloride solution were added in order to clarify the reaction mixture. After incubation at 25° for 2 h, the mixture was evaporated to dryness under nitrogen and treated with formic acid as described by Tamura *et al.*⁵, to give monodansyl histamine. The dried residue was dissolved in eluent F and added to the column.

Dansylation of the histamine fraction from a rat liver extract was performed as described above, with the use of double amounts of the reagents.

Preparation of histamine fraction from rat liver

Four grams of rat liver were homogenized in a glass homogenizer with 20 ml of 0.4 *N* perchloric acid and centrifuged at 30,000 *g* for 30 min. One eightieth of the supernatant fraction was added to a 0.32×2.8 -cm column of Dowex 50-X4 (Na^+) buffered at pH 5.0, washed with 5 ml of 1 *N* hydrochloric acid, and histamine was eluted with 1.6 ml of 2.5 *N* hydrochloric acid.

Preparation of the columns

Amberlite IRC-50 (A.G.) was pulverized, classified according to size and washed as described previously⁶. Particles of size ranges 35–40, 40–50 and 50–60 μm were used. The washed resin in the sodium form was buffered to the pH of the buffer used to prepare the eluent by adding either formic acid or citric acid solution to the resin suspension. The buffered resin was washed with the eluent described in Table I,

TABLE I
COMPOSITION OF ELUENTS

Eluent	Composition*	Proportions (v/v)
A	Formate buffer, pH 4.00 (0.4 <i>N</i>)-tetrahydrofuran (THF)-methyl ethyl ketone (MEK)-acetone (Me_2CO)	15:1:3:3
B	Formate buffer, pH 3.15 (0.4 <i>N</i>)-THF-MEK- Me_2CO	14:1:3:3
C	2% Acetic acid-THF-MEK- Me_2CO	20:4:3:3
D	Citrate buffer, pH 5.60 (0.1 <i>M</i>)-THF-MEK- Me_2CO	14:1:3:3
E	Formate buffer, pH 4.00 (0.4 <i>N</i>)-THF-MEK- Me_2CO	9:1:2:4
F	Citrate buffer, pH 5.60 (0.1 <i>M</i>)-THF-MEK- Me_2CO	10:1:3:3

* 0.25% (v/v) of thiodiglycol was added after mixing.

poured into a tube with the eluent used to equilibrate the resin and allowed to settle under gravity. When the resin of smaller particle size was used, it was packed into short chromatographic tubes with a column adjuster and two or three of these tubes were connected in series, in which the tube packed with the smaller resin was connected to the tubes containing the larger one. By this means, development of excessive back-pressure could be avoided. The sizes of the columns are shown in Table II.

TABLE II
CONDITIONS OF THE CHROMATOGRAPHIC SEPARATION

Figure	Eluent	Form of resin	Size of column (mm)*	Particle size of resin (μm)	Temperature of column ($^{\circ}\text{C}$)	Flow-rate (ml/h)
1a	A	Na^+	Top: 155 Middle: 105 Bottom: 110	40–50 35–40 35–40	46	6
1b	B	Na^+	Top: 160 Middle: 120 Bottom: 105	40–50 35–40 35–40	37	6
1c	C	H^+	550	50–60	37	6
1d	D	Na^+	440	50–60	40	6
2	E	Na^+	Top: 100 Bottom: 100	40–50 40–50	37	9
3a	F	Na^+	200	40–50	37	6
3b	F	Na^+	200	40–50	37	6

* Diameter of column = 8 mm.

Chromatographic separation and detection

Samples were dissolved in the eluent to be used for the separation and added to the column.

The buffer change system and constant flow pump of a JEOL 6AH amino acid analyzer were utilized for the elution of the dansyl derivatives, and eluent was pumped into the column at a flow-rate of either 6 or 9 ml/h. The eluate from the column was monitored with an L.D.C. Model 1209 fluoroMonitor or a JEOL FL-detector, and a back-pressure was applied so as to prevent the formation of bubbles in the flow cell. Amounts of 10^{-9} – 10^{-10} mole of the dansyl derivative could be detected with this assembly of equipment.

RESULTS AND DISCUSSION

As shown in Fig. 1a, most of the dansyl amino acids could be separated with eluent A, at 46° and a flow-rate of 6 ml/h, within 23 h.

Those dansyl amino acids which could not be separated with eluent A could be separated from each other by using eluent B (Fig. 1b), C (Fig. 1c) or D (Fig. 1d). Therefore, when the analysis of the dansyl amino acids present in the acid hydrolyzate of a dansylated protein with eluent A gave an ambiguous result, the analysis of the other aliquot of the sample with eluent B, C or D generally yielded sufficient results for the identification of the dansyl amino acid in question.

The positions in the elution pattern of dansyl-arginine, ϵ -dansyl-lysine, mono-

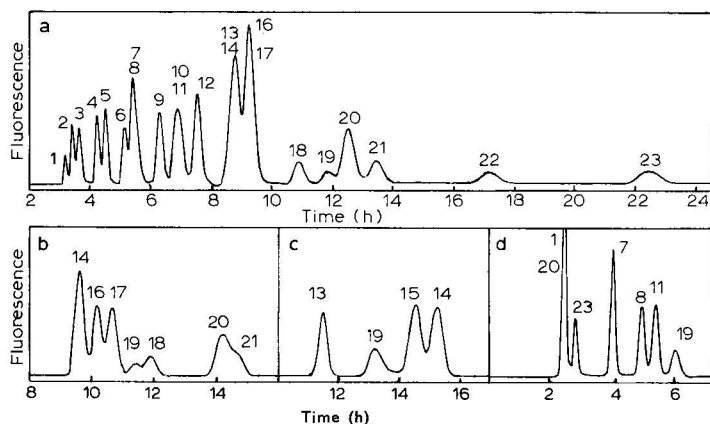


Fig. 1. Elution of dansyl amino acids. Chromatographic conditions are given in Table II. The numbers on the peaks represent the dansyl derivatives of aspartic acid (1), glutamic acid (2), serine (3), threonine (4), glycine (5), alanine (6), lysine (7, ϵ -dansyl), histidine (8, monodansyl), methionine (9), proline (10), arginine (11), valine (12), ammonia (13), leucine (14), tryptophan (15), isoleucine (16), phenylalanine (17), Val-Val (18), tyrosine (19, o -dansyl), lysine (20, didansyl), Ile-Val (21), Ile-Ile (22) and tyrosine (23, didansyl). Dansyl-tryptophan overlapped with dansyl-leucine and dansyl-Val-Ile overlapped with dansyl-Ile-Val under the chromatographic conditions of Figs. 1a and 1b. 1-Dimethylaminonaphthalene-5-sulphonic acid was eluted ahead of all of the above dansyl derivatives.

dansyl-histidine, dansyl-amide and o -dansyl-tyrosine relative to the other dansyl amino acids were very sensitive to changes in the pH of the eluent. In this chromatographic system, therefore, the pH of the buffer of eluent A was adjusted so as to permit the elution of o -dansyl-tyrosine ahead of didansyl-lysine, and the pH of the buffer of the eluent B was adjusted so as to permit the elution of o -dansyl-tyrosine just after dansyl-phenylalanine.

Dansyl derivatives of serotonin and catecholamines could be separated with eluent E containing a larger proportion of the organic solvents (Fig. 2). Peaks that eluted faster than dansyl-serotonin were also found in the dansylation mixture without amines, and these are probably the dansylated products of impurities present in the reaction mixture. The small peak that was eluted after dansyl-dopamine is the

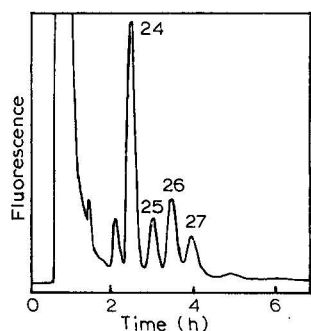


Fig. 2. Elution of dansyl amines. Chromatographic conditions are given in Table II. The numbers on the peaks represent the dansyl derivatives of serotonin (24), noradrenaline (25), adrenaline (26) and dopamine (27).

product derived from noradrenaline when it was dansylated with a large excess of dansyl chloride.

Monodansyl-histamine has a positive charge at pH 5.60, so that it could be separated from other dansyl amino acids and dansyl amines, which have a negative charge or no net charge at all (Fig. 3a).

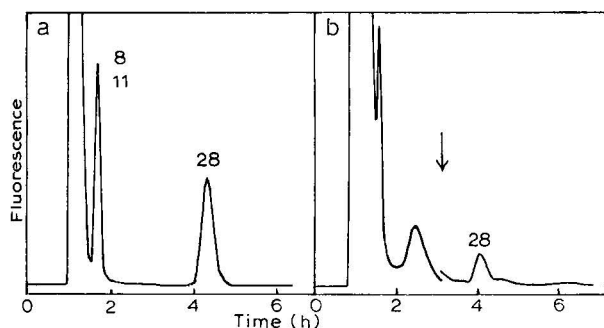


Fig. 3. (a) Elution of some dansyl amino acids, dansyl-catecholamines and monodansyl-histamine. Dansyl catecholamines were eluted in the first peak. (b) Elution of dansylated histamine fraction of rat liver. Chromatographic conditions are given in Table II. The numbers on the peaks represent the dansyl derivatives of histidine (8, monodansyl), arginine (11) and histamine (28). Sensitivity of the detector was doubled at the time indicated by an arrow.

From the elution patterns shown in Figs. 1–3, it may be inferred that non-polar interaction between the solute and the resin matrix, and ion exclusion from the resin phase of more negatively-charged dansyl derivatives, play an important role in this type of separation.

The application of this method to the determination of dansyl amino acids in the acid hydrolyzate of dansylated peptides and proteins is in progress. Its application to the quantitative determination of catecholamines in extract of mouse brain has not been successful so far, but the quantitative determination of histamine as its monodansyl derivative has been successful. The height of the peak of monodansyl-histamine was proportional to the amount of histamine dansylated (1–5 nmole). Analysis of the dansylated histamine fraction from a rat liver extract showed a peak of monodansyl-histamine well separated from the larger preceding peak.

ACKNOWLEDGEMENTS

We thank Dr. T. Inui for supplying the dipeptides, Mr. M. Taneda and Mr. Y. Kamisaki for the preparation of the histamine fraction from rat liver, and Prof. J. L. Gaylor of Cornell University for advice in the preparation of the manuscript. We also thank Japan Electron Optics Laboratory Co. Ltd. and Mitsumi Scientific Industry Co. Ltd. for the loan of equipment. This work was supported in part by a grant from the Tanabe Amino Acid Research Foundation.

REFERENCES

- 1 W. R. Gray and J. F. Smith, *Anal. Biochem.*, 33 (1970) 36.
- 2 N. Seiler, *Methods Biochem. Anal.*, 18 (1970) 259.
- 3 Z. Deyl and J. Rosmus, *J. Chromatogr.*, 69 (1972) 129.
- 4 W. R. Gray, *Methods Enzymol.*, 11 (1967) 139.
- 5 Z. Tamura, T. Nakajima, T. Nakajama, J. J. Pisano and S. Udenfriend, *Anal. Biochem.*, 52 (1973) 595.
- 6 T. Seki and K. Matsumoto, *J. Chromatogr.*, 27 (1967) 423.

CHROM. 7717

COMBINED APPLICATION OF ION-EXCHANGE CHROMATOGRAPHIC METHODS FOR THE STUDY OF "MINOR BASIC AMINO ACIDS"

E. TYIHÁK

Research Institute for Medicinal Plants, Budakalasz (Hungary)

S. FERENCZI, I. HAZAI and S. ZOLTÁN

Chinoin-Nagyteteny, Budapest (Hungary)

and

A. PATTHY

Research Institute for Pharmaceutical Chemistry, Budapest (Hungary)

SUMMARY

A two-dimensional ion-exchange thin-layer chromatographic method is described for the separation of all methylated basic amino acids from biological fluids or protein hydrolysates; development is carried out on Fixion 50-X8 plates, which contain a resin of the Dowex 50-X8 type. An automatic amino acid analyzer was used for quantitative analysis of the minor basic amino acids.

INTRODUCTION

Enzymic methylation of the side-chains of protein molecules after genetic translation yields, among other compounds, N^ε-methylated lysines, guanidino-methylated arginines and imidazole-N-methylated histidines^{1,2}. These methylated basic amino acids are generally found in histones, muscle proteins, cytochrome *c* and brain proteins, but they occur in insignificant amounts; in this respect, these compounds are "minor amino acids". Various methylated basic amino acids also occur free in brain, thymus, plasma and urine^{1,2}; these are probably derived from the hydrolysis of methylated proteins *in vivo*³.

These minor basic amino acids (both in free and bound forms) have important functions in living organisms, *e.g.*, they exert tumour-promoting and retarding effects⁴⁻⁶.

We have found that a combination of ion-exchange chromatographic methods offers a suitable approach to the study of these amino acids.

MATERIALS AND METHODS

Authentic amino acids

The compounds N^ε-monomethyl-DL-lysine hydrochloride (MML), N^ε,N^ε-dimethyl-DL-lysine hydrochloride (DML) and N^ε,N^ε,N^ε-trimethyl-DL-lysine dihy-

drochloride (TML) were prepared by total synthesis^{7,8}; the guanidino-methylated arginines N^G-monomethyl-L-arginine (MMA), N^G,N^G-dimethyl-L-arginine (DMA) and N^G,N^G-dimethyl-L-arginine (DMA') were gifts and partly prepared by synthesis⁹. Other authentic amino acids and their derivatives were obtained from various foreign firms.

Chromatoplates

Most experiments were performed on Fixion 50-X8 (Na⁺) containing Dowex 50-X8 type resin (Chinoin-Nagy-tétény, Budapest, Hungary). Identical results were obtained when Ionex 25 SA (Na⁺) chromatoshets (Macherey, Nagel and Co., Düren, G.F.R.) were used. The plates were equilibrated with sodium citrate buffer (pH 3.28, 0.02 *N* in Na⁺) as previously described¹⁰, and development was carried out with the solvents listed in Table I.

TABLE I

COMPOSITION, PER LITRE, OF DEVELOPING SOLVENTS FOR TLC

Component	Buffer solution		
	A (pH 6.0)	B (pH 5.28)	C (pH 6.0)
Hydrated citric acid, g	100.0	24.6	105.0
Hydrochloric acid (sp. gr. 1.19), ml	14.0	6.5	—
Sodium hydroxide, g	60.0	14.0	60.0
Sodium chloride, g	—	—	58.5
Sodium ions, <i>N</i>	1.5	0.35	2.5

Ninhydrin spray reagent. To prepare this reagent, 0.5 g of ninhydrin and 0.05 g of copper sulphate were dissolved in 100 ml of acetone.

Amino acid analyzer methods

A Japan Electron Optical Ltd. automatic amino acid analyzer (type JLC-5AH) was used; the minimum material requirement of the instrument was less than 1 nmole. The single-column method was used for complete analysis, the temperature of the column being maintained at 40° for 25 min from the beginning of the analysis and then raised to 60°.

When only the methylated lysines were examined, 0.35 *N* citrate buffer was used, with a 10-cm column containing LC-R-1 resin and operated at 25° and pH 6.5; the buffer velocity was about 30 ml/h. For the separation of guanidino-methylated arginines, we used a modification of the method of Kakimoto and Akazawa¹¹; the arginine and its methylated derivatives were eluted from a 55-cm column containing LC-R-1 resin (Mitsubishi Chemical Industries, Japan) with 0.51 *M* sodium chloride in 0.20 *M* sodium citrate buffer of pH 3.25 at a flow-rate of 100 ml/h at 60°.

RESULTS AND DISCUSSION

Table II shows $R_F \times 100$ values for the 30 amino acids so far identified in proteins by the proposed TLC method. The results show that these buffer systems,

TABLE II

$R_F \times 100$ VALUES OF 30 AMINO ACIDS SO FAR IDENTIFIED IN PROTEINS ON FIXION 50-X8 CHROMATOPLATE

Amino acid	Developing buffer		
	A	B	C
Asp	80	79	82
Thr	79	78	80
Ser	80	80	81
Glu	80	79	80
Gly	78	64	79
Ala	72	60	72
Pro	51	49	51
Val	65	61	65
Met	58	50	57
Ile	52	49	52
Leu	53	50	53
Tyr	51	41	50
Phe	54	50	55
Try	10	—	11
Asn	69	—	70
Gln	61	—	60
Cys	77	—	79
(Cys) ₂	60	—	62
HyPro	75	—	78
His	47	16	48
1-MeHis	37	15	36
3-MeHis	26	12	24
Lys	59	25	58
MML	38	19	39
DML	23	16	21
TML	14	12	13
Arg	29	8	28
MMA	21	8	20
DMA	14	9	13
DMA'	15	8	16

chiefly used for the separation of aromatic and basic amino acids, are very suitable for our purpose.

On the basis of the one-dimensional experiments with buffers A, B and C on the Fixion 50-X8 chromatoplates, a two-dimensional ion-exchange method was devised for the separation of all the methylated basic amino acids; the results are shown in Fig. 1. This method offers possibilities for studying minor basic amino acids from several biological fluids and protein hydrolysates. In Fig. 2 is shown the "layer-fingerprinting" of normal human urine with this method. Further, this thin-layer chromatographic method can conveniently be used for detecting aromatic amino acids, *e.g.*, in cases of phenylketonuria.

For the determination of methylated basic amino acids, we used the automatic amino acid analyzer. With this instrument, we could well separate the three guanidino-methylated arginines (MMA, DMA and DMA') from arginine; this is shown in Fig. 3, a chromatogram obtained for normal human urine. It is especially interesting

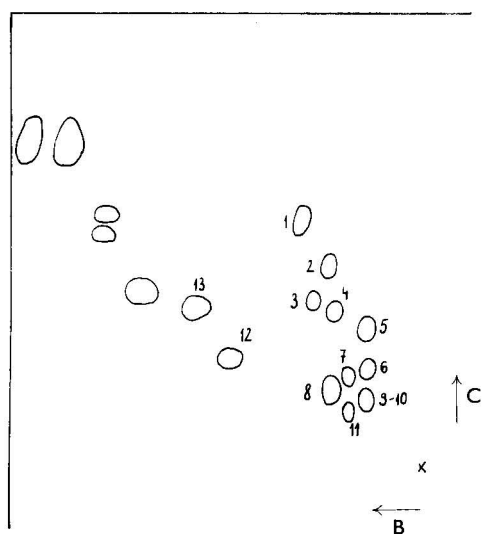


Fig. 1. Two-dimensional separation of aromatic and basic amino acids on a Fixion 50-X8 chromatoplate, with buffer solution B as solvent for the first dimension and buffer C as solvent for the second dimension. 1, Lys; 2, His; 3, MML; 4, 1-MeHis; 5, Arg; 6, MMA; 7, 3-MeHis; 8, DML; 9-10, DMA and DMA'; 11, TML; 12, Phe; 13, Tyr (each 2 μ g).

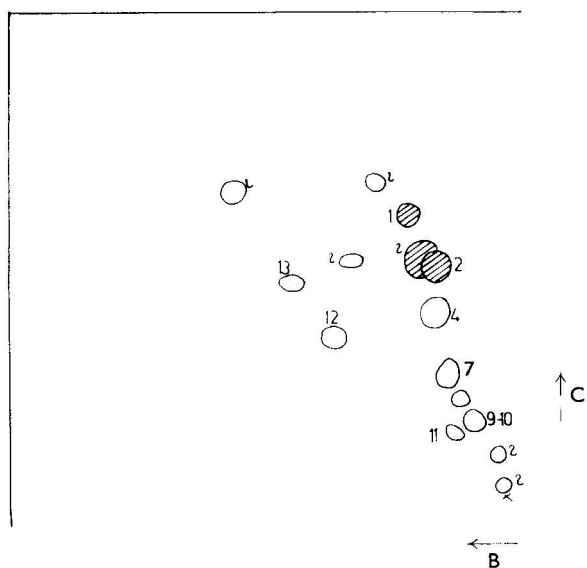


Fig. 2. Two-dimensional separation of aromatic and basic amino acids from normal human urine on a Fixion 50-X8 chromatoplate; conditions and abbreviations as for Fig. 1. The amounts used for analysis corresponded to 0.2 ml of urine after lyophilization and dissolution in methanol-1 *N* HCl (4:1).

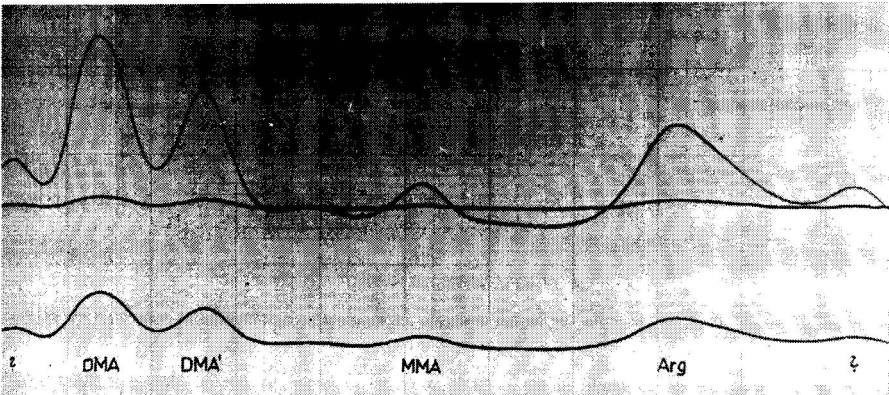


Fig. 3. The separation of guanidino-methylated arginines and arginine from normal human urine on the automatic amino acid analyzer. Retention times: Arg, 325 min; MMA, 275 min; DMA', 235 min; DMA, 215 min.

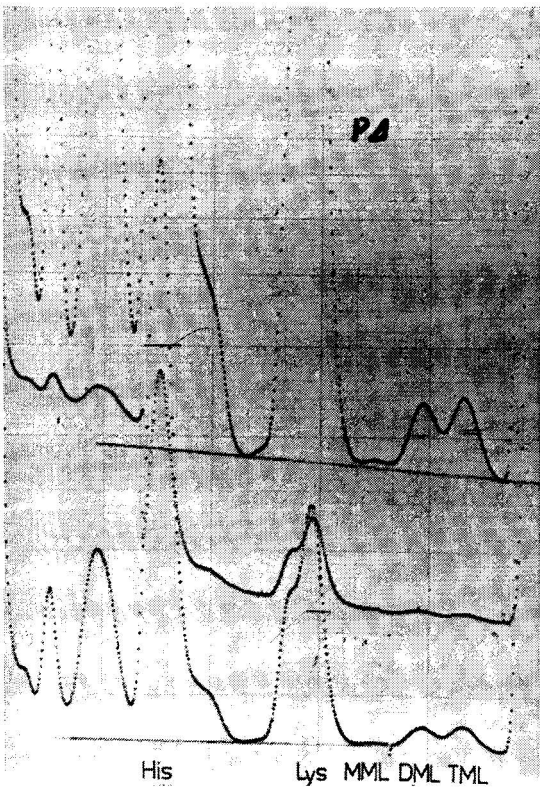


Fig. 4. The separation of N-methylated lysines and lysine from normal human urine on the automatic amino acid analyzer. Retention times: Lys, 75 min; MML, 85 min; DML, 90 min; TML, 95 min.

to note the separation of MMA from arginine; Kakimoto and Akazawa¹¹ could not separate these two amino acids.

In Fig. 4 is shown the separation of N^ε-methylated lysines (MML, DML and TML) from human urine. We have found that only a small amount of MML is present in normal urine.

We have so far not found an analyzer method suitable for the simultaneous separation of all the methylated basic amino acids. However, the proposed ion-exchange TLC method, used in conjunction with an automatic analyzer, achieves this object.

REFERENCES

- 1 W. K. Paik and S. Kim, *Science*, 174 (1971) 114.
- 2 E. Tyihák, *Magy. Kém. Lapja*, 27 (1972) 549.
- 3 V. G. Allfrey, E. Faulkner and A. E. Mirsky, *Proc. Nat. Acad. Sci. U.S.*, 51 (1964) 786.
- 4 B. Szende, E. Tyihák, L. Kopper and K. Lapis, *Neoplasma*, 17 (1970) 433.
- 5 L. Kopper, B. Szende, K. Lapis and E. Tyihák, *Neoplasma*, 18 (1971) 251.
- 6 E. Tyihák and A. Patthy, *Acta Agron. Acad. Sci. Hung.*, 22 (1973) 445.
- 7 J. Puskás and E. Tyihák, *Period. Polytech., Chem. Eng.*, 13 (1969) 261.
- 8 J. Puskás and E. Tyihák, in preparation.
- 9 S. Bajusz and A. Patthy, *Process for the Production of Guanidino-methylated Arginines*, Hung. Pat. GO 1189 (1972).
- 10 T. Dévényi, *Acta Biochim. Biophys. Acad. Sci. Hung.*, 5 (1970) 435.
- 11 Y. Kakimoto and S. Akazawa, *J. Biol. Chem.*, 245 (1970) 5751.

CHROM. 7716A

THE USE OF THE AMPHOTERIC ION-EXCHANGE RESIN RETARDION 11A8 FOR INORGANIC SEPARATIONS

RAJMUND DYBCZYŃSKI and ELŻBIETA STERLIŃSKA

Department of Analytical Chemistry, Institute of Nuclear Research, ul. Dorodna 16, 03-195 Warszawa (Poland)

SUMMARY

The use of the “snake in a cage” amphoteric ion-exchange resin Retardion 11A8 for various separations of inorganic ions was investigated.

Clean separations of Ga(III)–In(III)–Tl(III), Pt(II)–Pd(II), and Na(I)–Ni(II)–Cu(II)–Zn(II) mixtures have been achieved. In acidic media, in which the resin acts mainly as an anion exchanger, some residual activity of the acrylate polyanion seems to exist, resulting in significant changes in distribution coefficients in comparison with standard anion-exchange resins. In the case of elements that can exist as both cations and anions in solution (*e.g.*, Ni, Co, Cu and Zn), the amphoteric properties of Retardion 11A8 permit more specific isolation of certain elements from complex mixtures than would be possible with the use of monofunctional ion exchangers.

INTRODUCTION

Retardion 11A8, which is a “snake in a cage” type of amphoteric ion-exchange resin containing carboxylic and quaternary ammonium exchange groups, was first described in 1957 and has been used since then for the separation of electrolytes from non-electrolytes, desalting of amino acids, etc., by ion retardation^{1–3}. Fractionation of some inorganic salt mixtures using water as the eluent has also been reported¹. The resin has not been used so far for typical radiochemical or analytical separations of inorganic ions, and the investigation of its utility for this purpose was the aim of the present work.

EXPERIMENTAL

Ion-exchange resin

The properties of Retardion 11A8 resin used in this study are summarized in Table I. Methods of grinding, fractionating and microscopic determination of particle size have been described earlier⁴. The resin was conditioned by passing successively 2 *N* sodium hydroxide, water and 2 *N* hydrochloric acid through it and finally washing it with a large excess of water until it was free from chlorides. The total anion-

TABLE I

PROPERTIES OF RETARDION 11A8 RESIN USED IN THIS STUDY

Exchange capacity (mequiv./g dry resin, self-absorbed)			Bed density (g of dry resin, self-absorbed, per ml of bed), d_z	Particle size of fraction used for for column studies
Total	Excess of anion-exchange groups			
	From HCl	From NaCl		
2.95	0.14	0.09	0.420	20 μm $\leq \varnothing \leq$ 45 μm 40 μm $\leq \varnothing \leq$ 60 μm

exchange capacity (milliequivalents per gram of dry resin, self-absorbed) was determined by placing resin with a pre-determined water content in a special centrifuge tube⁵, washing it with 1 *N* hydrochloric acid and then with 0.1 *N* hydrochloric acid, centrifuging at 3000 rpm (*ca.* 900 g) for 15 min, displacing chlorides with 1 *N* sodium hydroxide and titrating them by Volhard's method. The results were corrected for the residual amount of hydrochloric acid retained at the interface of the beads⁵. The exchange capacity due to anion-exchange groups being in excess with respect to carboxylic groups was determined by treating the resin (self-absorbed) with 1 *N* hydrochloric acid or sodium chloride solution, washing with water until free from chlorides, displacing chloride ions with 1 *N* sodium hydroxide and determining them as described above.

The bed density (d_z) refers to the self-absorbed form of the resin in pure water.

Radioactive tracers and reagents

The following radioactive tracers were used: ¹³⁴Cs ($T_{1/2}$ = 2.07 years), ⁷²Ga ($T_{1/2}$ = 14.3 h), ^{114m}In ($T_{1/2}$ = 50 days), ²⁰⁴Tl ($T_{1/2}$ = 3.56 years), ¹⁰⁹Pd ($T_{1/2}$ = 13.5 h), ¹⁹⁷Pt ($T_{1/2}$ = 20 h), ⁶⁵Ni ($T_{1/2}$ = 2.56 h), ⁶⁰Co ($T_{1/2}$ = 5.26 years), ⁶⁴Cu ($T_{1/2}$ = 12.8 h), ⁶⁵Zn ($T_{1/2}$ = 245 days) and ²⁴Na ($T_{1/2}$ = 15.0 h). Most of the isotopes were prepared by neutron irradiation of spectrally pure metals, oxides or nitrates, in the Polish reactor EWA. ¹⁰⁹Pd and ¹⁹⁷Pt tracers were purified from ¹¹¹Ag and ¹⁹⁹Au isotopes, respectively (formed from target material by (n, γ), β^- reactions) by methods described earlier^{6,7}. ¹³⁴Cs and ²⁴Na were prepared by irradiation of the respective chlorides and purified from ³²P when necessary⁸.

In order to obtain trivalent thallium tracer, irradiated TlNO₃ was acidified with hydrochloric acid and chlorine gas was bubbled through the resulting suspension of TlCl until it was completely dissolved.

All reagents were of the highest grade available commercially.

Apparatus and procedure

Distribution coefficients were determined by batch equilibration and column experiments using the techniques described earlier^{4,5,9}. Jacketed glass columns of *ca.* 2 mm I.D. were used and the apparatus for the drop-elution technique was the same as described earlier^{4,5,9}. When necessary, the identity of the elution peaks or of the activity remaining on the resin was checked by γ -ray spectrometry.

RESULTS AND DISCUSSION

Separation of Ga-In-Tl mixtures

Weight-distribution coefficients, λ (amount per gram of dry resin, self-absorbed/amount per millilitre of solution) of Ga, In and Tl on Retardion 11A8 in hydrochloric acid medium are shown in Fig. 1. The differences in the values of the distribution coefficients are sufficiently high to permit the clean separation of Ga-In-Tl mixtures by stepwise elution (Fig. 2). Thallium, which shows high distribution

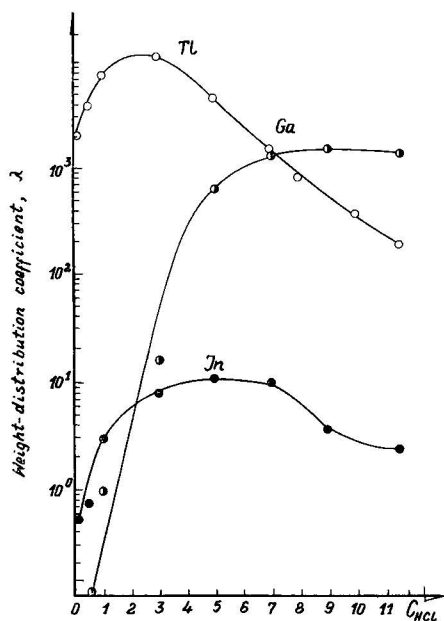


Fig. 1. Weight-distribution coefficients of Ga(III), In(III) and Tl(III) in the system Retardion 11A8-HCl (aq.).

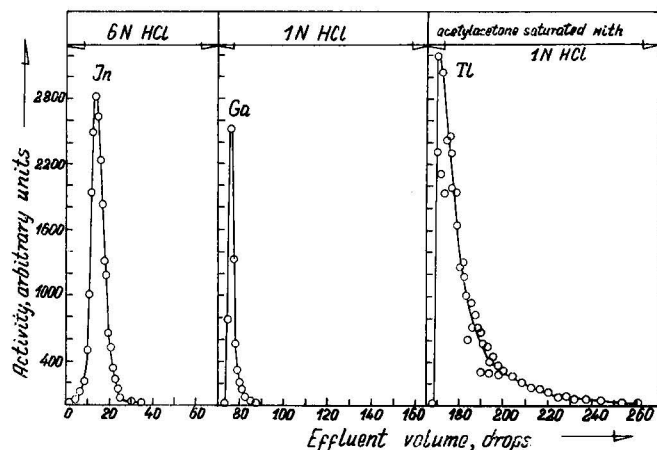


Fig. 2. Separation of In, Ga and Tl. Column: $2.50 \text{ cm} \times 0.0350 \text{ cm}^2$, Retardion 11A8 (20–45 μm). Temperature: 25° . Flow-rate: 2 cm/min.

coefficients over the whole range of hydrochloric acid concentrations, could be quantitatively eluted with acetylacetone saturated with 1 *N* hydrochloric acid. Surprisingly, some other organic solvents which are even more effective in the liquid-liquid extraction of Tl(III), *e.g.*, diethyl ether, failed to elute Tl from the resin.

Comparing the above ion-exchange behaviour with that reported by Kraus *et al.*¹⁰ for group IIIB elements on Dowex 1-X10 resin in hydrochloric acid medium, both similarities and differences in the general character of the $\log \lambda - C_{\text{HCl}}$ curves were observed. The curve for Tl on Retardion 11A8 has a distinct maximum at $C_{\text{HCl}} \approx 2.5$ (*cf.*, Fig. 1), which is absent when Dowex 1-X10 resin is used and the maximum values of λ_{Ga} are lower than those for Dowex 1-X10 by more than two orders of magnitude¹⁰. The inversion in selectivity between Tl and Ga occurs at $C_{\text{HCl}} \approx 4.5$ for Dowex 1-X10 and at $C_{\text{HCl}} \approx 8$ for Retardion 11A8. It is difficult to state unambiguously at present whether the presence of acrylate polyanions or merely the lower nominal degree of cross-linking (Retardion 11A8 is made from Dowex 1-X8 resin¹¹) are the reasons for these differences. There is no doubt, however, that much better separations of Ga-In-Tl mixtures can be obtained with this resin (*cf.*, Fig. 2) than those reported¹⁰ for Dowex 1-X10.

Separation of the pair Pt-Pd

Weight-distribution coefficients of these elements are shown in Fig. 3. It seemed feasible to elute Pd first with hydrochloric acid and then Pt with another suitable

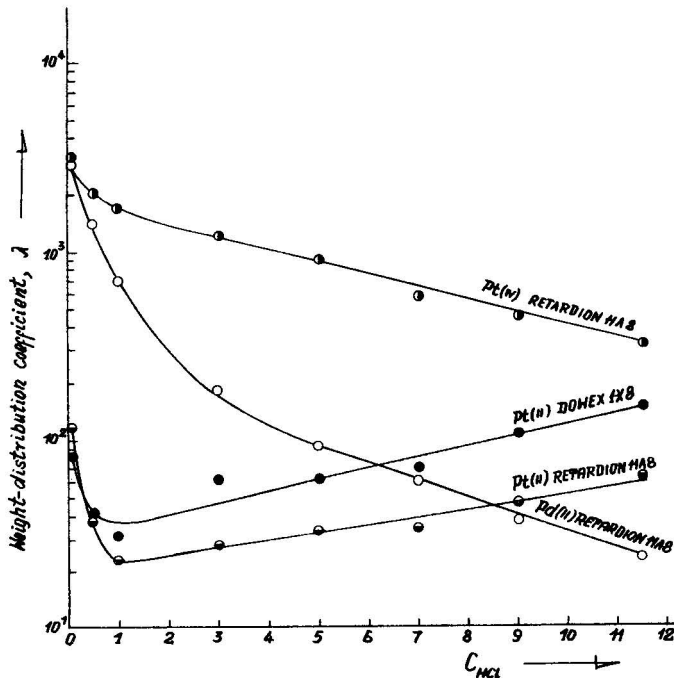


Fig. 3. Weight-distribution coefficients of Pt(IV) (after oxidation with aqua regia), Pt(II) (after reduction with $\text{N}_2\text{H}_4 \cdot \text{HCl}$) and Pd(II) in the systems Retardion 11A8-HCl and Dowex 1-X8-HCl(aq.).

eluent. Unexpectedly, however, it was found that some of the platinum was eluted in a reproducible manner with a distribution coefficient exceeding only slightly that of Pd, while the remainder (*ca.* 50%) remained firmly on the column. Moreover, elution of Pd with hydrochloric acid is a lengthy procedure owing to its relatively high distribution coefficient.

Addition of hydrazinium hydrochloride reduced Pt to the divalent state, which resulted in a considerable decrease in its distribution coefficient. Platinum was then eluted first and could be separated from Pd on a very short column (*cf.*, Fig. 4).

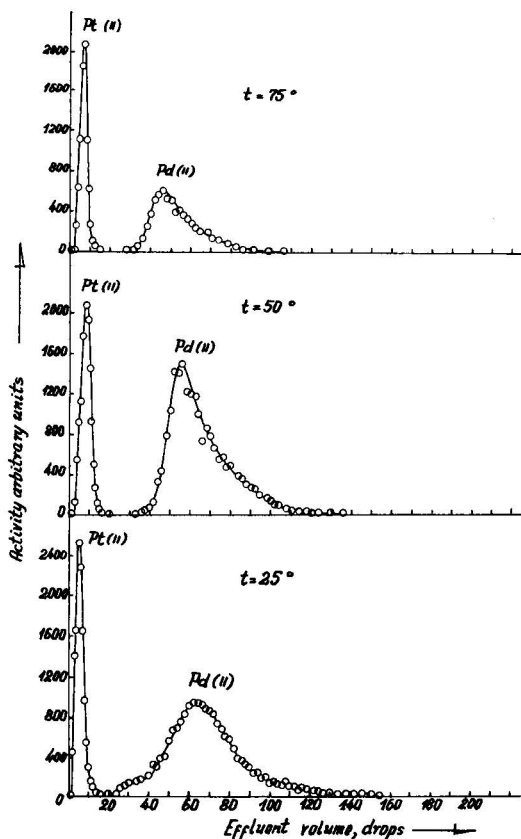


Fig. 4. Effect of temperature on the separation of Pt(II) and Pd(II). Column: 1.0 cm \times 0.0305 cm², Retardion 11A8 (20–45 μ m). Eluent: 3.4 N HCl. Flow-rate: 2 cm/min.

The effect of temperature on this separation was investigated by repeating the runs at 25, 50 and 75°. Separation factors, $\alpha_{\text{Pt}}^{\text{Pd}}$, were calculated from the elution curves by the equation

$$\alpha_{\text{Pt}}^{\text{Pd}} = \frac{U_{\text{max. (Pd)}} - (U_0 + V)}{U_{\text{max. (Pt)}} - (U_0 + V)} \quad (1)$$

where $U_{\text{max. (Pd)}}$ and $U_{\text{max. (Pt)}}$ are the retention volumes (ml) of the two elements in question, U_0 is the dead volume of the column and V is the free volume of the resin

bed. U_0 and $V = i \cdot V_b$ (where i is the fractional free volume of the bed and V_b is the bed volume) were determined from separate experiments in which a non-adsorbable tracer (^{134}Cs) was eluted from the same column having two different resin bed lengths, and calculated as described earlier^{4,12}. Mathematical analysis of the results confirmed the assumption that in the system Retardion 11A8-hydrochloric acid λ_{Cs} is approximately zero. Plate heights, H , were calculated from the relationship¹³

$$H = \frac{L \cdot W^2}{8 (U_{\text{max.}} - U_0)^2} = \frac{L \cdot \sigma^2}{(U_{\text{max.}} - U_0)^2} \quad (2)$$

where

L = length of the resin bed;

W = width of the peak for the $M = M_{\text{max.}}/e = 0.368 M_{\text{max.}}$ ordinate;

$\sigma = W/2\sqrt{2}$ = standard deviation of the chromatographic peak.

The resolution of the Pt-Pd pair, $R_3^{\text{Pt-Pd}}$, was calculated from the equation¹³

$$R_3^{\text{Pt-Pd}} = \frac{U_{\text{max. (Pd)}} - U_{\text{max. (Pt)}}}{3 (\sigma_{\text{Pt}} + \sigma_{\text{Pd}})} \quad (3)$$

The results are summarized in Table II.

TABLE II

EFFECT OF TEMPERATURE ON THE SEPARATION OF Pt-Pd IN THE SYSTEM: RETARDION 11A8-HCl + $\text{N}_2\text{H}_4 \cdot \text{HCl}$

Temperature (°C)	H_{Pt} (cm)	H_{Pd} (cm)	$\alpha_{\text{Pt}}^{\text{Pd}}$	$R_3^{\text{Pt-Pd}}$
25	3.05	0.06	63.2	1.15
50	0.47	0.04	15.1	1.26
75	0.49	0.05	17.4	1.15

Although very short columns had to be used in order to complete the elution of the Pd band in a reasonable time and therefore the results calculated from the Pt peak may be inaccurate, some conclusions are straightforward. An increase in temperature up to 50° has a favourable effect on the separation owing to a decrease in plate height, despite a simultaneous decrease in the separation factor. A further increase in temperature is undesirable. For practical purposes, however, it was preferred to use longer columns at room temperature and to elute the Pd with a 1% thiourea solution as a sharp band (*cf.*, Fig. 5). In another experiment, 5 mg of Pt were similarly separated from trace amounts of Pd.

It is interesting to note (see Fig. 3) that the $\log \lambda\text{-C}_{\text{HCl}}$ curve for Pt(II) on Retardion 11A8 is distinctly lower than the corresponding curve determined for Dowex 1-X8.

The apparent decrease in distribution coefficients, especially at higher hydrochloric acid concentrations, is larger than expected on the basis of differences in exchange capacity alone, if direct proportionality between distribution coefficients and exchange capacity is assumed. It would seem, therefore, that the presence of polyacrylate in the resin phase decreases the bond strength between the metal chloro-complex and the quaternary ammonium functional group.

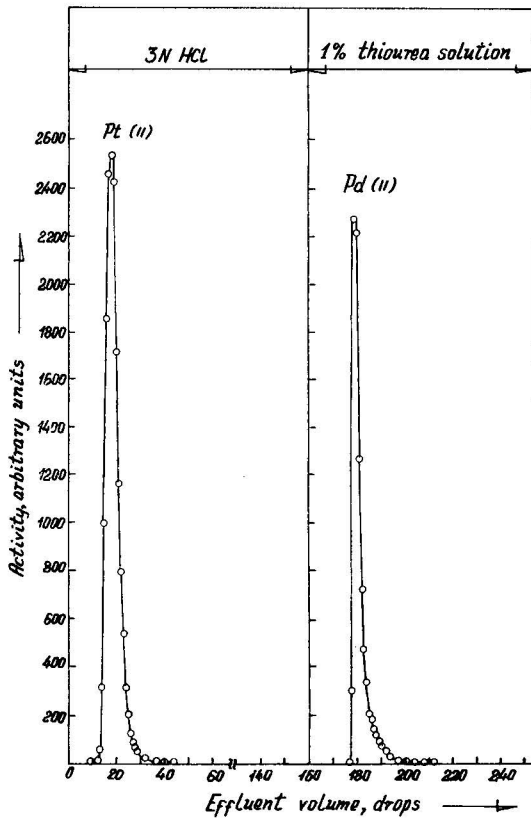


Fig. 5. Separation of Pt(II) (0.52 mg) and Pd(II) (0.0015 mg) by stepwise elution. Column: 4.30 cm \times 0.0305 cm², Retardion 11A8 (20–45 μ m). Temperature: 25°. Flow-rate: 2 cm/min.

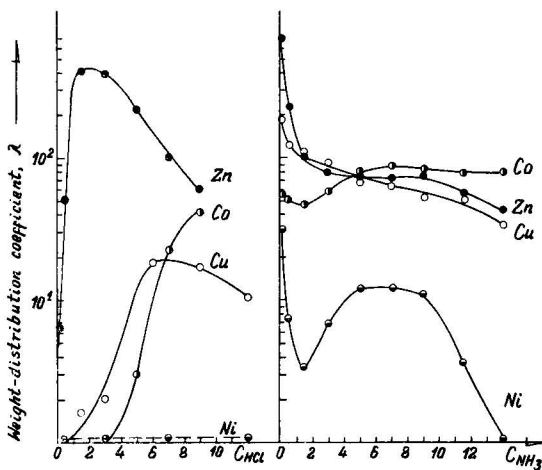


Fig. 6. Weight-distribution coefficients of Ni(II), Cu(II), Co(II) and Zn(II) in the systems Retardion 11A8–HCl (aq.) and Retardion 11A8–NH₃(aq.).

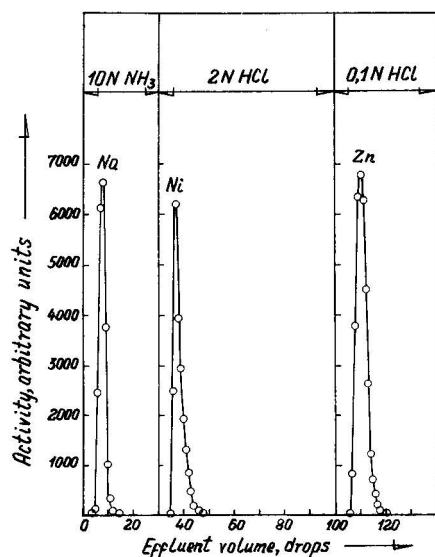


Fig. 7. Separation of Na, Ni and Zn. Column: $5.0 \text{ cm} \times 0.0306 \text{ cm}^2$, Retardion 11A8 (40–60 μm). Temperature: 25° . Flow-rate: 0.80 cm/min.

Separation of Na, Ni, Cu and Zn

In the separations discussed above, Retardion 11A8 acted mainly as an anion exchanger, although some influence of the acrylate polyanion on the distribution coefficients of metal chloride complexes and probably also on the elution behaviour seems to exist. In the case of metals that can form both cationic ammine complexes and anionic chloride complexes¹⁴, the amphoteric properties of the resin can be fully demonstrated.

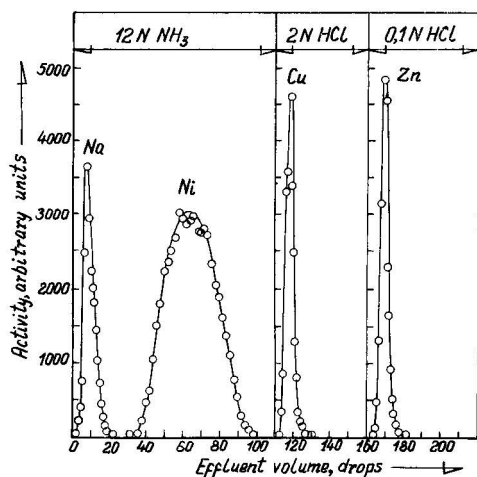


Fig. 8. Separation of Na, Ni, Cu and Zn. Column: $5.0 \text{ cm} \times 0.0324 \text{ cm}^2$, Retardion 11A8 (40–60 μm). Temperature: 25° . Flow-rate: 0.90 cm/min.

Weight-distribution coefficients of Ni, Zn, Cu and Co on Retardion 11A8 in both hydrochloric acid and ammonia solution are shown in Fig. 6. Two separations demonstrating the flexibility of the system are presented in Figs. 7 and 8.

Nickel, which cannot be separated from alkali metals on anion-exchange resins in hydrochloric acid medium, can be taken up here as a cation while sodium passes through, and is subsequently eluted with either hydrochloric acid or ammonia solution. It is interesting to note that elements such as Zn, which have a high affinity to the resin in both the cationic and anionic forms over almost the whole concentration range, can withstand the change in eluent from basic to acidic without any detectable leakage. Such behaviour may be the basis for selective isolation of certain elements from mixtures in a much more specific way than when making use of standard resins with only one type of functional group (cationic or anionic).

CONCLUSIONS

The results clearly show that Retardion 11A8 can be very useful in radio-chemical and analytical separations. In acidic media, in which the resin acts mainly as an anion exchanger, some residual effect of the polyacrylate in the resin phase seems to exist, resulting in changes in both the distribution coefficients and in the shape of the $\log \lambda_{\text{HCl}}-C_{\text{HCl}}$ plot in comparison with standard anion-exchange resins.

The amphoteric properties of the resin can be effectively exploited towards elements that can exist both as cations and as anions in solution, depending on the ligands present, pH, etc. It is hoped that in some instances more specific isolation of certain inorganic ions (*e.g.*, those which show amphoteric properties) from complex mixtures can be achieved than that attainable with monofunctional ion exchangers. Further work is needed in order to demonstrate all the possibilities that may be offered by this resin in various inorganic separations.

ACKNOWLEDGEMENT

The authors thank Mrs A. Kolyga for skilful technical assistance.

REFERENCES

- 1 M. J. Hatch, J. A. Dillon and H. B. Smith, *Ind. Eng. Chem.*, 49 (1957) 1812.
- 2 F. Wolf and H. Mlytz, *J. Chromatogr.*, 34 (1968) 59.
- 3 C. Rollins, L. Jensen and A. N. Schwarz, *Anal. Chem.*, 34 (1968) 711.
- 4 R. Dybczyński, Institute of Nuclear Research, Warsaw, Report No. 1115 (VIII) C, 1969.
- 5 R. Dybczyński, *J. Chromatogr.*, 50 (1970) 487.
- 6 H. Maleszewska and R. Dybczyński, *Radiochem. Radioanal. Lett.*, 6, No. 1 (1971) 7.
- 7 R. Dybczyński and H. Maleszewska, *Analyst (London)*, 94 (1969) 527.
- 8 A. Sterliński and R. Dybczyński, *Nukleonika*, 11 (1966) 533.
- 9 R. Dybczyński, *J. Chromatogr.*, 71 (1972) 507.
- 10 K. A. Kraus, F. Nelson and G. W. Smith, *J. Phys. Chem.*, 58 (1954) 11.
- 11 Bio-Rad Laboratories, Richmond, Calif., U.S.A., *Catalogue Y*, 1973.
- 12 J. Minczewski, J. Chwastowska and R. Dybczyński, *Analiza Śladowa Metody Rozdzielania i Zagęszczania*, WNT, Warsaw, 1973.
- 13 R. Dybczyński, *J. Chromatogr.*, 31 (1967) 155.
- 14 J. Bjerrum, G. Schwarzenbach and L. G. Sillen, *Stability Constants*, The Chemical Society, London, 1957.

CHROM. 7957

SEPARATION OF METAL IONS BY MIXED COLUMN ION-EXCHANGE CHROMATOGRAPHY

TAKEO YAMABE and TETSU HAYASHI

Institute of Industrial Science, University of Tokyo, Roppongi 7-chome, Minato-ku, Tokyo (Japan)

SUMMARY

The separation of metal ions with organic hydroxy acids at a definite pH was carried out by changing the mixing ratio (γ) of the cation- and anion-exchange resins. By using 0.25 *M* tartaric acid, the best separation of alkaline earth metals was obtained at pH 4.1 and $\gamma = 2$. The effect of γ on the separability is discussed by considering the equation for the distribution ratio in a mixed column.

INTRODUCTION

Although mixed bed deionization is commonly used to prepare water of high purity, it had not been employed in separations by ion-exchange chromatography until we used a mixed column that contained both cation- and anion-exchange resins in 1964¹. At first, we carried out the separation of metal ions on mixed columns with hydrochloric acid. In this process, however, we had only limited success with the separation of some heavy metal ions². We then tried to use organic hydroxy acids as eluents, and we had great success by selecting a definite pH and by changing the mixing ratio (γ) of the cation- and anion-exchange resins³⁻⁵. In this paper, we report the separation of alkaline earth metal ions, and discuss the effect of γ on the separability by considering the equation for the distribution ratio in a mixed column.

EXPERIMENTAL

Preparation of mixed column

The cation- and anion-exchange resins used were strongly acidic and strongly basic (Diaion SK and SA, $<25\ \mu\text{m}$, respectively) and were conditioned with hydrochloric acid and sodium hydroxide solution in the usual manner. After conditioning, appropriate amounts of the resins were mixed in a concentrated electrolyte solution, such as 20% sodium chloride solution, so as to avoid violent aggregation in pure water³.

Column operation and determination of metal ions

The total amount of the resins in the column was about 4 ml and the height of the resin in the 5-mm I.D. column was 200 mm. A 0.5-ml volume of *ca.* 10^{-3} *M* sample solution was added to the upper part of the column with a microsyringe and

then developed with an eluent consisting of a mixture of an organic hydroxy acid and sodium chloride at a definite pH adjusted with sodium hydroxide solution at a flow-rate of 60 ml/h (ref. 3).

The concentration of each metal ion was determined continuously by coulometry with a Hitachi Coulometric Monitor, Type 030. The principle of this instrument involves the coulometry of mercury or copper ions isolated by the reaction of metal ions with the EDTA complex of mercury or copper, and therefore the identification of a peak is achieved by comparison with the elution of a single metal ion.

RESULTS

Fig. 1 shows typical elution curves of metal ions with a definite pH and various mixing ratios (γ) of cation- and anion-exchange resins.

As shown by Hayashi and Yamabe⁴, for the separation of the yttrium group of rare earth elements, the best result was obtained with an eluent consisting of 0.50 *M* lactic acid and 0.06 *M* sodium chloride at pH 2.8 and $\gamma = 85/15$.

As shown in Fig. 1, for the separation of alkaline earth metals, the best result was obtained with an eluent consisting of 0.25 *M* tartaric acid, 0.07 *M* sodium chloride at pH 4.1 and $\gamma = 2$. Four metals (calcium, magnesium, strontium and barium) were almost separated within 90 min.

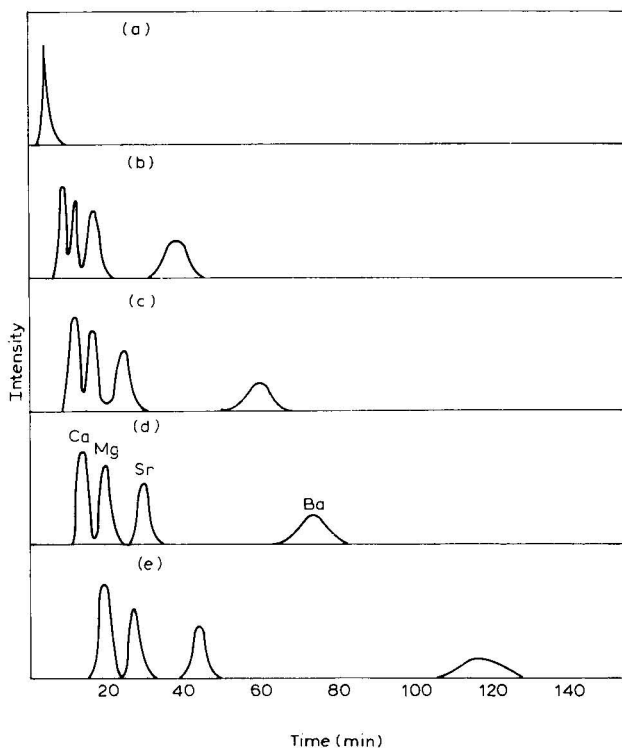


Fig. 1. Separation of alkaline earth metal ions with tartaric acid at pH 4.1 using mixed columns with Diaion SK:Diaion SA ratios of (a) 0:1; (b) 1:2; (c) 1:1; (d) 2:1; and (e) 1:0.

THEORETICAL

In ion-exchange chromatography, the following equation is obtained:

$$V_e = V_0 + K_d^M \cdot V_R \quad (1)$$

where V_e is the elution volume and V_0 the volume of the mobile phase, V_R the resin volume and K_d^M the distribution ratio in the mixed column. K_d^M can be defined as

$$K_d^M = \frac{V_R^+ \cdot K_d^+ + V_R^- \cdot K_d^-}{V_R} \quad (2)$$

where the distribution ratios for the cations and anions are K_d^+ and K_d^- and the volumes of the cation- and anion-exchange resins are V_R^+ and V_R^- , respectively.

If the equilibrium in the process forming a complex between a metal ion M^{3+} (for example, a rare earth metal ion) and Y^- (for example, lactate ion) is assumed to be



then the stability constant, K_c is given by

$$K_c = \frac{[MY_6^{3-}]}{[M^{3+}][Y^-]^6} \quad (4)$$

If the dissociation constant of lactic acid is K_a , then $[Y^-]$ is

$$\begin{aligned} [Y^-] &= C_Y \cdot \frac{K_a}{K_a + [H^+]} \\ &\doteq C_Y \cdot \frac{K_a}{[H^+]} \quad (\text{if } [H^+] \gg K_a) \end{aligned} \quad (5)$$

where C_Y is the total concentration of lactic acid. Therefore, if $K_c [Y^-]^6 \gg 1$, then

$$\begin{aligned} K_d^+ &= \frac{[M^{3+}]}{C_M} \cdot K_d^{0+} (M^{3+}) \\ &= \frac{1}{1 + K_c [Y^-]^6} \cdot K_d^{0+} (M^{3+}) \\ &\doteq \frac{K_d^{0+} (M^{3+})}{K_c [Y^-]^6} \end{aligned} \quad (6)$$

$$\begin{aligned} K_d^- &= \frac{[MY_6^{3-}]}{C_M} \cdot K_d^{0-} (MY_6^{3-}) \\ &\doteq K_d^{0-} (MY_6^{3-}) \quad (K_c [Y^-]^6 \gg 1) \end{aligned} \quad (7)$$

where C_M is the total concentration of metal, and K_d^{0+} and K_d^{0-} the values when only M^{3+} or MY_6^{3-} exists in the solution. Then, K_d^M is given by

$$\begin{aligned}
 K_d^M &= K_d^+ - \frac{1}{V_R} \cdot (K_d^+ - K_d^-) V_R^- \\
 &= \frac{K_d^0 + (M^{3+})}{K_c [Y^-]^6} - \frac{1}{V_R} \left(\frac{K_d^0 + (M^{3+})}{K_c [Y^-]^6} - K_d^0 - (MY_6^{3-}) \right) \cdot V_R^- \quad (8)
 \end{aligned}$$

DISCUSSION

It is considered that the best separability is obtained with the shortest elution time under the conditions of complete separation. We will discuss the separability from the point of view of the relationship between elution time or K_d^M and the various factors.

First, we can consider the effect of pH on elution time. From eqn. 5, an increase in pH causes a large increase in $[Y^-]$ and therefore a large decrease in K_d^+ . As shown earlier³, the yttrium group of rare earths is completely separated at pH 2.8 in a single column of cation-exchange resin, but gadolinium shows considerable tailing. If we adopt a pH value of 3.0, lutetium, thulium, erbium, holmium and dysprosium show mutual interference, because an increase in pH decreases considerably K_d^+ or the elution time to similar extents for all metals⁴.

For the increase in V_R^- , we must consider the difference in the K_c values of the metals in eqn. 8.

In the case of rare earth and alkaline earth metals, K_d^+ is usually larger than K_d^- and the elution behaviour resulting from an increase in V_R^- is similar to that resulting from an increase in pH. However, as shown in Fig. 1, the decrease in elution time in the case of metals of smaller K_d such as calcium, is less than that of a metal of larger K_d such as barium. Therefore, at $\gamma = 2$, complete separation is obtained because an appropriate decrease in elution time is obtained for all metals. From eqn. 7, if $K_d^0 - (MY_6^{3-})$ is almost equal for rare earth and alkaline earth metals, the peak position in the single column of anion-exchange resin occurs at almost the same position for all metals, as shown in Fig. 1, but from the above discussion it is obvious that the anion-exchange resin in the mixed column does not act as a diluent.

In conclusion, the effects of the mixing ratio on the elution behaviour of metal ions are different from the effect of pH or a simple decrease in the content of cation-exchange resin, and therefore we can expect to obtain the best separability by using mixed columns with appropriate mixing ratios.

REFERENCES

- 1 T. Yamabe and K. Honda, *Seisan-Kenkyu*, 16 (1964) 316.
- 2 T. Yamabe, *Seisan-Kenkyu*, 24 (1972) 431.
- 3 T. Yamabe and T. Hayashi, *J. Chromatogr.*, 76 (1973) 213.
- 4 T. Hayashi and T. Yamabe, *J. Chromatogr.*, 87 (1973) 227.
- 5 T. Yamabe, *J. Chromatogr.*, 83 (1973) 59.

CHROM. 7716

ÉCHANGE D'ANIONS DES ÉLÉMENTS SUR UNE RÉSINE ÉCHANGEUSE ANIONIQUE DE FAIBLE BASICITÉ EN MILIEU DE L'ACIDE BROMHYDRIQUE

LUDMIŁA WÓDKIEWICZ et RAJMUND DYBCZYŃSKI

Département de Chimie Analytique, Institut de Recherches Nucléaires, Varsovie (Pologne)

SUMMARY

Anion-exchange behaviour of some elements on a weakly basic anion exchanger in hydrobromic acid medium

The adsorbability of several elements has been studied in the system weakly basic anion exchange resin Amberlite IRA-68 (Br^-)-HBr + Br_2 . Distribution coefficients of more than 30 elements were determined by batch equilibration in the HBr concentration range 0.01–12 M. In most instances the distribution coefficients increase with increase in acid concentration. Some elements, such as Cu, Co, Fe, Mn, In, Ga and U, are adsorbed only at acid concentrations greater than 4 M. Pt, Hg, Ag and, to a somewhat smaller extent, Au, Tl and Re, show high distribution coefficients in dilute HBr solution. In general, the adsorbabilities of elements on Amberlite IRA-68 in the bromide system are lower than the adsorbabilities in an analogous system with strongly basic Dowex 1 resin. The observed differences in distribution coefficients are high enough for some interesting separations to be obtained. The possibility of column separations of several mixtures, such as Eu-U, Zn-Cd-Hg and Cu-Ag-Au, was demonstrated. The influence of temperature on the separation of the latter mixture was studied and the most important chromatographic parameters (distribution coefficients, separation factors, resolutions and plate heights) were calculated.

INTRODUCTION

Contrairement aux résines échangeuses d'anions fortement basiques, les échangeurs d'anions faiblement basiques ont été généralement peu utilisées à la séparation des éléments minéraux en chimie analytique et en radiochimie. Des résultats intéressants ont été obtenus par des chercheurs japonais^{1,2} qui ont étudié l'adsorption en milieu HCl et H_2SO_4 de certains éléments sur une résine anionique à structure de condensation (Amberlite CG-4B). La séparation de certains éléments a été également effectuée sur un échangeur de cellulose faiblement basique^{3,4}. Dans le présent travail, on étudie les échanges d'anions d'une série d'éléments dans un système de la résine échangeuse anionique de polymérisation de faible basicité Amberlite IRA-68-solution aqueuse de HBr.

PARTIE EXPÉRIMENTALE

Résine

Une résine d'anions faiblement basique était utilisée: Amberlite IRA-68 (fabriquée par Rohm & Haas, Philadelphia, Pa., États-Unis) à structure polyacrylique réticulée, hautement poreuse et possédant les groupements fonctionnels $-N(R_2)$, avec granulométrie $2\text{ mm} > \varnothing > 0.33\text{ mm}$ (sur le produit commercial) et $0.08\text{ mm} > \varnothing > 0.06\text{ mm}$ (sur le produit broyé).

Le conditionnement préalable et l'obtention de la fraction granulométrique voulue ont été décrits précédemment⁵. La capacité d'échange, Z_c , déterminée par la méthode décrite⁶, est de 5.06 méquiv./g de la résine sèche (Br^-). Il a été constaté que plusieurs cycles d'utilisation et de régénération de la résine diminuent faiblement la capacité d'échange. La densité du lit est 0.27 g de la résine sèche par 1 cm³ de lit.

Indicateurs radioactifs

Les radioisotopes ont été obtenus par irradiation par neutrons thermiques, dans un réacteur des nitrates ou des oxydes des métaux étudiés.

Solution étalon

Pour les éléments ne possédant pas de radioisotopes utilisables (U, Pb, V), on emploie les solutions de bromures.

Appareillage

Il comprend une colonne en verre de diamètre 0.2 cm, hauteur 15 cm, entourée d'une double enveloppe de verre, thermostatée. L'élément étudié est distribué par une burette sous pression. L'autre appareillage était un collecteur des fractions (Unipan 206B), un compteur de Geiger-Müller, un compteur de scintillation de puits $1 \times 1\text{ in. NaI (TI)}$, un analyseur d'amplitude à 4000 canaux DIDAC muni d'un détecteur Ge/Li, et un spectrophotomètre Specol.

Méthodes analytiques

On mesure l'activité des échantillons marqués. Quant aux échantillons inactifs ils sont analysés de la manière suivante:

l'U(VI): par la méthode spectrophotométrique (peroxydique)⁷;

le V(V): par spectrophotométrie à l'aide de BFHA (N-benzoylphenylhydroxylamine)⁸;

le Pb: par volumétrie à l'EDTA⁹.

Détermination des coefficients de partage

Le coefficient de partage de masse, λ (mole par gram de la résine sèche (Br^-)/mole de la solution) est déterminé par la méthode d'équilibre comme on a publié précédemment^{5,10,11}. Le coefficient de partage plus bas est déterminé par la méthode de colonne^{12,13}.

TABLEAU I

COEFFICIENTS DE PARTAGE DES ÉLÉMENTS DANS LE SYSTÈME RÉSINE ANIONIQUE FAIBLEMENT BASIQUE AMBERLITE IRA-68 (Br⁻)-HBr(aq.)

Elément	$c_{\text{HBr}} (M)$								
	0.01	0.05	0.1	0.5	1.0	4.0	6.8	10	12
Pt(IV)	10 000	4100	3800	1600		147	130		150
Hg(II)	5 500	4100	3800	1600	570	110	27	23	24
Ag(I)	5 000	3680		640	200	16	7	3.8	3
Au(III)		450	200	138	131	67	46	49	47
Tl(III)			1002	474	287	118	87	69	
Re(VII)	464		142	32		9	6.5		
Ir(IV)	287		128		128		22	13	17
W(VI)	300*	340*	280*		150	115	90		25
Mo(VI)	107*	80*	42*	19	4	11	32		77
Nb(V)	71*	105*	37*	7*		13	35	56	82
Sn(IV)	26*	44*	60*	70		91	96	99	117
Hf(IV)	28*		28*		15*	0.5	1	1.5	18
Zr(IV)	35*	12*	2*	5*	5	12	13		77
Pb(II)	24	23	39	59	37	14	18	23	
Ga(III)	0	0	0	2.6	0.9	4	35	46	118
Cd(II)	27		33	40	25	20	16	22	17
Zn(II)	0	0	0	0	1.1	42	35	35	32
U(VI)	0	0	0	0	1	14	32	48	67
Sb(V)	2.4*	0.8*		1	6	10	8.6		10.2
In(III)	0	0	0	0	5	18	27	46	
Tm(III)	0	0	1	1	1	5	7	11	24
V(IV)	0	0	0	0	1.8	1.9	1.8	1.9	2.4
Mn(II)	0	0	0	0	0	0	1.8	2.8	17
Fe(III)	0	0	0	0	0	0	3.1	22	17
Co(II)	0	0	0	0	0	0	0	20	25
Cr(III)	0	0	0.9	1.4	1.2	1	1.7	2	1.6
Cu(II)	0	0	0	1.3	1.5	1.5	2.5	6	8
Cs(I)	0	0	0	0	0	0	0	0	0
Ca(II)	0	0	0	0	0	0	0	0	0

* Les résultats ne sont pas reproductibles à cause de l'hydrolyse.

RÉSULTATS

Le Tableau I rassemble les résultats des déterminations pondérales des coefficients de partage entre une résine anionique faiblement basique et une solution aqueuse de HBr dans un domaine de concentration de 0.01–12 *M*. Pour les éléments ne s'adsorbant pas sur la résine dans ce domaine de concentration de HBr, on indique $\lambda = 0$. En se basant sur les résultats obtenus, on procède à une série de séparations radiochimiques. Des exemples pratiques d'utilisation de l'Amberlite IRA-68 pour la séparation sont montrés sur les Figs. 1, 2 et 3. La Fig. 4 montre l'influence de la température sur le processus de séparation d'une solution de Cu, Ag et Au à 25, 50 et 75°.

Le facteur de séparation d'une solution $\alpha_1^2 = \lambda_2/\lambda_1$, est calculé à partir des courbes d'élution. De même: l'hauteur du plateau théorique

$$H = \frac{L}{N} = \frac{L \sigma}{(V_{\text{max.}} - V_0)}$$

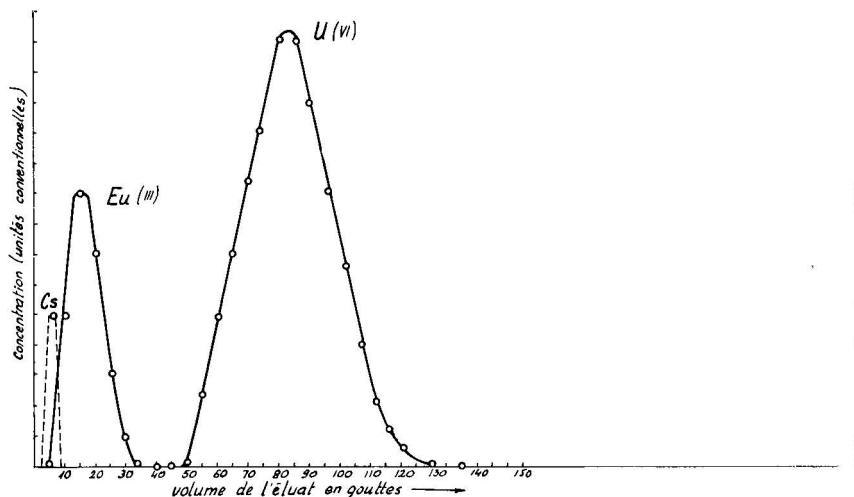


Fig. 1. Séparation de l'euprimum(III) avec l'uranium(VI). Amberlite IRA-68 (Br^-), $20\ \mu\text{m} \leq \varnothing \leq 80\ \mu\text{m}$; colonne, $6\ \text{cm} \times 0.031\ \text{cm}^2$. Éluant: $6.8\ \text{M HBr} + 0.004\ \text{M Br}_2$. Vitesse d'élution: $0.6\ \text{cm/min}$.

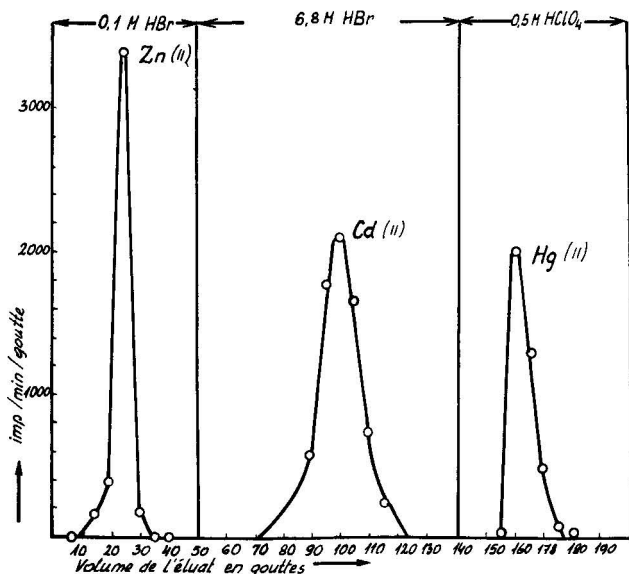


Fig. 2. Courbe d'élution du Cd(II) , Zn(II) et Hg(II) . Amberlite IRA-68 (Br^-), $20\ \mu\text{m} \leq \varnothing \leq 80\ \mu\text{m}$; colonne, $6\ \text{cm} \times 0.031\ \text{cm}^2$. Éluant: $0.1\ \text{M HBr}$, $6.8\ \text{M HBr}$ et $0.5\ \text{M HClO}_4$. Vitesse d'élution: $0.65\ \text{cm/min}$.

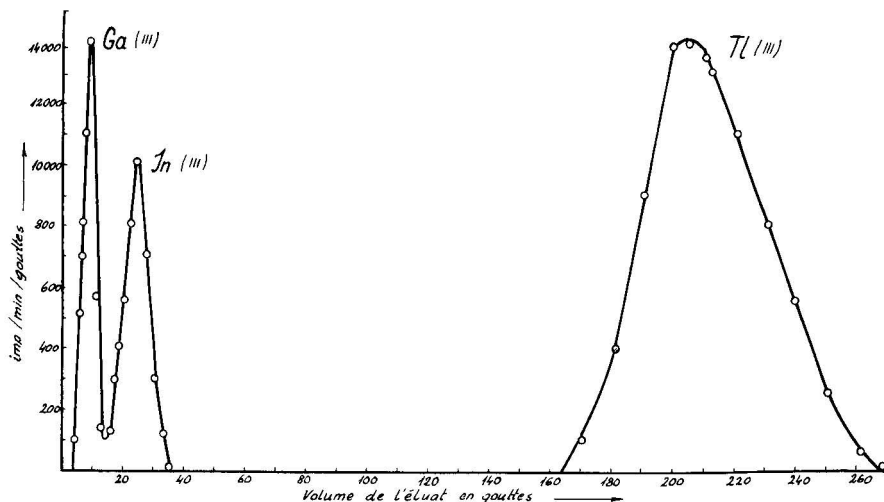


Fig. 3. Courbe d'élution du Ga(III), In(III) et Tl(III). Amberlite IRA-68 (Br^-), $20 \mu\text{m} \leq \varnothing \leq 80 \mu\text{m}$; colonne, $6 \text{ cm} \times 0.031 \text{ cm}^2$. Éluant: 4 M HBr . Vitesse d'élution: 0.6 cm/min .

où

- L = hauteur de la colonne de résine;
- N = nombre des plateaux théoriques;
- V_{max} = volume de la rétention;
- V_0 = volume mort de la colonne;
- σ = écart type d'un pic donné.

La résolution des pics, R_3 , est

$$R_3 = \frac{U_{\text{max.}(1)} - U_{\text{max.}(2)}}{3(\sigma_1 - \sigma_2)}$$

Les valeurs numériques de ces paramètres sont indiquées sur la Fig. 4. La Fig. 5 montre les variations du facteur de séparation et de la résolution en fonction de la température. Cette figure montre également la hauteur du plateau théorique normalisé pour une valeur donnée du coefficient de partage volumique λ' .

DISCUSSION

D'après les résultats rassemblés dans le Tableau I on peut classer les éléments étudiés en quatre groupes quant à leur propriété d'échange d'anions dans le système étudié:

- (1) Les éléments non absorbés par la résine dans tout le domaine de concentration en HBr. Ces éléments appartiennent aux IA et IIA de la classification périodique.
- (2) Les éléments dont les coefficients de partage augmentent avec la concentration en HBr. Cependant λ reste zéro pour les concentrations inférieures à 1 M .

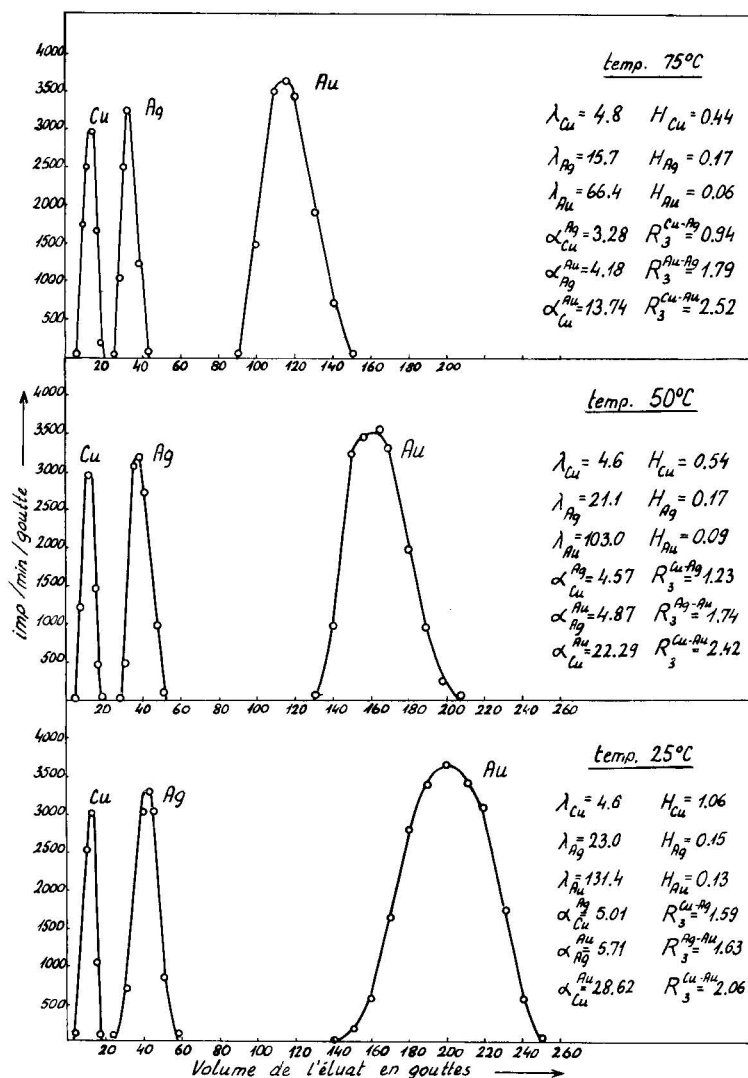


Fig. 4. Influence de la température sur la séparation du cuivre(II), de l'argent(I) et de l'or(III). Amberlite IRA-68 (Br^-), $20 \mu m \leq \varnothing \leq 80 \mu m$; colonne, $6 \text{ cm} \times 0.031 \text{ cm}^2$. Éluant: $3.204 \text{ M HBr} + 0.004 \text{ M Br}_2$. Vitesse d'élution: 0.65 cm/min .

Ce sont les éléments de terres rares, Zr, V, Nb, Cr(III), Mo, U(VI), Mn, Fe, Co, Ni, Cu, Ga, In, Sb et Sn.

(3) Les éléments dont le coefficient de partage diminue dans le domaine indiqué de concentration de HBr, quand la concentration de ce dernier augmente. Il faut mentionner ici Ag, Au, Hg, Pt, Ir, Re et Tl(III).

(4) Les éléments présentant un maximum du coefficient de partage pour certains concentrations de HBr. Ce sont Cd, Zn et Pb.

En comparant les résultats obtenus avec les données d'Andersen *et al.*¹⁴ concernant l'adsorption des éléments sur une résine fortement basique en milieu

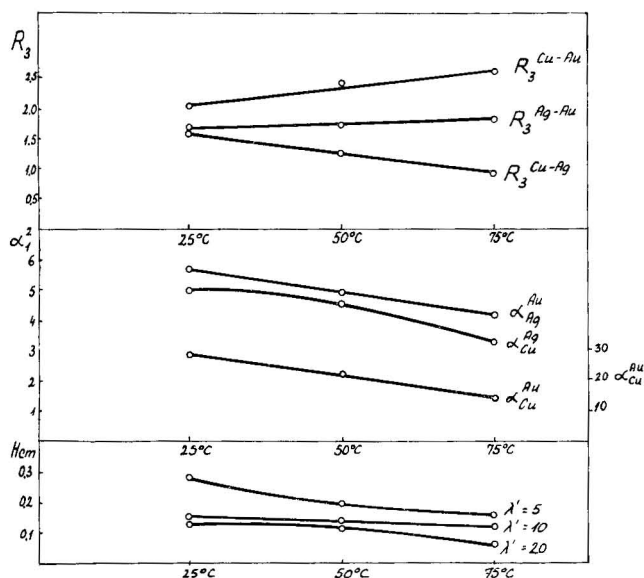


Fig. 5. Les coefficient de partage, facteurs de séparation, résolutions des pics et l'hauteur du plateau théorique pour la séparation du Cu, Ag et Au au système Amberlite IRA-68 (Br^-)-3.204 M HBr + 0.004 M Br_2 en fonction de la température.

HBr, on peut constater qu'une résine faiblement basique montre généralement une affinité plus faible pour la plupart des éléments.

Grâce à cette propriété, certains éléments à coefficient de partage élevé vis à vis d'une résine fortement basique dans la totalité du domaine de concentration de HBr, peuvent être éliminés de l'échangeur faiblement basique à l'aide d'un volume raisonnable d'éluant.

L'allure des courbes dans le système des coordonnées $\log \lambda/c_{HBr}$ est dans les deux cas similaire. Cependant, exceptionnellement la courbe de Ga, contrairement à l'adsorption sur une résine anionique fortement basique, ne montre pas ici de maximum. Il en est de même en milieu HCl avec une autre résine faiblement basique, Amberlite CG-4B¹¹. L'adsorption de cet élément croît rapidement pour les concentrations de HBr supérieures à 4 M.

Les éléments suivants démontrent les coefficients de partage exceptionnellement élevés dans un domaine de faibles concentrations de HBr: Pt, Hg, Ag; et dans plus faible mesure: Ir, Au, Re et Tl(III). Ils appartiennent au troisième groupe de la classification indiquée.

Le Pb, le Zn et le Cd montrent un maximum d'adsorption pour la concentration de HBr de 0.5–4 M. Il en est de même sur Amberlite CG-4B en milieu chlorhydrique et aussi sur une résine de forte basicité Dowex 1 en solution de HBr et HCl.

Des possibilités de séparation de certains éléments sur la résine étudiée résultent des différences relativement élevées sur du coefficient de partage. L'Eu (et les autres terres rares) est séparé à partir de l'U à l'aide de HBr de 6.8 M.

Le Zn, Cd et Hg peuvent être séparés sur l'Amberlite IRA-68 à l'aide des solutions de HBr de 0.1 et 6.8 M et $HClO_4$ de 0.5 M. Un autre exemple est celui de la

séparation de Ga, In et Tl. L'acide bromhydrique retire ces éléments de la colonne avec un rendement satisfaisant.

L'étude de l'influence de la température sur la séparation d'une solution de Cu, Ag et Au permet de déduire des conclusions intéressantes. Ils sont illustrés sur les Figs. 4 et 5. Le facteur de séparation, α , des éléments examinés diminue lorsque la température augmente. Les hauteurs des plateaux théoriques diminuent aussi mais à un degré différent pour des diverses valeurs de λ' . La résolution R_3 , qui est une fonction du coefficient de séparation et du nombre des plateaux de colonne, diminue et parfois augmente légèrement suivant l'un de deux facteurs qui domine dans la détermination de la valeur de R_3 ^{5,12} (cf., Fig. 5). Le coefficient de partage de l'élément élué en dernier (Au) décroît lorsque la température augmente; cela signifie qu'à une température supérieure il est parfois possible d'effectuer la séparation plus rapide, sans perte et même en augmentant la résolution.

Globalement, il faut constater que l'emploi des résines anioniques de faible basicité crée parfois des nouvelles possibilités de séparation. Les travaux dans cette direction seront poursuivis.

La différence relativement élevée de la possibilité d'échange d'anions d'éléments appartenant au même groupe de la classification périodique fait, que le système Amberlite IRA-68-HBr peut être utilisé pour une série des séparations d'une grande importance dans l'analyse chimique et radiochimique. La possibilité d'éluer dans un temps raisonnable, presque tous les éléments étudiés au moyen des concentrations courantes de HBr constitue un avantage réel.

REMERCIEMENTS

Nous tenons à remercier Mme. M. Marecka pour sa collaboration technique dans l'élaboration du présent travail.

RÉSUMÉ

Une étude est effectuée sur le comportement des certains éléments dans le système: la résine échangeuse d'anions de faible basicité Amberlite IRA 68 (Br^-)-HBr + Br_2 . Les coefficients de partage de 30 éléments en fonction de la concentration en HBr (0.01–12 M) ont été déterminés. Pour la plupart des éléments les coefficients de partage croissent avec l'augmentation de la concentration en acide. Pt, Hg, Ir, Au, Ag, Tl(III) et Re démontrent les coefficients de partage exceptionnellement élevés surtout dans le domaine de faible concentration en HBr. Leur adsorption sur la résine diminue avec l'augmentation de la concentration en acide. Généralement la résine étudiée montre l'affinité plus faible pour la plupart des éléments vis à vis de la résine fortement basique comme Dowex 1. Les différences entre les coefficients de partage des certains éléments sont suffisamment élevées pour effectuer des séparations intéressantes. On a présenté plusieurs exemples des séparations de colonne des métaux (Eu–U, Zn–Cd–Hg, Cu–Ag–Au). L'influence de la température sur la séparation du mélange de Cu–Ag–Au a été étudiée et les plus importantes valeurs (coefficients de partage, facteurs de séparation, résolution et l'hauteur du plateau théorique) ont été calculées.

BIBLIOGRAPHIE

- 1 R. Kuroda, K. Ishida et T. Kiriya, *Anal. Chem.*, 40 (1968) 1502.
- 2 R. Kuroda, K. Oguma, N. Kono et Y. Takahashi, *Anal. Chim. Acta*, 62 (1972) 341.
- 3 R. Kuroda et K. Ishida, *Anal. Chem.*, 39 (1967) 212.
- 4 R. Kuroda et N. Yoshikuni, *Talanta*, 18 (1971) 1123.
- 5 R. Dybczyński, *Inst. Bad. Jad.*, *Rapport*, 1115/C/VIII/1969.
- 6 Z. Błaszowska et R. Dybczyński, *Przem. Chem.*, 38 (1959) 168.
- 7 C. J. Rodden, *Analytical Chemistry of the Manhattan Project*, McGraw Hill, New York, 1960, p. 91.
- 8 D. E. Ryan, *Analyst (London)*, 85 (1960) 569.
- 9 H. Flaschka, *Mikrochim. Acta*, 39 (1952) 315.
- 10 R. Dybczyński, *J. Chromatogr.*, 14 (1964) 79.
- 11 R. Dybczyński, *Rocz. Chem.*, 41 (1967) 1689.
- 12 R. Dybczyński, *J. Chromatogr.*, 31 (1967) 155.
- 13 L. Wódkiewicz et R. Dybczyński, *J. Chromatogr.*, 68 (1972) 131.
- 14 T. Andersen et A. B. Knutsen, *Acta Chem. Scand.*, 16 (1962) 849.

CHROM. 7710

CHELATE SORBENTS FOR CONCENTRATION AND SEPARATION OF NOBLE METALS

S. B. SAVVIN, I. I. ANTOKOLSKAJA, G. V. MYASOEDOVA, L. I. BOLSHAKOVA and O. P. SHVOEVA

V.I. Vernadsky Institute of Geochemistry and Analytical Chemistry, U.S.S.R. Academy of Sciences, Moscow (U.S.S.R.)

SUMMARY

Chelate sorbents based on aminopolystyrene and chloromethylated and amino derivatives of styrene–divinylbenzene copolymers have been synthesized. The sorbents are of interest for the selective concentration of platinum-group elements. The sorption of the microgram amounts of Pd, Pt, Rh, Ir and Au has been investigated. The sorption of chloro-containing complexes of Pd(II), Pt(II), Pt(IV), Rh(III) and Ir(III) on sorbents with 8-aminoquinoline groups was studied. The difference in sorption may be explained by the formation of strong cyclic complexes of Pd and Pt with chelate groups of the resin. The sorbent can be used for the separation of milligram amounts of Pd, Pt and Au from microgram amounts of Rh and Ir and also for the selective concentration of Pd, Pt and Au from strongly acidic solutions containing large amounts of Cu, Fe, Ni and Co.

INTRODUCTION

Noble metals are usually found in natural materials in very low concentrations and, for their determination, a preliminary concentration for their separation from large amounts of other elements is required. For this purpose, the use of chelate sorbents is a promising technique¹.

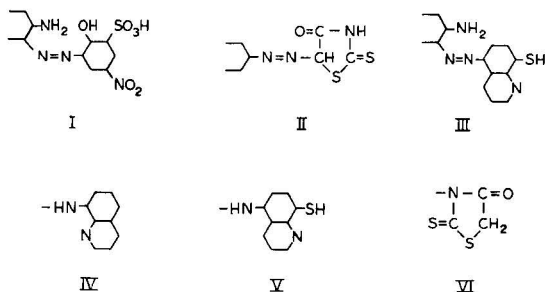
The selective properties of chelate sorbents depend on the nature of the functional groups that they contain. The sorbents with donor N and S atoms in the functional group are most significant for the noble metals^{2,3}. These groups form stable cyclic complexes with ions of the noble metals⁴.

New chelate sorbents for the concentration and separation of the noble metals have been synthesized in this laboratory in the light of known data about the formation of complexes of these metals with monomeric organic reagents.

EXPERIMENTAL

Aminopolystyrene and chloromethylated and amino derivatives of styrene–divinylbenzene macroporous copolymers have been used as polymer matrices for the

syntheses of these sorbents. The sorbents synthesized contain the following functional groups:



The sorbents were synthesized by known polymer transformation methods⁵. The sorbents are powdery or spherical granulated materials coloured yellow, brown or black; they are stable when heated in a strongly acidic solution.

The sorption of the noble metals was studied under static conditions from 0.5–10 *N* HCl, H₂SO₄ and HClO₄. Standard chloride complexes of the noble metals and their aquohydroxychlorides were prepared according to previous work^{6–9}. The experimental technique was described by Myasoedova *et al.*³.

RESULTS AND DISCUSSION

The investigation of the sorption properties of the chelate resins has shown that all of the sorbents synthesized can be used for the concentration of microgram amounts of Au and Pd from strongly acidic solutions. The sorption of Pt is most complete from hydrochloric acid solution. The sorption of Rh and Ir is effective on heating with resins with chelate groups III and V (Table I). Table I gives results for the extent of sorption of noble metals from 1 *N* HCl by resins synthesized on the basis of styrene–divinylbenzene copolymers.

The sorbents with III and V functional groups are the most interesting for the concentration of the noble metals. These sorbents have high selectivity for Al, Ca, Mg, Co, Ni, Fe and Cu. For instance, the extent of sorption of Ir is independent of

TABLE I

EXTENT OF SORPTION (%) OF PLATINUM-GROUP METALS

100 μ g of metals; 50 mg of resin; 10 ml of 1 *N* HCl; 2 h contact.

Chelate group	At room temperature (20°)					With heating (100°)	
	Au	Pd	Pt	Rh	Ir	Rh	Ir
I	90	100	25	20	—	—	—
II	100	100	40	26	15	69	—
III	100	100	96	39	40	88	95
IV	100	96	100	10	16	60	60
V	100	100	88	34	40	94	87
VI	100	92	50	—	—	83	46

the presence of Cu and Fe (10 mg/ml), Al (25 mg/ml) and Ca, Mg, Ni and Co (50 mg/ml) (Fig. 1). This result permits sorbents with III and V groups to be used for the concentration of the noble metals from complicated salt solutions. A considerable difference in the extent of sorption of the noble metals by sorbents with I and IV groups can be used for their separation. In this connection, the sorption properties of the above two sorbents have been thoroughly investigated and optimal conditions for the separation of Pd and Pt from Rh and Ir have been found. A sorbent based on amino-polystyrene with I groups was described by Dedkov *et al.*¹⁰.

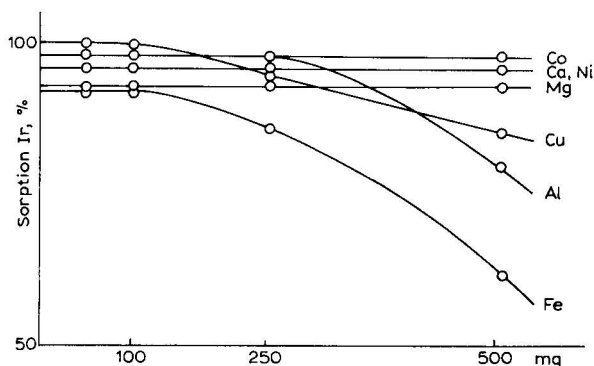


Fig. 1. Sorption of Ir in the presence of non-noble metals: 100 μ g of Ir; 20 mg of resin; 10 ml of 1 N HCl; 2 h contact; temperature *ca.* 100°.

Results are given here of the investigation of the sorption of chloro complexes of Pd, Pt, Rh and Ir by a resin containing IV groups (Table II). This sorbent was synthesized by aminating a chloromethylated styrene-divinylbenzene copolymer with 8-aminoquinoline. The presence of $-NH$ groups in the 8-position and a heterocyclic nitrogen atom ($-N\leq$) favour the formation of cyclic complexes with the noble metals. The chloro complexes $[PdCl_4]^{2-}$, $[Pt(II)Cl_3H_2O]^-$ and $[PtCl_4]^{2-}$ are completely adsorbed by the resin, independent of the nature of the acids, but the Pt(IV) complexes $[PtCl_6]^{2-}$ and $[PtCl_5OH]^{2-}$ are adsorbed completely only from hydrochloric and sulphuric acids. The sorption of Pt from perchlorate solutions is slight. A

TABLE II

EXTENT OF SORPTION (%) BY RESIN WITH IV GROUPS USING DIFFERENT ACIDS
100 μ g of metals; 50 mg of resin; 10 ml of solution; 2 h contact; temperature *ca.* 20°.

Metal	State in solution	1 N HCl	0.5 N H ₂ SO ₄	1 N HClO ₄
Pd(II)	$[PdCl_4]^{2-}$	100	100	100
Pt(IV)	$[PtCl_6]^{2-}$	99	88	15
	$[PtCl_5OH]^{2-}$	100	100	28
Pt(II)	$[PtCl_3H_2O]^-$	100	100	100
Rh(III)	$[RhCl_6]^{3-}$	—	—	—
	$[RhCl_5H_2O]^{2-}$	10	—	—
	$[RhCl_3(H_2O)_3]$	0	0	0
Ir(III)	$[IrCl_5H_2O]^{2-}$	15	15	0

comparison of the results obtained with those reported in the literature permits the possibility of reducing Pt(IV) to Pt(II) during the sorption from hydrochloric and sulphuric acids, while in perchloric acid Pt(IV) is not reduced. This explains the low extent of sorption. In the context of previous results^{8,11-13}, a greater extent of sorption of Rh and Ir may be expected than actually occurs (Table I). This result can probably be explained by the fact that under the experimental conditions used, Rh(III) and Ir(III) complexes retain an octahedral configuration. The sorption of these complexes is hindered because of steric factors that result from the interaction between these complexes and chelate groups of the resins.

Hence the difference in the sorption of noble metals is due to a dissimilar ability of the metals to give stable cyclic chelate complexes with functional groups of the resin, depending on the composition and electronic structure of the complexes.

It is the difference in the sorption abilities of these elements that enabled us to devise a method for the separation of milligram amounts of Pd, Pt and Au from microgram amounts of Rh and Ir. The separation is achieved by passing a solution of the noble metals in 3 *N* HCl through a sorbent-filled column. For the regeneration of the sorbent, a hot solution of thiourea in 0.1 *N* HCl is suitable. The dynamic capacity of the sorbent for Pt is 20 mg/g, and for Au 100 mg/g.

Separation of Rh from Pd, Pt and Au

A column of 0.5 cm diameter and 10 cm height packed with resin (*ca.* 1 g, the particle size being 0.25–0.5 mm) is washed with 3 *N* HCl. Then 1–5 ml of a solution containing the noble metals in 3 *N* HCl is passed through the sorbent layer at the rate of 0.5 ml/min. The column is then washed with 50 ml of 3 *N* HCl. The eluate is evaporated to dryness, 1–2 ml of a 1:2 mixture of concentrated HClO₄ and HNO₃ is added and the mixture is evaporated to dryness in order to decompose the organic material. The residue is treated with 2 ml of aqua regia and then twice with concentrated HCl. After evaporation to dryness, the residue is dissolved in 2 ml of 1 *N* HCl and Rh is determined.

This method of separation of Rh from Pd and Pt was checked on an artificial mixture of these elements and in the determination of Rh in some alloys. The Rh is determined by a spectrophotometric method with the new organic reagent 5-sulpho-allythiox (allyl ester of 5-sulpho-8-mercaptoquinoline)^{14,15}.

REFERENCES

- 1 G. V. Myasoedova, O. P. Eliseeva and S. B. Savvin, *Zh. Anal. Khim.*, 26 (1971) 2172.
- 2 G. V. Myasoedova, O. P. Eliseeva, S. B. Savvin and N. I. Uryanskaya, *Zh. Anal. Khim.*, 27 (1972) 2004.
- 3 G. V. Myasoedova, L. I. Bolshakova, O. P. Shvoeva and S. B. Savvin, *Zh. Anal. Khim.*, 28 (1973) 1550.
- 4 V. K. Gustin and T. R. Sweet, *Anal. Chem.*, 35 (1963) 44.
- 5 G. V. Myasoedova, L. I. Bolshakova and S. B. Savvin, *Zh. Anal. Khim.*, 26 (1971) 2081.
- 6 S. I. Ginsburg, K. A. Gladishevskaya, H. A. Ezerskaya, N. V. Ivonina, N. V. Fedorenko and A. N. Fedorov, *Rukovodstvo po Khimicheskomu Analizu Platinovih Metallov i Zolota*, Nauka, Moscow, 1965.
- 7 A. A. Grinberg, and G. A. Shagicultanova, *Zh. Inorg. Khim.*, 5 (1960) 280.
- 8 Y. S. Kononov, A. I. Popov and M. K. Makarov, *Izv. Akad. Nauk SSSR, Ser. Khim.*, 9 (1971) 133.

- 9 S. I. Ginsburg, N. A. Eserskaya, I. V. Prokofeva, N. V. Fedorenko, V. I. Shlenskaya and N. K. Belski, *The Analytical Chemistry of the Platinum Metals*, Nauka, Moscow, 1972.
- 10 Y. M. Dedkov, O. P. Eliseeva, A. N. Ermakov, S. B. Savvin and M. G. Slotinzeva, *Zh. Anal. Khim.*, 27 (1972) 726.
- 11 S. S. Berman and W. A. E. McBryde, *Can. J. Chem.*, 36 (1958) 833.
- 12 K. A. Burkov, E. A. Busko and L. S. Lilish, *Probl. Sovrem. Khim. Coord. Soedin.*, 3 (1970) 127.
- 13 G. Koster and G. Schmuckler, *Anal. Chem. Acta*, 38 (1967) 179.
- 14 Y. M. Dedkov and M. G. Slotinzeva, *Zh. Anal. Khim.*, 28 (1973) 2367.
- 15 G. V. Myasoedova, I. I. Antokolskaja, L. I. Bolshakova, O. P. Shvoeva and S. B. Savvin, *Zh. Anal. Khim.*, 29 (1974) 2097.

CHROM. 7735

EXTRACTION CHROMATOGRAPHY WITH LIQUID ION EXCHANGERS AS STATIONARY PHASE

C. TESTA and A. DELLE SITE

Radiotoxicological Laboratory, Medical Service, CNEN-CSN Casaccia, Rome (Italy)

SUMMARY

The use of Kel-F (polytrifluorochloroethylene) and Microthene-710 (microporous polyethylene) supporting some liquid ion exchangers is described. Solutions of tri-*n*-octylamine (TNOA), Aliquat-336 and di(2-ethylhexyl)phosphoric acid (HDEHP) have been used as stationary phases.

Many separations were carried out both by column chromatography and by batch extraction. This technique can be used successfully as a selective pre-concentration step for the determination of many radionuclides in aqueous solutions and biological samples.

The possibility of supporting an organic redox agent together with the liquid ion exchanger is also described.

Finally, the possible advantages of this technique when used in connection with liquid scintillation counting are discussed.

INTRODUCTION

Many analytical separations have been obtained in our laboratory by supporting liquid ion exchangers (tri-*n*-octylamine, TNOA; a quaternary ammonium salt, Aliquat-336; di(2-ethylhexyl)phosphoric acid, HDEHP) on microporous polymers such as polytrifluorochloroethylene (Kel-F) and microporous polyethylene (Microthene-710)^{1–3}. This paper summarizes some practical applications of this technique. In addition, the advantages of supporting a redox agent together with the extractant and of using extraction chromatography in connection with liquid scintillation counting are discussed.

EXPERIMENTAL AND RESULTS

Choice of the inert support

Six commercially available microporous polymeric compounds were considered¹, viz., Kel-F, Microthene-710, Algofton (polytetrafluorochloroethylene), Moplen (isotactic polypropylene), Vipla (polyvinyl chloride) and Corvic (polyvinyl chloride-polyvinyl acetate copolymer). All of these materials gave good results as supporting

agents; Kel-F was used in the first experiments, but it was then replaced with Microthene-710 because of its lower cost and ready availability.

Extraction chromatography with liquid anion exchangers

Separation of Fe(III)–Co(II)–Ni(II) in aqueous solutions with a Kel-F–TNOA column¹. The feeding solution is 8 M HCl. Nickel is not retained, cobalt is eluted with 2 M HCl and iron(III) with 1 M HNO₃.

Separation of U–Th in aqueous solutions with a Kel-F–Aliquat-336 column¹. When a 4 M HNO₃ feeding solution is used, uranium is not retained and thorium can then be eluted with 8 M HCl. When the feeding solution is 8 M HCl, thorium is not retained and uranium can then be eluted with 0.5 M HNO₃.

Determination of plutonium in urine with a Kel-F–TNOA column⁴. After co-precipitation of plutonium with magnesium and calcium phosphates, the precipitate is dissolved in 2 M HNO₃ and the solution is percolated through a Kel-F–TNOA column. After washing with 1 M HNO₃, the radionuclide is eluted by reduction to Pu(III) with H₂SO₃. Plutonium is then electroplated and counted with a solid-state detector for alpha-particles. The final yield is 90.5% and the sensitivity limit is 0.04 pCi for a 24-h urine sample.

Extraction chromatography with HDEHP liquid cation exchangers

Separation of Am–Pu in aqueous solutions with a Microthene–HDEHP column. The column consists of Microthene supporting 50% HDEHP in xylene. Both the radionuclides are retained on the column in 0.05 M HNO₃ solution; americium is then eluted with 1 M HCl and plutonium(IV) with 12 M HCl, as shown in Fig. 1.

Determination of Sr-90 in urine with a Microthene–HDEHP column⁵. This method is based on the retention of yttrium-90 at its equilibrium with strontium-90 on a column of Microthene supporting 1.5 M HDEHP in toluene. The urine is wet mineralized with HNO₃ and the pH is brought to 0.5; the solution is percolated through the column; strontium-90 is not retained and, after washing, the isolated yttrium-90 can then be eluted with 6 M HNO₃.

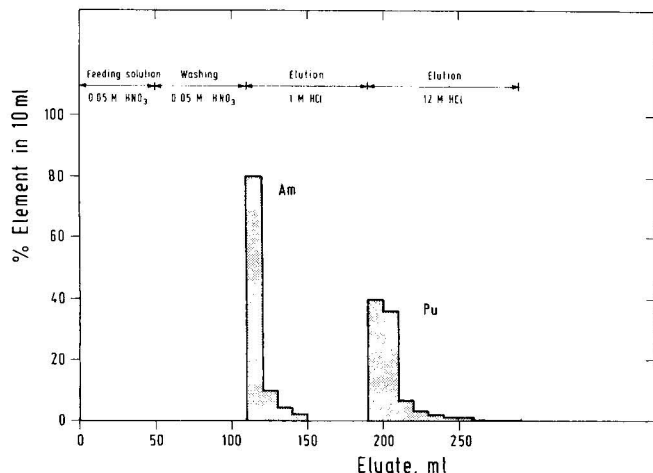


Fig. 1. Separation of Am(III)–Pu(IV) with a Microthene–HDEHP column.

Yttrium is precipitated as yttrium oxalate at pH 1.5 and counted in a low-background beta-detector. The final yield is 92% and the sensitivity limit is 5 pCi for a 24-h urine sample.

*Determination of Fe-55 in fall-out samples with a Microthene-HDEHP column*⁶. After the isolation of uranium, thorium and plutonium obtained by passing 7.5 M HNO₃ through an anion-exchange resin, the eluate containing iron-55 is immediately percolated through a Microthene-HDEHP column; iron is retained on the column and can be eluted with 6 M HCl. After an electroplating procedure, iron-55 is determined by counting its X-ray emission.

*Determination of Am-241 in urine by a batch extraction with Microthene-HDEHP*⁷. After wet mineralization of the urine with HNO₃ and H₂O₂, the pH is brought to 3 with ammonia solution; a batch extraction of the americium is then performed by stirring the urine solution with Microthene-HDEHP for 45 min. The slurry is transferred to a chromatographic column; after washing with 0.001 M HNO₃, americium is eluted with 3 M HNO₃, electroplated and alpha-counted with a solid-state detector. The final yield is 85.9%, the sensitivity limit is 0.04 pCi and the decontamination factors from the other alpha-emitters are as follows: 70 from thorium, 60 from protactinium, 80 from uranium and 100 from neptunium and plutonium.

Fig. 2 shows the americium-241 extraction as a function of pH (no DTPA curve); some extraction curves with urine containing diethylenetriaminopentaacetic acid (DTPA) are also reported. The results show that a sufficient recovery of americium-241 can also be obtained from urines of persons treated with this chelating agent for therapeutic reasons⁸.

Column redox-extraction chromatography

The possibility of supporting an organic redox compound together with the extractant was studied. When a solution of iron(II) in 6 M HCl is passed through a

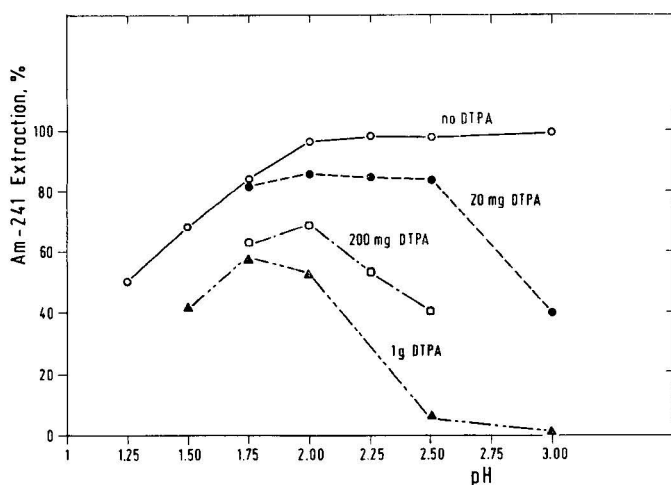


Fig. 2. Batch extraction of Am(III) in urine with a Microthene-HDEHP slurry as a function of pH and DTPA concentration.

column of Microthene supporting TNOA and tetrachlorohydroquinone (TCHQ), iron is in the iron(II) form and is not retained on the column. When the same solution is passed through a TNOA–tetrachloroquinone (TCQ) column, iron(II) is oxidized to iron(III), which remains on the column in the form of an anionic hydrochloride complex (Fig. 3).

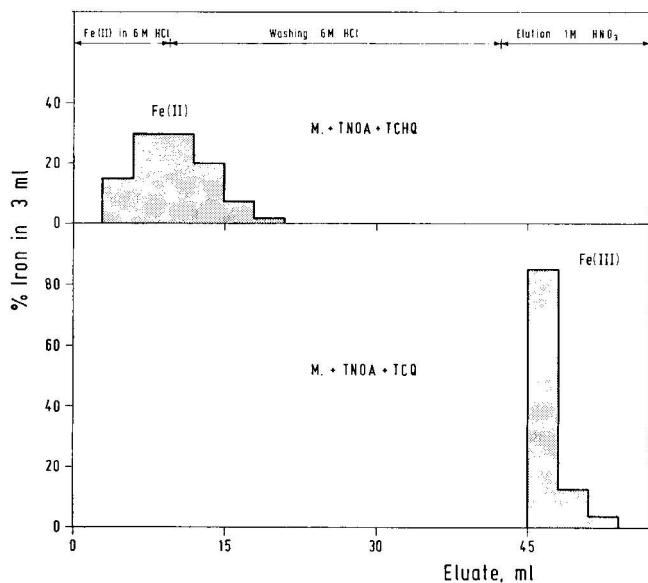


Fig. 3. Elution diagram of Fe(II) with a Microthene–TNOA–TCHQ column and with a Microthene–TNOA–TCQ column.

Some separations of actinide elements have been obtained by supporting, together with the extractant tri-*n*-octylphosphine oxide (TOPO), some reducing agents such as tetrachlorohydroquinone, 2,5-dichloronaphthaquinone, 2,5-di-*tert*-butylhydroquinone and 2,5-di-*tert*-phenylhydroquinone (DTPHQ). These compounds can reduce plutonium(IV) and plutonium(VI) to plutonium(III) and neptunium(V) and neptunium(VI) to neptunium(IV).

By using a Microthene–TOPO–DTPHQ column, the quantitative separations plutonium(III)–neptunium(IV), plutonium(III)–uranium(VI) and americium(III)–neptunium(IV) in 6 *M* HCl were obtained⁹. Fig. 4 shows the behaviour of plutonium and neptunium in 6 *M* HCl with a Microthene–TOPO column and with a Microthene–TOPO–DTPHQ column.

Extraction chromatography and liquid scintillation counting

By using this type of chromatography, it is possible to avoid the elution of alpha- or beta-emitters from the column if a liquid scintillation counting step is introduced. In fact, a Microthene–TNOA or Microthene–HDEHP slurry containing the extracted radionuclide can be transferred into a scintillation vial; the scintillation liquid is then added and the counting is carried out. The counting yields are good, as

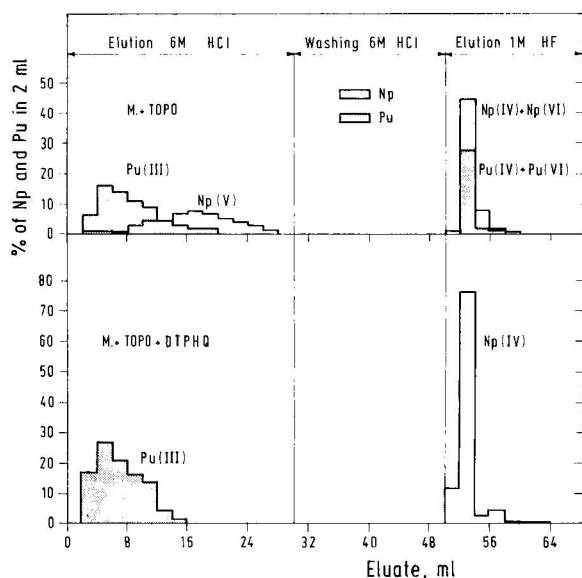


Fig. 4. Separation of Pu-Np with a Microthene-TOPO column and with a Microthene-TOPO-DTPHQ column.

shown in Table I; the background is about 15 c.p.m. Similar results could not be obtained with ion-exchange resins. Work is now in progress to prepare some extraction-scintillating columns by supporting an insoluble scintillating compound together with the extraction agent.

TABLE I

LIQUID SCINTILLATION COUNTING OF THE COLUMN AFTER ADDITION OF 10 ml OF INSTA-GEL

Radionuclide	Column	Aqueous solution	Counting yield (%)
Pu-239 (α)	3.5 g Microthene + 2.5 ml TNOA	2 M HNO_3	91.6
U-233 (α)	3.5 g Microthene + 2.5 ml TNOA	6 M HCl	94.2
Am-241 (α)	3.5 g Microthene + 2.5 ml HDEHP	0.001 M HNO_3	97.6
Y-90 (β)	3.5 g Microthene + 2.5 ml HDEHP	0.3 M HNO_3	90.0
U-233 (α)	3.5 g Dowex 1-X2	6 M HCl	19.2
U-233 (α)	3.5 g Dowex 2-X10	6 M HCl	10.0

REFERENCES

- 1 C. Testa, CNEN Report RT/PROT(65)33, 1965.
- 2 C. Testa, *Anal. Chim. Acta*, 50 (1970) 447.
- 3 C. Testa and L. Staccioli, *Analyst (London)*, 97 (1972) 525.
- 4 C. Testa, *Minerva Nucl.*, 10 (1966) 202.
- 5 C. Testa and G. Santori, *Energ. Nucl.*, 17 (1970) 320.

- 6 G. Bagliano, M. Castaldo, V. Marchionni and C. Testa, *Proc. 16th AIFSPR Congress, Florence, 1970*.
- 7 A. Delle Site, G. Santori and C. Testa, *Proc. 18th AIFSPR Congress, Rome, 1973*, in press.
- 8 A. Delle Site, G. Santori and C. Testa, *Proc. 3rd International Radiation Protection Association Congress, Washington, 1973*, in press.
- 9 A. Delle Site and C. Testa, *Anal. Chim. Acta*, 72 (1974) 155.

CHROM. 7734

EXTRACTION CHROMATOGRAPHY WITH LIQUID ION EXCHANGERS

G. GHERSINI

CISE, P.O. Box 3986, 20100 Milan (Italy)

SUMMARY

After a brief outline of the potential of extraction chromatography involving liquid anion and cation exchangers as a means for the quantitative separation of inorganic substances, the theoretical approaches to the technique are presented and criticized. Known limiting factors to theoretical interpretations of extraction chromatographic results are discussed, and additional factors are suggested.

INTRODUCTION

Suitable solid supports, loaded with liquid compounds normally used for the extraction of metals from aqueous solutions, enable one to obtain chromatographic systems that advantageously reproduce the same processes as liquid–liquid extraction. Although relatively recent, this technique, generally called extraction chromatography, has found increasing popularity in inorganic analytical laboratories, as indicated in several of the many reviews on the subject^{1–6}. Columns permit easy and satisfactory separations of microgram to milligram amounts of ions, while treated thin layers or paper are versatile materials for rapid investigations on the behaviour of the different stationary phases or for qualitative analysis.

In this paper, extraction chromatographic systems involving the so-called liquid anion and cation exchangers are briefly considered and compared with conventional ion-exchange resins, and the most recent theoretical approaches to the technique are critically outlined.

LIQUID ANION EXCHANGERS

The salts of long-chain aliphatic amines extract inorganic species from aqueous solution through the exchange of their original anion with an anionic species containing the element of interest, present in the aqueous phase. The nature of the amine affects the overall values of the resulting distribution coefficients, but apparently has little influence on the relative extractability of the different anionic species. Therefore, all extractants of this class display the same selectivity features, strictly comparable to those of conventional anion-exchange resins.

The most popular liquid anion exchangers are tri-*n*-octylamine (TNOA) and Aliquat 336 (methyltricaprylammonium chloride). A large number of other amines

TABLE I

LIQUID ANION EXCHANGERS USED IN COLUMN EXTRACTION CHROMATOGRAPHY

Type	Exchanger
Primary	Primene JM-T (trialkylmethylamine, 18–24 carbon atoms)
Secondary	Amberlite LA-1 (<i>n</i> -dodecyltrialkylamine, 24–27 carbon atoms) Amberlite LA-2 (<i>n</i> -dodecyltrialkylamine, 24–27 carbon atoms)
Tertiary	Alamine 336 (tricaprylylamine; caprylyl = <i>n</i> -octyl, <i>n</i> -decyl) methyldioctylamine tri- <i>n</i> -hexylamine trilaurylamine triisooctylamine tri- <i>n</i> -octylamine (TNOA)
Quaternary	Aliquat 336 (methyltricaprylylammonium chloride) Hyamine-1622 (diisobutylphenoxyethoxyethyltrimethylbenzylammonium chloride) trialkylbenzylammonium nitrates methyltrilaurylammonium salts

have been screened for their behaviour toward metals in laminar extraction chromatography^{2,3}, while relatively few of them have been applied as stationary phases for columns.

Amines and ammonium compounds used in columns are listed in Table I, while Table II lists materials most commonly used as supports. Accurate optimization of chromatographic parameters (amount of extractant loaded on the support; nature, grain-size and porosity of the support material; column packing and dimensions; flow-rate of the eluting solution; temperature) permit 0.2–0.4-mm theoretical plate heights, hydrophobized Kieselguhr or silica gel being the most suitable supports.

Because of their close similarity to conventional anion-exchange resins, amine stationary phases can represent an advantageous alternative to resins only when a

TABLE II

SUPPORTS USED IN COLUMN EXTRACTION CHROMATOGRAPHY

Cellulose powder
Glass beads or powder
Polyethylene: Microthene
Polystyrene: Amberlyst XAD-2
Polytetrafluoroethylene: Fluoroplast-4
Teflon
Polytrifluorochloroethylene: Hostaflon
Kel-F
Plaskon
Voltalef
Polyurethane foams
Poly(vinyl chloride–vinyl acetate) copolymer: Corvic
Silicon dioxide: silanized Kieselguhr
Celite
Hyflo Supercel
Chromosorb W
silica gel
Styrene–divinylbenzene copolymer granules

"tailor-made" retention power or particularly small plate heights are required, when the use of a particular extractant permits a small but important enhancement of the separation factor between closely similar elements (as in the case of several actinides), and in applications to high-pressure column chromatography, as pointed out by Huber⁷.

Among the most interesting column chromatographic separations obtained with liquid anion exchangers, Am-Cm, F^- - Cl^- - Br^- - I^- and Cr-W-Mo are particularly noteworthy.

LIQUID CATION EXCHANGERS

Water-insoluble liquid organic compounds that extract by exchanging protons for cationic species originally present in the aqueous phase are generally called "liquid cation exchangers".

The extractants of this class used in column extraction chromatography are listed in Table III; among them, acidic organophosphorus compounds are the most popular, in particular di(2-ethylhexyl)phosphoric acid (HDEHP). Supports used for columns are the same as those mentioned for liquid anion exchangers.

TABLE III

LIQUID CATION EXCHANGERS USED IN COLUMN EXTRACTION CHROMATOGRAPHY

Dinonylnaphthalenesulphonic acid (HDNNS)
Di- <i>n</i> -butylphosphoric acid
Di- <i>n</i> -octylphosphoric acid
Diisoamylphosphoric acid
Di(2-ethylhexyl)phosphoric acid (HDEHP)
2-Ethylhexylphenylphosphonic acid
2-Ethylhexylphosphoric acid
2,6,8-Trimethylnonyl-4-phosphoric acid

Acidic organophosphorus compounds extract through a mechanism that can be assumed to be cation exchange, but their selectivity is remarkably affected by the solvating properties of their $P \rightarrow O$ groups, and for strictly related metals generally increases as the ionic radius of the metal decreases. This makes their use very attractive as an alternative to sulphonic resins.

The popularity of HDEHP derives from its very advantageous separation factors for rare earths (the average value for an adjacent pair is 2.5). Using hydrophobized Kieselguhr, silica gel or polytetrafluoroethylene powder as the support material, HDEHP columns having theoretical plate heights as low as 0.1 mm can be obtained. Outstanding examples of separations obtained with HDEHP columns include all rare earths among themselves, transuranium elements, Ba-Sr-Ca and Tl-Ga-In-Al.

2-Ethylhexylphenylphosphonic acid displays even better separation factors than HDEHP for rare earths and was advantageously used for this purpose, supported on Kieselguhr. 2,6,8-Trimethylnonyl-4-phosphoric acid allowed for successful column separations of alkali metals among themselves.

Other cation exchangers, such as carboxylic acids and phenols, have so far found little popularity in extraction chromatography. This applies also to dinonylnaphthalenesulphonic acid (HDNNS), whose selectivity is closely similar to that of conventional cation-exchange resins.

THEORETICAL APPROACHES TO EXTRACTION CHROMATOGRAPHY

Extraction chromatographic systems are generally treated in terms of liquid-liquid extraction phenomena. On the basic assumption that the processes are fundamentally the same in both instances and that the spatial boundaries of the two chromatographic phases are well defined, the distribution coefficient, D , of the eluted species is related to the chromatographic parameters through the classical partition equations

$$D = \frac{V_R - V_m}{V_s} \quad (1)$$

and

$$D = \frac{A_m}{A_s} \cdot \left(\frac{1}{R_F} - 1 \right) \quad (2)$$

eqn. 1 referring to columns (V_R being the volume of eluate to the peak maximum, V_m and V_s the volumes of the mobile and stationary phases in the column, respectively) and eqn. 2 to paper and thin layers (A_m and A_s being the cross-sectional areas of the mobile and stationary phases, respectively, assumed to be constant along the whole chromatogram).

In turn, D can be related to the chemical parameters of the two phases. The extraction of a metal ion M^{n+} by an acidic extractant, for example, can be expressed by a cation-exchange equilibrium:



having an equilibrium constant

$$K = \frac{\gamma_{add}}{\gamma_M} \cdot \frac{[MX_n \cdot (m-n)HX]_{org} \{H^+\}_{aq}^n}{[M^{n+}]_{aq} \{HX\}_{org}^m}$$

where brackets and braces denote concentrations and activities, respectively, and γ_{add} and γ_M are the activity coefficients of the metal-containing species (adduct and ion) in the two phases.

If the above equilibrium is the only reaction responsible for the extraction of the metal, and M^{n+} and $MX_n \cdot (m-n)HX$ are the only metal-containing species present in the system, then

$$D = \frac{[MX_n \cdot (m-n)HX]_{org}}{[M^{n+}]_{aq}} = K \frac{\gamma_M}{\gamma_{add}} \cdot \frac{\{HX\}_{org}^m}{\{H^+\}_{aq}^n}$$

By combining this equation with eqns. 1 and 2, correlations are obtained be

tween the chromatographic results and the chemical parameters of the two phases, which in a logarithmic form appear as follows:

$$\log \left(\frac{V_R}{V_m} - 1 \right) = \log \frac{\gamma_M}{\gamma_{add}} + m \log \{HX\}_{org} - n \log \{H^+\}_{aq} + \log \frac{V_s}{V_m} + \text{constant} \quad (3)$$

$$\log \left(\frac{1}{R_F} - 1 \right) = \log \frac{\gamma_M}{\gamma_{add}} + m \log \{HX\}_{aq} - n \log \{H^+\}_{aq} + \log \frac{A_s}{A_m} + \text{constant} \quad (4)$$

Such correlations enable information to be gained on the reaction actually responsible for the retention of metals, by slope analysis of the plots of the results obtained varying only one of the chemical parameters involved; in general, the ratio of activity coefficients is assumed to be constant, and straight lines are expected.

Slope analysis has often been applied to extraction chromatographic results, especially when obtained by means of laminar chromatographic techniques. Often, however, these slopes are not in agreement with the reaction coefficients assessed or deduced from liquid-liquid extraction data; sometimes, slopes apparently have non-integer values, or abruptly change within the concentration range studied².

In many instances, reasonable explanations have been given for such poor results, based essentially on the lack of validity of the assumptions implied in eqns. 3 and 4, because of (at least) one of the following causes:

(1) more than one metal-containing species exist in one or both phases; most often, complexing in the aqueous phase is put forward, which reduces the validity of the correlation between distribution coefficients and equilibrium constant;

(2) the metal-containing species extracted in chromatography is not the same as that which appears to be extracted in normal liquid-liquid experiments; this may actually occur, as the aqueous phase concentration range involved in chromatography usually does not correspond to that used in liquid-liquid extraction;

(3) as a limiting case of the preceding item, a completely different mechanism may be responsible for extraction in chromatography, in addition to or instead of the one expected from liquid-liquid extraction experience; this is the case, for example, of the extraction of iron(III) and gallium by HDEHP from concentrated hydrochloric acid solutions⁸, noticed in chromatography and subsequently confirmed by liquid-liquid extraction;

(4) in addition to the extractant, the support materials also display some retention power for a particular metal;

(5) slow kinetics do not permit equilibrium to be reached between the two chromatographic phases; very little is known about extraction rates, especially when the distribution is relatively fast but still sufficiently slow to affect the chromatographic process: slow rates could complicate the interpretation of chromatographic results considerably, especially when obtained by ascending laminar techniques in which the elution speed varies as the eluent front runs up.

In the opinion of the author, other phenomena could be important causes of disagreement between chromatographic and liquid-liquid results in almost all extraction systems.

Liquid-liquid data are generally obtained at very low extractant loadings, *i.e.*, the amount of metal extracted is much lower than that required to saturate the extractant. On the other hand, the very few data available for extractions carried out at high extractant loadings demonstrate that in many instances the extraction process differs remarkably from that which occurs at low loadings; for example, iron(III) can be extracted with HDEHP as $\text{Fe}(\text{DEHP-HDEHP})_3$ and as $\text{Fe}(\text{DEHP})_3$ at low and high extractant loadings, respectively. When the extractant displays a relatively strong retention for a given metal, the whole amount of metal that is chromatographed is retained by a very limited portion of stationary phase, so that high extractant loadings are likely to occur easily. As the retention decreases (*i.e.*, R_F increases or V_R decreases) the system gradually turns to low extractant loading conditions. It is obvious how such a system can hardly fit a simple extraction scheme, and can differ appreciably from low extractant loading liquid-liquid results.

Laminar (and especially paper) chromatographic results can also be affected by appreciable variations of the A_m/A_s ratio along the chromatogram. In some instances, variations in the eluent composition can also take place, near to the front of the eluent. Both of these experimental uncertainties can considerably affect the results of slope analysis.

Extension of slope analysis to a study of the influence of the stationary phase parameters is very difficult because of the lack of knowledge of the actual physical and chemical properties of the combination extractant plus support. Two different approaches have been followed, one regarding the stationary phase as a sort of "solution" of the extractant in the support material, the other one considering the extractant as a well defined liquid phase invading the pores and filming on the surface of the solid support².

In the former case, variations of extractant loading per unit weight of support should change the activity of the stationary phase. If these activities could be estimated, slopes should approach the value of coefficient m in the extraction equation; in any event, log-log plots of results against the amount of loaded extractant need not necessarily give straight lines. In the latter case, the activity should keep constant for any extractant loading within a reasonable range, and log-log plots of results against extractant loading should give straight lines of slope $+1$, because of the linear variations of V_s (or A_s) in the right-hand sides of eqns. 3 and 4.

The problem has not been studied thoroughly. Most available results support the latter approach, but there are also data that undoubtedly indicate a dependence of the stationary phase activity on the amount of loaded extractant. Attempts have been made to derive a relationship between the activity of the extractant and its amount loaded on the support², but apparently they are not completely satisfactory: the seemingly good results were probably derived from a "vicious circle". Very recently, Siekierski⁹ has discussed theoretically the activity of an extractant that is fixed onto a support as a definite liquid phase. As the outer film of extractant is in equilibrium with that portion of it which enters the pores of the solid material, the activity can be derived from that of the free liquid extractant by calculating the change in chemical potential for forming capillary liquid from free liquid. For supports that have particularly small pore diameters, such as silica gel, the activity of the fixed extractant should be considerably lower than that of the free liquid, but this would have little effect on the distribution coefficient of metals, as a comparable decrease is also expected in the activity coefficient of the extracted species.

In the author's opinion, the actual physical meaning of the stationary phase probably depends on the nature of the supporting material. In most cases, the extractant should be considered as definitely separated from the support, and filmed on it: this applies reasonably to systems involving polytetrafluoroethylene, polytrifluorochloroethylene, polyethylene, Kieselguhr, silica gel, glass and probably cellulose. With other materials, such as styrene-divinylbenzene and vinyl chloride-vinyl acetate copolymers and polyurethane foams, the extractant is likely to be "dissolved" in the support.

The theoretical interpretation of extraction chromatographic results could be even more complicated than outlined above, as the applicability to such systems of the classical partition theories can also be considered. Actually, stationary phases in extraction chromatography have polar groups that give them an electrical nature very similar to that of the aqueous solutions used as the mobile phase, and the ion-containing species that undergo partition between the two phases often result from the simultaneous coordination of ions by molecules of both the stationary and mobile phases. This led Bark and Duncan¹⁰ to express "some doubt concerning the absolute chromatographic and physical boundaries of the two phases", on the existence of which all classical chromatographic equations are based.

From experiments carried out with thin layers loaded with different extractants, Bark and Duncan¹⁰ proposed the following general correlation between R_F and D :

$$D = A \left(\frac{1}{R_F} - 1 \right) - B \quad (5)$$

differing from the Martin and Synge equation not only in the existence of an additional term B , but also in the possible large disagreement between the A values and the corresponding ratio of the cross-sectional areas of the two phases, as determined experimentally.

Bark and co-workers interpreted eqn. 5 in the light of both partial mutual solubility of the two phases and of possible inactivity in the chromatographic process of a part of the active groups of the stationary phase, consumed in binding to the support. Most probably, at least three layers build up (stationary phase-interface-eluent), instead of the two definite layers considered in ideal liquid-liquid chromatographic conditions¹¹. A fourth layer could also exist, consisting of a portion of stationary phase bound to the support and unavailable for extraction. The volumes of stationary and mobile phases should take into account the volume variations that apparently occur in liquid-liquid extraction, and their ratio would therefore depend on the composition of the aqueous phase; the nature of the interface and its role in the dynamic chromatographic process are rather obscure.

The author developed Bark's result in the hypothesis of a portion of mobile phase that does not move with the rest of the eluent, as a reasonable simplification of the interfacial layer model. Although the available data were not sufficient to draw any conclusion, the resulting volumes of the different layers were reasonably consistent among themselves, and with the additional information available from Bark's work and from liquid-liquid extraction experience.

Unfortunately, in spite of the interesting implications of eqn. 5 for both laminar and column chromatography, no further investigation was carried out to

check the above interpretations or to define better the parameters possibly involved in the non-ideality of the system. It is worth pointing out that the term B in eqn. 5, which implies a partial retention also for elements whose distribution coefficient is zero, is in sharp contrast with the experimental evidence of spots running with the front of the eluent in most thin-layer extraction chromatographic systems, if one does not assume that the extracted metal itself is the main species responsible for the existence of the interfacial layer. This assumption finds support in the inverse relationship between R_F values and A_m/A_s ratios ($\approx A$ term) calculated by Bark by comparing distribution coefficients and chromatographic results for each element (see Table IV in ref. 10). Therefore, it is rather unsatisfactory to assess definite A and B values by averaging data obtained with different elements, having different R_F values, as done in ref. 10 and in the above-reported development of those data made by the present author.

CONCLUSIONS

Extraction chromatography with liquid anion and cation exchangers as the stationary phase appears to be a very attractive means for the separation of inorganic substances for analytical purposes, and often gives consistent advantages as an alternative to conventional ion-exchange resins.

Suitable development of extraction chromatographic results will enable useful information to be obtained on the mechanism underlying the distribution of elements between the two chromatographic phases, so as to permit one either to check qualitatively the validity of already well known liquid-liquid extraction processes, or to investigate the chemistry of new extraction systems.

However, theoretical developments are severely limited by several factors (more or less recognized by extraction chromatography investigators), the most important of which are the very scarce knowledge of the actual physical and thermodynamic status of extractant plus support combinations, and reasonable doubts on the applicability of the classical partition equations to such chromatographic systems. The interest that extraction chromatography has, both in itself and because of its potential usefulness as an aid in understanding liquid-liquid extraction processes, should lead to future systematic investigations that could throw light on the many theoretical aspects that are still unexplored.

REFERENCES

- 1 I. Stroński, *Oesterr. Chem.-Ztg.*, 68 (1967) 5.
- 2 E. Cerrai and G. Ghersini, *Advan. Chromatogr.*, 9 (1970) 3.
- 3 U. A. Th. Brinkman, in E. S. Perry and C. J. van Oss (Editors), *Progress in Separation and Purification*, Vol. 4, Wiley-Interscience, New York, 1971, p. 241.
- 4 P. Markl, *Extraktion und Extraktions-Chromatographie in der anorganischen Analytik*, Akademische Verlagsgesellschaft, Frankfurt/M., 1972.
- 5 G. S. Katykhin, *Zh. Anal. Khim.*, 27 (1972) 849.
- 6 T. Braun and G. Ghersini (Editors), *Extraction Chromatography*, Akadémiai Kiadó, Budapest, 1975, in press.
- 7 J. F. K. Huber, *3rd Symposium on Ion Exchange, Balatonfüred, 1974*, paper P03.
- 8 G. Ghersini, in T. Braun and G. Ghersini (Editors), *Extraction Chromatography*, Akadémiai Kiadó, Budapest, 1975, Ch. 4, in press.

- 9 S. Siekierski, in T. Braun and G. Gherisni (Editors), *Extraction Chromatography*, Akadémiai Kiadó, Budapest, 1975, Ch. 1, in press.
- 10 L. S. Bark and G. Duncan, *J. Chromatogr.*, 49 (1970) 278.
- 11 L. S. Bark, personal communication, 1973.

CHROM. 7736

THE USE OF AQUEOUS THIOCYANATE SOLUTIONS IN LIQUID-LIQUID EXTRACTION AND REVERSED-PHASE EXTRACTION CHROMATOGRAPHY. I

U. A. Th. BRINKMAN, G. DE VRIES, R. JOCHEMSEN and G. J. DE JONG

Free Reformed University, Amsterdam (The Netherlands)

SUMMARY

Ten ions have been chromatographed on thin layers of cellulose impregnated with Aliquat 336, Alamine 336 S, Amberlite LA-1 or Primene JM-T, and on non-impregnated cellulose. Solutions of 0.3–7 *M* thiocyanate acidified with 0.01–1.0 *N* hydrochloric acid are used as eluents. R_F spectra and a number of separations are reported. Percentage extraction *versus* NCS^- molarity data and results of maximum-loading and spectroscopic measurements for the systems liquid anion exchanger–Co(II)– NCS^- and liquid anion exchanger–Ni(II)– NCS^- are also reported.

The sorption strength/extraction efficiency of the exchangers increases in the order Primene < Amberlite < Alamine < Aliquat. Increasing the acidity of the aqueous phase generally decreases the sorption/extraction of the complex metal-thiocyanato anions to a considerable extent. Sorption proceeds through anion exchange for all ions investigated. The Co(II)-containing species extracted into the organic phase is $(\text{R}_3\text{R}'\text{NH}^+)_2\text{Co}(\text{NCS})_4^{2-}$ (R, alkyl; R', alkyl or H). Nickel is present in the organic phase predominantly as $\text{Ni}(\text{NCS})_6^{4-}$; however, depending upon the diluent used, $\text{Ni}(\text{NCS})_4^{2-}$ may also be present.

INTRODUCTION

Extraction of metal-thiocyanato complexes from aqueous solutions into water-immiscible solvents has been known for over 100 years. In 1863, Braun¹ showed that the coloured thiocyanato complex of molybdenum, which is formed upon reduction (however, see ref. 2) of molybdic acid with zinc in the presence of thiocyanate salts, is extracted by diethyl ether. Since that data, over 400 papers on thiocyanate extraction have been published, as can be ascertained from a recent literature review by Sultanova *et al.*³. Still, as these authors state, relatively little progress has been made in the elucidation of the mechanism(s) involved in thiocyanate extraction systems. Actually, results are rather meagre even as regards the extraction behaviour of HNCS itself. In recent years, high-molecular-weight amines and substituted quaternary ammonium salts, so-called liquid anion-exchangers, have shown high potential for use in liquid-liquid extraction and reversed-phase chromatography. However, here too, thiocyanate systems have been little exploited, despite promising

features such as the fact that metal-thiocyanato complexes are often more completely extracted than are, for example, metal-chloro complexes. In this paper, preliminary results of a systematic investigation of the liquid anion exchanger-NCS⁻ system are reported.

MATERIALS AND METHODS

Data on the anion exchangers used in the present study are given in Table I.

TABLE I
CHARACTERISTICS OF SOME LIQUID ANION EXCHANGERS

Type	Name	Composition	Mean mol. wt.	Manufacturer
Primary	Primene JM-T	Trialkylmethylamine	310	Rohm and Haas*
Secondary	Amberlite LA-1	Dodecenylntrialkylmethylamine	372	Rohm and Haas*
Tertiary	Alamine 336 S	Tri- <i>n</i> -(octyl + decyl)amine	392	General Mills**
Quaternary	Aliquat 336	Methyltri- <i>n</i> -(octyl + decyl)- ammonium chloride	475	General Mills**

* Philadelphia, Pa., U.S.A.

** Kankakee, Ill., U.S.A.

Chromatography

Chromatography was carried out as described in previous papers, using microcrystalline cellulose (Avicel TG104, Macherey, Nagel & Co., Düren, G.F.R.) as support. Amines are converted into their thiocyanate salts by equilibrating a 0.1 *M* solution in chloroform with an aqueous 2 *M* ammonium thiocyanate solution containing 0.12 *N* hydrochloric acid. Quaternary ammonium chlorides are converted into the corresponding thiocyanates by three consecutive equilibrations with 2 *M* ammonium thiocyanate solution containing 0.02 *N* hydrochloric acid. Suspensions of impregnated cellulose are prepared by thoroughly mixing the solution in cellulose-chloroform (1:4, w/v). The suspension is stored overnight and agitated again before use. Chromatoplates are prepared by dipping ordinary microscope slides into the suspension. After evaporation of the chloroform, a thin film of impregnated support material adheres to the slides; superfluous material is wiped off the back. Subsequently, a series of scores is made in the thin layer; as a result, six *ca.* 3.5-mm wide tracks appear on the chromatoplate, and small margins remain along the edges. Six spots (diameter *ca.* 1 mm) are applied on to each plate using a pointed paper wick partly impregnated with the solution to be analyzed. Sample solutions of the ions (as their chloride or nitrate salts) contain 1–10 mg/ml of cation. Ascending chromatography is carried out for a 3-cm run in suitable vessels, *e.g.*, Hellendahl staining jars. The development is terminated when the eluent reaches a previously applied groove in the cellulose layer. After drying the plates in the air, detection of all ions except Ag(I) and Cr(III) is achieved using a 0.2% solution of 4-(2-pyridylazo)resorcinol (PAR) in 80% ethanol, and subsequent treatment with ammonia vapour. Ag(I) is identified by spraying with a freshly prepared 0.2% solution of dithizone in 80% acetone, followed by treatment with ammonia. The spots of Cr(III) are made visible by spraying with

a 0.2% solution of diphenylcarbazone in 80% ethanol and subsequent heating to 200°. Details of the experimental procedure and the apparatus required are reported elsewhere⁴.

Extraction

An aqueous Co(II) or Ni(II) solution of suitable composition is shaken for 20 min with an equal volume of a solution of a liquid anion exchanger (as its thiocyanate salt) in toluene. After separation of the phases, an aliquot of the organic phase is pipetted into an erlenmeyer flask and the metal ion content is determined titrimetrically using the extractive end-point determination described below (Co and Ni) or spectrophotometrically at $\lambda = 630$ nm (Co only). UV-visible spectra are recorded on a Perkin-Elmer 402 spectrometer.

RESULTS AND DISCUSSION

Chromatography

In order to study the dependence of the extraction efficiency of the liquid anion exchangers on their structure, reversed-phase chromatography was performed for ten ions, viz., Al(III), Fe(III), Co(II), Ni(II), Zn(II), Ag(I), Cd(II), Pb(II), Th(IV) and U(VI). Solutions of 0.3–7 *M* ammonium thiocyanate acidified with 0.3 *N* hydrochloric acid were used as eluents. The results obtained with four exchangers, representing primary to tertiary amines and quaternary ammonium salts, are presented in Fig. 1. When using non-impregnated cellulose, all ions move with the solvent front over the whole NCS⁻ concentration range investigated.

The results in Fig. 1 agree favourably with literature results obtained by reversed-phase paper (tertiary amines⁵) and thin-layer (secondary amine⁶) chromatography. They clearly demonstrate that the sorption strength of the exchangers in-

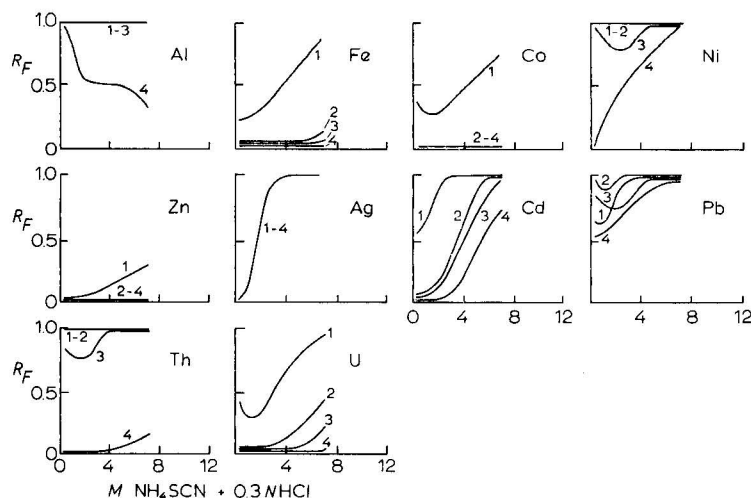


Fig. 1. R_F versus molarity of NH_4NCS spectra for ten ions, using cellulose impregnated with 1, Primene; 2, Amberlite LA-1; 3, Alamine 336 S; or 4, Aliquat 336.

creases in the order primary < secondary < tertiary < quaternary. This result contrasts with literature data on halide⁷ and nitrate⁸ systems. In these systems, sorption also increases from primary to tertiary exchangers; however, the behaviour of tertiary and quaternary exchangers usually does not differ significantly. In order to ascertain whether the divergent behaviour of tertiary and quaternary exchangers is a characteristic of thiocyanate systems, next to Aliquat and Alamine, three further pairs of structurally related tertiary and quaternary exchangers were studied. With Adogen 464 and 368 (mean mol.wt. 430; Archer-Daniels-Midland, Minneapolis, Minn., U.S.A.), which have a composition roughly comparable with that of Aliquat and Alamine, respectively, the sorption strength of the quaternary compound also surpasses that of its tertiary analogue. However, when using extractants with lower molecular weights, such as tri- and tetra-*n*-butyl- and tri- and tetra-*n*-hexylammonium thiocyanates, the differences in sorption strength between the two classes of exchangers disappear. No satisfactory explanation for these phenomena (experimental details of which will be published elsewhere⁹) can as yet be forwarded. However, in itself it is noteworthy that tri- and tetrabutylammonium salts can serve as useful impregnants in reversed-phase chromatography in thiocyanate systems; for it is known¹⁰ that in chloride systems, for example, the butylammonium salts dissolve in the aqueous mobile phase and appear as a dark, oily band immediately behind the solvent front.

In order to study the influence of the acidity of the mobile phase on the R_F values of the metal ions, experiments were performed on Aliquat-impregnated cellulose, using solutions of ammonium thiocyanate containing 0.01–1.0 *N* hydrochloric acid as eluents. The R_F spectra in Fig. 2 indicate that increasing the acidity of the eluent decreases the sorption of all ions except Ag(I). No results are included for Fe(III), Co(II) and Zn(II), because these ions have $R_F = 0.0$ in all instances. Their movement is negligibly small even when Aliquat is replaced with the much weaker sorbing Amberlite LA-1. Obviously, changing the acidity of the eluent is a powerful means of creating suitable conditions for metal ion separations.

As regards Ag(I), its R_F values at a fixed ammonium thiocyanate concentration vary neither with the type of exchanger selected for impregnation of the support nor with the acidity of the mobile phase. Usually, such behaviour indicates that the

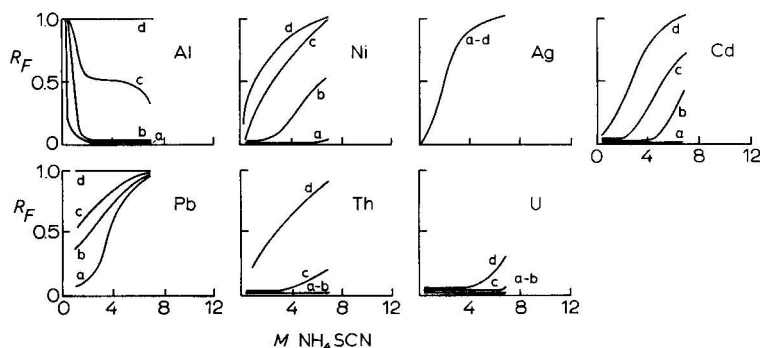
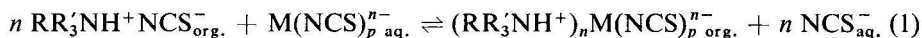


Fig. 2. Dependence of R_F values on acidity of the mobile phase. Stationary phase: cellulose impregnated with Aliquat 336. Mobile phase: solutions of NH_4NCS containing the following concentrations of HCl : a, 0.01 *N*; b, 0.1 *N*; c, 0.3 *N*; d, 1.0 *N*.

anion exchangers do not play a significant role, *i.e.*, phenomena such as adsorption to the support and precipitation of insoluble metal salts govern the sorption process. However, in the present case, Ag(I) moves with the solvent front on non-impregnated cellulose. Therefore, one must conclude that a specific interaction of the silver-thiocyanato complex ion with the liquid anion exchangers does occur.

The overall results indicate that for the ions under investigation, the sorption process may be represented by



(R, alkyl; R', alkyl or H).

It is interesting to note that in most instances the R_F values increase monotonously with increasing acid and thiocyanate concentration. This is in marked contrast with the results reported for exchanger-hydrochloric acid systems⁷, in which sorption often increases with increasing hydrochloric acid concentration. Obviously, strong complexation between metal ions and NCS^- often already occurs at low NCS^- concentrations. Desorption at higher concentrations may be attributed to factors such as the strong competition due to the uptake of HNCS in excess of the amount necessary for stoichiometric neutralization of the amine, *i.e.*, to the formation of $\text{RR}'_3\text{NH}^+\text{NCS}^- \cdot x\text{HNCS}$, increasing competition of the excess of NCS^- itself, and/or the formation of higher metal-thiocyanato complexes, which are expelled from the organic phase on account of their high negative charge.

Lastly, as regards eqn. 1, direct proof of the nature of the sorbed metal-thiocyanato complex was obtained in the case of Co(II). A spot of the metal ion, applied to cellulose impregnated with Aliquat⁺ NCS^- and eluted with an aqueous ammonium thiocyanate solution, was scanned over the range 270–750 nm using a Zeiss PMQ II spectrometer with a thin-layer attachment. The UV-visible absorption spectrum of the spot is virtually identical with that recorded for Co(II)-containing extracts obtained in liquid-liquid extraction: maxima occurring at 630, 592 (shoulder) and 333 nm demonstrate that the sorbed complex ion is $\text{Co}(\text{NCS})_4^{2-}$ (see below).

Separations. Some examples of separations are shown in Fig. 3. Particular attention is drawn to the analysis of the mixture of Al(III), Cr(III) and Ni(II). For most chromatographic systems, the separation of these ions meets with considerable problems, owing to their weak complexing tendency with inorganic ligands. It is

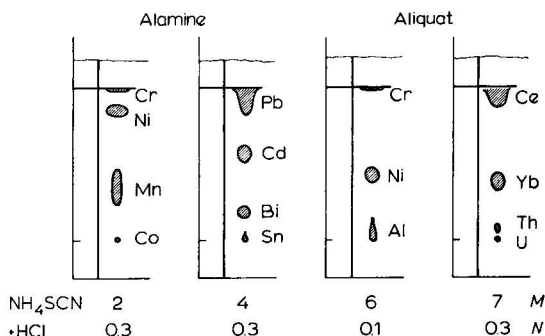


Fig. 3. Examples of thin-layer separations in two liquid anion exchanger- NH_4NCS systems.

interesting to note that in the present system, Cr(III), the very ion known to form a series of well defined anionic thiocyanato complexes, moves with the solvent front. Obviously, under the conditions of the system studied, $[\text{Cr}(\text{H}_2\text{O})_6]^{3+}$ is kinetically inert, so that replacement of the water ligand with the thiocyanato ligand does not take place^{6,11}.

Extraction of Co(II) and Ni(II)

Titrimetric determination. One of the few disadvantages of the use of liquid anion exchangers is the time-consuming back-extraction that is usually necessary in order to complete the determination of an extracted metal ion. In the present study, therefore, a two-phase titration with extractive end-point was used, based on a procedure originally described by Cameron and Gibson¹² for the determination of Co(II), Ni(II), Cr(III) and several other ions. A known excess of EDTA is added to the titration mixture, and back-titration is carried out with standard Co(II) solution, using thiocyanate ions as indicator in the presence of a solution of triphenylarsonium chloride (or tetra-*n*-hexylammonium chloride¹³) in chloroform. At the end-point, a blue ion-association complex is extracted into the organic phase. The results in Fig. 4 indicate that the extraction of Co(II) by Aliquat is quantitative under suitable conditions, so that this inexpensive, technical-grade product can also be used to help indicate the end-point.

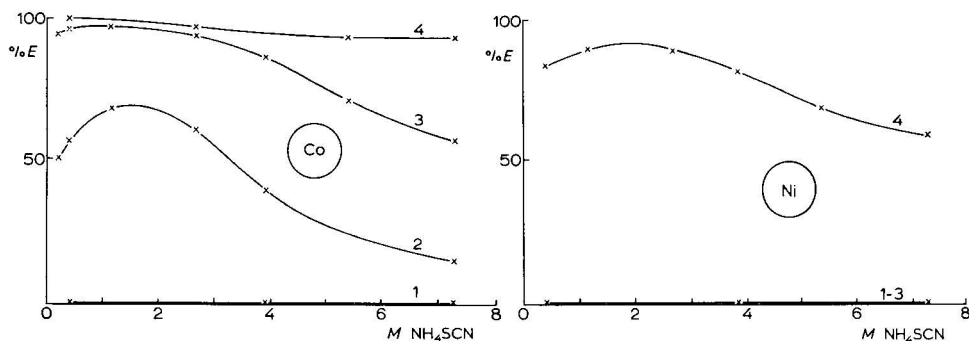


Fig. 4. Percentage extraction *versus* molarity of NH_4SCN curves for Co(II) and Ni(II). Organic phase: 0.1 *M* solution of a liquid anion exchanger (thiocyanate form) in toluene. Aqueous phase: 0.02 *M* Co(II) in *x M* NH_4SCN + 0.3 *N* HCl; 0.02 *M* Ni(II) in *x M* NH_4SCN + 0.02 *N* HCl. 1, Primene; 2, Amberlite LA-1; 3, Alamine 336 S; 4, Aliquat 336.

As liquid-liquid extractions are often performed in diluents such as toluene or xylene, which have a lower density than water, the titration procedure forces one to change the composition of the organic phase. This problem is adequately solved by using a solution of Aliquat in carbon tetrachloride, adding this to the organic metal-containing extract in a volume ratio of 1:1. Irrespective of the presence or absence of another liquid anion exchanger, provided it is not too highly coloured, a sharp colour change marks the end-point of the titration.

The complete procedure is as follows. A 5-ml volume of the Co(II)- or Ni(II)-containing organic extract is pipetted into a stoppered erlenmeyer flask. After the addition of 5 ml of a 0.1 *M* solution of Aliquat (chloride) in carbon tetrachloride, a

known excess of EDTA and 10 ml of 2 *M* potassium thiocyanate solution, dilute ammonia is added until an alkaline reaction is observed. Subsequently, the mixture is shaken for a few minutes in order to effect complexation of the metal ion with EDTA. Back-titration is carried out with a standard Co(II) solution until a permanent light blue colour persists in the organic phase. The mixture must be shaken vigorously near the end-point.

Extraction and separation. Results on the extraction of Co(II) and Ni(II) by solutions of each of the four liquid anion exchangers in toluene are presented in Fig. 4. Obviously, the extraction efficiency increases in the same order as the sorption strength in reversed-phase chromatography. This result, which is to be expected on the basis of the relationship $D = k (1/R_F - 1)$ (D = distribution coefficient; k = constant), has amply been verified for, e.g., chloride, bromide and nitrate systems¹⁰.

It is apparent from Fig. 4 that the extraction of Co(II) by solutions of Alamine is quantitative when suitable acid and thiocyanate concentrations are used, whereas the extraction of Ni(II) is negligible. Therefore, trace amounts of cobalt can be successfully removed from concentrated solutions of nickel salts without any loss of nickel. As the Co(II)-containing complex present in the organic phase has a high molecular extinction coefficient ($\epsilon_{630} = 1750$; see below), the amount of Co(II) present can easily be determined.

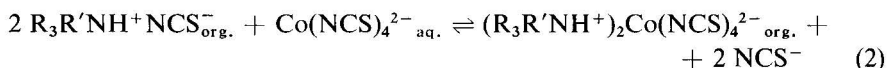
In a typical set of experiments, a 1 *M* solution of nickel chloride in 0.2 *M* ammonium thiocyanate + 0.02 *N* hydrochloric acid, containing 10^{-2} – 10^{-5} *M* Co(II), was shaken with an equal volume of a 0.1 *M* solution of AlamineH⁺NCS[−] in toluene. After extraction and phase separation, the spectrum of the organic extract was recorded and the percentage of Co(II) extracted calculated. When using 10^{-3} *M* or even more dilute cobalt solutions, a single extraction suffices for quantitative ($\geq 99.9\%$) removal of cobalt. With 10^{-2} *M* Co(II) solutions, two consecutive extractions are necessary in order to achieve this result. As the detection limit of cobalt can easily be lowered by about an order of magnitude by changing the volume ratio $V_{\text{org.}}:V_{\text{aq.}}$ to ca. 1:10, liquid–liquid extraction can be used to remove 1 – $10^{-4}\%$ of cobalt from nickel salts and determine it quantitatively.

Nature of the complexes. Data on the composition of the extracted Co(II)–thiocyanato complex are meagre and, moreover, conflicting. According to Selmer-Olsen¹⁴, who used triisooctylamine, the extracted species is $[\text{Co}(\text{SCN})_4]^{2-} \cdot 2 \text{R}_3\text{NH}^+ \cdot 2 \text{R}_3\text{NHCl} \cdot 2 \text{HSCN}$. Watanabe and Akatsuka¹⁵, however, on the basis of maximum-loading data, concluded that the blue-coloured species extracted with tri-*n*-octylamine in various diluents is $(\text{R}_3\text{NH}^+)_2\text{Co}(\text{SCN})_4^{2-}$. Lastly, Laskorin and Timofeeva¹⁶, who used the method of continuous variation and of maximum loading, reported that the extracted species has a Co:NCS[−]:amine ratio of 1:2:2.

In this study, the composition of the extracted Co(II)-containing species was determined using both Aliquat and Alamine, as it has occasionally been observed in anion exchanger– M^{n+} – X^- systems that additional molecules of exchanger are attached to a tertiary alkylammonium complex metal salt, whereas such a phenomenon is never encountered with substituted quaternary alkylammonium salts (examples: Fe^{3+} – Cl^- ; In^{3+} – Cl^- ; UO_2^{2+} – NO_3^- ; refs. 17–19).

UV–visible spectra of Co(II)-containing extracts show a characteristic absorption band with $\lambda_{\text{max.}} = 630$ nm and a shoulder at 592 nm. An intense absorption peak at 330 nm, which occurs in the spectra of many metal–thiocyanato complexes,

can most probably be attributed to intraligand transitions²⁰. Determination of the ratio [Co(II):exchanger]_{org.} as a function of the aqueous metal ion concentration, the concentrations of the exchanger and (excess) NCS⁻ being kept constant, yields a maximum-loading value of $1:2.0 \pm 0.1$, irrespective of the use of Aliquat or Alamine. The same result is obtained when determining the ratio Co(II):exchanger of the extracted species by the construction of mole-ratio plots; here, the concentration of the exchanger is increased at constant concentrations of the metal ion and (excess) NCS⁻. In conclusion, the extraction of Co(II) by Aliquat and Alamine may be represented by



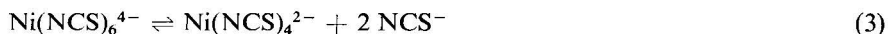
thereby confirming Watanabe and Akatsuka's results. As regards the different conclusions reached by Selmer-Olsen, we have re-investigated some of her experiments in our laboratory, the substitution of triisooctylamine by Alamine being the only important change. According to our results, under the conditions used by Selmer-Olsen, the ratio Co:amine:NCS⁻ is indeed 1:4:6. However, instead of Cl⁻, NO₃⁻ is present in the organic phase; moreover, maximum loading of the organic phase has not yet been reached. Probably the organic extracts analyzed by Selmer-Olsen contained free R₃NH⁺ (NCS⁻, NO₃⁻) · xH⁺ (NCS⁻, NO₃⁻) next to (R₃NH⁺)₂Co(NCS)₄²⁻. The rather implausible results obtained by Laskorin and Timofeeva can possibly be explained in an analogous way.

The relatively low extraction efficiency of secondary and primary amines does not allow one to extend the present investigation to Amberlite and Primene. However, the identical shape of the UV-visible spectra of Co(II)-containing extracts obtained with all four liquid anion-exchangers demonstrates that the complex metal anion is Co(NCS)₄²⁻ in all instances. In this context, it is interesting to note that the molar extinction coefficient ϵ_{630} has a value of 1850 in the case of Aliquat, whereas distinctly lower values are obtained with the amines, *e.g.*, 1750 in the case of Alamine. A similar phenomenon has been observed for the exchanger-Co(II)-Cl⁻ system^{21,22}. Probably the lowering of the ϵ values observed is due to a disturbance of the symmetry of the tetracoordinated complex metal ion, caused by the formation of hydrogen bonds of the type N-H...SCN and N-H...Cl.

The study of the nature of the nickel-thiocyanato complex has, for obvious reasons, been limited to systems containing Aliquat. The UV-visible spectra of Ni(II)-containing extracts show peaks at 710 and 420 nm, irrespective of the aqueous thiocyanate concentration used in the extraction procedure. These results may be compared with those recorded by De Haas²³ in his study of dilute solutions of nickel thiocyanate in molten dimethylsulphone containing mixtures of potassium and tetrabutylammonium thiocyanate. According to De Haas, both octahedrally and tetrahedrally coordinated nickel-thiocyanato complexes exist in solution, which show absorption peaks at 720 and 400 nm and 670 and 600 nm, respectively. On the basis of his interpretation, we may conclude that in the Aliquat extracts nickel is present as Ni(NCS)₆⁴⁻.

In a separate set of experiments, it was demonstrated that increasing the polarity of the organic phase by adding (increasing) amounts of, *e.g.*, nitrobenzene or acetophenone to toluene changes the absorption spectrum considerably: the peak at

710 nm gradually disappears, while new peaks emerge at 670 and 630 nm. That is, with increasing polarity of the organic phase, the equilibrium



shifts to the right.

The extraction efficiency of solutions of Aliquat in toluene towards nickel is small compared with that towards cobalt (see the legend to Fig. 4). Moreover, usually this efficiency strongly decreases when increasing polarity of the organic phase. Therefore, the maximum-loading and the mole-ratio techniques are of limited value in the Aliquat–Ni(II)–NCS[−] system. As a consequence, no quantitative correlation has yet been established between the percentage of more polar solvent added to toluene and the value of the ratio Ni(NCS)₆^{4−}:Ni(NCS)₄^{2−}.

REFERENCES

- 1 C. D. Braun, *Z. Anal. Chem.*, 2 (1863) 36.
- 2 I. P. Greenland and E. G. Lillie, *Anal. Chim. Acta*, 69 (1974) 335.
- 3 Z. Kh. Sultanova, L. K. Chuchalin, B. Z. Iofa and Yu. A. Zolotov, *J. Anal. Chem. USSR*, 28 (1973) 369.
- 4 G. de Vries and U. A. Th. Brinkman, *J. Chromatogr.*, 64 (1972) 374.
- 5 S. Przeszlakowski, *Chem. Anal. (Warsaw)*, 12 (1961) 57.
- 6 R. J. T. Graham and A. Carr, *J. Chromatogr.*, 46 (1970) 301.
- 7 U. A. Th. Brinkman, G. de Vries and E. van Dalen, *J. Chromatogr.*, 22 (1966) 407.
- 8 U. A. Th. Brinkman, G. de Vries and E. van Dalen, *J. Chromatogr.*, 23 (1966) 287.
- 9 G. J. de Jong and U. A. Th. Brinkman, in preparation.
- 10 U. A. Th. Brinkman, *Progr. Sep. Purif.*, 4 (1971) 241.
- 11 B. E. McClellan, M. K. Meredith, R. Parmelee and J. P. Beck, *Anal. Chem.*, 46 (1974) 306.
- 12 A. J. Cameron and N. A. Gibson, *Anal. Chim. Acta*, 25 (1961) 24 and 429.
- 13 H. M. N. H. Irving and R. H. Al-Jamah, *Chem. Anal. (Warsaw)*, 17 (1972) 779.
- 14 A. R. Selmer-Olsen, *Anal. Chim. Acta*, 31 (1964) 33.
- 15 H. Watanabe and K. Akatsuka, *Anal. Chim. Acta*, 38 (1967) 547.
- 16 B. N. Laskorin and V. K. Timofeeva, *Zh. Prikl. Khim.*, 36 (1963) 37.
- 17 U. A. Th. Brinkman, G. de Vries and E. van Dalen, *J. Chromatogr.*, 31 (1967) 182.
- 18 A. D. Nelson, J. L. Fasching and R. L. McDonald, *J. Inorg. Nucl. Chem.*, 27 (1965) 439.
- 19 P. R. Danesi, F. Orlandini and G. Scibona, *J. Inorg. Nucl. Chem.*, 27 (1965) 449.
- 20 Zs. Szabó-Ákos, V. Izvekov and E. Pungor, *Mikrochim. Acta*, (1974) 187.
- 21 M. G. Kuzina, A. A. Lipovski and S. A. Nikitina, *Russ. J. Inorg. Chem.*, 16 (1971) 1313.
- 22 H. R. Leene and U. A. Th. Brinkman, unpublished results.
- 23 K. S. de Haas, *Inorg. Nucl. Chem. Lett.*, 9 (1973) 947.

CHROM. 7708

SEPARATION OF METALS ON ION-EXCHANGE RESINS BY MEANS OF α -HYDROXYISOBUTYRONITRILE AS COMPLEXING AGENT

LÁSZLÓ LÉGRÁDI

26 Sagariu Street, 8184 Füzfőgyártelep (Hungary)

SUMMARY

α -Hydroxyisobutyronitrile (acetone cyanohydrin, ACH) reacts with metals in ammoniacal medium and yields cyano complexes of negative charge. On this basis, Ni^{2+} , Cu^{2+} , Hg^{2+} , Zn^{2+} , Cd^{2+} and Fe^{2+} can be separated on a strongly basic anion exchanger in the chloride form as cyano complexes from Mg^{2+} , Ba^{2+} , Ca^{2+} , Na^{+} and K^{+} . The structures of complexes were examined on a strongly basic anion exchanger in the Cl^{-} form and on a strongly acidic cation exchanger in the H^{+} form. In slightly ammoniacal medium, $\text{Cu}(\text{CN})_4$, $\text{Co}(\text{CN})_{3.6}$ and $\text{Ni}(\text{CN})_{3.2}$ were found. The complex adsorbs on the anion exchanger in the Cl^{-} form as a divalent $[\text{NH}_4\text{Cu}(\text{CN})_4]^{2-}$ or a monovalent $[\text{NH}_4\text{Zn}(\text{CN})_4]^{-}$ complex ion.

INTRODUCTION

In an earlier paper¹, α -hydroxyisobutyronitrile (acetone cyanohydrin, ACH) was recommended as a masking agent to replace potassium cyanide in complexometric analysis. Cu^{2+} , Ni^{2+} , Hg^{2+} and Zn^{2+} can be masked with ACH in complexometric titrations. With 1 mole of $\text{Cu}(\text{NH}_3)_4\text{SO}_4$ complex 4 moles of ACH react to give a colourless $\text{Cu}(\text{CN})_4^{3-}$ complex. On this basis, ACH can be determined by titrating $\text{Cu}(\text{NH}_3)_4\text{SO}_4$ solution with ACH solution until the blue colour disappears. The disadvantage of the use of ACH as a masking agent in comparison with potassium cyanide is that fewer metals can be masked. This difficulty can be overcome by the use of an anion exchanger in the Cl^{-} form.

EXPERIMENTAL

Stock solutions

Preparation of alkaline copper cyano complex solution. Dissolve 2.4968 g of $\text{CuSO}_4 \cdot 5\text{H}_2\text{O}$ in 100 ml of water, add 3.4 g of ACH and ammonia until the precipitate formed re-dissolves and the blue colour of the solution disappears (pH = 9).

Preparation of neutral copper cyano complex solution. The preparation is the same as above. Add 4–5 ml of strongly acidic cation-exchange resin in the H^{+} form to the solution to adsorb the excess of ammonia. Filter the solution and dilute to 1 l (pH = 7).

Preparation of zinc cyano complex solution. Dissolve 1.363 g of ZnCl_2 and 3.4 g of ACH in 50 ml of water and add ammonia until the precipitate formed re-dissolves, then proceed as in the previous section. The solution can be neutralized only to pH 8 because of the precipitation of zinc hydroxide. The solution does not contain free zinc ions according to the complexometric determination. The excess of ACH can be detected by a colour reaction described below.

Determination of ACH

Titrimetric. Prepare 0.1 *M* copper tetra-amino complex solution as follows. Dissolve 2.4968 g of $\text{CuSO}_4 \cdot 5\text{H}_2\text{O}$ in 70 ml of water, add 10 ml of 25% ammonia solution, filter and dilute to 100 ml. To 10 ml of this solution, add 100 ml of water and 3 drops of ammonia solution and titrate with 0.4 *M* aqueous ACH (3.4 g per 100 ml) solution until the blue colour disappears; 10 ml of copper tetra-amino complex solution is equivalent to 10 ml of 0.4 *M* ACH solution.

Complexometric. To 10 ml of 0.01 *M* copper tetra-amino complex solution add 4–10 mg of ACH in aqueous solution, 2 ml of ammoniacal buffer and titrate the copper with 0.01 *M* EDTA using murexide as indicator.

In the presence of cyano complex. First prepare diazotized *p*-nitroaniline as follows. Dissolve 0.54 g of *p*-nitroaniline in 5 ml of 65% H_2SO_4 and dilute to 100 ml. Filter off the insoluble matter. To 5 ml of the *p*-nitroaniline solution add 1 ml of 17% H_2SO_4 and 4 ml of NaNO_2 solution (0.34 g per 100 ml). To 10 ml of the solution to be analyzed add 0.5 ml of diazonium salt solution and 0.8 ml of 2 *N* sodium hydroxide. In the presence of ACH an orange colour appears, and in its absence a yellow colour. The range for measurements is 0.2–6 mg of ACH.

Determination of copper and zinc cyano complexes

To 10–30 ml of a 0.01 *M* solution of the complex to be analyzed add 0.5–1.0 ml of 1 *N* H_2SO_4 and 0.2–0.3 g of ammonium peroxydisulphate and heat until the solution becomes clear. In the case of the zinc cyano complex the solution must be boiled for at least 5 min. Neutralize the solution with ammonia and titrate the metal content with 0.01 *M* EDTA.

Ion-exchange columns

In all experiments the same type of column of 6 mm I.D. was used. The height of the resin bed was 8 cm. The strongly basic resin used was Varion AD and the strongly acidic resin was Varion KS (Nitrokémia, Hungary) of the polystyrene-divinylbenzene type with a grain size of 20–50 mesh. The capacity of the anion-exchange columns was determined by the usual method and was found to be 3.2 mequiv.

Determination of Mg^{2+} in the presence of Ni^{2+} , Cu^{2+} , Hg^{2+} , Zn^{2+} , Cd^{2+} and Fe^{2+} on ion-exchange resin

To a solution containing about 10 ml of 0.01 *M* of interfering metals add 2 drops of 25% ammonia solution and 4 drops of ACH and allow the mixture to flow through the Cl^- -form column. To the effluent add 3 ml of ammoniacal buffer and titrate with EDTA using Eriochrome Black T as indicator.

Investigation of formation of cyano complexes on the anion exchanger

Allow 10 ml of 0.01 *M* metal salt solution to flow through 10 ml of Cl^- -form resin and titrate the metal content in the effluent complexometrically. Repeat the operation in the presence of 2 drops of 25% ammonia solution and 4 drops of ACH.

Investigation of formation of cyano complexes on the cation exchanger

Allow 10 ml of 0.01 *M* metal salt solution to flow through 10 ml of H^+ -form resin and titrate the effluent with 0.1 *N* sodium hydroxide using methyl orange as indicator. Repeat the operation in the presence of 2 drops of 25% ammonia solution and 4 drops of ACH.

Determination of breakthrough capacity

Allow a solution of 0.01 *M* metal cyano complex to flow through Cl^- -form resin of 3.2 mequiv. Collect the effluent in 50-ml fractions for analysis. On the basis of the obtained data construct the breakthrough curves. The concentrations found by analysis in the fractions are plotted against the volume of the effluent.

RESULTS

Investigation of complex formation on the anion-exchange resin

On the basis of the experiments carried out by Inczédy and Frankow², it was found that considerable adsorption of cyanide and also of metal complex cyanide ions took place on the hydroxide- and chloride-form resin beds only. As hydroxide-form resin cannot be employed because of the precipitation of metal hydroxide on the resin, a strongly basic resin in the chloride form was used. In the presence of ACH, metals will be adsorbed partly or completely as complex anions on the resin, depending on the affinity between the metals and ACH. If a metal does not react with ACH, it will not be held on the resin. According to our investigation, Zn^{2+} , Ag^+ , Hg^{2+} , Cd^{2+} , Ni^{2+} , Cu^{2+} and Fe^{2+} can be adsorbed quantitatively on the resin as complex anions. The binding of Co^{2+} is not complete in the presence of other metals. Pb^{2+} , Mn^{2+} , Sr^{2+} , Al^{3+} and Bi^{3+} react only partly with ACH. In the case of the last two metal ions, total binding can be obtained on the resin but mostly in the hydroxide form. Ca^{2+} , Ba^{2+} , Mg^{2+} , K^+ and Na^+ do not react with ACH on the resin. ACH itself can be adsorbed on the resin to the extent of only about 25%.

Investigation of complex formation on the cation-exchange resin

The metal salt solution passes through the column of H^+ -form resin and the acid content of the effluent is titrated with sodium hydroxide. In the presence of ammonia, the metal reacts with ACH and a cyano complex is formed:



Ammonia is adsorbed by the H^+ -form resin and a complex acid is formed. Consequently, the amount of sodium hydroxide consumed is increased by the reaction with ACH. If the metal does not react with ACH, then the amount of titrant consumed does not change. From the increase in the amount of sodium hydroxide consumed one can propose a structure for the complex. When a tetracyano complex is formed,

the amount of titrant consumed will be double in the case of a divalent metal as a consequence of the reaction of the metal with ACH. When the increase in the amount of titrant consumed is less, the formation of the tetracyano complex is incomplete. For example, if a tricyano complex is formed, the amount of sodium hydroxide consumed increases only by 50% according to the following equation:



On the basis of our investigation, the amount of titrant consumed did not increase in the case of Ba^{2+} , Ca^{2+} and alkali metals, indicating that these metals did not react with ACH. On the same basis, it appeared that Mn^{2+} , Sr^{2+} and Pb^{2+} react only slightly with ACH. This result agrees with those obtained on anion-exchange resins. In addition, in the case of Co^{2+} we found the structure to be $\text{Co}(\text{CN})_{3.6}$ and for Ni^{2+} the structure is $\text{Ni}(\text{CN})_{3.25}$. This means that the formation of the tetracyano complexes is not complete for these metals. In the case of other metals, interference effects appeared. With Ag^+ , Cu^{2+} , Zn^{2+} and Cd^{2+} , metal cyanide precipitates were formed on the resin owing to the acidic medium. In the case of Fe^{2+} , a blue solution occurred because of oxidation of hexacyanoferrate(II) to hexacyanoferrate(III).

Adsorption of complex cyanide on the anion-exchange resin

Neutral and alkaline copper and alkaline zinc cyano complex solutions were adsorbed on the Cl^- -form resin. These complex ions break through the columns quickly, especially in alkaline solution. The cyano complex ions appeared in the effluent at 85, 10 and 40 ml, respectively (Figs. 1 and 2). At the breakthrough points, the capacity of the column was utilized to the extents of only 18, 2 and 8%, respectively. At the end of the saturation process the extents of utilization were found to be 98, 85 and 86%, respectively. According to our analysis, 157 ml of 0.01 *M* copper cyano complex in neutral medium and 137 ml in alkaline solution, and 275.2 ml of

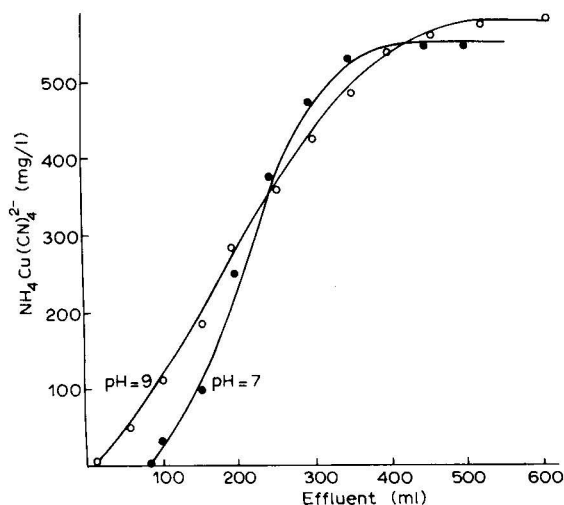


Fig. 1. Breakthrough curves of $\text{NH}_4\text{Cu}(\text{CN})_4^{2-}$ on anion-exchange resin in the chloride form.

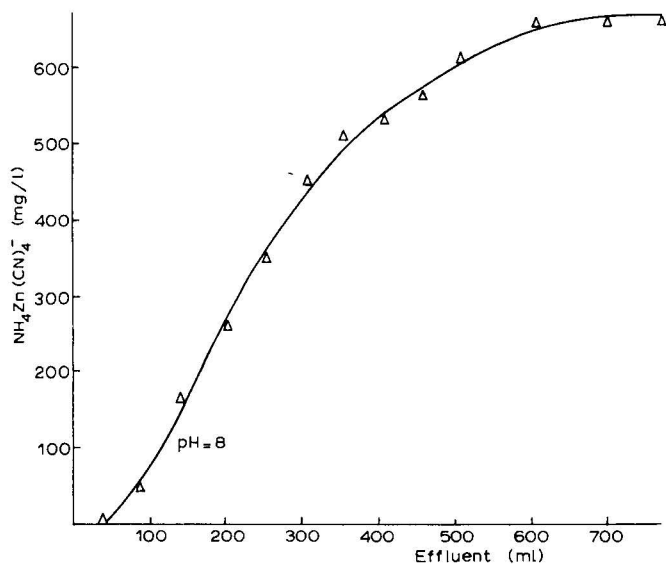


Fig. 2. Breakthrough curve of $\text{NH}_4\text{Zn}(\text{CN})_4^-$ on anion-exchange resin in the chloride form.

0.01 *M* zinc cyano complex, respectively, were bound to the columns. Considering the total capacity of the resin columns (3.2 mequiv.) and the amounts of the two species adsorbed, one must assume that a divalent copper and a monovalent zinc cyano complex were adsorbed with the compositions $\text{Cu}(\text{CN})_3^{2-}$ or $\text{NH}_4\text{Cu}(\text{CN})_4^{2-}$ and $\text{Zn}(\text{CN})_3^-$ or $\text{NH}_4\text{Zn}(\text{CN})_4^-$. The latter structure is the more probable in each case, as decomposition was not observed. On the basis of the results one can establish the order of adsorbability of metal cyano complexes: copper in neutral solution > copper in alkaline solution > zinc in alkaline solution.

DISCUSSION

The interaction between metals and ACH studied by means of anion and cation exchangers yielding tetracyano complexes occurs quantitatively in slightly ammoniacal medium only with copper. This is proved by the fact that ACH can be determined complexometrically with the aid of copper. To ACH is added $\text{Cu}(\text{NH}_3)_4\text{SO}_4$, the excess of which is measured. This determination of ACH is not possible with other metals. On the other hand, if ammonia is employed in large excess, then the reaction proceeds quantitatively with other metals also. For example, in the case of Zn^{2+} , the process takes place only to the extent of 25% in the complexometric determination, while in presence of a large excess of ammonia the tetracyano complex is formed quantitatively. In this case, the excess of ACH can be determined by a colour reaction with diazotized *p*-nitroaniline. On this basis, copper is the only metal suitable for the complexometric determination of ACH.

ACH can be used not only more satisfactorily than potassium cyanide for the masking of metals, but also for the preparation of cyano complexes and for the separation of metals on anion exchangers.

REFERENCES

- 1 L. Légrádi, *Z. Anal. Chem.*, 271 (1974) 284.
- 2 J. Inczédy and F. Frankow, *Period. Polytech., Chem. Eng. (Budapest)*, 11 (1967) 53.

CHROM. 7715

NEUARTIGE KATIONENAUSTAUSCHER AUF KIESELGELBASIS

I. DARSTELLUNG UND EIGENSCHAFTEN

NORBERT WEIGAND, IMRICH SEBESTIAN und ISTVÁN HALÁSZ

Angewandte Physikalische Chemie, Universität Saarbrücken (B.R.D.)

SUMMARY

New types of cation exchanger based on silica gel. I. Preparation and properties

The preparation and the properties of cation exchangers based on silica gel chemically modified with alkyl groups ("brushes" with $\equiv\text{Si}-\text{C}\equiv$ bond) are described. A maximum exchange capacity with a minimum cleavage of the $\equiv\text{Si}-\text{C}\equiv$ bond was achieved after sulfochloration by a gas-solid reaction. The exchange capacity depends on the specific surface of the silica gel carrier (250 $\mu\text{equiv./g}$ with 300 m^2/g).

The cation exchangers are stable against high pressure, and neither swell nor shrink. The bed volume is independent of the pH value and the ionic strength is independent of the eluent. The exchangers are stable in the pH range 0-8; their temperature stability is excellent.

EINLEITUNG

Die in der Säulenchromatographie verwendeten Ionenaustauscher mit organischer Matrix sind u.a. wegen ihrer relativ geringen Druckstabilität und ihrem Quellverhalten in Abhängigkeit von der Eluentenzusammensetzung für die Hochdruckflüssigchromatographie (HPLC) nur bedingt einsetzbar. Daher wurden für die HPLC druckstabile Ionenaustauscher entwickelt, bei denen auf einem inkompressiblen und nicht porösen Kern (Glaskugel) eine dünne Schicht eines organischen Ionenaustauschers aufgebracht wurde (pellicular ion exchanger)¹⁻³. Trotz ihrer niedrigen Kapazität (ca. 10 $\mu\text{equiv.}$) gelangen mit derartigen Austauschern vor allem auf dem Gebiet der Nucleinsäuren eine Vielzahl von Trennungen innerhalb weniger Minuten (zur Übersicht vgl. Lit. 4). Auch bei den anderen, teilweise handelsüblichen, Ionenaustauschern, die alle auf Dünnschichtkügelchen (z.B. auf Zipax, Corasil, u.a.) aufgebracht bzw. chemisch verankert sind, ist die Kapazität nicht oder nur unwesentlich grösser.

In der HPLC wird hauptsächlich Kieselgel als Adsorbens oder als Träger für die stationäre Phase verwendet. Werden Siebfraktionen mit kleinen Teilchendurchmessern verwendet, so erhält man Trennsäulen mit ausgezeichneter Trennleistung und hohen möglichen Analysengeschwindigkeiten. Zum anderen bietet gerade das Kiesel-

gel die Möglichkeit, durch einfache Reaktionen an der Oberfläche organische Moleküle mit verschiedenen funktionellen Gruppen chemisch zu verankern⁵⁻⁷. Die guten chromatographischen Trenneigenschaften und die mechanische Stabilität des Kieselgels bleiben bei derartigen Reaktionen erhalten, während die Selektivität auf Grund der neu eingeführten funktionellen Gruppen verändert wird. Wegen der hohen spezifischen Oberfläche von Kieselgel ist zu erwarten, dass die Zahl der eingeführten funktionellen Gruppen, d.h. die Ionenaustauschkapazität, relative gross sein wird.

Für die Darstellung von Ionenaustauschern ist allerdings die Verankerung von organischen Resten über $\equiv\text{Si}-\text{C}\equiv$ Bindungen erforderlich. Die Ionenaustauschgruppen werden nachträglich in die auf dem Kieselgel verankerten organischen Reste eingeführt. Am einfachsten ist die Sulfonierung von Arylgruppen, die auf dem Kieselgel über $\equiv\text{Si}-\text{C}\equiv$ Bindung verankert sind. Derartige Ionenaustauscher wurden bereits mehrfach beschrieben⁸⁻¹¹. Bei der Sulfonierung derartiger mit Aromaten bedeckter Kieselgele scheint jedoch immer ein nicht zu vernachlässigender Anteil der $\equiv\text{Si}-\text{C}\equiv$ Bindungen an der Oberfläche gespalten zu werden, so dass neben den gewünschten stark sauren Sulfogruppen auch die schwach sauren Silanolgruppen am Ionenaustausch beteiligt sind.

Nachdem die $\equiv\text{Si}-\text{C}\equiv$ Bindung zu aliphatischen organischen Resten stabiler ist als zu aromatischen Gruppen¹², wurde versucht auf Kieselgeloberflächen, die mit aliphatischen Resten bedeckt waren, Kationenaustauscherguppen (Sulfogruppen) mittels in Substanz bekannter Reaktionen der organischen Chemie einzuführen. Dabei wurde die Sulfonierungsreaktion sowohl in Richtung maximalem Sulfonierungsgrad als auch in Richtung minimalster $\equiv\text{Si}-\text{C}\equiv$ Spaltung optimiert. Durch Veränderung der Eigenschaften des Ausgangsträgermaterials konnte die Kapazität der synthetisierten Austauscher variiert werden.

EXPERIMENTELLES

In Tabelle I sind die physikalischen Eigenschaften der verwendeten Kieselgele (Merck, Darmstadt, B.R.D.) zusammengefasst.

TABELLE I

PHYSIKALISCHE EIGENSCHAFTEN DER VERWENDETEN KIESELGELE (MERCK)*

Kieselgel	Poren-Durchmesser (Å)	Spezifische Oberfläche (m ² /g)	Poren- volumen (ml/g)	Teilchengrösse, d_p (µm)
SI 100	100	300	1.0	36-40
SI 100	100	350	1.0	10
SI 200	180-200	150	0.7	40-63
SI 500	500	35	0.9	10
SI 1000	1000	10	0.75	10

* Die physikalischen Daten wurden den Datenblättern der Firma Merck entnommen.

Silanisierungsreaktion

Die handelsüblichen Kieselgele wurden mit konzentrierter Schwefelsäure gereinigt, mit destilliertem Wasser säurefrei gewaschen und bei 200° getrocknet. Die

Umsetzung des gereinigten Kieselgels mit den Chloralkylsilanen erfolgte in siedendem Toluol. Nach Beendigung der Reaktion wurde mit Toluol, Methanol, Methanol-Wasser (1:1), Wasser, Methanol und Äther in der hier angegebenen Reihenfolge gewaschen und anschliessend bei 110° im Vakuum getrocknet. Zeigte das Produkt infolge nicht umgesetzter Silanolgruppen noch Methylrotadsorption¹³, so wurde so lange mit Hexamethyldisilazan bzw. Bis(trimethylsilyl)acetamid nachsilanisiert bis der Test negativ ausfiel.

Sulfonierung

Sulfurylchlorid. Das silanisierte Kieselgel (25 ml) wurde mit 20 ml Sulfurylchlorid in Tetrachlorkohlenstoff bei verschiedenen Temperaturen zur Reaktion gebracht. Neben der Temperatur wurde auch die Reaktionsdauer variiert.

Chlorsulfonierung. Zur Chlorsulfonierung mit Chlor und Schwefeldioxid wurde ein drehbar gelagertes Glasrohr (13 cm Durchmesser, 25 cm lang) verwendet. Um eine gute Durchmischung der Probe während der Chlorsulfonierung zu gewährleisten, wurde das Reaktionsgefäss in einem 2-Sekundenrhythmus jeweils um 270° hin und her gedreht. Innerhalb des Reaktionsgefässes befand sich eine wassergekühlte 100 W UV-Lampe (Typ TQ 150; Heraeus). Eine im Reaktionsgefäss befindliche Kühle spirale erlaubte die Thermostatisierung auch auf Temperaturen unterhalb Raumtemperatur. Die Gase wurden über H₂SO₄ getrocknet und anschliessend auf 0° abgekühlt. Bei einem Gesamtgasstrom von 5–10 ml/min war das SO₂:Cl₂-Verhältnis auf etwa 3:2 eingestellt.

Bestimmung der Austauschkapazität

1 g des trockenen Austauschers in der H⁺-Form wurde mit 50 ml 5% KCl-Lösung versetzt. Nach einigen Minuten wurde die Lösung abgesaugt und die freigesetzte Menge HCl mit 0.1 N NaOH Lösung bestimmt. Bei direkter Titration des Austauschers wurden die gleichen Kapazitätswerte ermittelt.

DISKUSSION DER ERGEBNISSE

Die Übertragung der aus der klassischen organischen Chemie bekannten Reaktionen auf an der Oberfläche von Kieselgel gebundenen Silane gestaltet sich schwierig. Vor allem bei den Substitutionsreaktionen von Bromalkylsilanen mit Sulfit, Bisulfit und Sulfiden mit nachfolgender Oxydation zu Sulfogruppen war die erzielte Austauschkapazität gering, während die Spaltung der $\equiv\text{Si}-\text{C}\equiv$ Bindung auch unter den hier relativ milden Bedingungen nicht unerheblich war.

In Tabelle II sind die durchgeführten Substitutionsreaktionen mit den verwendeten Bedingungen sowie der erreichten Austauschkapazität zusammengestellt. In der letzten Spalte ist der Anteil der $\equiv\text{Si}-\text{C}\equiv$ Spaltung angegeben, wie er aus den Werten der C,H-Analyse vor und nach der Reaktion errechnet wurde. (Es soll jedoch darauf hingewiesen werden, dass die Aussagekraft der C,H-Analyse im Falle der Bestimmung von Kohlenstoff auf Kieselgeloberfläche nur beschränkte Gültigkeit hat, da der relative Fehler der C,H-Analyse in diesen Fällen gross ist!)

Die höchste Austauschkapazität, die auf diese Art erzielt wurde, lag bei 100 $\mu\text{equiv./g}$ (spezifische Oberfläche des Silikagels: 150 m²/g), wenn ein Alkylmerkaptan

TABELLE II

DARSTELLUNGSMETHODEN DER KATIONENAUSTAUSCHER DURCH SUBSTITUTIONSREAKTIONEN

Träger SI 200.

Funktionelle Gruppe am Kieselgel	Reaktionspartner	Reaktionsbedingungen*	Austauschkapazität (equiv./g)	$\equiv\text{Si}-\text{C}\equiv$ Spaltung (%)
Si-C ₄ Br	NaHSO ₃	DMSO/24 h/60°	0	40
Si-C ₄ Br	Na ₂ SO ₃	DMSO/24 h/60°	0	30
Si-C ₄ Br	(NH ₄) ₂ SO ₃	Autoklav/4 h/150°	66	40
		Autoklav/10 h/150°	65	65
Si-C ₄ Br	NaHS	Abs. Äthanol/24 h/55°	—	—
Si-C ₄ SH	H ₂ O ₂ /Eisessig	2 h/25°	20	25
		3 h/25°	54	30
		15 h/25°	103	50
		1 h/70°	64	40
	20% HNO ₃	3 h/25°	15	40

* DMSO = Dimethylsulfoxid.

(gebunden auf der Oberfläche) mit H₂O₂ in Eisessig oxydiert wurde. Dabei wurde allerdings etwa die Hälfte der vorhandenen $\equiv\text{Si}-\text{C}\equiv$ Bindungen gespalten.

Einen besseren Umsetzungsgrad erhielt man durch Sulfochlorierung mit Sulfonylchlorid in Tetrachlorkohlenstoff und anschliessender Hydrolyse mit Natriumsulfitlösung (pH 8). Konstante Werte der Austauschkapazität wurden bereits nach einer Reaktionsdauer von 2 h erzielt. Bei einer Reaktionstemperatur von 10° war die erzielte Kapazität im Endprodukt höher als bei höheren Temperaturen (bis 55°). Bei einem Kieselgel mit einer spezifischen Oberfläche von 370 m²/g und Butylgruppen an der Oberfläche wurde eine maximale Austauschkapazität von 260 $\mu\text{equiv.}/\text{g}$ erhalten. Waren an der Oberfläche Octadecylgruppen gebunden, so wurde unter den gleichen Reaktionsbedingungen eine Austauschkapazität von 360 $\mu\text{equiv.}/\text{g}$ erzielt. Derartige Austauscher mit "C₁₈-Bürsten" sind allerdings für flüssigchromatographische Zwecke weniger geeignet, da die Oberfläche trotz der eingeführten Sulfonsäuregruppen immer noch hydrophob ist. Ausserdem schien die Diffusion der Probenmoleküle in die Poren behindert zu sein, was sich durch weit schlechtere *h*-Werte als bei den "Butylbürsten" mit gleicher Korngrössenverteilung bemerkbar machte. Für die flüssigchromatographischen Untersuchungen wurden daher ausschliesslich Austauscher mit *n*-Butylgruppen verwendet.

Die höchsten Austauschkapazitäten bei vergleichbar geringer $\equiv\text{Si}-\text{C}\equiv$ Spaltung wurden jedoch bei der Sulfochlorierung mit SO₂/Cl₂ in einer Gas-Festkörper-Reaktion erhalten. Die erzielte Austauschkapazität war abhängig von der Leistung der Bestrahlungslampe. Mit der 100 W-Lampe wurde eine um etwa 20% höhere Austauschkapazität erzielt als mit einer 8 W-Lampe. Bei Temperaturen unterhalb Raumtemperatur (0–5°) war die erreichte Austauschkapazität ebenfalls grösser (ca. 30%) als bei 20°.

In Tabelle III sind die Austauschkapazitäten der mittels Gasphasen-Sulfochlorierung synthetisierten Kationenaustauscher mit den verschiedenen Kieselgelträgern zusammengestellt.

TABELLE III

EIGENSCHAFTEN DER KATIONENAUSTAUSCHER, HERGESTELLT MIT GASPHASEN-SULFOCHLORIERUNG

Kieselgel	Korngrösse, d_p (μm)	Oberflächenkonzentration ($\mu\text{Mol}/\text{m}^2$)		Austausch- kapazität ($\mu\text{equiv.}/\text{g}$)	Sulfonierungsgrad
		Vor Sulfonierung	Nach Sulfonierung		
SI 100	10	4.86	3.16	254	0.23
SI 100	36–40	4.26	3.18	230	0.24
SI 200	40–63	6.93	4.85	120	0.165
SI 500	10	13.10	8.05	43	0.153
SI 1000	10	13.0	11.4	18.5	0.11

Der Ionenaustauscher auf SI 100 hat etwa die doppelte Austauschkapazität als der auf SI 200, was in etwa den Verhältnissen der spezifischen Oberflächen entspricht. Die erzielte Austauschkapazität ist unabhängig von der Teilchengrösse, gleiches Ausgangsmaterial vorausgesetzt, was für die heterogene Oberflächenreaktion unter UV-Bestrahlung nicht vorauszusetzen war. Erstaunlich hoch ist die Oberflächenkonzentration der organischen Reste an den weitporigen Kieselgelen. Bei dem insgesamt sehr niedrigen Gesamtkohlenstoffwert (*ca.* 2%) führen geringfügige Verschiebungen der C-Analyse zu grossen Änderungen der Oberflächenkonzentrationswerte. Derartige Werte sind daher nur bedingt verwendbar und nur qualitativ zu betrachten.

Die Austauschkapazität dagegen kann sehr exakt gemessen werden. Da der Sulfonierungsgrad bei den weitporigen Kieselgelen trotz des hohen C-Gehaltes, im Gegensatz zu den Erwartungen, nur etwa halb so gross ist wie beim relativ engporigen SI 100, deutet dies auf einen Fehler entweder der C-Analyse oder der Oberflächenbestimmung hin.

Der Sulfonierungsgrad zeigt an, dass maximal nur jeder fünfte Butylrest eine Sulfogruppe enthält. Weder durch Verlängerung der Reaktionszeit, noch durch Variation des Schwefeldioxid/Chlor-Verhältnisses konnte diese Austauschkapazität erhöht werden. Als optimale Versuchsbedingungen erwiesen sich: SO_2/Cl_2 -Verhältnis 3:2; Temperatur $+5^\circ$; Lampenleistung 100 W bei 90 Min Reaktionsdauer.

Eigenschaften der Kationenaustauscher

Die Austauschkapazität der Ionenaustauscher, bestimmt nach der Verseifung der Sulfochloride mit Natriumsulfidlösung, nimmt mit jedem Regenerierungszyklus ab. Erst nach mehr als fünfzehn Beladungs- und Regenerationszyklen wird immer die gleiche Austauschkapazität bestimmt. (Nur diese konstanten Werte wurden in den Tabellen als Austauschkapazität angegeben). Ähnliches wird von Arylsulfonsäureaustauscher auf Kieselgelbasis berichtet¹¹ und auf physikalisch adsorbierte Organosiloxane mit sauren Gruppen zurückgeführt, die bei den Zyklen langsam ausgewaschen werden. Es ist denkbar, dass derartige Produkte bei der Photoreaktion in unserem Falle auch entstehen. Auch Säure, die in sehr engen Poren des Kieselgels festgehalten wird und nur sehr langsam herausdiffundieren kann, mag für den anfänglichen Abfall der titrimetrisch bestimmten Austauschkapazität verantwortlich sein.

Fig. 1 zeigt eine potentiometrische Titrationskurve eines Kationenaustauschers mit *n*-Butylgruppen auf SI 100, der eine konstante Austauschkapazität von 250 $\mu\text{equiv./g}$ hatte. Bis pH 5 erfolgte die Gleichgewichtseinstellung sehr rasch. Bei $\text{pH} > 5$ verlangsamte sie sich zunehmend, bis bei $\text{pH} > 8$ eine Gleichgewichtseinstellung nicht mehr möglich war, da die Natronlauge zur Hydrolyse des Kieselgelträgers verbraucht wurde. Sehr langsam war vor allem die Gleichgewichtseinstellung bei der Titration des zum Vergleich mit angegebenen "nackten" Kieselgels.

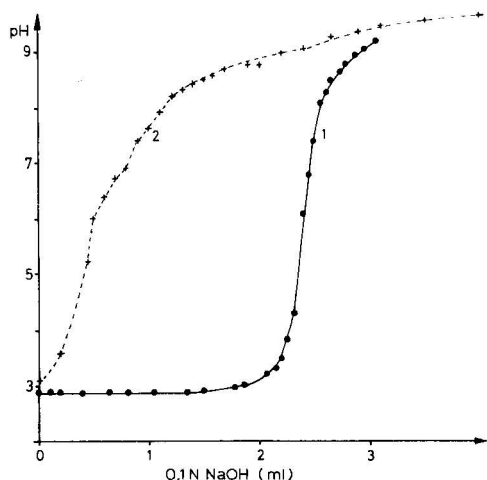


Fig. 1. Potentiometrische Titrationskurven. 1 = Kationenaustauscher: *n*-Butylsulfonsäure auf SI 100; 250 $\mu\text{equiv./g}$. 2 = Kieselgel SI 200, "nackt". Titriert wurde jeweils 1 g suspendiert in 30 ml Wasser mit 0.1 *N* NaOH. Gleichgewichtsänderungen nach 30 sec wurden nicht erfasst.

Die Kationenaustauscher sind im pH-Bereich von 0–8 gegen Säuren und Laugen stabil. Das Bettvolumen in der gepackten Säule ist unabhängig vom pH-Wert und der Konzentration des Eluenten. Nur bei $\text{pH} > 8$ beginnt die Kieselgelmatrix zu quellen, sich aufzulösen und die Permeabilität der Trennsäule bei fixiertem Bett nimmt ab.

In trockenem Zustand konnten die Austauscher auch längere Zeit Temperaturen um 150° ausgesetzt werden, ohne dass merkliche Veränderungen des C-Gehaltes und (oder) der Austauschkapazität festgestellt werden konnten. Die Differentialthermoanalyse zeigt erst bei Temperaturen $> 250^\circ$ merkliche Zersetzung an. In Gegenwart von Eluenten (Pufferlösungen unterschiedlichen pH-Wertes) wurde selbst bei längerem Arbeiten bei Temperaturen von 80–90° keine Veränderung der Austauschkapazität beobachtet.

Fig. 2 zeigt die Anwendung der hier beschriebenen Ionenaustauscher bei der Trennung von Nucleinsäurederivaten. Die *h*-Werte lagen bei dieser Trennsäule um 0.7 mm ($u = 0.4 \text{ cm/sec}$), das entspricht in der 30 cm langen Säule etwa 400 theoretischen Böden, bei einem Teilchendurchmesser (d_p) von 10 μm . Obwohl in nichtwässrigen Systemen mit dem gleichen Teilchendurchmesser wesentlich niedrigere *h*-Werte bestimmt werden, ist die Trennleistung für Ionenaustauschchromatographie ausreichend. Mit weitporigen Kieselgelträgern wurden bei gleicher Eluentengeschwindig-

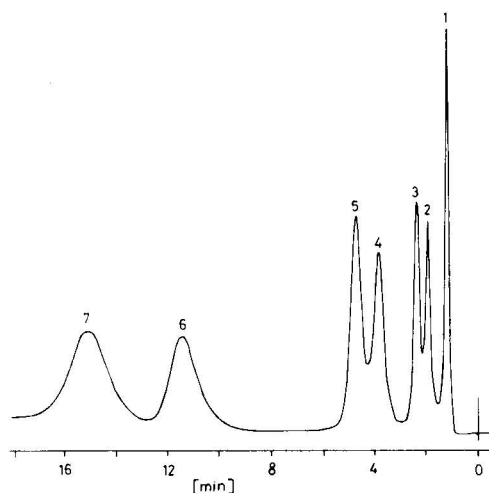


Fig. 2. Trennung von Nucleinsäurederivaten. Stationäre Phase: *n*-Butylsulfonsäure auf SI 100; 250 $\mu\text{equiv./g}$; $d_p = 10 \mu\text{m}$. Eluent: 0.1 *M* Natriumphosphatpuffer pH 4.7. Säule: 30 cm \times 4.2 mm I.D.; Lineargeschwindigkeit, $u = 0.36 \text{ cm/sec}$; Druckabfall, $\Delta p = 100 \text{ atm}$. 1 = Guanosintriphosphat (Kapazitätsverhältnis, $k' = 0$); 2 = Uracil (0.46); 3 = Guanosin (0.8); 4 = Guanin (1.85); 5 = Adenosin (2.44); 6 = Cytosin (7.35); 7 = Adenin (10.0).

keit bedeutend niedrigere h -Werte erhalten (0.1–0.2 mm). Über die anderen chromatographischen Eigenschaften dieser Ionenaustauscher wird in einer folgenden Arbeit berichtet.

DANK

Wir danken der Deutschen Forschungsgemeinschaft für ihre Unterstützung im Rahmen des Sonderforschungsbereiches 52, Analytik, Saarbrücken.

ZUSAMMENFASSUNG

Die Darstellung und die Eigenschaften von Kationenaustauschern auf der Basis von chemisch mit Alkylgruppen modifiziertem Kieselgel ("Bürsten" mit $\equiv\text{Si}-\text{C}\equiv$ Bindung) werden beschrieben. Die höchsten Austauschkapazitäten bei minimaler Spaltung der $\equiv\text{Si}-\text{C}\equiv$ Bindung wurden durch Sulfochlorierung in einer Gas-Festkörper-Reaktion erzielt. Die Austauschkapazität ist abhängig von der spezifischen Oberfläche des Kieselgelträgers (250 $\mu\text{equiv./g}$ bei 300 m^2/g).

Die erhaltenen Kationenaustauscher sind druckstabil und nicht quellbar. Dadurch ist das Bettvolumen unabhängig vom pH-Wert und von der Ionenstärke des Eluenten. Die Austauscher sind im pH-Bereich 0–8 stabil; ihre Temperaturstabilität ist ausgezeichnet.

LITERATUR

- 1 C. Horvath, B. Preiss und S. R. Lipsky, *Anal. Chem.*, 39 (1967) 1422.
- 2 C. Horvath und S. R. Lipsky, *Anal. Chem.*, 41 (1969) 1227.

- 3 C. Horvath, in J. A. Marinsky, und Y. Marcus (Herausgeber), *Ion Exchange and Solvent Extraction* Vol. 5, Marcel Dekker, New York, 1973, p. 207.
- 4 P. R. Brown, *High Pressure Liquid Chromatography, Biochemical and Biomedical Applications*, Academic Press, New York, 1973.
- 5 I. Halász und I. Sebastian, *Angew. Chem.*, 81 (1969) 464.
- 6 O.-E. Brust, I. Sebastian, und I. Halász, *J. Chromatogr.*, 83 (1973) 15.
- 7 I. Sebastian und I. Halász, *Chromatographia*, 8 (1974) 371.
- 8 K. Unger und K. Berg, *Z. Naturforsch.*, 24b (1969) 454.
- 9 K. Unger, W. Thomas und P. Adrian, *Kolloid-Z. Z. Polym.*, 251 (1973) 45.
- 10 K. Unger, K. Berg, D. Nyamah und Th. Lotte, *Kolloid-Z. Z. Polym.*, 252 (1973) 317.
- 11 K. Unger und D. Nyamah, *Chromatographia*, 7 (1974) 63.
- 12 W. Noll, *Chemie und Technologie der Silikone*, Verlag-Chemie, Weinheim, 1968.
- 13 I. M. Kolthoff und I. Shapiro, *J. Amer. Chem. Soc.*, 72 (1950) 776.

CHROM. 7905

SEPARATION OF ACIDIC COMPOUNDS BY HIGH-PRESSURE LIQUID-LIQUID CHROMATOGRAPHY INVOLVING ION-PAIR FORMATION

J. C. KRAAK and J. F. K. HUBER*

Laboratory of Analytical Chemistry, University of Amsterdam, Nieuwe Achtergracht 166, Amsterdam (The Netherlands)

SUMMARY

The distribution of acidic compounds in the phase system tri-*n*-octylamine–aqueous perchloric acid was investigated. The distribution equilibrium can be expressed by a simple formula which describes the dependence of the distribution coefficient on the single equilibrium constants, pH and ion concentration in the aqueous phase. The theoretical expression was shown to agree well with the experimental data. The distribution of strong acids was caused mainly by ion-pair formation and for weaker acids at low pH by the liquid–liquid distribution of the acid, while at larger pH ion-pair formation can also be involved in the distribution equilibrium. Special selectivity effects can be obtained by changing the temperature, pH or type and concentration of the anion in the aqueous phase.

It is shown that the tri-*n*-octylamine–aqueous perchloric acid system is very suitable for separation of acidic compounds like sulphonic and carboxylic acids by high-pressure liquid–liquid chromatography.

INTRODUCTION

The acid-binding properties of long-chain aliphatic amines have been used for 25 years in the extraction of anions from aqueous solutions with organic solvents¹. This type of extraction is based on the formation of an ion pair between the acid and the amine. In most instances, the ion pair is insoluble in aqueous phases but is readily soluble in organic solvents. Schill and co-workers have made extensive studies on the ion-pair extraction of acids and discussed the extraction conditions and side-reactions that can occur². Few papers have been published about ion-pair formation used in high-pressure column liquid chromatography^{3–7}.

The analytical separation of aromatic sulphonic acids is a problem that has not yet been solved satisfactorily. Most work in this field has involved the use of ion-exchange chromatography^{8–10}. Several pairs of aromatic sulphonic acids were separated by liquid–liquid chromatography on columns packed with Chromosorb impregnated with tricaprylamine (Alamine 336) using aqueous hydrochloric acid for the elution

* Present address: Institut für Analytische Chemie, Universität Wien, Währinger Strasse 38, Vienna, Austria.

of the first acid and aqueous perchloric acid as the mobile phase for the elution of the second acid¹¹.

The potential of high-pressure liquid chromatography¹²⁻¹⁴, which has been developed in recent years, has not previously been exploited in the separation of aromatic sulphonic and carboxylic acids. Also, the distribution equilibrium of this type of compound has not been investigated in liquid-liquid systems consisting of an aqueous and an amine phase. The results of such a study are presented in this paper, including phenols as an example of very weak acids.

EXPERIMENTAL

Apparatus

The liquid chromatographic experiments were carried out on a high-pressure liquid chromatograph (Siemens SP 200, Siemens, Karlsruhe, G.F.R.) with a UV spectrophotometer or refractive index detector fitted on custom-made straight thick-walled glass columns. The feed lines for the eluent were constructed from stainless-steel 316 tubes and Swagelock couplings in order to resist the acidic medium. In addition to a septumless injector (Siemens), a custom-made septum injection port and a 10- μ l syringe (Hamilton 701 N) were also used. The thick-walled borosilicate glass columns had an I.D. of 3.0 mm and a length of 185 mm. In order to prevent loss of stationary phase, a stainless-steel pre-column (50 \times 1 cm) was used. The wavelength of the detector in most experiments was adjusted to 263 nm.

Materials

The materials used were tri-*n*-octylamine (TOA; Fluka, Buchs, Switzerland); 70% (w/w) aqueous perchloric acid (Merck, Darmstadt, G.F.R.); diatomite (Kieselgur, Merck) washed with 1 *M* aqueous perchloric acid, ground and classified to a particle size range of 5–10 μ m by means of an air classifier (Alpine MZR, Augsburg, G.F.R.); low-surface-area silica (Spherosil XOC 005, Rhone-Progil, Neuilly sur Seine, France); sulphonic acids (Merck; Fluka); carboxylic acids (Merck, Fluka); and phenols (Fluka).

Procedures

The chromatographic capacity factor, κ_i , of a component *i* for a given column was derived from measurements of its retention time, t_{Ri} , and the retention time, t_{R0} , of a non-retarded component. It is determined by the distribution coefficient, K_i , and the volume ratio, *q*, of the stationary and the mobile phase:

$$\frac{(t_{Ri} - t_{R0})}{t_{R0}} = \kappa_i = K_i \cdot q \quad (1)$$

The selectivity factor (relative retention), r_{ji} , of two compounds was calculated from their capacity ratios:

$$\kappa_j / \kappa_i = r_{ji} \quad (2)$$

In order to prepare the columns, the glass tubes were dry-packed with small portions of coated acid-washed diatomite (Kieselguhr) or low-surface-area silica. The pre-column was similarly filled with acid-washed diatomite (100–200 μ m) coated with 10% TOA.

The aqueous perchloric acid solutions were prepared by diluting a weighed amount of the 70% (w/w) standard solution of perchloric acid with distilled water. The strength of this solution was determined by titration with aqueous borax solution. The pH of the mobile phase was measured with a pH meter (Radiometer, Copenhagen, Denmark). Perchlorate solutions containing 0.05 M ClO_4^- but having different pH values were prepared from 0.05 M perchloric acid by adding sodium hydroxide until the required pH was attained. The eluents containing different concentrations of perchlorate or additional anions were prepared by dissolving the sodium salt of the anions in 0.05 M perchloric acid.

The samples were dissolved in the mobile phase and injected into the top of the column with a 10- μl syringe through a septum or with the septumless injector.

THEORETICAL

Total distribution coefficient of an acid

The distribution of an acid HX between an aqueous phase containing a strong acid HA and an organic phase consisting of a long-chain aliphatic amine B depends on a number of competing equilibria. By considering only the most important equilibria, a simple expression for the total distribution coefficient can be derived. The following equilibria are considered:

(1) Liquid-liquid distribution of the undissociated acid HX between the stationary and the mobile phases. HX is assumed to be a component of the sample.

$$\begin{aligned} (\text{HX})_m &\rightleftharpoons (\text{HX})_s \\ K_{\text{HX}} &= \frac{[\text{HX}]_s}{[\text{HX}]_m} \end{aligned} \quad (3)$$

where K_{HX} = liquid-liquid distribution coefficient of HX; the square brackets denote the concentration of the component concerned; and the subscripts m and s refer to the mobile (aqueous) and the stationary (organic) phase, respectively.

(2) Dissociation of the acid HX in the mobile phase.

$$\begin{aligned} (\text{HX})_m &\rightleftharpoons (\text{H}^+)_m + (\text{X}^-)_m \\ K_1 &= \frac{[\text{H}^+]_m [\text{X}^-]_m}{[\text{HX}]_m} \end{aligned} \quad (4)$$

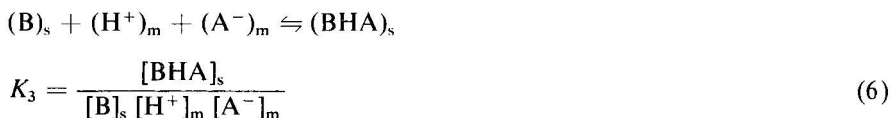
where K_1 = dissociation constant of HX.

(3) Ion exchange of the anion X^- in the mobile phase with the ion pair BHA in the stationary phase.

$$\begin{aligned} (\text{X}^-)_m + (\text{BHA})_s &\rightleftharpoons (\text{BHX})_s + (\text{A}^-)_m \\ K_2 &= \frac{[\text{BHX}]_s [\text{A}^-]_m}{[\text{X}^-]_m [\text{BHA}]_s} \end{aligned} \quad (5)$$

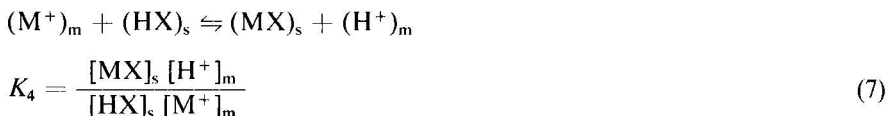
where K_2 = ion-exchange constant for the anion X^- in the mobile phase and the ion pair BHA in the stationary phase.

(4) Ion-pair formation between the dissociated acid HA in the mobile phase and the amine B in the stationary phase. The acid HA is a constituent of the eluent and is assumed to be a strong acid.



where K_3 = formation constant of the ion pair BHA in the stationary phase.

(5) Exchange of the proton of the acid HX in the stationary phase for the cation M^+ in the mobile phase which is assumed to be a constituent of the eluent.



where K_4 = ion-exchange constant for the cation M^+ in the mobile phase and the acid HX in the stationary phase.

Under the usual analytical chromatographic conditions, the sample is present in the mobile phase in very dilute solution, so that it can be assumed that its concentration in the stationary phase is also very low. Further, it is assumed that the components B and BHA of the stationary phase are insoluble in the mobile phase. Under these circumstances, the overall concentration of the stationary phase is given by the relationship

$$[B]_s + [BHA]_s = C \quad (8)$$

where C is constant. According to eqns. 3–8, the total distribution coefficient of X is given by the expression

$$K_X = \frac{[HX]_s + [BHX]_s + [MX]_s}{[HX]_m + [X^-]_m} \quad (9)$$

where K_X = total liquid-liquid distribution coefficient of the constituent X. From eqns. 3–9, an expression can be derived that describes the total distribution coefficient as the sum of three terms:

$$K_X = \Delta K_{X_1} + \Delta K_{X_2} + \Delta K_{X_3} \quad (10)$$

where

$$\Delta K_{X_1} = K_{HX} \cdot \frac{1}{1 + K_1/[H^+]_m}$$

$$\Delta K_{X_2} = K_2 \cdot C \cdot \frac{1}{([A^-]_m + 1/K_3 [H^+]_m) (1 + [H^+]_m/K_1)}$$

$$\Delta K_{X_3} = K_{HX} K_4 \cdot \frac{[M^+]_m}{[H^+]_m + K_1}$$

The first term describes the distribution of the acid, the second term the effect of ion-pair formation with the amine and the third term the effect of ion-pair formation with a monovalent cation. Eqn. 10 describes the dependence of the total distribution coefficient on the concentrations of the eluent anion, of the eluent cation and the pH of the mobile phase.

RESULTS AND DISCUSSION

The capacity ratio describes the migration of a compound in a chromatographic system, and can be determined from the retention time of this compound and that of a non-retarded compound. The values of the capacity ratio for different compounds on the same column are proportional to their distribution coefficients, the phase ratio being the proportionality constant. The selectivity of a phase system with respect to the distribution of two compounds is described by the selectivity factor, which is given by the ratio of the capacity ratios of the two compounds. For a number of phenols, carboxylic acids and sulphonic acids, the capacity ratio and the selectivity factor for successively eluting components were determined on a column containing tri-*n*-octylamine as stationary phase and aqueous perchloric acid with the eventual addition of a salt as the mobile phase.

The effects of temperature, perchloric acid concentration, pH and concentration and nature of the salt were investigated.

Influence of temperature

The temperature dependence of the capacity ratio on a given column is determined primarily by the temperature dependence of the distribution coefficient, although a minor effect can arise from a change in the phase ratio with temperature. The influence of temperature on the total distribution coefficient is determined according to eqn. 10 by the temperature dependence of the distribution coefficient K_{HX} of the species HX, and of the chemical equilibrium constants K_1 , K_2 , K_3 and K_4 .

The influence of temperature on the capacity ratio was studied in the phase system tri-*n*-octylamine-0.05 *M* perchloric acid. In this system, the third term in eqn. 10 vanishes, as $[M^+]_m$ is zero. In order to be certain that no stationary phase was stripped from the column during the sequence of measurements at different temperatures, the capacity ratios of some standard compounds were measured on the same column at the same temperature before and after the series of experiments. As shown in Table I, the capacity ratio was found to be constant with high accuracy.

From Table II, it can be seen that the change in the capacity ratio with temperature was found to be insignificant in some instances and to be substantial in others in which the capacity ratio partially decreases and partially increases with temperature. This behaviour can be explained by means of eqn. 10. If the first term in this equation is dominant, then the temperature dependence of the total distribution coefficient will be determined mainly by the partial distribution coefficient K_{HX} of the species HX. If the second term is dominant, then the ion-exchange constant K_2 will determine the temperature dependence of the total distribution coefficients. Depending on the enthalpy change, due to the dominating process, the corresponding equilibrium constant will increase or decrease with temperature and so will the total distribution coefficient. It can be assumed that the distribution coefficient K_{HX} de-

TABLE I

CONTROL OF THE CONSTANCY OF THE CAPACITY RATIO AT 25° BEFORE AND AFTER THE SERIES OF EXPERIMENTS

Phase system: tri-*n*-octylamine-0.05 *M* perchloric acid.

Compound	κ_t	
	Before	After
4-Nitrobenzoic acid	1.95	1.93
4-Nitrobenzenesulphonic acid	2.36	2.37
4-Methylbenzoic acid	4.30	4.27

TABLE II

INFLUENCE OF TEMPERATURE ON THE CAPACITY RATIO, κ_t , AND SELECTIVITY FACTOR, r_{ji} , FOR THE PHASE SYSTEM TRI-*n*-OCTYLAMINE-0.05 *M* PERCHLORIC ACID AT pH 1.5

Compound	25°		45°		65°	
	κ_t	r_{ji}	κ_t	r_{ji}	κ_t	r_{ji}
Phenol	1.03	—	0.89	—	0.72	—
3-Methylphenol	3.03	2.94	2.50	2.81	1.92	2.67
4-Methylphenol	3.13	1.03	2.61	1.04	1.99	1.04
2-Methylphenol	3.35	1.07	2.82	1.08	2.13	1.07
4-Nitrophenol	3.49	1.04	2.60	1.08	1.85	1.15
2-Nitrophenol	5.16	1.48	4.08	1.57	2.95	1.59
2,6-Dimethylphenol	6.05	1.17	5.63	1.38	4.41	1.49
2,5-Dimethylphenol	8.33	1.38	7.06	1.25	5.10	1.16
2,4-Dihydroxybenzoic acid	0.49	—	0.37	—	0.27	—
Benzoic acid	0.85	1.73	0.72	1.94	0.57	2.11
4-Nitrobenzoic acid	1.09	1.28	0.98	1.36	0.73	1.28
2-Hydroxybenzoic acid	1.73	1.59	1.43	1.46	1.12	1.53
4-Methylbenzoic acid	2.43	1.40	2.02	1.41	1.50	1.40
2-Amino-4-nitrobenzoic acid	2.89	1.19	1.99	1.01	1.29	1.16
Cinnamic acid	3.03	1.05	2.39	1.20	1.71	1.33
Benzenesulphonic acid	0.42	—	0.62	—	0.82	—
4-Nitrobenzenesulphonic acid	1.34	3.19	1.69	2.73	1.97	2.40
4-Toluenesulphonic acid	1.37	1.02	1.95	1.15	2.40	1.22
2-Naphthol-6-sulphonic acid	2.82	2.06	2.90	1.49	2.92	1.22
1-Naphthol-2-sulphonic acid	3.30	1.17	3.85	1.33	4.00	1.37
1-Naphthol-4-sulphonic acid	3.37	1.02	3.81	1.01	3.95	1.01
1-Naphthol-5-sulphonic acid	4.10	1.22	4.80	1.26	4.97	1.26
1-Naphthol-3-sulphonic acid	10.17	2.48	9.54	1.99	7.33	1.47
1-Naphthol-3,6-disulphonic acid	0.45	—	0.69	—	0.98	—
4,5-Dihydroxy-2,7-naphthalene-disulphonic acid	0.53	1.18	0.75	1.09	1.05	1.07
2-Naphthol-3,6-disulphonic acid	2.00	3.77	3.85	5.13	6.72	6.40
1-Naphthol-3,8-disulphonic acid	15.14	7.57	22.61	5.87	28.37	4.22

creases with temperature whereas the ion-exchange constant K_2 increases with temperature.

For phenols and carboxylic acids at pH 1.5, it can be concluded that the liquid-liquid distribution of these compounds is the major process, because their capacity ratios decrease with temperature. For sulphonic acids, it can be concluded that ion-pair formation is the major process at pH 1.5 as the capacity ratios of these compounds increase with temperature.

A special case arises with naphtholsulphonic acids, which have both a phenolic group and a sulphonic acid group. These compounds show an insignificant dependence of the capacity ratio on temperature, except for 1-naphthol-3-sulphonic acid, which behaves as a phenol. The behaviour of the other naphtholsulphonic acids suggests that liquid-liquid distribution and ion-pair formation have about the same influence owing to the presence of a phenolic and a sulphonic acid group in the same molecule. The overall effect of temperature on the capacity ratio is small in this instance as the phenolic group causes a decrease in the total distribution coefficient while the sulphonic acid group causes an increase. In the case of naphtholdisulphonic acids, the sulphonic acid function dominates because of the presence of the second sulphonic acid group, and therefore the capacity ratio increases with increase in temperature.

From Table II, it can be seen that in most instances the selectivity factors of successively eluting components within a group of compounds change significantly with temperature.

Influence of pH

The influence of pH can be explained by means of eqn. 10.

The first term in eqn. 10 has a constant value of K_{HX} at $[H^+]_m \gg K_1$. When K_1 is large, this value cannot be achieved because $[H^+]_m$ is limited in practice. In the range where $[H^+]_m$ is of the order of K_1 , the first term declines to zero. A further change in the first term is caused by the change in the distribution coefficient of the undissociated compound due to the change in the composition of the liquid phase with pH. According to eqn. 6, the stationary liquid consists predominantly of BHA at low pH and of B at high pH. This prediction was checked by determining the composition of the stationary liquid at low pH.

Tri-*n*-octylamine was mixed with aqueous perchloric acid and the decrease in the amount of perchloric acid in the aqueous phase was determined by titration. At pH 3, it was found that the decrease in the amount of perchloric acid was equivalent to the amount of tri-*n*-octylamine, which supports the prediction of eqn. 6. For sulphonic acids ($K_1 \approx 1$), the first term may be expected to be zero because of the high value of the dissociation constant. For carboxylic acids ($K_1 \approx 10^{-4}$), the first term should have the value of the liquid-liquid distribution coefficient at low pH and should decrease to zero at a pH about equal to the dissociation constant. For phenols ($K_1 \approx 10^{-10}$), the first term should have the value of the liquid-liquid distribution coefficient at low pH, decline in a certain pH range according to eqn. 6 and decrease to zero at a pH about equal to the dissociation constant.

The second term in eqn. 10 has a maximum at $pH = -\frac{1}{2} \log K_1/K_3 [A^-]_m$ and decreases to zero at low and high pH. The exact shape of the curve describing the dependence of the second term on pH depends on the relative magnitude of the

equilibrium constants K_1 , K_2 and K_3 . Depending on the value of the constants, the second term can have a sharp or a flat maximum.

From Fig. 1b, in which the values of the capacity ratio calculated from eqn. 10 are plotted as function of pH, it can be seen that the experimental curves shown in Fig. 1a can be approached by the theoretical curves (except for phenol), with an appropriate choice of the values for the equilibrium constants and the phase ratio. The decrease in the capacity ratio of phenol which can be seen in Fig. 1a is not described

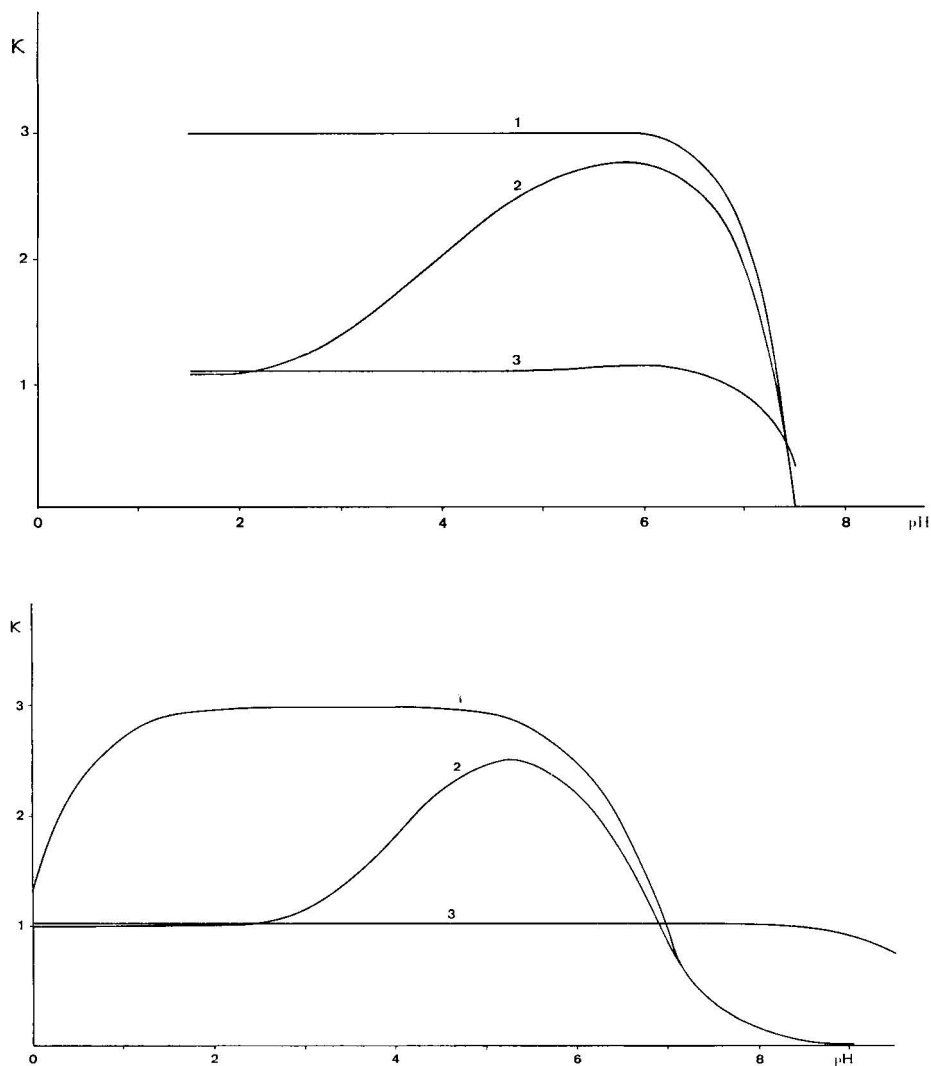


Fig. 1. pH Dependence of the capacity ratio. (a) Experimental results. Sample: (1) 2-naphthol-6-sulphonic acid; (2) 4-nitrobenzoic acid; (3) phenol. Column: TOA, 0.04 g per gram of solid support; 0.05 M HClO_4 . (b) Calculated according to eqn. 10. (1) $K_1 = 1$, $K_2 = 2$, $K_3 = 10^8$, $K_{\text{HX}} = 0$, $q = 0.030$, $C = 2.3$, $[\text{A}^-]_{\text{m}} = 0.05$; (2) $K_1 = 10^{-4}$, $K_2 = 2$, $K_3 = 10^8$, $K_{\text{HX}} = 36.2$, $q = 0.030$, $C = 2.3$, $[\text{A}^-]_{\text{m}} = 0.05$; (3) $K_1 = 10^{-10}$, $K_2 = 0$, $K_3 = 10^8$, $K_{\text{HX}} = 37.0$, $q = 0.030$, $C = 2.3$, $[\text{A}^-]_{\text{m}} = 0.05$.

by the effect of $K_1/[H^+]_m$ on the value of the first term but by the decrease in the distribution coefficient K_{HX} . Assuming $K_3 = 10^8$, the capacity ratio decreases in the pH range 5–8 according to eqn. 6. Its value beyond pH 8, being the distribution coefficient for tri-*n*-octylamine as stationary phase, is not known, however.

From the dependence of the capacity ratio on pH, it can be concluded that the effect of ion-pair formation is predominant for sulphonic acids, whereas distribution of the undissociated compound is predominant for phenols. In the case of carboxylic acids, both processes are significant.

For compounds with small dissociation constants, such as phenols, the capacity ratio approaches a constant value at low pH, as can be seen from Table III

TABLE III

pH DEPENDENCE OF THE CAPACITY RATIOS, κ_i , AND SELECTIVITY FACTORS, r_{ji} , OF PHENOLS, CARBOXYLIC ACIDS AND SULPHONIC ACIDS ON A COLUMN CONTAINING TOA AS STATIONARY PHASE AND 0.05 *M* PERCHLORIC ACID AS MOBILE PHASE AT 25°

Compound	pH									
	1.5		2.5		4.1		6.0		7.5	
	κ_i	r_{ji}	κ_i	r_{ji}	κ_i	r_{ji}	κ_i	r_{ji}	κ_i	r_{ji}
Phenol	1.07	—	1.07	—	1.07	—	1.11	—	0.34	—
3-Methylphenol	3.03	2.83	3.05	2.85	3.06	2.86	3.16	2.85	0.94	2.76
4-Methylphenol	3.18	1.05	3.21	1.05	3.26	1.06	3.33	1.05	0.93	1.01*
2-Methylphenol	3.34	1.05	3.35	1.04	3.37	1.03	3.51	1.05	1.28	1.38
4-Nitrophenol	3.41	1.02	3.41	1.02	3.48	1.03	4.29	1.22	0.31	4.12*
2-Nitrophenol	5.15	1.51	5.17	1.52	5.12	1.47	5.52	1.29	0.15	2.07*
2,6-Dimethylphenol	6.57	1.28	6.57	1.27	6.62	1.29	6.93	1.26	1.82	12.13
2,5-Dimethylphenol	8.50	1.29	8.53	1.30	8.59	1.30	9.03	1.30	3.25	1.79
2-Aminobenzoic acid	0	—	0.11	—	0.14	—	0.02	—	0	—
2,4-Dihydroxybenzoic acid	0.53	—	0.58	5.27	0.80	5.71	0.83	—	0	—
Benzoic acid	0.85	1.60	0.92	1.59	0.85	1.06	0.77	1.08*	0	—
4-Nitrobenzoic acid	1.05	1.24	1.17	1.27	2.07	2.43	2.74	3.56	0	—
2-Hydroxybenzoic acid	1.69	1.61	3.12	2.67	5.62	2.71	5.48	2.00	0	—
4-Methylbenzoic acid	2.43	1.44	2.47	1.26*	2.53	2.22*	2.04	2.69*	0	—
Cinnamic acid	3.15	1.30	3.12	1.26	3.37	1.33	3.20	1.57	0	—
Benzenesulphonic acid	0.43	—	0.43	—	0.46	—	0.42	—	0	—
1-Naphthol-3,6-disulphonic acid	0.44	1.02	0.42	1.02*	0.46	1.00	0.40	1.05*	0	—
4-Toluenesulphonic acid	1.25	2.84	1.18	2.81	1.45	3.15	1.30	3.25	0	—
3-Nitrobenzenesulphonic acid	1.36	1.09	1.31	1.11	1.44	1.01	1.35	1.04	0	—
2-Naphthol-3,6-disulphonic acid	2.04	1.50	1.98	1.51	2.29	1.59	1.92	1.42	0	—
2-Naphthol-6-sulphonic acid	2.94	1.44	2.96	1.49	2.97	1.30	2.97	1.55	0	—
1-Naphthol-2-sulphonic acid	3.64	1.24	3.70	1.25	3.68	1.24	3.65	1.23	0	—
1-Naphthol-4-sulphonic acid	3.68	1.01	3.61	1.02*	3.68	1.00	3.63	1.01*	0	—
1-Naphthol-5-sulphonic acid	4.56	1.24	4.55	1.26	4.67	1.27	4.71	1.30	0	—
1-Naphthol-3-sulphonic acid	11.08	2.43	10.53	2.31	10.65	2.28	10.22	2.17	0	—
1-Naphthol-3,8-disulphonic acid	14.53	1.31	14.51	1.38	15.23	1.43	14.75	1.44	0	—

* Successive capacity ratios are reversed.

and Fig. 1a. At higher pH values, the capacity ratio was found to decrease sharply. For compounds with medium dissociation constants, such as carboxylic acids, it was found that the capacity ratio approaches a constant value at low pH, has a maximum value at medium pH and decreases to zero at higher pH, as can be seen from Table III and Fig. 1a. For compounds with large dissociation constants, such as sulphonic acids, it can be seen from Table III and Fig. 1a that the capacity ratio is about constant at low pH and decreases sharply to zero at higher pH.

Influence of the nature and concentration of salts

In principle, the addition of a salt can influence the distribution equilibrium of an acidic compound between an organic and an aqueous liquid phase in two ways. On the one hand, the anion of the salt will compete with the anion of the sample with respect to protonation and ion-pair formation, while on the other hand, the cation of the salt can also form an ion pair with the anion of the sample. As a result of the addition of a salt, one can therefore expect a change in the total distribution coefficient if ion-pair formation is involved (or if the salt is derived from a weak acid or base). A number of salts of strong acids and bases were added to a liquid-liquid system consisting of TOA and 0.05 *M* perchloric acid. The influence of these additions on the capacity ratio can be seen from Table V.

The addition of sodium perchlorate causes a significant decrease in the capacity ratio with increasing sodium perchlorate concentration if a strong acid group (*e.g.*, sulphonic acid) is present in the sample molecule. A plot of the capacity ratio as a function of the reciprocal of the anion concentration gives a linear relationship for monovalent acids according to eqn. 10, as shown in Table IV. For divalent acids, a linear relationship is obtained if the total distribution coefficient is plotted as a function of the reciprocal of the square of the anion concentration, as can be seen from Table IV. This suggests, according to eqn. 10, that ion-pair formation with the amine dominates and the liquid-liquid distribution of the protonated anion and ion-pair formation with the sodium cation play a minor role so far as strong acids are concerned. For phenols or carboxylic acids, the change in the capacity ratio was found to be insignificant. For these weak acids, the partition of the undissociated molecules must be assumed to be the predominant process. The effect of the variation of the type of anion at constant concentration is shown in Table V. It can be seen that the capacity ratio changes

TABLE IV

DEPENDENCE OF THE CAPACITY RATIOS, κ_i , OF SULPHONIC ACIDS ON THE PERCHLORATE CONCENTRATION IN THE MOBILE PHASE

a = intercept; b = slope; r = regression coefficient.

Compound	Linear regression of κ_i versus $([A^-])^{-n}$			
	n	a	b	r
2-Naphthol-3,8-disulphonic acid	2	0.0135	0.0054	0.9971
1-Naphthol-3,8-disulphonic acid	2	-0.0051	0.0375	0.9999
2-Naphthol-6-sulphonic acid	1	-0.0038	0.2035	0.9990
1-Naphthol-2-sulphonic acid	1	0.0759	0.2530	0.9994
1-Naphthol-4-sulphonic acid	1	-0.0026	0.2581	0.9993
1-Naphthol-3-sulphonic acid	1	-0.1669	0.5098	0.9991

TABLE V

INFLUENCE OF THE NATURE AND CONCENTRATION OF SALTS ON THE CAPACITY RATIO, κ_i

Compound	Mobile phase	NaClO_4 (mole/l)				
		0	0.025	0.050	0.100	0.200
Phenol	0.05 M HClO_4 + NaClO_4 (pH \approx 1.5)	1.78	1.82	1.78	1.90	1.91
2,4-Dihydroxybenzoic acid		0.85	0.84	0.81	0.84	0.85
Benzoic acid		1.45	1.42	1.41	1.43	1.55
2-Methylbenzoic acid		3.91	3.87	3.74	4.04	4.17
3-Methylbenzoic acid		5.04	5.06	4.88	5.26	5.46
4-Methylbenzoic acid		4.48	4.42	4.34	4.87	5.07
2-Naphthol-3,8-disulphonic acid		2.22	0.88	0.58	0.32	0.08
2-Naphthol-6-sulphonic acid		4.03	2.74	2.11	1.29	0.80
1-Naphthol-2-sulphonic acid		5.10	3.46	2.69	1.75	1.04
1-Naphthol-4-sulphonic acid		5.14	3.42	2.68	1.66	1.02
1-Naphthol-3,8-disulphonic acid		15.00	6.71	3.61	1.62	0.61
1-Naphthol-3-sulphonic acid		10.17	6.44	4.85	3.25	1.99
Compound	Mobile phase	$X=\text{ClO}_4^-$ *	$X=\text{NO}_3^-$	$X=\text{Br}^-$	$X=\text{Cl}^-$	$X=\text{SO}_4^{2-}$
Phenol	0.05 M HClO_4 + 0.25 M NaX (pH \approx 1.5)	1.91	2.96	2.76	2.42	2.33
2,4-Dihydroxybenzoic acid		0.85	3.34	2.09	1.72	1.48
Benzoic acid		1.55	2.25	1.98	2.03	2.13
2-Methylbenzoic acid		4.22	6.85	5.99	5.98	6.65
3-Methylbenzoic acid		5.56	8.76	7.76	7.80	8.67
4-Methylbenzoic acid		5.07	7.80	6.83	6.82	7.67
1-Naphthol-3,6-disulphonic acid		0	0.09	0.21	0.29	0.39
4,5-Dihydroxynaphthalene-2,7-disulphonic acid		0	0.10	0.21	0.31	0.45
2-Naphthol-3,8-disulphonic acid		0.08	0.32	0.82	1.08	1.54
Benzenesulphonic acid		0.11	0.18	0.36	0.51	0.64
1-Naphthol-3,8-disulphonic acid		0.61	2.32	4.69	7.80	10.00
2-Naphthol-6-sulphonic acid		0.80	2.10	3.50	4.26	3.85
1-Naphthol-4-sulphonic acid		1.02	2.94	4.56	5.20	6.07
1-Naphthol-2-sulphonic acid		1.04	2.98	4.56	5.11	5.92
1-Naphthol-3-sulphonic acid		1.99	4.64	10.11	10.18	13.87

(Continued on p. 344)

TABLE V (continued)

Compound	Mobile phase	$M = \text{Li}^+$	$M = \text{Na}^+$	$M = \text{K}^+$
Phenol	0.05 <i>M</i> HClO_4	2.53	2.42	2.64
Benzoic acid	+ 0.25 <i>M</i> MCl	2.10	2.03	2.11
2-Methylbenzoic acid	(pH \approx 1.5)	5.81	5.98	5.82
3-Methylbenzoic acid		7.54	7.80	7.62
4-Methylbenzoic acid		6.72	6.81	6.79
2,6-Dihydroxybenzoic acid		0	0	0
3,4,5-Trihydroxybenzoic acid		0.06	0.10	0.13
3,5-Dihydroxybenzoic acid		0.09	0.10	0.10
3,4-Dihydroxybenzoic acid		0.11	0.14	0.12
2,5-Dihydroxybenzoic acid		0.64	0.67	0.73
4-Hydroxybenzoic acid		0.65	0.68	0.64
2,4-Dihydroxybenzoic acid		1.47	1.55	1.63
2-Hydroxybenzoic acid		5.21	5.33	5.42
4,5-Dihydroxynaphthalene-2,7-disulphonic acid		0.28	0.30	0.38
1-Naphthol-3,6-disulphonic acid		0.35	0.29	0.39
Benzenesulphonic acid		0.45	0.51	0.52
2-Naphthol-3,8-disulphonic acid		1.07	1.08	1.21
4-Toluenesulphonic acid		1.44	1.61	1.69
2-Naphthol-6-sulphonic acid		3.43	4.26	4.00
1-Naphthol-2-sulphonic acid		4.52	5.11	5.55
1-Naphthol-4-sulphonic acid		4.64	5.20	5.60
1-Naphthol-3,8-disulphonic acid		6.60	7.84	8.69
1-Naphthol-3-sulphonic acid		9.72	10.18	11.22

* $X = [\text{ClO}_4^-] = 0.20 \text{ M}$.

considerably with the nature of the anion for strong acids, where the effect of ion-pair formation prevails. It increases in the order $\text{ClO}_4^- < \text{NO}_3^- < \text{Br}^- < \text{Cl}^- < \text{HSO}_4^-$. This sequence is only partially correlated with the sequence of the dissociation constants of the corresponding acids, which is $\text{HClO}_4 > \text{HBr} > \text{HCl} \approx \text{H}_2\text{SO}_4 > \text{HNO}_3$. For weak acids (phenols, carboxylic acids), where the ion-pair formation was found to occur to a minor extent, the change in the capacity ratio with the type of anion is significantly smaller, as can be seen from Table V. In this case, the change in the activity coefficients in the aqueous phase due to the presence of different types of anions must be considered to be responsible for the change in the partition coefficient of the undissociated acid, which dominates the total distribution equilibrium.

The change in the capacity ratio that results from the variation of the type of

cation at constant concentration can be seen in Table V. Only a small effect can be found, which shows a uniform tendency only for strong acids. The distribution coefficient increases in the order $\text{Li} < \text{Na} < \text{K}$. For weak acids, a slightly irregular variation was noted, which can be explained in the same manner as the effect of the variation of the type of anion.

To summarize, it can be concluded that the influence of the addition of salts, like the influence of temperature and pH, indicates that strong ion-pair formation with a predominant influence on the total distribution coefficient occurs only for strong acids. The distribution process for weak acids is determined by the partition of the neutral molecules and dissociation in the aqueous phase.

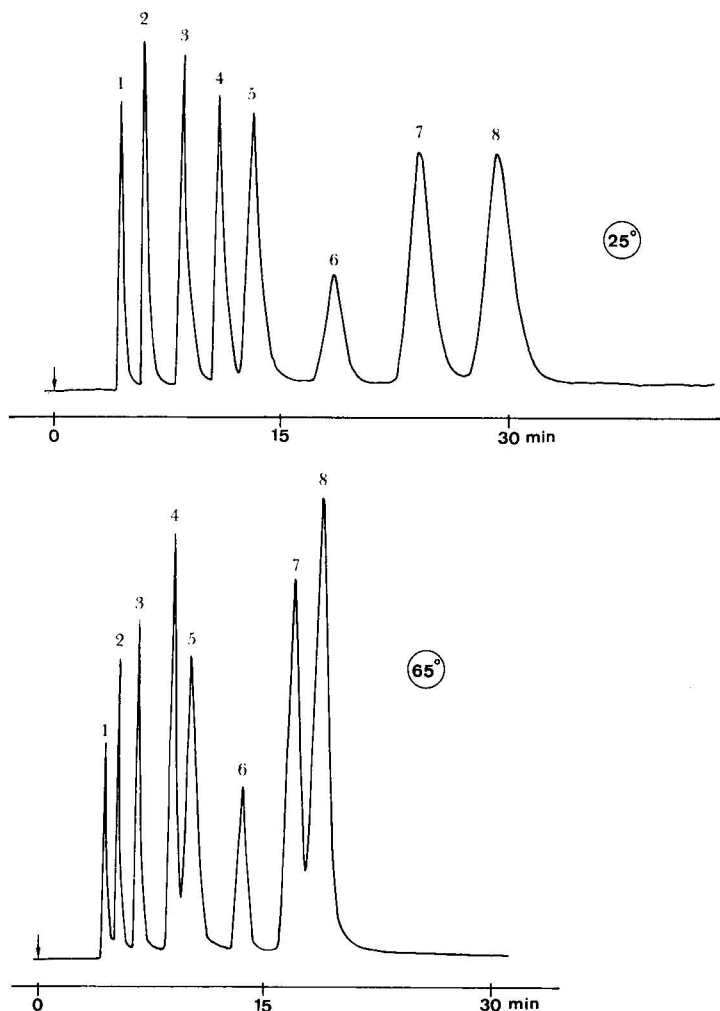


Fig. 2. Influence of temperature on the separation time and resolution of aromatic carboxylic acids at constant flow-rate: (a) 25°; (b) 65°. Sample: (1) 4-aminobenzoic acid; (2) 4-hydroxybenzoic acid; (3) 2,4-dihydroxybenzoic acid; (4) benzoic acid; (5) 4-nitrobenzoic acid; (6) 2-hydroxybenzoic acid; (7) 4-methylbenzoic acid; (8) cinnamic acid. Column: TOA, 0.04 g per gram of solid support; 0.05 *M* HClO_4 , pH 1.5. Flow-rate: 0.7 mm/sec.

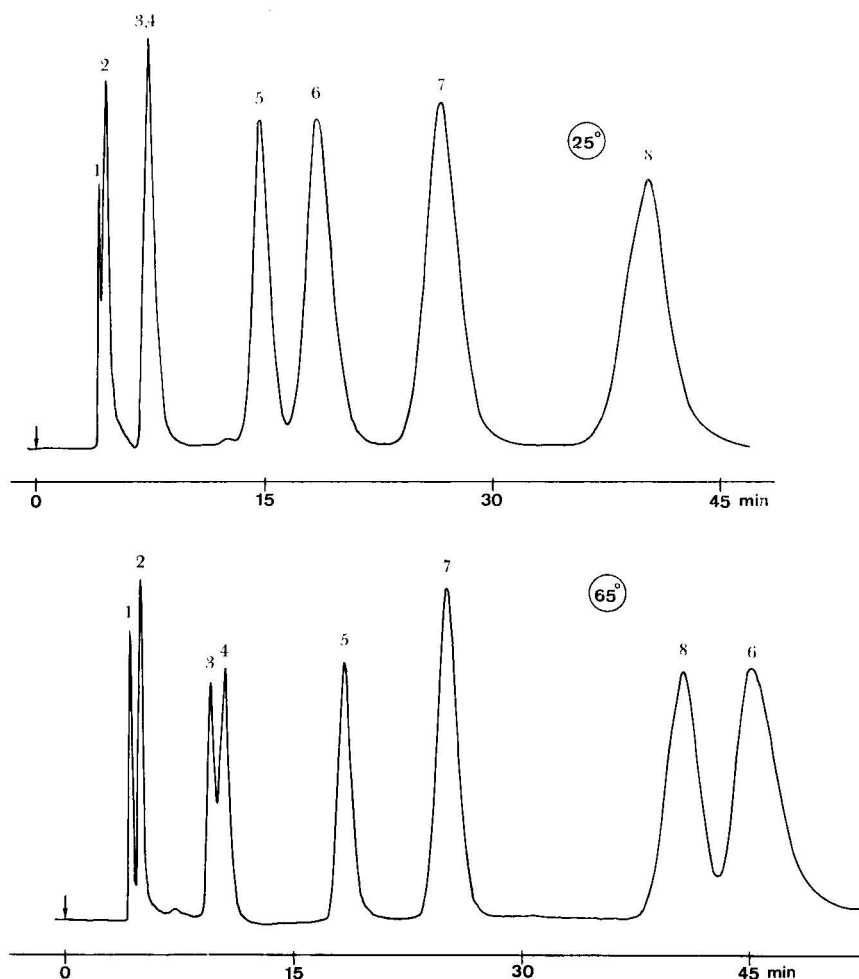


Fig. 3. Influence of temperature on the separation time and resolution of aromatic sulphonics acids at constant flow-rate: (a) 25°; (b) 65°. Sample: (1) 3-aminotoluenesulphonic acid; (2) 2-aminobenzenesulphonic acid; (3) benzenesulphonic acid; (4) 4,5-dihydroxy-2,7-naphthalenedisulphonic acid; (5) 4-nitrobenzenesulphonic acid; (6) 2-naphthol-3,6-disulphonic acid; (7) 2-naphtholsulphonic acid; (8) 1-naphthol-5-sulphonic acid. Column: as in Fig. 2.

Separation of test mixtures

In order to demonstrate the potential of the tri-*n*-octylamine-aqueous perchloric acid system and to show the effect of temperature and perchlorate concentration on the resolution and separation time, a number of separations were carried out.

Fig. 2 shows the influence of temperature on the separation time and resolution of carboxylic acids. The flow-rate was adjusted to the same value in both instances. It can be seen that the separation time decreases by one third without much resolution being lost when the temperature is raised from 25° to 65°. This change in the separation characteristics with temperature is typical of liquid-liquid chromatography when chemical equilibria are not predominant. It is caused essentially by the decrease in

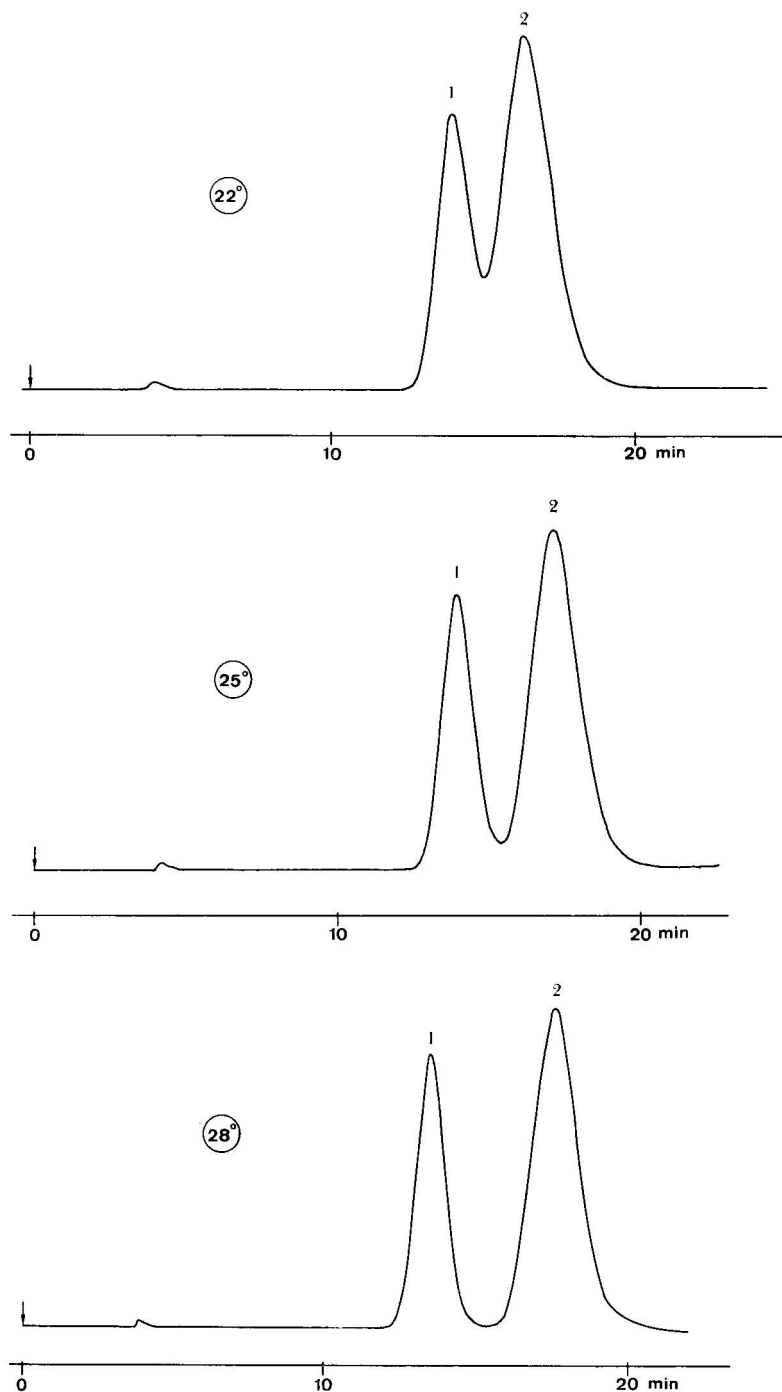


Fig. 4. Extreme example of the influence of temperature on the resolution of two aromatic sulphonic acids: (a) 22°; (b) 25°; (c) 28°. Sample: (1) 4-nitrobenzenesulphonic acid; (2) 2-naphthol-3,6-disulphonic acid. Column: as in Fig. 3.

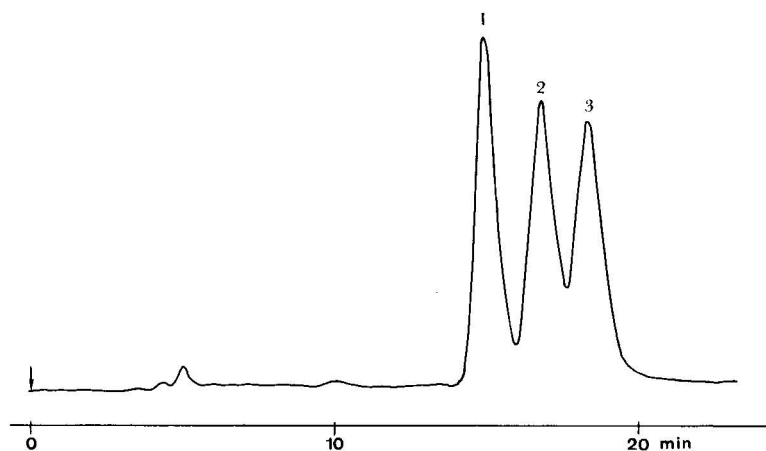


Fig. 5. Separation of methylbenzoic acid isomers. Sample: (1) 2-methylbenzoic acid; (2) 4-methylbenzoic acid; (3) 3-methylbenzoic acid. Column: as in Fig. 3. Temperature: 65°.

the capacity ratio and selectivity factor with temperature, as can be concluded from Table II.

Fig. 3 shows the influence of temperature on the resolution and separation time at constant flow-rate for sulphonic acids. It can be seen that the resolution changes considerably with temperature in some instances, whereas the separation time remains approximately constant. The resolution of benzenesulphonic acid and 4,5-dihydroxy-2,7-naphthalenedisulphonic acid, in particular, is not sufficient to show two peaks at 25°, and at 65° the two peaks are substantially resolved. This behaviour with respect to temperature changes is typical of liquid-liquid chromatography when ion-pair

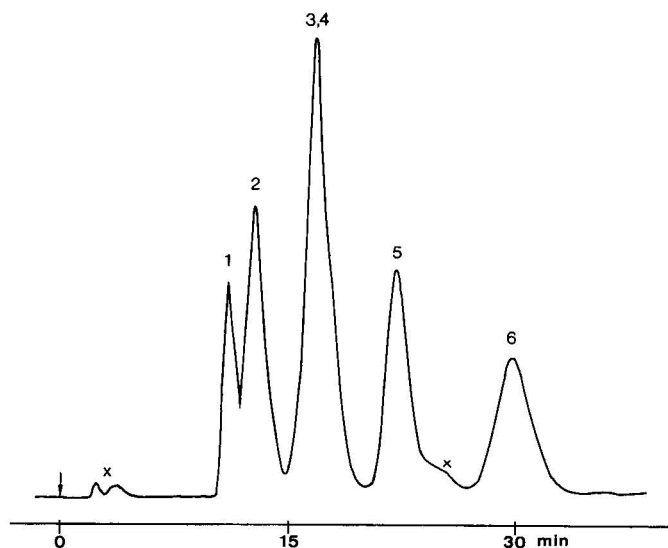


Fig. 6.

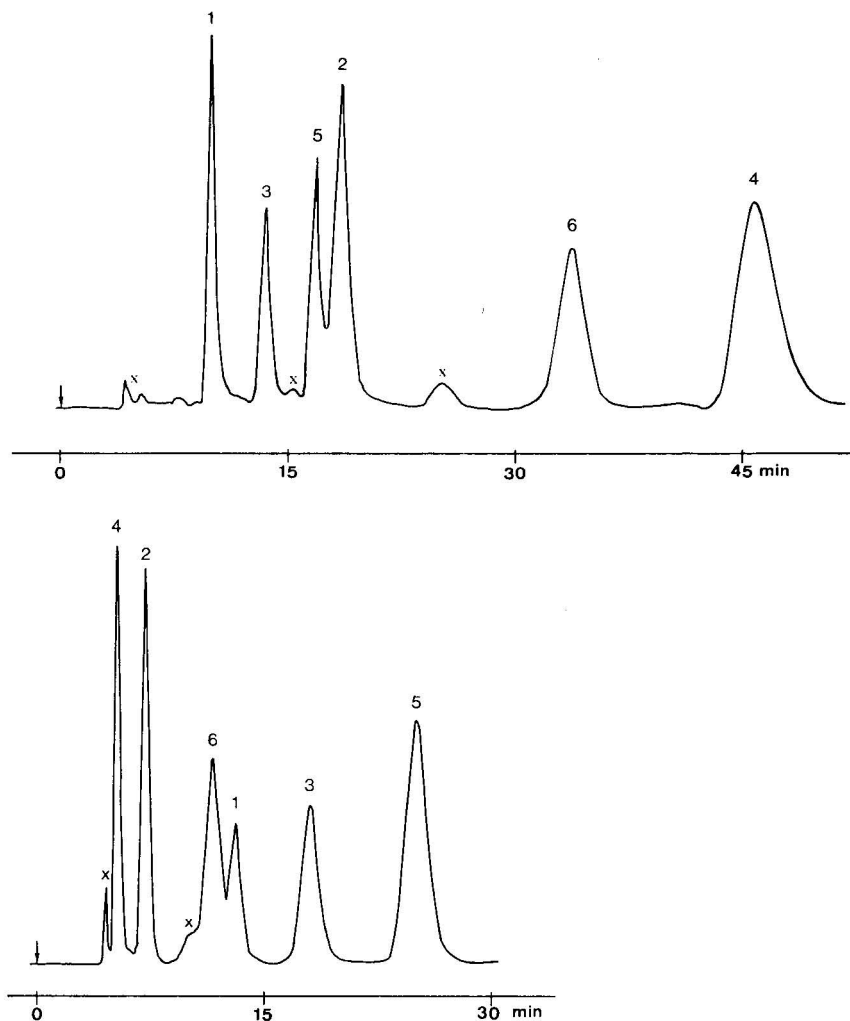


Fig. 6. Influence of temperature and anion concentration in the mobile phase on the group separation of aromatic sulphonic and carboxylic acids. Column: (a) TOA, 0.05 M $HClO_4$, pH 1.5; temperature, 25°. (b) TOA, 0.05 M $HClO_4$, pH 1.5; temperature, 65°. (c) TOA, 0.20 M $HClO_4$, pH 1.5; temperature, 25°. Sample: (1) 4-nitrobenzoic acid; (2) 4-nitrobenzenesulphonic acid; (3) 2-hydroxybenzoic acid; (4) 2-naphthol-3,6-disulphonic acid; (5) 4-methylbenzoic acid; (6) 1-naphthol-2-sulphonic acid. Impurities are marked with crosses.

formation is predominant. According to Table II, it can be explained mainly by the change in the capacity ratio and the selectivity factor with temperature.

An extreme example of the influence of temperature on the resolution is demonstrated in Fig. 4. It can be seen that a temperature increase of 6° causes an increase in resolution of about 80%.

The difficult separation of methylbenzoic acid isomers is shown in Fig. 5. Satisfactory resolution was achieved.

A group separation of carboxylic and sulphonic acids can be of practical importance and is demonstrated in Fig. 6. It can be seen that at 25° the different types of acids are eluted in an irregular sequence and at 65° they are separated in groups, the carboxylic acids being eluted first. An analogous group separation can be achieved by increasing the perchlorate concentration in the mobile phase, when the sulphonic acids are eluted first, as shown in Fig. 6c.

Fig. 7 shows a rapid separation of a five-component mixture of sulphonic acids in which the flow-rate was increased to the limit possible with the glass columns used.

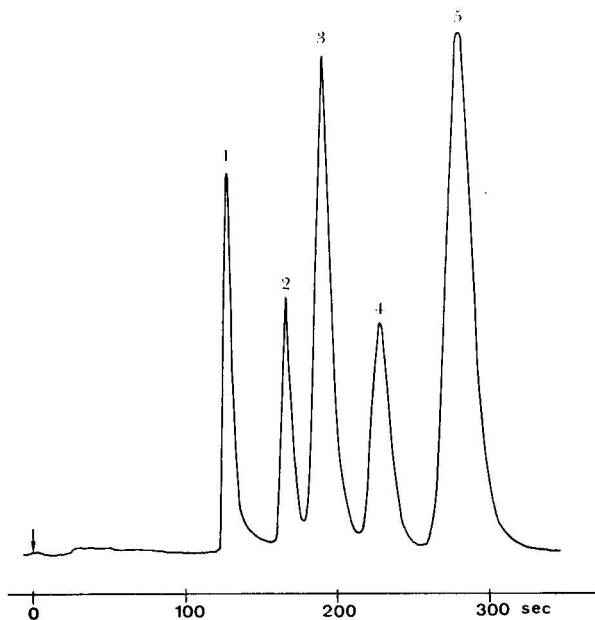


Fig. 7. Rapid separation of five aromatic sulphonic acids. Sample: (1) 3-aminotoluenesulphonic acid; (2) benzenesulphonic acid; (3) 4-nitrobenzenesulphonic acid; (4) 2-naphthol-3,6-disulphonic acid; (5) 2-naphthol-6-sulphonic acid. Column: TOA, 0.20 M HClO₄, pH 1.5. Flow-rate: 1.5 mm/sec. Temperature: 65°.

ACKNOWLEDGEMENTS

The authors are grateful for the assistance given by A. W. L. de Jong, K. Terwey-Groen and G. Szepesi.

REFERENCES

- 1 E. L. Smith and J. E. Page, *J. Soc. Chem. Ind., London*, 67 (1948) 48.
- 2 R. Modin, B.-A. Persson and G. Schill, in J. G. Gregory, B. Evans and P. C. Weston (Editors), *Proceedings of the International Solvent Extraction Conference 1971*, Vol. II, Society of Chemical Industry, London, 1971, p. 1211.
- 3 B.-A. Persson, *Acta Pharm. Suecica*, 8 (1971) 193.
- 4 S. Eksborg and B.-A. Persson, *Acta Pharm. Suecica*, 8 (1971) 605.
- 5 S. Eksborg, P. O. Lagerström, R. Modin and G. Schill, *J. Chromatogr.*, 83 (1973) 99.

- 6 S. Eksborg and G. Schill, *Anal. Chem.*, 45 (1973) 2092.
- 7 B.-A. Persson and B. L. Karger, *J. Chromatogr. Sci.*, 12 (1974) 521.
- 8 M. W. Scoggins and J. W. Miller, *Anal. Chem.*, 40 (1968) 1155.
- 9 R. H. Stehl, *Anal. Chem.*, 42 (1970) 1802.
- 10 J. A. Schmitt and R. A. Henry, *Chromatographia*, 3 (1970) 497.
- 11 J. S. Fritz and R. K. Gillette, *Anal. Chem.*, 40 (1968) 1777.
- 12 J. F. K. Huber, *Chimia*, Suppl. (1970) 24.
- 13 J. F. K. Huber and J. A. R. J. Hulsman, *Anal. Chim. Acta*, 38 (1967) 303.
- 14 J. F. K. Huber, J. C. Kraak and H. Veening, *Anal. Chem.*, 44 (1972) 1554.

CHROM. 7904

HIGH-PRESSURE LIQUID CHROMATOGRAPHY WITH ION-EXCHANGE CELLULOSES AND ITS APPLICATION TO THE SEPARATION OF ESTROGEN GLUCURONIDES

Sj. VAN DER WAL and J. F. K. HUBER*

Laboratory of Analytical Chemistry, University of Amsterdam, Nieuwe Achtergracht 166, Amsterdam (The Netherlands)

SUMMARY

The selectivity of a number of different types of anion exchangers for estrogen glucuronides was investigated. The effects of the nature of the exchanger anion, its concentration in the eluent, the pH of the eluent and temperature on the chromatographic resolution parameters for estrogen glucuronides on ECTEOLA-cellulose are discussed in detail.

The preparation of high-efficiency columns from ion-exchange celluloses was investigated and the influence of the particle size and temperature on the efficiency is discussed.

Several chromatograms of test mixtures are presented in order to demonstrate the performance of ion-exchange cellulose columns. Significant variations in efficiency and selectivity were found for different batches of the same type of ion exchanger.

INTRODUCTION

Steroids in urine are excreted as conjugates. Fig. 1 shows an example of the structure of a steroid conjugate, an estrogen glucuronide. Estrogen glucuronides constitute a major part of the urinary steroid hormones during pregnancy^{1–3} and give information on the physical condition of the foetus⁴.

Since the discovery that steroids are produced, transported and metabolized as conjugates⁵, the view has grown that physiological information is lost by hydrolysis of the conjugates. The formation of artifacts⁶ and loss of time⁷ during hydrolysis make it worthwhile to develop a method for the direct determination of these compounds.

Because of their low concentration and diversity, the separation of steroid conjugates must be performed in more than one step⁸:

(1) separation from other urine constituents;

* Present address: Institut für Analytische Chemie, Universität Wien, Währinger Strasse 38, Vienna, Austria.

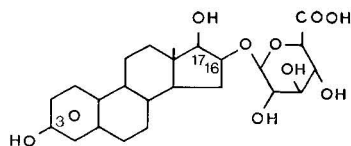


Fig. 1. Structure of estriol-16 α -glucuronide (E₃-16G).

- (2) separation into groups;
- (3) separation of the individual compounds.

So far, most attention has been paid to the first two steps. The present work is concerned with the separation of individual components.

Steroid conjugates are not sufficiently volatile to allow their direct gas chromatographic separation: a derivatization step has to be carried out prior to the separation by gas chromatography. Liquid chromatography, especially ion-exchange chromatography, taking advantage of the ionic character of the estrogen glucuronides, makes it possible to separate the steroid conjugates themselves, and it should therefore be the method of choice.

Disappointing results in the chromatographic separation of steroid conjugates have been reported⁹ for anion-exchange resins with hydrophobic polystyrene-divinylbenzene matrixes, probably because of interactions with the steroid skeleton.

Cellulose ion exchangers are promising with respect to their selectivity, but have a drawback in high-pressure liquid chromatography owing to their non-rigid structure. Few publications have been devoted to the packing of columns with these materials^{10,11}. Encouraged by the progress made in the packing of columns with rigid materials, an attempt was made to prepare highly efficient columns from ion-exchange cellulose materials.

EXPERIMENTAL

Apparatus

Two types of liquid chromatograph were used. One liquid chromatograph was assembled from commercial and custom-made parts and consists of a thermostated eluent reservoir, a high-pressure pump, a manometer, a flow resistance, a septum injection port, a separation column, a UV detector with an amplifier and a flat-bed potentiometric recorder. The pumping device is a reciprocating piston pump (Lewa FL 1). The flow pulses are eliminated by means of a flow-through Bourdon-tube manometer and a stainless-steel capillary flow resistance. The injection port, the separation column, its connections and the detector cell have been described in detail in previous publications¹²⁻¹⁴. The detector is a variable-wavelength spectrophotometer (Uicam SP 500), the output signal of which is amplified by an amplifier (Knick 72 W) and recorded by a linear potentiometric recorder (Servogor RE 511).

The other liquid chromatograph was a commercial apparatus (Hewlett-Packard 1010 A). This instrument was equipped with standard injection ports and two pumps. Stainless-steel columns (25 \times 0.3 cm) were used. The detector was a variable-wavelength UV spectrophotometer (HP 1030 B). The chromatograms were recorded by a linear potentiometric flat-bed recorder (Servogor RE 511).

The columns were packed using a pressurized slurry technique.

Chemicals

Samples. The glucuronides used were the sodium salts of testosterone- β -D-glucuronide (T-G), estrone- β -D-glucuronide (E₁-G), β -estradiol-3 β -D-glucuronide (E₂-3G), β -estradiol-17 β -D-glucuronide (E₂-17G), estriol-3 β -D-glucuronide (E₃-3G), estriol-16 α -(β -D-glucuronide) (E₃-16G) and estriol-17 β -(β -D-glucuronide) (E₃-17G) (all obtained from Sigma, St. Louis, Mo., U.S.A.). The molar absorptivity of estrogen glucuronides is about 10^3 at 275 nm and five times as high at 220 nm. Histamine was used as an unretarded tracer.

Column materials. Solutions of sodium chloride, sodium acetate, ammonium formate and citric acid in deionized water were used as eluents. The specified pH was adjusted by means of sodium hydroxide or acetic acid. All chemicals were of p.a. quality (Merck, Darmstadt, G.F.R.).

The following six types of anion-exchange materials were used as column packings: (i) Polydextran gel Sephadex G-15, Superfine (Pharmacia, Uppsala, Sweden), pre-swollen in deionized water and washed with pyridine¹⁵; (ii) dextran-based anion exchanger DEAE-Sephadex A-25 (Pharmacia), ion-exchange capacity (i.e.c.) 3.5 mequiv./g, left to swell for 1 week; (iii) polyalkylene amine-based anion-exchanger, Bio-Rex 5 (Bio-Rad Labs., Richmond, Calif., U.S.A.), i.e.c. 8.8 mequiv./g, swollen for 1 day; (iv) aminoethylcellulose Cellex AE (Bio-Rad), i.e.c. 0.37 mequiv./g; (v) diethylaminoethylcellulose Cellex D (Bio-Rad), i.e.c. 0.61 mequiv./g; (vi) ECTEOLA-cellulose Cellex E (Bio-Rad), i.e.c. 0.44 mequiv./g; MN 300 (Macherey, Nagel & Co., Düren, G.F.R.), i.e.c. 0.35 mequiv./g; Baker 300 (Baker, Deventer, The Netherlands), i.e.c. 0.35 mequiv./g; Servacel TLC p.a. (Serva, Heidelberg, G.F.R.), i.e.c. not specified; and Whatman ET 41 (W. & R. Balston, Maidstone, Great Britain), i.e.c. not specified. The cellulose ion exchangers were swollen by pre-cycling with 0.5 *N*

TABLE I

PARTICLE SIZES AND ION-EXCHANGE CAPACITIES OF ION-EXCHANGE MATERIALS USED AS COLUMN PACKINGS

Anion exchanger	Particle diameter range 10–90% (μ m)	Mean particle diameter (μ m)	Ion-exchange capacity (mequiv./g)
Cellex E	18–26	20	0.31
	15.5–24	18	
	7–17.5	12	
	5.5–12.5	9	
MN 300, batch A	11–19	14	0.04
MN 300, batch B	5–10	7	
Baker 300	12–27	19	0.27
	9–19	13	
	<14	8	
ET 41	16–26	20	0.23
	<17	10	
Servacel TLC	9–24	17	0.10
	7–18	11	0.05
	<12	7	0.03
Cellex AE	10.5–19	14	0.29
	5–13	9	

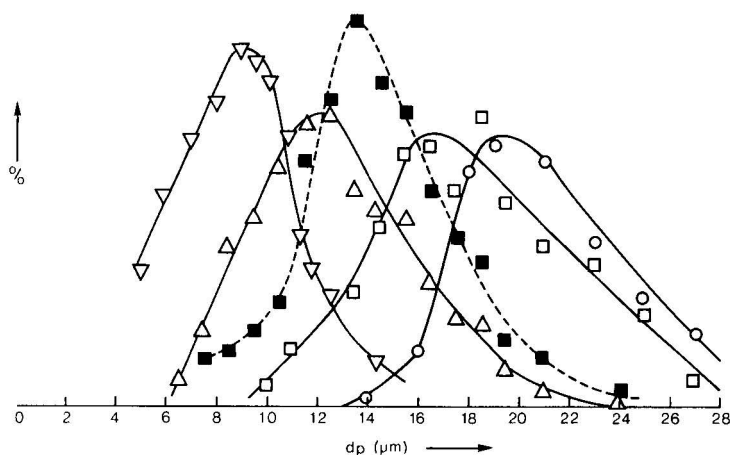


Fig. 2. Particle size distribution of air-classified fractions. —, Cellex E; ---, MN 300 (batch A). Mean particle diameter: ○, 20 μm ; □, 18 μm ; △, 12 μm ; ▽, 9 μm ; ■, 14 μm .

sodium hydroxide solution, 0.5 *N* hydrochloric acid and 0.5 *N* sodium hydroxide solution and rinsed with deionized water.

The ECTEOLA- and AE-celluloses were fractionated with an air classifier (Alpine Model 100 MZR) and the particle size distributions were determined with a Coulter Counter (Model D) (see Table I and Fig. 2).

The actual ion-exchange capacities were determined as the buffer capacity between pH 10 and pH 4 in 0.5 *N* sodium chloride solution (Table II). An automatic titrator (Radiometer TTT 1) was used.

RESULTS AND DISCUSSION

The choice of the phase system for a chromatographic separation should be based on the equation for the resolution, R_{ji} , of two components, j and i :

$$R_{ji} = (r_{ji} - 1) \cdot \frac{\kappa_i}{\kappa_i + 1} \cdot (N_i)^{\frac{1}{2}} \quad (1)$$

where

r_{ji} = selectivity factor = ratio of the capacity ratios of the components j and i in the phase system;

κ_i = capacity ratio of component i ;

$N_i = L/H_i$ = number of theoretical plates for component i ;

L = length of the column;

H_i = theoretical plate height for component i .

In a first approach, those phase systems should be selected for which the values of the factor $(r_{ji} - 1) \cdot [\kappa_i/(\kappa_i + 1)]$ for each pair of successively eluting components of the sample are largest, with the restriction that extremely high capacity ratios should be avoided, because otherwise the separation time becomes too long. The final choice of the appropriate phase system is made by taking into account the

column efficiency attainable with those phase systems which had been pre-selected because of their selectivity.

The capacity ratio was determined from the retention time, t_{Ri} , of the component i and the hold-up time, t_{R0} , of the eluent:

$$\kappa_i = \frac{t_{Ri} - t_{R0}}{t_{R0}} \quad (2)$$

The hold-up time was determined by means of an inert tracer (histamine).

Column selectivity

According to eqn. 1, the resolution of two components depends on the factor $(r_{ji} - 1) \cdot [\kappa_i / (\kappa_i + 1)]$, which is determined mainly by the distribution coefficients of the components, as the capacity ratio and the distribution coefficient, K , are proportional:

$$\kappa = q \cdot K \quad (3)$$

where the proportionality factor q is the phase ratio of the ion exchanger and the mobile phase.

From the equations describing the ion-exchange equilibrium of the anion X^- and the dissociation equilibrium of the protonated form HX , an expression for the overall distribution coefficient, K_x , of component X can be derived:

$$K_x = \frac{[X^-]_s}{[X^-]_m + [HX]_m} = \frac{K_1}{[A^-]_m (1 + K_2 [H^+]_m)} \quad (4)$$

where

$[X^-]_s$ = anion concentration of the sample component in the anion exchanger;

$[X^-]_m$ = anion concentration of the sample component in the mobile phase;

$[HX]_m$ = concentration of the undissociated sample component in the mobile phase;

$[A^-]_m$ = anion concentration of the counter ion of the ion exchanger in the mobile phase;

$[H^+]_m$ = hydrogen ion concentration in the mobile phase;

K_1 = ion-exchange equilibrium constant;

K_2 = formation constant of HX .

Influence of the type of anion exchanger. The ion-exchange equilibrium constant in eqn. 4 depends on, in addition to the nature of the sample anion, the nature of the matrix, the fixed ionogenic group and the mobile counter ion of the ion exchanger. A number of anion-exchange systems were screened for their selectivity with respect to estrogen glucuronides. The results are shown in Table II. The separation of a pair of compounds becomes difficult when the factor $(r_{ji} - 1) \cdot [\kappa_i / (\kappa_i + 1)]$ is less than 0.1.

It can be seen that the nature of the matrix, the fixed cationic group and the mobile counter anion of the ion exchanger have little influence on the elution order, which is determined primarily by the nature of the sample. The site of conjugation

in the estrogen conjugates was found to be more important than the type of steroid. Estrogen-3-glucuronides are eluted first, followed by 17- and then 16-glucuronides. The elution order according to the type of steroid is estriol, estrone and estradiol, except on Bio-Rex 5, where the order is estrone, estriol and estradiol. The separation of the pair E_3 -17G and E_3 -16G is difficult on all ion-exchange systems shown in Table II, whereas the separations of E_1 -G and E_3 -3G as well as of E_3 -17G and E_2 -3G are difficult only on certain systems. The separations of the other pairs of estrogen conjugates in Table II give no serious problems. Resolutions involving E_3 -17G are of minor interest from the clinical point of view, as this conjugate is reported not to occur in human urine in significant concentrations². Therefore, the discussion of the choice of an optimal phase system will be focused on the resolution of E_1 -G and E_3 -3G and occasionally E_3 -16G and E_2 -3G.

The separation of estrone and estradiol conjugates on DEAE-Sephadex has been reported earlier^{16,17}. From Table II, it can be concluded that the selectivity of this type of anion exchanger is insufficient when estriol conjugates are present.

ECTEOLA- and AE-cellulose ion exchangers were found to be more rigid and therefore more suited for high-pressure liquid chromatography than the other materials. They were chosen for further investigations, although polydextran gel would be more favourable in terms of overall selectivity. The variation of the properties of different batches of the same type of anion exchanger was investigated for six batches of ECTEOLA-cellulose, the particle sizes and ion-exchange capacities of which are given in Table I. Their selectivity data are given in Table III. It can be seen that the ion-exchange capacity and also the selectivity factor change significantly from batch to batch. An exact interdependence between the two parameters does not exist, however. The selectivity for E_1 -G- E_3 -3G, for instance, is smallest on ET 41, although its ion-exchange capacity is intermediate. The materials Baker 300 and MN 300/A appear to be identical, while MN 300/B resembles Servacel TLC. The ion-exchange capacity of Servacel TLC was found to be strongly dependent on the particle size, whereas that of Baker 300 was found to be constant, as reflected in the capacity ratios.

The effect of the nature of the mobile counter anion of the anion exchanger was studied in more detail. The results are presented in Table IV, from which it can be concluded that the nature of the counter anion has a significant influence on the absolute value of the capacity ratio but has a less distinct influence on the relative value, the selectivity factor.

Effect of eluent composition. According to eqn. 4, the distribution coefficient and with it the capacity ratio depend on the concentrations of the ion-exchanger counter anion and the hydrogen ion in the eluent.

The influence of the anion concentration was studied for chloride anions (Table V). In agreement with eqn. 4, it can be seen that the anion concentration has an insignificant influence on the selectivity factor. The reciprocal inter-relationship between the capacity ratio and the anion concentration is confirmed by the plots shown in Fig. 3. Extrapolation to infinitely large anion concentration gives significant residue values, which make it likely that the distribution process involved is a mixed mechanism including ion exchange and adsorption.

The influence of the pH of the eluent in an ion-exchange process is also described by eqn. 4, which predicts that the distribution coefficient is independent of

TABLE III
CAPACITY RATIOS AND SELECTIVITY FACTORS OF SUCCESSIVE COMPONENTS FOR ESTROGEN GLUCURONIDES ON DIFFERENT BATCHES OF ECTEOLA-CELLULOSE AT 70°
Number of repetitive measurements, 3; relative standard deviation of measurement, 2%.

Conditions		Ion exchanger																									
		Cellex E			MN 300			ET 41			Baker 300			Baker 300			Servacel TLC			Servacel TLC							
Mean particle size (μm)	Eluent	18	14	7	7	50 mM	chloride + acetate	20	250 mM	chloride + acetate	19	125 mM	chloride + acetate	13	125 mM	chloride + acetate	8	125 mM	chloride + acetate	17	125 mM	chloride + acetate	11	125 mM	chloride + acetate	7	50 mM
pH		5.0	5.0	5.0	5.0	5.0	5.0	5.0	5.0	5.0	5.0	5.0	5.0	5.0	5.0	5.0	5.0	5.0	5.0	5.0	5.0	5.0	5.0	5.0	5.0	5.0	5.0
Component		K_n	$r_{(n+1)n}$	K_n	$r_{(n+1)n}$	K_n	$r_{(n+1)n}$	K_n	$r_{(n+1)n}$	K_n	$r_{(n+1)n}$	K_n	$r_{(n+1)n}$	K_n	$r_{(n+1)n}$	K_n	$r_{(n+1)n}$	K_n	$r_{(n+1)n}$	K_n	$r_{(n+1)n}$	K_n	$r_{(n+1)n}$	K_n	$r_{(n+1)n}$	K_n	$r_{(n+1)n}$
T-G		0.66	1.57	0.62	1.37	0.48	1.40	0.89	1.59	0.96	1.35	0.94	1.33	0.88	1.30	0.88	1.39	0.88	1.30	0.88	1.39	0.88	1.39	0.24	1.62	0.35	1.61
E ₃ -3G		1.04	1.15	0.84	1.11	0.67	1.31	1.42	1.06	1.29	1.12	1.25	1.13	1.11	1.15	1.22	1.21	1.22	1.21	1.11	1.15	1.22	1.21	0.39	1.29	0.56	1.31
E ₁ -G		1.19	1.67	0.94	1.52	0.88	1.68	1.50	1.52	1.45	1.47	1.41	1.47	1.28	1.51	1.48	1.61	1.48	1.61	1.28	1.51	1.48	1.61	0.50	1.65	0.74	1.69
E ₂ -3G		1.98	1.30	1.42	1.14	1.48	1.25	2.29	1.16	2.13	1.08	2.08	1.07	1.93	1.06	2.38	1.26	2.38	1.06	1.93	1.06	2.38	1.26	0.83	1.31	1.25	1.31
E ₃ -17G		2.56	1.04	—	—	—	—	2.65	1.04	2.30	1.02	2.21	1.02	2.21	1.02	2.04	1.02	3.00	1.01	3.00	1.01	3.00	1.01	1.09	1.01	1.64	1.08
E ₃ -16G		2.70	1.26	1.62	1.30	1.85	1.19	2.76	1.19	2.34	1.29	2.28	1.30	2.28	1.30	2.07	1.33	3.03	1.27	3.03	1.27	3.03	1.27	1.10	1.29	1.78	1.28
E ₂ -17G		3.36	—	2.17	—	2.20	—	3.28	—	3.03	—	2.96	—	2.96	—	2.76	—	3.84	—	2.76	—	3.84	—	1.42	—	2.28	—

TABLE IV
DEPENDENCE OF THE CAPACITY RATIO AND THE SELECTIVITY FACTOR OF SUCCESSIVE COMPONENTS ON THE FORM OF THE ANION EXCHANGER
Number of repetitive measurements, 3; relative standard deviation of measurement, 2%.

Conditions	Ion exchanger				Cellex AE			
	Cellex E		Formate		Acetate		Chloride	
Eluent	1.0 M formate	1.0 M acetate	0.5 M acetate	0.5 M acetate	0.05 M formate	0.05 M acetate	0.125 M chloride + 0.05 M acetate	0.125 M chloride + 0.05 M acetate
pH	5.0	5.0	5.0	5.0	6.7	5.0	5.0	5.0
Temperature (°C)	25	25	25	25	30	25	25	25
Component	Cellex E		Formate		Acetate		Chloride	
	K_n	$r_{(n+1)n}$	K_n	$r_{(n+1)n}$	K_n	$r_{(n+1)n}$	K_n	$r_{(n+1)n}$
T-G	0.85	2.31	1.26	1.82	1.79	1.87	0.57	2.10
E ₃ -3G	1.82	1.18	2.29	1.23	3.35	1.18	1.20	1.16
E ₁ -G	2.15	1.48	2.82	1.54	3.95	1.53	1.39	1.59
E ₂ -3G	3.29	1.53	4.35	1.45	6.05	1.50	2.21	1.57
E ₃ -17G	5.25	1.04	6.32	1.13	9.10	1.09	3.46	1.08
E ₃ -16G	5.77	1.26	7.15	1.10	9.95	1.17	3.73	1.25
E ₂ -17G	6.61	—	7.88	—	11.60	—	4.68	—
					5.59	1.10	6.13	—
					11.89	1.07	12.7	—
					2.52	1.07	2.70	—
					1.07	1.07	2.34	1.08
					2.34	1.03	11.56	1.03
					6.94	1.67	5.22	1.33
					5.12	1.02	3.81	1.34
					2.46	1.02	1.01	1.09
					1.86	1.32	0.82	1.24

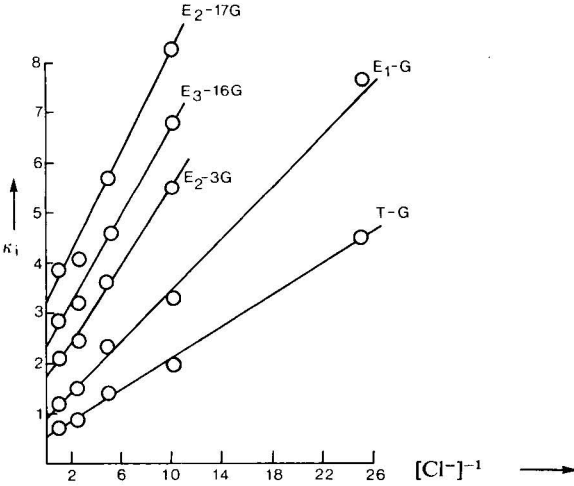


Fig. 3. Dependence of the capacity ratio on the anion concentration in the eluent. Phase system: Cellex E; chloride + 0.05 M acetate, pH 4.7; 70°.

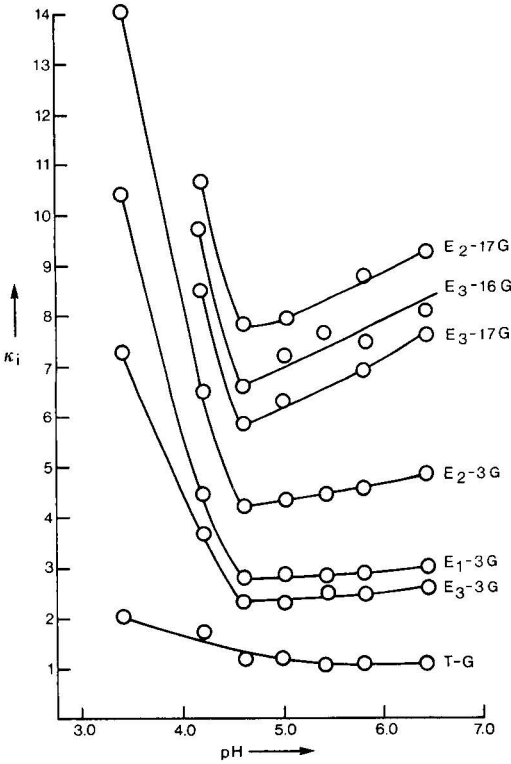


Fig. 4. Dependence of the capacity ratio on the pH of the eluent. Phase system: Cellex E; 1.0 M acetate; 25°.

TABLE VI
DEPENDENCE OF THE CAPACITY RATIO AND THE SELECTIVITY FACTOR OF SUCCESSIVE COMPONENTS ON THE PH OF THE ELUENT
Number of repetitive measurements, 3; relative standard deviation of measurement, 3%.

Phase system: Cellex E; 0.5 M chloride + 0.05 M acetate; 70°													
Component	pH 3.0	pH 4.0	pH 4.5	pH 5.0	pH 5.5	pH 6.0	pH 6.5	pH 7.0					
	K_n	$r_{(n+1)n}$	K_n	$r_{(n+1)n}$	K_n	$r_{(n+1)n}$	K_n	$r_{(n+1)n}$	K_n	$r_{(n+1)n}$	K_n	$r_{(n+1)n}$	K_n
T-G	0.83	1.40	0.64	1.61	0.64	1.56	0.66	1.58	0.67	1.57	0.66	1.52	0.65
E ₃ -3G	1.16	1.10	1.03	1.16	1.00	1.16	1.04	1.15	1.05	1.14	1.00	1.15	0.98
E ₁ -G	1.27	1.69	1.20	1.63	1.16	1.67	1.19	1.66	1.20	1.67	1.15	1.67	1.10
E ₂ -3G	2.14	1.08	1.96	1.29	1.94	1.30	1.98	1.30	2.00	1.31	1.92	1.34	1.84
E ₃ -17G	2.30	1.05	2.52	1.07	2.52	1.04	2.56	1.05	2.61	1.04	2.57	1.04	2.52
E ₃ -16G	2.42	1.45	2.69	1.24	2.62	1.27	2.70	1.25	2.71	1.25	2.67	1.25	2.58
E ₂ -17G	3.52	—	3.34	—	3.33	—	3.36	—	3.38	—	3.35	—	3.36
Phase system: Cellex E; 1.0 M acetate; 25°													
Component	pH 3.4	pH 4.2	pH 4.6	pH 5.0	pH 5.4	pH 5.8	pH 6.4						
	K_n	$r_{(n+1)n}$	K_n	$r_{(n+1)n}$	K_n	$r_{(n+1)n}$	K_n	$r_{(n+1)n}$	K_n	$r_{(n+1)n}$	K_n	$r_{(n+1)n}$	K_n
T-G	2.05	3.6	1.67	2.20	1.18	1.97	1.26	1.82	1.07	2.34	1.16	2.07	1.11
E ₃ -3G	7.25	1.42	3.67	1.20	2.33	1.18	2.29	1.23	2.50	1.13	2.39	1.20	2.55
E ₁ -G	10.4	1.31	4.4	1.48	2.75	1.54	2.82	1.54	2.83	1.57	2.86	1.60	2.92
E ₂ -3G	13.65	—	6.52	1.30	4.23	1.38	4.35	1.45	4.46	—	4.58	1.51	4.77
E ₃ -17G	—	—	8.45	1.15	5.83	1.13	6.32	1.13	—	—	6.90	1.09	7.60
E ₃ -16G	—	—	9.7	1.09	6.57	1.19	7.15	1.10	7.63	—	7.51	1.16	8.17
E ₂ -17G	—	—	10.6	—	7.8	—	7.88	—	—	—	8.75	—	9.25
Phase system: Cellex E; 1.0 M formate; 25°													
Component	pH 3.4	pH 4.0	pH 5.0	pH 5.6									
	K_n	$r_{(n+1)n}$	K_n	$r_{(n+1)n}$	K_n	$r_{(n+1)n}$	K_n	$r_{(n+1)n}$	K_n	$r_{(n+1)n}$	K_n	$r_{(n+1)n}$	K_n
T-G	1.38	2.12	0.86	2.31	0.85	2.14	0.85	2.03					
E ₃ -3G	2.93	1.17	1.99	1.18	1.82	1.18	1.73	1.21					
E ₁ -G	3.43	1.48	2.35	1.48	2.15	1.53	2.10	1.53					
E ₂ -3G	5.07	1.45	3.48	1.53	3.29	1.60	3.21	1.68					
E ₃ -17G	7.37	1.31	5.34	1.04	5.25	1.10	5.38	1.10					
E ₃ -16G	7.34	1.00	5.55	1.26	5.77	1.15	5.94	1.14					
E ₂ -17G	9.65	—	7.00	—	6.61	—	6.78	—					

pH when the formation constant is much smaller than the reciprocal of the hydrogen ion concentration. It is obvious that in this case the selectivity factor is constant. When the formation constant K_2 is of the order of or larger than the reciprocal of the hydrogen ion concentration, the distribution coefficient decreases with decreasing pH. In this pH range, a change in the selectivity factor with pH occurs if the formation constants differ. For the case when the protonated form HA is a weak acid, the A^- concentration will decrease with decreasing pH and consequently the distribution coefficient increases.

The results in Table VI and Fig. 4 can be explained by the prediction of eqn. 4, considering the proportionality of the capacity ratio and the distribution coefficient. For the chloride anion, the capacity ratio is about constant, while for the

TABLE VII

EFFECT OF TEMPERATURE ON THE CAPACITY RATIO AND THE SELECTIVITY FACTOR OF SUCCESSIVE COMPONENTS

Component	Phase system: Cellex E; 0.5 M chloride + 0.05 M acetate; pH 4.5					
	40°		50°		75°	
	K_n	$r_{(n+1)n}$	K_n	$r_{(n+1)n}$	K_n	$r_{(n+1)n}$
T-G	1.20	1.65	1.20	1.54	1.20	1.40
E ₃ -3G	1.98	1.23	1.85	1.21	1.68	1.17
E ₁ -G	2.44	1.58	2.24	1.60	1.96	1.60
E ₂ -3G	3.86	1.33	3.58	1.28	3.13	1.20
E ₃ -17G	5.14	1.07	4.58	1.06	—	—
E ₃ -16G	5.51	1.30	4.83	1.32	3.76	1.34
E ₂ -17G	7.17	—	6.37	—	5.04	—

Component	Phase system: Baker 300; 0.125 M chloride + 0.05 M acetate; pH 5.0							
	25°		40°		55°		70°	
	K_n	$r_{(n+1)n}$	K_n	$r_{(n+1)n}$	K_n	$r_{(n+1)n}$	K_n	$r_{(n+1)n}$
T-G	0.92	1.38	0.92	1.35	0.89	1.31	0.87	1.29
E ₃ -3G	1.26	1.25	1.24	1.21	1.16	1.18	1.11	1.15
E ₁ -G	1.58	1.40	1.50	1.44	1.38	1.45	1.28	1.51
E ₂ -3G	2.21	1.13	2.17	1.09	2.00	1.09	1.93	1.05
E ₃ -17G	2.49	1.07	2.38	1.07	2.18	1.03	2.03	1.02
E ₃ -16G	2.65	1.35	2.55	1.33	2.23	1.34	2.07	1.33
E ₂ -17G	3.59	—	3.39	—	2.99	—	2.76	—

Component	Phase system: Cellex AE; 0.125 M chloride + 0.05 M acetate; pH 5.0			
	25°		70°	
	K_n	$r_{(n+1)n}$	K_n	$r_{(n+1)n}$
T-G	0.82	1.24	0.73	1.15
E ₃ -3G	1.01	1.09	0.84	1.04
E ₁ -G	1.10	1.26	0.87	1.32
E ₂ -3G	1.39	1.68	1.15	1.37
E ₃ -17G	2.34	1.08	1.57	1.06
E ₃ -16G	2.70	—	1.65	1.00
E ₂ -17G	2.52	1.07	1.66	—

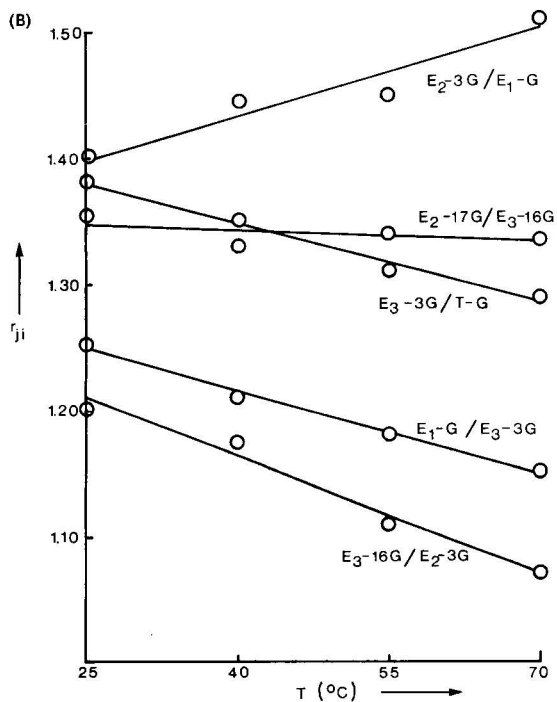
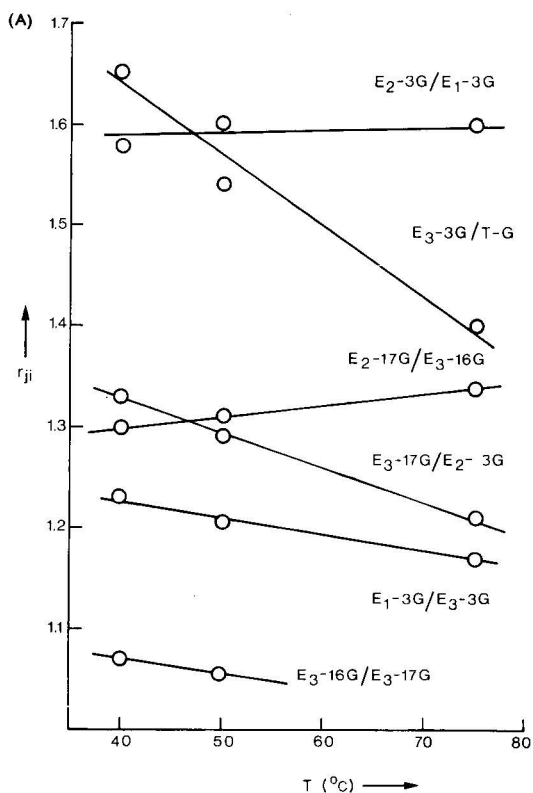


Fig. 5. The effect of temperature on the selectivity factor. Phase systems: A, Cellex E; 0.5 M chloride + 0.05 M acetate, pH 4.5; B, Baker 300; 0.125 M chloride + 0.05 M acetate, pH 5.0.

acetate anion the capacity ratio increases when the pH decreases beyond the pK_a of the acetic acid. The selectivity factor is only slightly influenced by the pH.

Effect of temperature. Capacity ratios and selectivity factors were measured at different temperatures on three ion-exchange systems with ECTEOLA- and AE-cellulose. The results are presented in Table VII and Fig. 5. It can be seen that the capacity ratio decreases with temperature, as usual. In some instances, the selectivity factor changes only slightly with temperature, while in others significant changes can be seen. In terms of resolution, the changes in the selectivity factors are mostly not very important, as they are either small or the values of the selectivity factors and those of the corresponding capacity ratios are relatively large, making the separation easy. An exception is the selectivity factor of E_3 -16G and E_2 -3G on Baker 300 ECTEOLA-cellulose, which increases from 1.07 at 70° to 1.20 at 25°.

Column efficiency

Theoretical plate height versus fluid velocity. In routine analysis, such as the determination of estrogens in urine, the speed of separation is of particular importance. An expression describing the retention time required for a given resolution is derived by substituting the theoretical plate number in eqn. 1 by means of the expression $NH_i = t_{Ri} \cdot v/(\kappa_i + 1)$:

$$t_{Ri} = \left(\frac{R_{ji}}{r_{ji} - 1} \right)^2 \cdot \frac{(\kappa_i + 1)^3}{\kappa_i^2} \cdot \frac{H_i}{v} \quad (5)$$

where v = average velocity of the eluent.

The ratio H/v should be made as small as possible when high-speed separation is required. It decreases with increasing fluid velocity and decreasing particle size. In

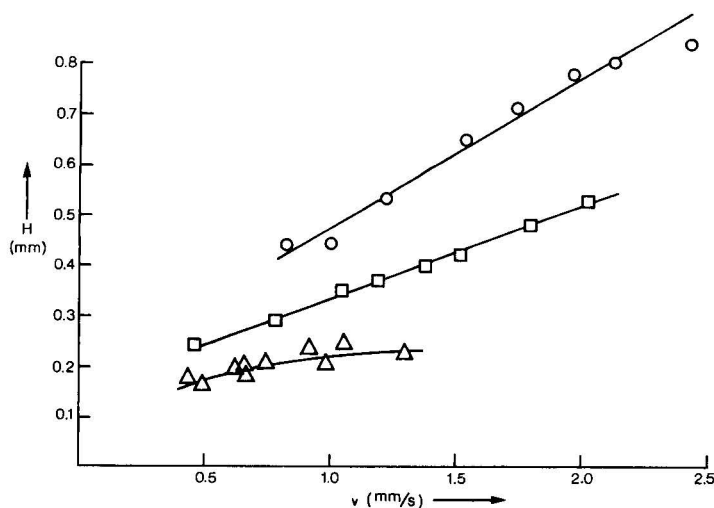


Fig. 6. H versus v curves for ECTEOLA-celluloses of different average particle size: ○, 20 μ m; □, 18 μ m; △, 12 μ m. The test component is E_3 -3G with $\kappa = 0.99$ (20 μ m), 1.36 (18 μ m) and 1.18 (12 μ m). Phase system: Cellex E; 0.5 M chloride + 0.05 M acetate, pH 5.0; 70°.

TABLE VIII
COMPARISON OF THE EFFICIENCIES OF COLUMNS PACKED WITH DIFFERENT TYPES OF ANION EXCHANGERS

Property	Anion exchanger		
	Servacel TLC	MN 300/A (Baker 300)	Cellux E
Mean particle diameter (μm)	11	14	12
Eluent	0.125 M chloride + 0.01 M acetate	0.5 M chloride + 0.05 M acetate	0.5 M chloride + 0.025 M acetate
pH	5.0	5.0	5.0
Temperature ($^{\circ}\text{C}$)	70	70	70
κ ($\text{E}_3\text{-3G}$)	0.5	0.8	1.18
v and H	v (mm/sec) H (mm)	v (mm/sec) H (mm)	v (mm/sec) H (mm)
	0.38 0.29	0.42 0.14	0.42 0.16
	0.82 0.48	0.87 0.18	0.88 0.19
	1.28 0.70	1.36 0.22	1.34 0.22
	1.64 0.76	1.74 0.25	— —
	2.11 0.99	— —	2.19 —
$(H/v)_{\text{min.}}$ (sec)	0.47	0.14	0.17
			0.13

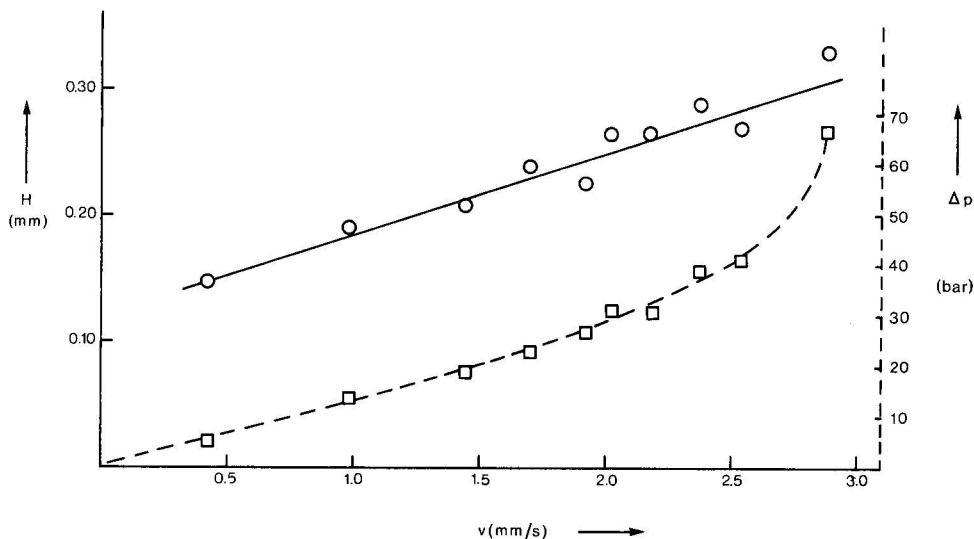


Fig. 7. H versus v (—) and Δp versus v (---) curves for aminoethylcellulose. Phase system: Cellex AE, $14\ \mu\text{m}$; $0.05\ M$ acetate, pH 5.0; 70° .

practice, the lowest attainable value, $(H/v)_{\min.}$, is determined by the maximum attainable fluid velocity, which is determined in the case of cellulose ion exchangers by the type of ion exchanger, its particle size and the pressure drop used during the packing of the column. Above the maximum fluid velocity, the column packing collapses as the pressure drop becomes too large.

Effect of particle size. The theoretical plate height was measured as a function of the fluid velocity at different average particle sizes for a given batch of ECTEOLA-cellulose, the columns being packed at 10 bar. The results are plotted in Fig. 6. Other batches of ECTEOLA-cellulose, with one exception, gave similar results, as can be seen from Table VIII. When an ECTEOLA-cellulose (Baker 300) with a mean

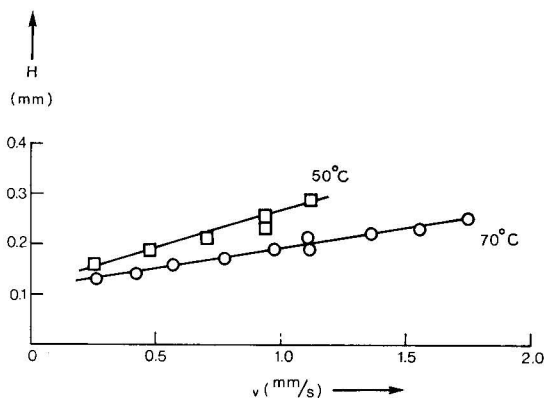


Fig. 8. H versus v curves at different temperatures. Test compound, E_3 -3G; $\kappa = 0.8$ (70°) and 0.9 (50°). Phase system: MN 300, $14\ \mu\text{m}$; $0.5\ M$ chloride + $0.05\ M$ acetate, pH 5.0.

TABLE IX
RESOLUTION PARAMETERS OF THE MOST DIFFICULT TO SEPARATE ESTROGEN GLUCURONIDES FOR SELECTED PHASE SYSTEMS

Property	Anion exchanger		Cellex E		Cellex AE	
	Baker 300					
Mean particle size (μm)	13		12		14	
Eluent	0.125 M chloride + 0.05 M acetate		0.5 M chloride + 0.05 M acetate		0.125 M chloride + 0.05 M acetate	
pH	5.0		4.5		5.0	
Temperature ($^{\circ}\text{C}$)	25		75		25	
Components: n	E ₃ -3G		E ₃ -3G		E ₃ -3G	
	E ₁ -G		E ₁ -G		E ₁ -G	
$(r_{(n+1)n} - 1) \kappa_n / (\kappa_n + 1)$	0.14		0.10		0.05	
	800		1700		8000	
$N_R = 4$	800		700		1400	
v_{max} (mm/sec)	1.5		1.3		1.3	
$(H_n/v)_{\text{min}}$ (sec)	0.27		0.17		0.28	
t_{R1} (min)	17		30		130	
$(\Delta P/L)_{\text{max}}$ (bar/cm)	0.65		0.60		2.5	
Components: n	E ₃ -17G		E ₃ -17G		E ₃ -17G	
	E ₃ -16G		E ₃ -16G		E ₃ -16G	
$(r_{(n+1)n} - 1) \kappa_n / (\kappa_n + 1)$	0.05		0.15		0.11	
	6000		700		1400	
$N_R = 4$	800		700		1400	
v_{max} (mm/sec)	1.5		1.3		1.3	
$(H_n/v)_{\text{min}}$ (sec)	0.27		0.17		0.28	
t_{R1} (min)	17		30		130	
$(\Delta P/L)_{\text{max}}$ (bar/cm)	0.65		0.60		2.5	
Components: n	E ₃ -3G		E ₃ -3G		E ₃ -3G	
	E ₁ -G		E ₁ -G		E ₁ -G	
$(r_{(n+1)n} - 1) \kappa_n / (\kappa_n + 1)$	0.14		0.10		0.05	
	800		1700		8000	
$N_R = 4$	800		700		1400	
v_{max} (mm/sec)	1.5		1.3		1.3	
$(H_n/v)_{\text{min}}$ (sec)	0.27		0.17		0.28	
t_{R1} (min)	17		30		130	
$(\Delta P/L)_{\text{max}}$ (bar/cm)	0.65		0.60		2.5	
Components: n	E ₃ -17G		E ₃ -17G		E ₃ -17G	
	E ₃ -16G		E ₃ -16G		E ₃ -16G	
$(r_{(n+1)n} - 1) \kappa_n / (\kappa_n + 1)$	0.05		0.15		0.11	
	6000		700		1400	
$N_R = 4$	800		700		1400	
v_{max} (mm/sec)	1.5		1.3		1.3	
$(H_n/v)_{\text{min}}$ (sec)	0.27		0.17		0.28	
t_{R1} (min)	17		30		130	
$(\Delta P/L)_{\text{max}}$ (bar/cm)	0.65		0.60		2.5	
Components: n	E ₃ -3G		E ₃ -3G		E ₃ -3G	
	E ₁ -G		E ₁ -G		E ₁ -G	
$(r_{(n+1)n} - 1) \kappa_n / (\kappa_n + 1)$	0.14		0.10		0.05	
	800		1700		8000	
$N_R = 4$	800		700		1400	
v_{max} (mm/sec)	1.5		1.3		1.3	
$(H_n/v)_{\text{min}}$ (sec)	0.27		0.17		0.28	
t_{R1} (min)	17		30		130	
$(\Delta P/L)_{\text{max}}$ (bar/cm)	0.65		0.60		2.5	
Components: n	E ₃ -17G		E ₃ -17G		E ₃ -17G	
	E ₃ -16G		E ₃ -16G		E ₃ -16G	
$(r_{(n+1)n} - 1) \kappa_n / (\kappa_n + 1)$	0.05		0.15		0.11	
	6000		700		1400	
$N_R = 4$	800		700		1400	
v_{max} (mm/sec)	1.5		1.3		1.3	
$(H_n/v)_{\text{min}}$ (sec)	0.27		0.17		0.28	
t_{R1} (min)	17		30		130	
$(\Delta P/L)_{\text{max}}$ (bar/cm)	0.65		0.60		2.5	
Components: n	E ₃ -3G		E ₃ -3G		E ₃ -3G	
	E ₁ -G		E ₁ -G		E ₁ -G	
$(r_{(n+1)n} - 1) \kappa_n / (\kappa_n + 1)$	0.14		0.10		0.05	
	800		1700		8000	
$N_R = 4$	800		700		1400	
v_{max} (mm/sec)	1.5		1.3		1.3	
$(H_n/v)_{\text{min}}$ (sec)	0.27		0.17		0.28	
t_{R1} (min)	17		30		130	
$(\Delta P/L)_{\text{max}}$ (bar/cm)	0.65		0.60		2.5	
Components: n	E ₃ -17G		E ₃ -17G		E ₃ -17G	
	E ₃ -16G		E ₃ -16G		E ₃ -16G	
$(r_{(n+1)n} - 1) \kappa_n / (\kappa_n + 1)$	0.05		0.15		0.11	
	6000		700		1400	
$N_R = 4$	800		700		1400	
v_{max} (mm/sec)	1.5		1.3		1.3	
$(H_n/v)_{\text{min}}$ (sec)	0.27		0.17		0.28	
t_{R1} (min)	17		30		130	
$(\Delta P/L)_{\text{max}}$ (bar/cm)	0.65		0.60		2.5	
Components: n	E ₃ -3G		E ₃ -3G		E ₃ -3G	
	E ₁ -G		E ₁ -G		E ₁ -G	
$(r_{(n+1)n} - 1) \kappa_n / (\kappa_n + 1)$	0.14		0.10		0.05	
	800		1700		8000	
$N_R = 4$	800		700		1400	
v_{max} (mm/sec)	1.5		1.3		1.3	
$(H_n/v)_{\text{min}}$ (sec)	0.27		0.17		0.28	
t_{R1} (min)	17		30		130	
$(\Delta P/L)_{\text{max}}$ (bar/cm)	0.65		0.60		2.5	
Components: n	E ₃ -17G		E ₃ -17G		E ₃ -17G	
	E ₃ -16G		E ₃ -16G		E ₃ -16G	
$(r_{(n+1)n} - 1) \kappa_n / (\kappa_n + 1)$	0.05		0.15		0.11	
	6000		700		1400	
$N_R = 4$	800		700		1400	
v_{max} (mm/sec)	1.5		1.3		1.3	
$(H_n/v)_{\text{min}}$ (sec)	0.27		0.17		0.28	
t_{R1} (min)	17		30		130	
$(\Delta P/L)_{\text{max}}$ (bar/cm)	0.65		0.60		2.5	
Components: n	E ₃ -3G		E ₃ -3G		E ₃ -3G	
	E ₁ -G		E ₁ -G		E ₁ -G	
$(r_{(n+1)n} - 1) \kappa_n / (\kappa_n + 1)$	0.14		0.10		0.05	
	800		1700		8000	
$N_R = 4$	800		700		1400	
v_{max} (mm/sec)	1.5		1.3		1.3	
$(H_n/v)_{\text{min}}$ (sec)	0.27		0.17		0.28	
t_{R1} (min)	17		30		130	
$(\Delta P/L)_{\text{max}}$ (bar/cm)	0.65		0.60		2.5	
Components: n	E ₃ -17G		E ₃ -17G		E ₃ -17G	
	E ₃ -16G		E ₃ -16G		E ₃ -16G	
$(r_{(n+1)n} - 1) \kappa_n / (\kappa_n + 1)$	0.05		0.15		0.11	
	6000		700		1400	
$N_R = 4$	800		700		1400	
v_{max} (mm/sec)	1.5		1.3		1.3	
$(H_n/v)_{\text{min}}$ (sec)	0.27		0.17		0.28	
t_{R1} (min)	17		30		130	
$(\Delta P/L)_{\text{max}}$ (bar/cm)	0.65		0.60		2.5	
Components: n	E ₃ -3G		E ₃ -3G		E ₃ -3G	
	E ₁ -G		E ₁ -G		E ₁ -G	
$(r_{(n+1)n} - 1) \kappa_n / (\kappa_n + 1)$	0.14		0.10		0.05	
	800		1700		8000	
$N_R = 4$	800		700		1400	
v_{max} (mm/sec)	1.5		1.3		1.3	
$(H_n/v)_{\text{min}}$ (sec)	0.27		0.17		0.28	
t_{R1} (min)	17		30		130	
$(\Delta P/L)_{\text{max}}$ (bar/cm)	0.65		0.60		2.5	
Components: n	E ₃ -17G		E ₃ -17G		E ₃ -17G	
	E ₃ -16G		E ₃ -16G		E ₃ -16G	
$(r_{(n+1)n} - 1) \kappa_n / (\kappa_n + 1)$	0.05		0.15		0.11	
	6000		700		1400	
$N_R = 4$	800		700		1400	
v_{max} (mm/sec)	1.5		1.3		1.3	
$(H_n/v)_{\text{min}}$ (sec)	0.27		0.17		0.28	
t_{R1} (min)	17		30		130	
$(\Delta P/L)_{\text{max}}$ (bar/cm)	0.65		0.60		2.5	
Components: n	E ₃ -3G		E ₃ -3G		E ₃ -3G	
	E ₁ -G		E ₁ -G		E ₁ -G	
$(r_{(n+1)n} - 1) \kappa_n / (\kappa_n + 1)$	0.14		0.10		0.05	
	800		1700		8000	
$N_R = 4$	800		700		1400	
v_{max} (mm/sec)	1.5		1.3		1.3	
$(H_n/v)_{\text{min}}$ (sec)	0.27		0.17		0.28	
t_{R1} (min)	17		30		130	
$(\Delta P/L)_{\text{max}}$ (bar/cm)	0.65		0.60		2.5	
Components: n	E ₃ -17G		E ₃ -17G		E ₃ -17G	
	E ₃ -16G		E ₃ -16G		E ₃ -16G	
$(r_{(n+1)n} - 1) \kappa_n / (\kappa_n + 1)$	0.05		0.15		0.11	
	6000		700		1400	
$N_R = 4$	800		700		1400	
v_{max} (mm/sec)	1.5		1.3		1.3	
$(H_n/v)_{\text{min}}$ (sec)	0.27		0.17		0.28	
t_{R1} (min)	17		30		130	
$(\Delta P/L)_{\text{max}}$ (bar/cm)	0.65		0.60		2.5	
Components: n	E ₃ -3G		E ₃ -3G		E ₃ -3G	
	E ₁ -G		E ₁ -G		E ₁ -G	
$(r_{(n+1)n} - 1) \kappa_n / (\kappa_n + 1)$	0.14		0.10		0.05	
	800		1700		8000	
$N_R = 4$	800		700		1400	
v_{max} (mm/sec)	1.5		1.3		1.3	
$(H_n/v)_{\text{min}}$ (sec)	0.27		0.17		0.28	
t_{R1} (min)	17		30		130	
$(\Delta P/L)_{\text{max}}$ (bar/cm)	0.65		0.60		2.5	
Components: n	E ₃ -17G		E ₃ -17G		E ₃ -17G	
	E ₃ -16G		E ₃ -16G		E ₃ -16G	
$(r_{(n+1)n} - 1) \kappa_n / (\kappa_n + 1)$	0.05		0.15		0.11	
	6000		700		1400	
$N_R = 4$	800		700		1400	
v_{max} (mm/sec)	1.5		1.3		1.3	
$(H_n/v)_{\text{min}}$ (sec)	0.27		0.17		0.28	
t_{R1} (min)	17		30		130	
$(\Delta P/L)_{\text{max}}$ (bar/cm)	0.65		0.60		2.5	
Components: n	E ₃ -3G		E ₃ -3G		E ₃ -3G	
	E ₁ -G		E ₁ -G		E ₁ -G	
$(r_{(n+1)n} - 1) \kappa_n / (\kappa_n + 1)$	0.14		0.10		0.05	
	800		1700		8000	
$N_R = 4$	800		700		1400	
v_{max} (mm/sec)	1.5		1.3		1.3	
$(H_n/v)_{\text{min}}$ (sec)	0.27		0.17		0.28	
t_{R1} (min)	17		30		130	
$(\Delta P/L)_{\text{max}}$ (bar/cm)	0.65		0.60		2.5	
Components: n	E ₃ -17G		E ₃ -17G		E ₃ -17G	
	E ₃ -16G		E ₃ -16G		E ₃ -16G	
$(r_{(n+1)n} - 1) \kappa_n / (\kappa_n + 1)$	0.05		0.15		0.11	
	6000		700		1400	
$N_R = 4$	800		700		1400	
v_{max} (mm/sec)	1.5		1.3		1.3	
$(H_n/v)_{\text{min}}$ (sec)	0.27		0.17		0.28	
t_{R1} (min)	17		30		130	
$(\Delta P/L)_{\text{max}}$ (bar/cm)	0.65		0.60		2.5	
Components: n	E ₃ -3G		E ₃ -3G		E ₃ -3G	
	E ₁ -G		E ₁ -G		E ₁ -G	
$(r_{(n+1)n} - 1) \kappa_n / (\kappa_n + 1)$	0.14		0.10		0.05	
	800		1700		8000	
$N_R = 4$	800		700		1400	
v_{max} (mm/sec)	1.5		1.3		1.3	
$(H_n/v)_{\text{min}}$ (sec)	0.27		0.17		0.28	
t_{R1} (min)	17		30		130	
$(\Delta P/L)_{\text{max}}$ (bar/cm)	0.65		0.60		2.5	
Components: n	E ₃ -17G		E ₃ -17G		E ₃ -17G	
	E ₃ -16G		E ₃ -16G		E ₃ -16G	
$(r_{(n+1)n} - 1) \kappa_n / (\kappa_n + 1)$	0.05		0.15		0.11	
	6000		700		1400	
$N_R = 4$	800		700		1400	
v_{max} (mm/sec)	1.5		1.3		1.3	
$(H_n/v)_{\text{min}}$ (sec)	0.27		0.17		0.28	
t_{R1} (min)	17		30		130	
$(\Delta P/L)_{\text{max}}$ (bar/cm)	0.65		0.60		2.5	
Components: n	E ₃ -3G		E ₃ -3G		E ₃ -3G	
	E ₁ -G		E ₁ -G		E ₁ -G	
$(r_{(n+1)n} - 1) \kappa_n / (\kappa_n + 1)$	0.14		0.10		0.05	
	800		1700		8000	
$N_R = 4$	800		700		1400	
v_{max} (mm/sec)	1.5		1.3		1.3	
$(H_n/v)_{\text{min}}$ (sec)	0.27		0.17		0.28	
t_{R1} (min)	17		30		130	
$(\Delta P/L)_{\text{max}}$ (bar/cm)						

particle size of 8 μm was used and the column was packed at a pressure of 30 bar, a theoretical plate height of 0.08 mm at a maximum allowable flow-rate of 0.4 mm/sec was achieved at a capacity ratio of 1.3. Another batch (MN 300/B) gave results similar to those with Servacel TLC.

An example of the results obtained with AE-cellulose is shown in Fig. 7, which demonstrates also the more than proportional increase of the pressure drop near to the maximum attainable fluid velocity.

Effect of temperature. An example of the influence of temperature on the theoretical plate height is shown in Fig. 8. The minimum attainable value of the ratio H/v increases in this case from 0.14 sec at 70° to 0.25 sec at 50°. In general, the minimum H/v ratio increases by a factor of about two when the temperature is decreased from 70° to 25°.

Choice of an optimum phase system for the separation of estrogen glucuronides

For a given selectivity factor and capacity ratio, a certain number of theoretical plates is required in order to achieve a given resolution. The theoretical plate number, N_R , required for the resolution R_{ji} can be calculated from eqn. 1:

$$N_R = \left(\frac{R_{ji}}{r_{ji} - 1} \right)^2 \left(\frac{\kappa_i + 1}{\kappa_i} \right)^2 \quad (6)$$

The corresponding length of the column is given by $L_R = N_R H$. In practice, the maximum length is limited by the pressure limit of the apparatus or the column packing.

The time in which the separation of the total mixture can be performed is given by the retention time of the last-eluting compound 1:

$$t_{R1} = \frac{N_R H_n}{v} \cdot (1 + \kappa_1) \quad (7)$$

where n refers to that component of the mixture which has the largest value of $N_R H_n/v$. In order to increase the speed of separation, the value of the capacity ratio, κ_1 , of the last-eluting component as well as the largest value of $N_R H_n/v$ occurring in the mixture should be minimized.

The required theoretical plate number, $N_{R=4}$, for a resolution of four was calculated for each successive pair of components from the data in Tables II–VII. The groups of values obtained under the same conditions were compared. Because E₃-17G is clinically unimportant, the comparison was made both inclusive and exclusive of this compound. The systems and temperatures which gave the lowest values for $N_{R=4}$ were further evaluated with regard to the practical minimum value of H/v and the minimum separation time was calculated according to eqn. 7. The results are summarized in Table IX, in which those components which are easily separated are not included. The following conclusions can be drawn from Table IX.

(1) The changes in the separation time are caused mainly by the changes in the factor $(r_{(n+1)n} - 1) \kappa_n / (\kappa_n + 1)$ and less by the changes in the value of $(H/v)_{\min.}$

(2) None of the phase systems is the best for the separation of each pair of estrogen glucuronides. E₁-G and E₃-3G are best separated in the first system, E₃-16G and E₂-3G in the second system and E₃-16G and E₃-17G at 25° in the third system.

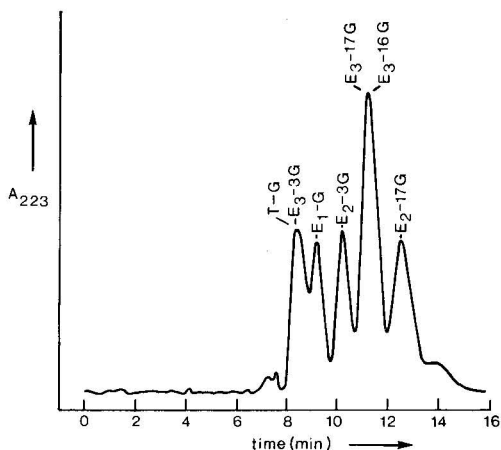


Fig. 9. Separation of a test mixture of estrogen glucuronides on an ECTEOLA-cellulose of low ion-exchange capacity. Phase system: MN 300, 7 μ m; 0.25 M chloride + 0.05 M acetate, pH 5.0; 70°.

The corresponding minimum separation times are 17, 12 and 25 min, respectively.

(3) The best system for the separation of all six estrogen glucuronides, representing a compromise, is the first system, although the separation of E₃-16G and E₃-17G is difficult and takes 130 min. Excluding E₃-17G, the separation can be performed in 17 min.

The choice of the best phase system and the best working conditions is illustrated by a number of chromatograms. Fig. 9 demonstrates an insufficient separation resulting from a too low capacity ratio due to the low ion-exchange capacity of the column packing. Fig. 10 shows the improvement in resolution that can be achieved with the same separation time with a better packing material. Fig. 11 demonstrates that the resolution can be improved further in a longer time. The most difficult separation, that of E₃-16G and E₃-17G, can be accelerated by using a system that is more selective for this pair of compounds, as shown in Fig. 12.

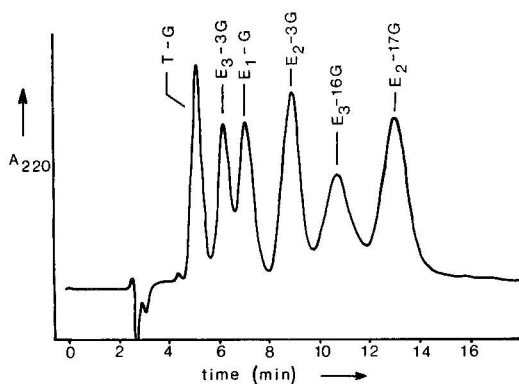


Fig. 10. Separation of a test mixture of estrogen glucuronides on an ECTEOLA-cellulose of high ion-exchange capacity. Phase system: Baker 300, 13 μ m; 0.125 M chloride + 0.05 M acetate, pH 5.0; 25°.

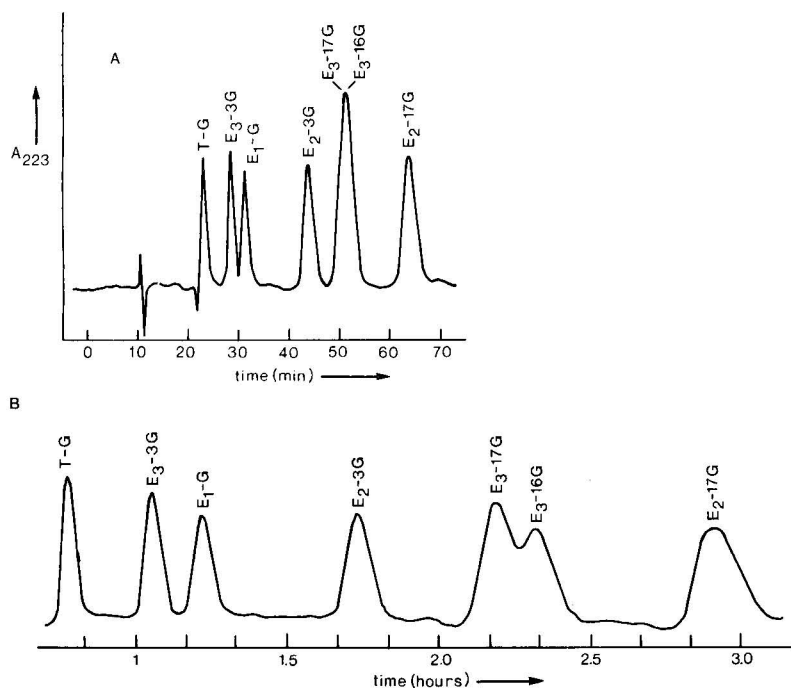


Fig. 11. Improvement in the resolution of a test mixture of estrogen glucuronides in a longer time. Phase system: Cellex E, $9\ \mu\text{m}$; $0.5\ \text{M}$ chloride + $0.05\ \text{M}$ acetate, pH 4.5; 75° (A) and 40° (B).

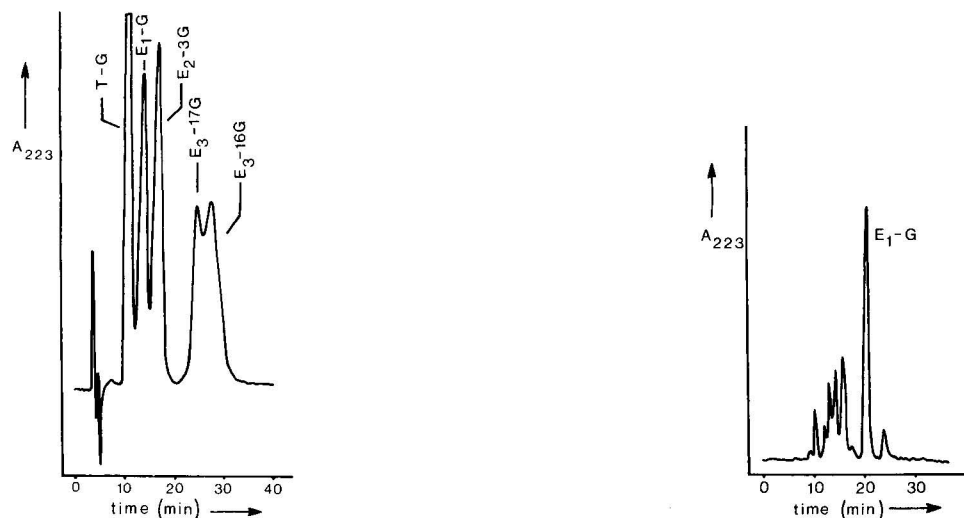


Fig. 12. Separation of a test mixture of estrogen glucuronides. Phase system: Cellex AE, $14\ \mu\text{m}$; $0.05\ \text{M}$ chloride + $0.05\ \text{M}$ acetate, pH 5.0; 25° .

Fig. 13. Purity control of a commercial product of $\text{E}_1\text{-G}$. Phase system: Baker 300, $8\ \mu\text{m}$; $0.125\ \text{M}$ chloride + $0.05\ \text{M}$ acetate, pH 5.0; 70° .

A first application is shown in Fig. 13. The chromatogram is the result of the purity control of a commercial product. This application illustrates the performance of the method in the analysis of steroid conjugates.

ACKNOWLEDGEMENTS

The authors are indebted to Mr. K. Camstra, whose technical skill was indispensable, and Messrs. L. T. M. Schilder, E. Endert and M. P. Uitendaal for their technical assistance.

REFERENCES

- 1 R. Hähnel and M. G. B. Abdul Rahman, *Biochem. J.*, 105 (1967) 1047.
- 2 E. R. Smith and A. E. Kellie, *Biochem. J.*, 104 (1967) 83.
- 3 J. Ahmed and A. E. Kellie, *J. Steroid Biochem.*, 3 (1972) 31.
- 4 H. Adlercreutz and T. Luukainen, *Ann. Clin. Res.*, 2 (1970) 365.
- 5 E.-E. Baulieu, C. Corpéchet, F. Dray, R. Emiliozzi, M. C. Lebeau, P. Mauvais-Jarvis and P. Robel, *Recent Progr. Horm. Res.*, 21 (1965) 411.
- 6 J. B. Brown, *Biochem. J.*, 60 (1955) 185.
- 7 S. L. Cohen, *Can. J. Biochem.*, 46 (1968) 563.
- 8 P. K. Siiteri, in S. Bernstein and S. Solomon (Editors), *Chemical and Biological Aspects of Steroid Conjugation*, Springer, New York, 1970, Ch. 4, p. 182.
- 9 R. Hähnel, *Clin. Chim. Acta*, 7 (1962) 768.
- 10 C. McMartin and J. Vinter, *J. Chromatogr.*, 41 (1969) 188.
- 11 C. M. Thompson, in H. Peeters (Editor), *Protides of the Biological Fluids*, Vol. 15, Elsevier, Amsterdam, 1967, p. 565.
- 12 J. F. K. Huber, *J. Chromatogr. Sci.*, 7 (1969) 85.
- 13 J. F. K. Huber, *J. Chromatogr. Sci.*, 7 (1969) 172.
- 14 J. F. K. Huber, F. F. M. Kolder and J. M. Miller, *Anal. Chem.*, 44 (1972) 105.
- 15 W. Paul, C. Stitt, W. J. Dignam and S. Kushinsky, *J. Chromatogr.*, 45 (1969) 381 and 392.
- 16 R. Hobkirk and M. Nilsen, *Anal. Biochem.*, 37 (1970) 377.
- 17 R. Hobkirk, P. Musey and M. Nilsen, *Steroids*, 14 (1969) 191.

CHROM. 7719

SEPARATION OF OPTICAL ISOMERS BY ION-EXCHANGE CHROMATOGRAPHY USING COPPER(II) IONS AS COMPLEX-FORMING AGENTS

J. GAÁL and J. INCZÉDY

Institute of Analytical Chemistry, University of Chemical Engineering, Veszprém (Hungary)

SUMMARY

On the basis of the differences between the stability constants of complexes of D- and L-aminodiols with copper(II) ions, an ion-exchange chromatographic method using copper(II) ions as complex-forming agents was developed for the quantitative separation of pairs of optical isomers. The stability constants of some complexes were determined. The distribution coefficients of two enantiomers were examined by static batch and elution methods. The optimal conditions of the separation and the composition of the eluent are discussed.

INTRODUCTION

The known methods for the separation of optical isomers are based mainly on reactions involving the formation of diastereoisomers. Using these reactions, ion-exchange and other chromatographic methods have been developed¹⁻³.

We have found that ion-exchange chromatography, in which the principle of separation is the difference between the stability constants of the two enantiomers formed with the same metal ion, can also be used for separations in a few cases. A chromatographic method has been developed for the separation of optical isomers (D- and L-forms) of racemic *threo*-1-(*p*-nitrophenyl)-2-amino-1,3-propanediol (D- and L-aminodiols) using copper(II) ions as complex-forming agents.

In order to determine the complex formation constants of D- and L-aminodiols, pH titrations were carried out. The stability constants of copper(II) complexes were determined by a modified graphical method of Leden⁴. We found that there are deviations in the values of the stability constants of the corresponding complexes.

In order to obtain information on the distribution properties of the two enantiomers between a cation-exchange resin and solutions containing copper and sodium ions, distribution experiments were carried out using the static batch method. We found that D-aminodiol complexes are more strongly bound than those of the L-isomer to the resin in the copper form if there is no copper in solution, corresponding to the order of the stability constants of the complexes. However, the distribution coefficients were found to be very high for separation. From the results of distribution measurements carried out with ion exchanger in the sodium form, it was found that the order of the distribution coefficients of the D- and L-aminodiols changes with

increasing concentration of copper(II) ions and the separation of optical isomers can be carried out under more favourable conditions if a resin in the mixed sodium and copper form is used instead of simply the copper form. For the separation, an eluent containing 0.14 mole of sodium acetate and 0.01 mole of copper(II) chloride was chosen.

In order to obtain information on the necessary size of the column, the plate height of the column was first calculated from the elution curve obtained by an elution experiment using Glueckauf's equation⁵. The required column length for quantitative separation were calculated using the following equation⁶:

$$L > 2\pi h \left[\frac{\left(\frac{D_2 + a}{D_1 + a} \right) + 1}{\left(\frac{D_2 + a}{D_1 + a} \right) - 1} \right]^2 \quad (1)$$

where D_1 and D_2 are the volume distribution coefficients of the two optical isomers, a is the void fraction, h the plate height and L the required length of the column.

EXPERIMENTAL AND RESULTS

Reagents

In all experiments, analytical-grade reagents were used.

Ion-exchange resin

Dowex 50-X8 resin (100–200 and 50–100 mesh) was used after extraction with methanol in Soxhlet apparatus.

Instruments

The pH was measured with a Radelkis pH meter (Budapest, Hungary), and the quantitative determination of the bases was carried out with a Spektromom 202 spectrophotometer (MOM, Budapest, Hungary).

Determination of the protonation and complex formation constants of D- and L-aminodiols

Volumes of 45 ml of 2×10^{-2} and 5×10^{-2} M alcoholic stock solutions of D- and L-aminodiols were titrated with 0.25 and 0.1 N sodium hydroxide solutions in the absence and presence (10^{-3} M) of copper(II) ions. The pH was measured using glass and calomel electrodes, and the concentration of the free copper(II) ions was determined with an ion-selective electrode⁷. During the titrations, nitrogen gas was bubbled through the solutions. From the titration curves, the protonation and complex formation constants were calculated. We found that the protonation constants of the two enantiomers are identical. ($\log K = 7.97 \pm 0.02$ and $\log K = 7.94 \pm 0.02$). It was found that the optical isomers form, in addition to regular 1:1 and 1:2 complexes, also protonated and mixed hydroxo-complexes with copper(II) ions. The logarithmic values of the stability constants are given in Table I.

TABLE I
LOGARITHMIC VALUES OF OVERALL STABILITY CONSTANTS

Composition of complexes	L-Aminodiol	D-Aminodiol
[Cu(LH)]	10.19 \pm 0.02	10.07 \pm 0.02
[CuL]	5.75 \pm 0.01	6.07 \pm 0.01
[CuL ₂]	9.45 \pm 0.02	10.51 \pm 0.02
[CuL(OH)]	11.45 \pm 0.02	13.93 \pm 0.02
[CuL(OH) ₂]	21.29 \pm 0.04	23.93 \pm 0.04

Determination of the distribution coefficients of D- and L-aminodiol

The determination of the distribution coefficients was carried out on room temperature in solutions containing 50% of methanol.

The solution containing the optically active base and the required salt or acetate buffer was equilibrated with ion-exchange resin in the copper form. After equilibration, the concentration of the base was determined by spectrophotometry and the distribution coefficients were calculated (before the spectrophotometric determinations, ammonia was added to the solution and the copper-ammine complex formed was removed by ion-exchange resin in the ammonium form). The distribution coefficients were calculated from the original and the final concentration values, and the results are given in Table II.

TABLE II
DISTRIBUTION COEFFICIENTS

Cation-exchange resin: 0.5 g of Dowex 50-X8 in the copper form.

Composition of solution	Distribution coefficients	
	D-Aminodiol	L-Aminodiol
10 ⁻³ mole of D-(or L)-aminodiol, pH 6.75	890	718
10 ⁻³ mole of D-(or L)-aminodiol and 10 ⁻² mole of copper(II) ions, pH 4.30	151	198

Distribution measurements were also carried out using resin in the sodium form and a constant concentration of sodium ions in which different amounts of copper(II) chloride were added to the solution. After equilibration, the solutions were analyzed as above and the distribution coefficients calculated. It was found that the difference between the distribution coefficients of D- and L-aminodiol is the most favourable if a solution containing of 0.01 mole of copper(II) ions and 0.14 mole of sodium ions is used.

Elution experiments

In the elution experiments, a 190 \times 6.5 mm ion-exchange column containing resin in the sodium form, prepared from Dowex 50-X8 cation-exchange resin, was used. The column was first equilibrated with the eluent solution by passing *ca.* 400

ml of eluent through it. The eluent consisted of sodium acetate and acetic acid buffer of pH 5, which contained 0.14 mole of sodium ions, 0.01 mole of copper(II) chloride and 50% of methanol.

After equilibration of the column, the methanolic solution of the optical isomers (0.20 ml) was placed on the column and elution was carried out with an eluent flow-rate of 22.0 ml/h. The effluent was collected in 2-ml fractions. The absorbance of the fractions was measured spectrophotometrically at 275 nm after addition of ammonia and removal of copper(II) ions with ion-exchange resin in the ammonium form⁸.

From the elution curves obtained, the plate height and the required plate number for quantitative separation were calculated.

Separation of D- and L-aminodiols

According to the calculation, a column 51 cm long was prepared. The composition of the eluent was the same as in the elution experiments. The feeding of the column and the continuous detection of the separated species in the effluent were carried out with an apparatus of our own design (Fig. 1). In the apparatus after the chromatographic column, ammonia solution was added continuously to the effluent and the solution was passed through a column containing resin in the ammonium form, thus removing copper(II) ions. The absorbance of the effluent from the latter column was measured spectrophotometrically at 275 nm using a flow cell. Under these conditions, the two optical isomers were resolved to the extent of 93% (Fig. 2).

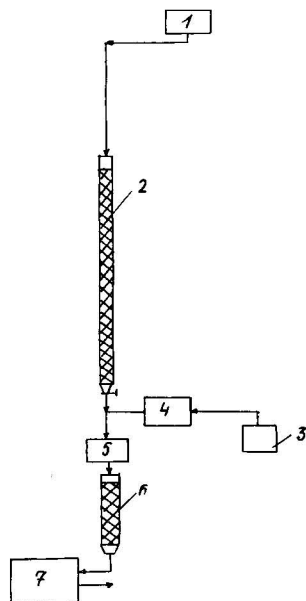


Fig. 1. Chromatographic apparatus for the separation of D- and L-aminodiols. 1 = Eluent; 2 = cation-exchange column of Dowex 50-X8 (mixed sodium-copper form; $L = 51.0$ cm, $\varnothing = 0.7$ cm); 3 = ammonia solution; 4 = peristaltic pump; 5 = mixing coil; 6 = cation-exchange column of Dowex 50-X8 (ammonium form); 7 = spectrophotometer.

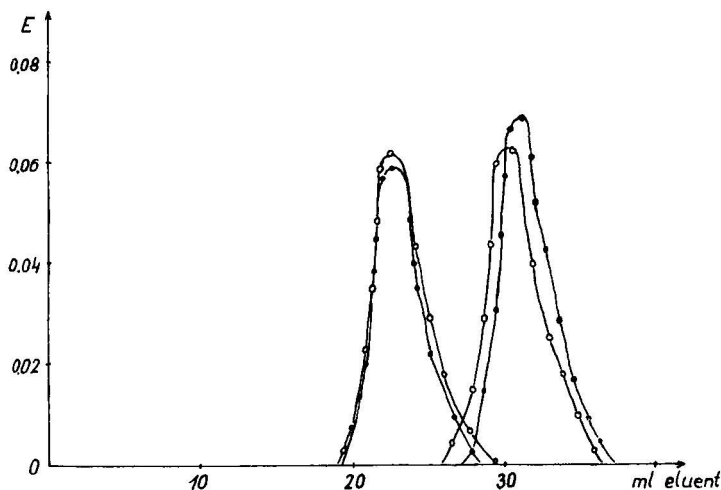


Fig. 2. Separation of D- and L-aminodiols. Eluent: ○, 0.01 *M* copper(II) chloride, 0.14 *M* sodium acetate, 50% methanol; ●, 0.01 *M* copper(II) chloride, 5×10^{-4} *M* D-aminodiol, 0.14 *M* sodium acetate, 50% methanol.

In order to increase the resolution, the earlier experiments were repeated under similar conditions but with an eluent that contained, in addition to 0.01 mole of copper(II) ions, also $5 \cdot 10^{-4}$ mole of D-aminodiol. In this manner we achieved a virtually quantitative separation of 0.11 mg of racemic aminodiol mixture.

DISCUSSION

A significant difference was found between the stability constants of D- and L-aminodiol complexes with copper(II) ions. The cause of this rare phenomenon may be explained by the fact that the compound has two asymmetric centres, and the groups coupling to asymmetric centres take part in the formation of the complexes. Other workers⁹ also found that the optically active isomers of some structurally similar compounds (adrenaline) form complexes of different stabilities with copper(II) ions.

Under the optimal experimental conditions, where the chromatographic separation was achieved, the following two dominating reactions may be assumed:



Eqn. 2 is the ion-exchange reaction, while eqn. 3 represents complex formation in the solution phase. According to calculation, complex formation inside the resin phase plays only a moderate role.

REFERENCES

- 1 D. R. Buss and T. Vermeulen, *Ind. Eng. Chem.*, 60, No. 8 (1968) 12.
- 2 G. Losse and K. Kuntze, *Z. Chem.*, 10 (1970) 22.
- 3 E. I. Klabunovski, *Usp. Khim.*, 27 (1958) 949.
- 4 I. Leden, *J. Phys. Chem.*, 188A (1941) 160.
- 5 E. Glueckauf, *J. Soc. Chem. Ind., London*, (1954) 34.
- 6 J. Inczédy, *J. Chromatogr.*, 50 (1970) 112.
- 7 J. Pick, K. Tóth and E. Pungor, *Anal. Chim. Acta*, 61 (1972) 169.
- 8 L. Láng and M. Vizessy, *Acta Chim. Acad. Sci. Hung.*, 56, No. 2 (1968) 109.
- 9 A. C. Andrens, T. D. Lyons and T. D. O'Brien, *J. Chem. Soc., London*, (1962) 1776.

CHROM. 7737

SEPARATION OF SOME CHLORAMPHENICOL INTERMEDIATES BY HIGH-PRESSURE ION-EXCHANGE CHROMATOGRAPHY

Gy. VIGH and J. INCZÉDY

Institute of Analytical Chemistry, University of Chemical Engineering, Veszprém (Hungary)

SUMMARY

High-pressure cation-exchange chromatography was used to separate three of the by-product compounds formed in the chloramphenicol production process. Base-line separation can be achieved within 8.5 min employing a 1-m column packed with Zipax SCX pellicular cation exchanger and 0.05 *M* sodium sulphate solution as eluent at pH 1.1 in a Varian Aerograph LC 4020 liquid chromatograph.

INTRODUCTION

This paper reports the separation of some chloramphenicol intermediates and by-products. These compounds are very polar, thermally labile and, owing to their low vapour pressure, cannot be analyzed by gas chromatography. A thin-layer chromatographic method has been applied for their analysis, employing a Kieselgel GF₂₅₄ layer and chloroform–methanol–glacial acetic acid (90:5:5) as developing solvent¹. However, good resolution and precise sub-microgram determinations of the compounds involved cannot be obtained. High-performance ion-exchange column chromatography was chosen in order to solve the separation problem.

EXPERIMENTAL

All experiments were carried out on a Varian Aerograph LC 4020 UV/RI liquid chromatograph (Walnut Creek, Calif., U.S.A.) equipped with some home-made units. Argon gas was used to pressurize the solvent container and to deliver the eluent. During the elutions, a high-pressure gas regulator (Lüedi, Zürich, Switzerland) kept the gas pressure constant. A 1 m × 1/16 in. O.D. stainless-steel capillary tube and a 0.5- μ m stainless-steel porous frit was used to maintain a back-pressure in the detector cells and to prevent bubbling out of the dissolved gas. By this means, the eluent could be delivered for about 2 h before the gas pressure had to be released and the eluent degassed.

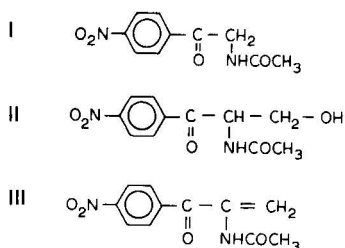
The starting-mark generating device² was used to determine the exact retention times of the compounds. The flow-rate was measured with a home-made bubble flow meter. Injection was made on-column through PTFE-laminated septa (Varian Aerograph) with a Hamilton HP 305 high-pressure microsyringe.

The columns were made of 1/8 in. O.D., 1.8 mm I.D. precision-bore stainless-steel tubing, equipped with a water jacket connected to a temperature-controlled water circulating bath (Type U10, MLW, Medingen, G.D.R.). The columns were dry-packed with Zipax SCX pellicular cation exchanger, (DuPont, Wilmington, Del., U.S.A.) employing a home-made machine similar to that described by Henry³.

All chemicals used were of reagent grade and were obtained from Reanal (Budapest, Hungary). The compounds to be separated were prepared and supplied by the EGYT Pharmaceutical Factory (Budapest, Hungary) and were considered to be of the highest available purity.

RESULTS

The compounds to be separated were:



Earlier experiments¹ showed that when these compounds are exposed to prolonged daylight or temperatures above 60°, they decompose and form red-coloured compounds. Therefore, all separations were carried out at 30° and sample solutions were freshly prepared each day.

The flow-rate of the eluent was kept constant at 0.40 ml/min while the corresponding gas pressure was varied between 62 and 75 atm. The eluent was distilled water containing 0.05 mole/l of sodium sulphate. The pH was adjusted by adding sulphuric acid.

The pH of the eluent was varied systematically so as to change the retention of the compounds to be separated. The results are shown in Fig. 1. We measured the



Fig. 1. Dependence of the retention volumes on the pH of the 0.05 M Na₂SO₄ eluent. Column: 1 m long packed with Zipax SCX, thermostatted to 30.0°, flow-rate 0.40 ml/min.

Fig. 2. Dependence of the square root of the peak width at 10% peak height on the retention volumes. Amounts injected were between 0.2 and 0.35 µg.

peak width at 10% height in each case. The change of the square root of this width as a function of the retention volume is shown in Fig. 2.

Down to pH 2, there was no significant change in the retention behaviour. The compounds were eluted so close together that their separation was not satisfactory.

Based on Figs. 1 and 2, we determined the pH of the eluent to be used in order to obtain resolution of at least 1.5 for each component pair. It was found that with an eluent of pH 1.1, the three compounds could be separated in 8.5 min. The chromatogram of the three components is shown in Fig. 3. The amounts injected were between 0.2 and 0.35 μg .

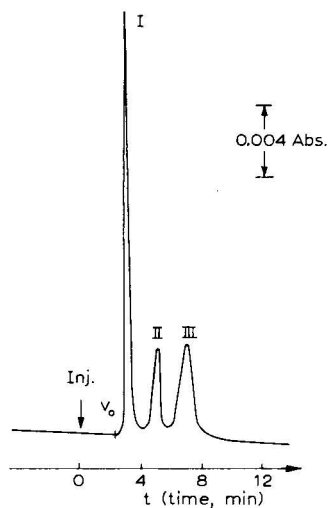


Fig. 3. Separation of compounds I, II and III. Amounts injected were 0.35, 0.20 and 0.25 μg in 3 μl respectively. Eluent: 0.05 M Na_2SO_4 at pH 1.1.

ACKNOWLEDGEMENT

The authors are grateful to the EGYT Pharmaceutical Factory for the samples and their permission to publish these results.

REFERENCES

- 1 EGYT Pharmaceutical Factory, Budapest, Hungary, personal communications, 1973.
- 2 Gy. Vigh, *J. Chromatogr.*, 74 (1972) 128.
- 3 R. A. Henry, in J. J. Kirkland (Editor), *Modern Practice of Liquid Chromatography*, Wiley-Interscience, New York, 1972, p. 74.

CHROM. 7738

APPLICATION OF LIGANDS WITH SULPHONIC GROUPS TO THE SEPARATION OF METAL IONS ON STRONGLY BASIC ANION EXCHANGERS

KRYSTYNA BRAJTER

Institute of Fundamental Problems of Chemistry, Warsaw University, Warsaw (Poland)

SUMMARY

The possibility of using bromopyrogallol red, chromotropic acid and alizarin red S as complexing agents for the selective separation of Ti and Zr from the other metal ions was investigated. Bromopyrogallol red was used for the separation of titanium(IV) from Co(II), Cu(II), Cr(III) and Fe(III), chromotropic acid for the separation of titanium from Ni, Cu and Fe, and alizarin red S for the separation of zirconium from Cu, Ni and Al.

Using chromotropic acid it is possible to separate titanium(IV) from large excess of metal ions giving weak complexes. By elution of metal ions which formed less stable complexes with the complexing agent no evidence of ligand in the eluate was discovered. This proves that very strong binding of ligand on anion-exchange resin occurs. It was found that for separation of Ti, chromotropic acid is more suitable than bromopyrogallol red.

INTRODUCTION

The selectivity of ion-exchange resins for metal ions can be increased by a suitable choice of the complexing agent. Aromatic complexing agents with sulphonic groups are very useful for the separation of metal ions on strongly basic anion-exchange resins, as was shown in previous papers^{1,2}. These compounds and their complexes with metal ions, owing to their aromatic character and the presence of sulphonic groups, have a great affinity for anion-exchange resins. When such a complexing agent is immobilized on the resin, it is transformed into a kind of specific resin preferring one (or a few) counter ion species much more strongly than any others according to its complexing ability.

This paper describes the possibility of using bromopyrogallol red (BPR), alizarin S and chromotropic acid as complexing agents for the separation of metal ions on strongly basic anion exchangers. The aim was to establish conditions for the separation of titanium and zirconium from other metal ions using the most selective complexing agent for these metal ions.

EXPERIMENTAL

The strongly basic anion exchangers Amberlite IRA 400 (capacity 3.55

mequiv./g), and Amberlite IRA 410 (capacity 3.0 mequiv./g) for alizarin S only, were used.

All the reagents used were of analytical grade. Solutions of metal ions were prepared from appropriate salts. Metal ions were determined by colorimetric methods.

Bromopyrogallol red (BPR) (dibromopyrogallolsulphonphthalein) as complexing agent

According to the literature^{3,4}, optimum conditions for the reaction of titanium with BPR occur at pH 2.2, for Cu^{2+} at pH 5, and for Co^{2+} above pH 5 (no stability constants for these metals are available). For Fe^{3+} , it was stated that the optimum conditions are close to pH 3. Those data show that it may be possible to separate titanium from Co^{2+} , Cu^{2+} and probably Fe^{3+} . No information was found in the literature about complexes with Cr^{3+} . Cr^{3+} was also used in this experiment because of its inert character.

In batch measurements, the correlation between the uptake of metal ions and the concentration of the ligand at pH values of 2.2 and 3.6 for Cu^{2+} , Co^{2+} and Cr^{3+} and for Fe^{3+} and TiO^{2+} also at pH 5.5 was established, using 200 mg of resin in the CH_3COO^- form and 20 ml of external solution. After equilibration, the external solutions were measured spectrophotometrically. In the external solution at pH 2.2 and 3.6, only free metal ions were present and the ligand was bound to the resin. However, at pH 5.5 it was noted that in the external solution BPR complexes with Fe^{3+} and TiO^{2+} ions exist.

At pH 2.2 and 3.6, Fe^{3+} ions starting from the ratio $\text{Fe}^{3+}:\text{ligand} = 1:2$ were bound to the resin to the extent of 90%. An increase in ligand concentration at these pH values does not change the uptake of Fe^{3+} . TiO^{2+} ions were bound quantitatively, starting from the ratio $\text{TiO}^{2+}:\text{ligand} = 1:2$ (Figs. 1 and 2). Co^{2+} , Cu^{2+} and Cr^{3+} are not bound.

The column conditions were as follows: height of packing, 17 cm; diameter, 1 cm; volumes of feed solutions, 10 ml. The solutions consisted of a mixture of TiO^{2+} ions with BPR; or Cu^{2+} , Cr^{3+} , Co^{2+} or Fe^{3+} ions with BPR or a pair of these ions with BPR (for instance, TiO^{2+} and Cu^{2+} ions); metal ion:BPR = 1:2.5; pH of solutions = 2.2.

The aim of these experiments was to check whether, under conditions given by both measurements, the separation of titanium from the other metal ions in column experiments would be possible.

The column experiments showed that at pH 2.2 titanium was bound quantita-

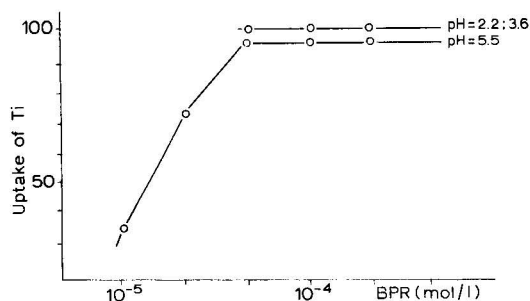


Fig. 1. Correlation between uptake of Ti and concentration of BPR at pH 2.2, 3.6 and 5.5.

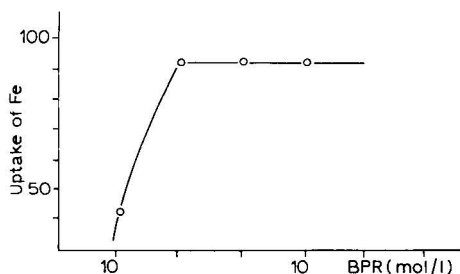


Fig. 2. Correlation between uptake of Fe and concentration of BPR at pH 2.2.

tively. Quantitative elution was obtained with 2 *N* hydrochloric acid (in order to elute 0.1 mg of titanium, 50 ml of acid are necessary). Cu^{2+} , Co^{2+} and Cr^{3+} , under conditions with which TiO^{2+} ions remained bound, passed to the effluent (found quantitatively in the effluent after washing the column with 50 ml of very dilute hydrochloric acid). But Fe^{3+} ions were partially bound to the resin under these conditions; Fe^{3+} ions passed to the effluent when 0.5 *N* hydrochloric acid was used. The results are summarized in Table I.

Chromotropic acid (ChH₄) (1,1-dihydroxynaphthalene-3,6-disulphonic acid) as complexing agent

ChH_4 is very convenient as a complexing agent for the separation of metal ions, because in a strongly acidic solution it gives complexes only with a limited number of metal ions, especially TiO^{2+} ions^{5,6,17}. Fe^{3+} ions^{7,8} also give complexes with ChH_4 in acidic solution, but not so strongly as TiO^{2+} ions. According to the literature⁹, Cu^{2+} ions give weak complexes with ChH_4 , while Ni^{2+} does not form such complexes¹⁰.

The conditions for the separation of TiO^{2+} ions from Fe^{3+} , Cu^{2+} and Ni^{2+} ions were investigated in batch and column experiments. These metal ions were chosen because of the different stabilities¹⁷ of their complexes with ChH_4 .

In batch measurements, it was noted that with a metal ion: ChH_4 ratio of 1:4 at pH 2 with anion exchangers in the acetate form (20 ml of solution, 200 mg of resin), TiO^{2+} ions were quantitatively bound to the anion exchangers.

There was no absorption of Ni^{2+} and Cu^{2+} ions under the above conditions. The absorption of TiO^{2+} , Cu^{2+} , Fe^{3+} and Ni^{2+} ions under these conditions of pH and metal ion: ChH_4 ratio was checked in column experiments.

TABLE I
SEPARATION OF Ti FROM Co, Cu, Cr AND Fe

Element	Amount of Ti (mg)	Amount of element (mg)	No. of determinations	Amount of Ti in effluent (mg)	Standard deviation
Cu	0.1	100	6	0.099	$7.0 \cdot 10^{-3}$
Co	0.1	100	6	0.099	$1.7 \cdot 10^{-3}$
Cr	0.1	100	6	0.098	$1.7 \cdot 10^{-3}$
Fe	0.1	0.5	3	0.098	

TABLE II

RESULTS OF ELUTION OF Ni^{2+} , Cu^{2+} AND Fe^{3+} USING CHROMOTROPIC ACID AS COMPLEXING AGENT

Element	Taken (mg)	Found (mg)	Column height (cm)	pH of solution	Excess of ChH_4	No. of determinations
Ni	0.50	0.52	13	2	6-fold	3
Cu	0.50	0.48	13	2	6-fold	3
Fe	0.50	0.49	13	2	6-fold	3

Column experiments. In column experiments, the absorption of single metal ions and the separation of mixtures of metal ions in different ratios were studied.

The feed solution equals 10 ml at equivalent metal ions ratio, at not equivalent larger ratio ($\text{Ti}:\text{Cu} = 1:16\ 000$ about 70 ml); metal ion: ChH_4 ratio = 1:3 1:4, 1:6, 1:60 or 1:80; pH = 2.0. The heights of the columns were 13, 15, 21 and 30 cm.

TiO^{2+} ions were quantitatively bound to the resin; 1.0 or 0.5 *N* perchloric acid was used to elute the TiO^{2+} ions. In order to elute Fe^{3+} ions, 0.2 *N* hydrochloric acid was used. Cu^{2+} and Ni^{2+} passed through the column without being bound, and for their quantitative elution very dilute hydrochloric acid was used.

The results of these experiments are summarized in Tables II and III.

TABLE III

SEPARATION OF Ti FROM Cu, Ni AND Fe USING CHROMOTROPIC ACID AS COMPLEXING AGENT

Element	Amount (mg)		Amount in effluent (mg)		Column height of packing (cm)	ChH_4 :Metal ion ratio	No. of determinations
	Element	Ti	Element	Ti			
Ni	0.5	0.5	0.48	0.51	15	6	3
Ni*	500	0.5	—	0.50	21	(Ti) 80	2
Ni**	2000	0.5	—	0.50	30	(Ti) 80	3
Ni**	8000	0.5	—	0.50	30	(Ti) 80	1
Cu	0.5	0.5	0.48	0.51	15	6	3
Cu***	530	0.5	—	0.50	30	(Ti) 60	1
Cu§	2000	0.5	—	0.50	30	(Ti) 60	1
Cu§	8000	0.5	—	—	30	(Ti) 60	2
Fe*	12	0.25	—	0.26	21	3	3
Fe*	25	0.25	—	0.26	21	3	3
Fe§§	50	0.25	—	0.26	30	4	4

* Ni^{2+} was eluted with 200 ml of very dilute HCl, pH 3–4. Ti^{4+} was eluted with 100 ml of 0.5 *N* HClO_4 .

** Ni^{2+} was eluted with 200 ml of very dilute HCl, pH 3–4. Ti^{4+} was eluted with 200 ml of 0.5 *N* HClO_4 .

*** Cu^{2+} was eluted with 200 ml of very dilute HCl, pH 3–4. Ti^{4+} was eluted with 200 ml of 0.5 *N* HClO_4 .

§ Cu^{2+} was eluted with 300 ml of very dilute HCl, pH 3–4. Ti^{4+} was eluted with 200 ml of 0.5 *N* HClO_4 (in cases not listed in these footnotes, Ti^{4+} was eluted with 50 ml of 1.0 *N* HClO_4).

§§ Fe^{3+} was eluted with 150 ml of 0.2 *N* HClO_4 .

Alizarin red S as complexing agent

Alizarin S gives, in strongly acidic solution, very strong complexes with zirconyl ions^{11,12}. Other metal ions, such as Al^{13,14}, also give comparatively strong complexes, but not as strong as those with Zr, and not as stable in acidic solution.

In this work, the conditions for the separation of Zr from Al, Cu^{15,16} and Ni were investigated. In batch measurements it was found that on Amberlite IRA 410 (Cl⁻) at a Zr:alizarin red S ratio of 1:5 (200 mg of resin, 20 ml of external solution), in 0.2 *N* hydrochloric acid Zr⁴⁺ is bound quantitatively, and in 2 *N* perchloric acid Zr⁴⁺ is not bound.

Column experiments. The height of the column was 17 cm and the Zr-alizarin S ratio was 1:5. The feed solution contained 0.2 mg of Zr in a volume of 10 ml (pH 1.0). It was found that 0.2 *N* perchloric acid does not elute Zr⁴⁺, 0.5–1.0 *N* perchloric acid partly elutes Zr⁴⁺ and 2 *M* hydrochloric acid elutes Zr⁴⁺ quantitatively. In order to elute 0.20 mg of Zr, 50 ml of 2 *N* perchloric acid were used; the amount found was also 0.20 mg with an error of 0% in four determinations.

Ni²⁺ and Cu²⁺ passed quantitatively through the column if the column was washed with very dilute hydrochloric acid. Al³⁺ was eluted with 30 ml of 5.0 · 10⁻³ *N* hydrochloric acid.

The results are summarized in Table IV.

TABLE IV

SEPARATION OF Al, Cu AND Ni FROM Zr, AND Zr FROM Al

Element	Amount (mg)		No. of determinations	Amount in effluent (mg)		Eluent
	Zr	Element		Zr	Element	
Cu	0.2	0.2	4	0.2	0.202	HCl (pH 5)
Ni	0.2	0.8	4	0.2	0.198	
Al	0.2	0.8	5	0.198	0.21	5 · 10 ⁻³ <i>N</i> HCl
Al	4.0	0.1	5	0.104		
Al*	10.0	0.1	6			

* Height of column 30 cm (7 layers of alizarin red S; each layer contain red 5 · 10⁻⁴ mole of alizarin red S).

REFERENCES

- 1 W. Kemula and K. Brajter, *Chem. Anal. (Warsaw)*, 15 (1970) 331.
- 2 K. Brajter, *Chem. Anal. (Warsaw)*, 18 (1973) 125.
- 3 V. Suk, I. Nemcova and M. Malat, *Collect. Czech. Chem. Commun.*, 30 (1965) 2538.
- 4 A. Janickova, V. Suk and M. Malat, *Chem. Listy*, 50 (1956) 760.
- 5 L. Sommer, *Z. Anal. Chem.*, 164 (1958) 299.
- 6 L. Sommer, *Bull. Soc. Chim. Fr.*, (1959) 862.
- 7 L. Sommer, *Chem. Listy*, 52 (1958) 1485.
- 8 J. Heller and G. Schwarzenbach, *Helv. Chim. Acta*, 34 (1951) 1876.
- 9 O. Janti, *Suom. Kem.*, 30B (1951) 136.
- 10 S. Ya. Schnaiderman and N. P. Mowchan, *Ukr. Khim. Zh.*, 19 (1953) 429.
- 11 E. M. Larsen and S. T. Hirozowa, *J. Inorg. Nucl. Chem.*, 3 (1956) 198.
- 12 G. Parissakis and J. Kantogandalos, *Anal. Chim. Acta*, 29 (1963) 220.

- 13 A. K. Mukherji and K. Deyel, *Vijanan Parishad Anusandhan Patrika*, 1 (1958) 23; *C.A.*, 56 (1962) 4351.
- 14 R. L. Seth and A. A. Dey, *J. Prakt. Chem.*, 19 (1963) 229.
- 15 S. P. Sangal, *J. Prakt. Chem.*, 30 (1965) 314.
- 16 A. K. Mukherji and A. K. Dey, *J. Indian Chem. Soc.*, 34 (1957) 461.
- 17 L. G. Sillen and A. E. Martell, *Stability Constants of Metal-ion Complexes*, Chemical Society, London, 1964.

ION-EXCHANGE TECHNOLOGY

CHROM. 7796

PREVENTION OF CALCIUM SULPHATE SCALE FORMATION IN EVAPORATION PLANTS BY ION EXCHANGE

GIANFRANCO BOARI*, LORENZO LIBERTI* and ROBERTO PASSINO**

Istituto di Ricerca Sulle Acque, Rome (Italy)

SUMMARY

A process has been developed that enables sulphate in sea-water feed to distillation plants to be replaced by chloride ions by means of weak anion-exchange resins. Calcium sulphate scales are thus prevented from forming on heat-exchange surfaces. Only the blow-down discharged from the evaporation plant is used to regenerate the resin. After a preliminary evaluation on a laboratory basis, pilot-plant tests, run for about 7500 h on a combined multflash–desulphation unit, fully confirmed the feasibility of the process. Based on these results, a 2000 m³/d advanced multflash plant will be erected near Bari with a maximum operating temperature of 150° and a recovery ratio of 20 kg of water per kg of vapour.

INTRODUCTION

Sea-water dealkalization enables distillation plants to be operated at 110–115° with a concentration ratio (n) of about 1.8. This corresponds to metastable conditions for the anhydrous calcium sulphate solubility, and frequent descaling maintenance operations are commonly scheduled in such plants. Fig. 1 shows, as an extreme case, a cross-section of a heat-exchange tube of a multflash evaporator run for about 700 h at 110° and $n = 1.8$; the tube is obstructed by calcium sulphate scale. Higher operating temperatures could theoretically reduce the cost of producing water¹, but it would produce intolerable scales.

In order to overcome this problem, systematic investigations have been carried out by IRSA with the aim of removing the sulphates from sea water by means of anion-exchange resins, using only concentrated sodium chloride solution discharged from the evaporation plants as regenerant. An extensive research programme has been carried out during the last 4 years, which first included basic investigations on the equilibrium and kinetic features of many anion-exchange resins toward the Cl⁻–SO₄²⁻ system. This led to the selection of a particularly suitable resin, which was subsequently characterized by laboratory tests so as to obtain design data for a pilot-scale evaluation of the process. A desulphation unit was then built in order to pre-

* Present address: IRSA-CNR, Via F. De Blasio, 70123 Bari, Italy.

** Present address: IRSA-CNR, Via Reno 1, 00198 Rome, Italy.

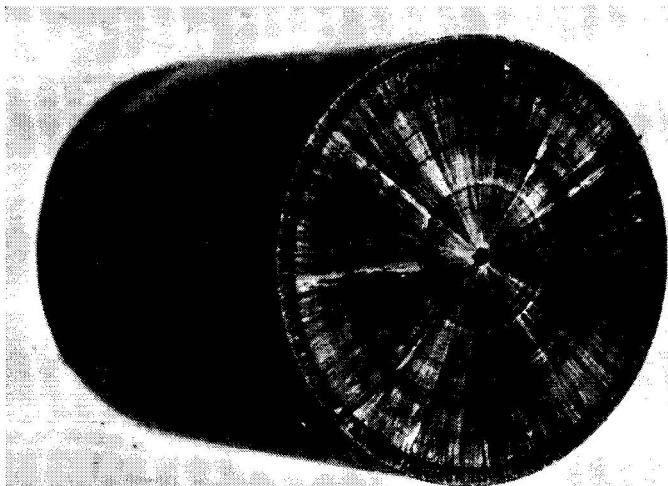


Fig. 1. Cross-section of a heat-exchange tube of a multflash evaporator encrusted by calcium sulphate scales. Operating temperature, 110° ; concentration ratio, $n = 1.8$.

treat the feed of a $100 \text{ m}^3/\text{d}$ multflash pilot plant. About 7500 h of effective service of the pilot unit, under various and severe operating conditions, definitely confirmed the suitability of the process. After this experience, a $2000 \text{ m}^3/\text{d}$ multflash plant with a desulphation unit has now been planned as the first industrial application of a high temperature, high recovery ratio evaporation plant.

This paper summarizes the main results obtained during each stage of the research programme.

BASIC INVESTIGATIONS

First, the thermodynamics and the kinetics of the Cl^- - SO_4^{2-} exchange on more than 30 anion-exchange resins have been investigated. Using the column equilibration procedure and the infinite batch technique for the selectivity and the kinetic measurements, respectively, equilibrium isotherms and the exchange rates were determined for each resin, with solution concentration ranging from $6 \cdot 10^{-3} \text{ N}$ (*i.e.*, $n = 10^{-2}$) to 1.8 N ($n = 3$), temperatures between 5 and 45° , and a pH of about 3.5. The resin performances were found to be essentially dependent, among the investigated parameters, on the fixed charge basicity, and the following sequences were obtained^{2,3} (Figs. 2 and 3):

(1) Selectivity sequence: $\text{IV}^{\text{ary}} < \text{III}^{\text{ary}} < \text{II}^{\text{ary}} < \text{I}^{\text{ary}}$ amino-type resins.

(2) Kinetic sequence: $\text{IV}^{\text{ary}} > \text{III}^{\text{ary}} > \text{II}^{\text{ary}} > \text{I}^{\text{ary}}$ amino-type resins.

The following conditions were also found to favour the process, although less significantly: high temperature; low pH; low solution concentration; hydrophilic, porous matrix; 10–12% cross-linking; high exchange capacity.

As a result of these investigations, a high-capacity, 11% cross-linked, acrylic resin with predominantly secondary (and primary) amino functional groups (Kastel A 102, produced by Montecatini Edison Co., Milan, Italy) was selected for further research development. This resin is characterized by the following features:

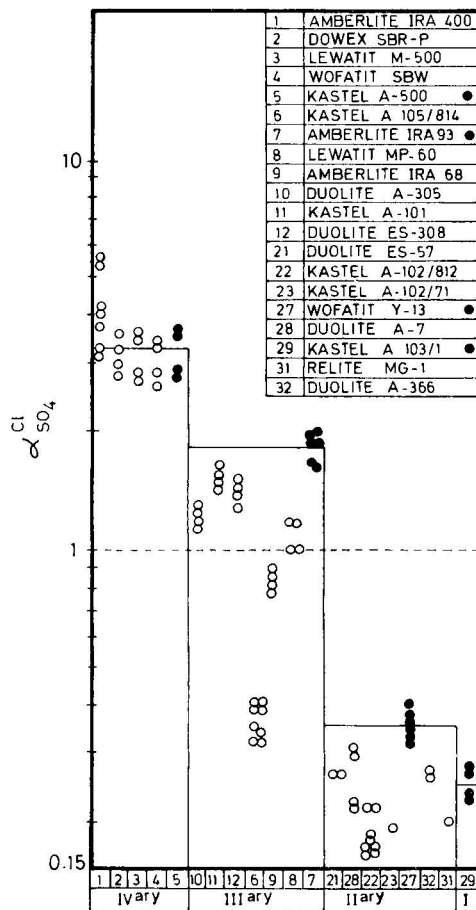


Fig. 2. Cl^- - SO_4^{2-} separation factors versus predominant functional group of anion-exchange resins. Separation factor, $\alpha < 1$, selectivity toward sulphates. Solution concentration, $C = 0.6 \text{ N}$; sulphate equivalent fraction in solution, $X = 0.5$; 25° .

- (a) extremely high selectivity toward sulphates at sea-water salinity (about $0.5 \text{ equiv. SO}_4^{2-}/\text{equiv. resin}$ under equilibrium conditions);
- (b) strong decrease in selectivity by increasing the solution concentration (more than a 50% decrease by a two-fold increase in the solution concentration);
- (c) very high exchange rate at solution concentrations equal to or higher than sea water (half-exchange times less than 1 min).

LABORATORY RUNS

More than 250 countercurrent exhaustion-regeneration cycles were run on a 5-l column filled with Kastel A 102 resin, with sea water (previously acidified at a pH 3.5) fed upwards. Synthetic sodium chloride solutions were used as regenerant. The dependence of resin performance on the main operating parameters (blow-down concentration, exhaustion and regeneration flow-rates) was characterized.

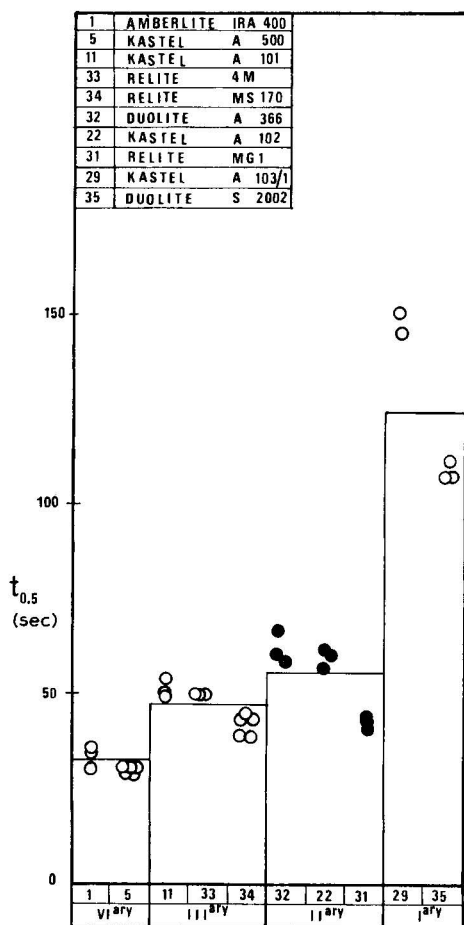


Fig. 3. Cl^- - SO_4^{2-} half-exchange times versus predominant functional group of anion-exchange resins. $C = 1.8 N$; 20–30 mesh; 25° .

Blow-down concentration

As the concentration ratio increases, higher degrees of desulphation may be obtained in the treated water (see Fig. 4). From a practical point of view, higher n values mean less sea water to be treated per unit volume of water produced and less heat to be discharged with the blow-down. On the other hand, corrosion problems and ebullioscopic losses make it difficult to use n values higher than 2.5–3.0 with traditional evaporation plants.

Exhaustion flow-rate

The determination of the breakthrough curves at different solution flow-rates (see Fig. 5) confirmed the very high exchange rates previously observed with this resin in batch experiments. At flow rates higher than 40 bed-volumes per hour, up to 20 bed-volumes of sea water may be treated with a degree of average desulphation $\geq 75\%$, depending on the blow-down concentration.

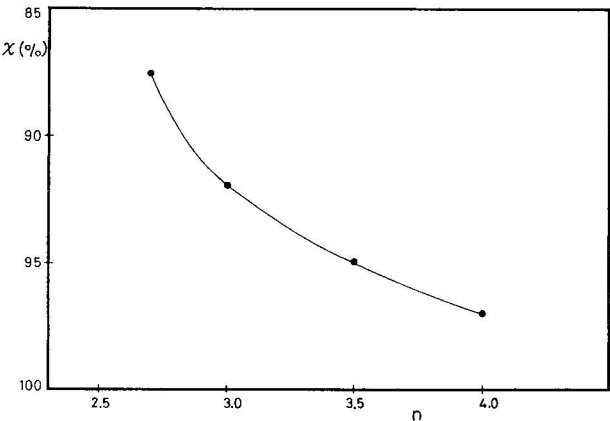


Fig. 4. Average degree of desulphation (χ) versus concentration ratio (n); each point represents the average of 10 cycles. Kastel A 102 resin; cycle volume of treated sea water, $V_{cs} = 16$ bed volumes; exhaustion flow-rate, $F_{cs} = 40$ bed volumes per hour; volume of blow-down, $V_{rig} = V_{cs}/n$.

Regeneration flow-rate

As the selected resin is still selective toward sulphates at $n = 4$, the regeneration step was thermodynamically unfavourable. Further, simplified plant operations (two columns in parallel, one regenerated while the other was being exhausted, no intermediate operations being necessary on a routine basis) made it necessary to assume equal times for regeneration and exhaustion operations.

The regeneration and exhaustion flow-rates were thus correlated, according to the equation

$$F_{rig} = F_{cs}/n \quad (1)$$

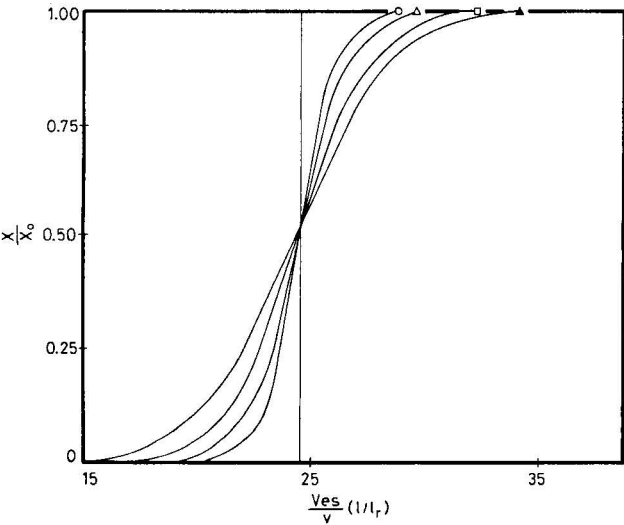


Fig. 5. Sulphate breakthrough curves during the exhaustion step. Kastel A 102 resin; $C = 0.6$ N; $c_{so} = 0.056$ equiv./l; sea-water pH = 3.5; $n = 3$. F_{cs} : ○, 5 bed volumes per hour; △, 10 bed volumes per hour; □, 20 bed volumes per hour; ▲, 40 bed volumes per hour.

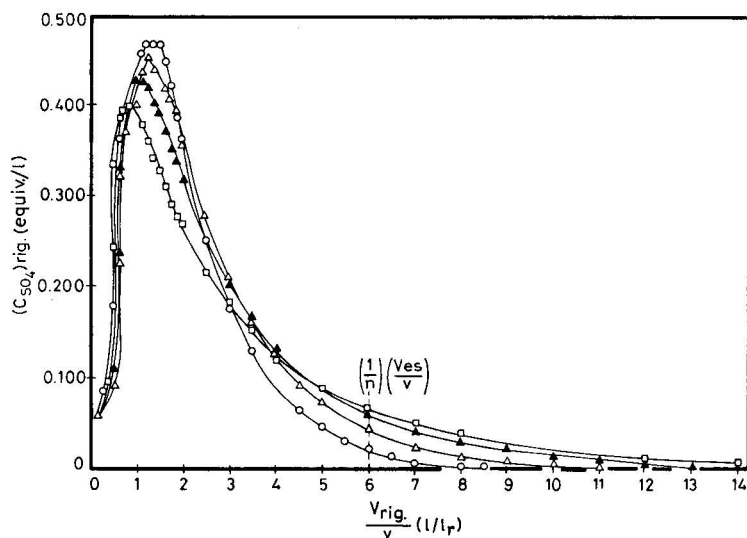


Fig. 6. Sulphate breakthrough curves during the regeneration step. Kastel A 102 resin; $n = 3.5$. F_{rig} : \circ , 0.5 bed volumes per hour; \triangle , 1 bed volume per hour; \blacktriangle , 5 bed volumes per hour; \square , 10 bed volumes per hour.

As indicated by the breakthrough curves obtained during this step (see Fig. 6), the blow-down regenerating capacity was strongly dependent on the liquid-solid contact time.

At each n value, according to eqn. 1 and based on sets of breakthrough curves as in Figs. 5 and 6, a suitable F_{es} value must be chosen that prevents sulphates from accumulating on the resin in each cycle. At the same time, only the last fraction (about 25%) of the (partially) exhausted blow-down was recovered in each run, to be used as first fraction in the subsequent regeneration so as to prevent dilution of the regenerant by the intraparticle bed solution. The laboratory runs demonstrated the suitability of the desulphation process and allowed design data for a larger, pilot unit to be obtained (Table I).

PILOT PLANT TESTS

A four-stage recirculation multistage plant, with an output capacity of about 100 m³/d, still existing at Breda Research Institute facilities in Bari, was served by a desulphating unit consisting of two columns in parallel, each containing about 300 l of Kastel A 102 resin. Fig. 7 shows the operating flow-sheet of the plant. Two series of runs were made, at "low" temperatures (operating temperature between 120 and 130°, $n = 2.5$ –2.0) and at "high" temperatures (145°, $n = 2.4$), for a total of 7500 h of effective service. The pH of sea water was maintained between 3.5 and 5.0, while after the degasifier a pH of about 7.2 was kept constant. No scales were observed during these runs, even at the highest temperatures.

The first series of runs confirmed the reliability of the desulphation process in conventional evaporation plants, indicating its capacity to re-adsorb occasional breakthroughs that occur as a result of accidental errors. The high-temperature tests

TABLE I

OPERATING CONDITIONS AND RESULTS FOR KASTEL A 102 ANION-EXCHANGE RESIN

Laboratory-scale plant.

Conditions	Concentration ratio, n					
	3.0		3.5		4.0	
Exhaustion flow-rate (l/l, h)	40.0		40.0		40.0	
Regeneration flow-rate (l/l, h)	13.3		11.4		10.0	
Sea-water pH	3.5		3.5		3.5	
Cycle volume of treated water (l/l,)	16.0	17.5	16.0	17.5	16.0	17.5
Cycle volume of brine (l/l,)	5.3	5.8	4.0	5.0	4.0	4.4
Average sulphate removal (%)	92.0	86.5	95.0	90.5	97.0	92.5
Recovered brine fraction	0.25		0.25		0.25	
Resin volume/product water flow-rate (l, h/m ³)*	75.0		70.0		66.6	
Cycle number per year**	3200	3500	3200	3500	3200	3500

* In two columns.

** 8000 h per year.

demonstrated the possibility of preventing, by means of this pre-treatment, the formation of calcium sulphate scales even under very severe conditions, thus allowing for the design of advanced evaporation plants.

Continuous control of the sulphate concentration in the brine, measurements of the fouling coefficient of the condenser tubes and periodic inspections of the heat-exchange surfaces (where sometimes small amounts of iron oxide scales, containing only traces of calcium sulphate, were found) and of the resin beads, fully confirmed the suitability of the desulphation process.

Particular attention was paid to control of the resin life during these tests. After about 7500 cycles (each complete cycle lasting for about 1 h), samples of resin were examined for total exchange capacity, granulometric analysis, etc., while internal

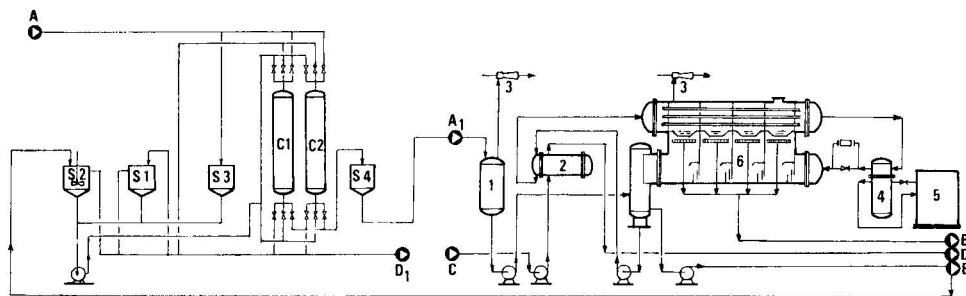


Fig. 7. Operating flow-sheet of the combined desulphation-multiflash pilot unit. A = feed water; A₁ = desulphated water; B = product water; C = cooling water inlet; D = cooling water outlet; E = brine outlet; D₁ = exhausted brine discharge; S1, S2, S3 = regenerant tanks; S4 = desulphated water tank; C₁, C₂ = ion-exchange columns; 1 = degasifier; 2 = brine cooler; 3 = ejectors; 4 = brine heater; 5 = steam generator; 6 = four-stage flash unit.

fouling was checked by X-rays and electronic scanning. All of these controls indicated the excellent features of the resin, as expected according to the very weak chemical and osmotic shocks that occurred during the process. No consumption of resin was detected at the end of the tests.

DEMONSTRATION PLANT

Based on the pilot-plant experiences, an advanced multistage plant with 68 effects, 2000 m³/d capacity is under construction in Bari's industrial area. A maximum operating temperature of 150° and a conversion ratio of 20 kg of water per kilogram of vapour have been adopted, while at n values near 2 the thermodynamic losses due to the elevation of the boiling point would be as in conventional evaporation plants.

Other than for demonstration purposes, the plant will provide data for the design and construction of high-temperature stages.

CONCLUSIONS

Laboratory and pilot-plant experiences have demonstrated the possibility of removing sulphates from sea-water feed to desalting evaporation plants by means of weak anion-exchange resins. These plants can thus be run at temperatures up to 150–160°, at the same concentration ratios as in conventional plants, without the formation of calcium sulphate scales.

A feasibility study on a 10,000 m³/d single-purpose multistage plant demonstrated that with this kind of pre-treatment, the cost of the product water can be de-

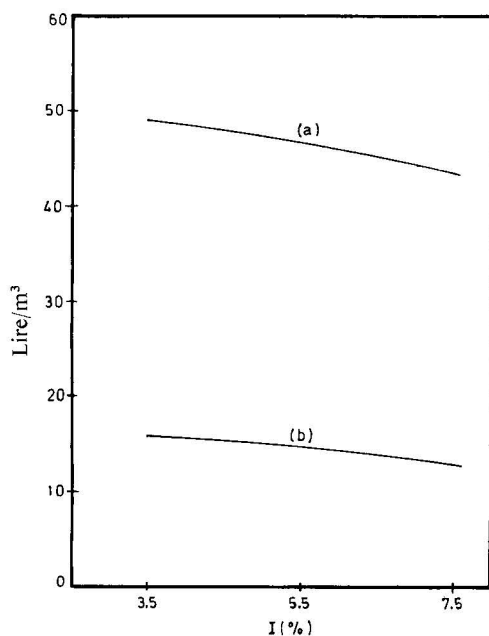


Fig. 8. Savings attainable with the desulphation process as a function of interest rate. Fuel costs: (a) 3500 Lire/10⁹ cal; (b) 1500 Lire/10⁹ cal.

creased considerably⁴. As indicated in Fig. 8, the savings are directly related to the fuel cost. With today's energy shortages, the actual savings are near the upper curve of this diagram, which means about 45 Lire/m³ (US\$0.30 per 1000 gal) of treated water. Even for dual-purpose evaporation plants, the desulphation process allows for appreciable savings owing to the possibility of raising the maximum operating temperature and of maintaining the heat-exchange coefficients at their maximum values.

ACKNOWLEDGEMENTS

The authors gratefully acknowledge the Istituto Ricerche Breda and Breda Termomeccanica Locomotive for their valuable contributions to the pilot-plant tests. Thanks are also due to Mr. Nicola Limoni and Mr. Lino de Girolamo, who contributed to the experimental work.

REFERENCES

- 1 G. K. Kunz, *Desalination*, 3 (1967) 362.
- 2 G. Boari, L. Liberti, C. Merli and R. Passino, *Desalination*, 15 (1974) 145.
- 3 L. Liberti and R. Passino, *J. Chromatogr.*, 102 (1974) 155.
- 4 Breda Termomeccanica & Locomotive, *Technical and Economic Study on Coupling of Desulphation and Multiflash Processes for Sea Water Desalination*, Final Report under Contract IRSA 35726, June 1973.

CHROM. 7766

SOME PROBLEMS IN THE SEPARATION OF COPPER AND IRON FROM MINE WATERS

ANNA SOPKOVÁ

Faculty of Sciences, Department of Inorganic Chemistry, P. J. Šafárik's University, Košice (Czechoslovakia)

KAREL VETEJŠKA

Ore Research Institute, Prague (Czechoslovakia)

and

JÁN BUBANEC

Faculty of Sciences, Department of Inorganic Chemistry, P. J. Šafárik's University, Košice (Czechoslovakia)

SUMMARY

Some copper mine waste waters contain, in addition to copper, also iron ions, the presence of which makes it difficult to recover copper by ion-exchange methods, particularly as the high acidity of the water lowers the capacity of weakly acidic ion exchangers. Using the proposed method, mine water samples were completely freed from iron and the $[\text{Cu}(\text{NH}_3)_4]^{2+}$ form was sorbed using the full capacity of the weakly acidic resin Ostion-KM (Na^+). After elution with sulphuric acid, we achieved a concentration of Cu^{2+} ions in solution, eliminating all of the iron present in the original sample.

INTRODUCTION

The isolation of copper from solutions, mainly from mine waters containing other metals, has always been a problem and remains so as far as ion-exchange methods are concerned. The most common metal in mine wastes is iron and its ions are simultaneously sorbed with copper ions, thus decreasing the capacity of the resin and hindering the concentration of copper ions. Therefore, in our studies on the behaviour of iron and copper ions in mine waters, we wished to decrease the amounts of iron and other metals present before treating the waters with resins. Common methods for the isolation of copper ions from low-grade copper ores and from copper wastes, such as leaching with dilute sulphuric acid and then winning the copper either by reduction with metal and electrolysis, or obtaining it in the form of crystalline copper sulphate or other forms¹, are useful also in the separation of copper from mine waters. However, with varying and low copper contents, and when other metals such as iron, magnesium, lead, manganese and zinc are present, the results are unsatisfactory.

The most commonly used and promising method for treating mine waters nowadays is the cementation method, which gives a 41 % copper recovery², using the lower standard redox potentials of iron ions.

The use of ion-exchange methods for the separation of copper from mine waters on a laboratory scale was first used by Quarm³. Before the use of Amberlite IRC-50, he pre-treated the water, containing 0.15–0.30 g/l of copper and 1.5–3.0 g/l of iron, by adding calcium carbonate. In this manner, he sorbed in the resin 84 % of copper and 20.1 % of iron.

Quarm³ also recovered similar amounts of copper and iron using a weakly acidic cation-exchange resin. Vránová⁴ studied the sorption of copper ions from mine waters from the Smolník locality and found that resin in the Mg^{2+} form was more useful than in the Na^+ or H^+ form.

We have treated samples of the same mine water containing lower contents of copper and also containing silica solids by sorption on a weakly acidic resin of Czechoslovak origin, namely Ostion KM (Na^+), and by floating the resin in order to separate it from the solids, recovering 66.7 % of the copper, and later⁵ we treated waters without solids, with a 92.2 % recovery of copper and a 20.53 % recovery of iron.

We then treated samples of mine water containing higher copper contents, by pre-treatment with calcium carbonate, and separated 95.2 % of the iron; we were then able to sorb 73.2 % of the copper on the Na^+ form of the resin and subsequently all of the remaining iron content by sorption on the Mg^{2+} form of the resin⁶. By elution, we achieved a 4.8-fold concentration of copper-containing mine water.

It is evident that the main disadvantages of the cementation method are low recovery, a great dependence on the variation in copper content in wastes, and also the quality of the copper metal obtained which is not satisfactory without a pre-treatment step. Ion-exchange methods, involving the use of pre-treated resin to permit the selective sorption of copper from mine waters, do not eliminate the possible sorption of other metal ions present in waters, which decrease the sorption capacity of the resin. The capacity of weakly acidic ion exchangers is also not fully utilized owing to the acidity of mine waters. Therefore, in this work we have investigated a more sensitive method for the pre-treatment of resins and also of the samples of mine waters.

EXPERIMENTAL

The resin used was weakly acid Ostion KM (Na^+), 0.315–0.8 mm, in a column containing 26 ml of resin.

The mine waters from the Smolník locality represented two concentration ranges:

Sample 1:

Original pH 2.24: 98.0 mg/l Cu^{2+} ; 142.0 mg/l Fe^{3+}

After pre-treatment to pH 10.10: 89.0 mg/l Cu^{2+} ; 0 mg/l Fe^{3+}

Sample 2:

Original pH 2.24: 156.5 mg/l Cu^{2+} ; 205.8 mg/l Fe^{3+}

After pre-treatment to pH 10.12: 140.1 mg/l Cu^{2+} ; 0 mg/l Fe^{3+}

The water, after establishing the optimal pH range for pre-treatment, was pre-treated with 25 % ammonia solution and, after filtering off the precipitate and all the Fe^{3+} formed, the solution with the remaining Cu^{2+} content was sorbed in the form

of $[\text{Cu}(\text{NH}_3)_4]^{2+}$ on the resin in the Na^+ form at a flow-rate of 0.123 ml/min per millilitre of resin and then eluted with sulphuric acid.

RESULTS

The copper content in mine waters after pre-treatment with various amounts of 25% ammonia solution was as shown in Fig. 1. The optimal pH value was found to be 10.12. Sample 1, after pre-treatment with 25% ammonia solution to this pH value, contained 89.0 mg/l of Cu^{2+} , all Fe^{3+} present being filtered off, and sample 2 at this pH value contained 140.1 mg/l of Cu^{2+} .

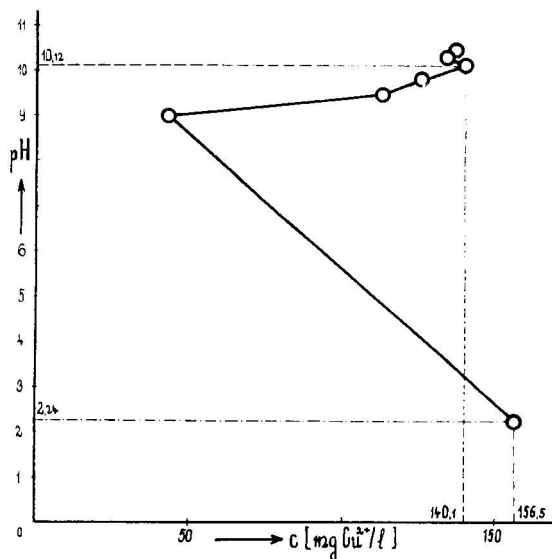


Fig. 1. Optimal value of pH after pre-treatment of mine water.

The sorption conditions of both samples are shown in Fig. 2. The amounts of copper sorbed were 74.6% in sample 1 and 71.3% in sample 2 and, after elution with the optimal⁶ concentration of 10% sulphuric acid, we achieved 9.5 and 5.3-fold concentrations, respectively, and recovered a solution of relatively pure copper sulphate.

A comparison of results from our previous methods with those from the proposed method is given in Table I.

DISCUSSION

For mine waters with varying copper and iron contents, we have developed a method of pre-treatment that eliminates the disadvantages of other methods with respect to the recovery grade, purity of isolated copper, time required and also the complete use of resin capacity. Pre-treatment of samples with ammonia solution to the optimal pH and subsequent sorption of the copper-containing solution on a weakly acidic resin in the $[\text{Cu}(\text{NH}_3)_4]^{2+}$ form eliminates the other metals present and,

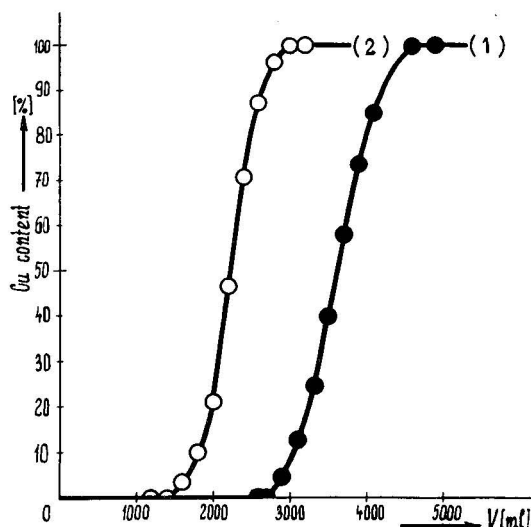


Fig. 2. Sorption of $[\text{Cu}(\text{NH}_3)_4]^{2+}$ from mine waters. (1) 89 mg/l of Cu^{2+} ; pH = 10.10. (2) 140 mg/l of Cu^{2+} ; pH = 10.12.

after 100% elution of Cu^{2+} ions⁶, satisfactory 9.5 and 5.3-fold concentrations of relatively pure copper solutions are achieved. We obtained more complete results by studying mine waters in the Smolník locality after different periods of rain, and found mainly two ranges of copper and iron contents in the waters.

TABLE I

COMPARISON OF RESULTS OBTAINED BY DIFFERENT METHODS

	Cementation ²	Ion exchange		Ion exchange (this work)			
		Cu	Fe	Cu	Fe	Cu	Fe
Water pretreated with to pH							
Concentration of original sample (mg/l)	121.5	199.2	262.1	98.0	142.0	156.5	205.8
Concentration of pre-treated water (mg/l)		195.0	12.5	89.0	—	140.1	—
Volume of sorbed water (ml)		525		4.600		3.000	
Sorbed (mg)		102.4	6.6	409.4	—	420.3	—
(%)		75.04	6.56	305.0	—	298.1	—
Eluted with 10% H_2SO_4 (mg)		73.5	99.4	74.6	—	71.3	—
Recovery from original water (%)	41	70.28	0.05	304.9	—	297.9	—
(concentration)		93.7	0.76	100	—	100	—
Recovery from pre-treated water (%)		67.1	0.04	67.7	—	63.5	—
(concentration)		3.5	—	8.6	—	4.8	—
Recovery from pre-treated water (%)		68.7	0.77	74.5	—	70.9	—
(concentration)		3.6	—	9.5	—	5.3	—

REFERENCES

- 1 H. Remy, *Anorganická Chémia*, Vol. II, SNTL, Prague, 1962.
- 2 V. Špaček and J. Beránek, *Výzkum a Využití Biologických Metod pro Úpravu Neroztných Surovin*, Ústav pro Výzkum Rud, Prague, 1970.
- 3 T. A. A. Quarm, *Bull. Inst. Min. Metall.*, 377 (1954) 109.
- 4 O. Vránová, *Úplný Hydrolog. Výzkum Těžebných Ložisk s Ohledem na Účinky Agresivních vod*, Dílčí Zpráva Evid. Č. ÚVZ 6220–23, Ústav pro Výzkum Rud, Prague, 1962.
- 5 A. Sopková, *Koncentrovane Kovových Iónov Flotáciou Ionexov, Vyrábaných v ČSSR. Thesis*, Vysoká Škola Chemicko-Technologická, Prague, 1969.
- 6 J. Bubanec, *Delenie Iónov Cu^{2+} a Fe^{3+} na Vymieňačoch Iónov. Dipl. práca*, Slovenská Vysoká Škola Technická, Bratislava, 1971.

CHROM. 7854

PURIWAT® APPARATUS*

A SYSTEM OF ION-EXCHANGE CELLULOSES FOR THE PRODUCTION OF HIGH-PURITY WATER

ZS. HORVÁTH

Institute of Inorganic and Analytical Chemistry, L. Eötvös University, H 1443 Budapest, P.O. Box 123 (Hungary)

SUMMARY

PURIWAT apparatus produces high-purity water for special purposes from distilled or deionized water. Contaminants at the parts per million level can be removed by passing the water through a column of sandwiched ion-exchange cellulose as filtering media. The volume of water to be purified can be programmed and the apparatus operates without supervision. The filtering media is disposable, and fillings for the purification of 50 or 100 l of water are available. The output of high-purity water is up to 6 l/h. When analysed by neutron activation analysis, the purified water is especially low in copper (0.0025 ppb**), while the contents of other heavy metals are less than 0.01 ppb.

INTRODUCTION

Advances in microelectronics, photography, trace chemical analysis and pharmaceutical syntheses are placing very high demands on water quality¹. The quality of water obtained by the usual techniques of deionization or distillation is inadequate for these purposes because of the high levels of certain elements (principally trace metals) and organics. Research laboratories impose additional requirements of freedom from specific materials, leading to a need for the so-called selectively pure water².

Distilled or deionized water contains a level of 100 ppb of metal impurities. Distilled water from a commercial metallic still is high in copper. For example, the distilled water in our laboratory analyzed by neutron activation analysis contains 5–50 ppb of copper, 10–60 ppb of iron, 0.2–100 ppb of zinc and 500 ppb of sodium. The quality of water is variable, depending on the quality of the feed water and the extent of corrosion of the still. This distilled water was purified by the PURIWAT apparatus, which is a new system for the production of high-purity water.

* PURIWAT® apparatus is manufactured by Gép-és Műszeripari Szövetkezet Co-operative for the Machine and Instrument Industries, 7130 Tolna, Hungary.

** Throughout this article the American billion (10⁹) is used.

EXPERIMENTAL AND RESULTS

It was shown in our recent investigations that ion-exchange celluloses in the form of loose fibres are very effective for the rapid removal of heavy metal impurities from distilled water. The purification, as proved by neutron activation analysis, was effective up to parts per 10^{12} concentrations³. Some types of dissolved organic compounds could also be removed from deionized water by ion-exchange celluloses⁴. Organic compounds dissolved from resins by water and metal contaminants in a colloidal form (Al, Cr, Sn, Pb, Fe, Cu, Ni, Zn) and particulates (dust, resin) in distilled or deionized water could be removed by ion-exchange celluloses. The chelate-forming ion-exchange cellulose iminodiacetic acid ethylcellulose prepared recently by us⁵ had the advantage over cationic and anionic ion-exchange celluloses that it formed chelates of high stability with the metallic contaminants in distilled water. It was shown that instead of a series of columns, consisting of alternate beds of loose fibres of cation- and anion-exchange cellulose, a new type of column system, which we called a "sandwich system", was more effective for the removal of the trace contaminants in distilled or deionized water.

The principle of the sandwich system of ion-exchange celluloses is as follows. In a special sequence, cation-exchange carboxymethylcellulose, anion-exchange diethylaminoethylcellulose and chelate-forming ion-exchange iminodiacetic acid cellulose are sandwiched in a column. The water to be purified is allowed to pass through the sandwiched ion-exchange celluloses, the so-called filtering media, at a rate of $1\text{--}1.5\text{ l/h}\cdot\text{cm}^2$. The PURIWAT apparatus holds a column consisting of the sandwiched ion-exchange celluloses as filtering media. The constructional materials of the apparatus that are in contact with the water are polyethylene and polymethacrylic ester. The housing or column holding the filtering media is made of polymethacrylic ester.

Fig. 1 shows the schematic diagram of the principle of operation of the PURIWAT apparatus.

Component 1 is the storage tank for the distilled or deionized water to be purified, 2 is the diaphragm tap and 3 is the centrifugal pump. When the diaphragm

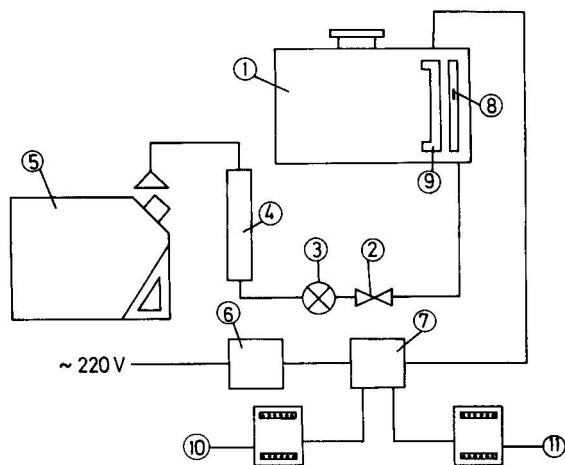


Fig. 1. Schematic diagram of the PURIWAT apparatus.

tap is opened and the operating switch is switched on, the centrifugal pump begins to deliver the water to be purified. The water passes through a plastic cartridge (4), which contains the sandwiched ion-exchange celluloses. A plastic can (5) serves to hold the effluent, the high-purity water. Components 6 and 7 are the supply unit and the relay. A magnetic float (8) indicates the decrease in the level of water in the storage tank. The volume of water flowing out of the storage tank is measured by a volume-measuring level sensor (9). The pulses given for each litre delivered are written out by a capacity indicator (10) and by a programme indicator (11) in the form of figures. The volume of water necessary for a certain purpose can be programmed on a programme indicating unit (11) and this automatically ensures operation without supervision. When the filtering media is exhausted, the apparatus programmed for the capacity of the filtering media produces sound and light signals and the centrifugal pump stops. The cartridge filling is disposable, and fillings for the purification of 50 or 100 l of distilled or deionized water are available. The filling can be exchanged within 1 min by pulling out the base connection, unscrewing the cartridge, discarding the old filling and replacing it with the new one. The output of high-purity water is up to 6 l/h.

DISCUSSION

The high-purity water produced from our laboratory distilled water by the PURIWAT apparatus was analyzed by neutron activation analysis. The metal content of the distilled water before passing it through the column is given in the Introduction. The purified water was especially low in copper content (0.0025 ppb). The iron content was 1, zinc 0.02–0.05 and sodium 20–30 ppb. The concentration of other elements such as calcium, cobalt, manganese, nickel, lead and antimony was less than 0.01 ppb, less than the sensitivity of the method for these elements.

Conductivity determinations cannot be used for the measurement of the purity of high-purity water as some elements that are present in particulate or colloidal form in the parts per 10^9 or 10^{12} concentration range are undetectable¹. For the evaluation of effluent quality, sensitive analytical methods such as neutron activation analysis and possibly flameless atomic-absorption spectroscopy are adequate. In the purified water, residues from the apparatus and degradation products of the ion-exchange celluloses after the purification of 100 l of distilled or deionized water could not be detected by the methods applied; the oxygen demand was measured by the potassium permanganate method and the transparency was measured up to the far UV region.

The PURIWAT apparatus produces an extremely high quality of high-purity water with the lowest levels of heavy metals and other contaminant ions that can be reached at present by the purification of distilled or deionized water. The high-purity water produced by the PURIWAT apparatus can be used in every research activity that demands extremely pure water, for example, in semiconductor, protein, enzyme and pharmacological research, in bacteriology, thin-layer chromatography, flame-emission and atomic-absorption spectrophotometry, making up analytical-grade reagents and for other purposes.

REFERENCES

- 1 R. C. Hughes, P. C. Müräu and G. Gundersen, *Anal. Chem.*, 43 (1971) 691.
- 2 G. Iwantscheff, *Das Dithizon und seine Anwendung in der Micro- und Spurenanalyse*, Verlag Chemie, Weinheim/Bergstr., 1972, p. 23.
- 3 Zs. Rempert-Horváth and M. Ördögh, *Mikrochim. Acta*, (1972) 491.
- 4 J. D. Guthrie, *Ind. Eng. Chem.*, 44 (1952) 2187.
- 5 Zs. Horváth and Gy. Nagydiósi, *J. Inorg. Nucl. Chem.*, in press.

CHROM. 7772

ÉCHANGE D'IONS EN LIT MOBILE À PLUSIEURS CONSTITUANTS

RECHERCHE D'UNE MÉTHODE DE CONCEPTION ET DE CALCUL POUR DES COLONNES PRÉPARATIVES DE PETITE DIMENSION

MICHEL BAILLY et DANIEL TONDEUR

Centre de Cinétique Physique et Chimique du C.N.R.S., Route de Vandoeuvre, 54600-Villers-les-Nancy (France)

SUMMARY

Multi-component moving-bed ion exchange. An approach to the design of small-scale preparative columns

It is shown how the theory of non-linear multi-component chromatography can be used for defining and designing continuous separation. The influence of kinetic and dispersion factors is studied. Preliminary experimental results are presented, comparing performance of a moving and a fixed bed.

INTRODUCTION

Nous nous proposons, à long terme, de développer des méthodes de conception et de calcul pour des séparations continues en lit mobile à petite échelle, par échange d'ions ou adsorption. Cette méthodologie est basée sur l'analogie de ces séparations avec les séparations chromatographiques non-linéaires. Nous pensons en effet, qu'à petite échelle, il est possible de concevoir des séparations continues avec une "efficacité" comparable à celle d'une colonne chromatographique (en plus des avantages inhérents au fonctionnement continu).

Dans cette optique, nous résumons ici les méthodes et résultats de nos travaux préliminaires, dirigés suivant trois axes: (i) L'application de la théorie de la chromatographie d'équilibre non-linéaire à plusieurs constituants^{1,2} à la définition et à l'étude d'une séparation en continu. (ii) L'évaluation de l'influence des effets dispersifs (cinétique de transfert, dispersion axiale) non pris en compte par le modèle d'équilibre ci-dessus. (iii) L'étude expérimentale comparative du lit fixe et du lit mobile justifiant les démarches ci-dessus.

THÉORIE DE L'ÉQUILIBRE APPLIQUÉE À UNE SÉPARATION

Nous nous proposons d'étudier la séparation par un ion éluant E de deux ions A et B, dont l'isotherme d'équilibre vérifie une loi d'action de masse à coefficients α_A et α_B constants.

$$\alpha_A = \frac{y_A}{y_E} \bigg/ \frac{x_A}{x_E} \text{ et } \alpha_B = \frac{y_B}{y_E} \bigg/ \frac{x_B}{x_E}$$

La théorie de l'équilibre^{1,2}, en négligeant tout effet dispersif, permet de montrer qu'au cours d'une opération de percolation, deux types de transition sont susceptibles de se développer dans une colonne: une transition stable, représentée par une discontinuité se déplaçant à une vitesse constante dans la colonne, et une transition dispersive, représentée par l'étalement d'un gradient de composition dans la colonne. Chacune de ces compositions est affectée d'une vitesse constante. Deux transitions successives sont séparées par un palier, de composition constante.

Cette théorie a été transposée au lit mobile³ par l'application du même traitement mathématique au bilan de matière en lit mobile sur chaque espèce ionique. Cette transposition montre que pour une même opération de percolation, les natures des transitions et la composition des paliers intermédiaires sont identiques en lit mobile et en lit fixe, mais que la vitesse des transitions stables et de chaque composition d'une transition dispersive est différente dans le cas du lit mobile et dépend d'un paramètre μ , égal au rapport des flux de capacité dans les deux phases.

Pour une valeur de ce paramètre μ , il sera possible de rendre nulle la vitesse d'un palier, d'une transition stable ou d'une composition d'une transition dispersive, et donc de stabiliser en régime permanent un de ces points dans la colonne.

Un lit mobile devra donc être considéré comme une succession de sections de colonne dans chacune desquelles sera stabilisé un des points particuliers décrits ci-dessus. Chacune de ces sections de colonne sera séparée de la suivante par une injection ou un soutirage de solution, de façon analogue à une opération de distillation et caractérisée par une valeur de μ .

Cette théorie de l'équilibre fournit donc un modèle très simple décrivant le régime de fonctionnement d'un lit mobile. Elle permet, en particulier, de choisir l'éluant en fonction de la séparation que l'on désire réaliser.

Supposons que le constituant A est préféré au constituant B par la résine.

On peut prétendre obtenir trois résultats à la séparation, si l'on ne dispose que des solutions E et A + B: (i) recueillir une fraction de B pur, (ii) recueillir une fraction de A pur et (iii) recueillir A et B séparés l'un de l'autre, mais mélangés à l'éluant E. Ces trois séparations type seront réalisées si l'on choisit l'éluant E tel que: (i) $\alpha_A > \alpha_B > 1$, (ii) $1 > \alpha_A > \alpha_B$ et (iii) $\alpha_A > 1 > \alpha_B$.

Nous avons porté, en Fig. 1, ces trois modes de fonctionnement du lit mobile: (1) sur un diagramme des caractéristiques (z , t), l'abscisse z représentant la longueur réduite de la colonne, l'ordonnée t le temps (pour obtenir plus de précisions sur cette représentation, on se reportera à la réf. 3) et (2) sur un diagramme de composition (z , x), les profils des titres de chaque espèce dans la colonne, en régimes transitoire et permanent.

Définissons, pour les deux premiers modes de fonctionnement, un rendement théorique de séparation, par le rapport du flux du produit pur soutiré au flux de ce même produit introduit dans le mélange d'alimentation. Nous avons montré, à l'aide du modèle considéré, que ce rendement théorique est indépendant de la composition de ce mélange et ne dépend que des relations d'équilibre.

En conclusion, la théorie de l'équilibre permet de définir le régime de fonctionnement du lit mobile, mais elle présente l'inconvénient de faire abstraction des

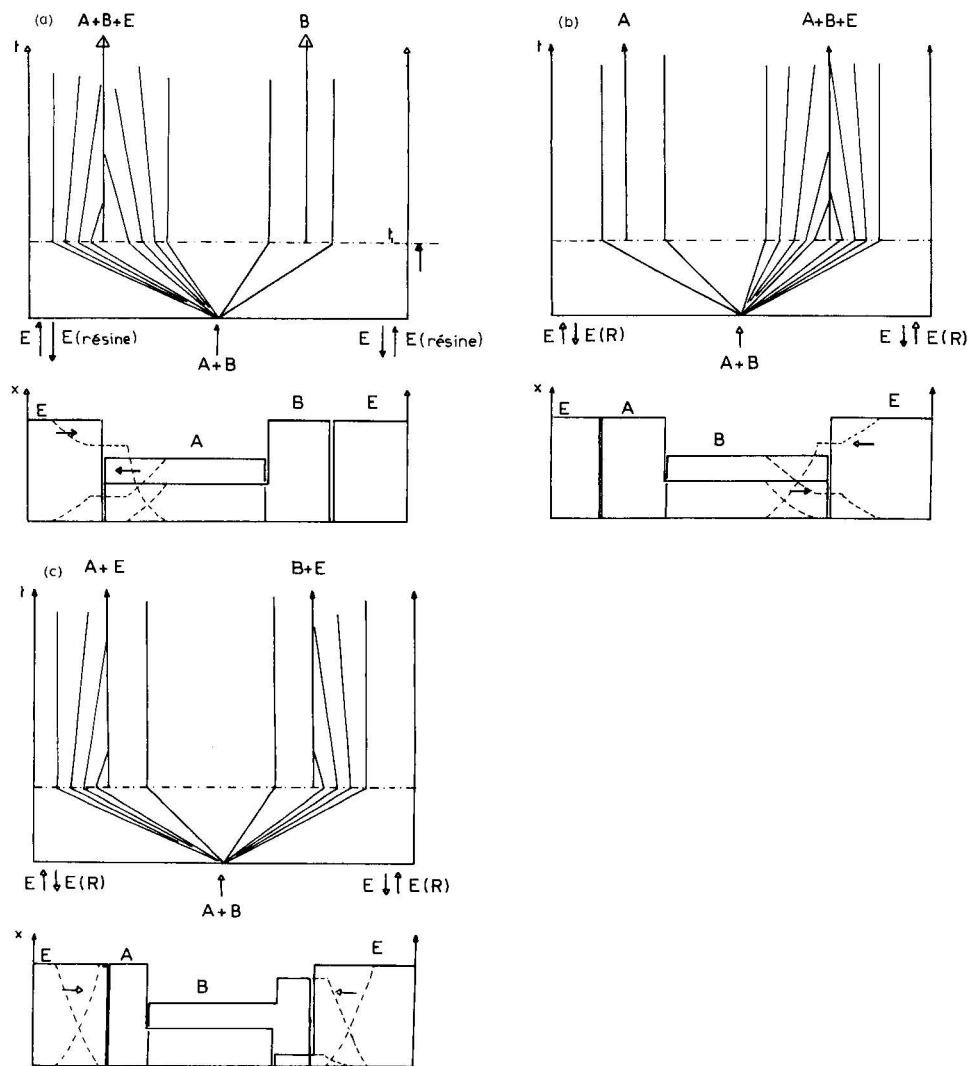


Fig. 1. Diagramme des caractéristiques et des profils en régimes transitoires ($t < t_1$) et permanent. —, t_∞ ; ---, t_1 . (a) $\alpha_A > \alpha_B > 1$; (b) $1 > \alpha_A > \alpha_B$; (c) $\alpha_A > 1 > \alpha_B$.

résistances au transfert de matière. Dans le cas d'une transition dispersive, il est couramment admis⁴ que la théorie de l'équilibre représente une bonne approximation du comportement réel du système. Par contre, dans le cas d'une transition stable, la description du comportement du système nécessaire à l'évaluation de son efficacité ne saurait être obtenue sans introduire les résistances au transfert de matière.

EXTENSION À UN SYSTÈME AVEC EFFETS DISPERSIFS

La non-linéarité de l'isotherme type loi d'action de masse ne permet pas d'obtenir une solution analytique de la transition dans la colonne. De nombreux auteurs

ont simplifié ce problème en supposant, pour un système à un constituant indépendant, par analogie avec une opération à contre-courant, que les effets dispersif de la résistance au transfert de matière, et compressif de l'isotherme, se compensent, et que la transition stable se déplace à vitesse constante dans la colonne, sans se déformer. Cette hypothèse simple dite de la solution asymptotique, assortie d'une grande variété de lois cinétiques, est à l'origine de nombreuses correlations publiées.

D'autre part, Amundson⁵ a étudié les conditions d'existence de cette solution asymptotique et a vérifié par intégration numérique que pour une loi de diffusion interne, avec dispersion axiale, le régime transitoire d'un système à un constituant indépendant approche rapidement la solution asymptotique. Nous avons, pour notre part, étendu partiellement cette démarche à un système à N constituants.

Ecrivons comme Amundson⁵, le bilan de matière dans la colonne sur chaque constituant, en présence de dispersion axiale et d'une loi cinétique quelconque

$$\frac{1}{Pe} \frac{\partial^2 x_i}{\partial z^2} - \frac{\partial x_i}{\partial z} + \mu \frac{\partial y_i}{\partial z} = \frac{\partial x_i}{\partial \tau} + \nu \frac{\partial y_i}{\partial \tau} \quad i = 1, \dots, N$$

$$\frac{\partial y_i}{\partial \tau} = G(x_i, y_i) \text{ avec } G(x_i, y_i) = 0 \text{ si } y_i = y_i^{\text{eq}}(x_i)$$

Si l'on introduit une représentation paramétrique, $\xi = z - \lambda\tau$, du système $[x_i(\xi), y_i(\xi)]$ et que l'on cherche les points singuliers de ce système $[(dx_i)/(d\xi) = (dy_i)/(d\xi) = 0; i = 1, \dots, N]$, on obtient une relation de compatibilité entre deux points singuliers successifs, k et $k + 1$

$$\frac{y_i^{\text{eq}}(k + 1) - y_i^{\text{eq}}(k)}{x_i(k + 1) - x_i(k)} = \Delta_{(k)}; i = 1, \dots, N$$

ainsi que la vitesse de la transition correspondante

$$\lambda_{(k)} = \frac{1 - \mu \Delta_{(k)}}{1 + \nu \Delta_{(k)}}$$

Ces relations sont les mêmes que celles que propose la théorie de l'équilibre, et, si on les assortit d'une condition de cohérence, relative aux vitesses des transitions,

$$\lambda(1) < \lambda(2) < \lambda(3) < \lambda(4) \dots$$

on peut tirer la conclusion suivante:

La solution asymptotique d'un système à plusieurs constituants, si elle existe, sera constituée d'une succession de transitions séparées par les mêmes paliers et se déplaçant à la même vitesse que ceux prédits par la théorie de l'équilibre.

La condition d'existence de cette solution ne pourra être obtenue que par l'étude de la stabilité du système d'équations différentielles obtenues. Nous avons effectué cette étude dans le cas d'un système à deux constituants indépendants en présence de dispersion axiale et nous avons toujours obtenu une solution asymptotique lorsque la théorie de l'équilibre prédit l'existence d'une transition stable. Nous avons, de plus, calculé la réponse d'une cascade de réacteurs agités à un échelon de composition engendrant deux transitions stables, et nous avons constaté que les deux solutions asymptotiques correspondantes représentaient rapidement la réponse de cette cascade (Fig. 2).

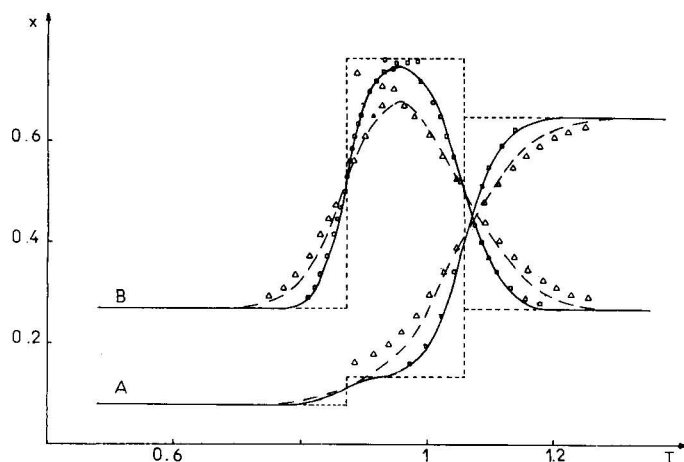


Fig. 2. Comparaison du régime transitoire d'une cascade de réacteurs agités à la solution asymptotique. $\alpha_A = 2.14$; $\alpha_B = 1.54$. ----, Théorie de l'équilibre. Régime transitoire: —, 100 réacteurs agités; ----, 50 réacteurs agités. Solution asymptotique: □, Péclet, 200; △, Péclet, 100.

Dans le cas général, nous pouvons de plus tirer deux conclusions qualitatives sur les performances relatives d'un lit fixe et d'un lit mobile: (1) La vitesse d'une transition est toujours plus faible en lit fixe qu'en lit mobile:

$$\lambda_{\text{lit mobile}} = \frac{1 - \mu \Delta_T}{1 + \nu \Delta_T} < \frac{1}{1 + \nu \Delta_T} = \lambda_{\text{lit fixe}}$$

(2) Dans les mêmes conditions d'alimentation, deux transitions successives sont plus distantes l'une de l'autre en lit mobile qu'en lit fixe:

$$\left(\frac{(z_1 - z_2)_{\text{lit mobile}}}{(z_1 - z_2)_{\text{lit fixe}}} \right)_T = 1 + \frac{\mu}{\nu} > 1$$

Une transition donnée est plus étalée en lit fixe qu'en lit mobile ainsi que l'a noté Amundson, pour une même valeur des paramètres caractérisant la dispersion axiale et le transfert de matière.

Par conséquent, si nous choisissons comme critère d'efficacité d'une colonne la longueur nécessaire à l'établissement d'un palier intermédiaire, nous pouvons conclure de l'étude de ce modèle que le lit mobile sera plus efficace que le lit fixe fonctionnant dans les mêmes conditions.

Nous nous proposons maintenant de vérifier s'il est réaliste de supposer que les effets dispersifs sont semblables en lit fixe et en lit mobile.

ÉTUDE DYNAMIQUE D'UN LIT MOBILE

Cet appareil (Fig. 3) est réalisé simplement par sédimentation des billes de résine à travers un orifice calibré. Le débit maximal de 5 cm^3 de solide peut être ajusté jusqu'à une valeur nulle à l'aide d'un contre-courant de solution à travers ce même orifice.

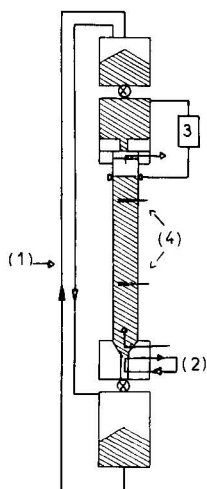


Fig. 3. Appareillage expérimental. (1) Recyclage de la résine; (2) régulation du débit de résine; (3) asservissement du niveau de résine; (4) sondes de conductivité.

Un détecteur photoélectrique permet d'ajuster en permanence le niveau supérieur du lit à une position constante.

Le débit de solution à contre-courant peut varier de 0 à 50 cm³/min. Cet appareil fonctionnant indifféremment en lit fixe ou en lit mobile, nous pourrions étudier *in situ* l'évolution de ses performances.

Dans la modélisation d'une opération de transfert de matière, trois types de résistances sont généralement mises en jeu, séparément ou simultanément: (1) La diffusion interne, qui n'est fonction que du diamètre des particules d'échangeur et du système ionique considéré: Elle ne sera donc pas affectée par le mode de mise en oeuvre de la résine. Nous avons évalué son importance par l'étude d'une réaction de neutralisation⁶ à forte concentration en réacteur agité fermé. (2) La dispersion axiale, qui est le paramètre le plus susceptible d'évoluer en cas de déplacement de la phase solide. Nous avons mesuré ce paramètre en lit fixe et en lit mobile par l'étude d'une injection d'un traceur adsorbable par la méthode des deux mesures. Nous avons constaté dans le domaine de débits étudiés que la dispersion axiale ne variait pas de façon notable, et, de plus, que la porosité du lit restait constante. (3) La diffusion externe: Sur un système échangeur d'ion, cette grandeur est difficile à atteindre indépendamment des autres résistances, et nous l'avons extrapolée à partir des paramètres optimisés d'un modèle de réaction irréversible⁷.

Ce modèle suppose, dans le cas d'une opération de percolation avec neutralisation que: (1) Le régime asymptotique est atteint. (2) La dispersion axiale intervient tout au long de l'échange. (3) À faible concentration, le transfert de matière est régi par la diffusion externe, $(\partial y)/(\partial t) = k_e C$. (4) Il est régi par la diffusion interne à forte concentration $(\partial y)/(\partial t) = k_i(y - 1)$.

L'extrapolation du paramètre de diffusion externe par optimisation de ce modèle sur des manipulations de neutralisation KOH/RH (Fig. 4) montre que dans les mêmes conditions hydrodynamiques, la résistance au transfert par diffusion externe est plus importante en lit mobile qu'en lit fixe. Cependant, la diminution de la vitesse

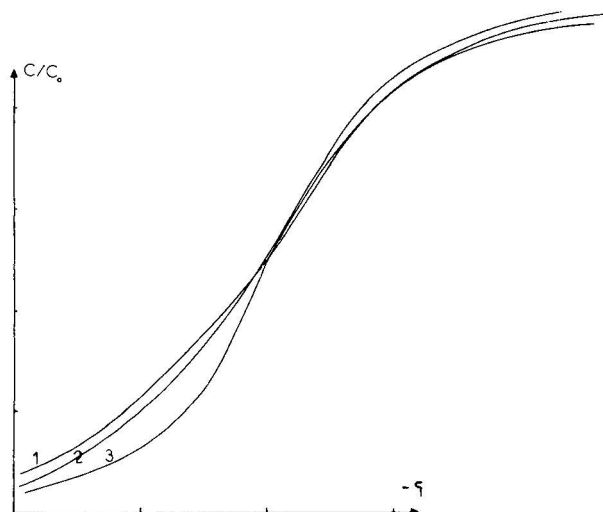


Fig. 4. Fronts de neutralisation KOH/H (résine) en lits fixe ($\mu = 0$) et mobile. (1) $\mu = 0$; (2) $\mu = 0.23$; (3) $\mu = 0.48$.

de propagation de la transition en lit mobile provoquant, ainsi que nous l'avons noté dans la section précédente, un effet opposé à celui de l'augmentation de la résistance au transfert par diffusion externe, nous avons constaté que la largeur de la zone d'échange était moins grande en lit mobile, donc que le régime lit mobile était plus "efficace" que le régime lit fixe.

CONCLUSION

On a montré que la théorie de la chromatographie non-linéaire en lit fixe, qui s'est considérablement développée récemment, permet de définir des modes de séparation continue et d'en calculer les caractéristiques essentielles (débits d'alimentation et de soutirage, rendement théorique de la séparation).

La présence d'effets dispersifs (cinétique de transfert) intervient pour le dimensionnement de l'appareil et la localisation des soutirages, et influe sur la pureté des produits. Mais pour des conditions de fonctionnement convenables, ces effets n'ont pas d'influence sur les débits prévus par le modèle d'équilibre.

RÉSUMÉ

On montre que la théorie de la chromatographie non-linéaire à plusieurs constituants peut être appliquée à la définition et au calcul d'opérations de séparation continues. Le rôle des facteurs dispersifs est analysé. On présente des résultats expérimentaux préliminaires comparant les performances en lit fixe et en lit mobile.

NOTATIONS

y_i = titre de l'espèce i en phase solide;

x_i = titre de l'espèce i en phase liquide;

Q = capacité totale de la phase solide par unité de volume;

C = concentration totale de la phase liquide;

v = vitesse de la phase solide;

u = vitesse de la phase liquide;

ε = porosité du garnissage;

$Pe = uL/D$ = critère de Péclet;

$v = \frac{Q(1 - \varepsilon)}{\varepsilon C}$;

$\mu = v\gamma/u$;

$\lambda_{(T)}$ = vitesse de déplacement de la transition;

$z = 1/L$ variable de position dans la colonne;

$\tau = ut/L$;

$T = (\tau - 1)v$;

L = longueur de la colonne.

BIBLIOGRAPHIE

- 1 D. Tondeur, *Thèse*, Nancy, 1969.
- 2 F. Helfferich et G. Klein, *Multicomponent Chromatography. Theory of Interference*, Marcel Dekker, New York, 1970.
- 3 N. R. Amundson, *Phil. Trans. Roy. Soc. London*, 269 (1971) 187.
- 4 E. Glueckauf, *J. Chem. Soc.*, (1949) 3280.
- 5 N. R. Amundson, *Chem. Eng. Sci.*, 28 (1973) 55.
- 6 F. Helfferich, *J. Phys. Chem.*, 69 (1965) 1178.
- 7 A. Rodrigues, *Thèse*, Nancy, 1973.
- 8 O. Levenspiel, *Chemical Reaction Engineering*, Wiley, New York, 1962.

CHROM. 7771

FONCTIONNEMENT CYCLIQUE D'UN LIT FIXE D'ÉCHANGE D'IONS AVEC TROIS CONSTITUANTS

G. GREVILLOT, D. TONDEUR et J. A. DODDS

Centre de Cinétique Physique et Chimique du C.N.R.S., Route de Vandoeuvre, 54600 Villers-les-Nancy (France)

SUMMARY

Cyclic operation of a fixed-bed ion-exchange column with three components

The cyclic operation of an ion-exchange or adsorption column, involving three components, is studied using the local equilibrium theory. The equilibrium relations are non-linear. The "regenerant" is the component of lesser affinity alone. The influences of the following factors on the periodic effluent history are investigated: equilibrium coefficients, saturant composition, extents of saturation and regeneration, length of column. A numerical example is presented.

INTRODUCTION

L'utilisation d'un lit fixe d'adsorption ou d'échange d'ions consiste toujours en pratique en une alternance de deux opérations: saturation et régénération. L'effluent de la colonne tend alors vers une distribution périodique des concentrations. L'objet de ce texte est l'étude des régimes cycliques de fonctionnement d'un tel lit.

Les cycles sont constitués de deux étapes à co-courant. On considère un système à trois ions échangeables (deux espèces indépendantes). Le régénérant (noté dans la suite ne contient qu'un seul ion, celui de plus faible affinité (l'ordre d'affinité est $1 > 2 > 3$). L'échange est gouverné par une loi d'équilibre non-linéaire du type facteur de séparation constant. Nous utilisons le modèle idéalisé de l'équilibre qui consiste à considérer la cinétique de transfert très rapide et l'absence de dispersion axiale. La théorie de ce modèle a été développée considérablement ces dernières années¹⁻⁵ pour des signaux relativement simples (échelons et créneaux en particulier). Nous nous appuyons donc sur ces théories pour l'étude du régime cyclique qui résulte d'une suite de créneaux.

RÉPONSE DE LA COLONNE À UN ÉCHELON UNIQUE

Le traitement mathématique, maintenant classique, de ce cas, conduit à plusieurs types de représentation des processus:

- (i) Le diagramme des caractéristiques dans le plan réel (z, t) (Fig. 1), chaque

caractéristique représentant la propagation d'une composition ou d'une discontinuité de concentration (choc) dans la colonne. Une section à $z = \text{cte}$ représente une "histoire" des concentrations à cette section et une coupe à $t = \text{cte}$ représente un profil de colonne à l'instant considéré.

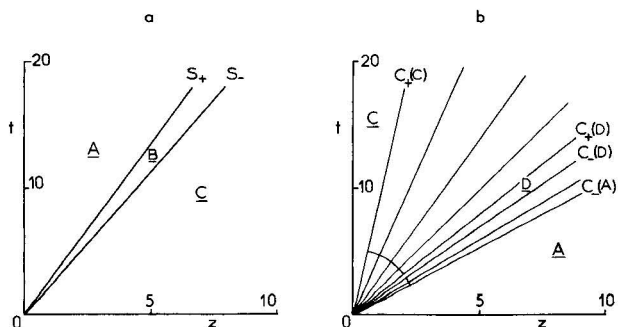


Fig. 1. Espace réel. (a) Échelon de A dans une colonne sous forme C (deux chocs). (b) Échelon de C dans une colonne sous forme A (deux transitions dispersives). \underline{B} = Zone de composition constante.

(ii) Le diagramme des caractéristiques dans le plan des concentrations (espace d'état) en phase mobile, x_1, x_2, x_3 que l'on représente dans un triangle équilatéral compte-tenu de la relation particulière à l'échange d'ions: $x_1 + x_2 + x_3 = 1$. Une histoire de l'effluent est représentée par un trajet dans ce diagramme, trajet qui suit en général les caractéristiques (Fig. 2). On montre qu'il existe deux familles de caractéristiques orientées Γ_+ et Γ_- . Un trajet porté par une caractéristique Γ_+ (resp. Γ_-) correspond dans l'espace réel à un choc S_- (resp. S_+) si le trajet est décrit dans le sens de Γ ou à une transition dispersive formée d'un faisceau de caractéristiques C_- (resp. C_+) si le trajet est décrit en sens inverse. Le trajet correspondant à la réponse à un échelon est constitué en général d'un segment de Γ_- et d'un segment de Γ_+ , celui-ci étant toujours en aval du premier.

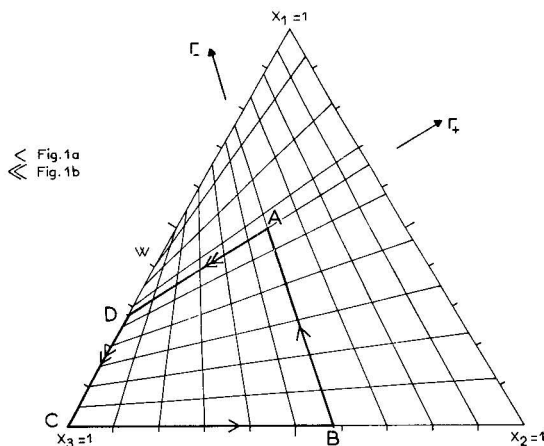


Fig. 2. Espace d'état (les flèches indiquent le sens du trajet dans l'histoire).

RÉPONSE À UN CRÉNEAU —INTERFÉRENCES

La réponse d'une colonne à un créneau de A de durée t_A (Fig. 3a) est déduite en partie de la réponse aux échelons de A et de C précédents. Les caractéristiques des deux échelons s'interceptent nécessairement ce qui indique des interactions, appelées interférences, entre les chocs et les transitions dispersives³⁻⁵. Les points d'intersection I sont définis sur la Fig. 3a. La transition dispersive C_- est transmise à travers le choc S_+ ; l'amplitude du choc, différence des compositions entre les bornes amont P et aval Q, varie et la caractéristique s'incurve (I_1 I_2).

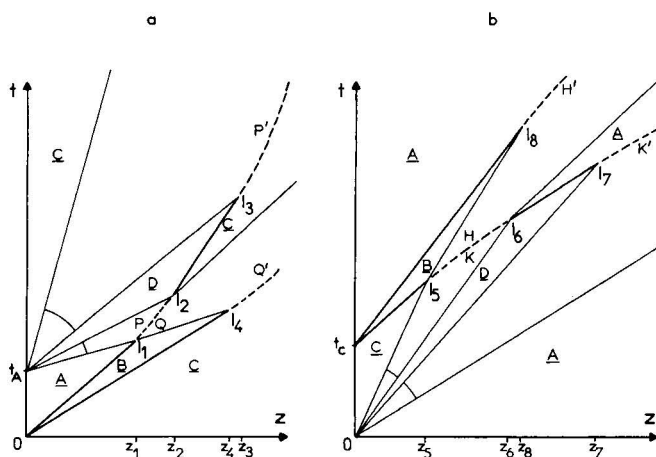


Fig. 3. Réponse d'une colonne à un créneau dans l'espace réel (schématique). (a) Créneau de A. (b) Créneau de C. — — —, Choc d'amplitude variable.

Dans l'espace d'état, l'histoire de l'effluent est représentée par le trajet $C \rightarrow B \rightarrow A \rightarrow D \rightarrow C$, si la longueur Z de la colonne est inférieure à z_1 . Si Z est compris entre z_1 et z_2 , le palier A n'existe plus et les paliers B et D sont reliés par le trajet $B \rightarrow Q \rightarrow P \rightarrow D$ (cf. Fig. 4).

À partir de I_2 , le choc retrouve une amplitude constante jusqu'au point I_3 où il rencontre la transition dispersive C_+ . Le choc et cette transition appartenant à la même caractéristique I_- , la transition dispersive est absorbée par le choc dont l'amplitude varie de nouveau par sa borne amont P' . Sa caractéristique s'incurve à partir de I_3 mais on montre qu'elle ne rattrape jamais $C_+(C)$. De manière semblable, le choc S_- absorbe indéfiniment la transition dispersive transmise C_- .

Considérons maintenant un créneau "inverse" du précédent, de composition C et de durée t_C (Fig. 3b). Il s'agit des mêmes chocs et des mêmes transitions qu'auparavant, mais maintenant les transitions sont en aval des chocs. La description des interférences ainsi que les correspondances entre espace d'état et espace réel établies ci-dessus sont intégralement et aisément transposables ici.

RÉGIME CYCLIQUE

La colonne est soumise à des variations cycliques de l'alimentation, un cycle étant constitué de la juxtaposition d'un créneau de A et d'un créneau de C.

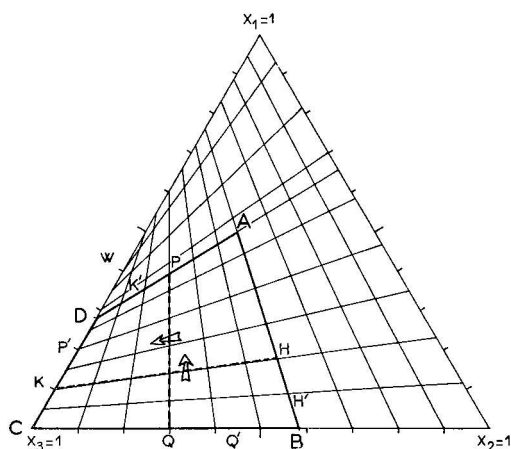


Fig. 4. Espace d'état correspondant à la Fig. 3.

Espace réel

Pour obtenir la configuration de l'espace réel en régime cyclique, amenons par translation les deux droites de choc S_+ et S_- de la Fig. 3a en coïncidence avec celles de la Fig. 3b. La configuration cyclique réelle ne peut pas être la simple superposition des deux diagrammes car il est physiquement impossible que chacun des deux chocs donne lieu simultanément et complètement aux deux types d'interférences correspondant aux deux types de créneau. Par exemple, si le point I_5 existe, le point I_4 n'existe pas; alors, si I_8 existe, I_1 n'existe pas et la caractéristique $C_-(A)$ (Fig. 3a) intercepte la ligne de choc issue de I_8 (Fig. 3b), et si I_1 existe, I_8 n'existe pas et les deux caractéristiques $C_-(B)$ et $C_+(B)$ se rejoignent (soit I_9 ce point d'intersection éventuel). Après I_9 , il y aurait une interférence entre les deux transitions dispersives transmises.

La configuration de l'espace réel en régime cyclique résulte donc de la compétition entre les différents points I_i et comporte d'autres interférences que celles décrites précédemment. Nous limiterons notre étude à la zone de l'espace réel où ne se produisent que les interférences illustrées par la Fig. 3 (en particulier les points I_4 et I_8 n'existent pas).

Combinaison des points I. L'étude topologique de l'espace réel de la Fig. 3 montre que les points suivants s'excluent mutuellement: I_1 et I_8 , I_5 et I_4 , I_2 et I_7 , I_3 et I_6 . On en déduit que dans la zone étudiée, les points I_1 , I_5 et I_9 existent toujours. La configuration cyclique est donc basée sur l'une des trois combinaisons de points I suivantes:

$$(I_1, I_5, I_9, I_2, I_3) \quad (C1)$$

$$(I_1, I_5, I_9, I_2, I_6) \quad (C2)$$

$$(I_1, I_5, I_9, I_6, I_7) \quad (C3)$$

Le choix de la combinaison s'effectue en comparant les abscisses des points

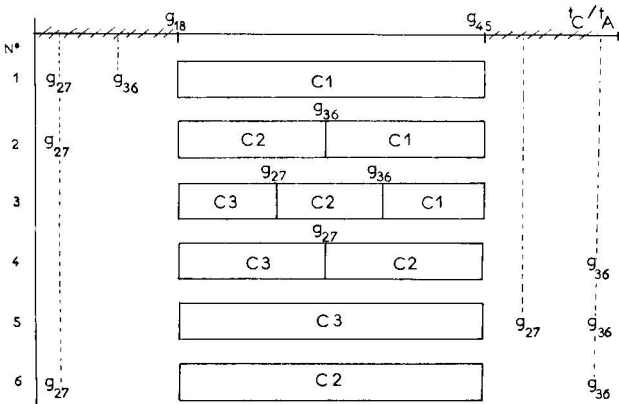
qui s'excluent mutuellement (le point à retenir est celui qui a l'abscisse la plus faible). On montre qu'il y a permutation de l'arrangement des points I_i et I_j pour :

$$\frac{t_c}{t_A} = g_{ij}(A)$$

où g est une fonction ne dépendant que de la composition du point A et des coefficients d'équilibre α_1 et α_2 . Ceci nous conduit à faire un classement des valeurs $g(A)$ sur une échelle t_c/t_A . On montre qu'il existe au maximum six types de classement définissant, dans la zone étudiée (qui correspond à l'intervalle $[g_{18}, g_{45}]$), la ou les combinaisons possibles (Tableau I).

TABLEAU I

COMBINAISONS POSSIBLES DANS LA ZONE ÉTUDIÉE SUIVANT LE CLASSEMENT DES g



Si α_1 et α_2 sont donnés, les g ne dépendent que de A ; on peut alors déterminer des domaines de composition de A dans le diagramme triangulaire correspondant à des types de classement (Fig. 5). Dans certaines conditions de coefficients d'équilibre α_1 et α_2 , certains types de classement peuvent ne pas exister, quelle que soit la composition de A .

Arrangements des points I. Plusieurs types de configuration de l'espace réel peuvent être obtenus pour chaque combinaison suivant l'arrangement des points I_i qui la constitue, en fonction de leur abscisse z_i (c'est ce classement qui est nécessaire si l'on s'intéresse à l'histoire de l'effluent, c'est-à-dire à la distribution des concentrations sur une droite $z = cte$). Le classement fait intervenir des quantités g_{ij} (où I_i et I_j sont deux points de la combinaison) que l'on peut placer sur l'axe t_c/t_A . Ces quantités définissent sur chaque segment de l'axe correspondant à une combinaison plusieurs sous-segments correspondants aux différents arrangements de la combinaison.

Si α_1 et α_2 sont donnés, un diagramme triangulaire du type de la Fig. 5 indique à quelles combinaisons on peut s'attendre ; la position de A indique la ou les combinaisons possibles. Alors le choix de t_c/t_A fixe l'arrangement des points I , c'est-à-dire la configuration cyclique de l'espace réel.

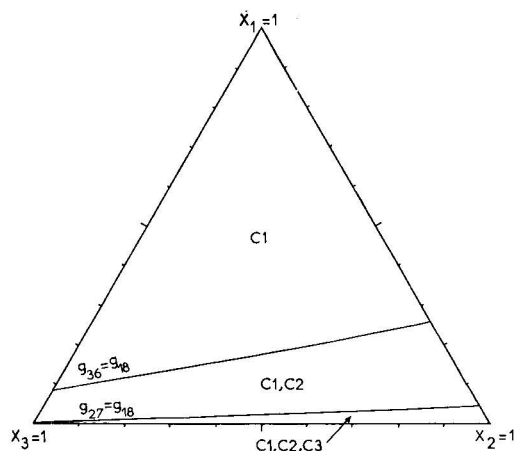


Fig. 5. Combinaisons possibles des points I pour $\alpha_1 = 8$ et $\alpha_2 = 2$.

Histoire de l'effluent

Pour une configuration donnée de l'espace réel, on peut obtenir différents types d'histoire suivant la longueur Z de la colonne. Par exemple, si Z est inférieur à tous les z_i , il ne se produit pas d'interférence dans la colonne et l'histoire est représentée dans l'espace d'état par le trajet $B \rightarrow A \rightarrow D \rightarrow C \rightarrow B$. Si Z devient supérieur à z_1 , le palier A disparaît et les paliers B et D sont alors reliés par le trajet $B \rightarrow Q \rightarrow P \rightarrow D$. On peut associer à chaque point I des modifications similaires du trajet suivi dans l'espace d'état, ce qui permet de déterminer très rapidement le trajet cyclique, pour une longueur Z donnée, par modifications successives en partant de $Z = 0$, sans qu'il soit nécessaire de tracer le diagramme (z, t) .

Dans l'espace d'état, le temps intervient comme paramètre variant sur le trajet cyclique. Il est souvent nécessaire de représenter l'histoire plus explicitement en portant les concentrations x en fonction de t . Pour les opérations cycliques, la représentation en coordonnées polaires (x = distance radiale; t = angle tel que $t_A + t_C = 2\pi$) est particulièrement concise. De plus, les quantités de matière y sont mesurées par des longueurs d'arcs ce qui peut être très pratique pour calculer des bilans de matière par exemple.

Exemple numérique

Avec les valeurs des coefficients d'équilibre $\alpha_1 = 8$ et $\alpha_2 = 2$, la Fig. 5 indique que pour A ($x_1 = 0.5$; $x_2 = 0.2$), la combinaison $C1$ existe seule sur l'intervalle $|g_{18}; g_{45}| = |4.15; 9.14|$. En choisissant $t_C = 67$ et $t_A = 12$, on obtient un rapport t_C/t_A qui appartient à l'intervalle. Sa valeur par rapport aux autres g_{ij} détermine l'arrangement des points I :

$$(I_1, I_5, I_2, I_9, I_3)$$

Si la longueur Z de la colonne est comprise entre z_5 et z_2 , on en déduit que l'histoire cyclique de l'effluent est représentée dans l'espace d'état par un trajet en boucle croisée du type (cf. Fig. 4):



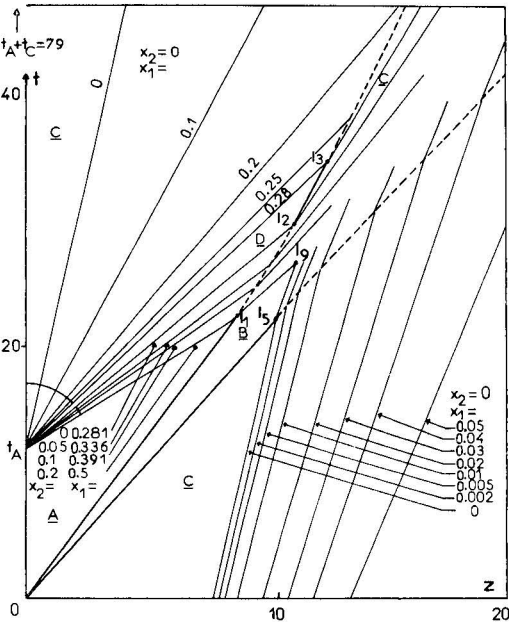


Fig. 6. Exemple de configuration cyclique de l'espace réel. $\alpha_1 = 8$; $\alpha_2 = 2$; $x_1(A) = 0.5$; $x_2(A) = 0.2$; $t_A = 12$; $t_C = 67$.

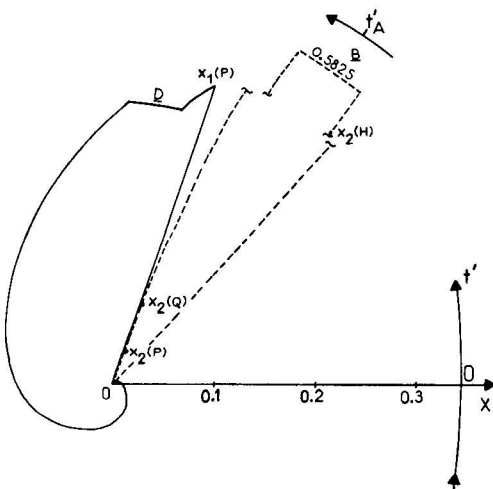


Fig. 7. Histoire cyclique de l'effluent en coordonnées polaires pour $Z = 10$ cm dans les conditions de la Fig. 6. —, x_1 ; ---, x_2 .

Ceci est illustré par les Fig. 6 et 7 qui représentent respectivement la configuration cyclique de l'espace réel et l'histoire cyclique de l'effluent pour $Z = 10$ cm.

CONCLUSION

On a appliqué la théorie de l'équilibre à une colonne d'échange d'ions en

fonctionnement cyclique. La méthode présentée permet de prévoir les influences respectives des coefficients d'équilibre, de la composition du saturant et du rapport des durées de saturation et de régénération sur la configuration cyclique de l'espace réel. On a étudié ensuite l'influence de la longueur de la colonne sur l'histoire de l'effluent. Cette méthode est encore restreinte à un intervalle de valeurs de t_c/t_A . Diverses extensions peuvent être envisagées: en particulier en dehors de l'intervalle (interférences multiples), pour du régénérant non-pur et dans le cas d'un changement éventuel des conditions d'équilibre entre les deux étapes du cycle.

L'importance des opérations cycliques d'échange d'ions ou d'adsorption justifie à notre avis de telles études.

NOTATIONS

- g_{ij} = fonction adimensionnelle = $(z_i/z_j)/t_c/t_A$;
 t = temps, sec;
 t' = temps normalisé par la durée du cycle (ad.);
 t_A = durée du créneau de composition A, sec;
 t_C = durée du créneau de composition C, sec;
 x_i = fraction équivalente de l'ion i dans la phase mobile (ad.);
 y_i = fraction équivalente de l'ion i dans la phase fixe (ad.);
 z = abscisse depuis l'entrée du lit, cm;
 z_i = abscisse du point I_i , cm (voir bibl. 4, p. 384);
 α_1, α_2 = facteurs de séparation: $\alpha_1 = (y_1/x_1)/(y_3/x_3)$ et $\alpha_2 = (y_2/x_2)/(y_3/x_3)$.

RÉSUMÉ

On étudie le fonctionnement cyclique d'une colonne d'échange d'ions ou d'adsorption, dans le cas d'un système à trois constituants, en s'appuyant sur la théorie de l'équilibre. Les relations d'équilibre sont non-linéaires. Le régénérant du cycle est le constituant de plus faible affinité, pur. On montre les influences respectives des coefficients d'équilibre, de la composition du saturant, des durées de régénération et de saturation et de la longueur de la colonne sur l'histoire périodique de l'effluent. Un exemple numérique est présenté.

BIBLIOGRAPHIE

- 1 D. Tondeur, *J. Chim. Phys.*, 68 (1971) 311.
- 2 D. Tondeur, *Chim. Ind. Génie Chim.*, 100 (1968) 1058.
- 3 R. Aris et N. R. Amundson, *Mathematical Methods in Chemical Engineering*, Vol. 2, Prentice Hall, Englewood Cliffs, N.J., 1973.
- 4 F. Helfferich et G. Klein, *Multicomponent Chromatography: Theory of Interference*, Marcel Dekker, New York, 1970.
- 5 H. K. Rhee, R. Aris et N. R. Amundson, *Phil. Trans. Roy. Soc. London, Ser. A*, 267 (1970) 419.

CHROM. 7740

ELUTION OF URANIUM FROM AN ANION-EXCHANGE RESIN BY EXTRACTION WITH AN ORGANIC EXTRACTANT IN THE PRESENCE OF AN AQUEOUS PHASE

M. ERDÉLYI and B. CZEGLÉDI

Mecseki Ércbányászati Vállalat (Mecsek Ore Mining Enterprise), Pécs (Hungary)

and

M. VIGVÁRI

Fémipari Kutató Intézet (Research Institute for Non-Ferrous Metals), Budapest (Hungary)

SUMMARY

The elution of uranium from anion-exchange resins by dilute sulphuric acid has many advantages, but as a consequence of unfavourable distribution values it has limited value. However, if the sulphuric acid phase serves only as a medium phase, and elution is carried out by organic extraction, the advantages of both elution and extraction are combined, while the undesirable factors can be eliminated.

The concentration of uranium from leach liquor or pulp by using an anion-exchange resin is a well known process. Uranium is extracted from the solution obtained by elution of the saturated resin with an organic solvent. The overall recovery is improved by the combination of these two processes.

Elution of uranium from an anion-exchange resin can be carried out with dilute hydrochloric, nitric or sulphuric acid. The eluting qualities of hydrochloric and nitric acids are satisfactory, while the application of sulphuric acid, which is desirable in many respects, has certain disadvantages.

Of the elution and extraction processes the former takes more time in the first place because of the slow diffusion. Fig. 1 shows the isotherm of elution by dilute sulphuric acid and it can be seen that the unfavourable conditions of equilibrium also contribute to the long time required for elution. The distribution ratio of uranium between the resin and the aqueous phase is about 10 when dilute sulphuric acid is used as the eluent. Hence the elution should be carried out with a large volume of solution or the number of theoretical plates should be increased, although even at an infinite number of plates the uranium concentration in the eluate is limited by the convex character of the isotherm.

One of the techniques for solving the problem is the so-called Eluex method, which makes the application of a large volume of eluting solution possible.

Another method is to perform the elution directly with an organic solvent (for example, di-2-ethylhexylphosphoric acid) in the presence of the aqueous phase which

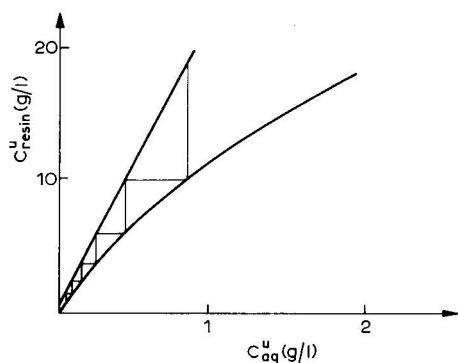


Fig. 1. Isotherm of uranium in the system resin-dilute sulphuric acid.

mediates in the mass transfer. In this case, the distribution ratio of uranium between the resin phase and the organic solvent is given by the proportion of those of elution and extraction:

$$D_m = \frac{C_{\text{resin}}^{\text{U}}}{C_{\text{org}}^{\text{U}}} = \frac{D_{\text{elution}}}{D_{\text{ext}}}$$

The line of the isotherm of uranium distribution between the resin and organic solvent differs from that between the resin and aqueous phase, as shown in Fig. 2, being concave on the side of the work-line of elution; this is highly favourable for the required number of theoretical plates. Its concave character permits the efficient utilization of the uranium capacity of the organic phase, and thus the number of plates can be significantly reduced by carrying out elution in countercurrent reactors, as shown by the scheme in Fig. 3.

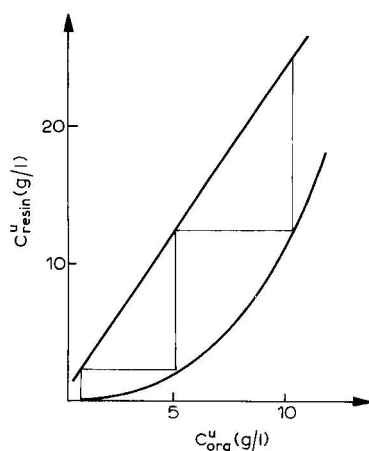


Fig. 2. Isotherm of uranium in the system resin-organic solvent.

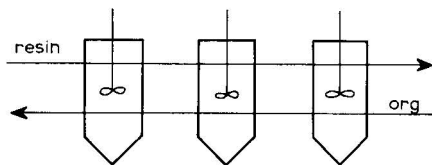


Fig. 3. Three-phase elution in a line of reactors.

The purpose of the aqueous phase, as the mediating phase, is to restrain the organic solvent from being absorbed into the resin by hindering the direct connection between the resin and organic phases. This is important in order to decrease both the loss of solvent and the corrosion of the resin.

This technique of elution can also be carried out in a pulsing column.

CHROM. 7739

COUNTERCURRENT ELUTION OF URANIUM(VI) AND IRON(III) FROM AN ANION-EXCHANGE RESIN

M. VIGVÁRI

Fémipari Kutató Intézet (Research Institute for Non-Ferrous Metals), Budapest (Hungary)

and

M. ERDÉLYI and B. CZEGLÉDI

Mecseki Ércbányászati Vállalat (Mecsek Ore Mining Enterprise), Pécs (Hungary)

SUMMARY

A countercurrent elution method for the separation of uranium and iron has been developed. The separation is based on changing the solution composition along the anion-exchange column and on the difference in the stability constants¹ and the ion-exchange distribution coefficients of the sulphate complexes of uranium and iron.

The sulphate complexes of iron(III) are adsorbed on a strongly basic anion-exchange resin together with uranium(VI) complexes from the leach solution obtained in uranium ore processing². By countercurrent elution of the saturated resin, all of the iron passes into the effluent. This impurity results in many difficulties during further treatment of the effluent. An elution process has been developed for the separation of uranium from the iron, using an acidic sodium chloride solution as the eluent.

The countercurrent elution process is performed in a vertical tower in which the saturated resin feed enters at the top and the eluent feed enters at the bottom of the column³. The maximum concentration of the sulphate ions is at the inlet of the resin feed and the maximum concentration of the chloride ions is at the inlet of the eluent. Between these two feed points, the sulphate:chloride concentration ratio varies continuously along the column (Fig. 1).

The countercurrent elution of the sulphate complexes of uranium and iron is based on the exchange process between SO_4^{2-} , HSO_4^- and Cl^- ions. The formation of the complexes and their distribution coefficients between the resin and solution phases are determined at every position in the column by the actual concentration of the SO_4^{2-} , HSO_4^- and H^+ ions. The selectivity of these ions is as follows: $\text{Cl}^- > [\text{UO}_2(\text{SO}_4)_2]^{2-} > [\text{UO}_2(\text{SO}_4)_3]^{4-} > \text{HSO}_4^- > [\text{Fe}(\text{SO}_4)_2]^- > \text{SO}_4^{2-}$.

Considering that the exchange of the SO_4^{2-} , HSO_4^- and Cl^- ions is the basic process, the distribution coefficients of the uranium and iron were measured at different concentrations of sulphate and chloride ions. The total salt concentrations of the solutions were 1 mole/l and the sulphate:chloride ratio was varied. The determinations were performed at different concentrations of uranium, iron and hydrogen ions.

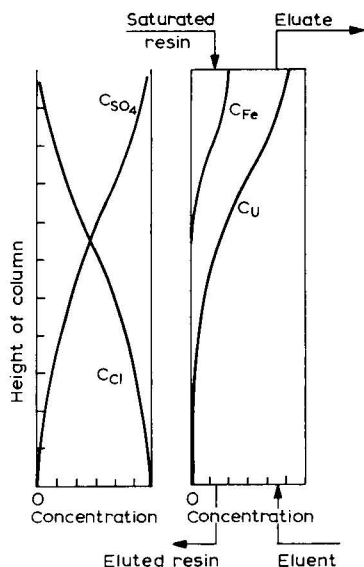


Fig. 1. Countercurrent column and concentration profile along the column.

A typical example is illustrated in Fig. 2. The value of the distribution coefficients (D_U , D_{Fe}) is plotted as a function of solution composition. It can be seen that the sorption of iron decreases rapidly with increasing chloride concentration. At a chloride concentration of 0.15 mole/l, the distribution coefficient of iron becomes less than unity. Alterations in the chloride concentration have only a slight effect on the distribution of uranium if the chloride concentration is less than 0.8 mole/l. The decrease in the distribution coefficient of uranium becomes significant only at the higher Cl^- concentrations. According to the analysis of the resin phase, the $[UO_2(SO_4)_2]^{2-}$ complex is mainly adsorbed. The sulphate:uranium ratio varies between 2 and 2.5.

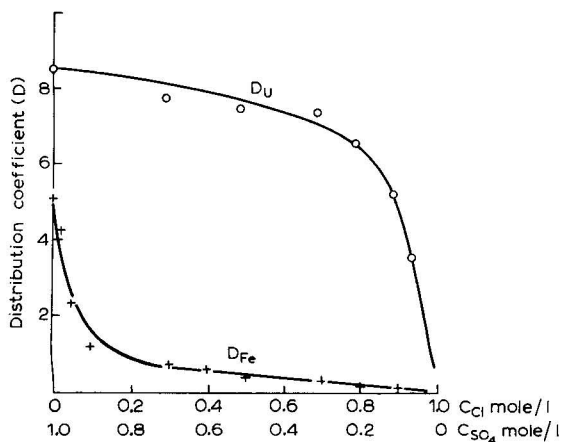


Fig. 2. Effect of the composition of the solution on the distribution coefficients of uranium and iron. \circ , D_U ($C_U = 0.03$ mole/l); +, D_{Fe} ($C_{Fe} = 0.03$ mole/l).

At low chloride and high sulphate concentrations, the value of D_U does not depend on the iron concentration in the solution. On the other hand, the distribution coefficient of uranium depends strongly on the uranium concentration in these solutions ($D_U = 10-100$). At high chloride and low sulphate concentrations, the distribution coefficient of uranium is nearly independent of the uranium concentration in the solution.

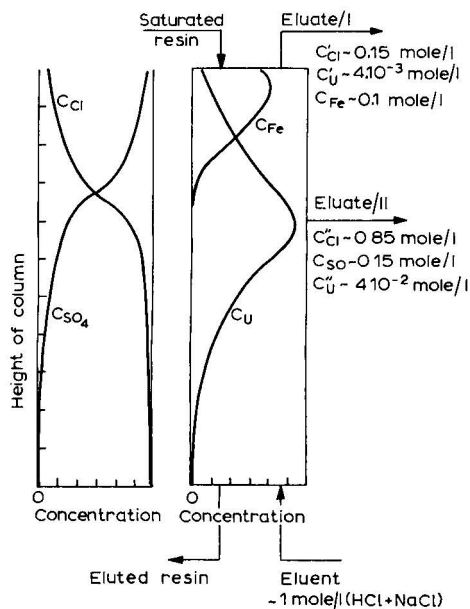


Fig. 3. Fractional column and the concentration profile along the column.

Consequently, if there are two outlets for the effluent on the countercurrent ion-exchange column, the concentration of sulphate and chloride ions can be regulated along the column by changing the flow ratio of the two effluent fractions, so that the chromatographic separation of iron from uranium should be possible. The scheme of this column and the concentration profile in the resin bed are shown in Fig. 3. The chloride and uranium concentrations are low in the "eluate 1" solution. On the other hand, the sulphate concentration is low and the chloride and uranium concentrations are high in the "eluate II" fraction. The eluate:resin flow volume ratio is equal to the distribution coefficient of uranium in the range of chloride concentrations in "eluate II":

$$\frac{\text{eluent flow volume}}{\text{resin flow volume}} = \frac{L}{G} = D_U''$$

The flow volume ratio of "eluate I" to resin flow volume is equal to the distribution coefficient of iron at $C_{Cl} = 0.1$ mole/l.

$$\frac{\text{"eluate I" flow volume}}{\text{resin flow volume}} = \frac{L'}{G} = D_{Fe}'$$

The chloride concentration in the eluent (C_{Cl}^0) should be calculated by the following equation:

$$C_{Cl}^0 = \frac{GQ_{eq} + L' C'_{Cl} + L'' C''_{Cl} \text{ mole/l}}{L}$$

where Q_{eq} = equivalent capacity of the resin. The elution process should be regulated by changing the flow ratio of the eluent and "eluate II" at constant eluent:resin ratio.

The process has been used successfully in a pilot plant.

REFERENCES

- 1 L. G. Sillen and A. E. Martell, *Stability Constants of Metal-Ion Complexes*, Chemical Society, London, 1964.
- 2 J. W. Clegg and D. D. Foley, *Uranium Ore Processing*, Addison Westley Publ. Co., Reading, Mass., 1958.
- 3 B. N. Laskorin, *At. Energ.*, 9 (1960) 286.

CHROM. 7866

ION EXCHANGE IN AGITATED BEDS

SIMULATION OF AN ION-EXCHANGE COLUMN BY A MODEL OF AGITATED TANKS IN CASCADE

A. E. RODRIGUES

Department of Chemical Engineering, University of Luanda, Luanda (Angola)

SUMMARY

Ion exchange in a stirred reactor is considered in terms of the influence of the non-linearity of the equilibrium isotherm on the outlet concentration. This study is supported by experimental results for the Cl^- - OH^- exchange accompanied by neutralization.

An iteration method is presented for calculation of the state of the column in the cyclic mode. For this, the column is simulated by a "tanks-in-series model" and two concepts are considered: (1) width of the mass transfer and (2) saturation factor and regeneration factor.

INTRODUCTION

For calculations on ion-exchange columns, it is important to know the breakthrough curves. The prediction of such curves (histories of concentration) is an important step in the calculation. The earliest model is the "theoretical plate model" of Martin and Synge¹, developed in 1941, but this model fails in the prediction of zone dispersion as a function of the different variables (flow-rate, particle size, etc.). Furthermore, the equilibrium isotherm is linear in the Martin and Synge work.

The "tanks-in-series model", used in chemical reactor theory², is equivalent to the plate model. The utilization of the tanks-in-series model is advantageous because the separation of the contribution of the zone spreading from the axial dispersion, film diffusion, etc., is possible.

In the case of ion-exchange operation, the most important parameter is the useful capacity of the column in the cyclic mode, because the saturation and regeneration steps are not completed. In this situation the Martin and Synge approach is not suitable. In our work, we assume that the equilibrium isotherm is, in general, non-linear.

In the first part of this paper we discuss the elementary cell of the model, the stirred reactor, particularly for the case of ion exchange accompanied by neutralization. In the second part, an iteration method is presented for the calculation of any state of the column, such as the cyclic mode of operation. The major assumption is the instantaneous establishment of equilibrium at the solid-liquid interface. This means that the axial dispersion, measured by N (number of cells), is the controlling mechanism of the operation ($N = \text{Peclet number}/2$).

THEORETICAL STUDY OF ION EXCHANGE IN AN AGITATED BED

We consider a stirred reactor that contains two phases: the solid phase (resin) and the liquid phase (solution). The material balance can be written in the form

$$Uc_0 = Uc_1 + V_S \cdot \frac{dc_1}{dt} + V_R \cdot \frac{dq}{dt} \quad (1)$$

We assume that the equilibrium isotherm is of the "law of mass action" type, $q = f(c)$, with

$$K = \frac{q(c_0 - c_1)}{(Q - q)c_1} \quad (2)$$

By introducing the dimensionless variables

$$\tau = \frac{V_S}{U}$$

$$\frac{1 - \varepsilon}{\varepsilon} = \frac{V_R}{V_S}$$

$$F = \frac{c_1}{c_0}$$

and

$$\theta^* = \frac{t}{t_{ST}}$$

the system of eqns. 1 and 2 can be reduced to the equation

$$\frac{dF}{d\theta^*} = \frac{1 - F}{g(F)} \quad (3)$$

An analysis of the influence of different factors (ε , c_0 and K) is possible after integration (numerical or analytical)³ of eqn. 3.

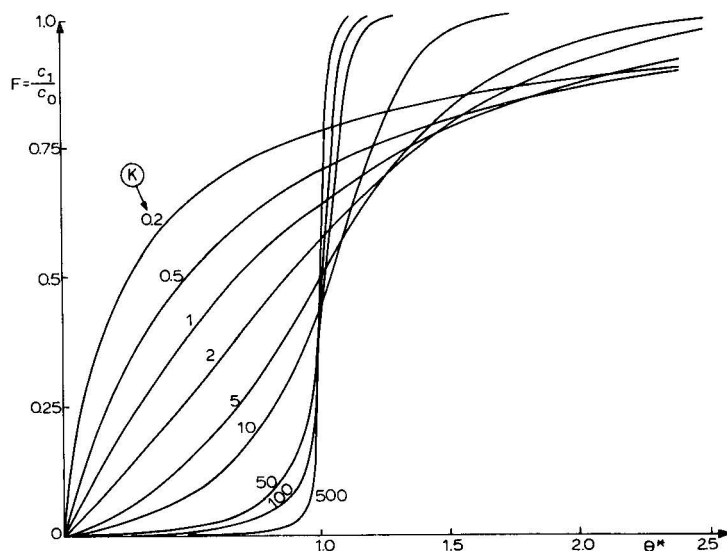


Fig. 1. Influence of K on the response of a stirred reactor, $\varepsilon = 0.4$; $Q = 1.4 N$; $c_0 = 0.05 N$.

Fig. 1 shows the calculated results for a stirred reactor; the response of the system to a step change in the concentration at the entry is mainly dependent on K (K characterizes the non-linearity of the isotherm).

EXPERIMENTAL RESULTS FOR ANION EXCHANGE IN A STIRRED REACTOR

We have used the anionic resin Duolite a102 D produced by Diaprosim (Chauny, France) in the ROH^- form. The solution passed through the reactor was HCl ; the exchange between Cl^- and OH^- ions is accompanied by neutralization and the equilibrium becomes irreversible.

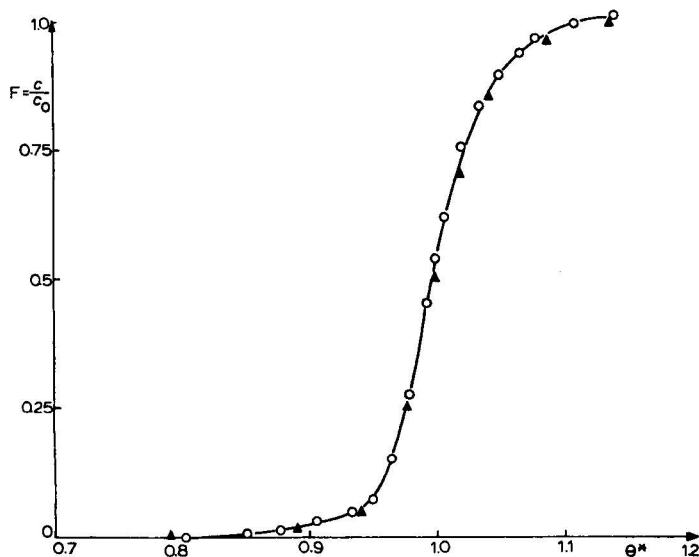


Fig. 2. Calculated (\blacktriangle) and experimental (\bigcirc) results. $V_{\text{reactor}} = 79$ ml; $V_R = 21$ ml; $c_0 = 0.01$ N; flow-rate = 13.44 ml/min.; $t_{ST} = 205.4$ min.

Fig. 2 represents experimental and calculated (for $K = 500$) results for different conditions. Apparently the hypothesis of instantaneous equilibrium is valid under the conditions of the present work.

SIMULATION OF AN ION-EXCHANGE COLUMN BY THE TANKS-IN-SERIES MODEL

We assume that the column is divided into a series of reactors; for reactor i , we can write

$$\frac{dF_i}{d\theta^*} = \frac{F_{i-1} - F_i}{f(F_i)} \quad (4)$$

Some numerical results of the integration of eqn. 4 by the fourth order Runge-Kutta method (the boundary conditions are: (1) at any time $c = c_0$ at the entry of the column and (2) at $t = 0$ the concentrations c and q are zero in the column) are shown in Figs. 3 and 4 (dispersive and stable fronts).

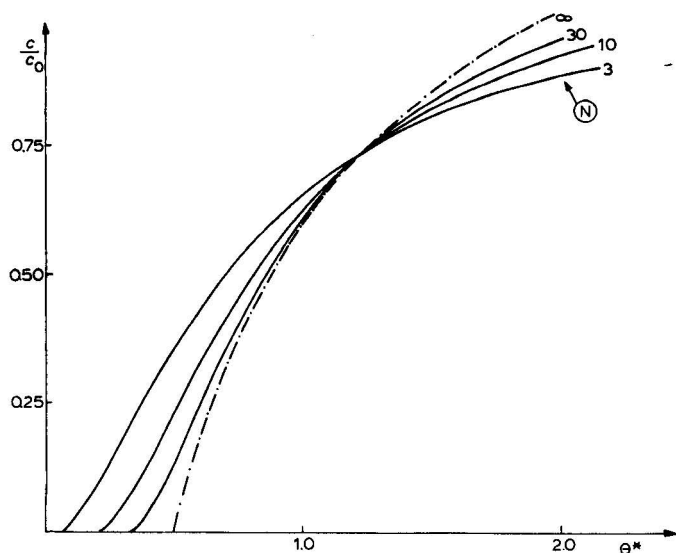


Fig. 3. Influence of N on the response of an anion-exchange column (tanks-in-series model) for $K = 0.5$, $c_0 = 0.05 N$; $Q = 1.4 N$; $\varepsilon = 0.4 N$. Broken line: equilibrium theory in absence of axial dispersion; $c/c_0 = (\sqrt{(r/T)} - r)/(1 - r)$.

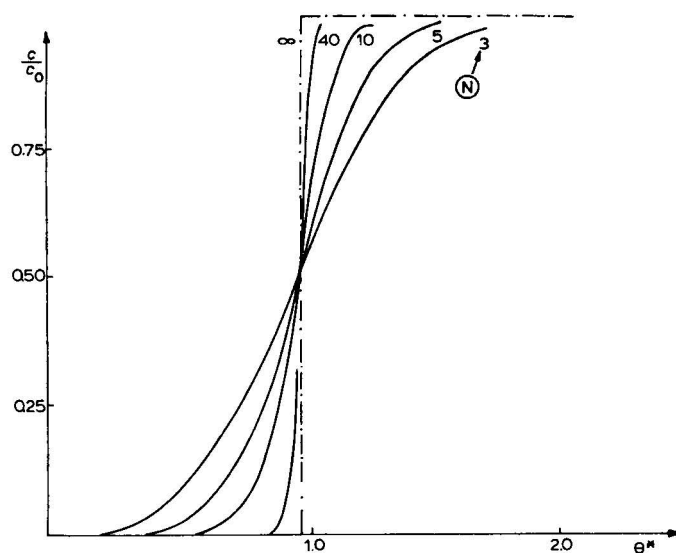


Fig. 4. Influence of N on the response of an anion-exchange column (tanks-in-series model) for $K = 2$, $c_0 = 0.05 N$; $Q = 1.4 N$; $\varepsilon = 0.4 N$. Broken line: equilibrium theory in absence of axial dispersion; $c/c_0 = H(\theta^* - 1)$, where H = Heaviside function.

For a breakthrough curve, we can define the "width of the mass transfer zone", Z_E (ref. 4), by

$$Z_E = L (\theta_S^* - \theta_E^*) \quad (5)$$

and obtain a relationship, for each K , between N and Z_E/L :

$$N = a \left(\frac{Z_E}{L} \right)^b \quad (6)$$

Now, for each step (saturation (S) or regeneration (R) of the column) we can calculate the saturation factor, F_S , and the regeneration factor, F_R , (ref. 5), respectively, defined by

$$F_{S \text{ (or } R)} = \int_0^{\theta^*} (1 - F_{1S \text{ (or } R)}) d\theta^*$$

and plot the curves $F_S = \varphi_1(\theta^*)$ and $F_R = \varphi_2(\theta^*)$. We assume that the shape of the saturation (or regeneration) front is independent of the regeneration (or saturation) level.

Next we can calculate the state of the column. We start with a completely regenerated column ($F_R = 0$, $F_S = 1$, in each "state" $F_{Ri} + F_{Si} = 1$); after partial saturation of the column we know the "available capacity of the resin", Q_0 (so t_{ST}^0) and by means of eqns. 5 and 6 we obtain N_0 . From the plot $F_S = \varphi_1(\theta^*)$ we obtain F_{S1} . The iteration method is presented in Table I.

TABLE I
ITERATION METHOD OF CALCULATION

State of the column	Parameters $F_R \quad F_S$	Steps of calculation
Initial		
At the end of saturation 1		$t_{ST_0} = \tau \frac{Q_0}{\varepsilon c_0} \rightarrow \left(\frac{Z_E}{L} \right)_0 \rightarrow N_0 \rightarrow F_{S1}$
At the end of regeneration 2		$t_{ST_1} = \tau \frac{Q_1}{\varepsilon c_0} \rightarrow \left(\frac{Z_E}{L} \right)_1 \rightarrow N_1 \rightarrow F_{R2}$
At the end of saturation 3		$t_{ST_2} = \tau \frac{Q_2}{\varepsilon c_0} \rightarrow \left(\frac{Z_E}{L} \right)_2 \rightarrow N_2 \rightarrow F_{S2}$

CONCLUSIONS

The ion-exchange operation in stirred reactors is of interest when the solid-liquid isotherm is favourable. In such a situation the performance is similar to that of a fixed bed, leading to a simpler design. The simulation technique of an ion-exchange column by the "tanks-in-series model" is the basis of the iterative calculation of a column "state"; for this purpose, it is necessary to determine the experimental saturation (and regeneration) fronts in a completely regenerated (or saturated) column.

SYMBOLS

c_0, c_1 solution concentrations at the entry and the exit of the reactor (mequiv./ml)
 L column length (cm)

q	concentration in the resin (mequiv./ml).
Q	capacity of the resin (mequiv./ml).
t_{ST}	stoichiometric time (sec); $t_{ST} = [\varepsilon c_0 + (1 - \varepsilon)Q]\tau/\varepsilon c_0$.
U	flow-rate of solution (ml/sec).
V_R, V_S	volumes occupied by the solid and liquid phases, respectively (ml).
$\theta_{S(or E)}^*$	stoichiometric time at $c = 0.95c_0$ (or $c = 0.05c_0$).

REFERENCES

- 1 A. J. P. Martin and R. L. M. Synge, *Biochem. J.*, 35 (1941) 1358.
- 2 J. Villiermaux, *Chem. Eng. Sci.*, 27 (1972) 1231.
- 3 A. Rodrigues, *Thèse Docteur-Ingénieur*, University of Nancy, Nancy, 1973.
- 4 J. Dodds and D. Tondeur, *Chem. Eng. Sci.*, 27 (1972) 1267.
- 5 A. Michaels, *Ind. Eng. Chem.*, 44 (1952) 1922.

CHROM. 7705

THE AKZO PROCESS FOR THE REMOVAL OF MERCURY FROM WASTE WATER*

G. J. DE JONG and C. J. N. REKERS

Akzo Zout Chemie Nederland B.V., P.O. Box 25, Hengelo (The Netherlands)

SUMMARY

Akzo Zout Chemie has developed a process for the removal of mercury from waste water, primarily in order to have a definite solution to the waste water problems of its own chlor-alkali plants. The Akzo process guarantees a very low concentration of mercury in the effluent even under strongly fluctuating conditions. The secondary pollution problems generated are extremely small compared with those in other processes. The mercury is efficiently recycled into the process. The process is competitive with other processes for the removal of mercury from waste water.

INTRODUCTION

The poisonous character of organic mercury compounds has been known for a long time. Organic mercurials have been used as fungicides, *e.g.*, for seed-dressing, and acute poisoning by organic mercurials occurred when contaminated corn seed was consumed.

Originally, inorganic mercury compounds were considered to be relatively harmless; calomel was once used as a laxative! This opinion changed when it was found that living organisms could transfer inorganic mercury into organically bound mercury, which penetrated the food chain algae → fish → man. The first case of poisoning of man by mercury from waste, due to the accumulation of mercurials in the food chain, was observed in Japan (Minimata disease).

This knowledge, when presented to industry, resulted immediately in greater efforts to decrease mercury losses to the environment. One of the main consumers of mercury is the chlor-alkali industry. Most of the mercury used in this industry ends up in waste streams, which are relatively well defined. Since 1970, the authorities have put strong pressure upon this branch of industry to reduce mercury losses. At that time, in most chlor-alkali plants, processes to reduce mercury losses, based on the favourable economics of the recovery of the expensive metal mercury, were already in operation, but further reduction of these losses required the introduction of a series of additional techniques.

* Also presented at the First International Mercury Congress, Barcelona, May 1974.

The protection of the environment against pollution is the main objective of these new techniques, and the value of regenerated mercury is no longer of importance with respect to the operational costs involved. For the evaluation of mercury pollution abatement processes, the following factors are considered to be important:

- (a) the residual mercury concentration in the treated effluent;
- (b) the secondary pollution problems generated by the processes under consideration;
- (c) possibilities for recycling the recovered mercury;
- (d) the relative cost of the various processes.

When trying to solve pollution problems in which pollutants of a persistent nature are involved, special attention should be paid to avoiding the concentration of a pollutant in a solution or solid that cannot be recycled.

SELECTION OF A PROCESS

Recognizing the fact that any method for solving a pollution problem generates a secondary problem, the following basic criteria for the selection of a suitable process for the removal of mercury from chlor-alkali waste water have been used at Akzo Zout Chemie:

- (a) secondary pollution problems should be minimal;
- (b) mercury should be recycled;
- (c) the residual mercury concentration in the treated effluent should be low enough to meet the most stringent regulations expected;
- (d) this residual mercury concentration should not be influenced by variations in the composition of the waste water, for chlor-alkali waste water concerns in particular the sodium chloride concentration.

Three basic possibilities for the removal of mercury from chlor-alkali plant waste water have been considered, *viz.*, precipitation as metallic mercury, precipitation as mercury(II) sulphide and ion exchange. Both of the precipitation processes have been discounted, mainly because of their secondary pollution problems. Fig. 1 shows the mercury flow in a precipitation process compared with that of an ion-exchange process.

In the precipitation process, mercury in the waste water is transferred to solid waste and, for the recovery of the mercury, this solid waste has to be treated. Dry distillation is commonly used for this purpose. During dry distillation, most of the mercury is transferred to the gas phase and a solid waste is obtained. The mercury-bearing gas is cooled, and both mercury and water vapour condense. The mercury phase and the water phase are separated, and the water is recycled to the start of the waste water process. The gas is still rich in mercury and is treated separately, *e.g.*, by iodised activated carbon. This carbon is then recycled to the solid waste treatment.

In an ion-exchange process, the mercury from the waste water is removed by an ion-exchange resin and, at the end of the cycle, the resin is regenerated and the regeneration liquid containing the mercury is returned to the process. The resin is re-used. A small amount of solids originally present in the waste water stream remains as solid waste, together with some spent resin. An ion-exchange process potentially meets the first two selection criteria (low secondary pollution and recycling of the mercury) better than the precipitation processes.

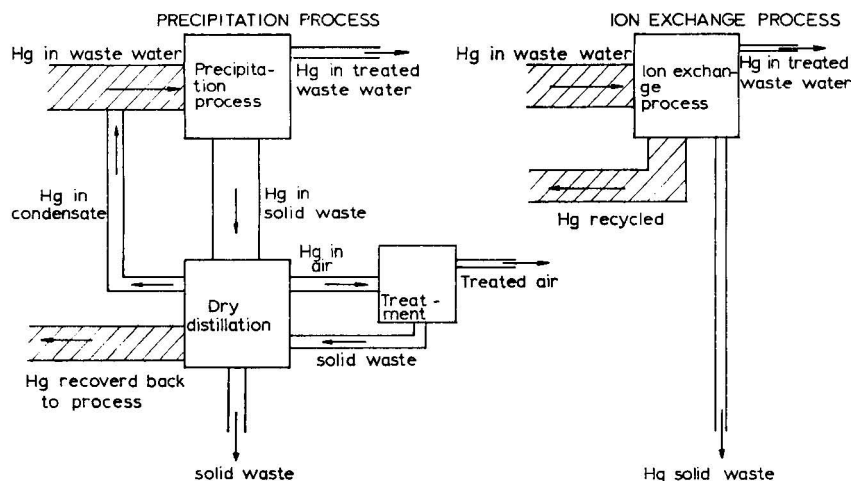


Fig. 1. Comparison of secondary problems in mercury-removing processes.

In 1970, anion-exchange resins capable of absorbing chloride-complexed mercury were available. The performance of these materials, however, was characterised by a restricted polishing power, generally resulting in a mercury level in the effluent higher than 100 ppb^{*}, and by a low sorption capacity, due to an unfavourable sorption isotherm in the areas of low mercury and high chloride concentration. These circumstances induced Akzo to start a screening programme with more specific mercury-sorbing resins. The material selected should have a strong polishing power in order to reduce mercury in the treated effluent down to a few parts per billion, and the performance should not be seriously influenced by fluctuations in pH, temperature and the concentrations of SO_4^{2-} and ClO_3^- ions.

In order to avoid secondary waste problems, it should nevertheless be possible to regenerate the resin with a liquid that can be re-introduced into the electrolysis process. The resin should be very specific for mercury, in order to avoid introduction of impurities, which are potentially detrimental to the electrolysis process, when recycling the regenerating solution with the mercury.

Nitrogen compounds can be very dangerous in the chlor-alkali industry, as they can form the highly explosive nitrogen trichloride. Therefore, the resin should not contain nitrogen in its molecule, in order to avoid all risks of contamination.

From these screening tests, which included the study of new commercial mercury-specific resins, a new resin, originating from our own synthetic work, evolved as the best material. It was decided to develop this material in close cooperation with Akzo's sorbent-producing group Imacti^{**} under the name Imac TMR.

IMAC TMR

Chemistry

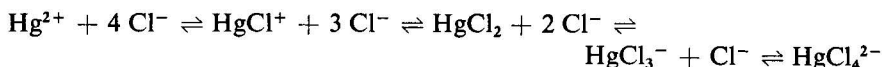
From the literature, it is known that the mercury-sulphur bond in HgS is very

^{*} Throughout this article the American billion (10^9) is used.

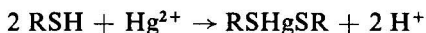
^{**} P.O. Box 4038, Amsterdam, The Netherlands.

strong and that the solubility product of this compound is extremely low. Organic compounds that contain $-SH$ groups are named mercaptans (derived from the Latin *mercurium captans*, seizing mercury). The Imac TMR resin developed by Akzo is a polymeric mercaptan in which thiol groups are attached to a chemically and mechanically highly inert matrix. The affinity of this thiol resin ($R-SH$) towards mercury proved to be very high, the strength of the resin-mercury bond being comparable to that of the mercury-sulphur bond in HgS . Thus the resin, even in saturated brine, can compete successfully with the very stable $HgCl_4^{2-}$ complex.

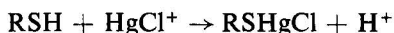
In brine, the following dissociation equilibria of mercury(II) chloride complexes exist:



Most of the mercury is then present as $HgCl_4^{2-}$ complex ions. The Imac TMR resin ($R-SH$) reacts preferentially with $HgCl^+$ or Hg^{2+} ions according to the reactions



and



During the reaction, the dissociation equilibria of the $HgCl_4^{2-}$ complex shift towards the $HgCl^+$ and Hg^{2+} side. Also, although these ions represent only a very small fraction of the total mercury, the affinity of the resin towards these ions is so strong that the total mercury level that remains in the liquid can be reduced to below 5 ppb, even in brine. This is illustrated by Fig. 2, which represents a breakthrough curve of an Imac TMR column on electrolysis-plant brine.

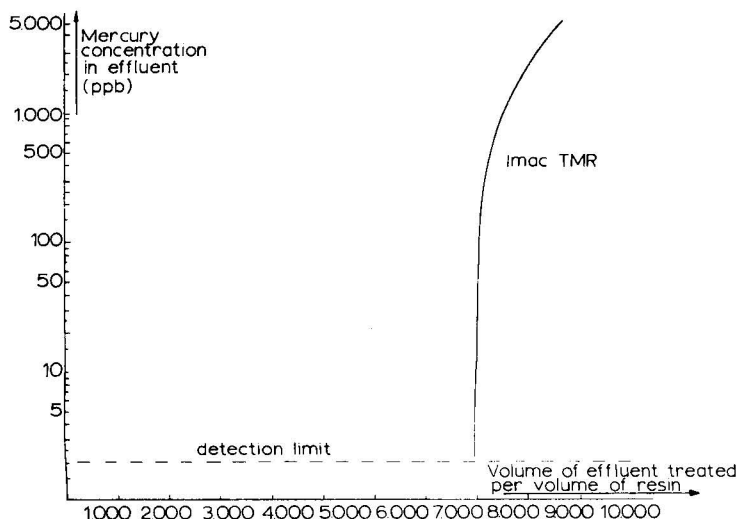


Fig. 2. Typical breakthrough curve. Chlor-alkali plant brine, pH 2. Mercury concentration in feed, 20–50 mg/l; space velocity, 10 bed volumes per hour; bed height, 1.5 m.

Capacity

The total capacity of Imac TMR is at least 1200 mequiv. of $-SH$ per litre, which, at full loading, is equivalent to 240 g of mercury per litre of resin. The equilibrium capacity of Imac TMR depends on the concentration of mercury in the liquid phase. In Fig. 3, the equilibrium curve of Imac TMR for mercury is given, which is valid for pH values between 1 and 14 and sodium chloride concentrations between 0 and 310 g/l.

From this curve, it can be calculated that at a mercury concentration in the feed of 10 ppm, 1 m³ of resin can treat 10,000 m³ of waste water in one cycle. Although the amount of mercury in the resin will increase with increasing concentration in the feed, the volume of waste water per cycle will, of course, decrease. The opposite is true for lower feed concentrations.

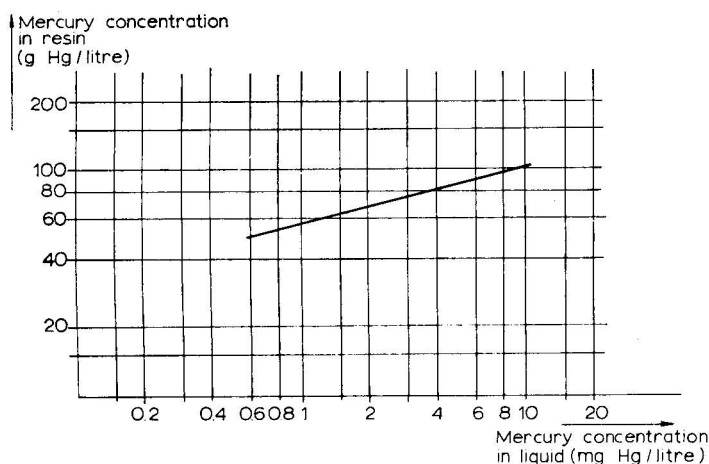


Fig. 3. Equilibrium curve for Imac TMR.

Selectivity

As mentioned earlier, the selectivity of the resin is of prime importance. Some impurities from the electrolysis process are disposed of by means of the waste water. These impurities are not necessarily detrimental for the environment. They can occur in the waste water in much higher concentrations than mercury itself and these impurities, e.g., iron, can be detrimental to the electrolysis process itself. Upon regeneration of a non-selective resin, these impurities would be re-introduced into the electrolysis process. Therefore, the ion-exchange resin to be used has a prime function of retaining the mercury while all other impurities pass through.

The affinity of Imac TMR towards metal ions is related to the solubility product of the metal sulphides: the metal with the smallest solubility product of its sulphide has the highest affinity towards the resin.

A column of Imac TMR has been fed with a solution containing 10 ppm each of Hg, Cu, Pb and Cd ions, and breakthrough curves are given in Fig. 4. It can be seen that the resin initially removes all metals from the liquid. After the initial period, Cd, Pb and Cu are subsequently replaced from the resin by mercury. The concentration of the three metals in the effluent equals the concentration in the feed long before

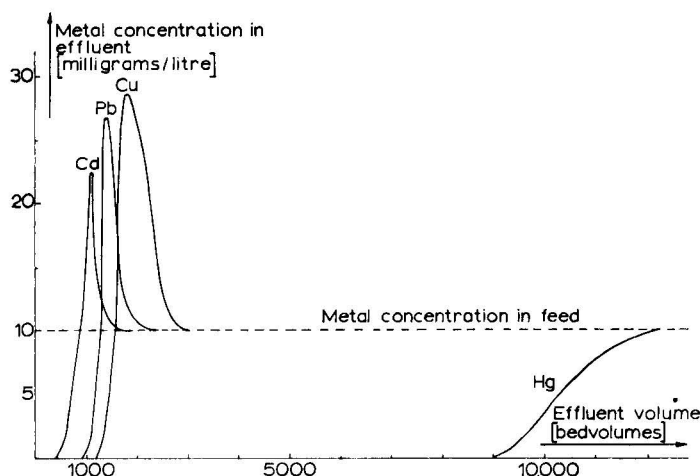
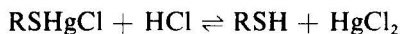


Fig. 4. Replacement of Cd, Pb and Cu ions by Hg ions when percolating a solution containing 10 ppm of each species.

mercury finally breaks through. The resin is therefore very selective for mercury in comparison with other metals.

Regeneration

Fortunately, the equilibrium of the reaction allows the resin to be regenerated with concentrated hydrochloric acid:



Hydrochloric acid is a common chemical in the chlor-alkali industry and is used in considerable amounts for pH adjustment of the brine circuit. The hydrochloric acid used for regeneration of the resin can serve this purpose equally well. The mercury is recycled into the electrolysis process.

THE AKZO PROCESS

In the above section, the special features of the Imac TMR were discussed. Although this resin constitutes the heart of the process, it cannot be used efficiently without appropriate pre-treatment of the waste water. This pre-treatment can determine the success of the whole operation to a large extent.

In chlor-alkali waste water, mercury can occur as metallic and as ionic mercury. This waste water can vary widely in pH and salt and chlorine content, and can contain considerable amounts of solids, including hydroxides which are difficult to filter. In some instances, the amount of waste water can fluctuate over a wide range. Coarse solids have to be removed prior to treatment, and sufficient buffer capacity has to be installed to guarantee an even flow of waste water. The Akzo Imac TMR process consists of the following stages (see Fig. 5): oxidation/pH adjustment; filtration; dechlorination; and ion exchange.

Oxidation

The resin reacts only with ionic mercury, and all metallic mercury in the waste water must therefore be oxidized. For this oxidation step, chlorine or hypochlorite is used. Although the resin is not sensitive to pH, the pH of the waste water is controlled at about 3 for other reasons.

Filtration

The Imac TMR resin has a long operating cycle. In order to prevent clogging of the resin beds, good filtration is essential; either sand filters or cloth filters are used for this purpose. Hydroxides which are commonly present in chlor-alkali waste water can cause filtration problems, particularly iron hydroxide. In order to avoid these problems, the pH of the waste water is controlled at about 3 so as to keep iron in solution. As a secondary function, the filter retains mercury droplets which might pass the oxidation reactor, these droplets being oxidized in the filter.

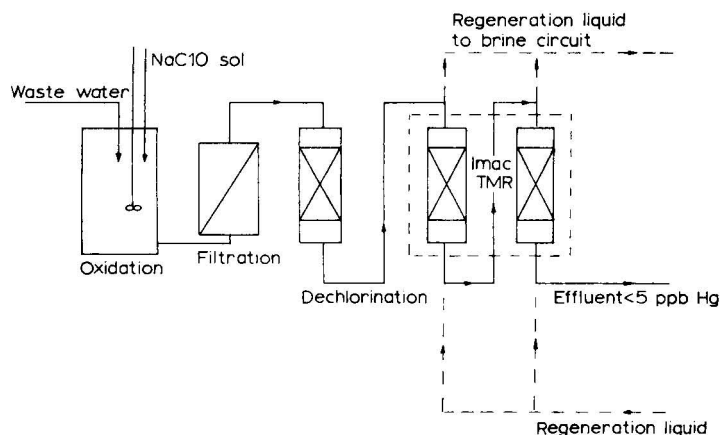


Fig. 5. Akzo Imac TMR process.

Dechlorination

The thiol groups of the resin are sensitive to oxidation and removal of the excess of oxidant is therefore necessary. In our plants, we use a column with a special activated carbon for this purpose; the column dimensions are the same as those of the ion-exchange columns.

Ion exchange

The ion-exchange columns are very similar to those used for water treatment. The flow-rate in the columns is, however, maintained at 10 volumes of waste water per volume of resin per hour. As long as a sufficient bed height of fresh resin is available, the effluent mercury concentration will be below 0.005 mg/l. There are two resin beds in series, which permits complete loading of the first resin bed in equilibrium with the influent mercury concentration. The long cycle time of the resin gives ample time to regenerate the first column before the second column starts to break through. After regeneration, the operating sequence of the columns is changed, the freshly

regenerated column acting as a second column for polishing the effluent of the first column.

The first unit of this process has been operating at the Akzo chlor-alkali plant in Delfzijl since May 1973. Four more plants are at the engineering stage.

Process economics

As mentioned in the Introduction, the process is not economic when based on the recovery of the mercury. A comparison of the investment and direct operating costs of this process with two alternative precipitation processes shows, however, a definite advantage over the precipitation processes (see Table I).

TABLE I

COMPARISON OF INVESTMENT AND DIRECT OPERATING COSTS OF MERCURY-REMOVING PROCESSES

Base case flow 10 m³/h; 6 mg Hg/l; amounts in Dutch currency.

	<i>Reduction/ filtration</i>	<i>Sulphide precipitation</i>	<i>Imac TMR treatment</i>
Product quality	0.1–0.3 g Hg/m ³	<0.1 g Hg/m ³	< 0.005 g Hg/m ³
Investment battery limits	Dfl 570,000	Dfl 600,000	Dfl 558,000
First resin and carbon charge	—	—	Dfl 70,000
Direct operating cost in cents/m ³ water:			
Electricity	7.2	12.0	8.4
Chemicals	68.6	52.6	17.2
Resin	—	—	20.0 (5 cycles)
Carbon	—	—	6.7
Less recovered mercury at 280 \$ per flask	—	—	12.6
Total	75.8	64.6	39.7
Secondary pollution problems	43 tons of solid waste, 80% moisture, with 525 kg of Hg per year	85 tons of solid waste, 80% moisture, with 525 kg of Hg per year	1 m ³ of spent resin with less than 100 g of Hg per year

CHROM. 7767

EINSATZMÖGLICHKEITEN VON PULVERFÖRMIGEN IONENAUSTAUSCHERN IN DER KONDENSATAUFBEREITUNG

REINHARD SCHAAF

VEB Chemiekombinat, 44 Bitterfeld (D.D.R.)

SUMMARY

Possible application of powdered ion exchangers in the treatment of condensate

Change-over from the natural circulation boiler to the forced circulation boiler requires feed-water of the highest possible purity. As far as the make-up treatment is concerned, this has been achieved by using ion exchangers in complete desalination plants. However, this extreme purity of water cannot be maintained during the operation, since degradation in the quality of the feed-water caused by dissolved, colloidal and suspended matter takes place. To guarantee the purity of the water-vapour circulation, treatment of the condensate is required.

The method of pre-coat filtration, using powdered ion exchangers, finds ever increasing application. This method became known under the name of "Powdex process" and appears to be a combination of filtration and ion exchange.

The characteristics of the Wofatit powdered exchangers are explained thoroughly on the basis of laboratory experiments. Detailed information is given on the relationships between granulation, mixture ratio and pre-coat behaviour. The ion-exchange and filtration characteristics of the powdered exchangers are described comprehensively. The efficiency of the Wofatit powdered resins is shown in the light of pilot plant experiments and technical results.

EINLEITUNG

Der Übergang zu modernen Grosskraftwerken in der heutigen Zeit ist dadurch gekennzeichnet, dass beim Bau neuer Blockeinheiten Dampferzeuger- und Turbinenleistung ständig erhöht werden. Wegen der zunehmenden Heizflächenbelastungen in den Zwangsdurchlaufkesselanlagen und der enormen Dampfdurchsätze in der Turbine wird eine hohe Speisewasserqualität gefordert. Diese Forderung wird erfüllt durch eine sorgfältige Aufbereitung sowohl des Zusatzwassers als auch des im Kreislauf zurückgeführten Kondensats. Nach herkömmlicher Weise besteht eine Kondensatreinigungseinheit aus mechanischem Vorfilter und Entsalzungsanlage, da das Kondensat einmal durch Korrosionsprodukte der vom Wasser-Dampf-Kreislauf berührten Metallteile, zum anderen durch Salzeinbrüche infolge Kondensatorleckagen verunreinigt wird.

Das Verfahren der Anschwemmfiltration unter Verwendung pulverförmiger Ionenaustauscher vereinigt nun mechanische Filtration und Ionenaustausch zu einer Stufe. Bei dieser Kondensatreinigungsmethode, welche in den letzten zehn Jahren unter der Bezeichnung "Powdex-Prozess" bekannt geworden ist, wird ein im Wasser suspendiertes Gemisch aus gepulverten Kationenaustauscher- und Anionenaustauscherharz mittels einer Pumpe in eine Anschwemmapparatur gebracht und an wasser-durchlässigen Kerzen oder Platten angeschwemmt, so dass ein 3–6 mm dicker Filterkuchen aus Ionenaustauschermaterial entsteht. Dieser übernimmt nach Beaufschlagung des Anschwemmfilters mit Kondensat die Funktion der gleichzeitigen Entfernung der in suspendierter, kolloidal und echt gelöster Form vorliegenden Kondensatinhaltsstoffe.

EIGENSCHAFTEN DER PULVERFÖRMIGEN IONENAUSTAUSCHER

Beim Zusammenbringen von pulverisierten Kationen- (H^+ -Form) und Anionenaustauscher (OH^- -Form) in Wasser tritt eine augenblickliche Agglomeration zu flockenähnlichen Gebilden ein, die durch elektrostatische Anziehungskräfte zwischen den extrem feinen Teilchen mit entgegengesetztem Ladungssinn hervorgerufen wird. Das Ausmass der Agglomerationserscheinungen wird hauptsächlich beeinflusst durch: (i) das Mengenverhältnis der beiden Austauscherharze, (ii) die unterschiedliche Korngrösse der Teilchen und (iii) die mehr oder weniger intensive Vermischung der Komponenten in der wässrigen Suspension.

Bei etwa gleichen Gewichtsanteilen an Kationen- und Anionenaustauschermaterial und damit annähernd gleicher Anzahl aktiver Oberflächenladungen ist die grösste Volumenzunahme zu erwarten. Überwiegt dagegen die eine Austauscherkomponente, beispielsweise bei einem Verhältnis der beiden Pulverharzkomponenten von 9:1, resultiert aus dem Überschuss an positiven oder negativen Ladungen eine kleinere Flockengrösse sowie eine Trübung der überstehenden Flüssigkeit. Einen grossen Einfluss auf die Flockengrösse und -festigkeit übt die Korngrössenzusammensetzung der Komponenten aus. Verhältnismässig grobe Körnungen ergeben lockere Flockengebilde, die sich durch Rühren leicht zerteilen lassen. Verschiebt sich der mittlere Korn-durchmesser der Teilchen auf $< 50 \mu m$, so nimmt die Stärke der gegenseitigen Beeinflussung der Pulverharzteilchen zu. Die Flocken werden stabiler und nach dem Absetzen der agglomerierten Teilchen bildet sich darüber eine klare Flüssigkeit aus. Diese Feststellung trifft nicht zu, wenn nur eine Komponente eine feinere Körnung aufweist, während die andere weitaus gröber vorliegt. Bei dem aufeinanderfolgenden Eintragen der beiden Pulverharzkomponenten im Wasser kommt es zufolge der augenblicklichen Agglomeration zu einer unregelmässigen Anordnung der unterschiedlich geladenen Teilchen bei ihrem ersten zufälligen Zusammentreffen. Es bilden sich voluminöse Gebilde aus. Eine Neuverteilung der gegenseitig sich beeinflussenden Teilchen innerhalb der Flocken kann nur durch intensives Rühren über einen längeren Zeitraum erfolgen. Die Teilchen liegen jetzt in einer regelmässigen Anordnung zueinander vor, die Flockengrösse wird dadurch kleiner.

ANSCHWEMMTECHNIK

Für das Erreichen der wirksamen Entfernung aller Kondensatinhaltsstoffe muss die Forderung einer gleichmässigen und vollständigen Beschichtung der Filterele-

mente erhoben werden. Erwartungsgemäss lässt sich eine solche Anschwemmung mit einer flockigen und voluminösen Masse viel schwerer erreichen als bei Verwendung konventioneller Anschwemm-Materialien. Die Agglomeration der Teilchen zu Flocken wirkt sich auf den Anfangsdruckverlust der mit Pulverharz beschichteten Filterelemente sehr günstig aus, jedoch muss die Flockengrösse in bestimmten Grenzen gehalten werden. Bei Ausbildung grosser voluminöser Gebilde lassen sich diese nur teilweise oder überhaupt nicht an den Filterelementen anschwemmen.

Folgende Forderungen müssen erfüllt sein, wenn brauchbare Anschwemmschichten erreicht werden sollen:

(1) Die verwendeten Pulverharzkomponenten müssen etwa dasselbe Korngrössenspektrum aufweisen. Nach unseren Erfahrungen muss der Hauptanteil der Teilchen eine Korngrösse zwischen 5 und $50\text{ }\mu\text{m}$ besitzen.

(2) Die im Ansetzgefäss vorliegende Pulverharzsuspension ist intensiv zu durchmischen, ehe mit dem Anschwemmprozess begonnen wird.

(3) Die Methode der sogenannten Dosieranschwemmung ist anzuwenden. Dabei wird mittels einer Kreiselpumpe das aus einem Behälter kommende Wasser über das Anschwemmfilter im Kreislauf gefahren. Die in einem zweiten Behälter befindliche gut durchmischte Pulverharzsuspension wird über eine Dosierpumpe in den Kreislauf gegeben.

Beim Passieren der Kreislaufpumpe werden die agglomerierten Gebilde vollständig zerschlagen. Infolge der starken Verdünnung im Kreislaufwasser kann sich das feinverteilte Harzmaterial nicht wieder zu einer voluminösen Flockenmasse vereinigen. Es erscheint eher als ein im Wasser suspendiertes Pulver. Erst wenn dieses auf den Filterelementen angeschwemmt worden ist, findet die Agglomeration zu grösseren Teilchen statt. Die Flocken müssen dann zwangsläufig in stark abgeplatteter Form erscheinen, was sich auf die Filtrationseigenschaften der Schicht günstig auswirkt.

(4) Das Anschwemmfilter muss einige konstruktive Besonderheiten aufweisen. Der lichte Abstand zwischen den einzelnen Filterelementen ist auf mindestens 50 mm zu begrenzen, um ein Zusammenwachsen der Filterschichten zu vermeiden. Turbulenzerscheinungen im Anschwemmfilter sind weitgehend zu unterdrücken, was z.B. durch konische Gestaltung des unteren Teiles bei Kerzenanschwemmfiltern erreicht werden kann. Ausserdem ist die Temperatur des Kreislaufwassers vor und während der Anschwemmphase niedrig zu halten und soll maximal 40° betragen.

Nach Erreichen einer vollständigen Pulverharzschicht an den Filterelementen ist die Anschwemmphase beendet, und das Reinigungssystem kann in den Kondensat-kreislauf des Kraftwerksblockes eingebunden werden.

VERSUCHE MIT PULVERHARZ-ANSCHWEMMFILTERN

Zwecks Austestung der pulverförmigen Wofatit-Ionenaustauscher zur Ermittlung der Filtrier- und Entsalzungseigenschaften wurden umfangreiche Untersuchungen an einer halbtechnischen Versuchsanlage sowie an Platten- und Kerzen-Anschwemmfiltern in verschiedenen Wärmekraftwerken angestellt. Zur Verfügung standen Anschwemmfilter mit einer Filterfläche von $0.15\text{--}10\text{ m}^2$. Die Filtrationsgeschwindigkeit lag zwischen 5 und 10 m/h. Die spezifische Anschwemm-Menge betrug 1 kg/m^2 Filterfläche (bezogen auf Trockensubstanz). Das Verhältnis Kationen- zu Anionenaustauscherharz wurde in den Grenzen zwischen 1:1 und 9:1 variiert.

Zur Ermittlung der Entsalzungseigenschaften der Pulverharze wurden vor Filtereingang verdünnte Kochsalzlösungen in den Kreislauf eindosiert. Die Natriumionenkonzentration und die Säureleitfähigkeit wurden vor und nach Filter über den gesamten Zeitraum des jeweiligen Versuches bestimmt. Das Aufnahmevermögen des Kationen- und Anionenaustauschers bis zum Erreichen einer bestimmten Restionenkonzentration im Filterablauf konnte errechnet werden. Tabelle I gibt einen Überblick über die erzielten Ergebnisse.

TABELLE I

NUTZBARE AUSTAUSCHKAPAZITÄTEN DER PULVERFÖRMIGEN WOFATIT-IONEN-AUSTAUSCHER BEI VERSCHIEDENEN IONENKONZENTRATIONEN IM FILTER-EINLAUF

Pulverharzmengen im Verhältnis 1:1.

<i>Filtereinlauf</i>		<i>Nutzbare Austauschkapazität (equiv./kg trockenes Pulverharz)</i>			
<i>Durchschnittliche Natriumkonzentration ($\mu\text{g/l}$)</i>	<i>Durchschnittliche Säureleitfähigkeit ($\mu\text{S/cm}$)</i>	<i>des Kationenaustauschers bis zu einem Natriumschlupf im Filterablauf von 20 $\mu\text{g/l}$</i>	<i>des Anionenaustauschers bis zu einer Säureleitfähigkeit im Filterablauf von</i>		
			<i>0.1 $\mu\text{S/cm}$</i>	<i>0.2 $\mu\text{S/cm}$</i>	<i>0.5 $\mu\text{S/cm}$</i>
350	5.5	2.81	1.75	2.20	2.50
—	7	—	1.35	2.05	2.35
630	10	1.57	1.00	1.70	2.25

Eine Abhängigkeit der nutzbaren Austauschkapazität von der im Filtereinlauf vorliegenden Salzkonzentration ist deutlich erkennbar. Da bei diesen Versuchen relativ hohe Salzeinbrüche simuliert wurden, wird die nutzbare Kapazität der Pulverharze bei geringen oder gar keinen Kondensatorleckagen höhere Werte annehmen. Bei alkalischer Fahrweise wird jedoch mit steigendem pH-Wert des Kondensates das Aufnahmevermögen des Kationenaustauschers für Natriumionen zurückgehen.

Für den Umgang mit Pulverharzen soll folgender Hinweis gegeben werden: Die Ionenaustauscher werden vom Produzenten im regenerierten Zustand hohen Grades geliefert. Es ist bekannt, dass stark basische Anionenaustauscher in der Hydroxylform beim Stehen an der Luft Kohlendioxid aufnehmen. Diese Eigenschaft ist besonders bei den feinteiligen Pulverharzen mit grosser äusserer Oberfläche ausgeprägt. Wird also dieser Tatsache keine Beachtung geschenkt und der Anionenaustauscher der Luft ausgesetzt, treten beim späteren Einsatz merkliche Kapazitätsverluste ein. Fig. 1 zeigt den Einfluss der Einwirkungsdauer vom Kohlendioxid der Luft auf die nutzbare Austauschkapazität.

Während des Anfahrprozesses eines Kraftwerkblockes muss wohl die Kondensatreinigungsanlage hauptsächlich die Funktion der mechanischen Filtration übernehmen. Die durch Stillstandskorrosion eingetretene Verschlechterung der Kondensatqualität ist in kurzer Zeit zu beseitigen, wenn Störungen am Verdampfer- und Turbinenanlagen vermieden werden sollen.

Wir haben uns dieser Problematik gewidmet und Untersuchungen angestellt über das Filtriervermögen pulverförmiger Wofatit-Ionenaustauscher. Insbesondere

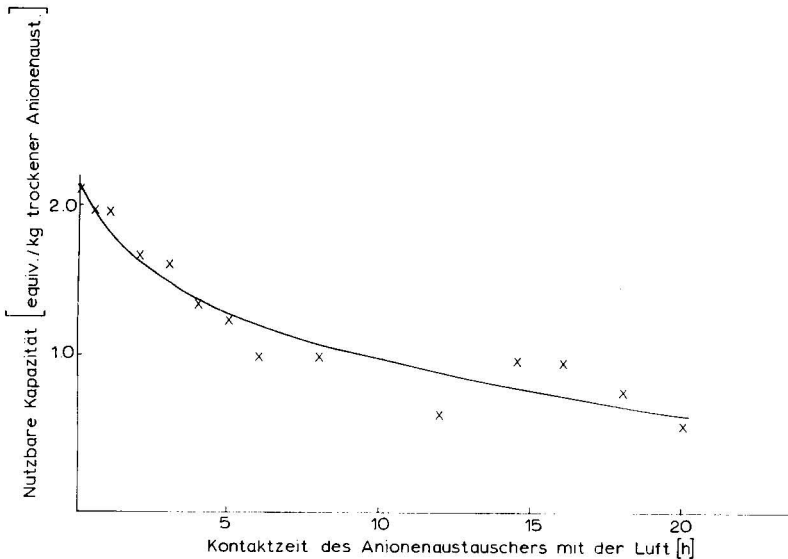


Fig. 1. Einfluss der Kohlendioxideinwirkung auf die erreichten nutzbaren Austauschkapazitäten beim Anionenaustauscher.

ging es um die Entfernbarekeit des Eisens, welches in diesem Falle teilweise als kolloidales und schwer filtrierbares Oxidhydrat im Kondensat vorliegt. Nach mehreren Versuchen, bei denen frisch gefälltes Eisen(III)hydroxid in den Kreislauf eingebracht worden war, musste festgestellt werden, dass infolge Rissbildung in der angeschwemmten Pulverharzschicht Filtrier- und Entsalzungswirkung nicht befriedigten. In einer Reihe von Laborversuchen konnten die Ursachen für das Entstehen der Risse ermittelt werden. Die stark ausgeprägten Oberflächenladungen von frischgefällten Metalloxidhydraten kompensieren einen Teil der Ladungen des Austauschers mit entgegengesetztem Vorzeichen. Dadurch werden die Wechselwirkungen zur anderen Pulverharzkomponente herabgesetzt. Die Folge ist eine Volumenkontraktion, die sich durch das Auftreten von Rissen in der angeschwemmten Schicht äussert.

Das Aufschwemmen einer inerten Deckschicht auf die Pulverharzschicht bot sich an. Als Anschwemm-Materialien wurden Filterzellulose Typ FNS und ein feinkörniges Styrol-Divinylbenzol-Copolymerisat verwendet. Die spezifische Anschwemm-Menge dieser Materialien lag bei 660 g/m^2 für Zellulose bzw. bei 2000 g/m^2 für das Copolymerisat. Bei der Erprobung dieser aufgeschwemmten Deckschicht zeigten sich günstige Ergebnisse. Die Rissbildung an den Filterelementen blieb aus, die gemeinsam in den Kreislauf eindosierten Eisenhydroxid- und Kochsalzmengen wurden wirksam entfernt. Eine Zusammenstellung der Versuchsergebnisse ist in Tabelle II zu finden. Die beobachtete Rissbildung der Pulverharzschicht ist bei der Verwendung von gleichen Anteilen der beiden Austauscherkomponenten am stärksten. Sie tritt nicht auf, wenn andere Modifikationen des Eisenoxides mit der Pulverharzschicht in Kontakt kommen. Beispielsweise lässt sich das Eisen in Form von Magnetit wesentlich besser abtrennen. Ausserdem ist ein Rückgang der Rissbildung zu verzeichnen, wenn das Mengenverhältnis der beiden Austauscherkomponenten stark nach der Seite des Kationenaustauschers verschoben wird. Wegen der geringen Anteile

TABELLE II

EINFLUSS DER INERTSTOFFANSCHWEMMUNG AUF DIE WASSERQUALITÄT IM FILTERABLAUF

Durchschnittliche Eisenkonzentration(EK) im Filtereinlauf: 250 µg/l.

Spezifische Pulverharz- menge (kg/m ²)	Harzver- hältnis (Trocken- massean- teile)	Spezifische Inertstoff- menge		Filterablauf			
		Zellulose (kg/m ²)	Copoly- merisat (kg/m ²)	Max. EK vor der Riss- bildung (µg/l)	Prozen- tuale Absenkung (%)	Max. EK nach der Rissbil- dung (µg/l)	Prozen- tuale Ab- senkung (%)
1	1:1	0	0	70	72	160	36
1	1:1	0.66	0	14	95	—*	95
1	1:1	0	2.0	20	92	—*	92

* — = keine Rissbildung beobachtet, maximale Eisenkonzentration im Filterablauf blieb konstant.

Anionenaustauscherharz nimmt natürlich das Entsalzungsvermögen der Pulverharzschicht sehr stark ab.

Es ist deshalb jedem Betreiber eines solchen Kondensatreinigungssystems zu empfehlen, die Zusammensetzung der angeschwemmten Materialien den jeweils vorliegenden Kondensatbedingungen anzupassen, um eine wirksame Entfernung aller Kondensatinhaltsstoffe zu erreichen.

ZUSAMMENFASSUNG

Der Übergang von Naturumlauf- zum Zwangsdurchlaufkessel stellt in bezug auf das Speisewasser die Forderung nach möglichst absoluter Reinheit. Für die Zusatzwasseraufbereitung ist dies durch den Einsatz von Ionenaustauschern in Vollentsalzungsanlagen erfüllbar geworden. Die extreme Reinheit des Wassers kann jedoch während des Betriebes nicht erhalten bleiben. Die Verschlechterung der Speisewasserqualität wird durch gelöste, kolloidale und suspendierte Stoffe hervorgerufen. Um nun die Reinhaltung des Wasser-Dampf-Kreislaufes zu gewährleisten, macht sich eine Aufbereitung des Kondensates erforderlich.

Immer mehr Verbreitung findet dabei die Methode der Anschwemmfiltration unter Verwendung pulverförmiger Ionenaustauscherharze, welche unter dem Namen "Powdex-Verfahren" bekannt wurde und eine Kombination von Filtration und Ionenaustausch darstellt.

Ausgehend von Laboruntersuchungen werden die Eigenschaften der Wofatit-Pulveraustauscher ausführlich erläutert. Auf Zusammenhänge zwischen Körnung, Mischungsverhältnis und Anschwemmverhalten wird ausführlich eingegangen. Die Ionenaustausch- und Filtrationseigenschaften der Pulveraustauscher werden umfassend dargestellt. An Hand von Technikumsversuchen und technischen Ergebnissen wird die Wirksamkeit der Wofatit-Pulverharze gezeigt.

CHROM. 7868

THE ION-EXCHANGE BEHAVIOUR OF ARSENIC(III) ON VARION ANION-EXCHANGE RESINS

I. BÁLINT-AMBRÓ

Radiochemistry Department, Research Institute for Heavy Chemical Industries, Veszprém (Hungary)

SUMMARY

The ion-exchange equilibrium of arsenic ions was studied on the strongly basic anion-exchange resins VARION AD, VARION AT-4 and VARION AT-6. The apparent equilibrium constants (K^*) and the distribution coefficients (D) were determined between the resin and the liquid phases in acidic and alkaline solutions. The effect of arsenic concentration on the course of chromatographic experiments was studied in terms of the breakthrough capacity of the ion-exchange column and the pH of the effluent. VARION AT-6 resin proved to be the most suitable for removing arsenic from highly alkaline solution.

INTRODUCTION

It is well known that arsenic is a very poisonous material, and therefore arsenic compounds from industrial processes must not be allowed to contaminate the waste water. There are a few industrial processes in which arsenic occurs in large amounts and in these cases it would be preferable to remove it from the by-products or the waste water and to recycle it into the process. By that means two problems could be solved: (1) removal of the arsenic, and (2) recycling it for economic reasons. In this paper, experiments are described in which arsenic in alkaline solutions was removed with the aid of ion-exchange resins and, after elution, recirculated into the initial industrial process.

EXPERIMENTAL

VARION AD, VARION AT-4 and VARION AT-6 anion-exchange resins with a polystyrene matrix, produced by Nitrokémia Works (Balatonfüzfő, Hungary) were used. The functional group of VARION AD resin is R_4N^+ Alkanol¹, and of the VARION AT resins it is $R(CH_3)_3N^+$, where R is an alkyl group; the numbers 4 and 6 refer to the degree of cross-linking, VARION AT-4 having a looser lattice. These resins have a high affinity for silicate and carbon dioxide. The silicate binding power of resin VARION AD is below that of the VARION AT types¹.

The resins were used in the Cl^- , SO_4^{2-} , HCO_3^- and OH^- forms. In the equi-

librium systems (*i.e.*, in the batch systems), they were used in a dry form, being dried to constant weight in an oven at 60°.

The arsenic(III) solutions were prepared by dissolving arsenic(III) oxide in 1 *M* potassium hydroxide solution; in other cases, the solutions were taken from the waste water of a factory. Demineralized water was used throughout. The liquid phase was labelled with the isotope ⁷⁶As. The sorption of arsenic was checked by measuring the specific activity of the solutions.

In the equilibrium experiments, 3 g of dried resin and 10 cm³ of the solution were used in each case, at pH values of 4.6 and 7.9. Hydrochloric acid and gaseous carbon dioxide were used to adjust the pH of the solutions.

The equilibrium samples were shaken for 24 h at ambient temperature (22–23°). According to our preliminary experiments, the systems examined attained ion-exchange equilibrium during this time. Then 1–2-cm³ volumes were removed from the solution for activity measurements. Activity measurements were made with a well-type counter and with a scaler (Type NK-108 from Gamma, Hungary).

From the specific activity (cpm/cm³) of the solutions, the amount of arsenic bound to the resin was calculated by the equation

$$\frac{A}{A_0} = \frac{C_{As}}{C_{0As}}$$

where A_0 is the initial specific activity of the solution, A is the specific activity of the solution at equilibrium, and C_0 and C are concentrations.

With a knowledge of the amounts of the resins (g) used in the experiments (namely 3.0 ± 0.002 g), their capacities (mequiv./g), the specific activities of the solutions (A_0 and A) and the initial concentration, the apparent equilibrium constant (K^*) and the distribution coefficients (D) could be calculated. The results of the equilibrium experiments are given in Table I.

The chromatographic experiments were carried out on ion-exchange columns of 80 or 165 cm height and 2 or 3 cm diameter. The solution was fed in at the top of the column (input), and had a volume velocity of 10 cm³/min or a linear velocity of 1.41 cm/min. The activity and pH of the effluent (output) were checked continuously during the sorption and elution. The results of these experiments are given in Table II and Fig. 1.

TABLE I

APPARENT ION-EXCHANGE EQUILIBRIUM CONSTANTS (K^*) AND DISTRIBUTION COEFFICIENTS (D) OF ARSENIC(III) ON VARION ANION-EXCHANGE RESINS

pH	Ionic form	K^*			D		
		VARION AD	VARION AT-4	VARION AT-6	VARION AD	VARION AT-4	VARION AT-6
4.6	Cl ⁻	27.1	8.6	13.1	0.98	0.77	0.77
	SO ₄ ²⁻	31.5	20.5	106.7	1.02	1.00	1.21
	HCO ₃ ⁻	127.9	237.8	303.9	1.34	1.72	1.39
	OH ⁻				2.66	3.34	>1000
7.9	Cl ⁻	43.1	4.1	8.8	1.09	0.6	0.70
	SO ₄ ²⁻	43.1	32.4	44.3	1.09	1.13	1.02
	HCO ₃ ⁻	104.0	469.3	182.2	1.30	1.93	1.30
	OH ⁻				2.16	3.34	1.86

TABLE II

pH AND BREAKTHROUGH CAPACITY IN REMOVAL OF ARSENIC WITH VARION AT-6 RESIN

$-\log K_w = 14.1969$; temperature = 20° (ref. 4). Chromatographic conditions: column length = 1.65 m; diameter = 0.03 m; flow velocity = $10 \text{ cm}^3/\text{min}$; linear velocity = 1.41 cm/min .

Expt. No.	Input		Output		n ($C_{\text{OH}^-}/C_{\text{As}}$)	Breakthrough capacity ($\text{g As}_2\text{O}_3 \pm 0.5$)
	$C_{\text{As}_2\text{O}_3}$ (g/l)	C_{As} (g-atom/l)	pH (± 0.05)	C_{OH^-} (g-equiv./l)		
1	0.4	$4.04 \cdot 10^{-3}$	11.8	$4.30 \cdot 10^{-3}$	1.064	24
2	0.8	$8.08 \cdot 10^{-3}$	12.1	$8.57 \cdot 10^{-3}$	1.061	24
3	1.0	$10.10 \cdot 10^{-3}$	12.2	$1.08 \cdot 10^{-2}$	1.069	26
4	4.0	$4.04 \cdot 10^{-2}$	12.7	$3.40 \cdot 10^{-2}$	0.817	30
5	40.0	$4.04 \cdot 10^{-1}$	13.7	$3.40 \cdot 10^{-1}$	0.842	10

RESULTS AND DISCUSSION

It can be seen from the distribution coefficients and equilibrium constants shown in Table I that the sorption affinity of the VARION AD resins for arsenic is weaker than that of the VARION AT resins. It has been established¹ that their sorption affinity is similar to that of silicate ions. All three resins in the OH^- form show the highest affinity for arsenic ions.

According to the equilibrium data, chromatographic experiments were planned on both laboratory and pilot-plant scales.

During these "dynamic" measurements, the effect of the "input" arsenic content was studied in terms of the pH of the effluent (output) and the breakthrough capacity. Some of the results are summarized in Table II and Fig. 1. The results show that in the steady-state sorption of arsenic from "input solution" the arsenic concen-

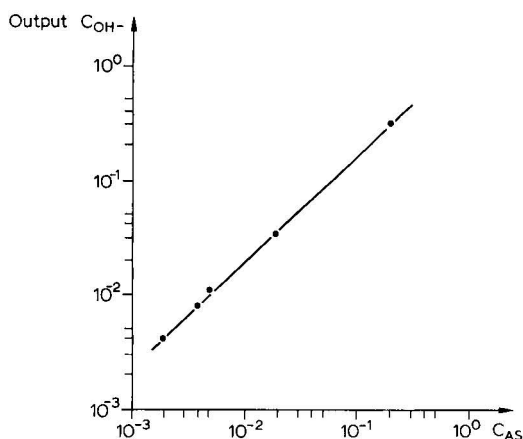


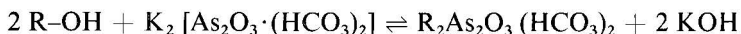
Fig. 1. OH^- concentration (C_{OH^-}) of the effluent versus arsenic content of the solutions fed into the VARION AT-6 ion-exchange column. Column height, 1.65 m; diameter, 0.03 m; volume of resin, 1.166 l.

tration determines the pH value in the "output". The ratio n of $C_{\text{OH}^-, \text{output}}$ to the arsenic concentration of the solution fed into the ion-exchange column, $C_{\text{As, input}}$, is almost unity (Table II, 6th column), *i.e.*, each equivalent of arsenic corresponds to one equivalent of hydroxide. Fig. 1 shows that there is a linear relationship between $\log C_{\text{OH}^-}$ and $\log C_{\text{As}}$. The slope of the graph can be evaluated according to the equation

$$\frac{\Delta \log (C_{\text{OH}^-, \text{output}})}{\Delta \log (C_{\text{As, input}})} = 1.001$$

which shows that one equivalent of hydroxide corresponds to one equivalent of arsenic in the sorption of arsenic on the anion-exchange resins in the OH^- form.

These results are in agreement with those of other workers. According to Stehlik², in strongly alkaline solution the metaarsenite form exists, and according to Ephraim³ it is able to form complex arsenic-carbonate compounds with the carbonate in the solution. In more strongly alkaline and concentrated solutions, the association of arsenic to produce diarsenite ions can be the cause of a decrease in n (Table II, experiments 4 and 5). Taking in consideration the above, the following equation could perhaps be assumed for an overall equilibrium:



where R is the resin matrix (cross-linked polystyrene).

Other experiments were carried out to study the effect of arsenic concentration on the breakthrough capacity of the ion-exchange column. The results given in the last column in Table II show that an increase in the arsenic concentration causes a decrease in the breakthrough capacity of the column.

When the column was loaded with a solution containing 40 g/l of arsenic(III) oxide, the pH of the effluent increased to 13.7. In this case the liberated OH^- ions prevent the necessary sorption of arsenic ions. According to the second column of Table II, working with an input concentration of arsenic(III) oxide of 4 g/l, the pH of the output is 12.7. The arsenic concentration in this effluent is 4 mg/l as arsenic(III) oxide, which is satisfactory for our purposes.

According to these experiments, a method has thus been developed for removing arsenic from alkaline waste water, by which the concentration of the arsenic can be reduced to less than 4 mg/l as arsenic(III) oxide⁵.

The elution of the sorbed arsenic from the resin was carried out with 1 M potassium hydroxide solution. By this means, the arsenic can be eluted with a sharp peak. After elution of the arsenic, the resin is in the OH^- form again and can be loaded repeatedly with arsenic.

REFERENCES

- 1 J. Bognar, *2nd Symp. on Ion Exchange, 10-14th Sept. 1969, Balantonszéplak*, Hungarian Chemical Society, Budapest, p. 37.
- 2 B. Stehlik, *Collect. Trav. chim. Tchecosl.*, 14 (1949) 241.
- 3 F. Ephraim, *Helv. Chim. Acta*, 3 (1920) 800.
- 4 B. E. Conway, *Electrochemical Data*, Elsevier, Amsterdam, 1952, p. 187.
- 5 I. Bálint-Ambró, *Research Report*, NEVIKI (Research Institute for Heavy Chemical Industries), Veszprém, 1968.

Author Index

- Abadie, A. 181
 Abramova, I. M. 83
 Alberti, G. 5
 Alekseenko, V. A. 235
 Alovitdinov, A. B. 89
 Antokolskaja, I. I. 287
 Bailly, M. 413
 Bálint-Ambró, I. 457
 Belyakov, V. N. 191
 Belyavskaya, T. A. 203
 Boari, G. 393
 Bogoczek, R. 131
 Bolshakova, L. I. 287
 Brajter, K. 385
 Brinkman, U. A. Th. 309
 Bubanec, J. 403
 Bunzl, K. 169
 Chmelíček, J. 89
 Chmielowiec, J. 197
 Corte, F. de 217
 Costantino, U. 5
 Czeglédi, B. 429, 433
 De Corte, D. 217
 De Jong, G. J. 309, 443
 Delle Site, A. 293
 Dévényi, T. 245
 De Vries, G. 309
 Dickel, G. 31
 Dodds, J. A. 421
 Duffy, S. C. 149
 Dybczyński, R. 263, 277
 Dyer, A. 95
 Erdélyi, M. 429, 433
 Ferenczi, S. 245, 257
 Gaál, H. 77
 Gaál, J. 375
 Chersini, G. 299
 Gorodnev, M. S. 83
 Grevillot, G. 421
 Halász, I. 325
 Häupke, K. 117
 Hayashi, T. 273
 Hazai, I. 245, 257
 Hecker, H. 135
 Hering, R. 141
 Horváth, Zs. 409
 Hoste, J. 217
 Huber, J. F. K. 333, 353
 Inczédy, J. 41, 165, 225, 375, 381
 Jha, S. K. 217
 Jochemsen, R. 309
 Jong, G. J. de 309, 443
 Kakihana, H. 47
 Kálmán, A. 109
 Kemula, W. 197
 Kočkarova, Ch. U. 89
 König, K.-H. 99
 Kraak, J. C. 333
 Lásztity, A. 203
 Légrádi, L. 319
 Liberti, L. 155, 393
 Lukas, D. 123
 Makhalov, E. M. 235
 Marhol, M. 89
 Marton, A. 165
 Mink, J. 109
 Myasoedova, G. V. 287
 Nagy, O. 77
 Nikashina, V. A. 235
 Ogden, A. B. 95
 Papp, E. 225
 Passino, R. 155, 393
 Patthy, A. 257
 Pientka, V. 117
 Rees, L. V. C. 149
 Rekers, C. J. N. 443
 Rodrigues, A. E. 437
 Roques, H. 181
 Rubanik, S. C. 191
 Rubinstein, R. N. 235
 Salát, J. 245
 Saldadze, G. K. 83
 Savvin, S. B. 287
 Schaaf, R. 451
 Schwachula, G. 123
 Sebestian, I. 325
 Seki, T. 251
 Senyavin, M. M. 235
 Shvoeva, O. P. 287
 Site, A. delle 293
 Sopková, A. 403
 Sterlińska, E. 263
 Strazhesko, D. N. 191
 Strelko, V. B. 191
 Szabó, J. 77
 Szirtes, L. 105, 109
 Testa, C. 293
 Thomas, J. D. R. 209
 Tondeur, D. 413, 421
 Tyihák, E. 257

- Van der Wal, Sj. 353
Varentsov, V. K. 83
Venitsianov, E. V. 235
Vetejška, K. 403
Vigh, Gy. 381
Vigvári, M. 429, 433
Vries, G. de 309
Wada, H. 251
Wal, Sj. van der 353
Walton, H. F. 57
Weigand, N. 325
Werner, G. 69
Wódkiewicz, L. 277
Yamabe, T. 273
Zoltán, S. 245, 257
Zsinka, L. 105, 109

Subject Index

- Acetone cyanohydrin
Separation of metals on ion-exchange resins by means of α -hydroxyisobutyronitrile as complexing agent 319
- Acidic compounds
Separation of — by high-pressure liquid-liquid chromatography involving ion-pair formation 333
- Alamine 336 S
The use of aqueous thiocyanate solutions in liquid-liquid extraction and reversed-phase extraction chromatography. I 309
- Aliquat 336
The use of aqueous thiocyanate solutions in liquid-liquid extraction and reversed-phase extraction chromatography. I 309
- Alizarin red S
Application of ligands with sulphonic groups to the separation of metal ions on strongly basic anion exchangers 385
- Alkaline earth metals
Separation of metal ions by mixed column ion-exchange chromatography 273
- Alkaloids
Liquid chromatography of organic compounds on ion-exchange resins 57
- Amberlite LA-1
The use of aqueous thiocyanate solutions in liquid-liquid extraction and reversed-phase extraction chromatography. I 309
- Amines
Chromatographic separation of dansyl amino acids and dansyl — on Amberlite IRC-50 251
- Amino acids
Chromatographic behaviour of — on cation-exchange resin-coated chromatoseeds in the H^+ form 245
- Amino acids
Chromatographic separation of dansyl — and dansyl amines on Amberlite IRC-50 251
- Amino acids, basic
Combined application of ion-exchange chromatographic methods for the study of "minor basic —" 257
- Aminodiol enantiomer-copper(II) complexing
Separation of optical isomers by ion-exchange chromatography using copper(II) ions as complex-forming agents 375
- Amphoteric resin, ion retardation
Synthesis and properties of some snake-cage ion-retardation resins 131
- Amphoteric resin, ion retardation
The use of the amphoteric ion-exchange resin Retardion 11A8 for inorganic separations 263
- Anion-exchange equilibria of maleic and fumaric acids
Investigation of — 165
- Anion exchange of metals
Anion exchange in ternary mixtures of aliphatic acids, mineral acids and water 217
- Anion-exchange resins, amino types
Chloride-sulphate exchange on —. Kinetic investigations. I 155
- Anion exchanger in hydrobromic acid medium
Anion-exchange behaviour of some elements on a weakly basic — 277
- Anion exchangers, strongly basic
Contribution to basicity testing of — 135
- Aqueous thiocyanate solutions
The use of — in liquid-liquid extraction and reversed-phase extraction chromatography. I 309
- Arsenic
The ion-exchange behaviour of — (III) on VARION anion-exchange resins 457
- Basicity testing
Contribution to — of strongly basic anion exchangers 135
- Bis-(4-vinylphenyl)-methane
Study on the preparation of strongly acidic cation exchangers based on copolymers of styrene and — 123
- Bromopyrogallol red
Application of ligands with sulphonic groups to the separation of metal ions on strongly basic anion exchangers 385
- Calcium sulphate
Prevention of — scale formation in evaporation plants by ion exchange 393
- Cation exchange on silica gels
Mechanism of — 191
- Cation exchanger based on silica gel
New types of —. I. Preparation and properties 325

- Cation exchangers, strongly acidic
 Study on the preparation of — based on copolymers of styrene and bis-(4-vinylphenyl)-methane 123
- Cerium
 The mobility of — ions in synthetic zeolites 95
- Cerium(IV) phosphate
 Recent progress in the field of synthetic inorganic exchangers having a layered or fibrous structure 5
- Cerium(IV) phosphate-sulphates
 On the selectivity of the cation exchange on crystalline — 99
- Chabazites
 Comparison of experimental and theoretical rates of ion exchange 149
- Chelate sorbents
 — for concentration and separation of noble metals 287
- Chemical equilibria
 — in ion-exchange chromatography 41
- Chloramphenicol
 Separation of some — intermediates by high-pressure ion-exchange chromatography 381
- Chloride-sulphate exchange
 — on anion-exchange resins. Kinetic investigations. I 155
- Chromatosheets in the H^+ form
 Chromatographic behaviour of amino acids on cation-exchange resin-coated — 245
- Chromotropic acid
 Application of ligands with sulphonic groups to the separation of metal ions on strongly basic anion exchangers 385
- Complex-forming agents
 Separation of optical isomers by ion-exchange chromatography using copper(II) ions as — 375
- Copolymers
 Study on the preparation of strongly acidic cation exchangers based on — of styrene and bis-(4-vinylphenyl)-methane 123
- Copper
 Some problems in the separation of — and iron from mine waters 403
- Copper(II)
 The extraction of — ions with liquid anion exchangers using salicylate as complex-forming agent 225
- Dansyl derivatives
 Chromatographic separation of dansyl amino acids and dansyl amines on Amberlite IRC-50 251
- Derivatography
 Examination of ion-exchange resins by — 77
- Dinitrobenzene
 Effect of cross-linking of a sulphonic cation-exchange resin and effect of temperature on the chromatographic separation of isomers of — 197
- Distribution coefficients of maleic and fumaric acids
 Investigation of anion-exchange equilibria of maleic and fumaric acids 165
- Donnan ions
 The phenomenon of osmosis in permeable membranes 31
- Drugs
 Liquid chromatography of organic compounds on ion-exchange resins 57
- Equilibrium constants
 Chemical equilibria in ion-exchange chromatography 41
- Estrogen glucuronides
 High-pressure liquid chromatography with ion-exchange celluloses and its application to the separation of — 353
- Evaporation plants
 Prevention of calcium sulphate scale formation in — by ion exchange 393
- Extraction chromatography
 — with liquid ion exchangers 299
- Extraction chromatography
 — with liquid ion exchangers as stationary phase 293
- Faujasites
 The mobility of cerium ions in synthetic zeolites 95
- Fixed-bed ion-exchange
 Cyclic operation of a — column with three components 421
- Fumaric acid
 Investigation of anion-exchange equilibria of maleic and — 165
- Glucuronides
 High-pressure liquid chromatography with ion-exchange celluloses and its application to the separation of estrogen — 353
- α -Hydroxyisobutyronitrile
 Separation of metals on ion-exchange resins by means of — as complexing agent 319
- Inorganic ion exchangers
 IR and X-ray measurements on various — 109
- Inorganic ion exchangers
 Preparation of some new — 105

- Ion exchange in agitated beds
—, Simulation of an ion-exchange column by model of agitated tanks in cascade 437
- Ion-exchange membranes, structure heterogeneity
Investigation of structure heterogeneity in — 83
- Ion-exchange processes, differential
Kinetics of — in a finite solution volume 169
- Ion-exchange processes, optimization
Determination of the optical conditions for ion-exchange processes 235
- Ion-exchange reactions
Comparison of experimental and theoretical rates of ion exchange 149
- Ion exchangers, inorganic
Preparation of some new — 105
- Ion exchangers, inorganic
Recent progress in the field of synthetic inorganic exchangers having a layered or fibrous structure 5
- Ion exchangers, nomenclature
A proposal for the nomenclature of exchangers 141
- Iron
Countercurrent elution of uranium(VI) and —(III) from an anion-exchange resin 433
- Iron
Some problems in the separation of copper and — from mine waters 403
- Isotope-exchange reactions
Ion exchange, isotope exchange and isotope separation 47
- Ligand-exchange chromatography
Liquid chromatography of organic compounds on ion-exchange resins 57
- Liquid ion exchangers
Extraction chromatography with — 299
- Liquid ion exchangers
Extraction chromatography with — as stationary phase 293
- Liquid ion exchangers
The use of — in extraction chromatography 69
- Maleic acid
Investigation of anion-exchange equilibria of — and fumaric acids 165
- Membranes, permeable
The phenomenon of osmosis in — 31
- Mercury, removal from water
The Akzo process for the removal of — from waste water 443
- Metal ions
Separation of — by mixed column ion-exchange chromatography 273
- Metal ions
The use of liquid ion exchangers in extraction chromatography 69
- Metals
Separation of — on ion-exchange resins by means of α -hydroxyisobutyronitrile as complexing agent 319
- Metals, divalent
Anion exchange in ternary mixtures of aliphatic acids, mineral acids and water 217
- Metals, divalent
Selective properties and analytical use of an ion-exchange resin based on α -phenylvinylphosphonic acid 89
- Metals, noble
Chelate sorbents for concentration and separation of — 287
- Mine waste waters
Some problems in the separation of copper and iron from mine waters 403
- Moving-bed ion exchange
Multi-component —, An approach to the design of small-scale preparative column 413
- Nomenclature of exchangers
A proposal for the — 141
- Organic compounds
Liquid chromatography of — on ion-exchange resins 57
- Osmosis
The phenomenon of — in permeable membranes 31
- α -Phenylvinylphosphonic acid-acrylic acid copolymer
Selective properties and analytical use of an ion-exchange resin based on — 89
- Pollutant, organic
Mass transfers in ion-exchange systems perturbed by simultaneous fixation of an — 181
- Powdered ion exchangers
Possible application of — in the treatment of condensate 451
- Preparative columns
Multi-component moving-bed ion exchange. An approach to the design of small-scale — 413
- Primene JM-T
The use of aqueous thiocyanate solutions in liquid-liquid extraction and reversed-phase extraction chromatography. I 309
- PURIWAT® Apparatus
—, A system of ion-exchange celluloses for the production of high-purity water 409

Resins

New results in the study on the porosity of styrene-divinylbenzene copolymers and ion-exchange — 117

Resins, thermal behaviour

Examination of ion-exchange resins by derivatography 77

Salicylate as complex-forming agent

The extraction of copper(II) ions with liquid anion exchangers using — 225

Silica gels

Mechanism of cation exchange on — 191

Silica gel, cation exchanger

New types of cation exchanger based on silica gel. I. Preparation and properties 325

Silicic acid

Mechanism of cation exchange on silica gels 191

Snake-cage ion-retardation resins

Synthesis and properties of some — 131

Snake-cage ion retardation resins

The use of the amphoteric ion-exchange resin Retardion 11A8 for inorganic separations 263

Sorption of ion-exchange resin

Some aspects of ion-exchange in non-aqueous and mixed solvents 209

Sorption of ions

Selective swelling of ion exchangers in mixed solvents and the effect of swelling on the — 203

Stability of ion-exchange resin

Some aspects of ion-exchange in non-aqueous and mixed solvents 209

Stationary phases

Extraction chromatography with liquid ion exchangers as — 293

Styrene

Study on the preparation of strongly acidic cation exchangers based on copolymers of — and bis-(4-vinylphenyl)-methane 123

Styrene-divinylbenzene copolymers

New results in the study on the porosity of — and ion-exchange resins 117

Sugars, amino

Liquid chromatography of organic compounds on ion-exchange resins 57

Sulphonic cation-exchange resin

Effect of cross-linking of a — and effect of temperature on the chromatographic separation of isomers of dinitrobenzene 197

Swelling of ion exchangers

Selective — in mixed solvents and the of swelling on the sorption of ions 203

Tellurate exchangers

Preparation of some new inorganic ion exchangers 105

Thiocyanate solutions

The use of aqueous — in liquid-liquid extraction and reversed-phase extraction chromatography 309

Titanium

Application of ligands with sulphonic groups to the separation of metal ions on strongly basic anion exchangers 385

Uranium

Countercurrent elution of —(VI) and iron (III) from an anion-exchange resin 433

Uranium

Elution of — from an anion-exchange resin by extraction with an organic extractant in the presence of an aqueous phase 429

Water purification

PURIWAT® apparatus. A system of ion-exchange celluloses for the production of high-purity water 409

Zeolites, synthetic

The mobility of cerium ions in — 95

Zirconium

Application of ligands with sulphonic groups to the separation of metal ions on strongly basic anion exchangers 385

Zirconium phosphate

Recent progress in the field of synthetic inorganic exchangers having a layered or fibrous structure 5

journal of chromatography news section

APPARATUS

N-556

ELECTROPHORESIS POWER SUPPLY

Bio-Rad announces the availability of a dual output power supply for both tube and slab gel electrophoresis. The Model 400 provides constant voltage or cross-over operation, 10x expansion on current adjustment for fine control of current level, voltage and current meters with 10x scale expansion for accurate readings and polarity reversing switches to eliminate cable reversals.

The Model 400 is designed to limit the amount of voltage that can be supplied at a given current, or the amount of current at a given voltage, in order to protect the gel from power levels that will cause excessive heating and poor separations. It has a constant voltage of 10-400 V DC and a constant current output of 2-80 mA DC.

N-555

UNIMETRICS CATALOG

Unimetrics announces a 32-page catalog giving information on its micro syringes, micro-pipetters, and chromatographic accessories. A number of new products are described including a repeating dispenser and a new series of fixed volume repeating syringes with capacities to 10 ml.

N-553

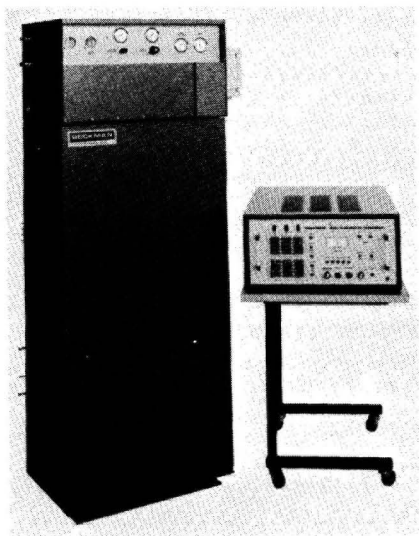
PROCESS GAS CHROMATOGRAPH

Beckman announces the first series of its Model 352 Process Gas Chromatograph. Designed for automatic composition analyses of process streams in refineries, chemical and petrochemical plants, the Model 352 incorporates an extensive chain of safety devices.

The system consists of four basic units - sample conditioner, analyzer, programmer and data acquisition device. The sample conditioner receives raw samples from the process streams and prepares them for introduction into the analyzer. As the process conditions vary widely from one application to another, a large variety of special components are available together with experienced engineering to offer solutions for most complex and heavy-duty requirements.

The analyzer, mounted on top of the sample conditioner, is a complete self-contained unit which can also be operated manually for ease of maintenance and to simplify startup. The large oven compartment offers maximum accessibility to the columns, the piston-operated switching valves and the thermal conductivity detectors or flame ionization detectors, all thermostated to any temperature from 50 to 200°. Amplification of the detector signal in the analyzer and the constant current signal transfer to the programmer help to eliminate transmission noise and signal loss errors. The quartz-controlled digital timer in the programmer unit, which is unaffected by frequency fluctuations in the power line, can control up to 20 functions in an analysis cycle which can be adjusted from 31.25 sec to 10,000 sec. The digital ICs are all of the Cos-Mos

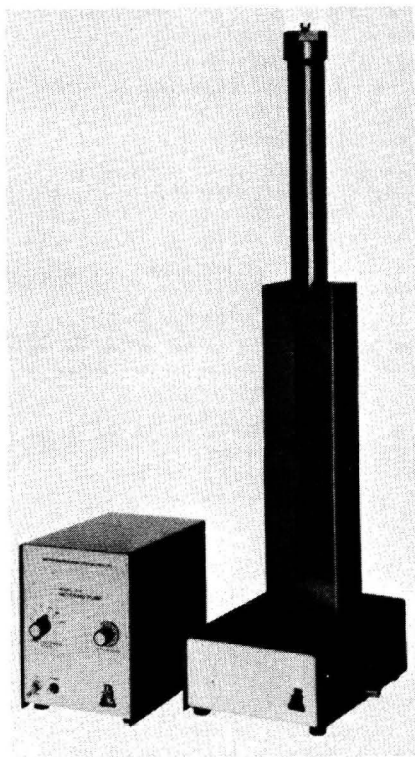
series for maximum noise immunity. The programmer, which can be used for either 6-stream thermal conductivity or flame ionization detector applications, is designed for relay-rack mounting and is directly computer-compatible for data acquisition via priority interrupt or long-term memory amplifiers.



N-558

SYRINGES FOR HPLC

A series of syringes, Model 88210S, from Hamilton for HPLC are gas- and liquid-tight and have been designed primarily for high-pressure liquid chromatography. Available in 50, 100, 250 and 500 μ l capacities, these syringes will withstand routine inlet pressures from 2000–3000 p.s.i. The syringes have a metal hub to use in holding and steadying the syringe during insertion, a plunger guide to prevent bending and stops to prevent plunger blowout during injection.



N-552

SYRINGE PUMP FOR HPLC

A redesign has increased operating pressure of the ISCO Model 314 syringe pump from 2,000 p.s.i. to 2,850 p.s.i. (200 kg/cm²). The Model 314 delivers constant flow from 0.8 to 200 ml/h regardless of back pressure, making it suitable for high performance liquid chromatography, reagent injection, and other applications requiring high pressure over wide, reproducible flow rates. The total capacity is 375 ml.

Single-stroke steel syringe construction and ultra-precision bearings provide pulseless delivery absolutely free of minute fluctuations. An optional electronic digital pressure monitor/regulator is available for the Model 314 metering pump and the companion Model 384 high pressure gradient pump.



N-565

MICROSYRINGE PIPET

A series of spring-loaded microsyringe pipets, which deliver samples in the 1- μ l range with 1% accuracy, has been developed by Hamilton. They are suited for electrophoresis sampling, RIA, and radioimmuno-diffusion.

The microsyringe pipets have a disposable tip at the end of the needle to avoid the possibility of cross-contamination. Pre-set volumes may be dispensed by simply pressing the plunger to an auxiliary stop prior to discharge. The sample to be dispensed is confined to the plastic tip.

They are available in the 10 μ l and 25 μ l models, with a permanently affixed needle.

N-578

CARLO ERBA "SHORT NOTES"

Carlo Erba Strumentazione in their July edition of "Short Notes" describe a number of items including a high-sensitivity thermionic detector suitable for the selective detection of heteroatoms (e.g. nitrogen, phosphorus) in organic molecules. An accessory for gas chromatography, designed especially to enable the accurate determination of solvent residues in food wrapping materials, is also described, as well as an automatic sampler for use in the routine determination of chlorinated, phosphorated and nitrogen pesticides. Further, a number of sampling systems for gases, liquids and solids are described.

N-574

AUTOMATED TLC ELUTION

Camag has designed an apparatus called Eluchrom which allows quantitative elution of thin-layer spots without scraping off the layer. Six spots can be eluted simultaneously by means of elution cells pressed tightly on the plate and transported each to a cuvette (for subsequent determination), provided that the distance between two spots is at least 2.5 mm and the spot diameter not greater than 20 mm.

N-577

HAMILTON CATALOG

A large part of Hamilton's catalog H-75 is devoted to their syringes. The 7000-series syringes are renewed and improved in order to handle samples against 400 atm. Several new high pressure syringes are introduced for volumes up to 50 μ l.

Of great importance for clinical laboratories and the pharmaceutical industry is the extended range of dispensers. They deliver volumes up to 10 ml and down to 0.5 μ l with a very high accuracy and reproducibility. Attention is paid to the special miniature inert valves, and a valve-driving system is introduced for remote and automatic operation of those Hamilton valves. Resins are described briefly.

N-567

UNIMETRICS CATALOG

Unimetrics Corporation's eight-page catalog describes a series of precision valves, connectors and chromatography equipment, all autoclavable and chemically inert. The connectors allow rapid joining of tubing of different diameters as well as different materials. Descriptions of equipment and the assembly of complete introductory kits for column chromatography are listed and pictured. Solid Teflon-valve bodies with EN58J stainless-steel keys as well as two-, three- and seven-way valves are described.

N-576

LIQUID CHROMATOGRAPHS

The Universal liquid chromatograph (ULC) from Tracor has both a syringe type (pressures up to 6000 p.s.i., flow-rates up to 100 ml/min) and a reciprocating type (up to 3000 p.s.i., up to 10 ml/min) pumping system. It incorporates a UV absorbance and a refractometer detector. The Model 8000 gradient elution chromatograph is another member of the Tracor LC Series and consists of a primary (2000 p.s.i.) and a secondary (1000 p.s.i.) pumping system, a stop-flow injection system and a UV absorbance detector.

N-571

CLINICAL ELECTROPHORESIS SYSTEM

Product Bulletin 331 from Gelman describes their 4 clinical electrophoresis systems and Gelman procedures for electrophoretic determination of serum proteins, lipoproteins, LDH-isozymes, and hemoglobins.

N-570

CTR COLUMNS

Alltech Associates' Bulletin 8700 describes CTR Columns, comprising of a column within a column. This concentric arrangement permits the analysis of certain chemical mixtures which up till now required switching valves or use of two separate analytical runs. The bulletin illustrates this point by reference to the problem of separating oxygen, nitrogen, carbon monoxide, carbon dioxide and methane which is shown to be complete in less than 10 min in one run, at room temperature.

N-572

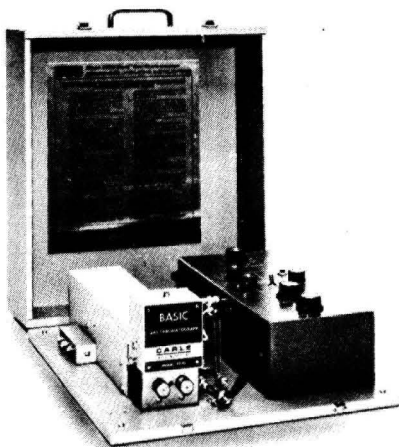
SEPRACHROMTM

In Product Bulletin 329 from Gelman a description is given of Seprachrom procedures (with disposable chambers) which can be used in drug screening and identification, as well as for determination of lecithin/sphingomyelin ratios in amniotic fluid. Seprachrom chambers can also be used in screening radiopharmaceuticals for impurities.

N-583

HPLC PRODUCTS

Newsletter 17 from Alltech Ass. describes high-performance liquid chromatography-products. Items described are pumps, solvents, septa, injection valves, syringes, LI-Chroma tubing, stainless-steel frits, special fittings, labels and books. A tool useful for cutting 1/16-in. O.D. stainless-steel tubing without danger of collapsing the inside hole, is also described.



N-580

MEASUREMENT OF VINYL CHLORIDE IN AIR

The Model 9500-P BasicTM Gas Chromatograph from Carle is designed to identify and measure trace amounts of toxic organic volatiles in any atmosphere. The instrument enables one to decide whether or not a peak is vinyl chloride with a sensitivity down to less than 1 ppm.

By the parallel column technique it is possible to discover interferences and ensure correct peak identification and quantitative accuracy.

The portable Model 9500-P is designed to measure toxic organics, particularly aromatic and chlorinated hydrocarbons. Amongst its attributes the Model 9500-P allows samples to be handled without any preconcentration techniques.

N-573

COMPUTING DENSITOMETER FOR ELECTROPHORESIS

The ACD-15 is a digital, solid state computing instrument for scanning serum proteins, LDH isozymes, lipoproteins, and alkaline phosphatase. The ACD-15 has the ability to scan all the major electrophoresis media. It has automatic or manual peak selection, a grating monochromator for dialing the wavelength desired, linearity from 0 to 2 O.D., a new heat-sensitive form with the complete scan automatically entered for a permanent record, "hot wire" printing and 15 second scans.

N-579

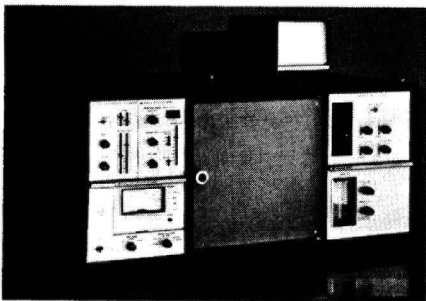
DUAL COLUMN, DUAL DETECTOR GAS CHROMATOGRAPH

A dual column, dual detector gas chromatograph with a dual differential electrometer is introduced by Hewlett-Packard. The Series 5730A instruments are available with thermal conductivity (TC), flame ionization (FI) and electron capture (EC) detector systems. Dual detector configurations available consist of FI/TC, FI/EC and EC/EC.

The differential electrometer with dual input and dual output capability is standard in all 5730A Series instruments. Switch-selectable operating modes are A or B and differential. The dual differential electrometer provides two independent channels for chromatographic runs or operation in the compensation mode. (Electrometer performance specifications are the same as those for Model 5711A instruments.)

The standard temperature control configuration for Series 5730A GC's consists of an isothermal controller for the column oven (programmer optional) and four independent temperature controllers; for two detectors, injection port and a heated accessory. (The optional oven temperature programmer (used in 5730A instruments) is identical to the digital programmer used in Series 5710A Gas Chromatographs.) Operation is fully automatic including cooldown and reset.

The instruments are equipped with dual flow controllers for carrier gas flow regulation. The instrument is equipped with an injection port for heated on-column injection or with heated metal liners for 1/8" or 1/4" columns. Liners with removable glass inserts for special applications are available as an option.



N-581

MINIATURE CENTRIFUGE

BECKMAN BULLETIN

Bulletin GR-6303 describes the table-top Microfuge B from Beckman that spins down blood samples and precipitates from micro samples in less than 60 sec. A 6-place rotor head permits centrifugation of up to 48 micro samples in a single run. The Microfuge B accepts the tapered-bottom 1.5-ml tubes as well as the standard 250- and 400- μ l tubes. Suitable for stat and routine lab. applications, the Microfuge B is useful in RIA methodology for carcinoembryonic antigen (CEA), serum or plasma separations for ultramicro- and micro-chemistry, electrophoresis serum and hemolysate preparation and clarifying cerebrospinal fluid concentrates.

N-582

VARIAN CHROMATOGRAPHY CATALOG

Chromatography Catalog No. 18 (72 pages) describes a wide range of items, dealing under the section "Gas Chromatography" with gas chromatographs, detectors, columns, automatic sampler etc. The section entitled "Data handling for GC and LC" provides information on a data system, integrators and recorders, while "Liquid Chromatography" deals with liquid chromatographs, detectors, columns, etc. A final section describes fittings for GC and LC.

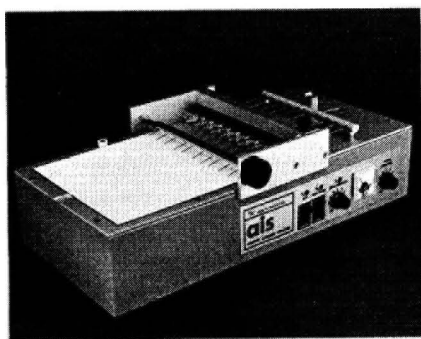
N-585

μ STYRAGEL PACKING

Because of the interest in high-speed/high-resolution size separations and size separations of small molecules (obtained by gel permeation chromatography employing μ Styragel as the size-separating packing material in the column), the autumn 1974 issue of "Chromatography Notes" from Waters Ass. is devoted to size separations employing μ Styragel. Included in this issue are discussions on separating and analyzing pharmaceuticals, natural products, essential oils, and polymers. References are given to other Waters' publications containing more complete coverage of each subject.

AUTOMATE THIN-LAYER SPOTTING

The TLC Multi-Spotter, a 16-spot unit, automatically applies the contents of sixteen 100- μ l syringes at variable rates, ranging from 5–30 min. A 9-spot unit has been specially designed for use with the Schoeffel spectrodensitometer. A built-in solvent evaporator allows large volumes to be concentrated in spots less than 3 mm in diameter. For labile compounds a special manifold for evaporation under a stream of nitrogen is available. Syringes designed for the TLC spotting are available in 10-, 25-, 50- and 100- μ l sizes.



N-557

PRODUCTS FOR HOSPITAL AND CLINICAL LABORATORY

The sixteen-page Bulletin GR-7500, "Beckman Products for the Hospital and Clinical Laboratory", summarizes the company's total capability in the health-care field. The section, "Instruments for clinical chemistries", describes the new System TR enzyme activity analyzer, the UV/Vis spectrophotometer, glucose/BUN analyzers, flame photometer, electrophoresis systems and enzyme reagents. Gamma-counting and liquid-scintillation instruments for radioimmunoassay, medical gas and oxygen analysis equipment for cardiopulmonary applications and EEG, echoencephaloscope and a dual-channel vascular analysis system are described and illustrated. The bulletin also covers centrifuges, pH meters and diagnostic reagents.

CHEMICALS

N-547

P-L BIOCHEMICALS CATALOGUE

An 160-page catalogue from P-L Biochemicals consists of 8 sections and an index. The products in the sections are alphabetically listed. The sections comprise: nucleotides, coenzymes, and related products; amino acids; carbohydrates; lipids; antibiotics; buffers; enzymes; diagnostic reagents.

N-548

ADSORBENTS FOR HPLC

PartisilTM is a microparticulate silica adsorbent for HPLC manufactured by Reeve Angel and described in their Bulletin No. 100. It is available in three mean particle sizes 5, 10, and 20 μ m, as loose media or in "PXS" prepacked columns. It has a mean pore size of 40–50 Å with a surface area of 400 m²/g. It is applicable as adsorbent in LSC and as solid support in LLC.

The liquid chromatography source book (Bulletin No. 103, Vol. 1) of Reeve Angel summarizes their adsorbents, ion-exchange resins, and accessories for HPLC.

N-549

RADIOIMMUNOASSAY NEWSLETTER

"Radioassay News", a monthly newsletter serving the clinical and biomedical fields, covers the latest news and information regarding radioimmunoassay and related techniques.

For further information concerning any of the news items, apply to the publisher, using the reply cards provided, quoting the reference number printed at the beginning of the item.

MEETINGS

THIRD INTERNATIONAL SYMPOSIUM ON THIN-LAYER CHROMATOGRAPHY

The third International Symposium on Thin-layer Chromatography will be held in London, England, May 5-7, 1975. The themes are: Separations (detection and practical aspects), Photodensitometry (qualitative and theoretical aspects) and Associated physico-chemical techniques (mass spectrometry).

Participants will be: A.A. Boulton (Saskatoon), T. Brodasky (Kalamazoo), P.E. Flinn (St. Louis, Mo.), F. Geiss (Ispra, Italy), R.R. Goodall (Macclesfield), O. Hutzinger (Halifax, N.S.), H. Jork (Saarbrücken), M. Lederer (Rome), N.N. Osborne (Göttingen), V. Pollak (Rio de Janeiro), K. Randerath (Houston, Texas), G. Rouser (Duarte, Calif.), B.G. Smith (Skokie, Ill.), G. Szekeley (Basel), N. Seiler (Frankfurt), L.R. Treiber (Sodertälje, Sweden).

The Proceedings of the meeting will be published in a special issue of the *Journal of Chromatography*. For further information contact Dr. A.A. Boulton, Psychiatric Research Unit, Room 508, University Hospital, Saskatoon, Saskatchewan S7N 0W8, Canada.

EIGHTH INTERNATIONAL SYMPOSIUM ON CHROMATOGRAPHY AND ELECTROPHORESIS

The eighth International Symposium on Chromatography and Electrophoresis will be held in Brussels, Belgium, May 28-30, 1975. The three main subjects to be discussed are the following: Sequential Analysis of Polypeptides and Nucleic Acids, Metabolites of Drugs and Specific Detectors.

The programme will be as follows:

Opening address: Prof. M. Lederer (Rome);

Prof. A.H. Beckett (London): Some problems in gas chromatography related to pharmacokinetic studies of bases;

Prof. W. Fiers (Ghent): The genetic information content: direct analysis and prospects;

Prof. A. Frigerio (Milan): Metaboliti dei farmaci studiati coi metodi gas cromatografici e di spettrometria di massa;

Dr. K. Han (Lille): Electrophorèse et chromatographie dans la détermination de la séquence des protéines;

Prof. G. Schill (Uppsala): Liquid chromatography with optical detection based on ion-pair technique;

Prof. J. Sjövall (Stockholm): Specific detection by mass spectrometry;

Dr. D.H. Williams (Cambridge): Application of mass spectrometry to the sequencing of proteins.

Participants who intend to contribute a communication or a demonstration should apply before January 1, 1975 to: Société Belge des Sciences Pharmaceutiques, rue Archimède 11, 1040 Brussels, Belgium. The latest date on which the registration form will be accepted is April 15, 1975 after which a tax of BFr 500 will be required. Registration before this date qualifies participants to receive the final programme. An exhibition of scientific apparatus is scheduled to take place during the symposium. The official languages are English, French, Dutch, German and Italian.

TOXICOLOGY WORKSHOPS

A series of seven regional toxicology workshops jointly sponsored by The American Association of Clinical Chemists, the Perkin-Elmer Corp. and Gelman, has been announced for 1974-75 in the U.S.A. The two-day workshops deal with UV/fluorescence spectroscopy, gas and thin-layer chromatography as far as they apply to toxicological analysis.

3rd INTERNATIONAL SYMPOSIUM ON MASS SPECTROMETRY IN BIOCHEMISTRY AND MEDICINE

The 3rd International Symposium on Mass Spectrometry in Biochemistry and Medicine will be held in Alghero, Sardinia, Italy, June 16th–18th, 1975. The Symposium will be devoted to topics such as the following:

- Gas Chromatography–Mass Spectrometry
- Stable Isotope Measurements
- Mass Fragmentography
- Field Ionization
- Field Desorption
- Chemical Ionization
- High Resolution Studies
- Data Acquisition and Processing

The areas of application will include biochemistry, medicine, toxicology, drug research, forensic science, clinical chemistry and pollution. The official language will be English.

Authors wishing to present a communication (approximately 20 minutes) are requested to submit the title and an abstract of maximal 200 words (in English) before February 28th, 1975. The abstracts should be typewritten using a format 21 × 29.7 cm with a 2.5-cm margin left above, below and on either side of the text. Tables and figures should be submitted as the originals.

A book exhibition and a display of manufacturers' literature on mass spectrometers and related instrumentation will be staged for the whole period of the Symposium.

Further information can be obtained from Dr. Alberto Frigerio (Symposium Organizer), 3rd International Symposium on Mass Spectrometry in Biochemistry and Medicine, Istituto di Ricerche, Farmacologiche "Mario Negri", 20157 Milan, Via Eritrea 62, Italy.

NEW BOOKS

Mass spectrometry in biochemistry and medicine, edited by A. Frigerio and N. Castagnoli, Jr., Raven Press, New York, and North-Holland, Amsterdam, 1974, ix + 389 pp., price Dfl. 97.00, US\$ 37.30.

Analyse extraterrestrischen Materials, edited by W. Kiesel and H. Malissa, Jr., Springer, Vienna, New York, 1974, ix + 326 pp., price DM 56.00, US\$ 22.90.

Handbook of commercial scientific instruments, Vol. 2, Thermoanalytical techniques, by W.W. Wendlandt, Marcel Dekker, New York, 1974, xii + 234 pp., price US\$ 14.75.

Rodd's chemistry of carbon compounds, supplement to the 2nd ed. of Vol. II (Alicyclic compounds), parts A and B, edited by M.F. Ansell, Elsevier, Amsterdam, xvi + 424 pp., price Dfl. 135.00, US\$ 51.90.

Rodd's chemistry of carbon compounds, supplement to the 2nd ed. of Vol. II (Alicyclic compounds), parts C, D and E, edited by M.F. Ansell, Elsevier, Amsterdam, xvii + 317 pp., price Dfl. 110.00, US\$ 42.30.

Advances in chromatography, Vol. 10, edited by J.C. Giddings and R.A. Keller, Marcel Dekker, New York, 1974, xi + 246 pp., price US\$ 19.75.

Proceedings of the International Symposium on Macromolecules, Rio de Janeiro, July 1974, edited by E.B. Mano, Elsevier, Amsterdam and New York, 1974, vii + 463 pp., price US\$ 46.25.

Spectroscopic and chromatographic analysis of mineral oil, by S.H. Kägler, Halsted Press (Wiley), New York, Toronto, and Israel Program for Scientific Translations, Jerusalem, London, 1974, xiii + 560 pp., price £ 25.40.

PUBLICATION SCHEDULE FOR 1975

Journal of Chromatography (incorporating *Chromatographic Reviews*)

MONTH	D 1974	J	F	M	A	M	J	J	A	S	O	N	D
JOURNAL	101/1 101/2 102	103/1 103/2 104/1	104/2 105/1 105/2	106/1 106/2	107/1 107/2	The publication schedule for the volumes 108-112 and 114 will be published later.							
REVIEWS*				113/1					113/2			113/3	

* Volume 113 will consist of *Chromatographic Reviews*. The issues comprising this volume will not be published consecutively, but will appear at various times in the course of the year.

GENERAL INFORMATION

(A leaflet *Instructions to Authors* can be obtained by application to the publisher.)

Types of Contributions. (a) Original research work not previously published in a generally accessible language in other periodicals (Full-length papers). (b) Review articles. (c) Short communications and Notes. (d) Book reviews; News; Announcements. (e) Bibliography of Paper Chromatography, Thin-Layer Chromatography, Column Chromatography, Gas Chromatography and Electrophoretic Techniques. (f) Chromatographic Data.

Submission of Papers. Three copies of manuscripts in English, French or German should be sent to: Editorial office of the Journal of Chromatography, P.O. Box 681, Amsterdam, The Netherlands. For *Review articles*, an outline of the proposed article should first be forwarded to the Editorial office for preliminary discussion prior to preparation.

Manuscripts. The manuscript should be typed with double spacing on pages of uniform size and should be accompanied by a separate title page. The name and the complete address of the author to whom proofs are to be sent should be given on this page. Authors of papers in French or German are requested to supply an English translation of the title. A short running title of not more than 50 letters (including spaces between the words) is also required for Full-length papers and Review articles. All illustrations, photographs, tables, etc., should be on separate sheets.

Heading. The title of the paper should be concise and informative. The title should be followed by the authors' full names, academic or professional affiliations, and addresses.

Summary. Full-length papers and Review articles should have a summary of 50-100 words. In the case of French or German articles an additional summary in English, headed by an English translation of the title, should also be provided. (Short communications and Notes will be published without a summary.)

Illustrations. The figures should be submitted in a form suitable for reproduction, drawn in Indian ink on drawing or tracing paper. Particular attention should be paid to the size of the lettering to ensure that it does not become unreadable after reduction. Sharp, glossy photographs are required to obtain good halftones. Each illustration should have a legend, all the *legends* being typed together on a *separate sheet*. Coloured illustrations are reproduced at the author's expense.

References. References should be numbered in the order in which they are cited in the text and listed in numerical sequence on a separate sheet at the end of the article. The numbers should appear in the text at the appropriate places using superscript numerals. In the reference list, periodicals¹, books², and multi-author books³ should be cited in accordance with the following examples:

- 1 A. T. James and A. J. P. Martin, *Biochem. J.*, 50 (1952) 679.
- 2 L. R. Snyder, *Principles of Adsorption Chromatography*, Marcel Dekker, New York, 1968, p. 201.
- 3 R. D. Marshall and A. Neuburger, in A. Gottschalk (Editor), *Glycoproteins*, Vol. 5, Part A, Elsevier, Amsterdam, 2nd ed., 1972, Ch. 3, p. 251.

Abbreviations for the titles of journals should follow the system used by *Chemical Abstracts*.

Proofs. Two sets of proofs will be sent to the author to be carefully checked for printer's errors. Corrections must be restricted to instances in which the proof is at variance with the manuscript. "Extra corrections" will be inserted at the author's expense.

Reprints. Fifty reprints of Full-length papers, Short communications and Notes will be supplied free of charge. Additional reprints can be ordered by the authors. An order form containing price quotations will be sent to the authors together with the proofs of their article.

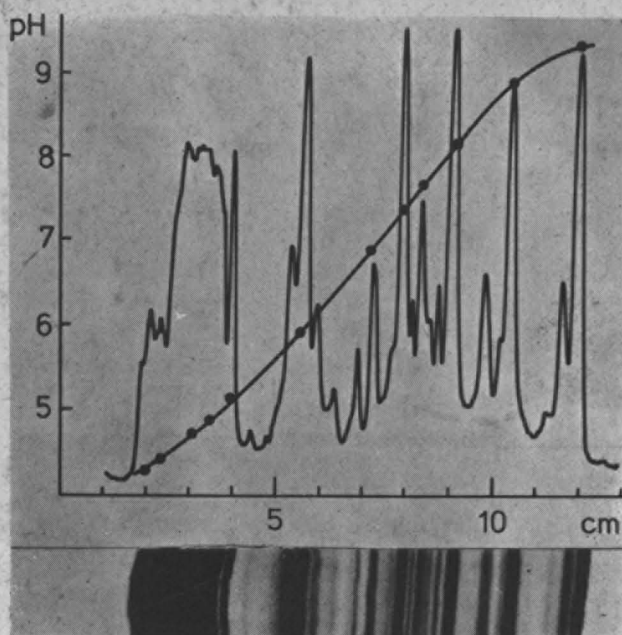
News. News releases of new products and developments, and information leaflets of meetings should be addressed to: The Editor of the News Section, Journal of Chromatography, Elsevier Scientific Publishing Company, P.O. Box 330, Amsterdam, The Netherlands.

Subscription orders. Subscription orders should be sent to: Elsevier Scientific Publishing Company, P.O. Box 211, Amsterdam, The Netherlands.

Publication. The *Journal of Chromatography* (including *Chromatographic Reviews*) appears fortnightly and has 14 volumes in 1975. The subscription price for 1975 [Vols. 101-114 and Supplementary Vol. 4 (Bibliography of Electrophoresis 1968-1972)] is Dfl. 1365.00 plus Dfl. 120.00 (postage). Subscribers in the U.S.A., Canada and Japan receive their copies by air mail. Additional charges for air mail to other countries are available on request. Back volumes of the *Journal of Chromatography* (Vols. 1 through 100) are available at Dfl. 100.00 (plus postage).

Advertisements. Advertisement rates are available from the publisher on request. The Editor of the journal accepts no responsibility for the content of the advertisements.

DESAGA



Isoelectric Focusing

The DESAGA TLE Double Chamber® – a versatile apparatus for a versatile method.

Isoelectric focusing ranks with the highest resolution among the separating methods. The separated components are identified by their isoelectric point. This method has revealed an unprecedented heterogeneity in many proteins, enzymes and other amphoteric substances.

Analytical Isoelectric Focusing

The DESAGA TLE Double Chamber® is suitable for thin-layer isoelectric focusing in continuously polymerized polyacrylamide gels or in granulated gels. You can run 20 – 30 proteins in two hours under identical conditions.

Preparative Isoelectric Focusing

With the DESAGA TLE Double Chamber® you can separate 0,01 – 10 g protein. The excellent resolution of analytical isoelectric focusing is also achieved in preparative separations.

The DESAGA TLE Double Chamber® has been specially designed with flexibility of operation in mind. We have constructed the apparatus so that you like can perfect your own particular separation process. Would you like to know how the best isoelectric focusing can be carried out in an analytical and preparative scale? Just contact us, we have the experience.

Maybe you are also interested in other separation techniques. The DESAGA TLE Double Chamber® can also be used for Thin-layer Electrophoresis, Preparative Electrophoresis and Paper Electrophoresis. You can buy this versatile apparatus at an extremely reasonable price.

Ask for product information 173.



World Hallmark
of Thin-layer
Chromatography
and Electrophoresis

C. DESAGA GmbH
Nachf. Erich Fecht
D 69 Heidelberg 1 · P.O.B. 10 19 69
Telephone (0 62 21) 8 10 13
Telex 04-61 736